DEVELOPMENT OF NOVEL NI-CATALYZED REDUCTIVE COUPLING REACTIONS OF AZIRIDINES

Dmitry Zimin

UNIVERSITAT ROVIRA i VIRGILI

Development of Novel Ni-Catalyzed Reductive Coupling Reactions of Aziridines

DMITRY ZIMIN

DOCTORAL THESIS
2024

Development of Novel Ni-Catalyzed Reductive Coupling Reactions of Aziridines

Dmitry Zimin

Doctoral Thesis

Supervised by Prof. Ruben Martin Romo

Institut Català d'Investigació Química (ICIQ)

Universitat Rovira i Virgili (URV)

Department of Analytical Chemistry and Organic Chemistry

UNIVERSITAT ROVIRA i VIRGILI

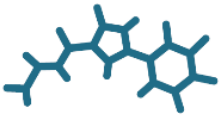

ICIQ

Institute of Chemical Research of Catalonia

UNIVERSITAT ROVIRA i VIRGILI

ICIQ Institute of Chemical Research of Catalonia

Prof. Ruben Martin Romo, Group Leader at the Institute of Chemical Research of Catalonia (ICIQ) and Research Professor of the Catalan Institution for Research and Advanced Studies (ICREA),

I STATE that the present study, entitled "Development of novel Ni-catalyzed reductive coupling reactions of aziridines", presented by Dmitry Zimin for the award of the degree of Doctor, has been carried out under my supervision at the Institute of Chemical Research of Catalonia (ICIQ).

Tarragona, April 3rd, 2024

Doctoral Thesis Supervisor

Prof. Ruben Martin Romo

Table of contents

Acknowledgements

First of all, I would like to thank **Prof. Ruben Martin Romo** for accepting me into the Martinis family. That decision truly became a life-changing for me. I am thankful for scientific guidance, but even more for full moral support during my PhD.

The studies presented in the Doctoral Thesis are conducted in collaboration with past group members, namely **Dr. Jacob Davies**, **Dr. Craig Day** and **Dr. Matthew Wakeling**. I was very lucky to collaborate with you guys and this thesis would never be finished without your help and contribution.

I would like specifically thank **Prof. Kathrin H. Hopmann** for her supervision and guidance while conducting DFT studies, which would never be done without her help.

I would like to thank present group members **Mr. Filip Meger** and **Dr. Alvaro Velasco** for their help with reading and correcting the Doctoral Thesis.

Finally, I would like to thank all past and present members of Martinis group as well as all the people I have met at ICIQ and URV for all great life moments we shared together.

List of abbreviations

EWG = Electron-withdrawing group

EDG = Electron donating group

EDO = Electron-deficient olefin

SET = Single electron transfer

HAA = Halogen Atom Abstraction

OA = Oxidative Addition

Alk = Alkyl

Ar = Aryl

Phen = Phenanthroline

Bipy = Bipyridine

Ts = Tosyl

Ns = Nosyl

TFE = 2,2,2-Trifluoroethanol

General introduction

A dream chemical transformation of medieval alchemists was the transmutation of lead into gold by using the so-called "Philosopher's Stone". In time, humanity has achieved extraordinary progress in the natural sciences including chemistry and these days we know that such a process was beyond possible. However, as humans never stop dreaming,[1] modern chemists have a dream akin to their alchemist predecessors. This dream can be described as an ability to access any molecule with specific properties. As the theoretical number of possible organic molecules is infinite the discussion of how realistic this dream is turns into a philosophical topic. Nevertheless, it does not stop scientists from pushing the horizons of this idea forward and we can point out two fundamental parts of it. The first part is how to predict the chemical structure of the molecule which potentially possesses the desired properties. The revolutionary idea in this field is the idea of "chemical space" when all potential chemical structures have their mathematical coordinates in conditional mathematical unity analogously to the coordinates of space objects in the space maps.[2,3] By "traveling" through this space we can discover compounds with specific properties and reveal their structures.[4] However, at this point the second part of modern chemists dream comes into play: how can we access these molecules in reality? Is the present stage of development of chemical methodology area enough to successfully perform the synthesis? Again, as mentioned above, the theoretical number of possible organic molecules is technically infinite, which means there is technically an infinite amount of chemical transformations. This is far beyond human mental capacities. To overcome this problem nowadays we seek the support of computer technologies with artificial intelligence as a particular example. According to the experts in the field, we are still at the point of generating big data which a crucial for chemical AI development.[5] Thus, still being on our own designing novel chemical transformations we use some sort of intellectual approximations to simplify our lives. We build our research around a particular idea, such as using a particular catalyst or reagent;[6] creating a synthetic concept with criteria which developed transformations have to fit, e.g. the so-called "Shuttle catalysis";[7] following a particular reaction mechanism;[8] etc. In prof. Ruben Martin's group the general theme of research is the activation of inert entities, specifically activation of CO_2, N_2O, and the activation of inert C-H, C-C, C-O, or C-N bonds. Once we have a general area of research we still need to develop it into a particular synthetic methodology. To achieve this, we use more specific generalizations. Among many different examples, the classic and reliable way to design a new chemical transformation is to choose a fixed structural organic moiety, which becomes the topic of research. From here we can think in two ways: (1) how many synthetic routes are there to make this moiety; (2) how many synthetic routes are there to modify this moiety? Every discovered synthetic transformation exists

within a particular theme of research and once published it fills a gap which previously existed before in our collective knowledge of chemistry.[9] Little by little, collecting our efforts and following Hegel's "law of transition from quantity to quality" we can ultimately expect breakthroughs at the level of our understanding of chemistry which will entirely change the way we think about this science.[10,11]

Nevertheless, we do not know when this transition will happen and we need to go back to a less lofty level of discussion. Within the context of this thesis, the fixed structural organic moiety is an aziridine ring – a three-membered nitrogen-containing heterocycle. Following our interest in the activation of inert entities we explored the activation of aziridine C-N bonds using nickel catalysis. The first project incorporated a CO_2 molecule into the aziridine moiety giving access to β-amino acids. In the follow-up project we used alkynes as coupling partners to form homoallylamines. We also performed numerous mechanistic experiments, supported by DFT analysis, to elucidate the mechanisms of the transformations developed. All our modest combined efforts are summarized on the following pages and represent our contribution to the search for modern "Philosopher's Stone".

I hope you enjoy the content.

Dmitry Zimin

Summary of the thesis

The thesis is structured based on the following order:

1) ***Chapter I.*** This chapter focused on providing a thorough introduction into aziridine chemistry. Firstly, the general properties of aziridines are discussed and a short overview of synthetic accessibility is given. Next, azanickellacyclobutanes and azapalladacyclobutanes are introduced through discussion of the reports by Gregory L. Hillhouse in 2002,[12] and by John P. Wolfe in 2006,[13] as these are the key reactive species crucial for synthetic methodologies developed afterward. Finally, a literature review detailing works focused on Ni- and Pd-catalyzed transformations using aziridines from 2002 to the state of the art is given. The chapter is concluded with a general summary and perspective showing the motivations behind the experimental chapters.

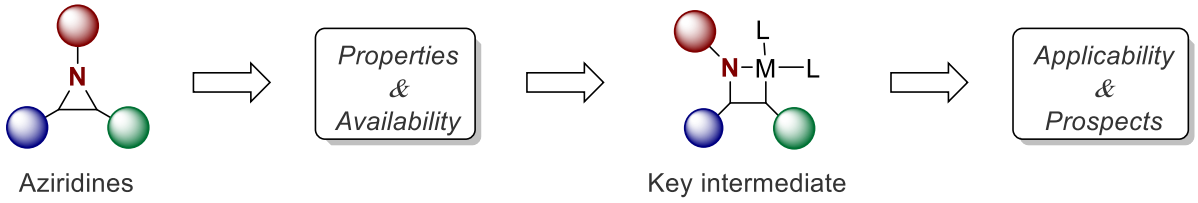

Figure I. Aziridines – a general overview

2) ***Chapter II.*** This chapter is focused on the Ni-catalyzed reductive carboxylation of aziridines using CO_2. First, fundamentals of Ni-catalyzed carboxylation are given for a better understanding of the developed methodology. Next, the main stages of research are described, starting from optimization of reaction conditions followed by an assessment of substrate scope. Finally, after a discussion of a series of control experiments, some general conclusions are made. The chapter ends with a corresponding experimental data section.

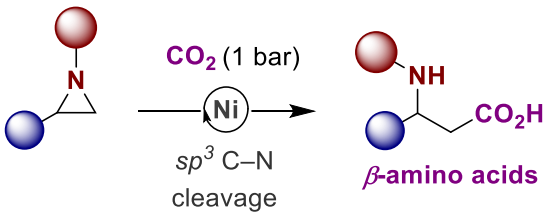

Figure II. Nickel-catalyzed aziridine carboxylation using CO_2

3) ***Chapter III.*** This chapter is focused on Ni-catalyzed aziridine hydroalkenylation, using alkynes as a coupling partners. First, fundamentals of Ni-catalyzed alkyne functionalization are given for a better understanding of the developed methodology. Next, the main stages of research are described, starting from optimization of reaction conditions and followed by the evaluation of the

reaction's synthetic applicability. Finally, after a discussion of a series of control experiments, some general conclusions are made. The chapter ends with the corresponding experimental data section.

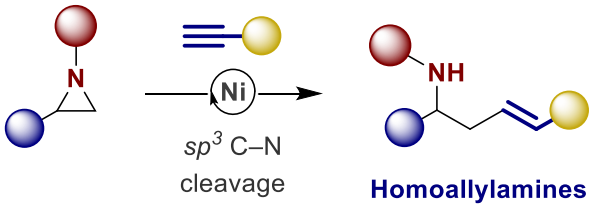

Figure III. Nickel-catalyzed aziridine hydroalkenylation using alkynes

4) ***Chapter IV.*** This chapter is focused on aziridine C-N bond activation with Nickel complexes and the reactivity of azanickellacyclobutane intermediate. Our mechanistic and computational investigation results are introduced step by step and discussed. The chapter ends with a corresponding experimental data section.

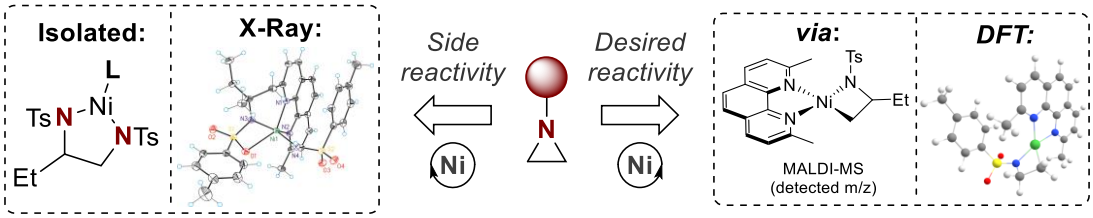

Figure IV. Transformations of aziridines under Nickel catalysis

5) ***Conclusions.*** At the end of the present thesis, conclusions are made to summarize our efforts in nickel-catalyzed transformations of aziridines.

Chapter I. Aziridines an overview

1.1 General chemical properties of aziridines

Aziridines are a saturated three-membered nitrogen heterocycle. As a cyclic compound of small ring size with bond angles of approximately 60° it possesses significant ring strain (Figure 1.1).[14–16]

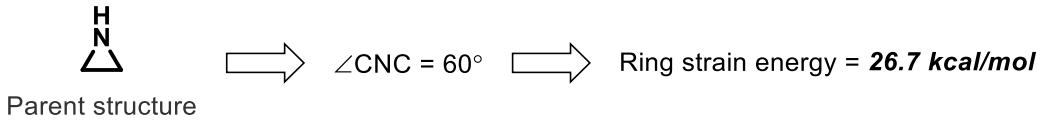

Figure 1.1 Aziridine and ring strain phenomenon

This strain energy and related physico-chemical properties of aziridine distinguish it from other saturated nitrogen heterocycles. For instance, the aziridine nitrogen atom has an increased s-character due to the specific hybridization of orbitals in the case of bent bonds and as a result reduced π-donor abilities and basicity (pK_a 8 in water), compared with acyclic amines (pK_a 11).[17] In addition, the nitrogen inversion barrier is also significantly higher compared with acyclic amines; consequently results such as dynamically-controlled aziridine functionalization have been achieved.[18,19] Most notably, aziridine rings undergo ring-opening reactions giving access to a tremendous amount of amines, and are widely used in organic synthesis and polymer chemistry.[20–22] The nature of these chemical transformations strongly depends on substituents present in the aziridine parent core. Thus, a substituent adjacent to the nitrogen atom can greatly change the mechanism of ring-opening activation. On the model reaction of nucleophilic ring-opening by CN^- anion the observed trend is that activation energy decreases with the increase of electron-withdrawing effect of the substituent (Figure 1.2).[23]

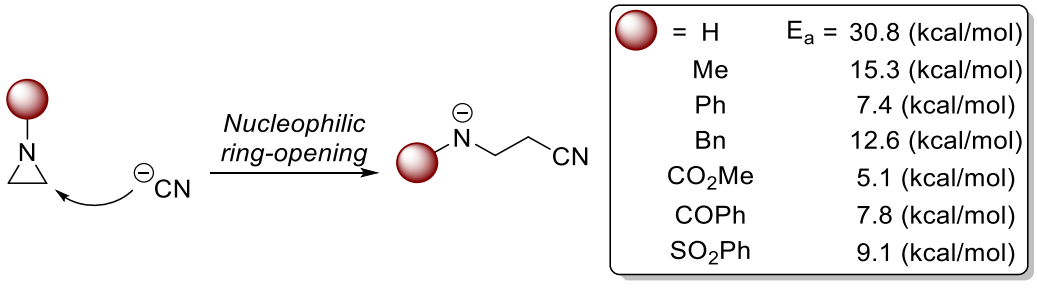

Figure 1.2 Calculated activation energies for nucleophilic ring-opening of aziridine depending on *N*-substituent

Following this trend we can distinguish aziridines into two groups. The first group is formally called “activated” aziridines, bearing the EWG group adjacent to the nitrogen. The second group

is formally called “unactivated” aziridines, where the nitrogen atom either has no substituent or is bonded with an aliphatic group. Even though, *N*-phenyl aziridine demonstrated the activation energy relative to *N*-sulfonyl and *N*-carbonyl-substituted aziridines, based on the experimental data accumulated in literature it demonstrates reactivity of both types and is formally considered as an “unactivated” aziridine.[24]

Thus, as shown above, “activated” aziridines undergo facile ring-opening in the nucleophilic substitution manner via an anionic path, whereas “unactivated” ring-opening requires electrophilic activation of aziridine via a cationic path (Figure 1.3).[25,26]

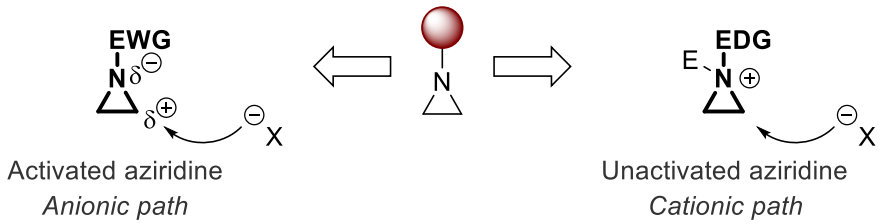

Figure 1.3 Reactivity of “activated” and “unactivated” aziridines

The situation gets more complex, once at least one substituent adjacent to the carbon of aziridine ring is introduced. With additional substituent two regioisomers resulting from nucleophilic attack are possible. The effects of a new substituent have to be taken into consideration when predicting the final product. For instance, when aziridine **1.1** bearing methyl group is attacked by CN^- anion, the nucleophilic substitution occurs at the least substituted carbon atom, due to the steric effect of methyl group (Figure 1.4).[23]

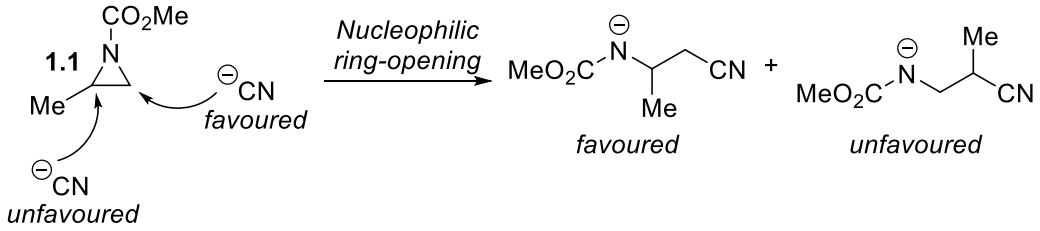

Figure 1.4 Nucleophilic ring-opening of aziridine **1.1**

In contrast, for the aziridine **1.2** bearing acyl group the nucleophilic substitution occurs at the most substituted carbon atom driven by the electronic effects of the substituent (Figure 1.5).[23]

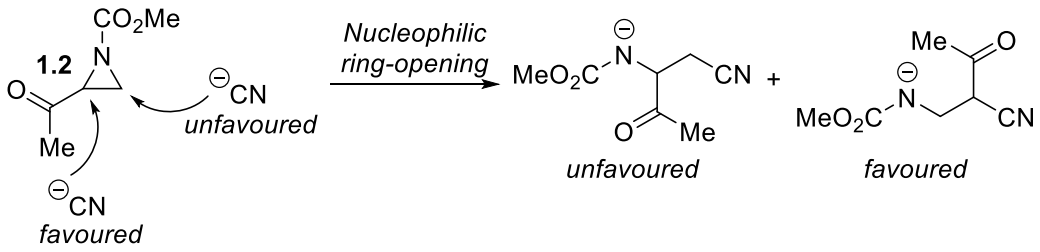

Figure 1.5 Nucleophilic ring-opening of aziridine **1.2**

Nevertheless, regioselectivity can be inverted in the presence of Lewis acids. However, the Lewis acid must be chosen carefully, as it can have either an oxophilic or azaphilic character resulting in the formation of different products (Figure 1.6).[27,28]

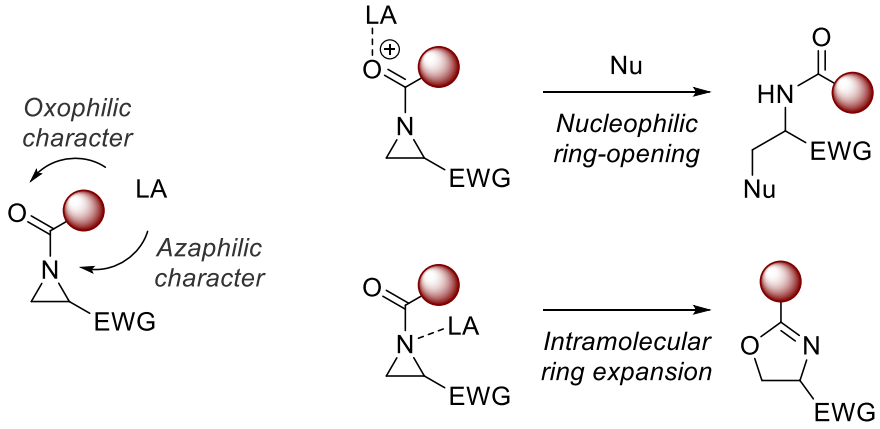

Figure 1.6 Aziridine reactivity based on Lewis acid oxophilic or azaphilic character

Another big area of aziridine chemistry involves using aziridines as dipoles in the cycloaddition reactions.[29,30] Aziridines act as dipoles through C-N cleavage event (Figure 1.7, left) or through C-C cleavage (Figure 1.7, right), depending on the substituents adjacent to the aziridine ring (Figure 1.7).

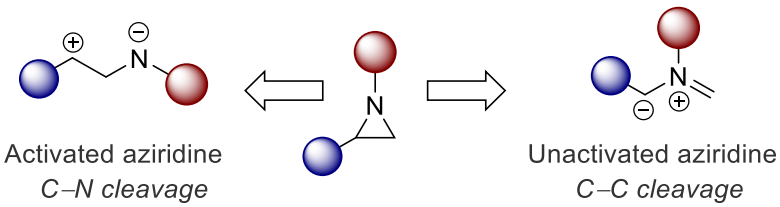

Figure 1.7 Aziridines as dipole synthons

Such a diverse variety of possible reactivity patterns with corresponding complexity of reactivity control can be achieved already with only two substituents in the aziridine ring. However, there are still three more substituents that can be added to the aziridine structure (Figure 1.8).

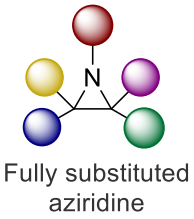

Figure 1.8 Fully substituted aziridine

Even simply considering the following set: H, Alk, Ar, EWG; placed around 5 available positions, we can think about an enormous amount of combinations, where each unique combination possesses its specific intricacies of reactivity.

In addition, as a cyclic compound aziridines are known to be a part of spiro,[31] fused,[32] and bridged polycyclic systems (Figure 1.9).[33]

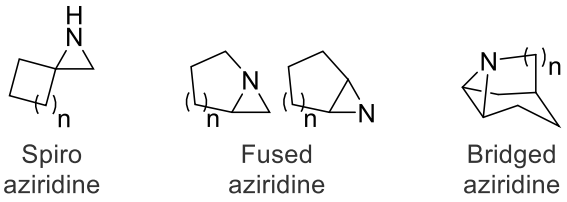

Figure 1.9 Spiro, fused, and bridged aziridines

Taking into account the abundance of aziridine motifs in natural products,[34] their interesting biological properties,[35] and diverse synthetic applicability,[20] including stereocontrolled chemical transformations,[36] it is not a surprise that aziridines attract significant attention in the literature. This growing interest results in a constantly increasing publication growth. For instance, approximately 2300 publications about aziridines were reported from 1991 to 2000. It went to 3800 publications in the period of 2001-2010 and almost 5000 publications during the last decade.[24] A significant amount of these publications are related to aziridine synthesis, which will be discussed in the following section.

1.2 Synthetic accessibility of aziridines

While trying to analyze retrosynthetic disconnections to access the aziridine ring, the most obvious one is the intramolecular cyclization of amines, bearing the leaving group at the β-position (Figure 1.10).

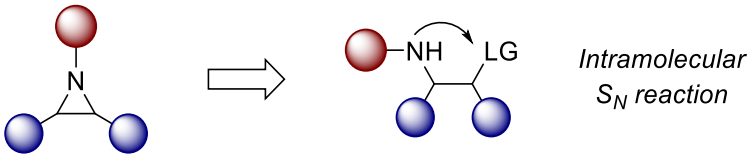

Figure 1.10 Synthesis of aziridine via intramolecular cyclization

One of the earliest processes of that type is Wenker synthesis,[37,38] which is used in the industrial synthesis of the simplest unsubstituted aziridine (ethylene imine).[39] A big advantage of this intramolecular cyclization approach is easy access to chiral aziridines starting from readily available enantiopure precursors.[36]

The other two most common retrosynthetic disconnections discussed in the literature are nitrene insertion into the olefin bond (Figure 1.11, left), or carbene insertion into the imine bond (Figure 1.11, right). This includes transformations with nitrene and carbene synthetic equivalents.[40–43]

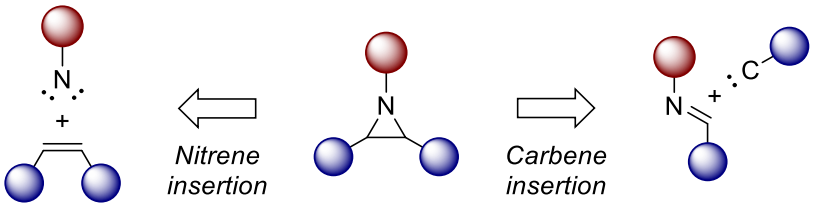

Figure 1.11 Synthesis of aziridine via nitrene or carbene insertions

Among the transformations of the first type, one of the most famous and well-spread methodologies is Evans aziridination.[44] The reaction is catalyzed by copper salts at ambient temperatures, the aziridination of olefins can be achieved using sulfonated iminoiodinanes giving a simple and reliable route to a series of sulfonated aziridines (Figure 1.12).

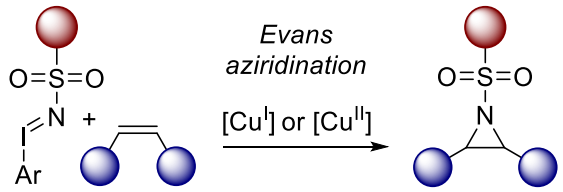

Figure 1.12 Evans aziridination

In the context of chemistry using carbenes, or carbene equivalents, an example of a highly reliable and well-developed methodology is a variation of Darzens reaction with imines, which is known as aza-Darzens reaction. The reaction proceeds stepwise with the formation of a C-C bond through nucleophilic attack at imine α-carbon followed by intramolecular cyclization forming the aziridine product (Figure 1.13).

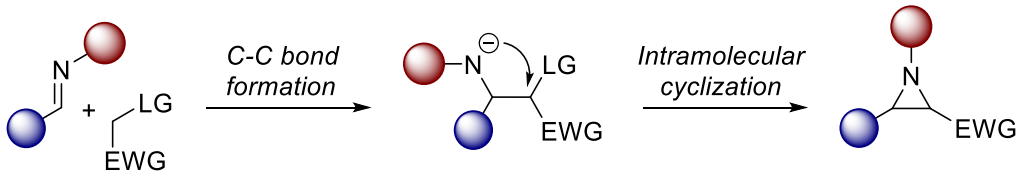

Figure 1.13 aza-Darzens reaction

It is worth mentioning, that the development of aziridination processes in an asymmetric manner based on these two types of transformations (direct or formal nitrene/carbene insertions) is an active field of research.[46,47] Thus, aziridines, including enantiopure ones, are becoming increasingly accessible.

Nevertheless, the field is not limited to the discussed transformations and novel methodologies with new creative synthetic ideas are published regularly, especially ones for accessing synthetically challenging unactivated aziridines. For instance, to highlight some recent examples we can consider protocols from Kurti (Nat. Catal. 2020),[48] Wickens (Nature 2021),[49] and Powers (Nat. Commun. 2022).[50]

In 2020 Kurti reported a metal-free aziridination protocol of unactivated olefins (Scheme 1.1).[48] According to the mechanistic studies, the reaction proceeds via *in situ* formation of oxazirdine **1.5** from amine transfer reagent **1.3** and dicarbonyl compound **1.4**. The compound **1.4** is used in catalytic amounts (20 mol%), as it is regenerated in the reaction after the aziridination event with **1.5** as active species. The reaction demonstrates excellent selectivity of aziridination for substrates containing multiple olefin bonds with products **1.6**, **1.7**, and **1.8** being formed in high yields.

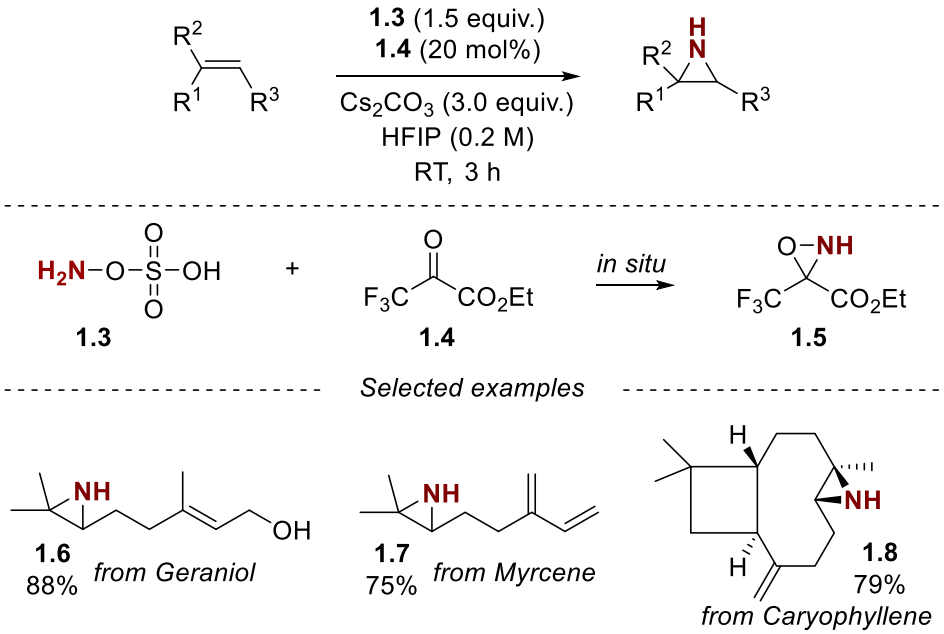

Scheme 1.1 Aziridination of unactivated olefins

In 2021 the Wickens group , developed an elegant *N*-alkyl aziridine synthesis, using thianthrene dicationic adducts with unactivated olefins **1.9**, formed via electrolysis from corresponding olefins and thianthrene respectively (Scheme 1.2).[49]

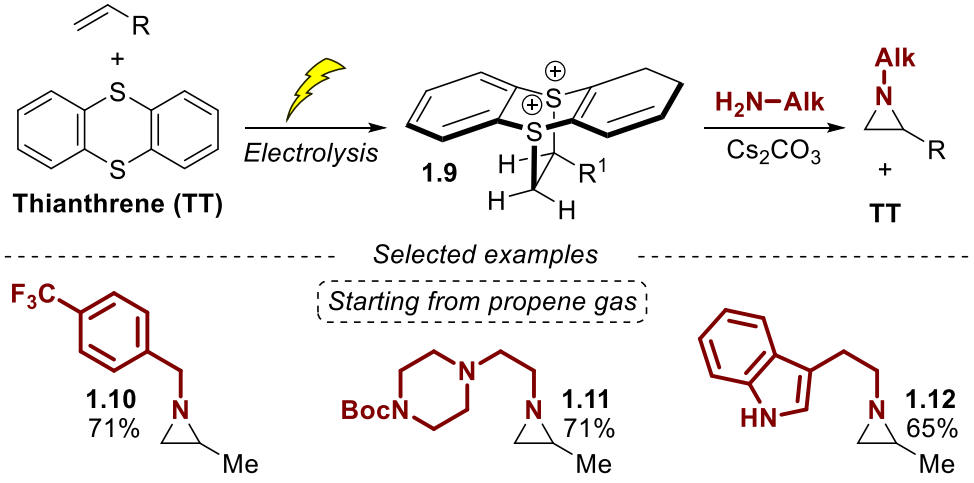

Scheme 1.2 Synthesis of *N*-alkyl aziridines using thianthrene dicationic adducts

The adduct **1.9** reacts with aliphatic amines in the presence of an inorganic base forming the desired aziridines. This procedure opens up a simple way to access an important class of *N*-alkyl aziridines and is suitable even for the simplest gaseous olefins, for instance products **1.10**–**1.12** were synthesized from propene gas.

Lastly, in 2022 by the group of Powers,[50] described the synthesis of *N*-aryl aziridines **1.15** through a sequential approach by forming first *N*-aminopyridinium reagents **1.13** and then applying them to the Ni-catalyzed C-N cross-coupling event with aryl boronic acids **1.14** (Scheme 1.13).

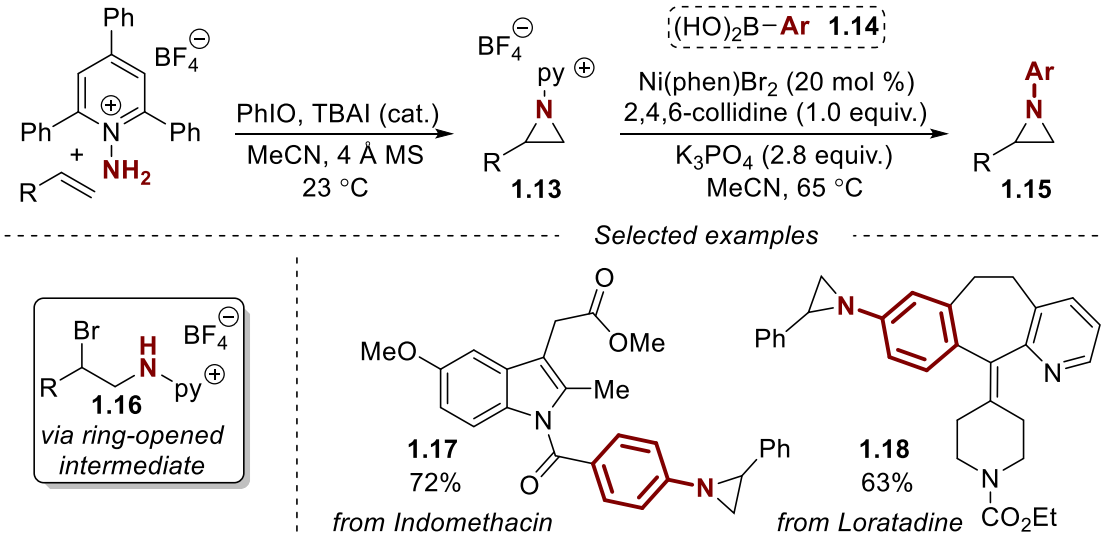

Scheme 1.3 Synthesis of *N*-aryl aziridines from *N*-aminopyridinium reagents

Based on mechanistic studies, the transformation proceeds through the *in situ* formation of the ring-opened intermediate **1.16**, which undergoes stepwise cross-coupling functionalization followed by aziridine ring-closure. To demonstrate the synthetic potential of the reported transformation, derivatives of pharmaceuticals were synthesized, specifically an Indomethacin derivative **1.17** and a Loratadine derivative **1.18**.

The discussed transformations serve as representative examples, introducing state of the art of methods for aziridine synthesis. At this point, bearing in mind the chemical properties of aziridine, especially the ring strain energy, and having a general idea of substrate synthetic availability, we can move to the discussion of aziridine synthetic utility in the context of transition-metal catalyzed reactions. To do so, in the following section the first precedents of aziridine C-N bond activation in the presence of metal complexes will be discussed in detail.

1.3 Reactivity of aziridines toward transition metal complexes

Once started, the area of transition metal-catalyzed transformations forming new bonds via the initial metal center oxidative addition step went through a natural evolution. Starting from revolutionary at the time Pd-catalyzed cross-coupling transformations with aryl halides, the area moved in the direction of substrates more challenging for transition metal oxidative addition event.[51,52] At this point, Nickel came to the fore with the ability to activate more inert pseudohalide bonds (Figure 1.14).[53,54]

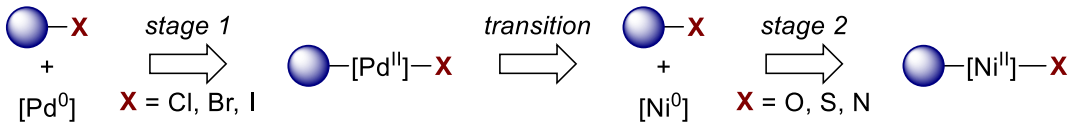

Figure 1.14 Evolution of transition metal-catalyzed cross-coupling transformations

The growing interest spawned a large amount of detailed mechanistic investigations including the preparation of Ni-complexes, containing metal-heteroatom bonds. It was found that many of them are stable and isolable, and can be studied for further reductive elimination events forming carbon-heteroatom bonds (Figure 1.15).[55–57]

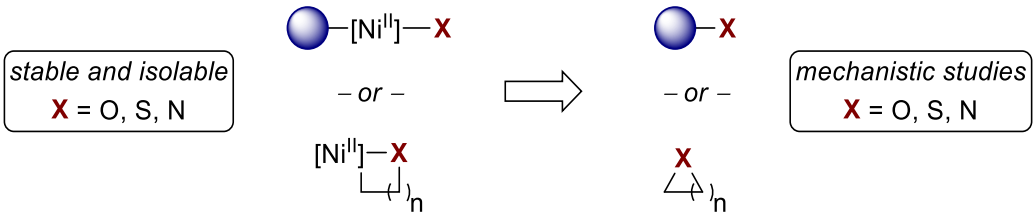

Figure 1.15 Stable Ni^{II} complexes and their applicability

Hence, a natural progression of this chemistry was application of aziridines in the metal-catalyzed transformations and in the synthesis of stable azametallacyclobutanes through the insertion into the C-N bond. The first examples started appearing in the early 80's. In 1981,[58] Alper and coworkers reported Pd-catalyzed carbonylation of azirines (*unsaturated* 3-membered N-heterocycle) and proposed the reaction mechanism proceeding via the formation of fused aziridine **1.19** as reaction intermediate, which undergoes oxidative addition with a Pd-carbonyl complex to form an azapalladacyclobutane **1.20** (Scheme 1.4).

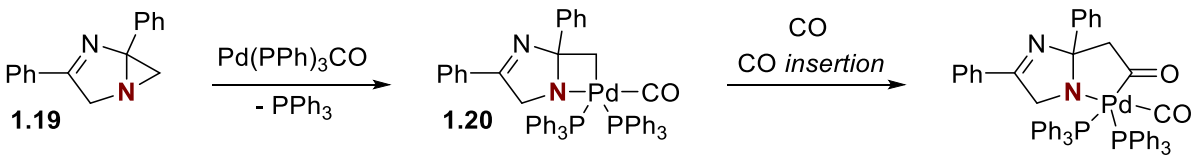

Scheme 1.4 Proposed formation of azapalladacyclobutane intermediate

However, later the same group showed this hypothesis was incorrect.[59] In 1983, Alper developed a carbonylation of aziridines to access *β*-lactams.[60] This was accomplished through a Rh-catalyzed carbonylation of 2-phenyl *N*-alkyl aziridines **1.21**, with azarhodacyclobutane **1.22** proposed as reaction intermediate (Scheme 1.5).

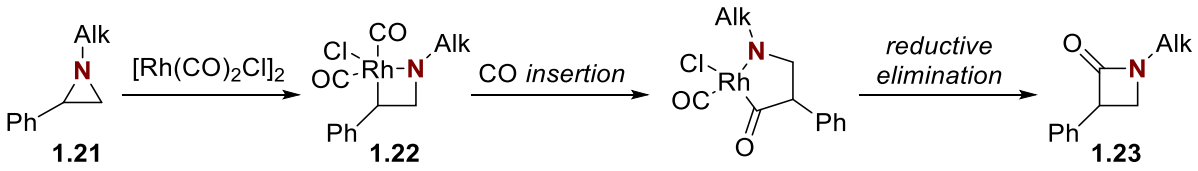

Scheme 1.5 Rh-catalyzed carbonylation of aziridines

The final product **1.23** was formed exclusively as a single regioisomer with the insertion of CO occurring at the most substituted carbon, which indicates that the regioselectivity of the proposed oxidative addition follows general trends discussed in Section 1.1. This reaction was the first example of direct aziridine ring expansion and carbonylation of an aziridine core.

Despite the fact, that in the following 20 years this reaction was well-explored and multiple aziridine carbonylation protocols were reported, applying different transition metals, such as Rh,[60,61] Co,[62] Pd,[63] and Ni,[64] the field was lacked evidence about the formation of azametallacyclobutanes. There was a single example of isolated and characterized azairidacyclobutane complex **1.24**, reported in 1988 by Bergman,[65] which was obtained in the indirect manner stepwise starting with C-H activation of *tert*-butylamine with Cp*(PMe$_3$)IrH$_2$ complex (Scheme 1.6).

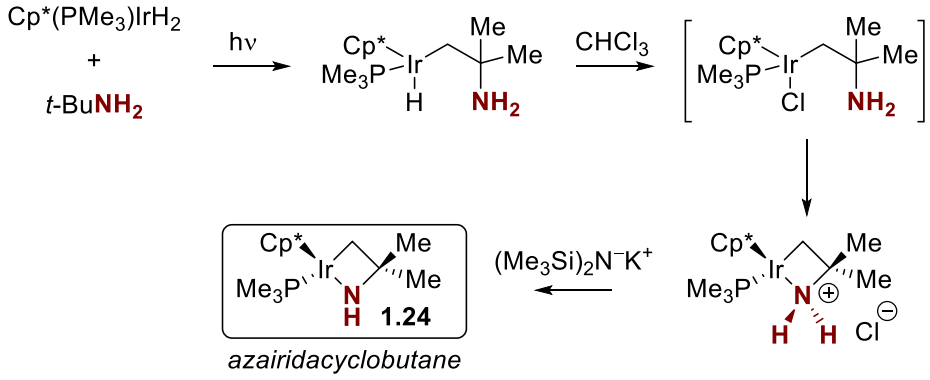

Scheme 1.6 Synthesis of azairidacyclobutane complex **1.24**

Nevertheless, the area of cross-coupling transformations was growing, and in the mid-90s the group of Hillhouse reported a series of protocols regarding studies of reductive elimination events at Ni-metal center forming C-N bond.[57,66,67] Stable amido complexes of Ni were prepared from the reaction between Ni alkyl species and tolylazide (Scheme 1.7).

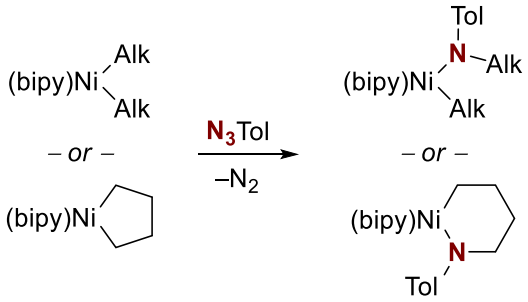

Scheme 1.7 Synthesis of stable amido complexes of Ni

Thus, following the keen interest in the studies of oxidative addition and reductive elimination events that break and make C-X bonds (X = O, S, N), in 2002 Hillhouse reported the interactions of aziridines with Ni complexes giving stable and isolable azanickellacyclobutanes.[12] This protocol became the first example of direct metallacycles synthesis via oxidative addition of metal center into aziridine C-N bond.

At the initial step a series of stable azanickellacyclobutanes **1.26** were synthesized from N-tosylaziridines **1.25** reacting with Ni(0) or Ni(II) complexes in THF under an inert atmosphere (Scheme 1.8).

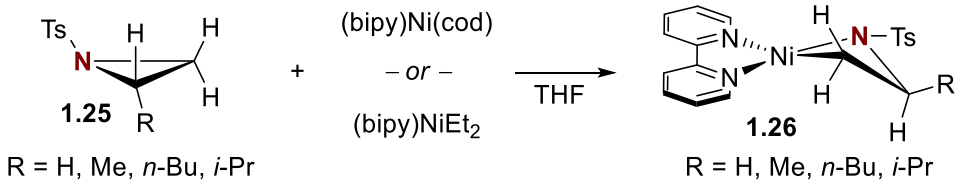

Scheme 1.8 Synthesis of stable azanickellacyclobutanes **1.26** from N-tosylaziridines **1.25**

In all cases, the formation of *only one* regioisomer was observed with oxidative addition occurring exclusively at the least-hindered C-N bond. The structure of 2-methyl N-tosyl aziridine was additionally confirmed by X-ray analysis showing the pyramidal character of nitrogen atom and amido type of Ni-N bond in the solid phase.

Next, the stereochemical course of the reaction was studied. For that purpose, a monodeuterated aziridine **1.27** was prepared using Evans aziridination and subjected to the reaction conditions (Scheme 1.9).

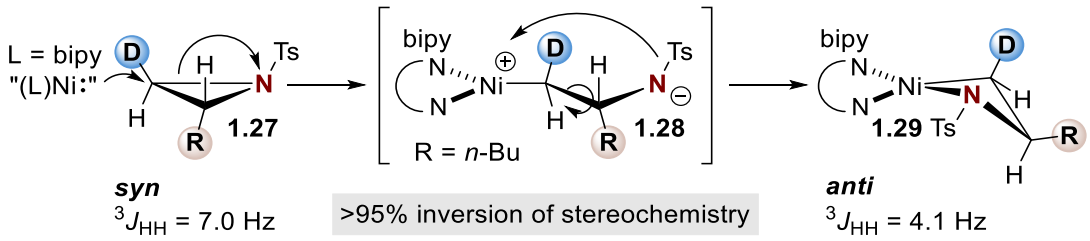

Scheme 1.9 The stereochemical course of aziridine ring-opening with Ni-complexes

Comparing the proton coupling constant of initial aziridine **1.27** ($^3J_{HH}$ = 7.0 Hz => ***syn*** arrangement) with the coupling constant of obtained metallacycle **1.29** ($^3J_{HH}$ = 4.1 Hz => ***anti*** arrangement) it was observed the *full inversion of stereochemistry* at the methylene carbon, once reaction occurred. To rationalize this observation, Hillhouse suggested an S_N2-type reaction mechanism involving nucleophilic attack of Ni center at the least hindered C atom with the formation of ring-opened intermediate **1.28**. The final product **1.29** is formed after the rotation of nitrogen about C-C bond and subsequent ring-closure. However, the obtained metallacycles were only studied for oxidatively induced reductive elimination reforming the aziridine ring by exposing them to an oxygen atmosphere. Any other types of potential azanickellacyclobutanes reactivities have not been explored.

Inspired by Hillhouse results and being interested in the azametallacycles reactivity, the group of Wolfe reported in 2006 their results regarding the synthesis and reactivity of azapalladacyclobutanes.[13] Thus, initial attempts to obtain azapalladacycle following Hillhouse's observations failed after screening multiple Pd(0) sources, and no reaction of aziridine **1.30** or only conversion of aziridine **1.30** into imine **1.31** was observed (Scheme 1.10).

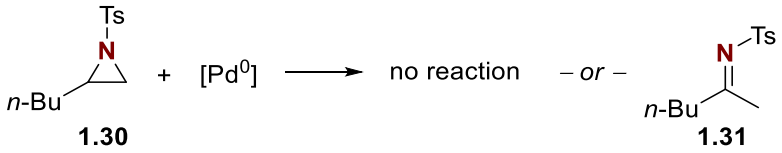

Scheme 1.10 Initial attempts for azapalladacyclobutane synthesis

To unlock the desired transformation it was crucial to have an unsaturated fragment at the α-substituent of aziridine. For instance, aziridine **1.32** reacted with a mixture of $Pd_2(dba)_3$/phenanthroline with the formation of the desired azapalladacyclobutane **1.33** (Scheme 1.11).

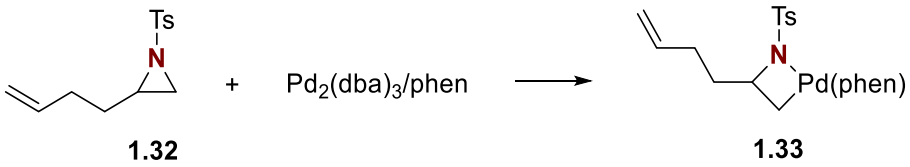

1.32 **1.33**

Scheme 1.11 Successful synthesis of azapalladacyclobutane

Interestingly, any other combinations of $Pd_2(dba)_3$ with chelate N (including bipyridine) or P ligands did not lead to the successful reaction.

Finally, it is worth mentioning, that 2-methyl *N*-Nosyl aziridine **1.34** was also reactive in the presence of $Pd_2(dba)_3$/phenanthroline mixture and metallacycle **1.35** was formed (Scheme 1.12).

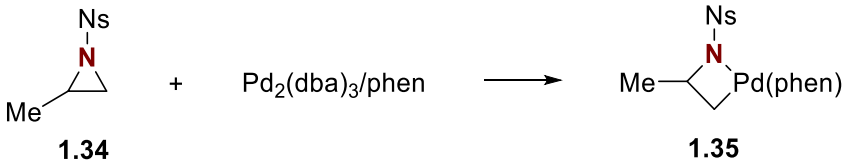

1.34 **1.35**

Scheme 1.12 Successful synthesis of azapalladacyclobutane **1.35** from *N*-Nosyl aziridine **1.34**

This result can be easily rationalized due to the stronger activating properties of the Nosyl group compared to the Tosyl one.

When the stereochemical course of the reaction was studied using deuterium labeled aziridine **1.36** the obtained results were in agreement with those previously reported by Hillhouse. Specifically, the oxidative addition occurred with clean inversion of configuration at the reacting methylene carbon observed in the product **1.37** (Scheme 1.13).

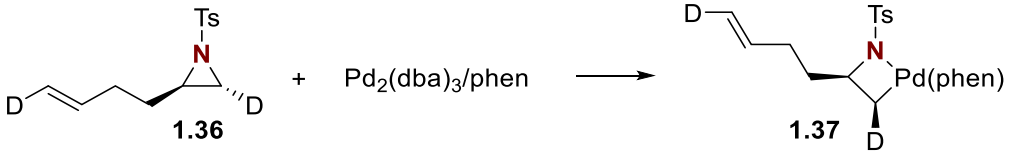

1.36 **1.37**

Scheme 1.13 The stereochemical course of the reaction between aziridines and Pd(0) complexes

Wolfe summarized all the results in the following mechanistic hypothesis. At the first step, the ability of a Pd(0) complex to undergo oxidative addition was dependent on the steric and electronic properties of the ligand used. Thus, using electron-poor ligands, or sterically bulky ligands lead to a lack of aziridine ring opening and no reaction was observed. The reaction is facilitated in the case of electron-rich Pd(0) complexes, however at the next step, when zwitterionic intermediate **1.38** is formed, it leads to a rapid and uncontrolled β-H elimination with the formation of enamine **1.39** in the anionic form (Scheme 1.14, left).

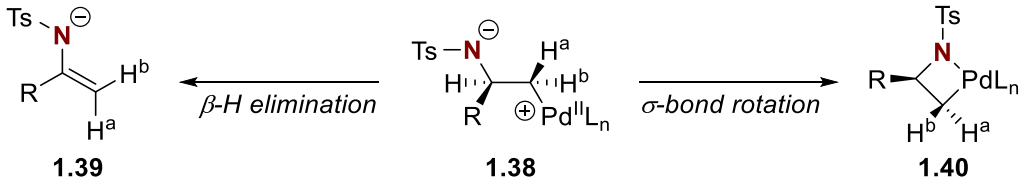

Scheme 1.14 Reactivity of zwitterionic intermediate **1.38**

In contrast, if the intermediate **1.38** is resistant to β-H elimination, then σ-bond rotation occurs with ring-closure of **1.38** into desired azapalladacyclobutane **1.40** (Scheme 1.14, right). In order to reach aforementioned stability the chelation effect of the ligands seems to be crucial.

Finally, investigating the reactivity of azametallacyclobutanes toward insertion of olefin bonds, the CuI catalyzed ring-expansion forming the product **1.43** was achieved in the case of azapalladacycle **1.41**, whereas analogous azanickellacycle **1.42** did not undergo intramolecular alkene insertion under similar conditions (Scheme 1.15).

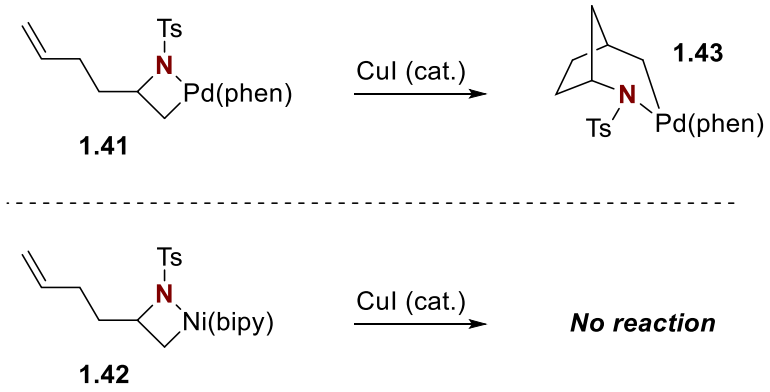

Scheme 1.15 Reactivity of azametallacyclobutanes toward intramolecular alkene insertion

At this point, two key mechanistic papers were covered. It is worth combing the following observations from previous sections together: (1) aziridines are readily available starting materials with a broad range of synthetic methodologies available for initial substrate design; (2) aziridines possess a high reactivity toward nucleophilic attack in general, and toward nucleophilic attack by transition metal centers in particular under mild conditions, driven by the release of ring strain energy; (3) in the case of aziridines monosubstituted at α-carbon the ring-opening event is fully regioselective and exclusively one regioisomer is formed; (4) the regioselectivity of oxidative-addition can be predicted based on general reactivity of aziridines toward the nucleophilic attack; (5) the successful synthesis and isolation of stable azanickellacyclobutanes and azapalladacyclobutanes by Hillhouse and Wolfe proves their stability as potential reaction intermediates and opens up a room for a subsequent design of transition-metal catalyzed cross-coupling transformations of aziridines based on general chemical theory for the reactivity of

$L_nNi(R)(X)$ and $L_nPd(R)(X)$ complexes. The discussion of such transformations starting from 2002 and up to the state of the art is presented in the following section.

1.4 Aziridines as a synthetic platform to access β-functionalized ethylamine core

The event of *β*-H elimination, which Wolfe discussed later in 2006 as an undesired side-process, was first turned into a synthetic feature. In 2003, a Pd-catalyzed transformation of aziridines into ketimines was reported.[68] This was accomplished by heating 2-alkyl aziridines **1.44** with catalytic amount of $Pd(PCy_3)_2$ forming ketimine product **1.45** (Scheme 1.16).

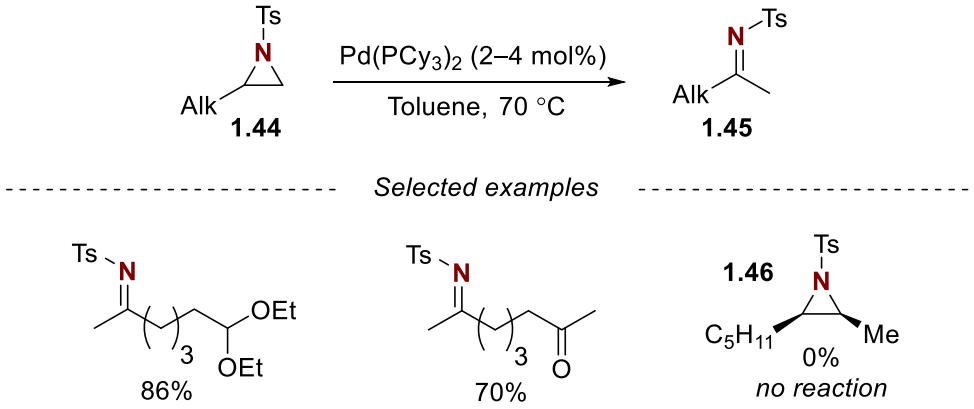

Scheme 1.16 Pd-catalyzed transformation of aziridines into ketimines

The reaction scope is narrow and does not possess many examples. However, among the observations made, it is worth mentioning that 2,3-dialkyl substituted aziridine **1.46** did not react and reaction was limited to monosubstituted aziridines.

Except for the example above the field was relatively inactive until 2012, when the group of Doyle reported the first example of a cross-coupling reaction using styrenyl aziridines as electrophiles in a Negishi-type protocol (Scheme 1.17).[69] This reaction gave access to valuable *β*-substituted amines synthesis and the stoichiometric reaction of azanickellacyclobutanes **1.50** with an organozinc reagent saw the formation of product **1.51**.

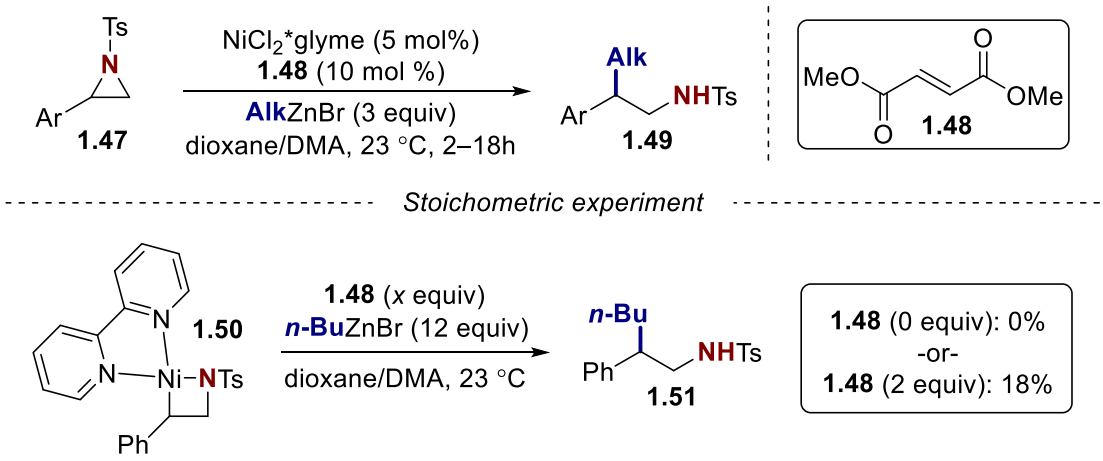

Scheme 1.17 Ni-catalyzed Negishi alkylation of styrenyl aziridines

Organozinc reagents were chosen based on their azaphilicity and the assumption that this would facilitate the transmetalation step. However, any phosphine or amine ligands tested did not lead to significant product formation. To favour the C-C bond forming reductive elimination step, forming products **1.49**, it was crucial to use an electron-deficient olefin (EDO) **1.48** as a ligand. The stoichiometric experiment with presynthesized nickellacycle **1.50** showed that no product was formed in the absence of **1.48**, however, in the presence of **1.48** the formation of the amine **1.51** was observed. These results were in agreement with previous reports of electron-deficient olefins accelerating reductive elimination by association with a metal center.[70,71]

Among important observation was the loss of enantiopurity in product **(*S*)-1.53**, which was synthesized starting from enantiopure aziridine **(*R*)-1.52** (Scheme 1.18).

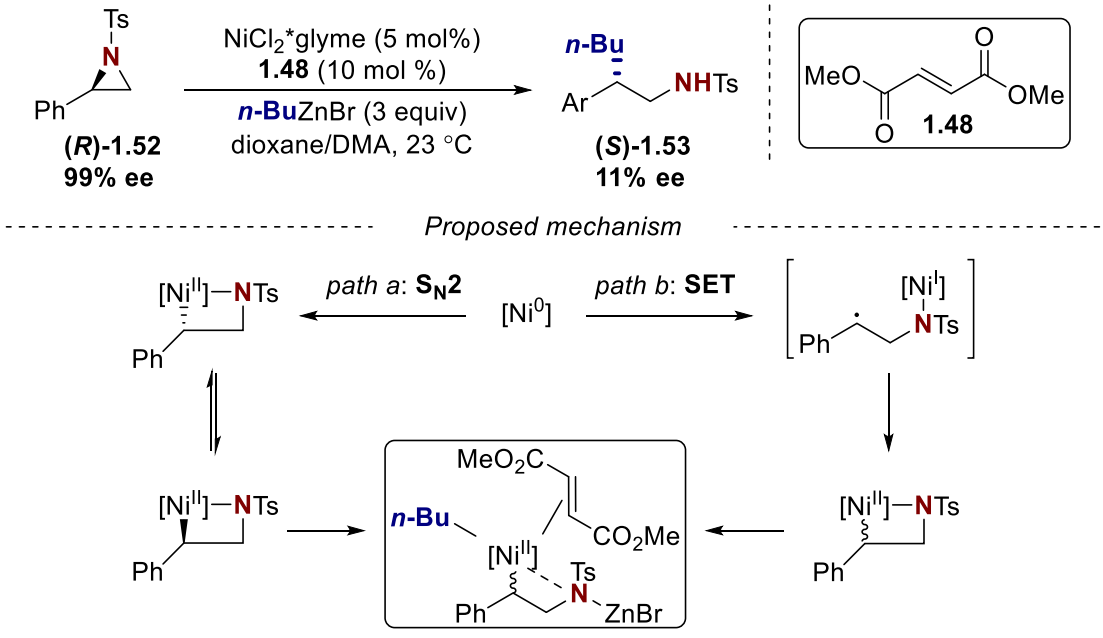

Scheme 1.18 Proposed mechanism of Negishi alkylation

To explain this phenomena, the SET step (Scheme 1.18, *path b*) was proposed analogously for Ni-catalyzed coupling reactions with alkyl halides.[72] However, as some enantiomeric excess still was observed, the S_N2 type ring-opening mechanism (Scheme 1.18, *path a*) could not be completely excluded. In this case, the mechanism of bond racemization is not clear. Either azanickellacyclobutane intermediate undergoes homolysis of Ni-C benzylic bond, or both paths (*path a* and *path b*) are competing within one catalytic cycle.

Nevertheless, the developed procedure was only suitable for styrenyl aziridines and the authors state that: "initial attempts to cross-couple unactivated alkyl aziridines under a range of conditions gave no desired product". Challenging this problem, in 2013, the Doyle group reported directed Ni-catalyzed Negishi cross-coupling of alkyl aziridines.[73] The group came up with a creative substrate design by adding an electron-deficient olefin into the sulfonyl group. This olefin fragment acts both as a directing group to activate substrate **1.54** toward oxidative addition of Ni-center and as a ligand to facilitate the C-C bond-forming reductive elimination event (Scheme 1.19).

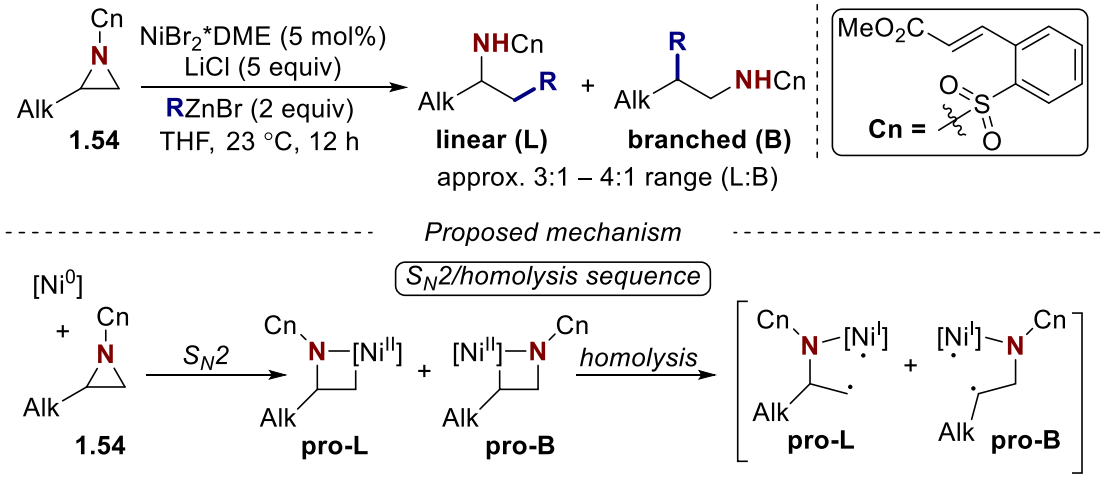

Scheme 1.19 Ni-catalyzed Negishi cross-coupling of 2-alkyl aziridines

Regardless of a unique reactivity this protocol achieved the formation of a mixture of linear and branched amines was observed with poor regioselectivity, which limited the synthetic applicability of the developed methodology. Nevertheless, it was noted by authors that this transformation represents "the first example of catalytic cross-coupling reaction using an electrophile bearing a non-benzylic or non-allylic C_{sp3}-N bond". Based on the results from mechanistic studies the sequence of S_N2-type ring-opening with homolysis/recombination of Ni-C bond under reaction conditions was proposed. The low configurational stability of azanickellacyclobutane intermediates was rationalized due to the absence of bidentate amino ligands which significantly stabilize the azanickellacyclobutane intermediate.

These initial reports by Doyle, attracted the attention of other scientific groups, and a few months later the Michael group reported a Pd-catalyzed Suzuki coupling involving 2-alkylaziridines as coupling partners with aromatic boronic acids.[74] The reaction was optimized using *N*-Nosyl aziridines **1.55**, and the product **1.56** was formed exclusively as a linear isomer (Scheme 1.20).

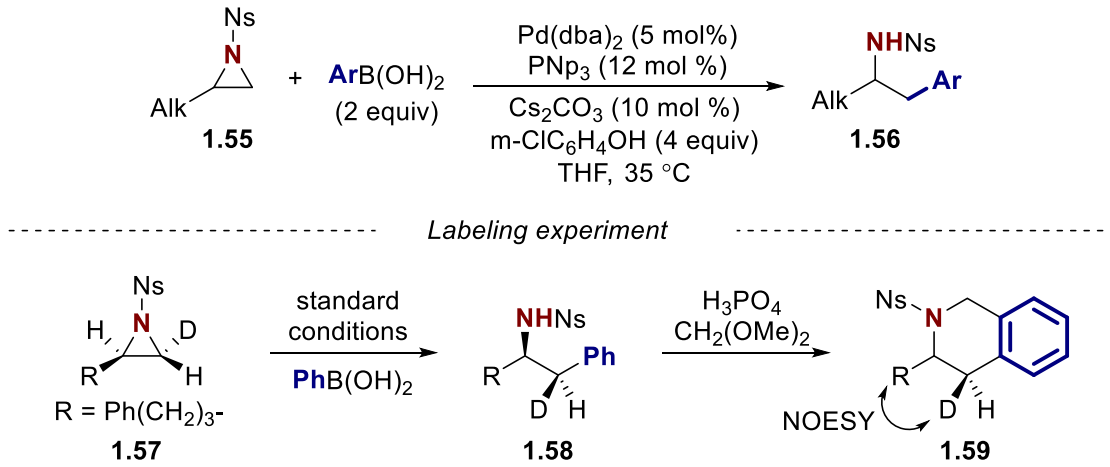

Scheme 1.20 Pd-catalyzed Suzuki cross-coupling of 2-alkyl aziridines

By performing the reaction with deuterium-labeled aziridine **1.57**, and after cyclizing the reaction product **1.58** into the tetrahydroisoquinoline derivative **1.59**, it was estimated by NOESY NMR experiment that alkyl substituent and deuterium atom are in the cis position. This result establish that ring opening occurred with a 100% inversion of stereochemistry at the methylene carbon via the S_N2-type ring-opening mechanism.

An interesting feature of the developed transformation is the presence of a proton source in the reaction media. As the reaction yield drops drastically in the absence of a proton source, Michael assumed that direct transmetalation of the azapalladacyclobutane **1.60** with the boronic acid is unfavorable. Instead, it was proposed the initial protonolysis of **1.60** with the formation of ring-opened Pd(II) alkoxide intermediate **1.61**, which then undergoes a transmetalation step resulting in the formation of the desired intermediate **1.62** (Scheme 1.21).

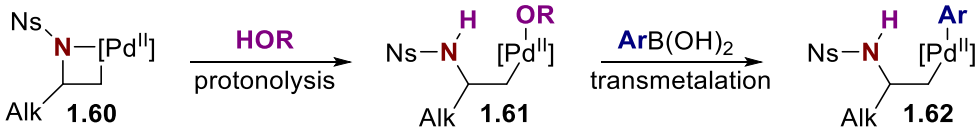

Scheme 1.21 Proposed azapalladacyclobutane **1.60** protonolysis

Motivated by the reliable reaction course for Pd-catalyzed Suzuki transformation of aziridines (full inversion of stereochemistry at the methylene position) compared with the results for Ni-catalyzed Negishi coupling (stereochemical scrambling), the Minakata group reported in 2014 a Pd-

catalyzed Suzuki arylation of enantiopure 2-arylaziridines **1.63** to access enantiopure 2-arylphenethylamine derivatives **1.64** (Scheme 1.22).[75]

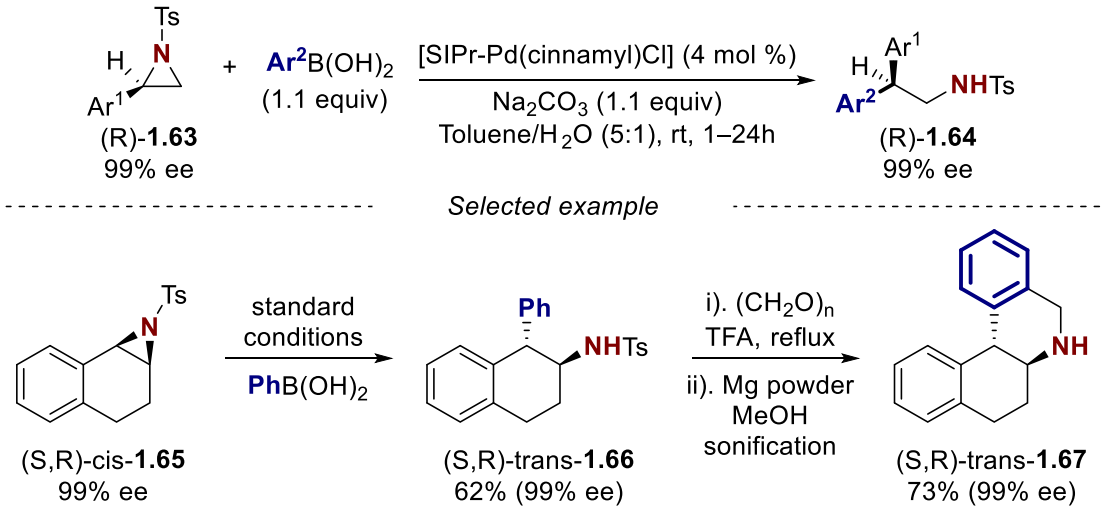

Scheme 1.22 Pd-catalyzed Suzuki cross-coupling of enantiopure 2-aryl aziridines

The absolute configuration of the product delivered from the model substrate was determined by X-ray crystallography confirming the complete stereo-inversion at the reacting benzylic carbon of aziridine. All the products **1.64** from the reaction scope were analyzed with chiral HPLC and were found to be enantiomerically pure (99% *ee*) in all cases. Interestingly, the developed protocol was not limited to monosubstituted aziridines, but 1,2-disubstituted substrates also reacted. For instance, aziridine **1.65** yielded the enantiopure amine **1.66**. The product **1.66** was transformed within 2 steps into synthetically relevant enantiopure cyclic amine **1.67**.

At this point, two main types of monosubstituted aziridines (2-alkyl and 2-aryl) have been used in cross-coupling transformations forming C_{sp3}-C_{sp2} and C_{sp3}-C_{sp3} bonds (Figure 1.16).

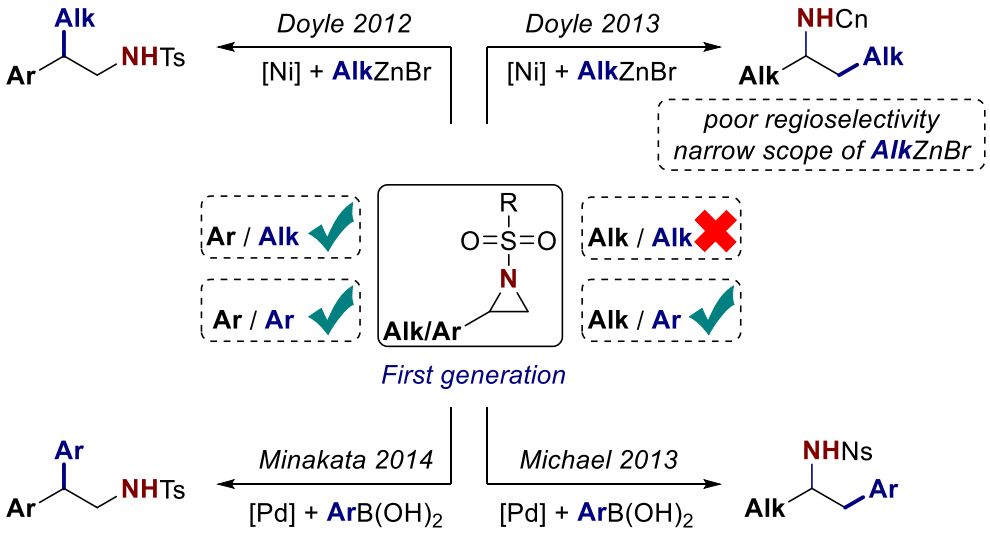

Figure 1.16 Cross-coupling transformation of monosubstituted aziridines

However, among possible combinations the Alk/Alk one has remained problematic. The procedure reported by Doyle is distinguished from the others by its poor regioselectivity (< 4:1 of linear/branch products ratio). In addition, the reaction scope contained only a few examples using alkylzinc reagents. Thus, the problem of regioselective alkylation of 2-alkyl aziridines has been remaining unsolved. In 2014 the Jamison group addressed this challenge reporting a procedure for fully regioselective Negishi coupling of 2-alkyl aziridines with alkylzinc reagents.[76] The key difference from the method developed by Doyle was the use of bidentate phenanthroline-derived ligands in the catalytic system. Aziridines **1.68** were reacted in the presence of $Me_4phen/NiCl_2$ (1.25:1) forming a broad scope of amines **1.69** with over 20:1 regioselectivity of the alkylation reaction (Scheme 1.23).

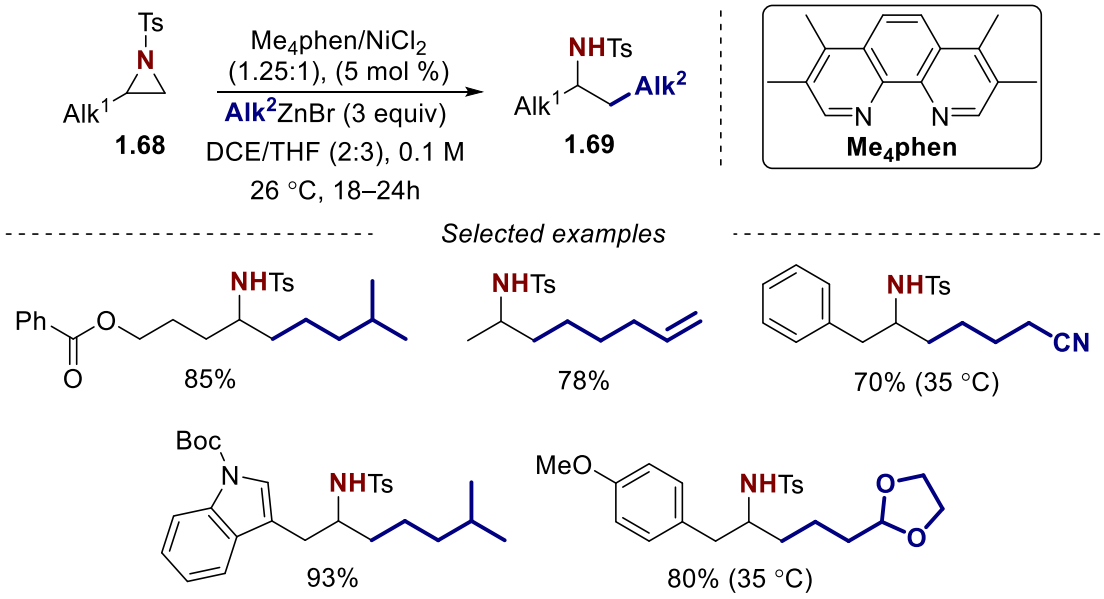

Scheme 1.23 Negishi coupling of 2-alkyl aziridines with alkylzinc reagents

A stoichiometric experiment with azanickellacyclobutane **1.70** and an organozinc reagent resulted in the formation of product **1.71** and $TsNH_2$ with 80% overall NMR yield (Scheme 1.24, top).

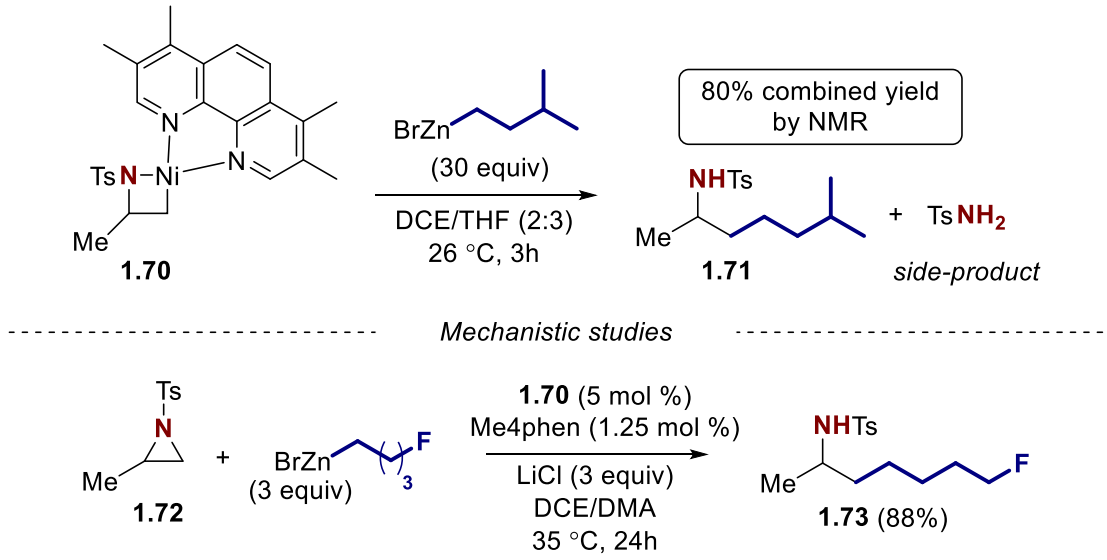

Scheme 1.24 Mechanistic studies

The obtained result is in drastic contrast with the results obtained by Doyle for azanickellacyclobutane **1.50** (Scheme 1.17), which only reacted with the alkyl zinc reagent in the presence of the electron-deficient olefin **1.48**.

In addition to the stoichiometric experiment, it was shown that azanickellacyclobutane **1.70** can catalyze the alkylation of aziridine **1.72** with the formation of desired product **1.73** in excellent yield (Scheme 1.24, bottom). Thus, the competent role of nickellacycle **1.70** as a reaction intermediate in the catalytic cycle was undoubtedly proved.

Finally, experiments with deuterium-labeled aziridine **1.74**, and with enantiopure aziridine **1.75** have shown that the reaction proceeds via an S_N2-type insertion without C-C bond scrambling at the terminal carbon, and without any erosion of enantiopurity at the tertiary carbon (Scheme 1.25)

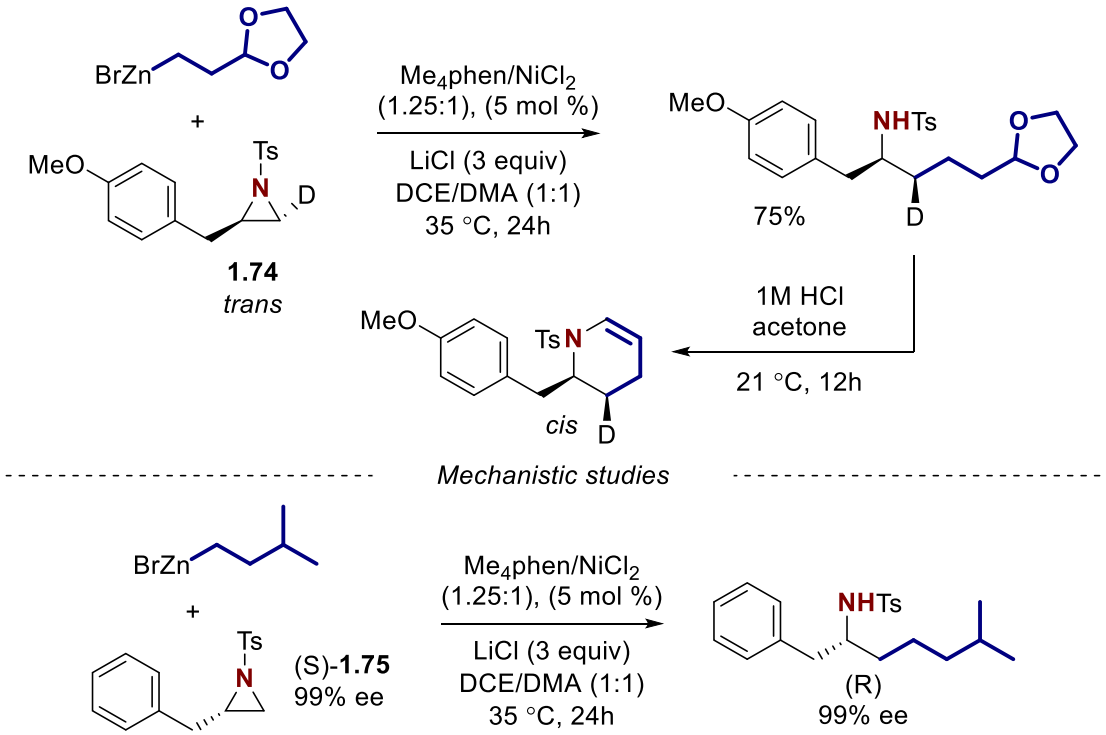

Scheme 1.25 Studies of stereochemical course of the Negishi alkylation

After the pioneering studies of Doyle and Jamison the potential for accessing *β*-functionalized amines through metal-catalyzed aziridine ring-opening became clear. However, many challenges remained. For instance, none of the aforementioned protocols used 2,2-disubstituted aziridines or reported sluggish reactivity upon their use. This was not surprising, as the cross-coupling with tertiary electrophiles is characterized by its slow reductive elimination step to form quaternary carbon centers.[77,78] Nevertheless, inspired by initial results applying EDOs as a ligand accelerating reductive elimination from Ni metal center, the group of Doyle reported in 2015 a successful design of EDOs structure, unlocking cross-coupling event between 2,2-disubstituted aziridines and organozinc reagents. Thus, using the EDO, which got the name **Fro-DO**, amines **1.77** with tertiary carbon center at the β-position could be synthesized, starting from aziridines **1.76** under mild catalytic conditions (Scheme 1.26).[79]

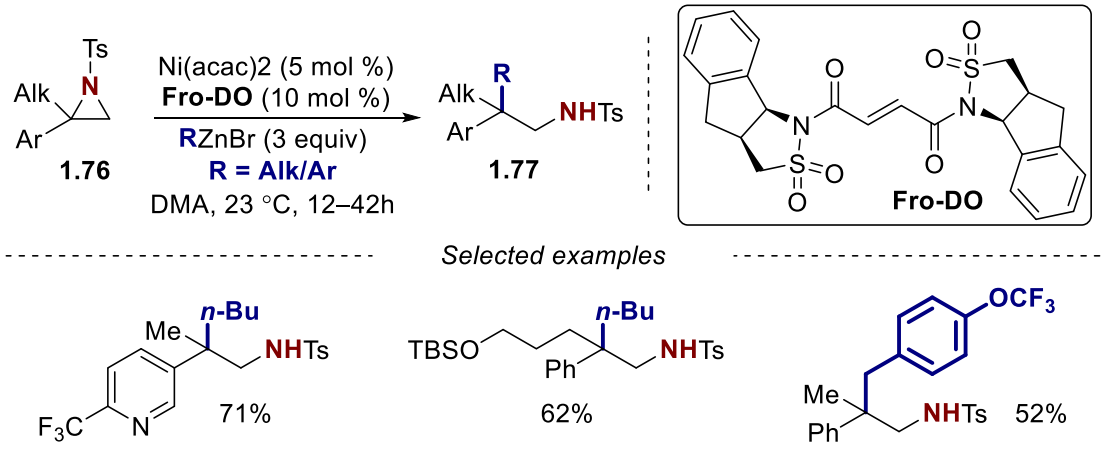

Scheme 1.26 Negishi alkylation of 2,2-disubstituted aziridines

One of the method's drawbacks is that it is still limited for styrene-derived aziridines, as at least one of the substituents in the aziridine has to be aromatic. In addition, while testing enantiopure aziridine **1.78** under reaction conditions erosion of enantiopurity was observed in the final product **1.79** (Scheme 1.27).

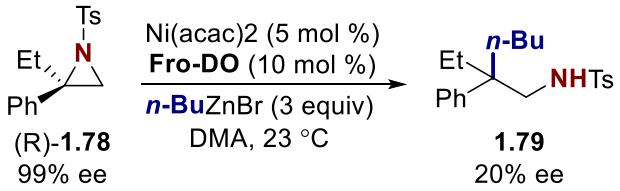

Scheme 1.27 Erosion of enantiopurity in the amine **1.79** starting from enantiopure aziridine **1.78**

This result is in agreement with previous observations made by the Doyle group. The low configurational stability of azanickellacyclobutane intermediates in the presence of EDOs and Ni-C bond scrambling is always observed.

Transition metal-catalyzed transformations are not limited by the formation of only C-C bonds. For example, one of the most widely used reactions is a transition metal-catalyzed borylation.[80,81] While exploring further the reactivity of aziridines under transition-metal catalyzed conditions, the Minakata group reported in 2016 regiodivergent borylation of 2-aryl aziridines **1.80** with the formation of unexpected linear regioisomers of *β*-amino alkylboronates **1.81** (Scheme 1.28).[82]

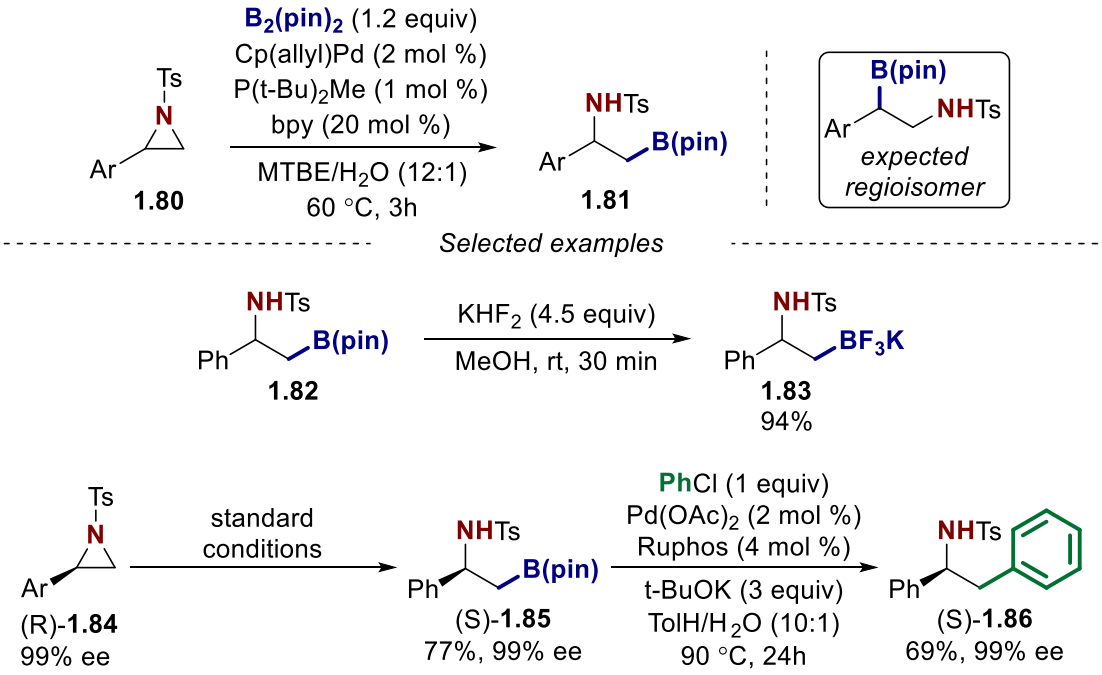

Scheme 1.28 Regiodivergent Pd-catalyzed borylation of 2-aryl aziridines

All previously reported transition-metal catalyzed transformations of styrene-derived aziridines **1.80** occur at the most substituted benzylic position. However, the catalytic system developed by Minakata led exclusively to the formation of a C-B bond at the least substituted carbon. The borylated product **1.82** was easily transformed into alkylfluoroborate **1.83**, which a widely used in cross-coupling reactions.[83] The enantiopure β-amino alkylboronate **1.85**, accessed upon standard conditions from enantiopure aziridine **1.84**, was involved directly in Pd-catalyzed Suzuki-Miyaura cross-coupling with PhCl to form product **1.86**. This sequential 2-step regiodivergent arylation of 2-aryl aziridines is complementary to the previously reported by Minakata direct Pd-catalyzed arylation of the same substrates.[75] Overall, the obtained results afford opportunities for stepwise regiodivergent functionalization of styrenyl aziridines **1.80** forming linear products.

Upon standard mechanistic studies with deuterium-labeled materials it was demonstrated that, despite the unusual regioselectivity, the reaction proceeds via S_N2-type aziridine ring-opening. The phenomena of reversed regioselectivity were additionally studied *ab initio* by applying DFT calculations (Figure 1.17).

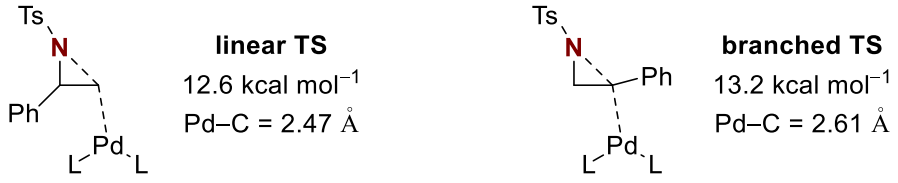

Figure 1.17 Difference between linear and branched TS from DFT calculations

According to the obtained results the liner transition state was 0.6 kcal mol^{-1} lower in energy than the branched transition state. The corresponding regioselectivity distribution calculated using the Boltzmann equation gave the value of 89:1. This number was in qualitative agreement with the experimental results of Minakata (99:1). The lower energy of the linear transition state was simply explained by steric repulsion. Thus, the nucleophilic attack of the Pd center at the least substituted carbon gives 2.47 Å of Pd-C bond distance in the optimized TS geometry. Whereas, the nucleophilic attack of the Pd center at the most hindered atom gives the Pd-C bond distance number of 2.61 Å. The shorter distance between the metal center and the aziridine substrate provides better charge interactions and stabilizes the kinetic complex formed before the ring-opening step.

In 2017 the group of Michael expanded previously reported Pd-catalyzed Suzuki arylation (using arylboronic acids) of 2-alkyl aziridines **1.87** to the scope of alkenylboronic acids **1.88** accessing homoallylic amines **1.89** (Scheme 1.29).[84]

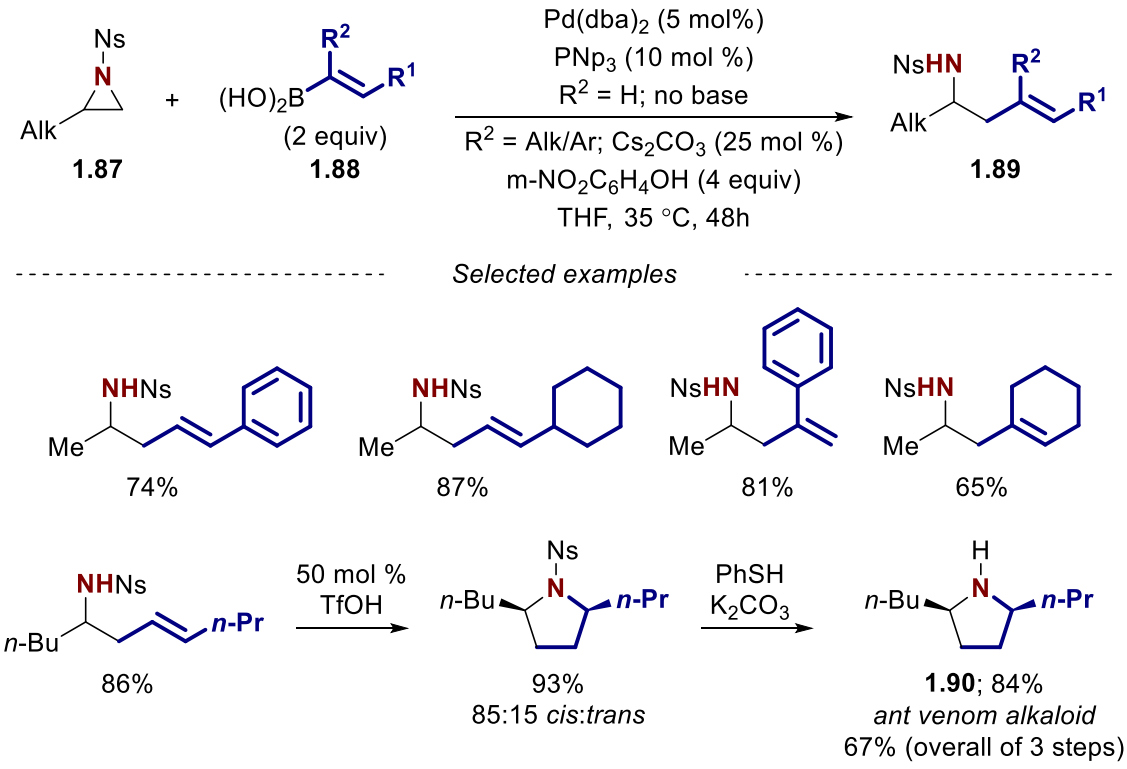

Scheme 1.29 Pd-catalyzed Suzuki coupling of 2-alkyl aziridines with alkenylboronic acids

The reaction worked well for terminal aromatic and aliphatic alkenylboronic acids, as well as for aromatic and aliphatic internal alkenylboronic acids. The ant venom alkaloid **1.90** was synthesized over 3 steps with an overall yield of 67%, starting from 2-*n*-Bu N-Nosyl aziridine, applying the developed methodology at the first step.

Even though the developed transformations discussed above demonstrate good synthetic applicability, they still use organometallic reagents, such as boronic acids or especially organozinc reagents. Consequently, while applying these reagents synthetic chemists have to face the unavoidable drawbacks and limitations of their application in practical synthesis. To expand the scope of possible coupling partners to transform aziridines into β-functionalized amines the groups of Sigman and Doyle combined their efforts to develop a reductive cross-coupling arylation styrenyl aziridines using aryl iodides.[85] Thus, in the presence of Mn as a stoichiometric reductant, arylation of aziridines **1.91** occurs at the benzylic position giving amines **1.92** (Scheme 1.30).

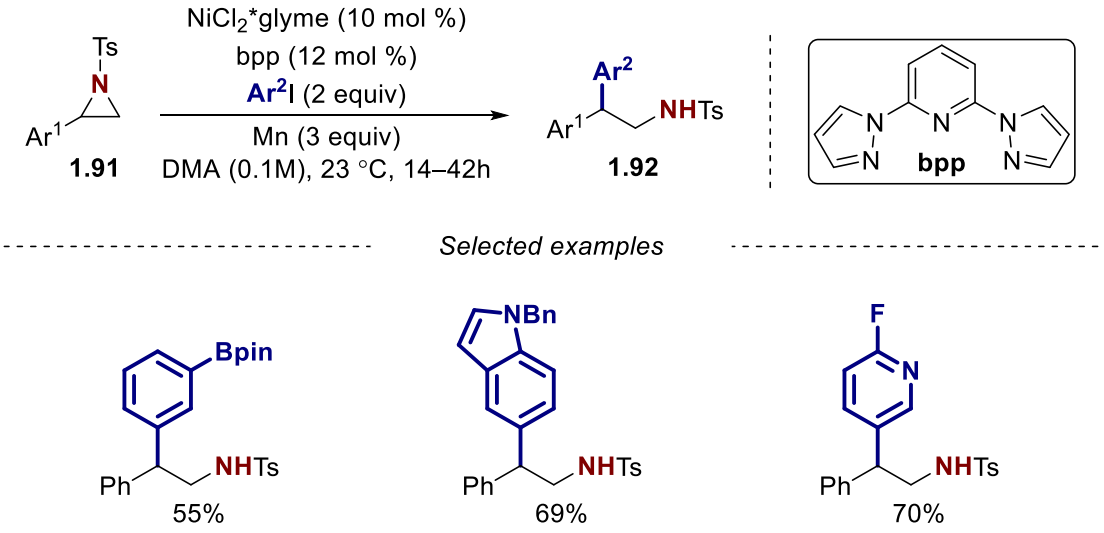

Scheme 1.30 Reductive Ni-catalyzed arylation of styrenyl aziridines by Sigman and Doyle

The reaction scope demonstrated a great range of compatible functional groups and the developed reaction has advantages over Negishi coupling developed by Doyle group earlier,[69,79] specifically the use of organozinc reagents is avoided. However, Pd-catalyzed Suzuki arylation of styrene aziridines by Minakata is still an alternative,[75] especially in the synthesis of amines bearing a chiral center at the *β*-position, due to the stereospecificity of the reaction.

Sigman and Doyle decided to challenge this advantage as they saw the potential of using racemic aziridines in the synthesis of enantioenriched amines. The assumption was made based on previously collected pieces of evidence of open-shell intermediates in the Ni/EDOs systems and in reductive cross-coupling systems.[86,87] In addition, some Ni-catalyzed asymmetric reductive couplings of secondary electrophiles were already reported by that time.[88–91] Upon testing enantiopure aziridine **1.93** under conditions optimized for racemic aziridines the product **1.94** was formed as a racemate with a complete loss of enantiopurity (Scheme 1.31).

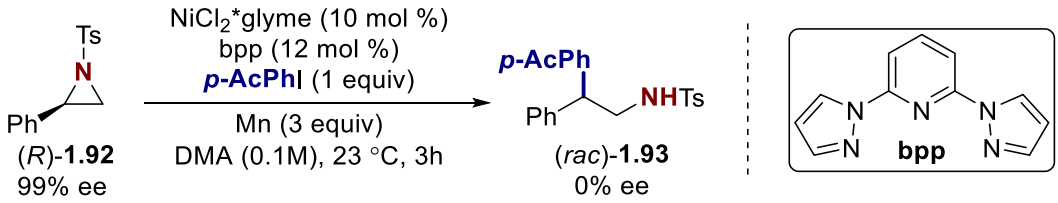

Scheme 1.31 Formation of racemic product **1.93** from enantiopure aziridine **1.92**

As the erosion of enantiopurity suggested the radical open-shell intermediate this result opened up room for the development of an enantioselective version of the desired transformation. After extensive screening of chiral ligands, the BiOx ligand framework was found to be the most promising. Next, a careful ligand design was performed by changing substituents in the ligand core. The conditions were reoptimized using the best ligand giving enantioenriched amines **1.95** with high *ee* values using racemic aziridines **1.94** as a starting material (Scheme 1.32).

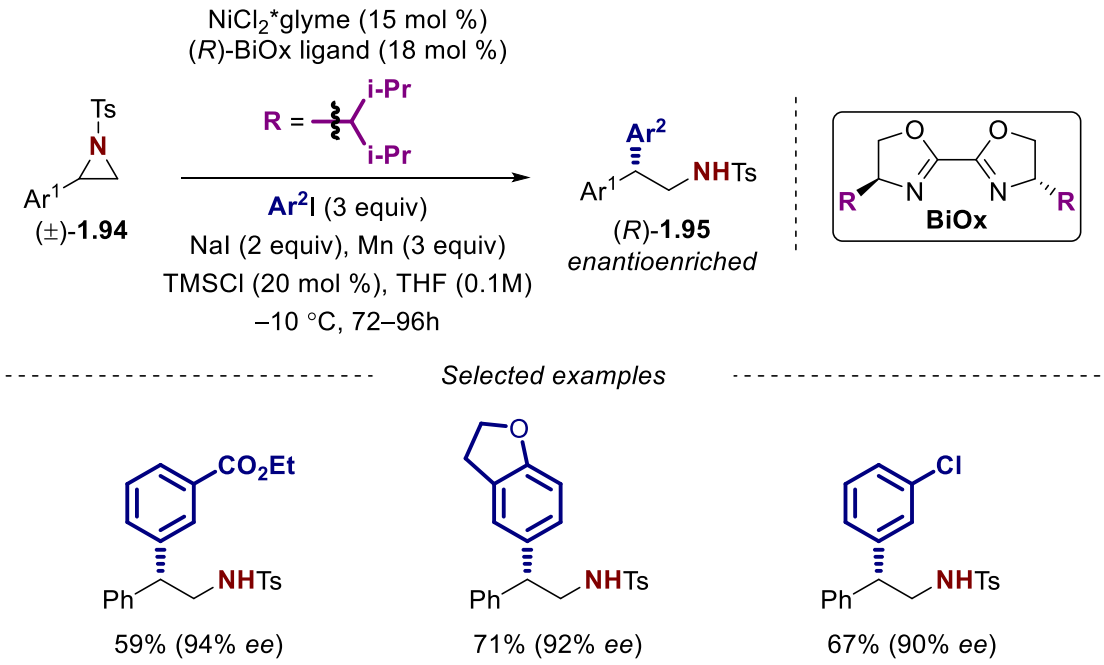

Scheme 1.32 Ni-catalyzed enantioselective reductive arylation of aziridines

Such a great result makes the developed transformation a valuable addition to the previously reported stereospecific transformations of aziridines using enantioenriched aziridines as starting materials.

Overall, the results reported by Sigman and Doyle have included aziridines as study objects in two important recent research topics: reductive cross-coupling of electrophiles and transition-metal catalyzed enantioselective transformations. Both topics will be widely explored in the context of aziridine reactivity in the following years.

In 2018 the group of Xiao reported a dual photoredox/Ni-catalyzed alkylation of 2-aryl aziridines **1.96** using benzytrifluoroborates **1.97** in the presence of an EDO ligand (Scheme 1.33).

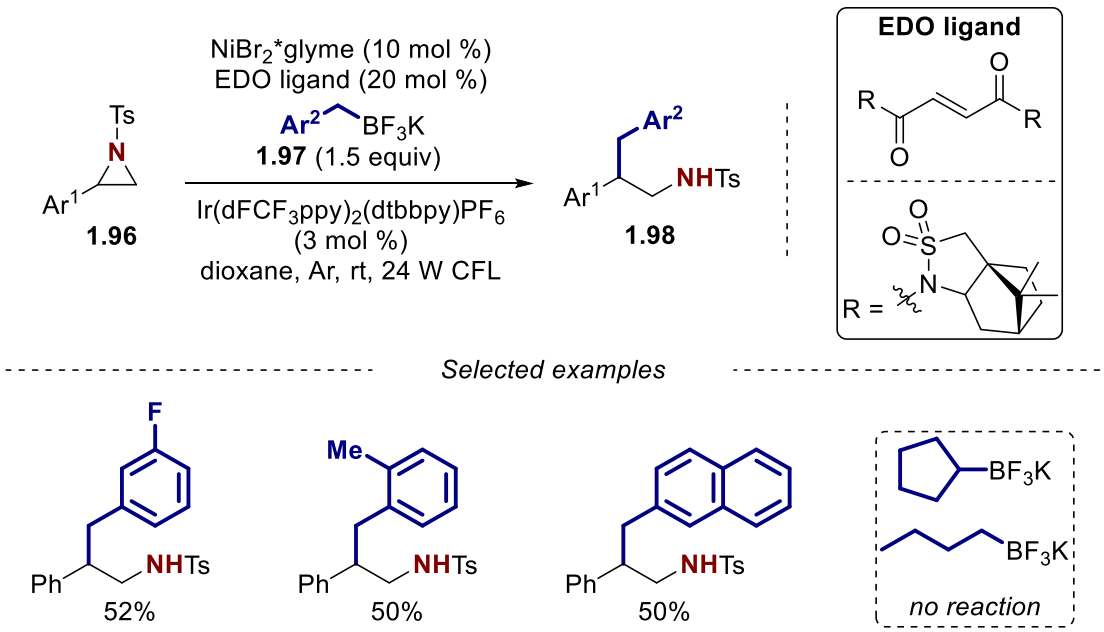

Scheme 1.33 Dual photoredox/Ni-catalyzed alkylation of 2-aryl aziridines

Unfortunately, as primary and secondary alkyltrifluoroborates did not demonstrate any reactivity toward the formation of product **1.98** under optimized conditions the synthetic application of such a transformation is limited.

An elegant approach to access ^{13}C-labeled *β*-amino acid derivatives was reported in 2019 by the group of Skrydstrup.[92] First, a series of azanickellacyclobutanes **1.99** was presynthesized from aziridines following the Hillhouse conditions (Scheme 1.34).

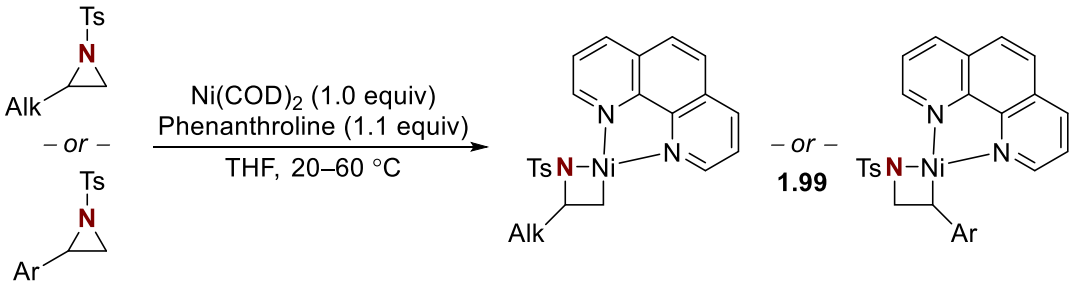

Scheme 1.34 Synthesis of azanickellacyclobutanes

The prepared metallacycles were subsequently subject to the two-chamber system (COware gas reactor) widely used by the Skrydstrup group for carbonylation reactions.[93] One chamber is used to generate ^{13}CO from ^{13}COgen reagent while the other contains the azanickellacyclobutanes **1.99**. The azanickellacyclobutanes **1.99** reacts with^{13}CO selectively inserting into weaker Ni-C bond forming an air stable cyclic aza-Ni-acyl complexes **1.100** (Scheme 1.35).

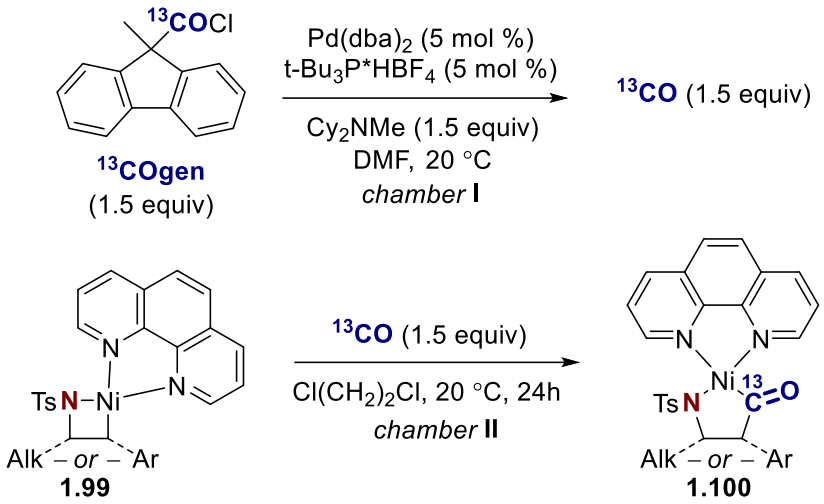

Scheme 1.35 Selective ^{13}CO insertion into azanickellacyclobutanes

The synthetic utility of the proposed labeling strategy was illustrated by accessing a broad range of ^{13}C-labeled *β*-amino acid derivatives from the corresponding Ni complex **1.101** (Scheme 1.36).

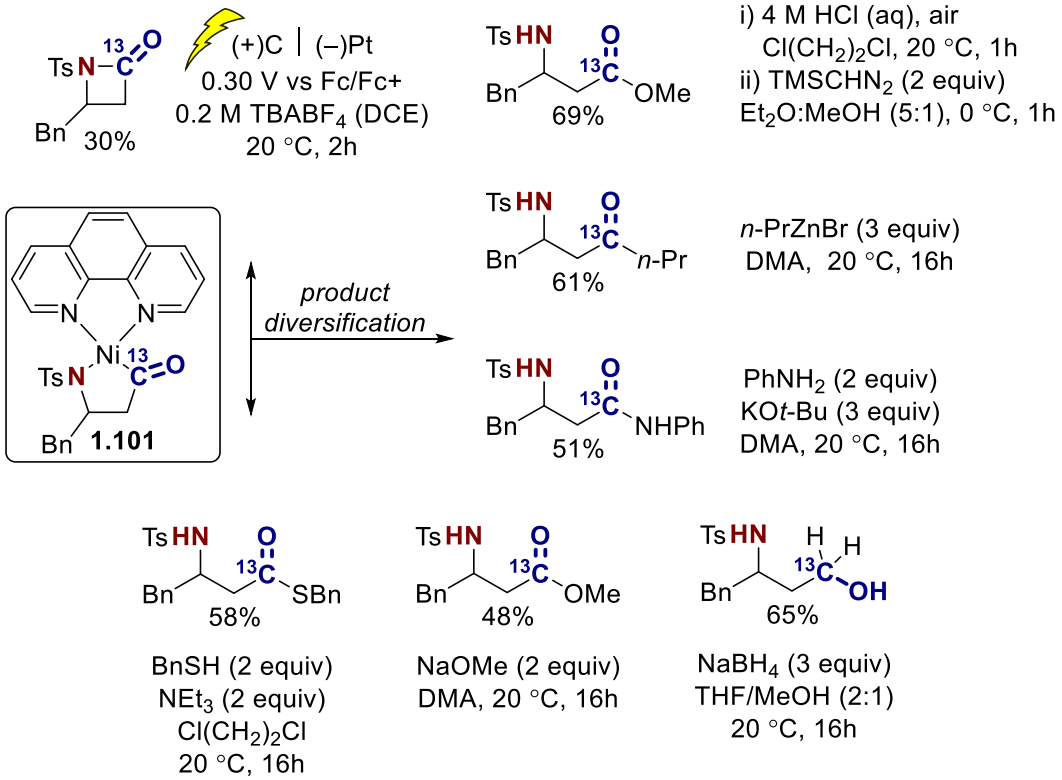

Scheme 1.36 Synthesis of ^{13}C-labeled *β*-amino acid derivatives

This study serves as an excellent representative case when the high stability of the reactive intermediate, which limits performing reaction catalytically, was turned into a synthetic feature and used in the design of a highly useful synthetic strategy.

In 2019, the Minakata group reported catalyst-controlled silylation of 2-aryl aziridines using sililborane. By using previously obtained experience in Pd-catalyzed arylation and borylation of aziridines, a fully regioselective reaction outcome was achieved for the formation of either linear **1.102** or branched **1.103** β-silyl amines upon a careful choice of catalytic cocktail (Scheme 1.37).

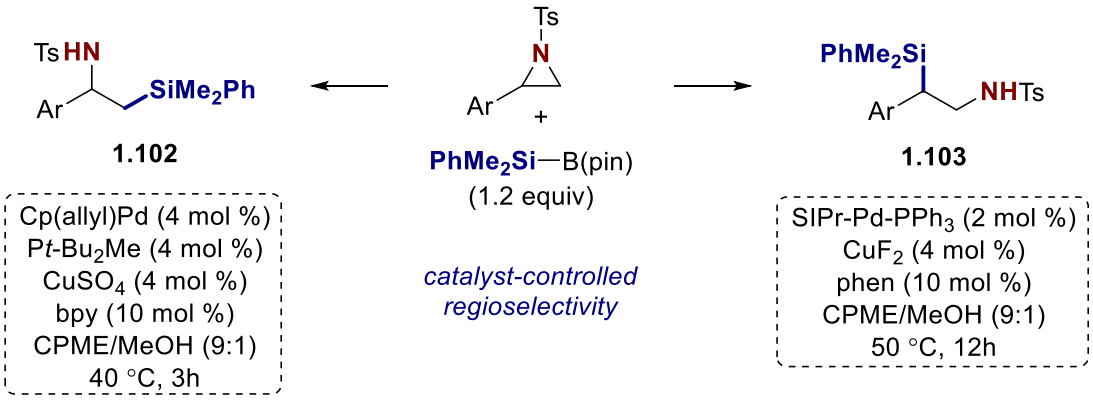

Scheme 1.37 Catalyst-controlled silylation of 2-aryl aziridines

The main side product observed upon the formation of branched regioisomers **1.103** under optimized conditions was the geminal silylation product **1.104** (Scheme 1.38).

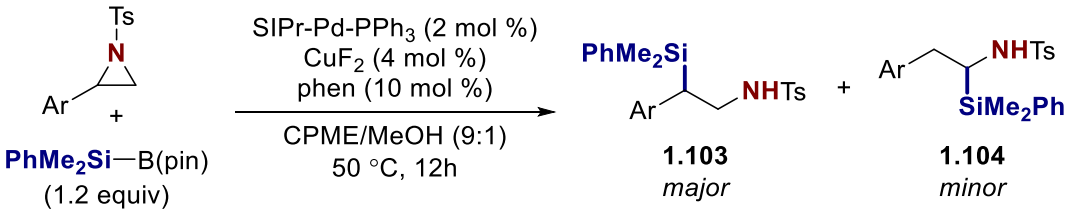

Scheme 1.38 Formation of unexpected geminal silylation product **1.104**

Upon further optimization of the reaction conditions a catalytic system to form exclusively product **1.104** was identified (Scheme 1.39).

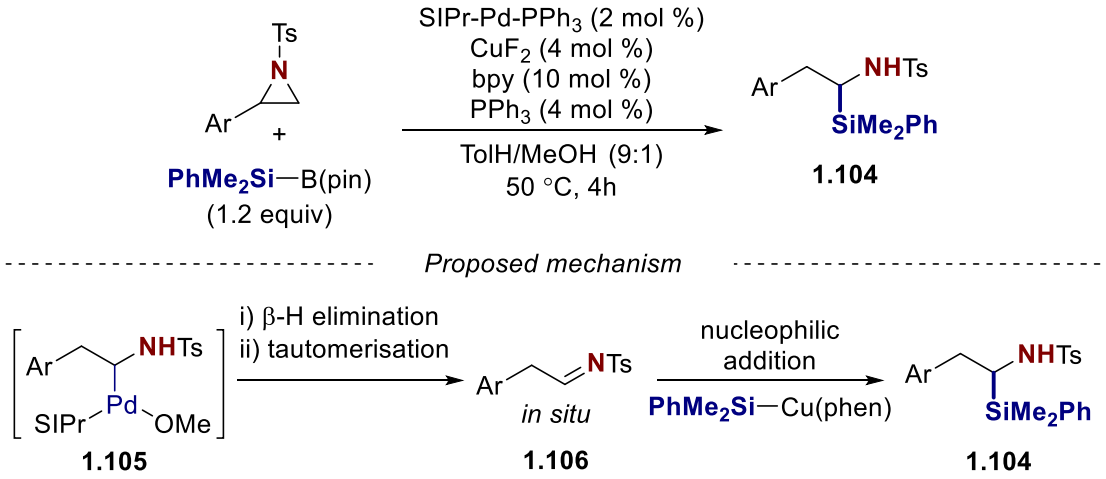

Scheme 1.39 Geminal silylation of aziridines

The mechanistic hypothesis proposed was the formation of imine **1.106** in situ after the *β*-H elimination event of intermediate **1.105** and subsequent tautomerization of the enamine. This assumption was supported by the independent subjection of compound **1.106** to the optimized reaction conditions, which led to the formation of product **1.104** in moderate yield. Imine **1.106** demonstrated reactivity toward nucleophilic addition of Si-Cu species and was confirmed to be a possible key reaction intermediate.

After successful cross-electrophile arylation of 2-aryl aziridines with aromatic iodides under reductive conditions,[85] the group of Doyle moved to the development of more challenging reductive cross-electrophile coupling of aryl iodides with 2-alkyl aziridines. Even though the Pd-catalyzed Suzuki arylation of 2-alkyl aziridines by Michael demonstrated good synthetic applicability it was crucial to expand the scope of arylation reagents, as Michael's protocol was limited to boronic acids.[74]

In 2020, Doyle and colleagues addressed this problem developing a Ni-catalyzed cross-electrophile coupling of aliphatic aziridines **1.107** and aryl iodides under photoredox conditions (Scheme 1.40).[94]

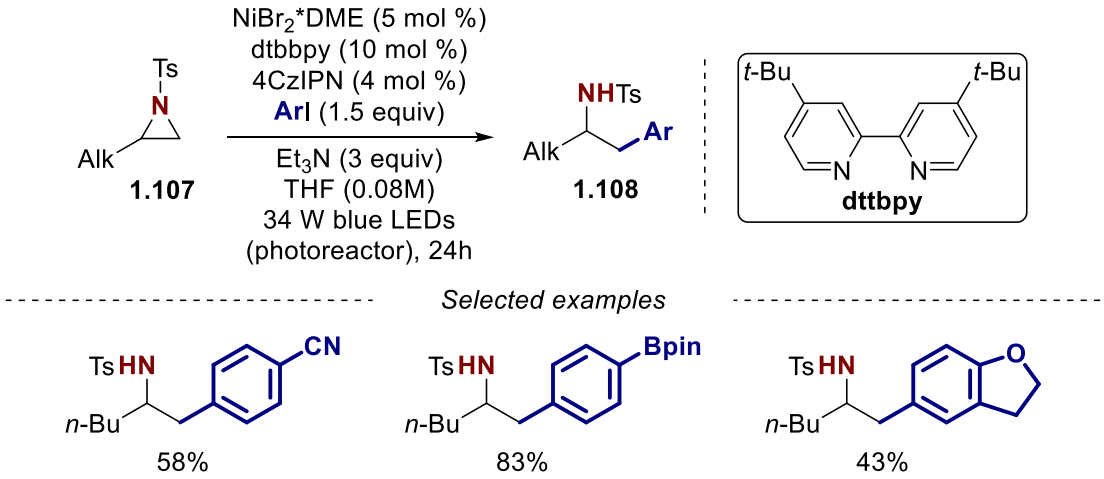

Scheme 1.40 Ni-catalyzed photoredox cross-electrophile arylation of aliphatic aziridines

Using developed reaction conditions, a broad scope of *β*-phenethylamine derivatives **1.108** were accessed with diverse substitution patterns. An unexpected result was observed upon subjecting 2-phenyl aziridine **1.109** under reaction conditions (Scheme 1.41).

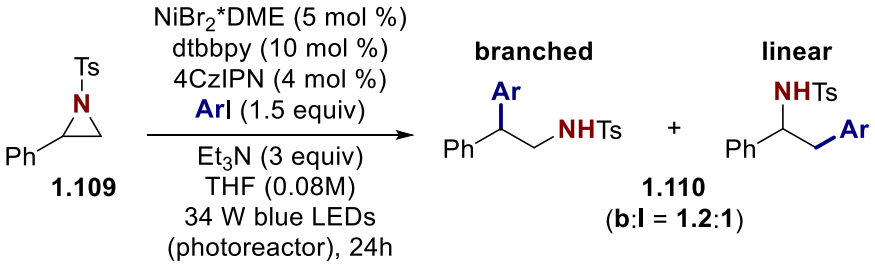

Scheme 1.41 Unexpected result of 2-phenyl aziridine arylation

Instead of forming exclusively the expected branched arylation isomer the product **1.110** was formed as a mixture of branched and linear regioisomers which was unprecedented in the case of Ni-catalyzed cross-coupling transformations with aziridines.

After careful studies of the reaction mechanism, it was elucidated that the actual electrophile involved in the cross-coupling event is the *in situ* formed *β*-iodo amine **1.111** (Scheme 1.42).

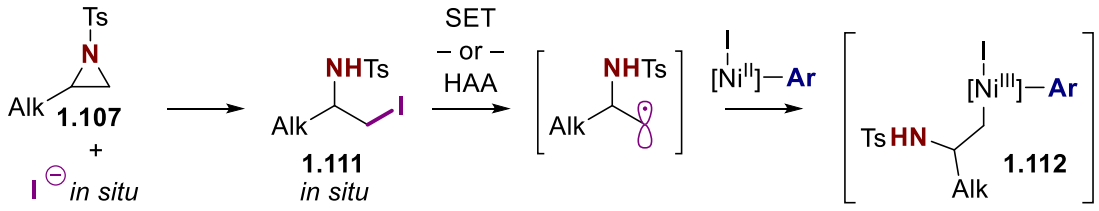

Scheme 1.42 Proposed mechanism for Ni-catalyzed photoredox cross-electrophile arylation of aliphatic aziridines

As proposed, this iodoamine next undergoes SET or HAA with the formation of an alkyl radical, which is trapped by the Ni(II) oxidative addition complex. The resulting Ni(III) species **1.112** then undergo reductive elimination to form the desired product.

Mechanistically, this result does not significantly contribute to the topic of the direct activation of the C-N bond in aziridines with transition metal complexes as the ring opening is achieved indirectly. However, from the synthetic standpoint, it opens up many options for the development of new synthetic methods using aziridines, which were not possible through direct oxidative addition of metal center to the aziridine ring.

In 2021 Wang and coworkers reported the synthesis of *β*-amino ketones **1.115** from aldehydes **1.113** and 2-aryl aziridines **1.114** (Scheme 1.43).[95]

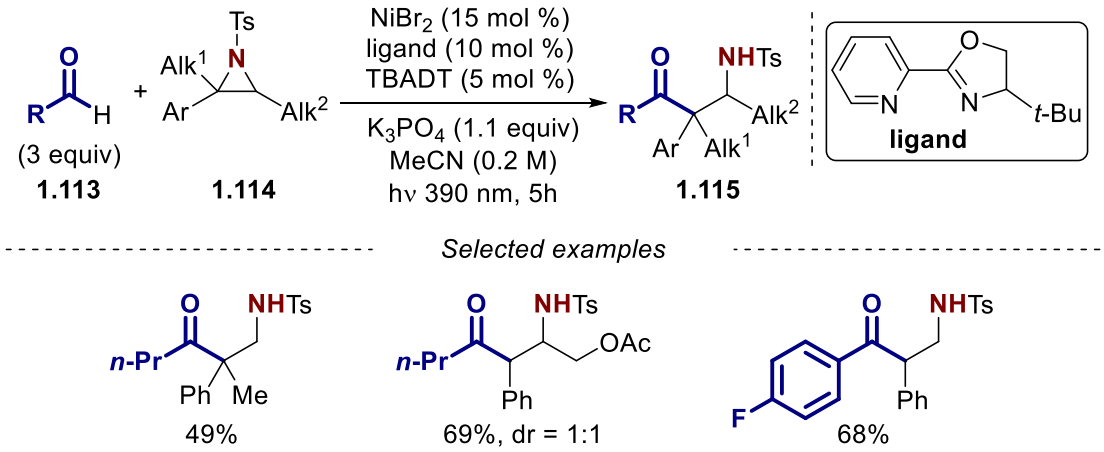

Scheme 1.43 Synthesis of *β*-amino ketones from aldehydes and 2-aryl aziridines

The reactivity of aldehydes **1.113** was unlocked upon a HAT event with TBADT forming acyl radicals. The reactivity of aziridines **1.114** resulted from the *in situ* formation of *β*-bromo amines **1.116**, analogously to the previously discussed protocol by Doyle (Scheme 1.44).

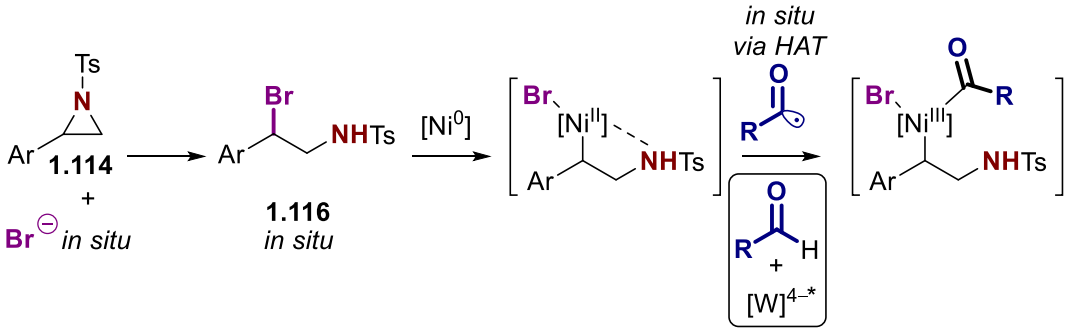

Scheme 1.44 Proposed mechanism of *β*-amino ketones synthesis from aldehydes and 2-aryl aziridines

The HAT activation of acetals **1.117** to form alkyl radicals after *β*-scission was used by Doyle and coworkers when in 2022 they reported a Ni-catalyzed alkylation of styrenyl aziridines **1.118** under photoredox conditions forming amines **1.119** (Scheme 1.45).[96]

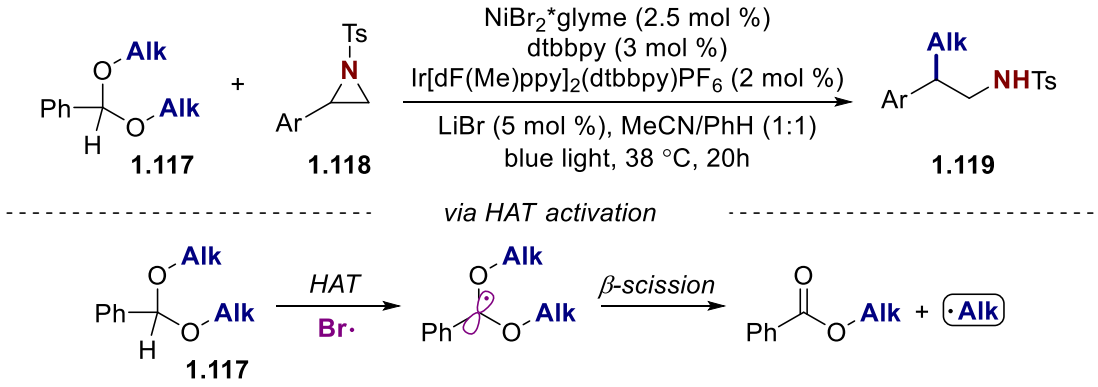

Scheme 1.45 Ni-catalyzed alkylation of styrenyl aziridines with acetals

As the bromine anion is present in the reaction media it was crucial to consider *β*-bromo amines as active reactive intermediates based on previous observations by Doyle and Wang. However, upon testing substrate **1.120** under optimized reaction conditions toward the formation of the product **1.121** practically no desired reactivity was observed (Scheme 1.46).

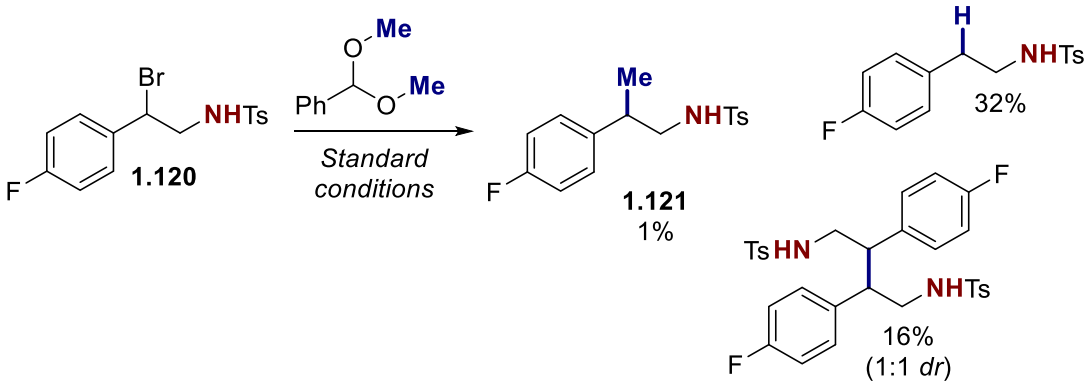

Scheme 1.46 Reactivity of β-bromo amine **1.120** toward Ni-catalyzed alkylation with acetals

Intrigued by this result the group of Doyle further studied the mechanism of the transformation and assessed that the key step of the catalytic cycle is a SET type oxidative addition of Ni(I)-alkyl species **1.122** to the aziridines with the stepwise formation of Ni(III) intermediate **1.123** (Scheme 1.47).

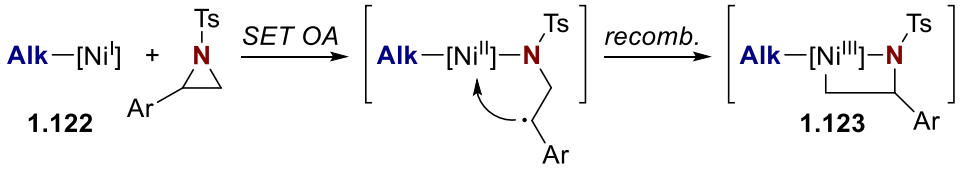

Scheme 1.47 Proposed SET oxidative addition step

Finally, it is worth mentioning that the reaction scope possesses a single example of alkylation of 2-methyl aziridine **1.124** (Scheme 1.48).

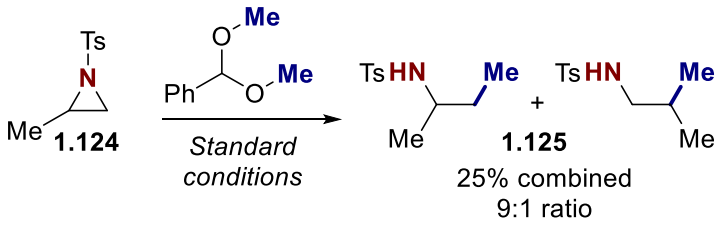

Scheme 1.48 Ni-catalyzed alkylation of 2-methyl aziridine with acetals

The final product **1.125** was formed in a low yield and as a mixture of two regioisomers, with the main isomer formed after methylation of less hindered carbon. This result is more consistent with the classical S_N2-type oxidative addition ring-opening mechanism. At the same time, the structure of the minor isomer is in agreement with the SET oxidative addition hypothesis as a more stable radical will be formed at the most substituted carbon. Overall, the reaction outcome indicates that in this particular case, the regioselectivity in the final product and the character of aziridine ring activation are dictated by the substitution pattern of the aziridine.

Nevertheless, this result can serve as an excellent starting point for the development of an efficient alkylation methodology of 2-alkyl aziridines under cross-electrophile coupling conditions which remains undeveloped up to date (Figure 1.18).

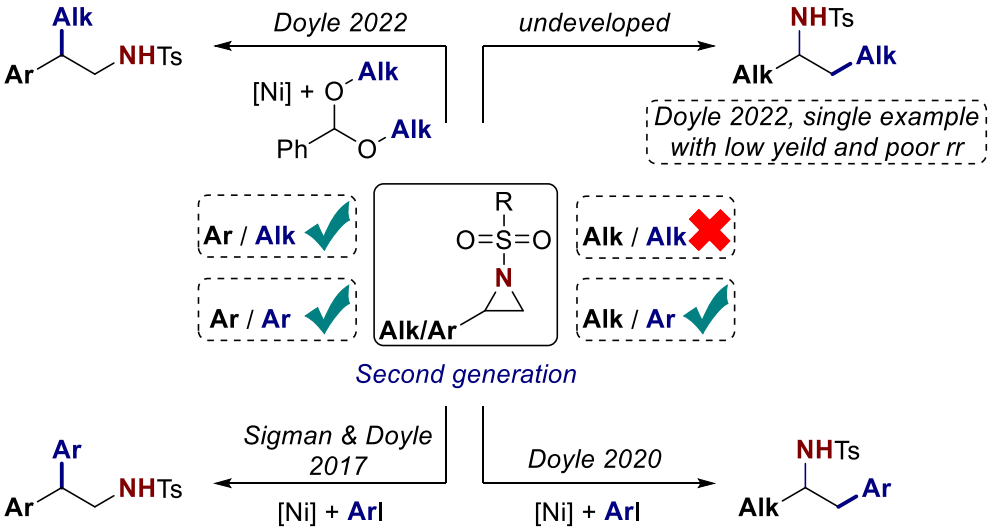

Figure 1.18 Aziridines as a coupling partners in the cross-electrophile coupling

Further expanding the cross-electrophile coupling with aziridines in 2023 the groups of Mei, Nevado, and Rueping, independently reported several electrochemically driven Ni-catalyzed transformations.

First, Mei and coworkers expanded the enantioselective arylation of racemic styrenyl aziridines (already reported by Doyle with stoichiometric Mn as a reductant) to the electrochemical reaction setup.[97] This approach compared to the use of heterogeneous reductant significantly improves reaction time (from days to hours) by accelerating the reduction step. Additionally, it leads to a simpler reaction workup resulting from the absence of stoichiometric metal in reaction media. Finally, using model substrate **1.126** it was demonstrated that this Ni-catalyzed enantioselective cross-coupling can be performed on the multi mmol scale, giving more than 1g of desired chiral amine **1.127** (Scheme 1.49).

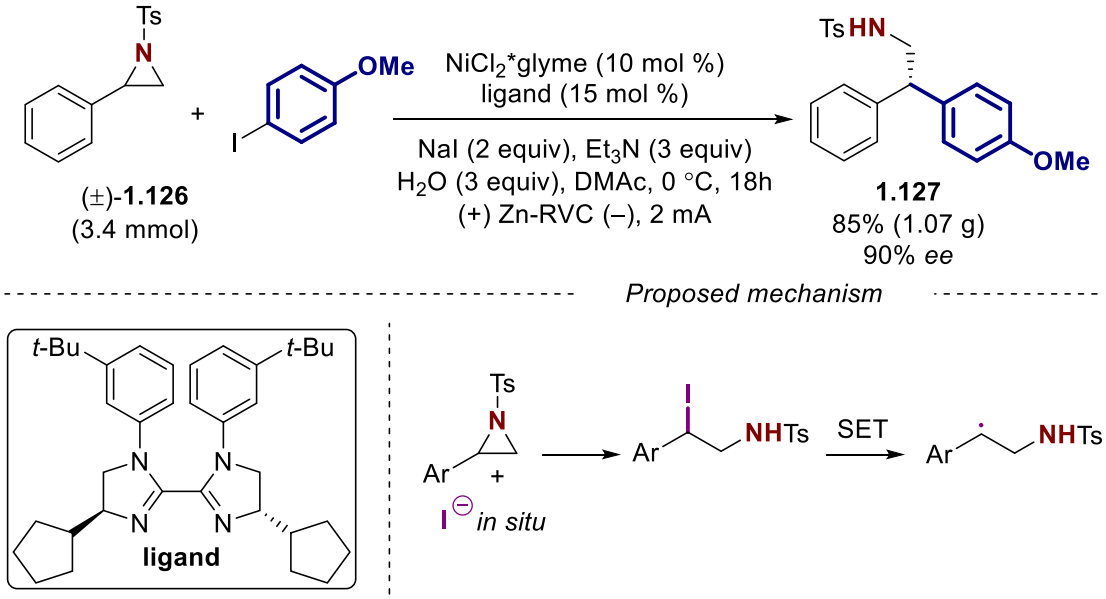

Scheme 1.49 Ni-catalyzed enantioselective arylation of aziridines under electrochemical conditions

The mechanistic studies revealed that under this particular reaction conditions, the actual electrophile involved in the catalytic cycle is *in situ* formed *β*-iodo amine.

Shortly afterwards, the group of Nevado reported Ni-catalyzed enantioselective electrochemical reductive cross-coupling of racemic 2-aryl aziridines **1.128** with alkenyl bromides **1.129**, thus, extending the scope of known electrophilic cross-coupling partners to access *β*-functionalized amines (Scheme 1.50).[98]

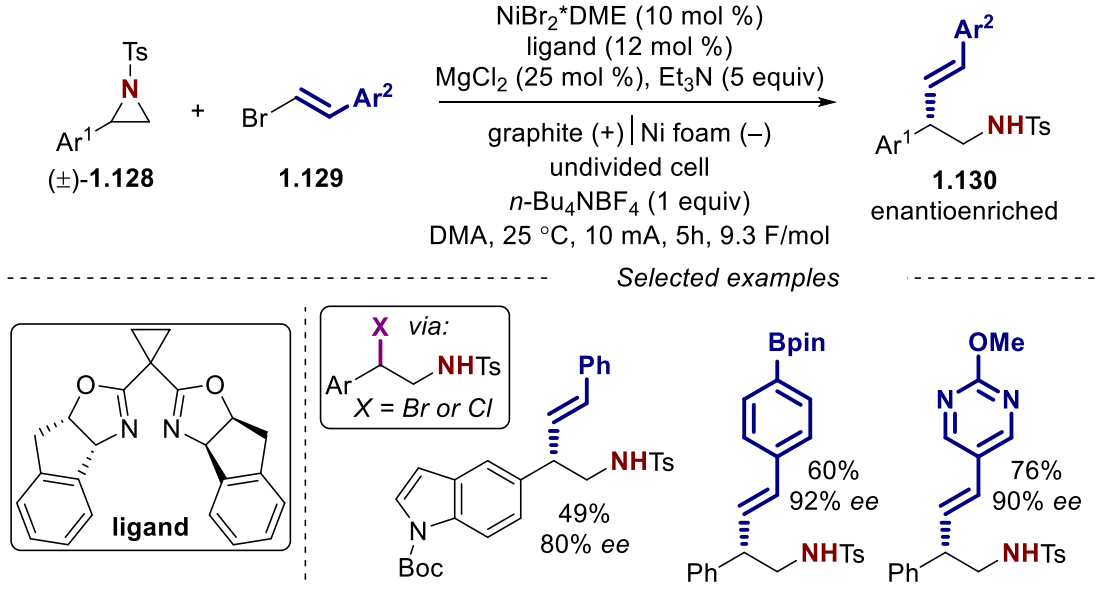

Scheme 1.50 Ni-catalyzed enantioselective electrochemical synthesis of *β*-aryl homoallylic amines

Using this method, a broad range of *β*-aryl homoallylic amines **1.130** can be accessed. The activation mode of C-N aziridine bond is similar to previously reported transformations of aziridines in the presence of halogen anion in the reaction media. Thus, *β*-halo amines are the actual electrophilic species involved in the formation of the desired products.

Finally, Rueping and coworkers applied electrochemical conditions and successfully expanded the list of electrophiles involved in the cross-electrophile coupling transformations with 2-aryl aziridines **1.131** to aryl bromides and alkyl bromides (Scheme 1.51).[99]

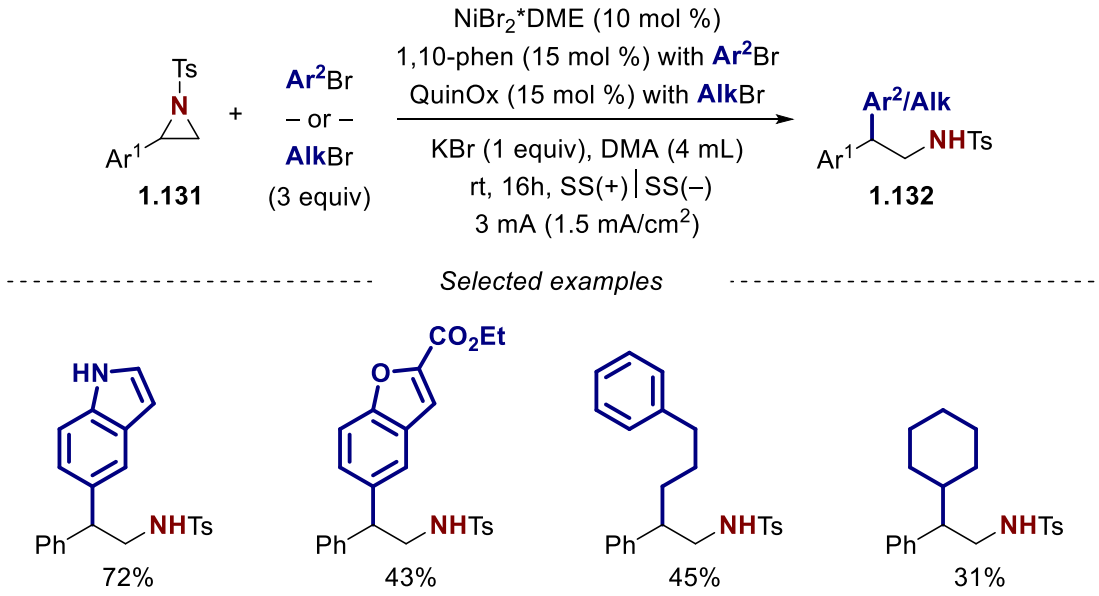

Scheme 1.51 Ni-catalyzed electrochemical arylation and alkylation of 2-aryl aziridines with aryl and alkyl bromides

Mechanistic studies revealed that the formation of product **1.132** was achieved via a unique process. Iron salts ($FeBr_2$ and $FeBr_3$) were generated *in situ* from stainless steel material of electrodes (an alloy of approx. 80% of Fe). These salts participate in the azanickellacyclobutanes **1.133** ring-opening leading to the formation of intermediates **1.134** (Scheme 1.52).

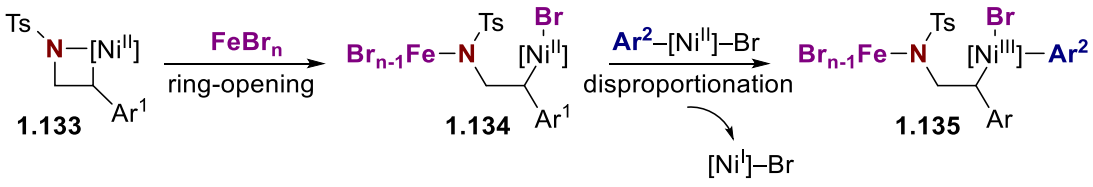

Scheme 1.52 Proposed ring-opening of azanickellacyclobutanes in the presence of iron salts

Finally, Ni(III) species **1.135** are formed after disproportionation of complex **1.134** with ArNi(II)Br oxidative addition complex and the final product **1.132** can be formed after the reductive elimination step.

The group of Fan reacted trifluoromethyl-substituted alkenes **1.136** with styrenyl aziridines **1.137** in the presence of a Ni-catalyst resulting in the formation of *δ-gem*-difluoroalkene-substituted amines **1.138** (Scheme 1.53).[100]

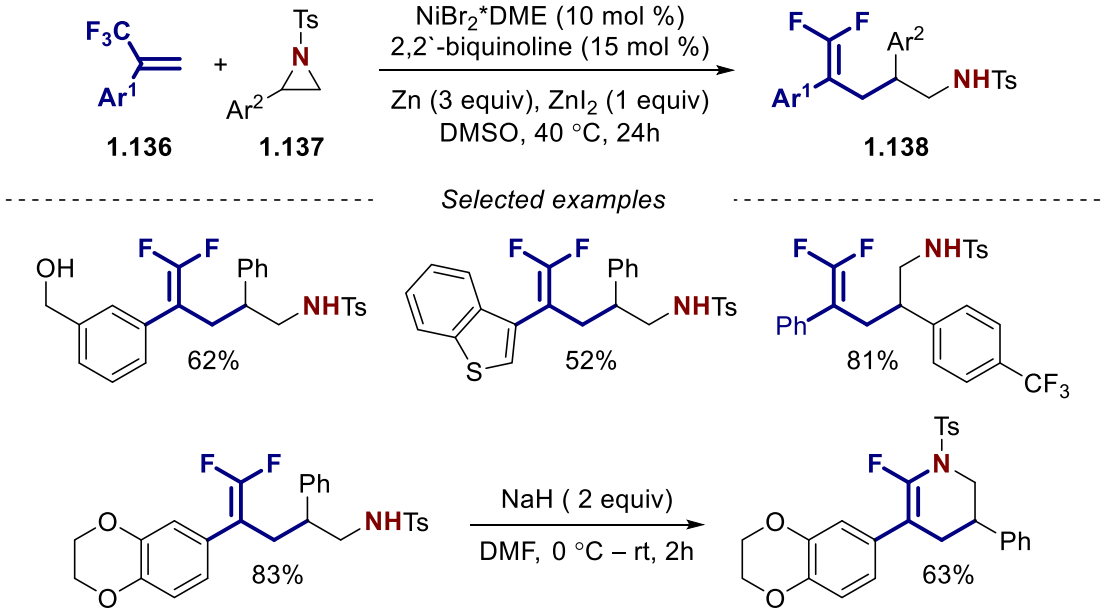

Scheme 1.53 Ni-catalyzed cross-electrophile *gem*-difluoroallylation of styrenyl aziridines

The products can be cyclized to a tetrahydropyridine core after a simple addition of base. During reaction optimization studies the ring-opening of aziridines was achieved only in the presence of metal iodides. After subjecting the *β*-iodo amine to the reaction conditions, but in the absence of ZnI_2, the formation of the desired product was observed, confirming that aziridine reactivity was unlocked upon iodolysis of the aziridine ring resulting in the formation of benzyl iodides as the actual reactive electrophiles.

Finally, the last protocol published up to date in the context of the synthesis of *β*-functionalized amines from aziridines under Ni- or Pd-catalyzed cross-coupling conditions is a unique approach developed by the Doyle group in 2023 changing regioselectivity of ring-opening for 2-alkyl substituted aziridines.[101]

The research was based on Ti-catalyzed radical ring-opening of aziridines reported by Lin and Gansauer.[102,103] Thus, upon coordination of Ti(III) metal center to the oxygen in the N-carbonyl fragment of aziridine the oxidation of Ti(III) to the Ti(IV) occurs followed by aziridine ring-opening with the formation of more stable radical species (Scheme 1.54).

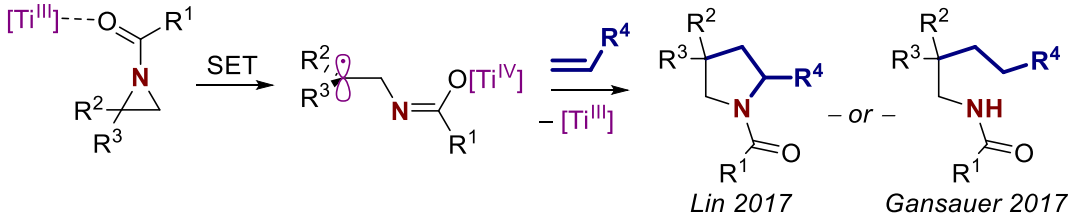

Scheme 1.54 Ti-catalyzed radical ring-opening of aziridines

The combination of Ti and Ni complexes in a dual redox catalytic system in the presence of a single reductant was already known in literature.[104] The group of Doyle proposed that by combining a Ti-catalyzed radical aziridine ring-opening approach with Ni-catalyst *β*-phenethylamine derivatives **1.140** can be accessed from 2-alkyl aziridines **1.139** and aryl iodides. Such an approach will be a complementary method to the previously reported alkylation of 2-aryl aziridines with acetals.

Even though, the desired reactivity mode was successfully achieved forming the desired product **1.140**, the regioselectivity of the transformation was not ideal as in many cases the formation of undesired linear product was observed (Scheme 1.55).[101]

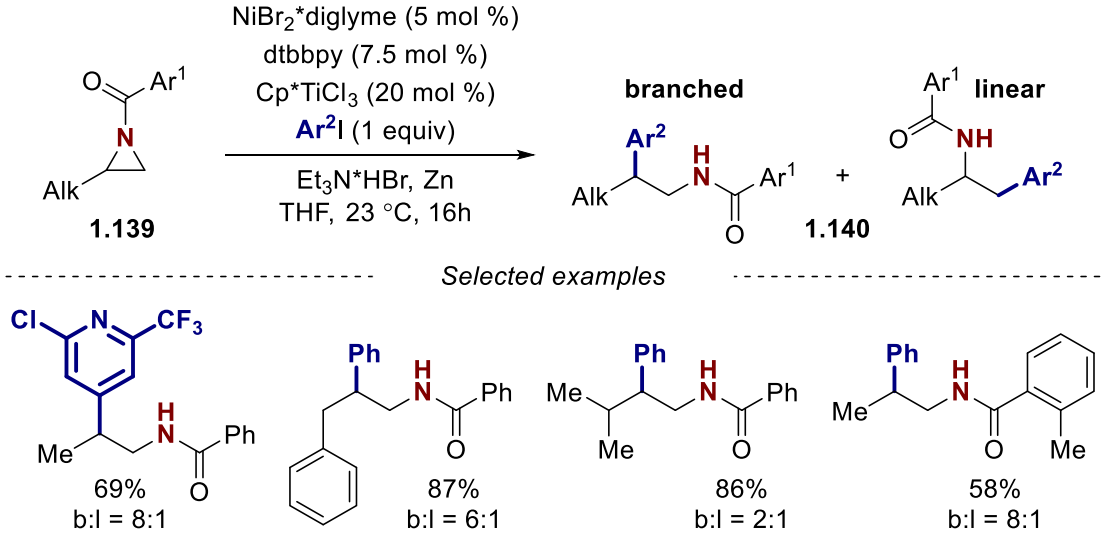

Scheme 1.55 Branched-selective dual Ti/Ni-catalyzed arylation of 2-alkyl aziridines

Nevertheless, conceptually this result is remarkable as it puts aziridines in line with radical retrosynthesis logic, which is gaining increased attention due to the large volume of literature coving radical reactivity.[105]

1.5 Mechanistic summary of the chapter

Herein, the current topic status and clarification of topic perspectives regarding existing gaps and challenges, and a summary generalizing reactivity trends and transformation types is given.

To begin with, reported protocols can be classified by the mode of C-N bond activation and the mechanism of aziridine ring-opening. Whereas a radical activation so far presented as a single example reported by Doyle using Ti catalyst, the vast majority of the transformations discussed above proceed via classical $2e^-$ S_N2-type nucleophilic substitution ring-opening pathway (Figure 1.19).

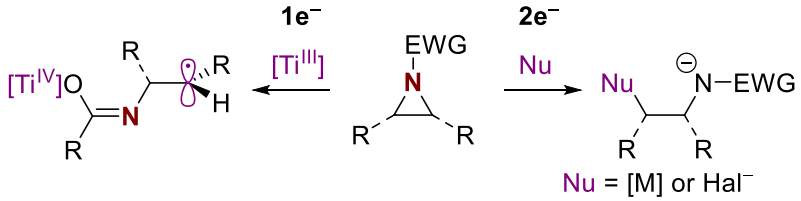

Figure 1.19 Radical type and $2e^-$ S_N2-type aziridine ring-opening

Among these $2e^-$ processes aziridine ring-opening is either achieved through oxidative addition of Ni or Pd complexes with the formation of azametallacyclobutane intermediates, or by nucleophilic attack of halide anion with the formation of *β*-halo amines.

The mechanism of the oxidative addition step differs depending on the metal, the ligand, the substitution pattern of aziridine, as well as the oxidative state of the metal center prior to the addition step.

Thus, for palladium, all reported transformations proceed through $2e^-$ S_N2-type nucleophilic substitution ring-opening mechanism with the azapalladacyclobutane formed after Ϭ-bond rotation (Figure 1.20).

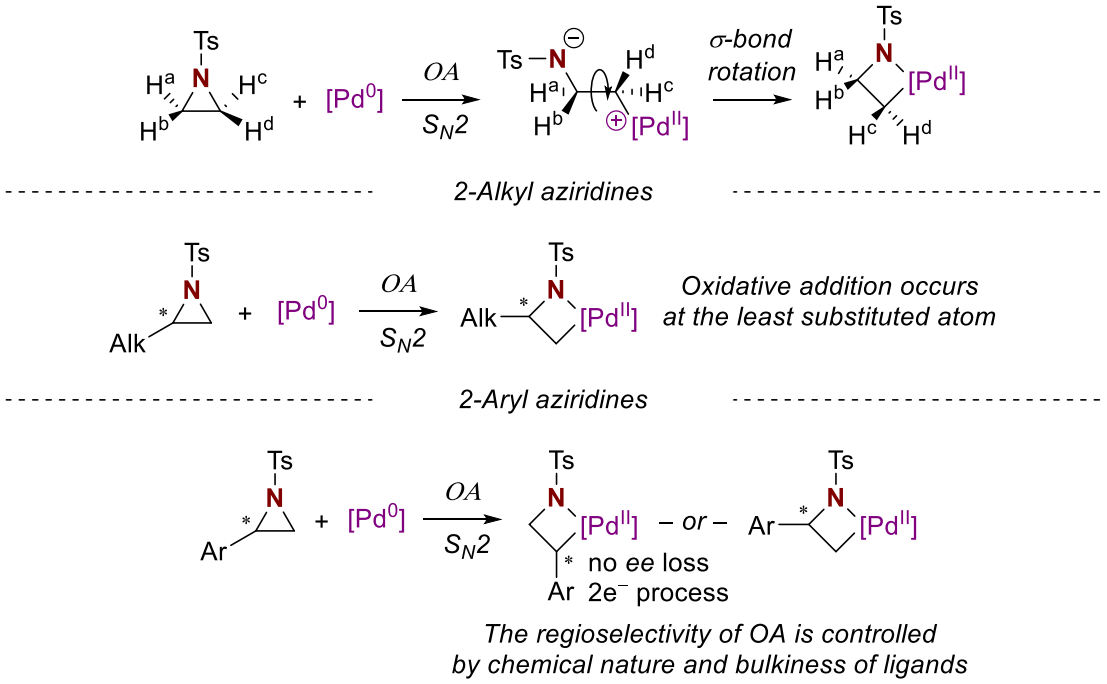

Figure 1.20 Ring-opening of aziridines with palladium

In the case of 2-alkyl aziridines the regioselectivity of ring-opening was always observed to occur at the least hindered carbon. The regioselectivity in the case of 2-aryl aziridines however in some cases can be controlled by a choice of different catalytic systems. With bulkier ligands the steric effect becomes more dominant than electronic, and instead of oxidative addition to the benzylic C-N bond the Pd center attacks more sterically available less substituted carbon. However, as it is still a 2e– process while breaking the benzylic bond in enantiopure 2-aryl aziridines the final product remains the enantiopurity.

The situation gets more complex for Ni-catalyzed aziridine ring-opening. Starting the discussion from 2-alkyl aziridines, the S_N2-type ring-opening mechanism at the least substituted carbon first observed by Hillhouse in 2002 seems to be predominant, and the use of *phen* or *bipy* families of ligands are required for the successful reaction (Figure 1.21).

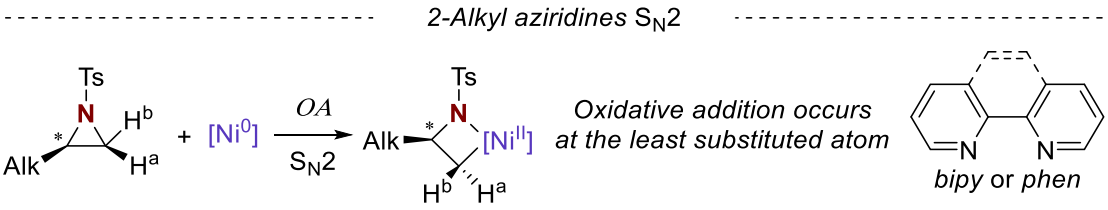

Figure1.21 S_N2-type ring-opening of 2-alkyl aziridines with nickel

However, it was observed by Doyle, that either in the presence of EDO ligands or in case of oxidative addition with Ni(I) species there is a stepwise mechanism and radical type species are formed via initial SET Ni(II)-N bond formation (Figure 1.22).

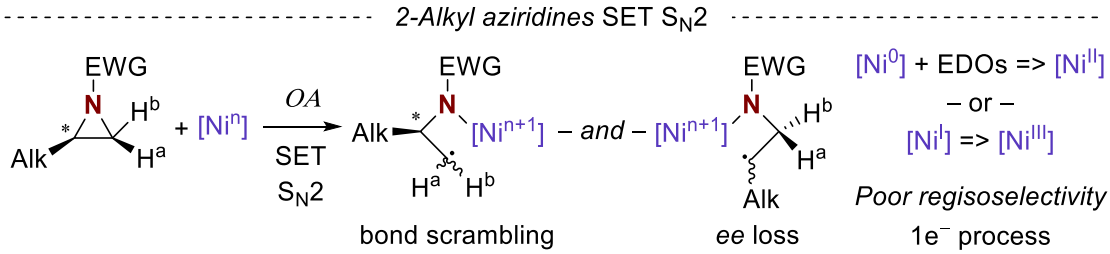

Figure 1.22 SET S_N2-type ring-opening of 2-alkyl aziridines with nickel

Once an aromatic substituent is introduced this mechanism of SET oxidative addition ring-opening becomes predominant, which leads to the loss of enantiopurity using enantiopure starting materials. On the other hand, the regioselectivity in all known cases is limited to the breaking of weaker benzylic bonds and the formation of more stable benzylic radicals (Figure 1.23).

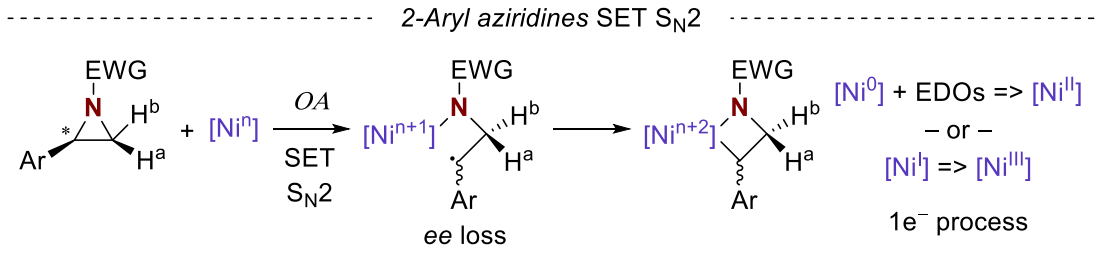

Figure 1.23 SET S_N2-type ring-opening of 2-aryl aziridines with nickel

Nevertheless, this mechanism opens up another unique opportunity – the development of Ni-catalyzed enantioselective C-C bond-forming cross-coupling transformations starting from racemic aziridines (Figure 1.24).

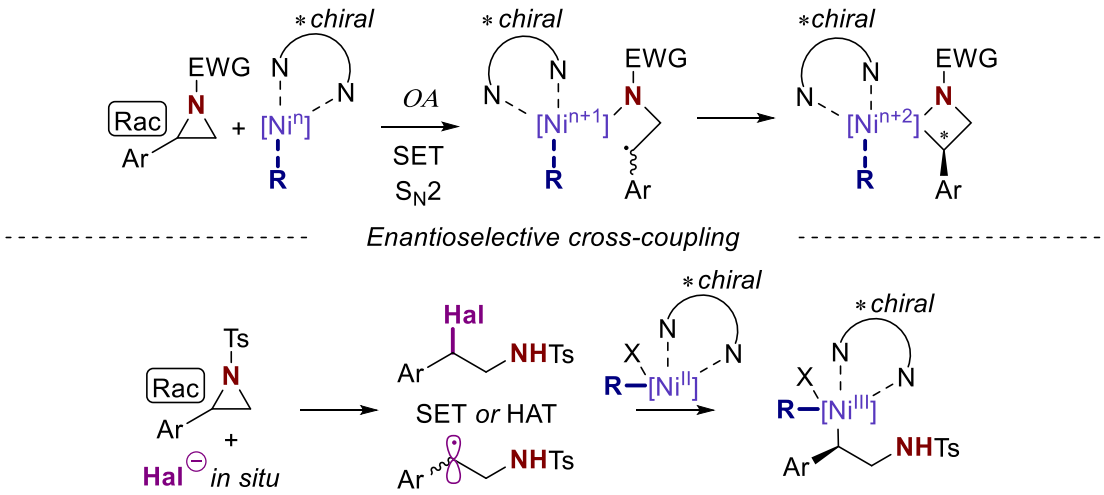

Figure 1.24 Enantioselective cross-coupling reactions of aziridines with nickel

The enantioselective cross-coupling can be also designed based on halogenolysis of racemic aziridines, as a reactive intermediate – the radical is formed from *β*-halo amines at the next step and then can be trapped by the Ni center.

Finally, it is worth discussing the reactivity of azametallacyclobutanes of Pd or Ni toward the formation of reaction intermediates capable of reductive elimination step.

For Pd-catalyzed reactions reported for aziridines, all reaction conditions possess one feature in common – the presence of a proton source in the reaction media. This leads to the protonolysis of azapalladacyclobutane with the formation of acyclic Pd complexes (Figure 1.25).

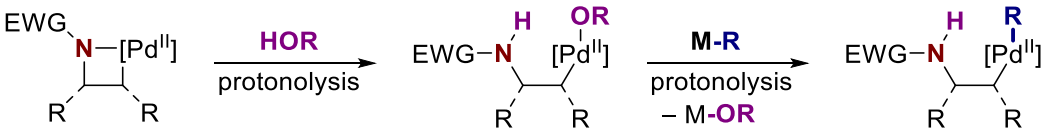

Figure 1.25 Protonolysis of azapalladacyclobutane

Surprisingly, that type of azanickellacyclobutanes activation is unknown, and when ring-opening of azametallacycles is proposed as a step of the catalytic cycle it is achieved rather by interaction with organozinc reagents, or in the presence of Fe(II/III) salts (Figure 1.26).

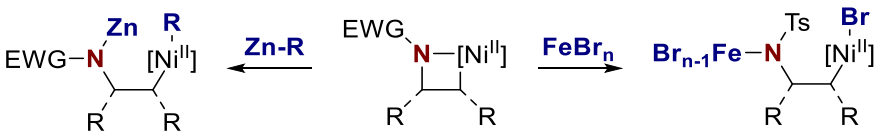

Figure 1.26 Activation of azanickellacyclobutane

Thus, the vast majority of Ni-catalyzed transformations with aziridines involve the aziridine ring halogenolysis step and do not involve the formation of azanickellacyclobutanes.

1.6 Synthetic summary of the chapter and future perspectives

After summarizing mechanistic aspects of Pd- and Ni-catalyzed transformations with aziridines all known data can be summarized by the type of products formed. To do so, the data can be split into two groups, based on which substitution pattern of aziridines was used, 2-aryl or 2-alkyl substituted ones.

All known products for the cross-coupling reactions of 2-aryl aziridines are shown on Figure 1.27.

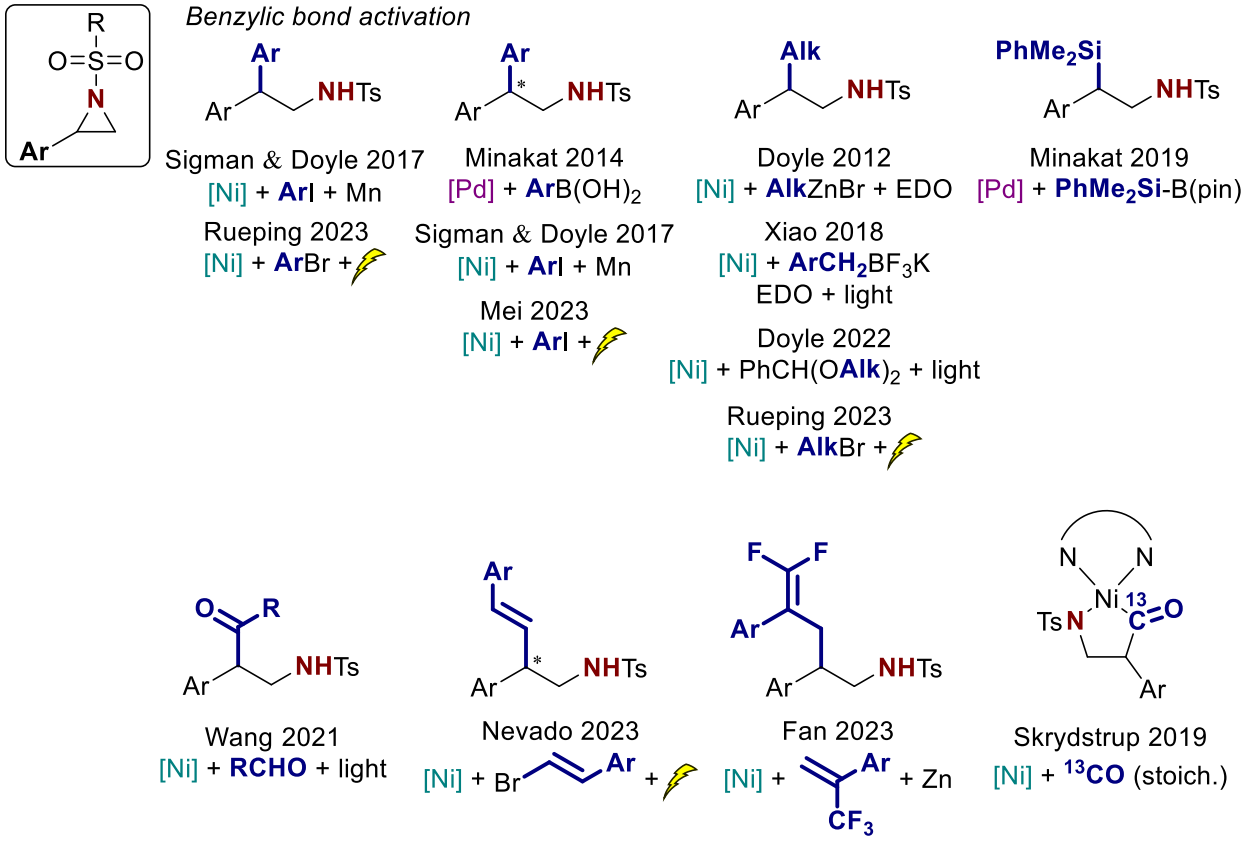

Figure 1.27 Known products for the cross-coupling reactions of 2-aryl aziridines

After careful evaluation of the table, we can point out several directions for further exploration of the topic. First, the list of known products can be expanded. For instance, some highly demanded in organic synthesis and medicinal chemistry programs structural moieties, such as homopropargyl amines, ethylenediamines, and γ-fluorinated amines may be accessed from aziridines under transition metal-catalyzed coupling reactions (Figure 1.28).

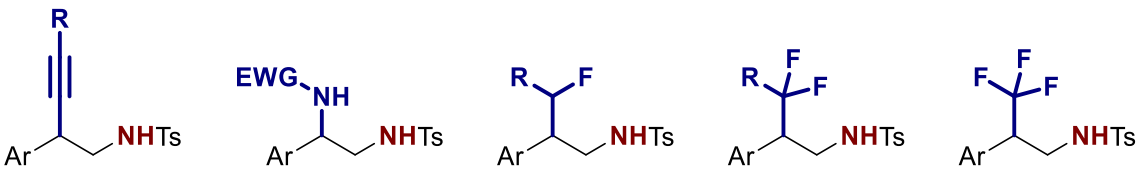

Figure 1.28 Compounds proposed for synthesis using cross-coupling reactions of aziridines

Secondly, the enantioselective versions of already known and proposed reactions need to be developed, as the current ones are limited to arylation and vinylation protocols. Finally, already known methodologies can be further expanded for a broader list of coupling partners and different reaction conditions (heterogeneous reductant/light/electricity driven).

Additionally, more attention can be paid to the development of regiodivergent cross-coupling reactions, and the geminal silylatition reported by Minakata seems underestimated as it remains a unique precedent in the literature so far (Figure 1.29).

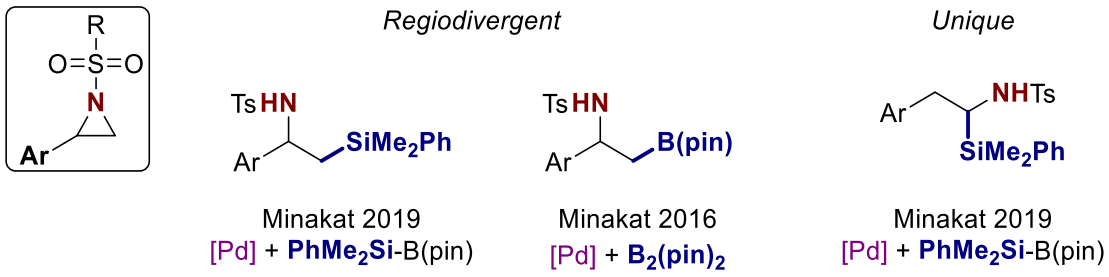

Figure 1.29 Specific Pd-catalyzed transformations of aziridines

Next, all known products for the cross-coupling reactions of 2-alkyl aziridines are shown on Figure 1.30.

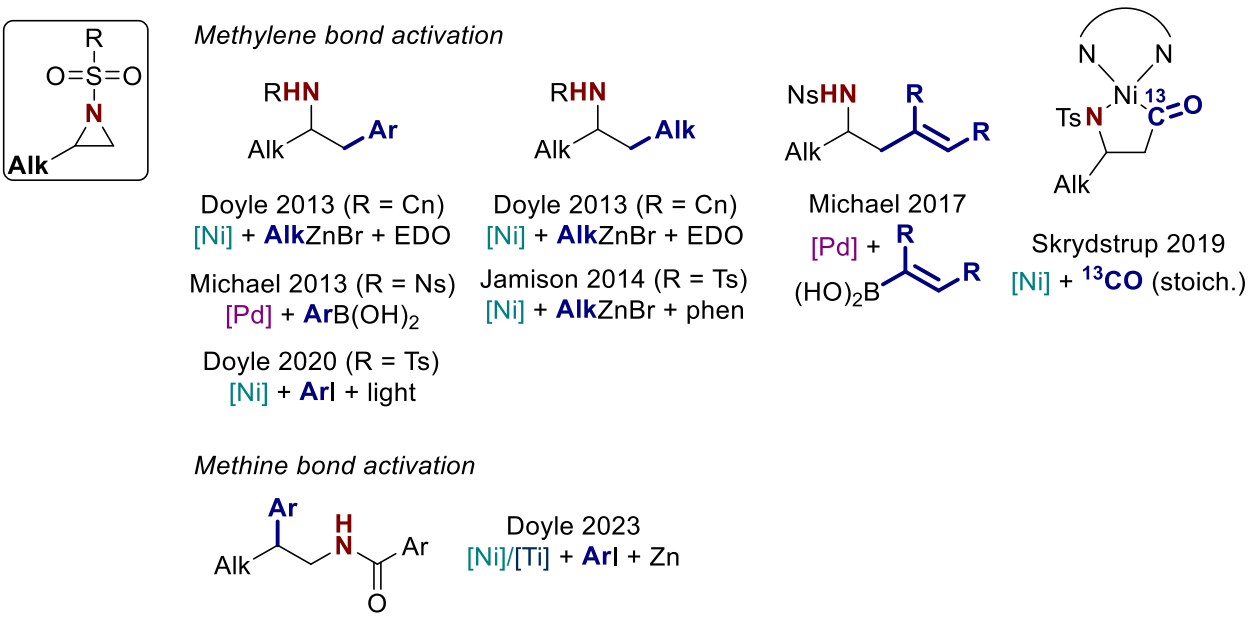

Figure 1.30 Known products for the cross-coupling reactions of 2-alkyl aziridines

After careful evaluation of the table, it is clear, that involvement of 2-alkyl aziridines in the cross-coupling events is more challenging, as the scope of known products so far is narrow. Same for 2-aryl aziridines, the list of known products can be significantly expanded. The groundbreaking

protocol by Doyle, opening aziridine ring at the most substituted position gives room for the development of enantioselective procedures.

1.7 Aim of the thesis

At this point, we come up with the contribution of the present thesis to the field. We achieved the reactivity of 2-alkyl aziridines toward the formation of highly valuable products namely *β*-amino acids and homoallylamines (Figure 1.31).

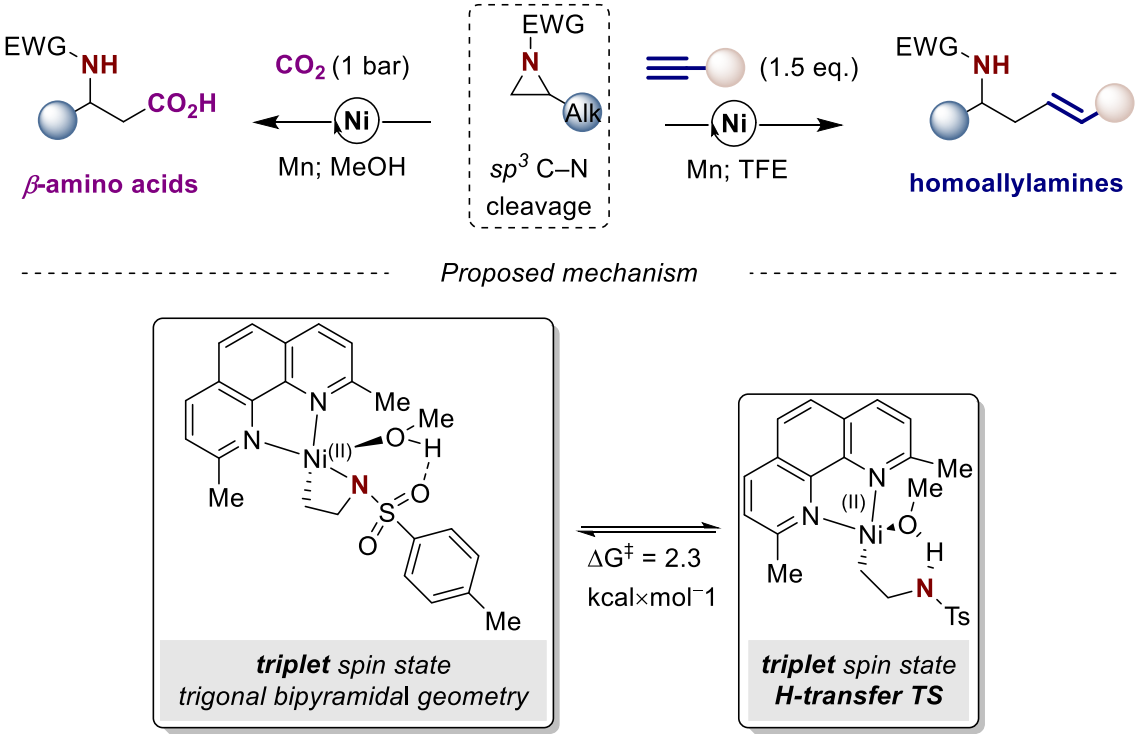

Figure 1.31 Novel Ni-catalyzed reductive coupling reactions of aziridines

A detailed discussion of the carboxylation methodology is presented in the following Chapter 2. A detailed discussion of the hydroalkenylation methodology is presented in Chapter 3. Upon collecting the results of our mechanistic investigation we claim, that the key mechanistic contribution of developed transformations to the field is the unique feature of Ni complexes bearing sterically hindered ligands to adopt its geometry by changing the metal center spin state. Thus, equilibrium between single and triplet azanickellacyclobutane complexes unlocks the protonolysis event and the subsequent formation of reaction intermediates. A detailed discussion of the reaction mechanism is presented in Chapter 4.

Chapter II. Ni-catalyzed reductive carboxylation of aziridines to access *β*-amino acids

2.1 Ni-catalyzed carboxylation of organic moieties using CO_2 and project hypothesis

For a better understanding of the project hypothesis, the carboxylation of organic moieties using CO_2 gas needs to be introduced first. All existing carboxylation methods can be split into 6 groups, based on the type of the key reaction intermediate or the substrate involved in the chemical transformation (Figure 2.1).[106]

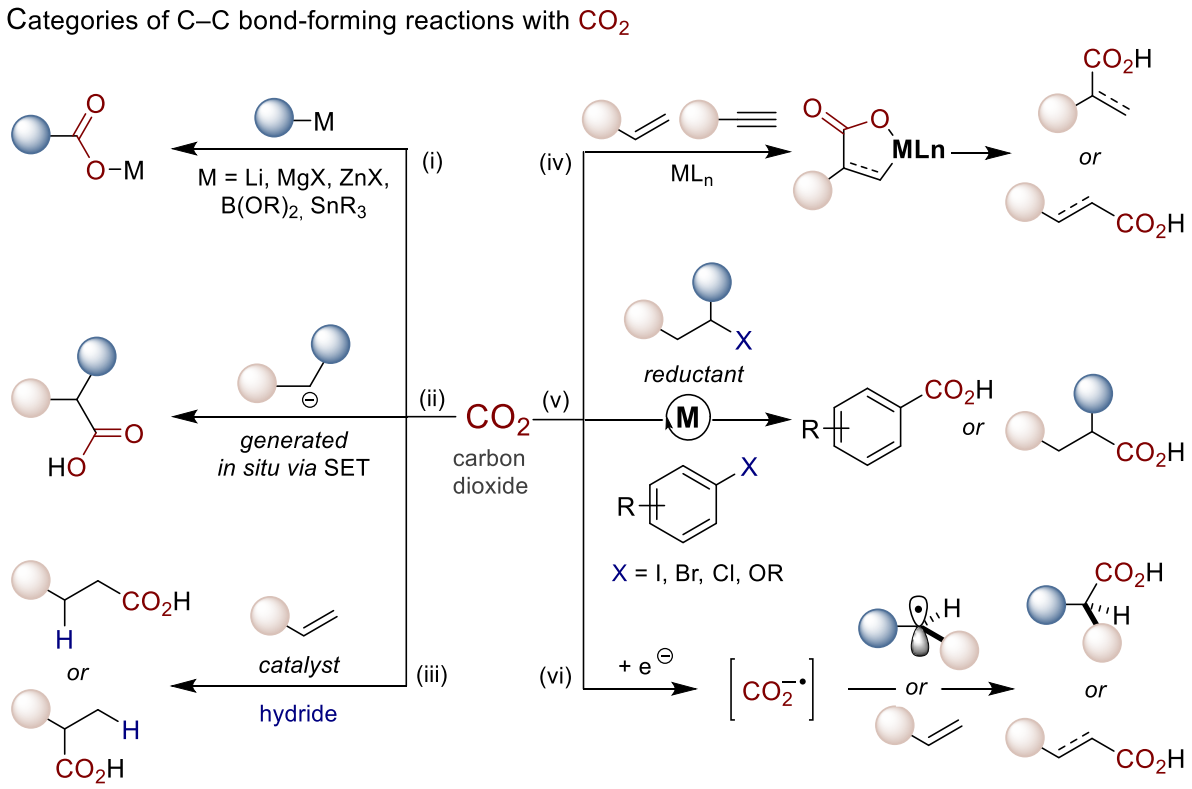

Figure 2.1 Carboxylation reactions arranged by the reactivity type

Among them are reactions of CO_2 with organometallic species (*route i*); with carbanions generated in situ from carbon radicals (*route ii*); carboxylation of olefins in the presence of metal hydride species (*route iii*); carboxylation of unsaturated bonds via a formation of metallalactones (*route iv*); reductive carboxylation of organic halides or pseudohalides, catalyzed by transition metal complexes (*route v*); carboxylation events involving CO_2 radical anion (*route vi*).

Within the lifetime of Prof. Ruben Martin's group significant expertise was gained in the carboxylation area following routes *iii* and *v*, applying Ni-based catalytic systems.[107,108] These transformations possess one important feature in common – the desired reactivity is unlocked while using sterically hindered bidentate N,N-ligands, namely phenantrolines and bypiridines (Figure 2.2).

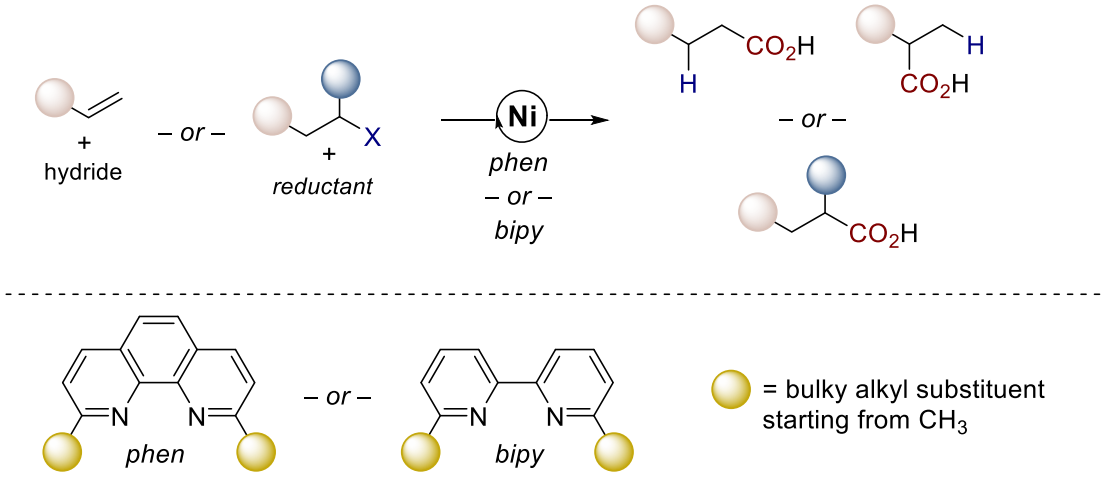

Figure 2.2 Common ligands in reductive Ni-catalyzed carboxylation reactions

For a long time, this phenomenon was rationalized with the hypothesis of increased stability of Ni(I)-Alk species, formed within a catalytic cycle, in the presence of mentioned bulky ligands and insertion of CO_2 to be occurring with these Ni(I) intermediates. This idea got experimental confirmation when in 2020 the isolation and characterization of respective reaction intermediates was finally reported (Figure 2.3).[109]

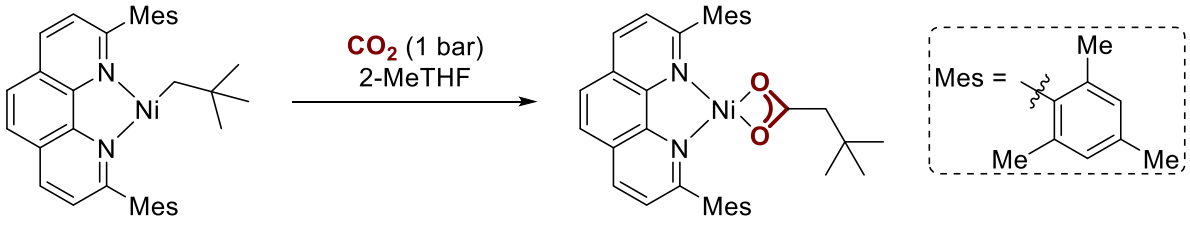

Figure 2.3 Insertion of CO_2 into Ni(I)-Alkyl bond

Based on well-built expertise gained through the years, we saw a potential in the aziridine core to be used as a coupling partner under Ni-catalyzed reductive carboxylation conditions using CO_2 gas. As a working hypothesis it was claimed that *on paper* in situ formed azanickellacyclobutanes can be reduced directly or with the support of additional additives in the presence of reductant, forming desired Ni(I)-Alk species. These species will *a priori* undergo insertion of CO_2 into Ni-C bond forming highly valuable products – *β*-amino acids (Figure 2.4).

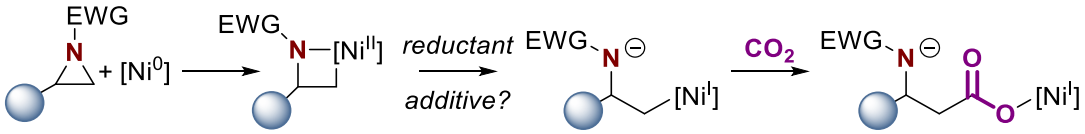

Figure 2.4 Proposed synthesis of *β*-amino acids from aziridines and CO_2

This initial proposal was successfully tackled by previous group member Dr. Daniel Janssen-Muller during initial reactivity tests and initial reaction conditions screenings. Some observations, key for the project, about reactivity trends made at that time are discussed in the following section.

2.2 Initial proof of concept and screening observations

As it was discussed in the previous section, based on the previous group's experience as an initial catalytic system for initial studies was chosen the system consisting of model substrate **2.1a**, Ni(II) precatalyst, N,N-ligand, solvent, Mn, and CO_2 gas (1 atm) with the idea to prove the proposed synthetic concept by forming desired product **2.2a** (Figure 2.5).

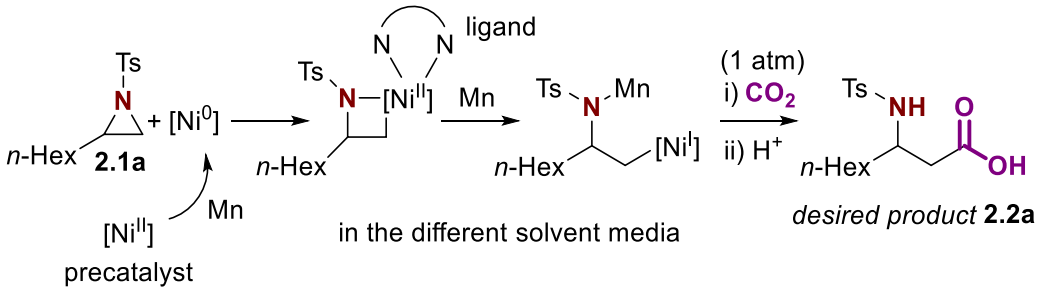

Figure 2.5 Initial attempts to form product **2.2a** from aziridine **2.1a**, combining Ni-catalyst and CO_2 in the presence of Mn reductant

However, the formation of the desired product was only observed in trace amounts by applying such a combination of reagents. Any change in Ni(II) precatalyst, ligand type or ligand structure, and solvent type did not lead to any improvement. Nevertheless, some minor conversion of SM normally was observed (10-20%), suggesting that oxidative addition of Ni-center occurs without further reaction continuation.

At this point the addition of extra additive was considered with the idea to facilitate the ring-opening of azanickellacyclobutane intermediate. The intense screening of a diverse list of potential additives, including Lewis acids, metal salts, and hydrogen sources was conducted. It was found that any kind of LAs or metal salts did not lead to the formation of the desired product in the amount of the product yield higher than traces.

Luckily, it was found that the reaction simply works upon the addition of alcohols, suggesting any sort of proton transfer or protonolysis to be among the key steps of the catalytic cycle. Among, proton sources tested the most promising performance was observed using MeOH. It is also worth mentioning that reaction only worked in the amide type family of solvents (Figure 2.6).

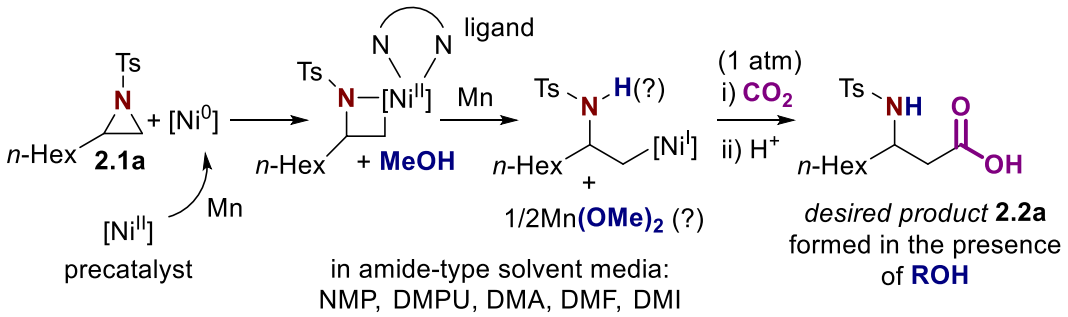

Figure 2.6 Formation of the desired product **2.2a** in the presence of ROH

After achieving this initial positive result, the screening process continued. The best conditions at that moment, obtained by Dr. Janssen-Muller, were as follows: $(neocuproine)_2Ni(ClO_4)_2$ (10 mol%) as Ni(II) precatalyst, extra amounts of neocuproine (6 mol%), Mn (3 equiv) as reductant, MeOH (5 equiv) as a proton source. The reaction was performed in DMPU (dry), under a pressure of CO_2 (1 atm), and at 10°C. These conditions resulted in approximately 50% product yield and 25% of $TsNH_2$ as the main side-product of the reaction (Scheme 2.1).

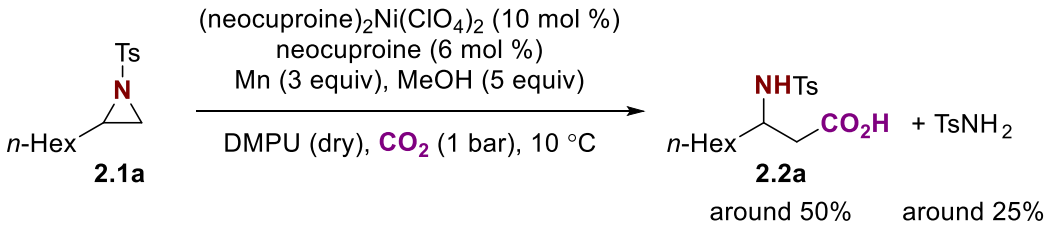

Scheme 2.1 Ni-catalyzed reductive carboxylation of aziridines; reaction conditions preoptimized using cationic Ni(II) precatalyst

Additionally, it was found that usage of $NiCl_2$*glyme – a non-cationic Ni(II) precatalyst led to similar results (Scheme 2.2).

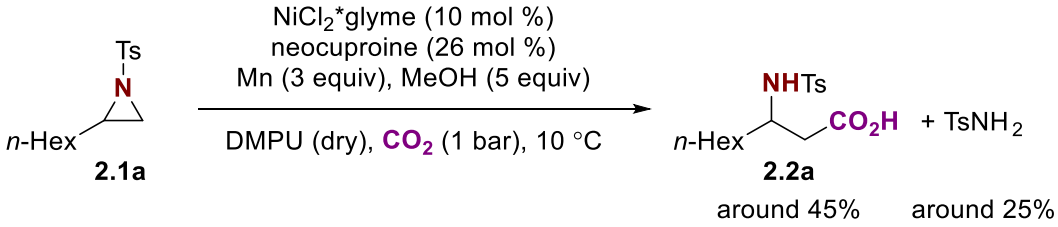

Scheme 2.2 Ni-catalyzed reductive carboxylation of aziridines; reaction conditions preoptimized using non-cationic Ni(II) precatalyst

At this step and with these mid-optimized conditions in hand, the project was carried further under the lead of Dr. Jacob Davies, with whom I had the pleasure of working together. Our combined efforts in the development of reductive Ni-catalyzed aziridine carboxylation methodology are discussed in the following sections.

2.3 Final optimization of reaction conditions

The study began with reproducibility approaches and the respective product reaction yields and $TsNH_2$ yields were observed (Scheme 2.3).

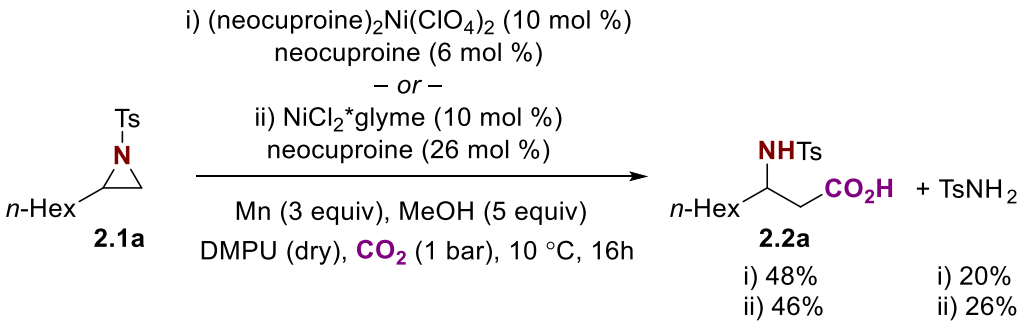

Scheme 2.3 Initial reproducibility approach

Among different observations made by Dr. Janssen Muller, it was mentioned that trace amounts of Cl^- aziridine ring-opening side-product were observed, potentially due to the formation of Cl^- anion from ClO_4^- in the presence of Mn. Our goal was to push the reaction yield over 50% and we considered the potential influence of this process on the overall reaction performance and tested the reaction conditions using $(neocuproine)_2Ni(BF_4)_2$ as precatalyst. Thus, upon testing the extra ligand loading it was noticed that no difference in the reaction yield was observed compared with $(neocuproine)_2Ni(ClO_4)_2$ precatalyst and that extra addition of neocuproine(**L5**) ligand did not lead to the reaction yield improvement (Table 2.1).

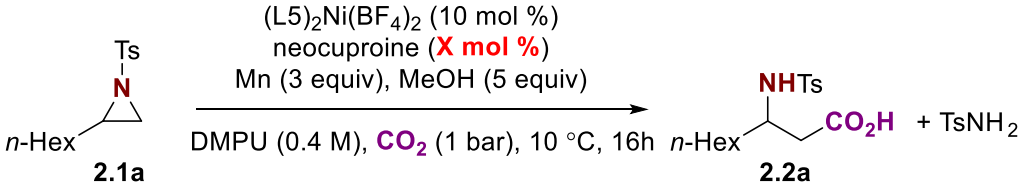

[Ni] (mol%) + ligand (mol%)	Conv. of 2.1a (%)	Product (%)	$TsNH_2$ (%)
$Ni(L5)_2(BF_4)_2$ (10) + L5 (8)	96	48	16
$Ni(L5)_2(BF_4)_2$ (10) + L5 (6)	98	49	19
$Ni(L5)_2(BF_4)_2$ (10) + L5 (4)	95	45	18
$Ni(L5)_2(BF_4)_2$ (10)	98	47	18

Table 2.1 Screening of extra additive of ligand effect on the reaction performance

Nevertheless, further optimization was continued with $(neocuproine)_2Ni(BF_4)_2$ precatalyst. Next, trying to reduce the amount of catalyst used or increase the reaction yield by using extra catalyst loading it was confirmed that 10 mol % of Ni(II) precatalyst is the optimal amount (Table 2.2).

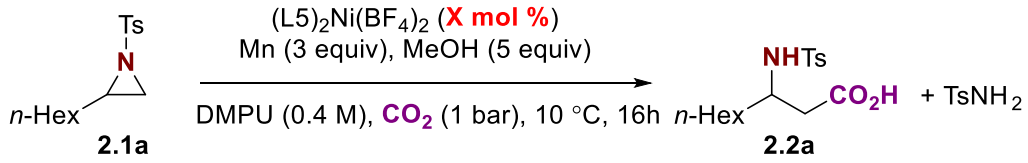

[Ni] (mol%)	Conv. of 2.1a (%)	Product (%)	$TsNH_2$ (%)
$Ni(L5)_2(BF_4)_2$ (2.5)	50	18	13
$Ni(L5)_2(BF_4)_2$ (5)	83	38	19
$Ni(L5)_2(BF_4)_2$ (10)	97	50	17
$Ni(L5)_2(BF_4)_2$ (20)	84	39	14

Table 2.2 Screening of extra additive of ligand effect on the reaction performance

As was mentioned in the previous section, the formation of the desired product was only observed using the amide-type family of solvents. Seeking for any improvement in the reaction yield we tested some other commercially available amide solvents (Table 2.3).

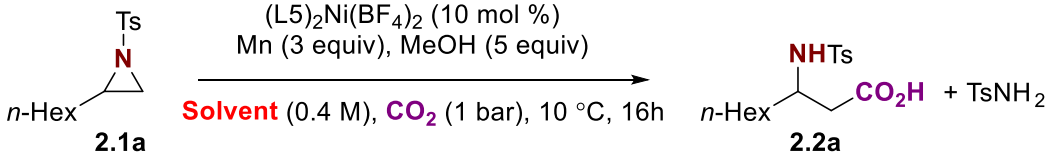

Solvent	Conv. of 2.1a (%)	Product (%)	$TsNH_2$ (%)
DMA	84	47	20
DMF	63	32	15
DMI	48	25	13
NMP	96	47	25

Table 2.3 Solvent screening

Promising results were obtained with DMA and NMP which gave similar product yield as DMPU. These three solvents were tested for dilution influence (Table 2.4).

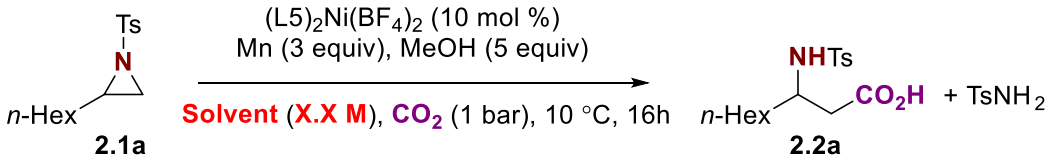

Solvent (M)	Conv. of 2.1a (%)	Product (%)	$TsNH_2$ (%)
DMPU (0.8)	100	47	25
DMPU (0.4)	98	49	15
DMPU (0.27)	81	40	11
DMA (0.8)	94	40	26
DMA (0.4)	89	41	18
DMA (0.27)	86	40	15
NMP (0.8)	100	43	32
NMP (0.4)	96	49	22
NMP (0.27)	92	46	17

Table 2.4 Dilution screening

Although less $TsNH_2$ was observed under higher dilution, the amount of product was unaffected. NMP performed similarly to DMPU.

Even though, MeOH was found to be the best proton source during initial proof of concept studies, the proton source screening was repeated (Table 2.5).

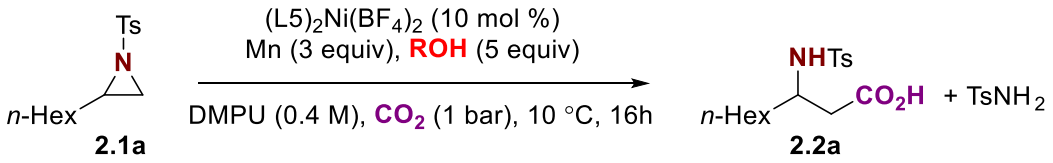

ROH	Conv. of 2.1a (%)	Product (%)	$TsNH_2$ (%)
EtOH (5)	44	15	6
TFE (5)	25	5	10
HFIP (5)	27	0	10
***i*PrOH** (5)	16	0	0
***t*BuOH** (5)	13	0	0
Phenol (5)	24	5	0

Table 2.5 Screening of various alcohols

Unfortunately, any of the alcohols tested did not demonstrate any promising result. An interesting observation, however, was made regarding the conversion of model substrate **2.1a**. The origin of such a drastic difference with MeOH is unclear, as usage of MeOH normally gives a near quantitative conversion of aziridine **2.1a**.

Upon screening addition of MeOH to the reaction in different quantities it was confirmed the amount of 5 equivalents to be the optimal (Table 2.6).

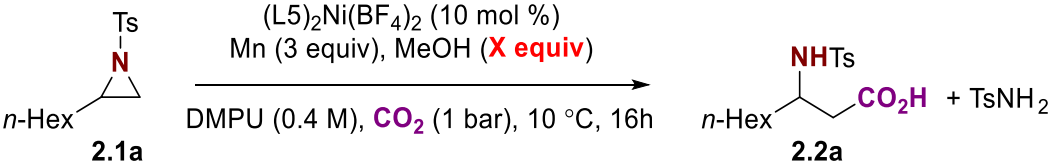

MeOH (equiv)	Conv. of 2.1a (%)	Product (%)	$TsNH_2$ (%)
MeOH (2.5)	85	40	13
MeOH (5)	99	55	19
MeOH (7.5)	94	45	18
MeOH (10)	92	49	18
MeOH (20)	61	28	12

Table 2.6 Screening of MeOH equivalents

No significant improvement in the reaction yield was achieved at this point. With the idea to affect the formation $TsNH_2$ side-product toward the formation of the desired product **2.2a** a systematic ligand screening was conducted. As performing screening with (L)Ni(II)$(BF_4)_2$ type of precatalyst would require an additional synthesis of a precatalyst in each case we switched our attention toward the result obtained with non-cationic $NiCl_2$*glyme. Using a simple Ni(II) source with ligand added to the reaction mixture an extra synthetic effort could be avoided, whereas possessing a qualitative screening.

Thus, upon testing ligand loading with $NiCl_2$*glyme we observed a highly promising result using 10 mol % of neocuproine(**L5**) (Table 2.7).

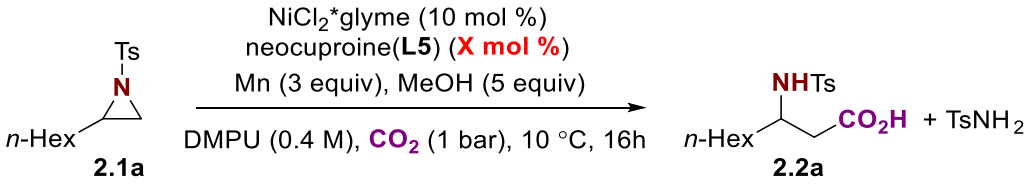

[Ni] (mol%) + ligand (mol%)	Conv. of 2.1a (%)	Product (%)	$TsNH_2$ (%)
$NiCl_2$*glyme (10) + L5 (20)	99	50	25
$NiCl_2$*glyme (10) + L5 (15)	97	50	19
$NiCl_2$*glyme (10) + L5 (10)	100	43	40

Table 2.7 Screening of ligand loading(**L5**) with $NiCl_2$*glyme

Even though an excess of ligand gave a higher yield, but a larger amount of $TsNH_2$ was produced at 10 mol % loading of neocuproine(**L5**). It was hypothesized that the yield of **2.2a** could be increased by modifying the ligand at this loading.

In addition, some other Ni(II) non-cationic precursors have been tested, but usage of $NiCl_2$*glyme remained the best option (Table 2.8).

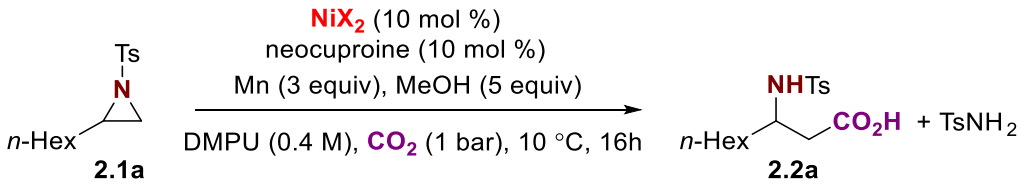

[Ni] (mol%) + ligand (mol%)	Conv. of 2.1a (%)	Product (%)	$TsNH_2$ (%)
$NiBr_2$glyme (10) + L5 (10)	97	35	26
$NiCl_2$ (10) + L5 (10)	37	11	5
$NiBr_2$ (10) + L5 (10)	29	-	-
NiI_2 (10) + L5 (10)	93	35	26

Table 2.8 Screening of non-cationic Ni(II) sources

We started the ligand screening from *phen* family of ligands (Table 2.9).

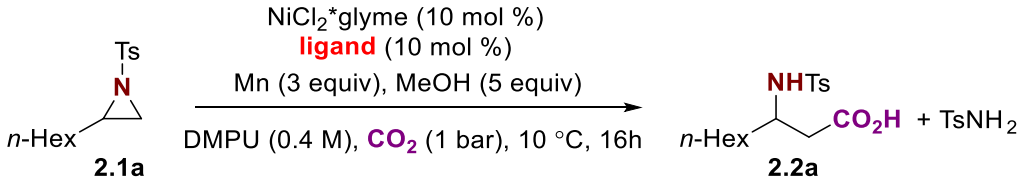

[Ni] (mol%) + ligand (mol%)	Conv. of 2.1a (%)	Product (%)	$TsNH_2$ (%)
$NiCl_2$glyme (10) + **L6** (10)	95	33	43
$NiCl_2$glyme (10) + **L7** (10)	98	40	38
$NiCl_2$glyme (10) + **L8** (10)	82	33	31
$NiCl_2$glyme (10) + **L9** (10)	99	41	38
$NiCl_2$glyme (10) + **L10** (10)	46	0	19
$NiCl_2$glyme (10) + **L11** (10)	97	42	32
$NiCl_2$glyme (10) + **L12** (10)	82	32	20

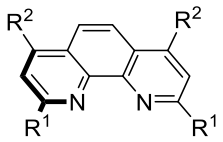

R^1=Et; R^2 = H (**L6**)
R^1=*n*Bu; R^2 = H (**L7**)
R^1=*i*Bu; R^2 = H (**L8**)
R^1=*n*Hex; R^2 = H (**L9**)

R^1=Me; R^2=Ph (**L10**)
R^1=Me; R^2= (2,4-OMe-C_6H_3) (**L11**)
R^1=Me; R^2=OMe (**L12**)

Table 2.9 Screening of *phen* family of ligands

Unfortunately, we did not observe any improvement or significant change in the overall reaction performance by increasing the steric hindrance of substituents R^1 (see **L6**-**L9**). While trying to

change electronics in the *phen* backbone some irrational results were obtained. Whereas **L10** completely suppressed desired reactivity, using **L11** and **L12** it was recovered, but with remarkable difference. This difference might be explained potentially by a difference of ligands solubility, resulting in the different solubility of Ni complexes in the reaction media.

Next, we moved to the screening of *bipy* family of ligands (Table 2.10).

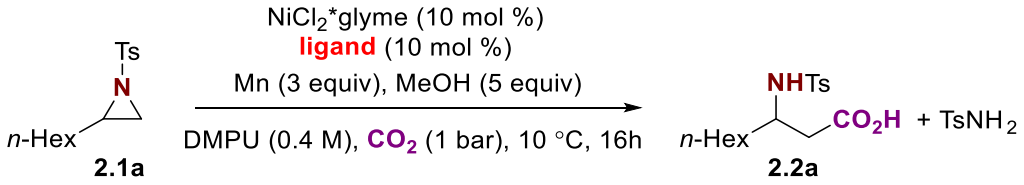

[Ni] (mol%) + ligand (mol%)	Conv. of 2.1a (%)	Product (%)	$TsNH_2$ (%)
$NiCl_2$glyme (10) + **L1** (10)	78	34	24
$NiCl_2$glyme (10) + **L2** (10)	98	50	32
$NiCl_2$glyme (10) + **L3** (10)	23	0	2
$NiCl_2$glyme (10) + **L4** (10)	32	2	8
$NiCl_2$glyme (10) + **L13** (10)	38	1	6
$NiCl_2$glyme (10) + **L14** (10)	40	2	9
$NiCl_2$glyme (10) + **L15** (10)	77	7	42
$NiCl_2$glyme (10) + **L16** (10)	85	23	43
$NiCl_2$glyme (10) + **L17** (10)	38	5	10
$NiCl_2$glyme (10) + **L18** (10)	53	12	18
$NiCl_2$glyme (10) + **L19** (10)	39	6	15
$NiCl_2$glyme (10) + **L20** (10)	48	22	7

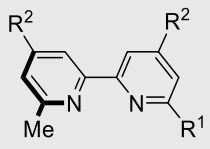

R^1=Me; R^2=OMe (**L1**)
R^1=Me; R^2= *t*Bu (**L2**)
R^1=Me; R^2 = Me (**L3**)
R^1=H; R^2 = OMe (**L4**)
R^1=H; R^2 = *t*Bu (**L13**)

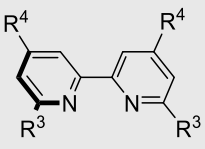

R^3=Me; R^4 = H (**L14**)
R^3=Me; R^4 = Ph (**L15**)
R^3=Me; R^4 = anisole (**L16**)
R^3=*i*Bu; R^4 = *t*Bu (**L17**
R^3=*n*Bu; R^4 = *t*Bu (**L18**)
R^3=*n*Hex; R^4 = *t*Bu (**L19**)

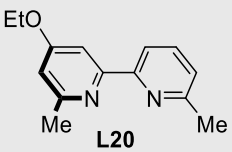

Table 2.10 Screening of *bipy* family of ligands

Electron-rich 4,4′-MeO-6,6′-Mebpy(**L1**) and 4,4′-tBu-6,6′-Mebpy(**L2**) were found to be promising. Variation in the *ortho*-sterics is detrimental with both reducing (**L4**, **L13**) and increasing (**L17-19**) bulk resulting in lower yields.

Other ligand classes screening resulted in trace or no product formation (Table 2.11).

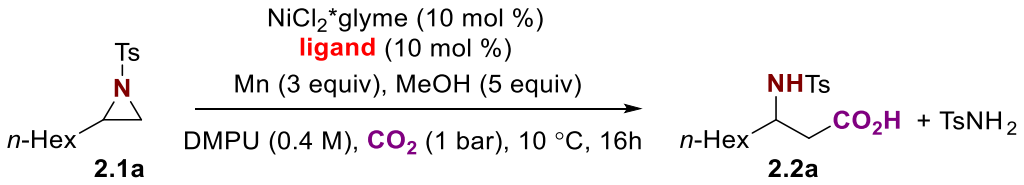

[Ni] (mol%) + ligand (mol%)	Conv. of 2.1a (%)	Product (%)	$TsNH_2$ (%)
$NiCl_2$glyme (10) + **L21** (10)	-	0	-
$NiCl_2$glyme (10) + **L22** (10)	18	2	2
$NiCl_2$glyme (10) + **L23** (10)	32	0	-
$NiCl_2$glyme (10) + **L24** (10)	18	4	2
$NiCl_2$glyme (10) + **L25** (10)	-	-	-

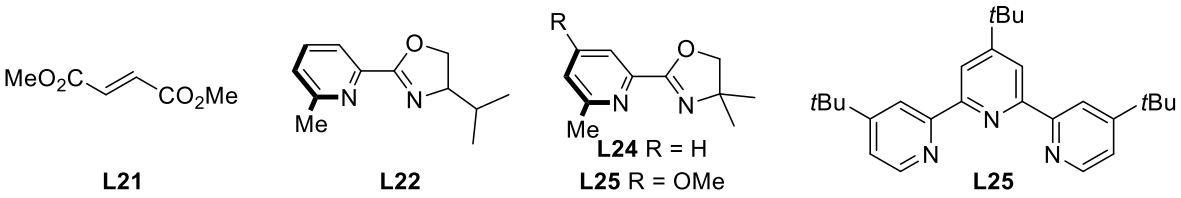

Table 2.11 Screening of other ligand classes

As it was observed that higher loading of **L5** gave higher product yield we decided to test the two most promising *bipy* ligands (**L1** and **L2**) for potential reaction outcome improvement with higher ligand loading (Table 2.12).

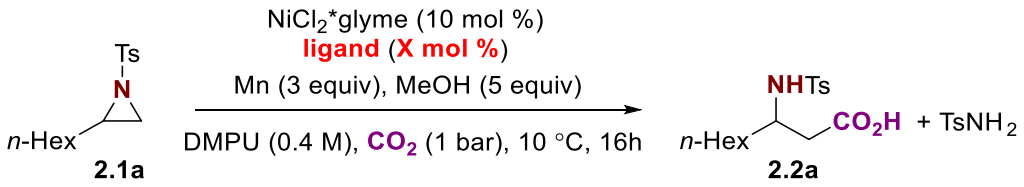

[Ni] (mol%) + ligand (mol%)	Conv. of 2.1a (%)	Product (%)	$TsNH_2$ (%)
$NiCl_2$glyme (10) + **L1 (12)**	100	51	30
$NiCl_2$glyme (10) + **L1 (15)**	99	55	24
$NiCl_2$glyme (10) + **L1 (20)**	100	62	23
$NiCl_2$glyme (10) + **L1 (25)**	100	49	25
$NiCl_2$glyme (10) + **L2 (10)**	98	50	32
$NiCl_2$glyme (10) + **L2 (15)**	100	53	30
$NiCl_2$glyme (10) + **L2 (20)**	97	53	34

Table 2.12 Screening of ligand loading for **L1** and **L2**

Whereas no difference was observed for different amounts of **L2**, while using **L1** at 20 mol % ligand loading we finally observed the desired improvement in the yield of **2.2a** (62% NMR yield).

At this stage, reproducibility issues between different batches of **2.1a** were encountered. Initially used in the optimization screening starting material possessed 95% purity by NMR and was mostly consumed to the moment. With higher purity aziridine **2.1a** prepared for further screening, the reaction was found to be slower but more selective for the desired product **2.2a** with only 10-15% $TsNH_2$ observed.

That was a crucial finding for the study. Finally, just simply increasing the reaction time up to 48 hours the yield of the desired product **2.2a** higher than 70% was achieved (Table 2.13).

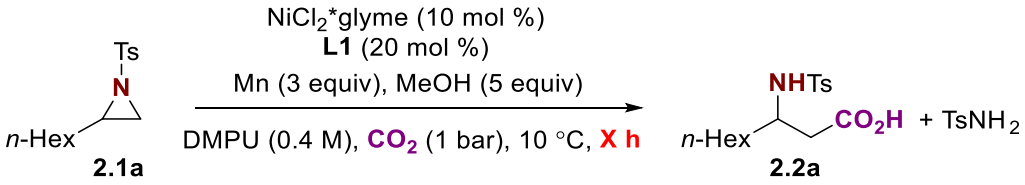

Time / h	Conv. of 2.1a (%)	Product (%)	$TsNH_2$ (%)
24	57	40	8
30	85	54	10
48	94	73	12
60	100	75	10

Table 2.13 Screening of reaction time with **L1**

By retesting neocuproine(**L5**) with the freshly prepared starting material **2.1a** we confirmed the advantage of using *bipy* ligand **L1** (Table 2.14).

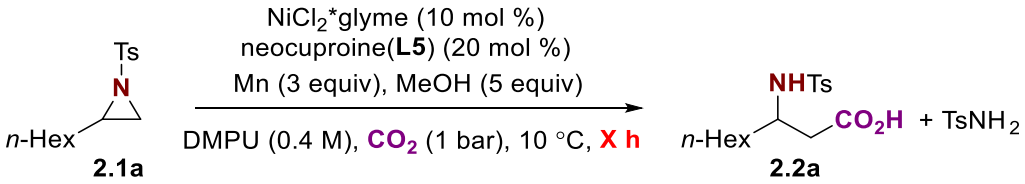

Time / h	Conv. of 2.1a (%)	Product (%)	$TsNH_2$ (%)
20	55	29	9
48	87	56	20

Table 2.14 Screening of reaction time with **L5**

With the idea to increase the reaction rate, we tried to increase the reaction temperature, however, that only led us to a drop in the reaction yield and increased formation of undesired $TsNH_2$ side-product (Table 2.15).

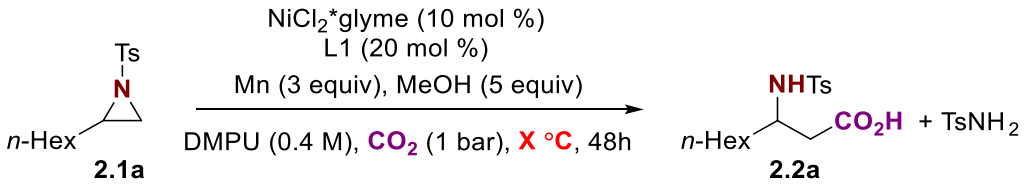

Temp. / °C	Conv. of 2.1a (%)	Product (%)	$TsNH_2$ (%)
10	90	73	12
15	93	70	15
25	86	53	20

Table 2.15 Screening of reaction temperature

Finally, we decided to test the influence of CO_2 pressure (Table 2.15).

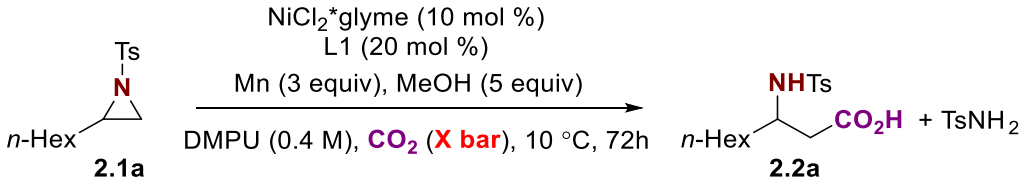

CO_2 (bar)	Conv. of 2.1a (%)	Product (%)	$TsNH_2$ (%)
0.5	93	71	20
1.0	94	76	12
1.75	80	69	10
2.5	76	65	9

Table 2.15 Screening of CO_2 pressure

It was observed, that the increased pressure slowed down the reaction, which can be rationalized as inhibited catalytic activity of Ni catalyst.

To summarize our efforts to the conclusion, the optimal conditions to continue with reaction scope investigation were as follows: $NiCl_2$*glyme (10 mol%) as Ni(II) precatalyst, **L1** at 20 mol % ligand loading, Mn (3 equiv) as reductant, MeOH (5 equiv) as a proton source. The reaction was performed in DMPU (dry, 0.4 M), under the pressure of CO_2 (1 atm), and at 10°C, for 48-72h for the model substrate **2.1a** to achieve a complete conversion (Scheme 2.4).

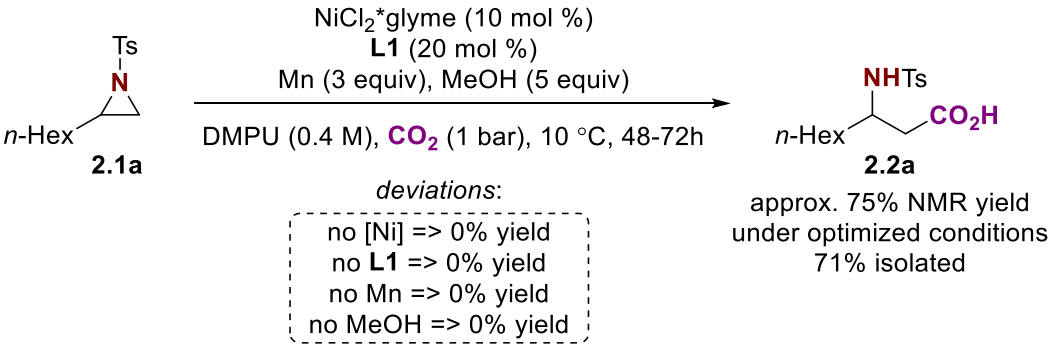

Scheme 2.4 Optimized conditions for Ni-catalyzed reductive carboxylation of aziridines using CO_2

By erasing from the catalytic cocktail one by one different components such as Ni(II) source, ligand, Mn, and alcohol we demonstrated that all of them are crucial for the successful reaction endeavor.

To conclude, the presence of H-source in the reaction media was found to be pivotal to unlocking the desired reactivity during preliminary studies. During the following optimization studies, the high yield of the desired product (>70% by NMR) was achieved upon carefully choosing the ligand, favoring the reaction direction to the formation of the desired product **2.2a** rather than $TsNH_2$. The reaction was found to be sensitive to the trace amounts of impurities (<5% by NMR) formed during the preparation of starting material **2.1a** and the substrate of very high purity (>99% by NMR) must be used to achieve the desired yield and avoid reproducibility issues.

The studies of reaction utility and limitations are presented in the following sections.

2.4 Investigation of the reaction scope

2.4.1 Reaction scope of natural α-amino acids homologs

In *Section 1.2* the three main synthetic pathways to access aziridines were introduced. Among them, intramolecular cyclization of amines containing the leaving group at the *β*-position and aziridination of olefins with nitrenes or nitrenoids were used for the preparation of starting materials in our study. Thus, *N*-Tosyl aziridines can be accessed upon treatment of *β*-amino alcohols with strong base in the presence of TsCl (Scheme 2.5).

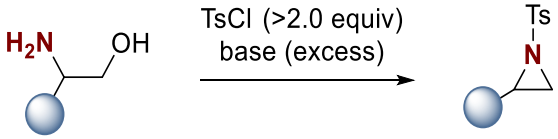

Scheme 2.5 Synthesis of *N*-Tosyl aziridines from *β*-amino alcohols

Meanwhile, *β*-amino alcohols can be derived from α-amino acids through reduction with $LiAlH_4$. Considering the entire retrosynthetic sequence then, we can determine our developed reaction as a stepwise homologation of α-amino acids using CO_2 (Figure 2.7).

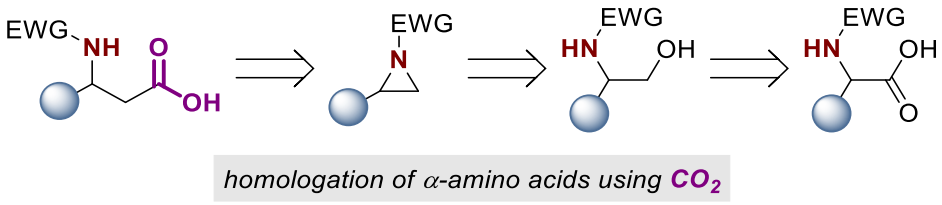

Figure 2.7 Retrosynthetic sequence for *α*-amino acids homologation through aziridine carboxylation using CO_2

For that reason, to initiate our reaction scope study, we attempted to synthesize some homologs of 20 natural amino acids. At first, we chose Glycine, Alanine, Valine, and Leucine as a case study to investigate how substituent steric effects influence reaction outcomes. Thus, after obtaining corresponding aziridines **2.1** we tested them under optimized reaction conditions (Scheme 2.6).

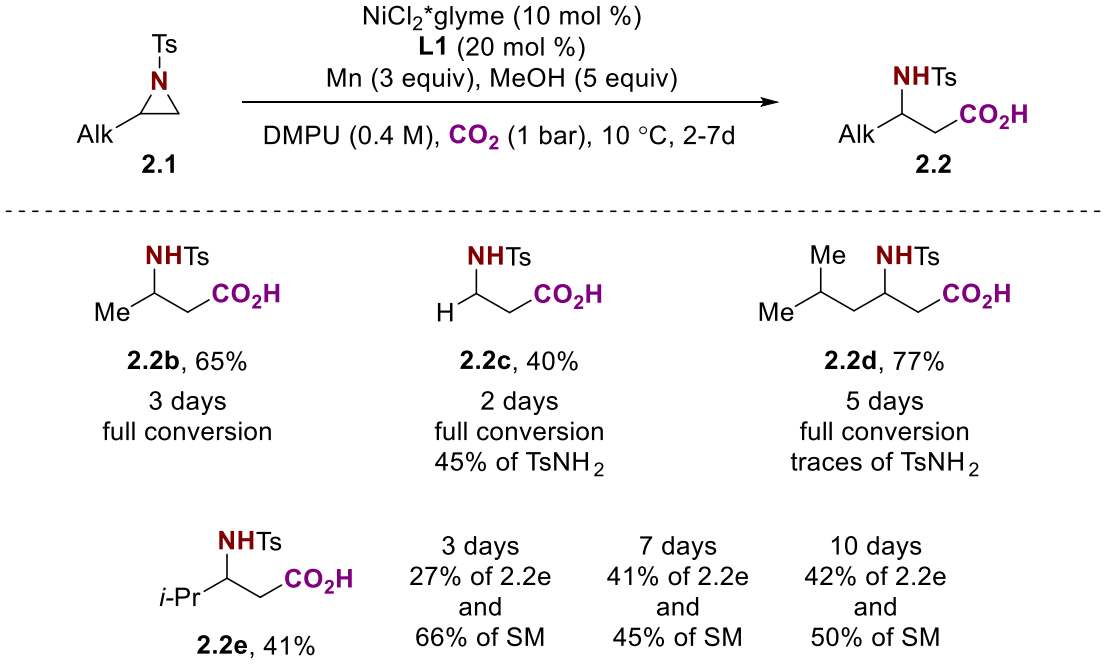

Scheme 2.6 Synthesis of *N*-Tosyl *β*-Glycine, *β*-Alanine, *β*-Valine, and *β*-Leucine

First, *N*-Tosyl *β*-Glycine **2.2b** was obtained as expected with a similar yield as the product **2.2a** delivered from the model substrate (65% vs 71%). However, after unsubstituted aziridine **2.1c** was tested in our conditions we observed a significant drop in the reaction yield of the product **2.2c** (40%) and the formation of a significant amount of $TsNH_2$ (45% by NMR). The aziridine **2.1d** has shown a significantly slower reaction rate (full conversion of **2.1d** achieved after 5 days) but at the same time a high selectivity toward the formation of the desired product **2.2d** over the formation of $TsNH_2$. The most sterically hindered aziridine **2.1e** demonstrated the slowest reaction rate with

a significant amount of SM remaining in the reaction mixture even after 10 days of reaction time (50% of SM by NMR). Any effort to push this result to a full substrate conversion by increasing catalyst or ligand loading, using less hindered ligands or raising the reaction temperature, unfortunately, did not lead to any improvement.

In addition, to demonstrate the synthetic potential of our reaction in the synthesis of *β*–amino acids on the scale larger than milligrams we successfully synthesized *N*-Tosyl *β*-Phenylalanine **2.2f** (62% isolated yield) starting from 1.0 mmol of aziridine **2.1f** (Scheme 2.7).

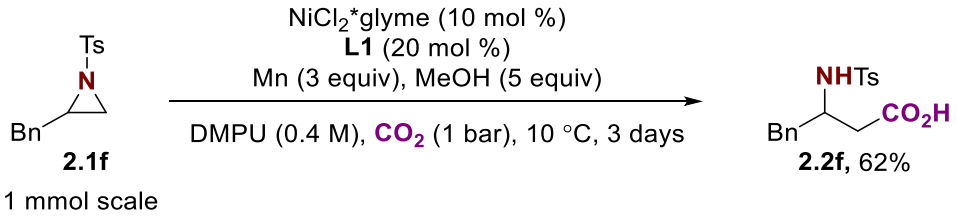

Scheme 2.7 Synthesis of *N*-Tosyl *β*-Phenylalanine **2.2f** from the aziridine **2.1f** on a 1.0 mmol scale

Next, we decided to approach the synthesis of *N*-Tosyl *β*-Tryptophan and *N*-Tosyl *β*-Histidine both possessing heterocyclic moiety in their structure. Luckily, aziridines **2.1g** and **2.1h** could be accessed from commercially available *β* amino alcohols upon cyclization in the presence of TsCl following literature procedures

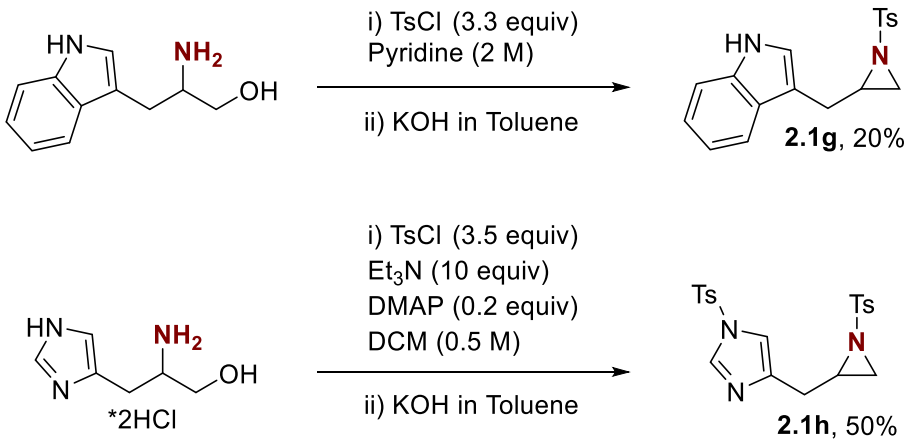

Scheme 2.8 Synthesis of aziridines **2.1g** and **2.1h** from *β*-amino alcohols

We immediately tested them under reaction conditions, however only in case of substrate **2.1g** the formation of the desired product *N*-Tosyl *β*-Tryptophan **2.2g** was achieved (Scheme 2.9).

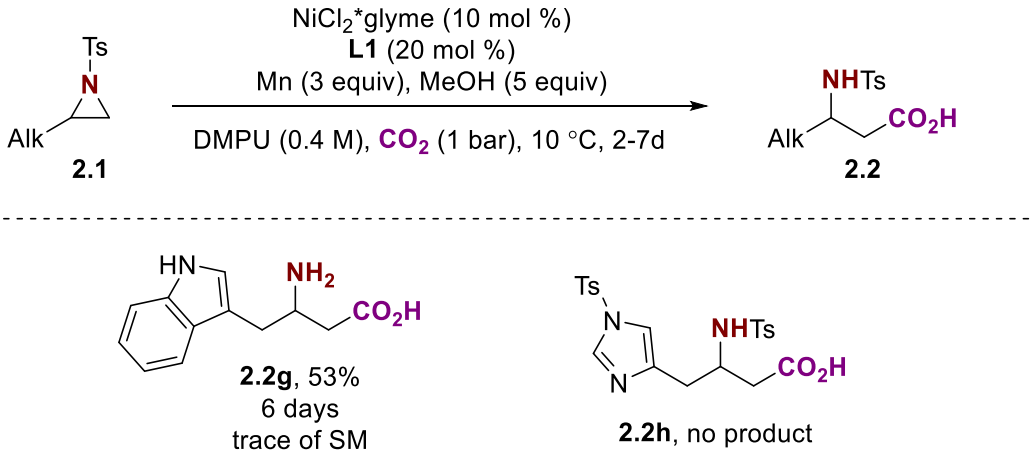

Scheme 2.9 Synthesis of *N*-Tosyl *β*-Tryptophan **2.2g** and *N*-Tosyl *β*-Histidine **2.2h**

The slower reaction time in that case can be explained by the coordination of the free indole nitrogen to the Ni-center, resulting in the inhibition of its catalytic activity.

Elevating further our study we challenged the synthesis of *β*-Tyrosine. However, from initial attempts to synthesize aziridine **2.1i** possessing free phenol –OH group we failed to access the product, following standard procedure with olefin aziridination using commercial reagent Chloramine-T*3H_2O (Scheme 2.10).

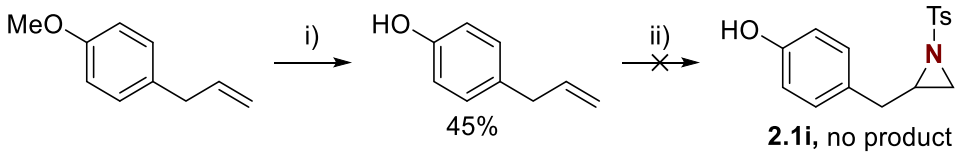

i) BBr_3, DCM, 0 °C; ii) Chloroamine-T*3H_2O, $PhMe_3N^+Br_3^-$ (cat.), RT, MeCN

Scheme 2.10 Synthesis of aziridine **2.1i**

Instead, we decided to approach the synthesis of different *O*-substituted *β*-Tyrosine derivatives. Initially, we intended to synthesize a TBS-protected aziridine **2.1j**, which was found to be unstable upon different standard purification techniques and we switched our attention to other *O*-substituted *β*-Tyrosine derivatives (Scheme 2.11).

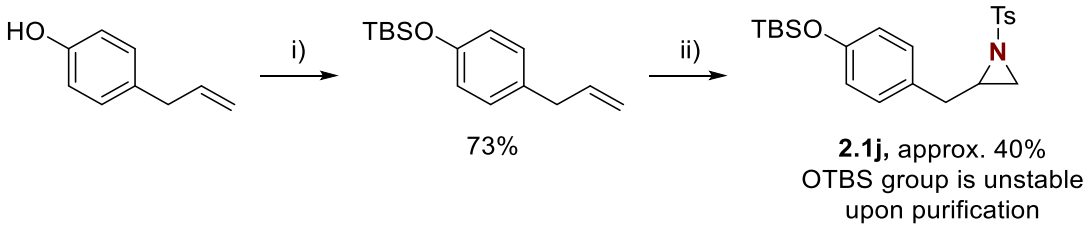

i) TBSCl, imidazole, DCM, 0 °C; ii) Chloroamine-T*3H_2O, $PhMe_3N^+Br_3^-$ (cat.), RT, MeCN

Scheme 2.11 Synthesis of aziridine **2.1j**

Thus, aziridine **2.1k** bearing *O*-methyl substituted phenyl ring gave desired product **2.2k** with good yield (49%) (Scheme 2.12).

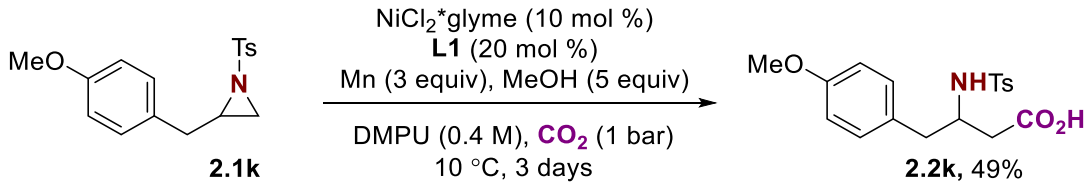

Scheme 2.12 Synthesis of aziridine **2.1j**

Next, we attempted demethylation of acid **2.2k** in the presence of BBr_3 (Scheme 2.13).

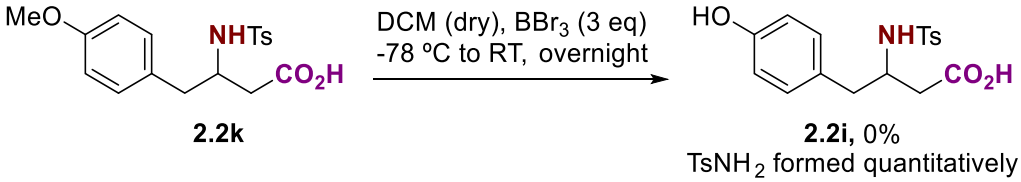

Scheme 2.13 Synthesis of *β*-Tyrosine **2.2i**

Unfortunately, no product formation was achieved. Instead, the $TsNH_2$ formed quantitatively, demonstrating that material **2.2k** is unstable under these conditions.

Finally, upon cyclization of commercially available Tyrosinol in the presence of TsCl, we obtained *O*-Tosyl-protected aziridine **2.1l** (Scheme 2.14).

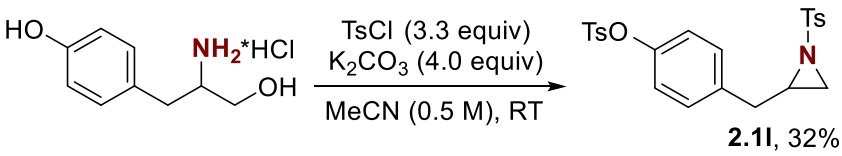

Scheme 2.14 Synthesis of aziridine **2.1l**

After subjecting this aziridine to the optimized reaction conditions we observed the formation of desired acid **2.2l** with moderate yield (41%) (Scheme 2.15).

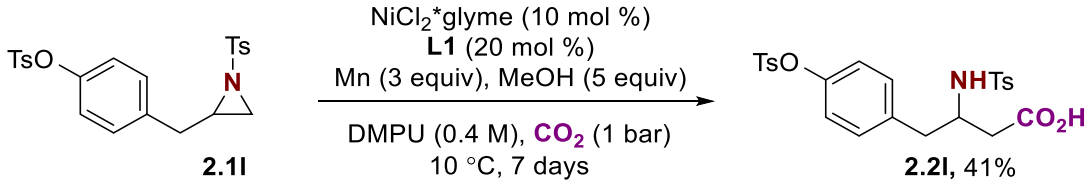

Scheme 2.15 Synthesis of *O*-Tosyl *β*-Tyrosine **2.2l**

The drop in the reaction yield is caused by the formation of multiple trace by-products, which were observed in the crude NMR before the purification step.

Next, we turned our attention to the *β*-Glutamic acid. Corresponding aziridine **2.1m** bearing methyl ester group was easily delivered from the commercial olefin, and the carboxylation procedure gave the desired methyl ester derivative **2.2m** of *β*-Glutamic acid in 53% isolated yield (Scheme 2.16).

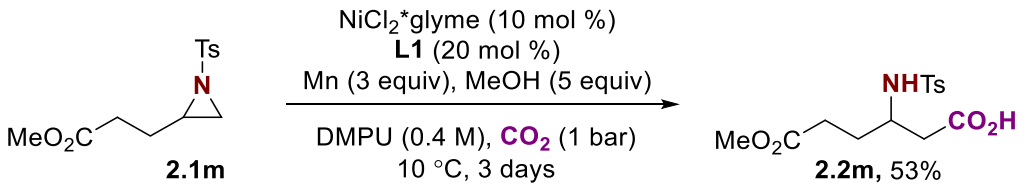

Scheme 2.16 Synthesis of *β*-Glutamic acid methyl ester derivative **2.2m**

Inspired by this result we expected to access *β*-Methionine **2.2n** next easily. Unfortunately for us, the developed catalytic system was found to be sensitive to the presence of sulfur in the low oxidation state, and together with the formation of Ni-black and Ni-mirror of the sides of the reaction flask, no product formation was detected (Scheme 2.17).

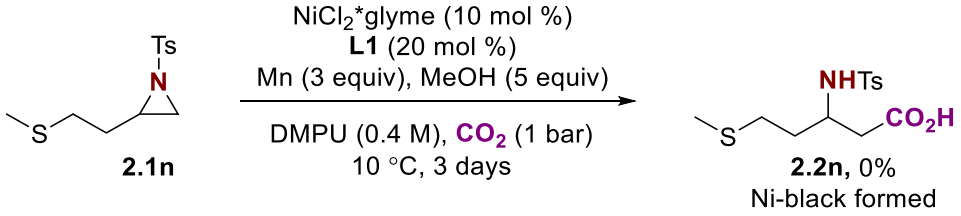

Scheme 2.17 Synthesis of *β*-Methionine **2.2n**

The synthesis of *β*-Serine **2.2o** was initially attempted from aziridine **2.1o** bearing non-protected –OH group and only 10% of the product formed were observed in crude NMR (Scheme 2.18).

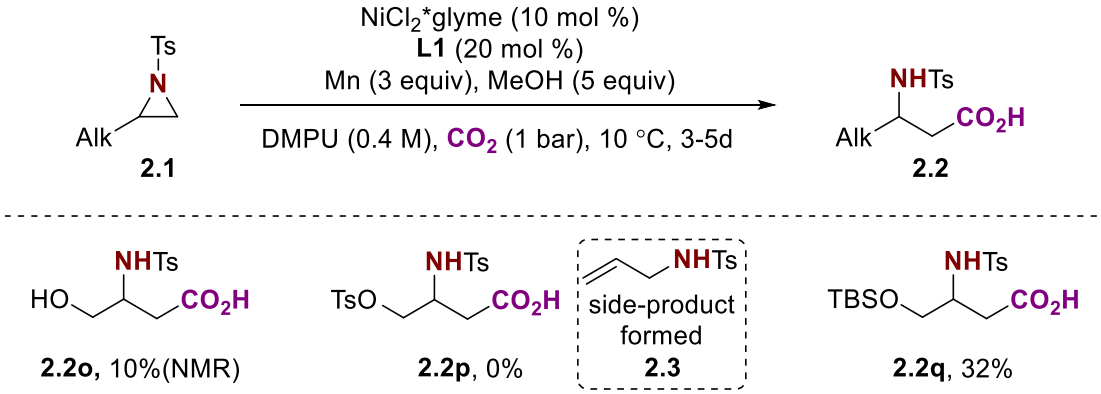

Scheme 2.18 Synthesis of *β*-Serine **2.2o** and *β*-Serine derivatives **2.2p** and **2.2q**

During attempts to achieve carboxylation of *O*-Tosyl protected aziridine **2.1p**, we observed that the reaction is biased towards forming the side-product **2.3** and no product **2.2p** was formed. Luckily, TBS-protected *β*-Serine **2.2q** was achieved with a moderate yield (32%).

For the synthesis of *β*-Lysine **2.2s**, we proposed from the beginning the use of a phthalimide-protecting group, which can give the desired product after the hydrolysis step (Scheme 2.19).

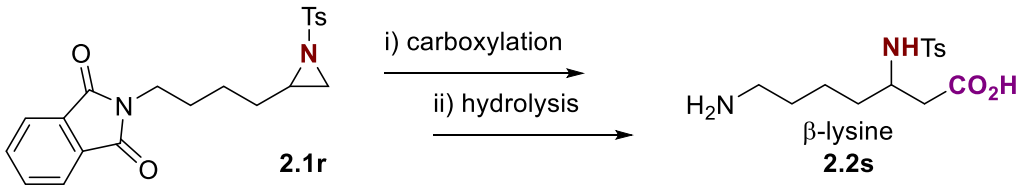

Scheme 2.19 Proposed synthesis of *β*-Lysine **2.2s** using phthalimide protecting group

Following this idea, we successfully synthesized the parent aziridine **2.1r** and subjected the obtained substrate under carboxylation conditions (Scheme 2.20).

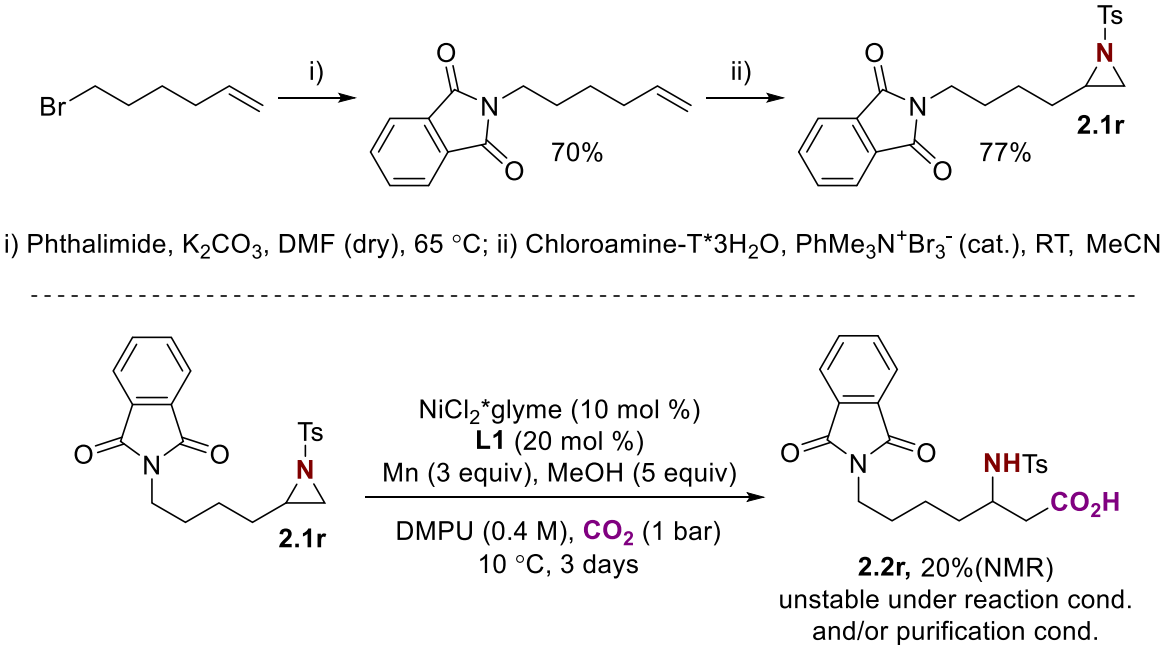

Scheme 2.20 Synthesis of *β*-amino acid **2.2r** bearing phthalimide protecting group

Even though the formation of the desired product **2.2r** was observed in the crude NMR, the number of the yield was unsatisfying (20% by NMR). While trying to purify the product we realized that phthalimide undergoes cleavage under reaction conditions and potentially during reaction workup and product purification, and the pure material was never isolated.

We proposed an alternative strategy by modifying the product with a suitable leaving group for potential amination reaction, instead of giving up on the result. Thus, upon testing aziridine **2.1t**, bearing chlorine atom at the terminal carbon under reaction conditions we obtained acid **2.2t**, showing additionally, that our method tolerates primary alkyl chloride moieties (Scheme 2.21).

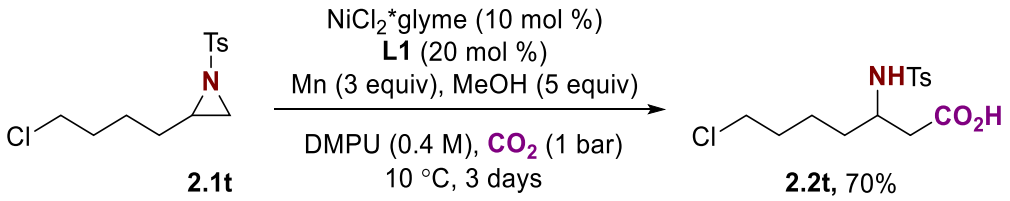

Scheme 2.21 Synthesis of *β*-amino acid **2.2t** bearing chlorine atom

To our triumph, the amination of the material **2.2t** toward the formation of desired *β*-Lysine **2.2s** was achieved by simply treating **2.2t** with NH_4OH excess under reflux (Scheme 2.22).

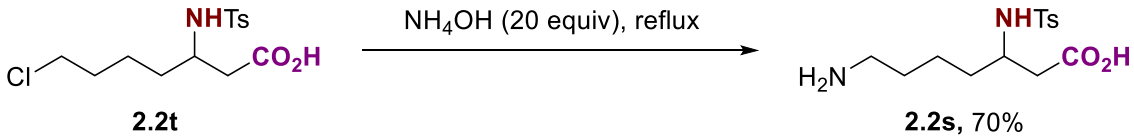

Scheme 2.22 Synthesis of *β*-Lysine **2.2s** from *β*-amino acid **2.2t**

Additionally, we saw another useful post-modification step regarding possible transformations of the product **2.2t**, and by treating it with NaH in DMF we accessed piperidin-2-yl-acetic acid **2.2u** after intramolecular cyclization (Scheme 2.23).

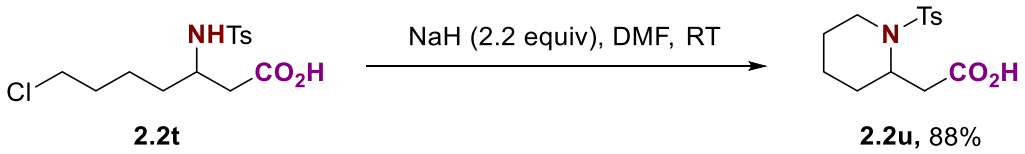

Scheme 2.23 Synthesis of piperidin-2-yl-acetic acid **2.2u** from *β*-amino acid **2.2t**

That was an important result for us, as by shortening the carbon chain in the parent aziridine by one carbon (compared to **2.2t**) we could think of accessing *β*-homoproline **2.2v** in a similar step-wise synthetic manner. Fortunately, the carboxylation of parent aziridine **2.1w** was successfully achieved and the obtained product **2.2w** was cyclized into the desired *β*-homoproline **2.2v** using the same procedure with NaH treatment (Scheme 2.24).

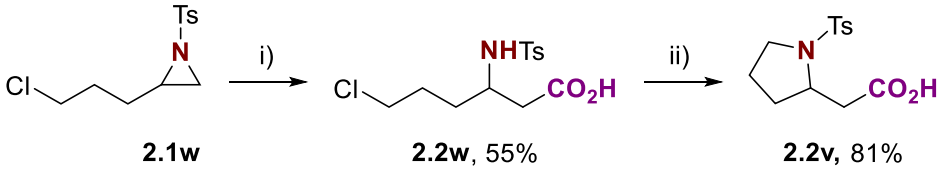

Scheme 2.24 Synthesis of *β*-homoproline **2.2v** from *β*-amino acid **2.2w**

At this point, we finished with the synthesis of natural amino acids homologs following our procedure, as the remaining acids possessed similar structures as products approached for the

synthesis already and their synthesis would not add extra enlightenment to our understanding of reaction limitations and synthetic utility.

Thus, to demonstrate further the synthetic potential of the developed transformation in the following section we moved to the testing of complex aziridines possessing diverse functional moieties under reaction conditions.

2.4.2 Remaining reaction scope, functional group tolerance and other limitations

We continued our study by testing the series of aziridines **2.1x-ab** bearing different substituents in the aromatic ring, placed in the aziridine side-chain (Scheme 2.25).

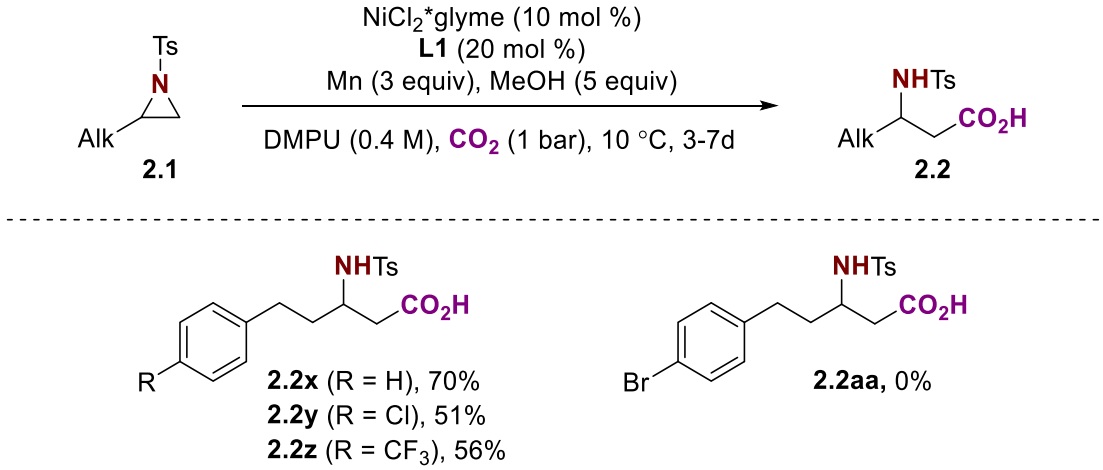

Scheme 2.25 Reaction scope and following studies with aziridines **2.1x-aa**

Whereas carboxylation products bearing *p*-Cl (**2.2y**) and *p*-CF_3 (**2.2z**) were obtained with good yields, no product possessing *p*-Br substituent (**2.2aa**) was formed. The oxidative addition of Ni-center into C-Br bond was found to be faster than insertion into the aziridine C-N bond. Nevertheless, the aziridine **2.1aa** was subjected to Suzuki coupling conditions to access more complex aziridines **2ab-ad** (Scheme 2.26).

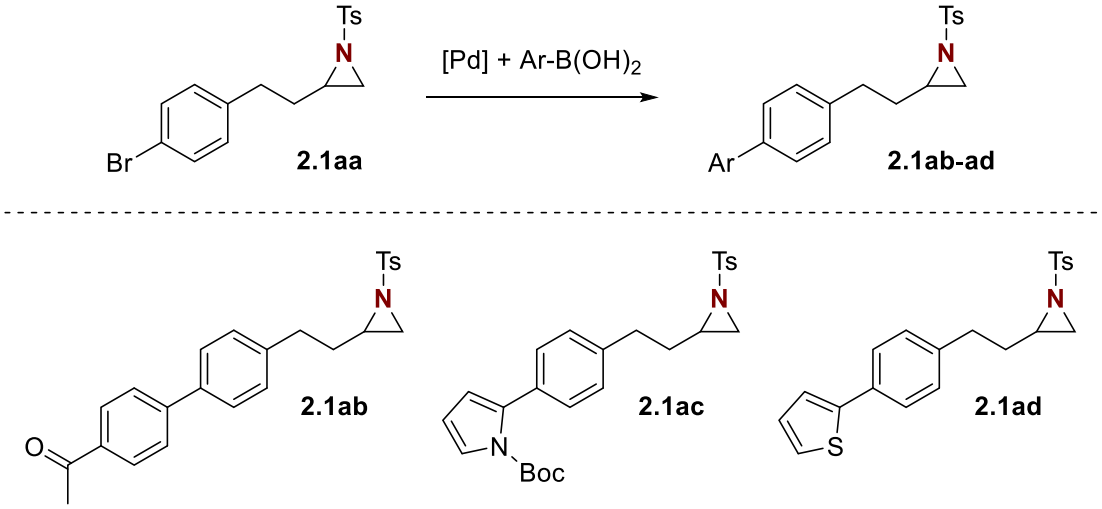

Scheme 2.26 Synthesis of aziridines **2ab-ad** from aziridine **2.1aa**

Once accessing the materials, we tested them under reaction conditions (Scheme 2.27).

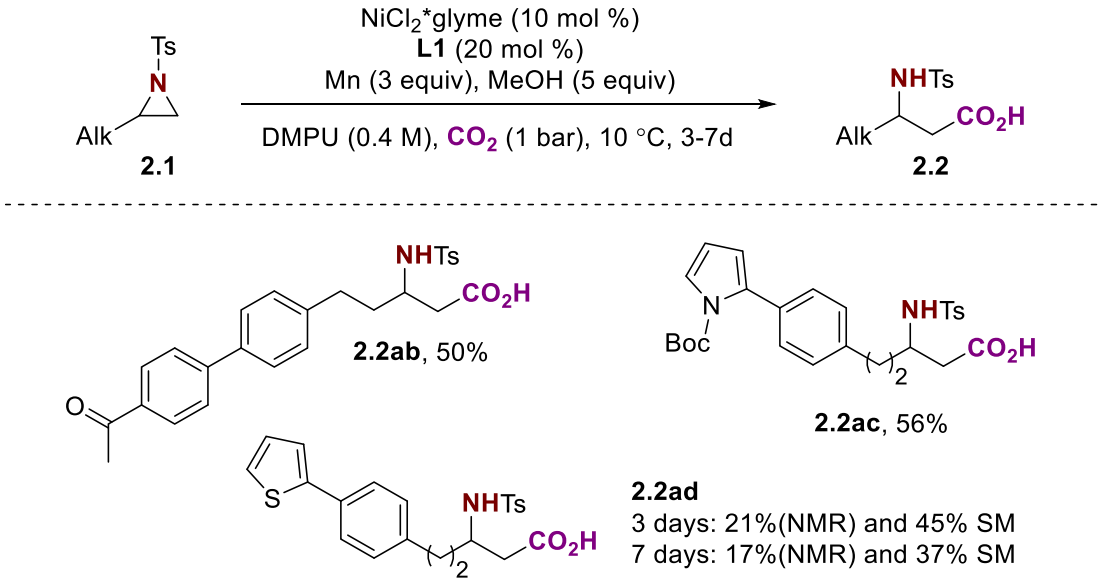

Scheme 2.26 Reaction scope and following studies with aziridines **2.1ab-ad**

Products bearing p-Ac (**2.2ab**) and *N*-Boc pyrrole (**2.2ac**) were obtained in good yields (50% and 56% respectively). The aziridine **2.1ad** bearing thiophene ring demonstrated poor results. With low reaction yield (21% by NMR) and uncompleted conversion of the starting material after the reaction being kept for 3 days under standard conditions, there was no improvement upon prolongation of the reaction time up to 7 days. This result is in agreement with catalyst poisoning observed in the case of *β*-Methionine **2.2n**.

Among different strategies to access complex aziridines for reaction scope studies and demonstrative purposes, the coupling of aromatic carboxylic acids with alcohol moiety was proposed (Scheme 2.27).

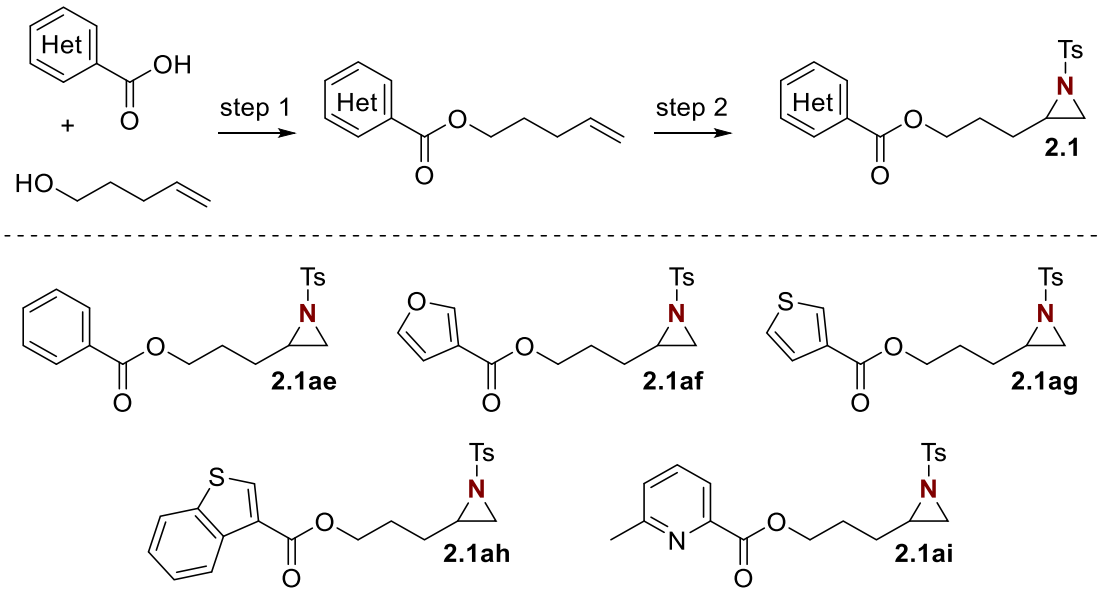

Scheme 2.27 Proposed coupling of aromatic carboxylic acids with alcohol moiety to access aziridines **2.1ae**-**2.1ai** bearing aromatic/heteroaromatic ester group

Following this strategy, we synthesized aziridines **2.1ae-ai** bearing phenyl (**2.1ae**), furan (**2.1af**), thiophene (**2.1ag**), benzothiophene (**2.1ah**), and pyridine (**2.1ai**).

When we tested this series of aziridines under standard conditions products **2.2ae** and **2.2af** were formed with similar good yields (66% and 65% respectively) (Scheme 2.28).

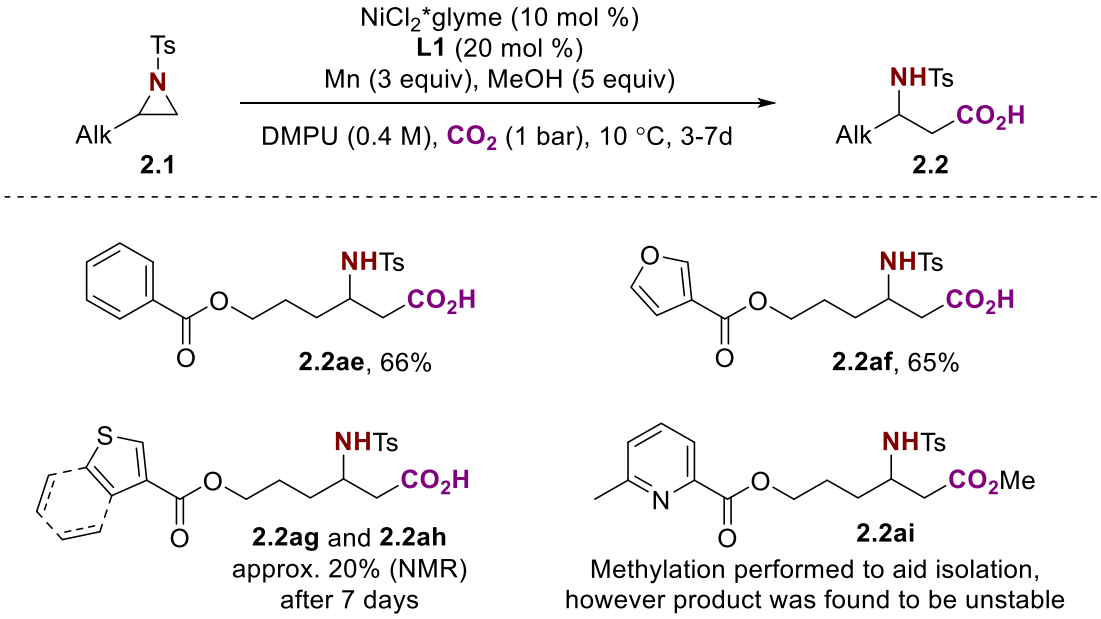

Scheme 2.28 Reaction scope and following studies with aziridines **2.1ae-ai**

A complementary to the product **2.2ad** result was obtained for acids **2.2ag** and **2.2ah** with low yields of desired products and low conversion of starting materials even after 7 days of reaction time. Even though the characteristic signals potentially for the product **2.2ai** were observed in the

crude NMR it was found to be unstable upon purification as some amount of organic material isolated didn't possess a pyridine ring in the structure.

Another strategy we used to access aziridines bearing diverse functional group set was the coupling of different phenols with alkyl bromide moiety (Scheme 2.29).

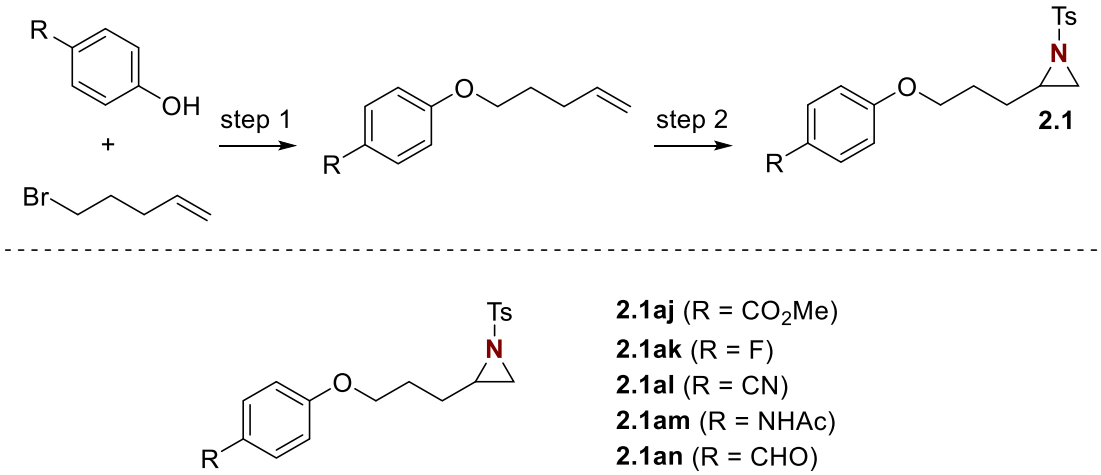

Scheme 2.29 Proposed coupling of phenols with alkyl bromide moiety to access aziridines **2.1aj-2.1an**

After testing these phenol-derived aziridines under standard reaction conditions we observed, in all cases, the formation of desired carboxylation products with yields from low to good (Scheme 2.30).

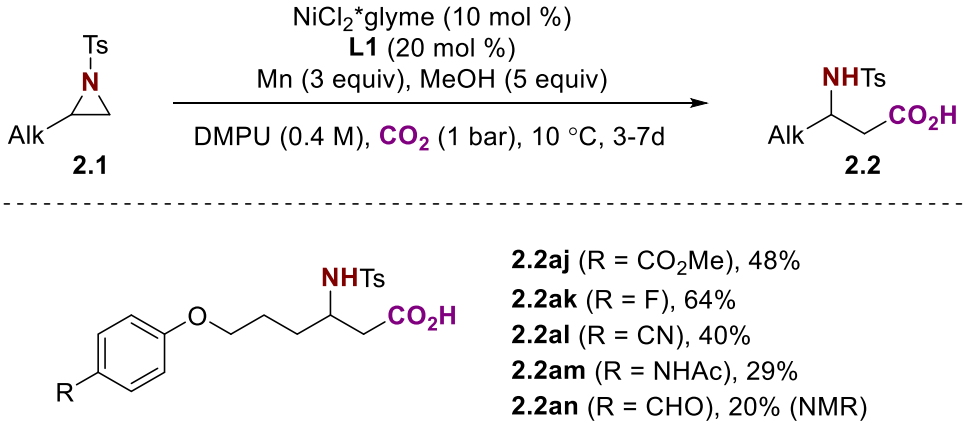

Scheme 2.30 Reaction scope and following studies with aziridines **2.1aj-2.1an**

Moderate yields in all cases are followed by a formation of significant amounts of side-products, especially in case of product **2.2an** (45% of terminal olefin detected in the crude NMR).

Finally, to accomplish our reaction scope studies regarding functional group tolerance we tested under reaction conditions the series of functionalized 2-alkyl aziridines **2.1ao-av** bearing a diverse set of functional groups adjacent to the aliphatic carbon (Scheme 2.31).

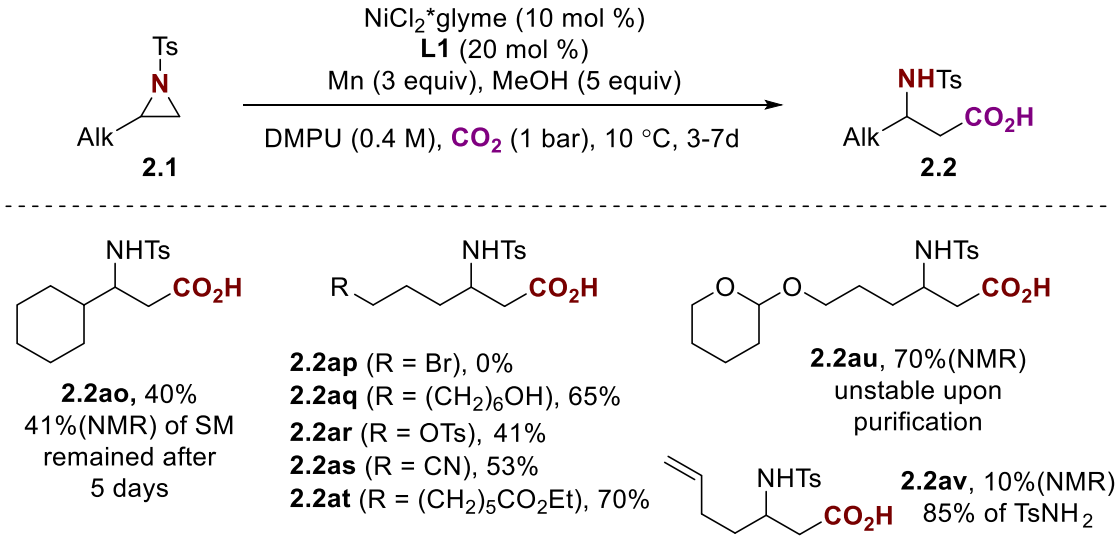

Scheme 2.31 Reaction scope and following studies with aziridines **2.1ao-2.1av**

First, the aziridine **2.1ao** gave the product **2.2ao** with a moderate yield (40%) and a significant amount of SM remaining in the crude mixture was observed. Prolongation of the reaction time didn't improve the reaction outcome and this result was found to agree with the result obtained for the synthesis of *β*-Valine **2.2e**. Next, when aziridine **2.1ap** bearing alkyl bromide moiety was tested under the reaction conditions no product formation was observed as the bromide group was found to be highly reactive in the presence of Ni-catalyst. Interestingly, when either the free alcohol group (aziridine **2.1aq**) or *O*-Tosyl group (aziridine **2.1ar**) were placed far from the actual reactive center (compared to aziridines **2.1o** and **2.1p**), corresponding carboxylation products **2.2aq** and **2.2ar** were successfully formed. Some functional groups like –CN (**2.2as**), alkyl ester (**2.2at**), and acetal (**2.2au**) also were demonstrated to be tolerant to the reaction conditions. However, the product **2.2au** was unstable under purification conditions and was not isolated. Finally, terminal olefin placed in the alkyl chain of aziridine **2.1av** accelerated *β*-H elimination event, and an 85% yield of $TsNH_2$ was observed with only a 10% yield of the desired product **2.2av** according to the crude NMR.

To demonstrate further the synthetic utility of our transformation of aziridines using CO_2 we decided to perform a labelling synthesis using ^{13}C labeled $^{13}CO_2$. As a carboxylation object, we chose to achieve from parent aziridine **2.1aw** pharmaceutically-relevant methylenedioxy-protected *β*-Homo-DOPA precursor **2.2aw** (Scheme 2.32).

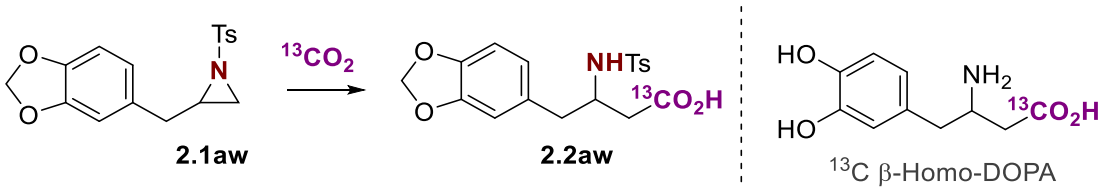

Scheme 2.32 Proposed synthesis of ^{13}C labeled *β*-Homo-DOPA precursor **2.2aw** from parent aziridine **2.1aw**

First, the starting material **2.1aw** was synthesized in 2 steps (Scheme 2.33).

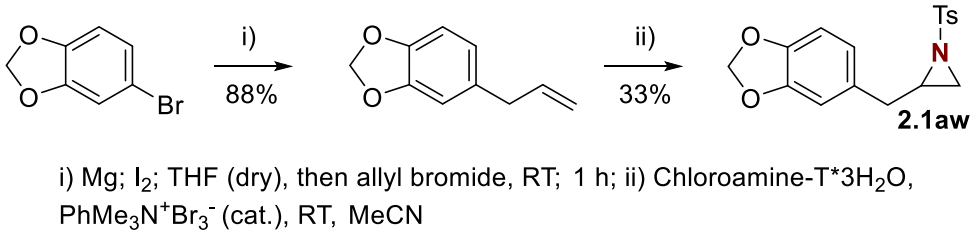

Scheme 2.33 Synthesis of *β*-Homo-DOPA parent aziridine **2.1aw**

Next, we tested the obtained aziridine first under standard conditions with CO_2. After achieving the desired product with 64% isolated yield we repeated the synthesis using $^{13}CO_2$ and obtained ^{13}C labelled *β*-Homo-DOPA precursor **2.2aw** with 62% isolated yield (Scheme 2.34).

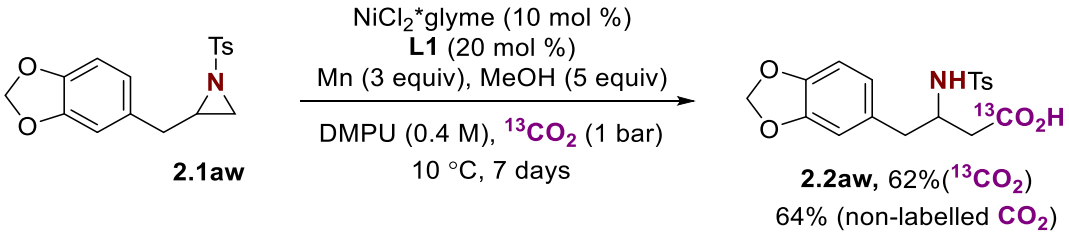

Scheme 2.34 Synthesis of ^{13}C labeled *β*-Homo-DOPA precursor **2.2aw**

Inspired by this result we decided to approach, using our carboxylation procedure, the synthesis of another pharmaceutically-relevant molecule possessing *β*-amino acid structural moiety – the so-called commercial drug *Sitagliptin* **2.4** (Scheme 2.35).

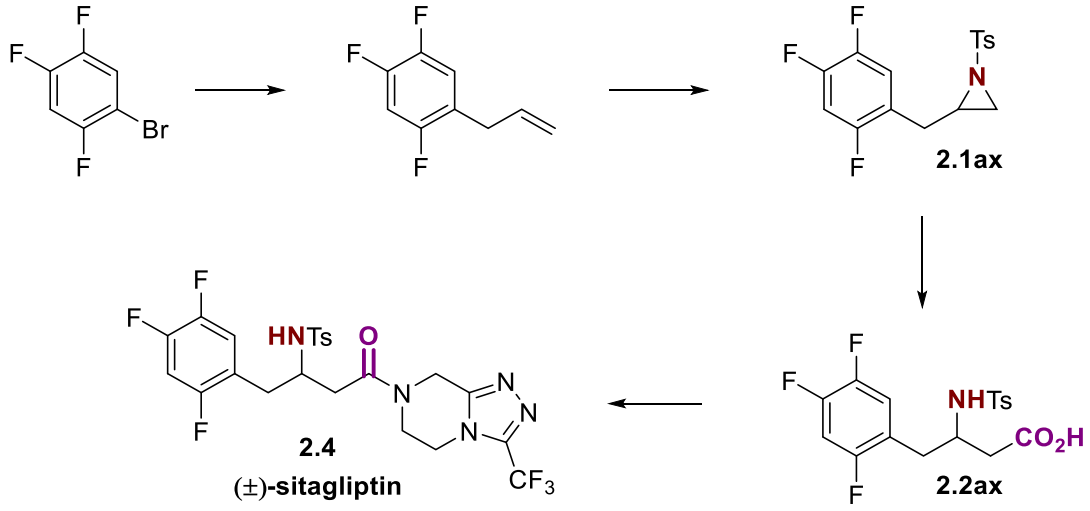

Scheme 2.35 Proposed synthesis of commercial drug Sitagliptin **2.4**

Thus, the synthesis of parent aziridine **2.1ax** was approached in 2 steps using Evans aziridination procedure for the formation of aziridine ring (Scheme 2.36)

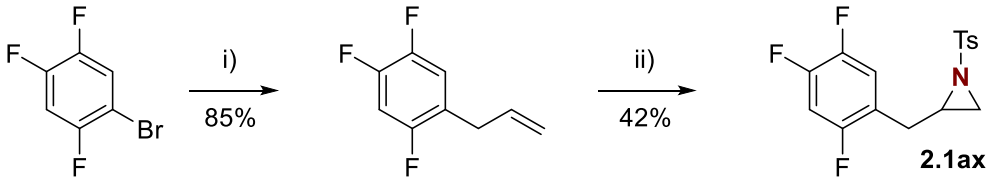

i) *i*-PrMgCl*LiCl (sol. in THF), then allyl bromide, –10 °C; ii) TsNIPh (1.0 equiv), $Cu(OTf)_2$ (20 mol %), MeCN (dry)

Scheme 2.36 Synthesis of Sitagliptin parent aziridine **2.1ax**

After subjecting the obtained aziridine **2.1ax** under standard reaction conditions we obtained the Sitagliptin parent *β*-amino acid **2.2ax** with 38% yield (Scheme 2.37).

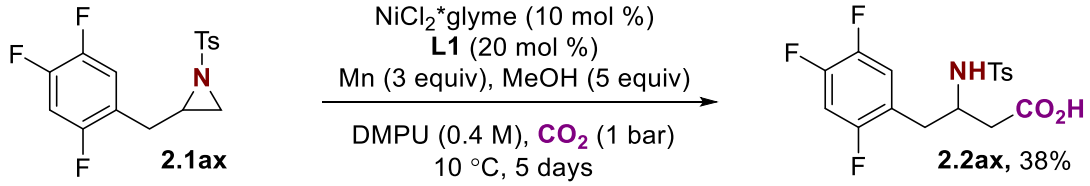

Scheme 2.36 Synthesis of Sitagliptin parent *β*-amino acid **2.2ax**

With the compound **2.2ax** in hand, we synthesized the desired molecule **2.4** by forming the amide bond in the presence of EDC*HCl (Scheme 2.37).

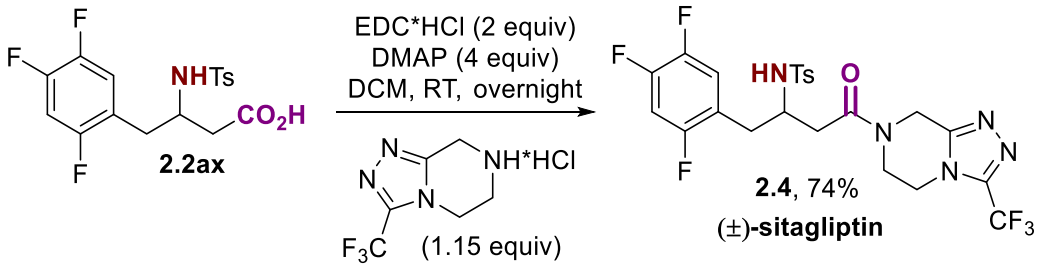

Scheme 2.37 Synthesis of Sitagliptin **2.4** from parent *β*-amino acid **2.2ax**

Expecting the electronic effect of a substituent in the *N*-sulfonyl group to affect the carboxylation event by influencing the strength of C-N aziridine bonds we tested the series of aziridines bearing different *N*-sulfonyl groups starting from strong electron-donating to the strong electron-withdrawing (Scheme 2.38).

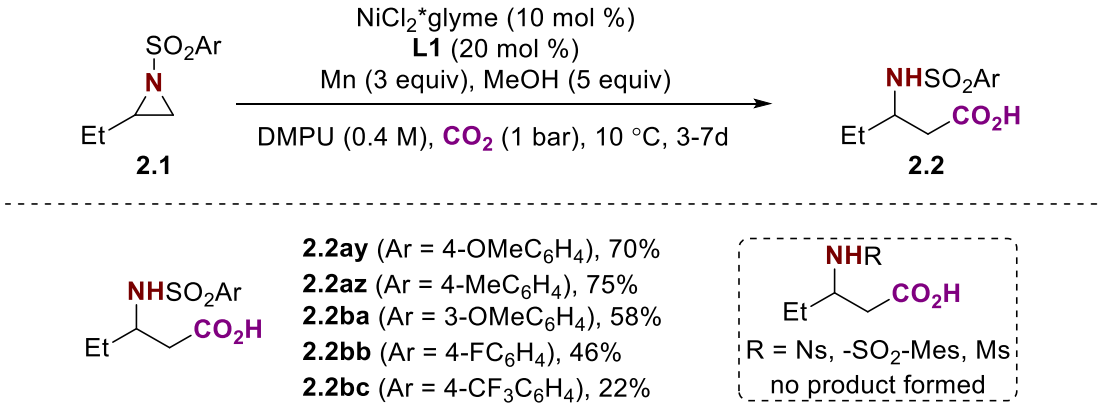

Scheme 2.38 Reaction scope and following studies with aziridines **2.1ay**-**2.1bc**

Thus, we observed the trend of the reaction yield dropping in the series of aziridines **2.1ay**-**2.1bc** upon increasing the electron-accepting properties of the substituent. No product formation was observed for the substrate bearing highly activated Nosyl group. This result, however, might be caused not only by the increased instability of the reaction intermediates toward the direction of the desired product formation, but also by a high reactivity if $-NO_2$ group in the presence of Mn reductant and Ni-center.[110] The sterically hindered sulfonyl group with mesityl substituent also did not lead to the formation of the desired acid. Surprisingly, the negative result regarding the desired product formation was observed for Mesyl-protected aziridine.

After completing the reaction scope study for 2-alkyl substituted aziridines **2.1**, we decided to explore the reaction of aziridines with other substitution patterns. We started by testing the reaction conditions on a styrene-derived aziridine **2.5** (Scheme 2.39).

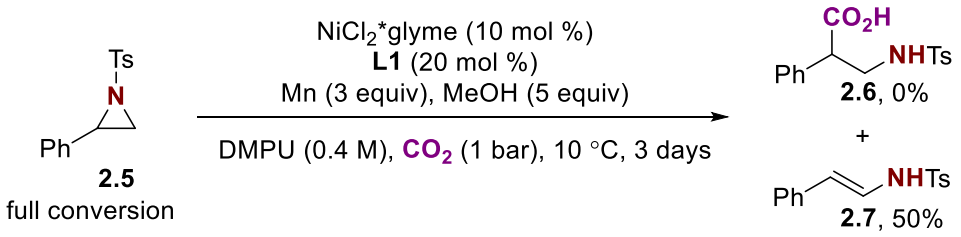

Scheme 2.39 Carboxylation attempt for the styrene-derived aziridine **2.5**

Within a full conversion of the starting material there was no formation of the desired product **2.6**; instead, the enamine **2.7** was formed due to a *β*-H elimination side reaction.

We tested next a series of 2,3-dialkyl substituted aziridines **2.8** (Scheme 2.40).

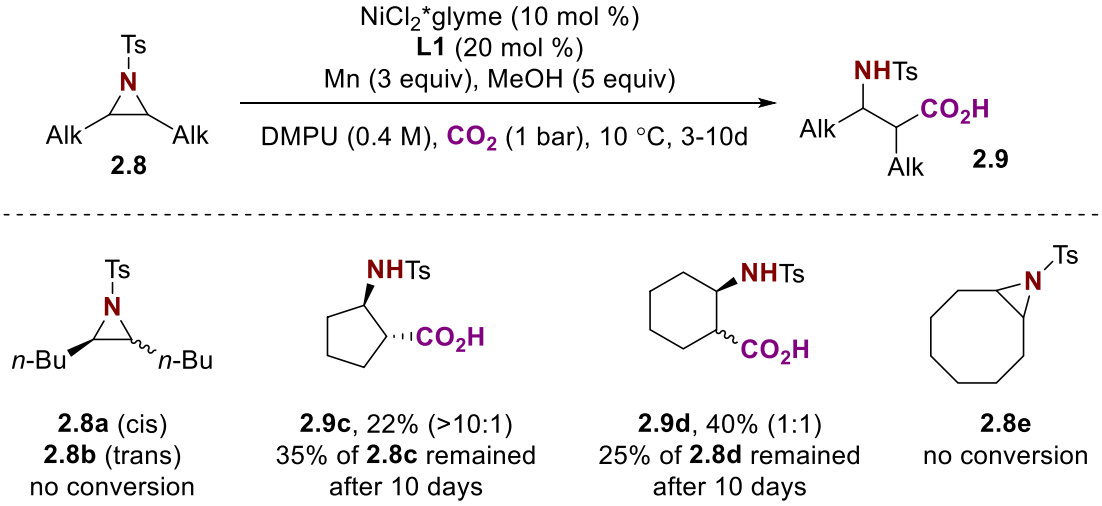

Scheme 2.40 Reaction scope and following studies with aziridines **2.8a-2.8e**

Non-fused aziridines **2.8a** and **2.8b** were inert under optimized reaction conditions and no conversion of aziridines was observed. In contrast, upon testing a series of fused aziridines starting from the substrate **2.8c** a formation of the desired acid **2.9c** was observed with low yield (22%) and as a mixture of diastereomers (dr = >10:1). The reaction rate was significantly slower compared to monosubstituted aziridines **2.1** and significant amounts of starting material **2.8c** remained in the reaction mixture even after 10 days of the reaction time. When the size of the fused carbon ring was increased by one carbon in the case of aziridine **2.8d** we observed a significant improvement in the reaction yield of **2.9d** (40%) but with a significant drop in the diastereomers ratio (dr = 1:1). While expecting the reaction rate to increase even more by increasing further the size of the fused carbon ring due to an increase in the substrate conformational flexibility we tested aziridine **2.8e** fused with a cyclooctane ring under reaction conditions. To our surprise, the opposite effect was achieved and no conversion of starting material was observed.

Finally, we tested a series of 2,2-dialkyl aziridines **2.10** under reaction conditions (Scheme 2.41).

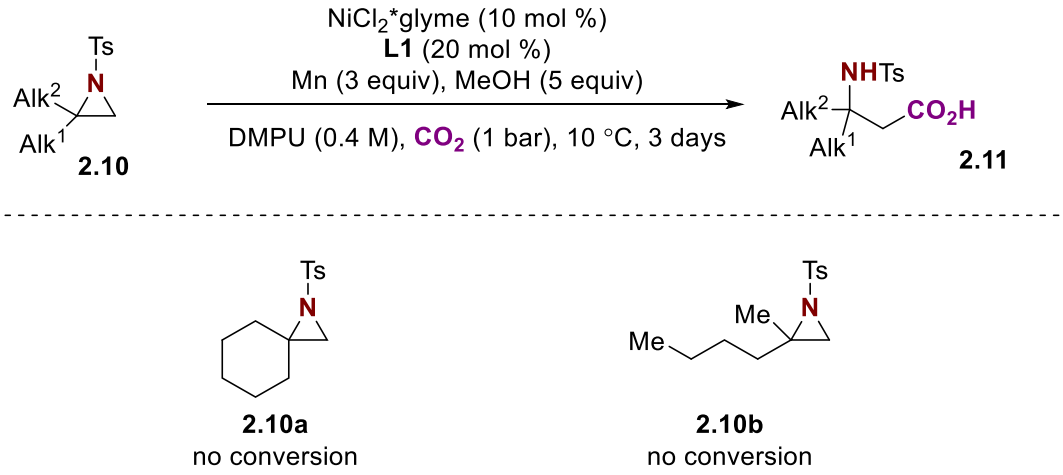

Scheme 2.41 Reaction scope and following studies with aziridines **2.10a** and **2.10b**

In both cases for spiro-aziridine **2.10a** and 2-methyl, 2-*n*-butyl-aziridine **2.10b** we observed the complete lack of reactivity due to the inertness of these aziridines toward the oxidative addition of Ni-center resulted in the complete lack of aziridines conversion.

To conclude our studies of the reaction scope it is worth mentioning that a homolog of aziridine – the so-called *azetidine* (saturated 4-membered nitrogen heterocycle) **2.12** was also tested under reaction conditions (Scheme 2.42).

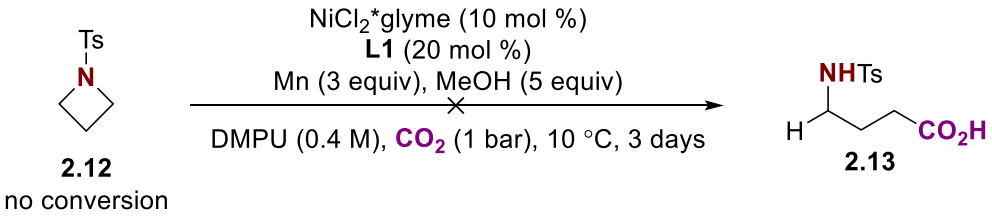

Scheme 2.42 Carboxylation attempt of azetidine **2.12**

Even though the azetidine ring is known to possess relatively similar ring-strain energy compared to aziridine (25.2 kcal/mol vs 26.7 kcal/mol),[16] the substrate **2.12** was completely inert under optimized reaction conditions and no conversion of the starting material was observed.

2.5 Control experiments

A series of control experiments were conducted to elucidate some mechanistic aspects of studied transformation prior a detailed mechanism studies.

First, for better understanding of side-reactions occurring in the catalytic system aziridine **2.1x** was tested under reaction conditions in the absence of CO_2 atmosphere (Scheme 2.43)

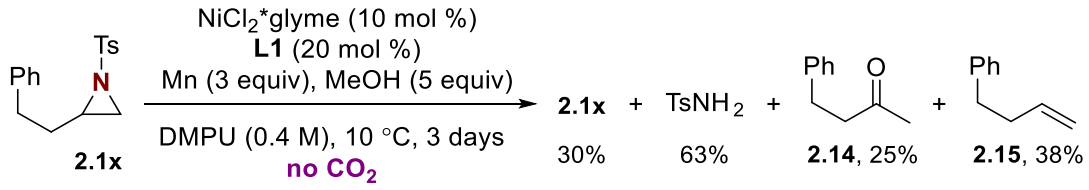

Scheme 2.43 Formation of side-products from aziridine **2.1x** in the absence of CO_2 atmosphere

Upon careful analysis of the crude reaction mixture the following compounds were identified: 30% of starting material **2.1x** remained; 63% of $TsNH_2$ formed; 25% of ketone **2.14**; 38% of olefin **2.15**. It can be easily noticed that the yield of $TsNH_2$ (63%) is equal to the combined yield of ketone **2.14** (25%) and olefin **2.15** (38%). Formation of $TsNH_2$ and ketone mixture after hydrolysis of parent ketimine formed as a by-product of *β*-H elimination step is widely discussed in literature (e.g. see Chapter 1, Scheme 1.14). However, formation of $TsNH_2$ and olefin mixture is unprecedented in literature regarding transformations with aziridines. This result was rationalized by proposed *β*-deamination side-reaction and discussed with more details in Chapter 4.

Next, it was assumed that the carboxylation event might occur via nucleophilic addition of in situ generated metalla-enamines onto CO_2. To probe this possibility, enantiopure (*S*)-**2.1f** was submitted to the reaction conditions and (*S*)-**2.2f** was isolated with complete preservation of the chiral integrity at the sp^3 C–N site (Scheme 2.44).

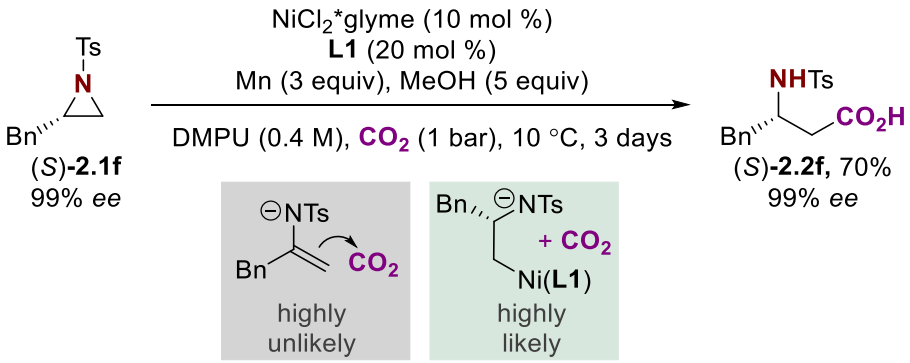

Scheme 2.44 Synthesis of enantiopure product (*S*)-**2.2f** from enantiopure aziridine (*S*)-**2.1f**

Therefore, it is highly unlikely that the reaction proceeds via the formation of an enamine intermediate. The insertion of CO_2 into the C-Ni bond, likely in oxidation state I, remained as a main working hypothesis and discussed in more details in Chapter 4.

Finally, the experiment with deuterium-labeled aziridine **2.1a-*d*$_1$** was conducted for studying the stereochemical course of the reaction and potential Ni-C(methylene) bond erosion events (Scheme 2.45).

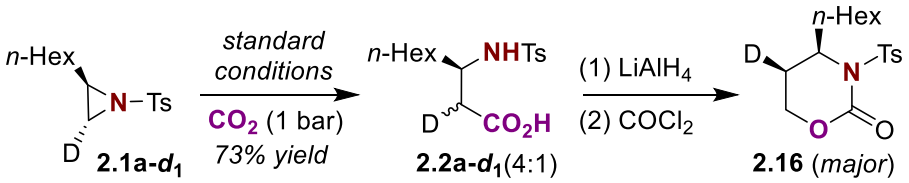

Scheme 2.45 Stereochemical course of the reaction via isotope-labelling

It was found that the carboxylation of *trans* **2.1a-*d*$_1$** followed by reduction and a cyclization events resulted in **2.16** with a 4:1 *cis/trans* ratio. It was possible that the product **2.2a-*d*$_1$** could isomerize under the reaction conditions so it was resubmitted to the standard reaction conditions in place of the aziridine. However, no change in the *cis/trans* ratio was observed. The formation of identified major product *cis*-**2.16** might be explained following Hillhouse mechanism through an S_N2-type insertion of Ni(0) into the aziridine backbone. However, the presence of the trans isomer, together with the lack of diastereocontrol in formation of **2.9c** and **2.9d** suggests that other conceivable pathways might come into play. Specifically, (1) single-electron transfer type oxidative addition or (2) homolytic cleavage/recombination events of Ni-intermediates.

2.6 Chapter conclusions

- A novel methodology for Ni-catalyzed reductive carboxylation of aziridines was developed
- Initially the formation of *β*-amino acids was achieved upon the addition of alcohols to the reaction media
- Optimal reaction yield was achieved through systematic ligand screening. It was demonstrated that the use of sterically hindered *phen* or *bipy* ligands is crucial for the formation of the desired product
- The reaction was found to be sensitive regarding the steric effect of substituent in the aziridine ring. The reaction rate was observed to get slower for aziridines bearing bulkier substituents
- The reaction was found to be sensitive to the presence of functional groups capable of coordination with the Ni-center. Placed close to the aziridine ring these FG either lead to catalyst inhibition or favor the formation of side-products. In some cases reactivity is recovered when FG is placed far from the aziridine ring.
- Diverse range of functional groups were found to be tolerant under reaction conditions demonstrating a high synthetic potential of the developed transformation
- The stereochemical course of the reaction was studied and reaction was found to be applicable for the synthesis of enantiopure *β*-amino acids from enantiopure aziridines

2.7 Experimental section

2.7.1 General remarks

Reagents. Commercially available materials were used as received without further purification. $NiCl_2$glyme (98% purity), Manganese powder (≥99.9 trace metal basis), DMPU (H_2O ≤0.03%), Chloramine T trihydrate and Trimethylphenylammonium tribromide were purchased from Aldrich. 6,6'-dimethyl-2,2'-bipyridine was purchased from Fluorochem. 4-Toluenesulfonyl chloride, anhydrous MeOH (99.8% purity), anhydrous *N, N*-Dimethylacetamide (99.5% purity) and anhydrous *N, N*-Dimethylacetamide (99.5% purity) were purchased from Acros.

Analytical methods. ^{1}H, ^{13}C NMR and ^{19}F spectra were recorded on Bruker 300 MHz, Bruker 400 MHz and Bruker 500 MHz at 20 °C. All ^{1}H NMR spectra are reported in parts per million (ppm) downfield of TMS and were calibrated using the residual solvent peak of $CHCl_3$ (7.26 ppm), unless otherwise indicated. All ^{13}C NMR spectra are reported in ppm relative to TMS, were calibrated using the signal of $CDCl_3$ (77.16 ppm). Coupling constants, *J*, are reported in Hertz. Melting points were measured using open glass capillaries in a Büchi B540 apparatus. Flash chromatography was performed with EM Science silica gel 60 (230-400 mesh). Thin layer chromatography was used to monitor reaction progress and analyze fractions from column chromatography. To this purpose, TLC Silica gel 60 F254 aluminium sheets from Merck were used and visualization was achieved using UV irradiation and/or staining with $KMnO_4$ or Bromocresol green solution.

2.7.2 Optimization of reaction conditions

General procedure for the optimization of **2.2a** *from aziridine* **2.1a**:

To an oven dried Schlenk tube in the glove box was added Ni(II) pre-catalyst, ligand and manganese (Mn). A stirrer bar was added and the Schlenk was capped before being removed from the glove box. An atmosphere of CO_2 was then generated by 3 cycles between vacuum (<1 mbar pressure) and CO_2 line (1 atm). Under a flow of CO_2, dry DMPU (or other solvent) was added followed by 1a (52 µl, 1 equiv. 0.2 mmol) and finally MeOH (or other alcohol). Note/ between each addition, the Schlenk tube was agitated for ~10 s to ensure the components were well dissolved. The Schlenk tube was then tightly capped and stirred at 10 °C (or other specified temperature) for the noted time. The reaction was quenched by careful addition of HCl (1.0 M, 2.0 ml) at 10 °C, diluted with EtOAc and then stirred at RT. Trimethoxybenzene (11 mg, 0.33 equiv.) internal standard was added as a stock solution in EtOAc, the layers were separated and the aqueous layer was extracted with EtOAc (3 × 5.0 ml). The combined organic layers were then washed twice with HCl (1.0 M, 15 ml), dried ($MgSO_4$), filtered and concentrated *in vacuo*. Quantification was carried out by integration of ^{1}H NMR against the TMB internal standard.

2.7.3 Synthesis of L1 and $LNiCl_2$ complexes

L3 (HETCAT) and **L5** (Aldrich) are commercially available and were used as received. **L2**,[111] **L4**,[112] **L5NiCl$_2$**[113] and **L5$_2$Ni**[114] were present in-house having been synthesized according to the described procedures.

Synthesis of 4,4'-dimethoxy-6,6'-dimethyl-2,2'-bipyridine (L1)

This ligand can be accessed via two routes depending on the quantity required. For synthesis of small quantities, a reductive cross-coupling of 2-chloro-4-methoxy-6-methylpyridine can be carried out.[115] The low efficiency of this reaction and the high cost of the starting pyridine precursor, however, meant an alternative route was selected for gram scale synthesis.

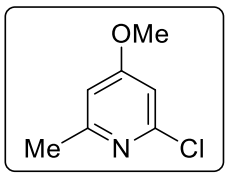

2-Chloro-4-methoxy-6-methylpyridine: To 2,6-chloro-4-methoxy-pyridine (1.0 g, 5.6 mmol) and $Fe(acac)_3$ (0.10 g, 0.28 mmol, 0.05 equiv.) in THF: NMP (25 ml: 6 ml) at 0 °C was added MeMgBr (3 M in Et_2O, 2.4 ml., 7.3 mmol) drop wise. The reaction was stirred for 30 minutes at this temperature before being quenched with NH_4Cl (sat.). The mixture was diluted with H_2O and extracted with EtOAc (3 × 25 ml). The combined organic layers were then washed with NaCl (sat.), dried ($MgSO_4$), filtered and reduced *in vacuo* to give 2-chloro-4-methoxy-6-methylpyridine (0.78 g, 88%) which was used in the next step without further purification. ^{1}H NMR (300 MHz, $CDCl_3$) δ 6.66 (d, *J* = 1.9 Hz, 1H), 6.59 (d, *J* = 2.1 Hz, 1H), 3.82 (s, 3H), 2.46 (s, 2H) ppm. ^{13}C NMR (101 MHz, $CDCl_3$) δ 167.7, 160.2, 151.7, 108.9, 106.8, 55.6, 24.5 ppm.

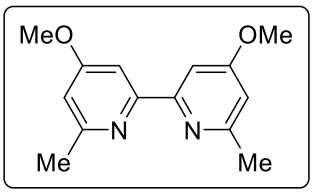

4,4'-Dimethoxy-6,6'-dimethyl-2,2'-bipyridine (L1): Following a modified literature procedure,[115] $Ni(PPh_3)_2Cl_2$ (0.65 g, 1.0 mmol, 0.20 equiv.), Zn powder (0.55 g, 8.4 mmol, 1.7 equiv.) and Bu_4NI (1.8 g, 4.9 mmol, 1.0 equiv.) were stirred in THF (0.25 M, 20 ml) for 30 minutes at room temperature. 2-chloro-4-methoxy-6-methylpyridine (0.78 g, 4.9 mmol) was then added as a solution in THF (20 ml) and the mixture was heated to 50 °C for 20 h. After allowing to cool to room temperature, the reaction mixture was poured into 2 M aqueous NH_3 solution (170 ml) and CH_2Cl_2 (280 ml) and stirred for 30 minutes. The resultant precipitate was removed by filtration, the phases were separated and the organic layer was dried ($MgSO_4$), filtered and reduced *in vacuo*. Purification by column chromatography (EtOAc) gave **L1** (0.30 g, 50%) as a white solid. ^{1}H NMR (400 MHz, $CDCl_3$) δ 7.79 (d, *J* = 2.4 Hz, 2H), 6.69 (d, *J* = 2.4 Hz, 2H), 3.93 (s, 6H), 2.58 (s, 6H) ppm. ^{13}C NMR (101 MHz, $CDCl_3$) δ 167.1, 159.3, 157.5, 109.9, 104.3, 55.4, 24.7 ppm. Spectroscopic data matched those previously reported in the literature.[116]

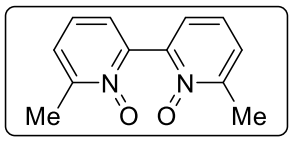

6,6'-Dimethyl-[2,2'-bipyridine] 1,1'-dioxide: Following literature procedure,[117] to 6,6'-dimethyl-2,2'-bipyridine (6.0 g, 33 mmol) in $CHCl_3$ (0.50 M) was added mCPBA (15 g, 2.6 equiv., 85 mmol) as a solution in $CHCl_3$. The use of excess mCPBA ensured compete consumption of the intermediate mono-*N*-oxide. After stirring for 48 h, the solvent was evaporated and the crude purified by flash chromatography (hexane:EtOAc) gave 6,6'-dimethyl-[2,2'-bipyridine] 1,1'-dioxide (4.4 g, 62%) as a white solid. ^{1}H NMR (400 MHz, $CDCl_3$) δ 7.42 – 7.34 (m, 4H), 7.29 – 7.21 (m, 2H), 2.58 (s, 6H) ppm. Spectroscopic data matched those previously reported in the literature.[118]

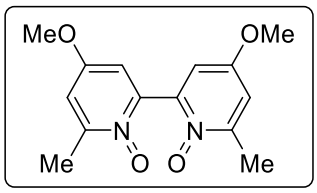

4,4'-Dimethoxy-6,6'-dimethyl-[2,2'-bipyridine] 1,1'-dioxide: Following literature procedure adapted to our substrate,[119] to 6,6'-dimethyl-4,4'-dinitro-[2,2'-bipyridine] 1,1'-dioxide (5.8 g, 19 mmol) dissolved in dry MeOH (190 ml) was added NaOMe (25% solution in MeOH, 3.5 equiv., 15 ml) drop wise. The mixture was then heated to 80 °C for 90 minutes. After allowing to cool to room temperature, the solution was neutralized with HCl (conc.) and the precipitate filtered off. The collected filtrate was concentrated *in vacuo* giving 4,4'-dimethoxy-6,6'-dimethyl-[2,2'-bipyridine] 1,1'-dioxide (4.1 g, 79%) as an orange solid which was used without and further purification.^{1}H NMR (400 MHz, $CDCl_3$) δ 6.93 (d, *J* = 3.5 Hz, 2H), 6.88 (d, *J* = 3.4 Hz, 2H), 3.83 (s, 6H), 2.54 (s, 6H) ppm. Spectroscopic data matched those previously reported in the literature.[116]

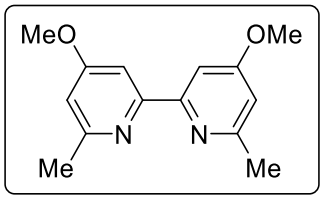

4,4'-Dimethoxy-6,6'-dimethyl-2,2'-bipyridine (L1): Following literature procedure,[119] to 4,4'-dimethoxy-6,6'-dimethyl-[2,2'-bipyridine] 1,1'-dioxide (4.1 g, 15 mmol)) dissolved in dry $CHCl_3$ was added PCl_3 (26.0 ml, 20.0 equiv.) drop-wise before being heated to reflux for 3 h. After allowing to cool to room temperature, the reaction mixture was poured onto ice (~500 g) and the chloroform was removed in vacuo. The resultant aqueous solution was basified with solid NaOH until pH~10 and then extracted with $CHCl_3$ (4 x 200 ml). The collected organic layers were dried ($MgSO_4$), filtered and evaporated. The resultant pale brown solid was carefully washed with cold EtOH to give 4,4'-dimethoxy-6,6'-dimethyl-2,2'-bipyridine (3.4 g, 92%) as a white powder. ^{1}H NMR (400 MHz, $CDCl_3$) δ 7.79 (d, *J* = 2.4 Hz, 2H), 6.69 (d, *J* = 2.4 Hz, 2H), 3.93 (s, 6H), 2.58 (s, 6H) ppm. ^{13}C NMR (101 MHz, $CDCl_3$) δ 167.1, 159.3, 157.5, 109.9, 104.3, 55.4, 24.7 ppm. Spectroscopic data matched those previously reported in the literature.[116]

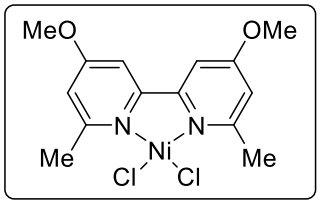

(4,4'-MeO-6,6'-Me-bpy)NiCl$_2$ (Ni-1): **L1** (0.30 g, 1.20 mmol) and $NiCl_2$ (0.15 g, 1.2 mmol) were dissolved in THF (0.10 M, 12 ml) and refluxed for 24 h. After this time, the reaction mixture was cooled to RT and filtered. The collected solid was then dissolved in CH_2Cl_2, precipitated with hexane, filtered again and dried *in vacuo* to give **Ni-1** (0.44 g, 98%) as a purple solid. Note: This complex is highly hygroscopic and should be stored under inert atmosphere. ^{1}H NMR (500 MHz, $CDCl_3$, paramagnetic) δ 79.2 (s, 2H), 59.9 (s, 2H), 47.8 (s, br, 6H), 12.6 (s, 6H) ppm.

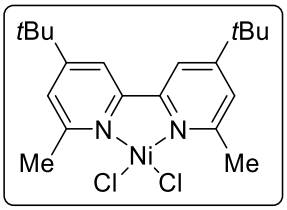

(4,4'-*t*Bu-6,6'-Me-bpy)NiCl$_2$ (Ni-2): **L2** (0.15 g, 0.52 mmol) and $NiCl_2$ (64 mg, 0.50 mmol) were dissolved in THF (0.10 M, 5.0 ml) and refluxed for 24 h. After this time, the reaction mixture was cooled to room temperature and filtered. The collected solid was then dissolved in CH_2Cl_2, precipitated with hexane, filtered again and dried *in vacuo* to give **Ni-2** (0.20 g, 94%) as a purple solid. Note: This complex is highly hygroscopic and should be stored under inert atmosphere. ^{1}H NMR (500 MHz, $CDCl_3$, paramagnetic) δ 76.9 (s, 2H), 60.6 (s, 2H), 31.1 (s, br, 6H), 1.9 (s, 18H) ppm.

2.7.4 Synthesis of aziridines

Note: The synthesis and characterization of aziridines **2.1** is only given for specific substrates when related final products **2.2** were successfully isolated and characterized.

General procedure 1 (GP1): Synthesis of (enantiopure) aziridines from amino alcohols

Following a literature procedure,[120] tosyl chloride (2.2 equiv.) was added portion wise at RT to a stirred mixture of the amino alcohol (1.0 equiv.) and K_2CO_3 (4.0 equiv.) in acetonitrile (0.50 M). After 6 h, the solid was filtered off and washed with EtOAc. The filtrate was concentrated *in vacuo* and purified by column chromatography on silica gel (hexane:EtOAc) to afford the pure *N*-tosyl aziridines.

General procedure 2 (GP2): Synthesis of (enantiopure) aziridines from amino alcohols

Following a literature procedure,[120] tosyl chloride (2.5 equiv.) was added portion wise at RT under vigorous stirring to a mixture of KOH (35 equiv.), the amino alcohol (1.0 equiv.), water (0.50 M) and CH_2Cl_2 (0.50 M). After 30 min, ice and water were added and diluted with CH_2Cl_2. The organic layer was separated and washed with water, dried ($MgSO_4$), filtered and concentrated *in vacuo*. Flash column chromatography on silica gel (hexane:EtOAc) afforded the pure *N*-tosyl aziridines.

General procedure 3 (GP3): Synthesis of racemic aziridines from alkenes

Following a literature procedure,[121,122] to a mixture of chloramine-T trihydrate (1.1 equiv.) and alkene (1.0 equiv.) in CH_3CN (25 mL) at ambient temperature was added $PhNMe_3Br_3$ (0.10 equiv.). The reaction was stirred vigorously for 16 h, the solid was filtered off and the filtrate was concentrated *in vacuo*. Flash column chromatography (hexane:EtOAc) afforded the pure *N*-tosyl aziridines.

General procedure 4 (GP4): Base cyclisation of aziridines containing uncyclized reaction intermediates

Note: In certain cases, cyclization to the aziridine was less favourable and trace uncyclized intermediates often co-eluted with the aziridine. A subsequent base cyclisation was performed to obtain high purity aziridine in these cases. The resulting material isolated from **GP1-3** was dissolved in MeCN (5-10 ml), K_2CO_3 (1.0 equiv.) was added and the mixture was stirred vigorously at 45 °C for 3 h. The mixture was cooled to RT, filtered and concentrated *in vacuo*. The material was then dissolved in CH_2Cl_2 (1 mL) and filtered through a short plug of silica gel, 3 × 4 cm, eluting with hexane:EtOAc 1:1.

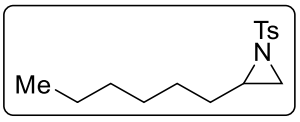

2-Hexyl-1-tosylaziridine (2.1a): Following **GP3** with 1-octene (15 mL, 100 mmol), purification by column chromatography on silica gel (hexane:EtOAc 95:5) afforded **2.1a** as a colorless oil (19 g, 68%). ^{1}H NMR (400 MHz, $CDCl_3$) δ 7.82 (d, *J* = 8.3 Hz, 2H), 7.33 (d, *J* = 7.7 Hz, 2H), 2.71 (tt, *J* = 7.3, 4.8 Hz, 1H), 2.63 (d, *J* = 7.0 Hz, 1H), 2.44 (s, 3H), 2.05 (d, *J* = 4.6 Hz, 1H), 1.57 – 1.47 (m, 1H), 1.39 – 1.10 (m, 9H), 0.85 (t, *J* = 7.0 Hz, 3H) ppm. ^{13}C NMR (126 MHz, $CDCl_3$) δ 144.5, 135.4, 129.7, 128.1, 40.6, 33.9, 31.7, 31.4, 28.8, 26.8, 22.6, 21.7, 14.2 ppm. Spectroscopic data for **2.1a** match those previously reported in the literature.[123]

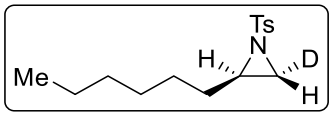

***trans*-2-Hexyl-1-tosylaziridine-3-*d* (2.1a-*d*$_1$)**: Following **GP3** with (*E*)-oct-1-ene-1-*d* (0.56 g, 5.0 mmol), which was synthesized using a literature procedure,[124] purification by column chromatography on silica gel (hexane:EtOAc 95:5) afforded **2.1a-*d*$_1$** as a colorless oil (0.30 g, 21%). ^{1}H NMR (400 MHz, $CDCl_3$) δ 7.87 – 7.79 (m, 2H), 7.37 – 7.30 (m, 2H), 2.71 (dt, *J* = 7.6, 4.8 Hz, 1H), 2.44 (s, 3H), 2.05 (d, *J* = 4.7 Hz, 1H), 1.55 – 1.49 (m, 1H), 1.39 – 1.09 (m, 9H), 0.85 (t, *J* = 7.0 Hz, 3H) ppm. ^{13}C NMR (101 MHz, $CDCl_3$) δ 144.5, 135.4, 129.8, 128.2, 40.6, 33.68 (t, *J* = 25.5 Hz), 31.8, 31.4, 28.8, 26.9, 22.6, 21.8, 14.2 ppm. Spectroscopic data for **2.1a-*d*$_1$** match with the non-deuterated analogue **2.1a**.

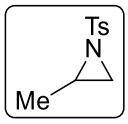

2-Methyl-1-tosylaziridine (2.1b): Following **GP1** with (±)-2-amino-1-propanol (1.5 g, 20 mmol), purification by column chromatography on silica gel (hexane:EtOAc 8:2) afforded **2.1b** as a white solid (0.93 g, 22%). ^{1}H NMR (400 MHz, $CDCl_3$) δ 7.82 (d, *J* = 8.3 Hz, 2H), 7.34 (d, *J* = 8.2 Hz, 2H), 2.90 – 2.76 (m, 1H), 2.61 (d, *J* = 7.0 Hz, 1H), 2.44 (s, 3H), 2.02 (d, *J* = 4.6 Hz, 1H), 1.25 (d, *J* = 5.6 Hz, 3H) ppm. ^{13}C NMR (101 MHz, $CDCl_3$) δ 144.5, 135.6, 129.8, 128.0, 36.0, 34.9, 21.8, 16.9 ppm. LRMS (ESI): 234 $(M+Na)^+$, 212 $(M+H)^+$. Spectroscopic data for **2.1b** match those previously reported in the literature.[125]

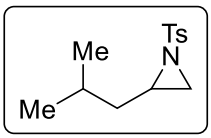

2-Isobutyl-1-tosylaziridine (2.1d): Following **GP1** with (±)-Leucinol (1.2 g, 10 mmol), purification by column chromatography on silica gel (hexane:EtOAc 9:1) afforded **2.1d** as a white solid (1.2 g, 48%). ^{1}H NMR (400 MHz, $CDCl_3$) δ 7.82 (d, *J* = 8.3 Hz, 2H), 7.33 (d, *J* = 7.9 Hz, 2H), 2.78 (tdd, *J* = 7.0, 5.9, 4.6 Hz, 1H), 2.62 (d, *J* = 7.0 Hz, 1H), 2.44 (s, 3H), 2.02 (d, *J* = 4.6 Hz, 1H), 1.67 – 1.55 (m, 1H), 1.40 – 1.26 (m, 2H), 0.88 (d, *J* = 6.7 Hz, 3H), 0.87 (d, *J* = 6.7 Hz, 3H) ppm. ^{13}C NMR (101 MHz, $CDCl_3$) δ 144.5, 135.4, 129.8, 128.1, 40.6, 39.2, 34.2, 26.9, 22.9, 22.06, 21.8 ppm. LRMS (ESI): 253, 238, 224, 212, 155, 139, 98, 91. Spectroscopic data for **2.1d** match those previously reported in the literature.[126]

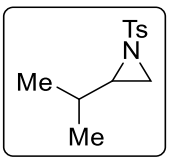

2-Isopropyl-1-tosylaziridine (2.1e): Following **GP1** with (±)-Valinol (1.0 g, 10 mmol), purification by column chromatography on silica gel (hexane:EtOAc 9:1) afforded **1e** as a white solid (1.6 g, 56%). ^{1}H NMR (400 MHz, $CDCl_3$) δ 7.83 (d, *J* = 8.3 Hz, 2H), 7.33 (d, *J* = 7.9 Hz, 2H), 2.61 (d, *J* = 7.0 Hz, 1H), 2.51 (ddd, *J* = 7.7, 7.0, 4.6 Hz, 1H), 2.43 (s, 3H), 2.10 (d, *J* = 4.6 Hz, 1H), 1.42 (dp, *J* = 7.5, 6.7 Hz, 1H), 0.90 (d, *J* = 6.9 Hz, 3H), 0.80 (d, *J* = 6.7 Hz, 3H). ^{13}C NMR (101 MHz, $CDCl_3$) δ 144.6, 135.3, 129.7, 128.2, 46.4, 32.9, 30.3, 21.8, 19.7, 19.2. LRMS (ESI): 239, 224, 155, 146, 139, 91, 84. Spectroscopic data for **2.1e** match those previously reported in the literature.[127]

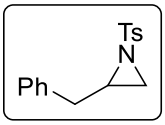

(±)-2-Benzyl-1-tosylaziridine (2.1f): Following **GP3** with allylbenzene (0.59 g, 5.0 mmol), purification by column chromatography on silica gel (hexane:EtOAc 9:1 → 5:1) afforded **2.1f** as a white solid (0.67 g, 47%).^{1}H NMR (400 MHz, $CDCl_3$) δ 7.71 – 7.67 (m, 2H), 7.24 – 7.20 (m, 2H), 7.18 – 7.13 (m, 3H), 7.07 – 7.02 (m, 2H), 2.95 (tdd, *J* = 7.0, 5.2, 4.5 Hz, 1H), 2.81 (dd, *J* = 14.5, 5.2 Hz, 1H), 2.73 – 2.66 (m, 2H), 2.42 (s, 3H), 2.16 (d, *J* = 4.5 Hz, 1H) ppm. ^{13}C NMR (101 MHz, $CDCl_3$) δ 144.4, 137.1, 135.0, 129.7, 128.9, 128.6, 128.0, 126.6, 41.3, 37.6, 33.0, 21.7 ppm. LRMS (ESI): 287, 172, 155, 132, 117, 105, 91, 77. Spectroscopic data for **2.1f** match those previously reported in the literature.[128]

HPLC: *rac* (CHIRALPAK® IC, hexane/ EtOH = 88:12, 1 mL/min, 220 nm, t_R= 17.644; 18.848).

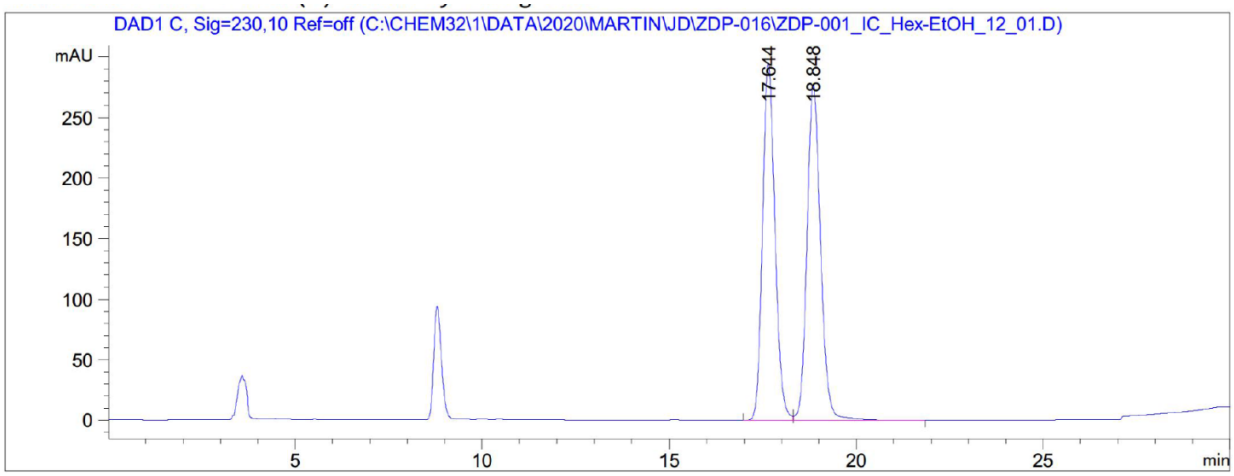

Peak #	RetTime [min]	Type	Width [min]	Area [mAU*s]	Height [mAU]	Area %
1	17.644	BV	0.3557	6820.63477	295.02158	49.3863
2	18.848	VB	0.3891	6990.15576	276.35837	50.6137
Totals :				1.38108e4	571.37994	

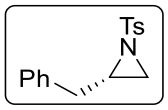

(S)-2-benzyl-1-tosylaziridine ((S)-2.1f): Following **GP1** with (−)-2-Amino-3-phenyl-1-propanol (0.60 g, 4.0 mmol), purification by column chromatography on silica gel (hexane:EtOAc 9:1 → 5:1) afforded (S)-**2.1f** as a white solid (0.72 g, 63%). ^{1}H NMR (400 MHz, $CDCl_3$) δ 7.69 (d, *J* = 8.3 Hz, 2H), 7.21 (d, *J* = 7.9 Hz, 2H), 7.20 – 7.10 (m, 3H), 7.09 – 7.00 (m, 2H), 2.95 (tt, *J* = 7.0, 5.0 Hz, 1H), 2.81 (dd, *J* = 14.5, 5.2 Hz, 1H), 2.74 – 2.64 (m, 2H), 2.42 (s, 3H), 2.16 (d, *J* = 4.5 Hz, 1H) ppm. ^{13}C NMR (101 MHz, $CDCl_3$) δ 144.4, 137.1, 135.0, 129.7, 128.9, 128.6, 128.0, 126.6, 41.3, 37.6, 33.0, 21.7 ppm. Spectroscopic data for (S)-**2.1f** match those previously reported in the literature.[128] HPLC: >99% *ee* (CHIRALPAK® IC, hexane/*i*-PrOH = 85/15, 1 mL/min, 220 nm, t_R= 18.835).

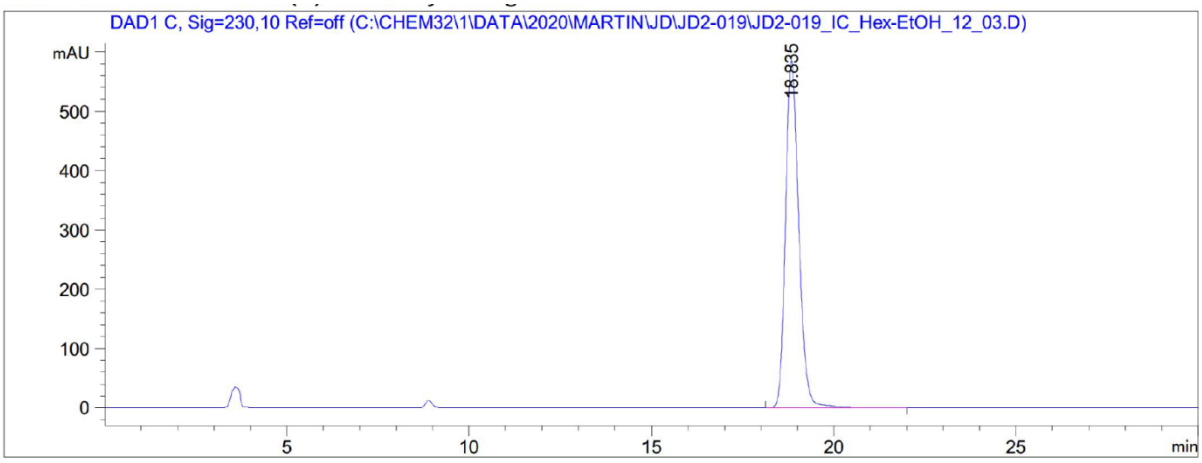

Peak #	RetTime [min]	Type	Width [min]	Area [mAU*s]	Height [mAU]	Area %
1	18.835	BB	0.3884	1.47844e4	585.94495	100.0000
Totals :				1.47844e4	585.94495	

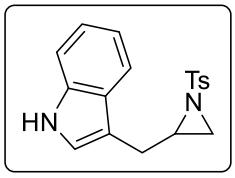

3-((1-Tosylaziridin-2-yl)methyl)-1H-indole (2.1g): Following literature procedure[129] with tryptophanol (0.48 g, 2.5 mmol), purification by column chromatography (hexane:EtOAc 8:2 → 6:4) afforded **2.1g** as a pale yellow solid (0.17 g, 20%). ^{1}H NMR (400 MHz, $CDCl_3$) δ 7.95 (s, br, 1H), 7.69 – 7.62 (m, 2H), 7.46 (dq, *J* = 7.9, 0.9 Hz, 2H), 7.31 (dt, *J* = 8.2, 0.9 Hz, 1H), 7.18 (ddd, *J* = 8.2, 7.0, 1.2 Hz, 1H), 7.17 – 7.09 (m, 1H), 7.07 (ddd, *J* = 8.0, 7.0, 1.0 Hz, 1H), 6.99 (d, *J* = 2.3 Hz, 1H), 3.11 – 3.05 (m, 1H), 3.01 (ddd, *J* = 15.1, 5.1, 0.9 Hz, 1H), 2.85 (ddd, *J* = 15.0, 6.8, 0.9 Hz, 1H), 2.71 (d, *J* = 6.7 Hz, 1H), 2.39 (s, 3H), 2.20 (d, *J* = 4.5 Hz, 1H). ^{13}C NMR (101 MHz, $CDCl_3$) δ 144.3, 136.2, 134.9, 129.5, 127.9, 127.3, 122.4, 122.2, 119.6, 118.7, 111.4, 111.2, 40.8, 33.5, 27.3, 21.8. LRMS: 349 $(M+Na)^+$, 327 $(M+H)^+$. Spectroscopic data for **2.1g** match those previously reported in the literature.[129]

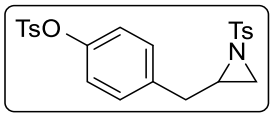

4-((1-Tosylaziridin-2-yl)methyl)phenyl 4-methylbenzenesulfonate (2.1l): Following **GP1** using L-tyrosinol hydrochloride (0.20 g, 1.0 mmol), purification by column chromatography on silica gel (hexane:EtOAc 9:1 → 6:4) afforded **2.1l** as a colourless oil (0.15 g, 32%). ^{1}H NMR (400 MHz, $CDCl_3$) δ 7.72 – 7.61 (m, 4H), 7.31 (d, *J* = 7.7 Hz, 2H), 7.23 (d, *J* = 7.8 Hz, 2H), 6.99 – 6.91 (m, 2H), 6.80 – 6.71 (m, 2H), 2.93 – 2.78 (m, 2H), 2.70 (d, *J* = 6.7 Hz, 1H), 2.56 (dd, *J* = 14.3, 7.4 Hz, 1H), 2.45 (d, *J* = 3.1 Hz, 6H), 2.12 (d, *J* = 4.3 Hz, 1H) ppm. ^{13}C NMR (101 MHz, $CDCl_3$) δ 148.5, 145.5, 144.9, 136.3, 134.9, 132.6, 130.0, 129.9, 129.8, 128.6, 128.0, 122.4, 41.0, 37.0, 32.9, 21.9, 21.8 ppm. HRMS calcd. for ($C_{23}H_{23}NNaO_5S_2$) $[M+Na]^+$: 480.0910 found 480.0909. This compound is reported in literature, but no spectroscopic data is provided.[120, 130]

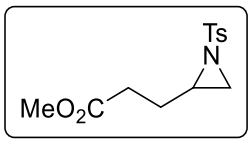

Methyl 3-(1-tosylaziridin-2-yl) propanoate (2.1m): Following **GP3** with methyl-4-pentanoate (0.23 g, 2.0 mmol), purification by column chromatography on silica gel (hexane:EtOAc 9:1 → 7:3) afforded **2.1m** along with uncyclized intermediate **2.1m'**[i]. This mixture was submitted to a base cyclisation step (**GP4**) to afforded **2.1m** (0.15 g, 22%) as a colourless oil. ^{1}H NMR (400 MHz, $CDCl_3$) δ 7.83 – 7.78 (m, 2H), 7.38 – 7.30 (m, 2H), 3.65 (s, 3H), 2.82 (ddt, *J* = 7.9, 6.9, 4.6 Hz, 1H), 2.65 (d, *J* =

[i] **2.1m'**: 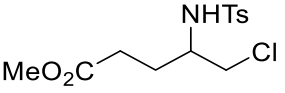

7.0 Hz, 1H), 2.45 (s, 3H), 2.36 – 2.19 (m, 2H), 2.11 (d, *J* = 4.5 Hz, 1H), 1.99 (dtd, *J* = 14.3, 7.7, 4.6 Hz, 1H), 1.55 (dtd, *J* = 14.0, 7.7, 6.1 Hz, 1H) ppm. ^{13}C NMR (101 MHz, $CDCl_3$) δ 172.8, 144.6, 134.8, 129.7, 128.0, 51.6, 39.1, 33.9, 30.8, 26.4, 21.6 ppm. IR (neat, cm^{-1}): 2999, 2953, 1732, 1597, 1494, 1438, 1365, 1320, 1206, 1156, 1091. HRMS calcd. for ($C_{13}H_{17}NNaO_4S$) $[M+Na]^+$: 306.0770 found 306.0770.

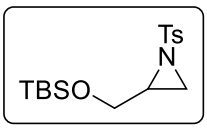

2-(((*tert*-Butyldimethylsilyl)oxy)methyl)-1-tosylaziridine (2.1q): Following **GP3** with (allyloxy)(tert-butyl)dimethylsilane (1.7 g, 10 mmol), purification by column chromatography on silica gel (hexane:EtOAc 9:1 → 5:1) afforded **2.1q** as a colorless oil (1.2 g, 36%). ^{1}H NMR (400 MHz, $CDCl_3$) δ 7.86 – 7.80 (m, 2H), 7.35 – 7.30 (m, 2H), 3.69 (dd, *J* = 11.6, 4.0 Hz, 1H), 3.59 (dd, *J* = 11.6, 5.3 Hz, 1H), 2.96 – 2.88 (m, 1H), 2.64 (d, *J* = 7.1 Hz, 1H), 2.44 (s, 3H), 2.20 (d, *J* = 4.5 Hz, 1H), 0.81 (s, 9H), –0.03 (s, 3H), –0.04 (s, 3H) ppm. ^{13}C NMR (101 MHz, $CDCl_3$) δ 144.6, 135.3, 129.8, 128.2, 62.5, 40.9, 30.7, 25.9, 21.8, 18.4, -5.3, -5.4. Spectroscopic data for **2.1q** match those previously reported in the literature.[131]

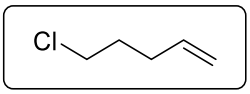

5-Chloropent-1-ene (S1): Following literature procedure,[132] pent-4-en-1-ol (10 g, 0.12 mol) was dissolved in the mixture of CH_2Cl_2 (30 ml) and pyridine (1.0 ml). The mixture was cooled to 10 °C, and $SOCl_2$ (15 g, 0.13 mol) was added drop wise with stirring. Vigorous gas evolution occurred. The reaction was stirred overnight at room temperature and poured over ice. Organic phase was separated and washed additionally with saturated $NaHCO_3$ and brine, dried ($MgSO_4$) and distilled under atmospheric pressure. The target product (B.P. = 104 – 105 °C) was obtained as a colorless liquid (1.5 g, 12%) and used in the next synthetic step without any further purification. ^{1}H NMR (400 MHz, $CDCl_3$) δ 5.78 (ddt, *J* = 16.9, 10.2, 6.7 Hz, 1H), 5.11 – 4.99 (m, 2H), 3.55 (t, *J* = 6.6 Hz, 2H), 2.26 – 2.17 (m, 2H), 1.92 – 1.82 (m, 2H). Spectroscopic data for **S1** match those previously reported in the literature.[133]

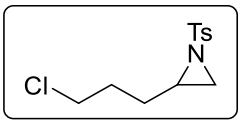

2-(3-Chloropropyl)-1-tosylaziridine (2.1w): Following **GP3** with 5-chloropent-1-ene **(S1)** (0.28 g, 2.7 mmol), purification by column chromatography on silica gel (hexane:EtOAc 9:1 → 5:1) afforded **2.1w** as a colorless oil (0.26 g, 36%). ^{1}H NMR (400 MHz, $CDCl_3$) δ 7.85 – 7.80 (m, 2H), 7.37 – 7.33 (m, 2H), 3.54 – 3.45 (m, 2H), 2.79 – 2.72 (m, 1H), 2.64 (d, *J* = 7.0 Hz, 1H), 2.45 (s, 3H), 2.09 (d, *J* = 4.5 Hz, 1H), 1.90 – 1.81 (m, 1H), 1.80 – 1.73 (m, 2H), 1.46 – 1.37 (m, 1H) ppm. ^{13}C NMR (101 MHz, $CDCl_3$) δ 144.8, 135.2, 129.9, 128.1, 44.1, 39.3, 34.0, 29.9, 28.7, 21.8 ppm. IR (neat, cm^{-1}): 2999, 2957, 2871, 1597, 1446, 1402, 1319, 1305, 1291, 1235, 1156, 1090, 929, 875, 815, 712, 690, 659, 567, 549. HRMS calcd. for ($C_{12}H_{16}ClNNaO_2S$) $[M+H]^+$: 296.0482 found 296.0479.

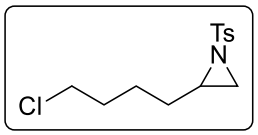

2-(4-Chlorobutyl)-1-tosylaziridine (2.1t): Following **GP3** with 6-chloro-1-hexene (0.66 mL, 5.0 mmol), purification by column chromatography on silica gel (hexane:EtOAc 9:1) afforded **2.1t** as a colorless oil (1.4 g, 91%). ^{1}H NMR (400 MHz, $CDCl_3$) δ 7.82 (d, *J* = 8.3 Hz, 2H), 7.34 (d, *J* = 7.8 Hz, 2H), 3.42 (td, *J* = 6.6, 1.0 Hz, 2H), 2.71 (tt, *J* = 6.9, 4.5 Hz, 1H), 2.64 (d, *J* = 7.0 Hz, 1H), 2.44 (s, 3H), 2.07 (d, *J* = 4.5 Hz, 1H), 1.84 – 1.54 (m, 3H), 1.48 – 1.22 (m, 3H) ppm. ^{13}C NMR (101 MHz, $CDCl_3$) δ 144.7, 135.2, 129.8, 128.1, 44.7, 40.1, 33.8, 31.9, 30.7, 24.3, 21.8 ppm. LRMS: 287 (M+), 252, 238, 210, 184, 172, 155, 132, 91. Spectroscopic data for **2.1t** match those previously reported in the literature.[121]

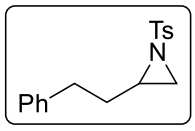

2-Phenethyl-1-tosylaziridine (2.1x): Following **GP3** with 4-phenyl-1-butene (4.5 mL, 30 mmol), purification by column chromatography on silica gel (hexane:EtOAc 9:1) afforded **2.1x** as a colorless solid (5.7 g, 63%). ^{1}H NMR (400 MHz, $CDCl_3$) δ 7.84 (d, *J* = 8.3 Hz, 2H), 7.37 – 7.32 (m, 2H), 7.30 – 7.24 (m, 2H), 7.21 – 7.16 (m, 1H), 7.14 – 7.10 (m, 2H), 2.78 (tt, *J* = 7.7, 4.7 Hz, 1H), 2.67 – 2.54 (m, 3H), 2.45 (s, 3H), 2.06 (d, *J* = 4.6 Hz, 1H), 1.93 – 1.83 (m, 1H), 1.73 – 1.62 (m, 1H) ppm. ^{13}C NMR (101 MHz, $CDCl_3$) δ 144.6, 140.8, 135.2, 129.8, 128.6, 128.4, 128.1, 126.2, 39.9, 34.0, 33.3, 33.1, 21.8 ppm. LRMS (ESI): 301 (M+), 260, 184, 155, 117, 91, 77. Spectroscopic data for **2.1x** match those previously reported in the literature.[123]

General procedure 5 (GP5): Synthesis of propenylated and butenylated arenes (S2-4)

To a flame-dried 250 mL round-bottom flask was added aryl or benzyl bromide (1.0 equiv.) and anhydrous THF (0.50 M). The reaction flask was cooled to 0 °C while under an atmosphere of nitrogen and allylmagnesium bromide was added drop wise (1.0 M in Et_2O, 1.1 equiv.). The reaction was stirred for 2 h at 0 °C and then allowed to warm to RT before being quenched with H_2O. The layers were separated and the aqueous layer was extracted with Et_2O (3 times). The combined organic fractions were washed with Na_2SO_4 (sat.), brine and dried ($MgSO_4$). Purification of the crude reaction mixture by column chromatography (hexane:EtOAc 99:1 → 97:3) was carried out when necessary.

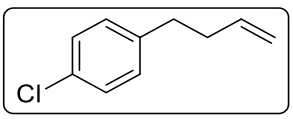

1-(But-3-en-1-yl)-4-chlorobenzene (S2): Following **GP5** with 4-chlorobenzyl bromide (3.1 g, 15 mmol, 1.0 equiv.), purification by column chromatography on silica gel (hexane:EtOAc 95:5) afforded **S2** (1.94 g, 78%) as a colourless oil. ^{1}H NMR (400 MHz, $CDCl_3$) δ 7.26 – 7.22 (m, 2H), 7.13 – 7.09 (m, 2H), 5.82 (ddt, *J* = 16.9, 10.2, 6.6 Hz, 1H), 5.08 – 4.94 (m, 2H), 2.68 (dd, *J* = 8.8, 6.7 Hz, 2H), 2.35 (qq, *J* = 7.8, 6.5, 1.4, 0.6 Hz, 2H) ppm. ^{13}C NMR (101 MHz, $CDCl_3$) δ 140.4, 137.8, 131.7,

129.9, 128.5, 115.4, 35.5, 34.8 ppm. Spectroscopic data for **S2** match those previously reported in the literature.[134]

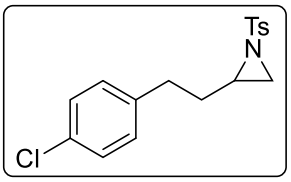

2-(4-Chlorophenethyl)-1-tosylaziridine (2.1y): Following **GP3** with **S2** (2.0 g, 12 mmol) purification by column chromatography on silica gel (hexane:EtOAc 9:1) afforded **2.1y** as a white solid (1.05 g, 26%). M.P: 46 - 48 °C. ^{1}H NMR (400 MHz, $CDCl_3$) δ 7.92 (d, *J* = 8.3 Hz, 2H), 7.44 (d, *J* = 7.9 Hz, 2H), 7.33 (d, *J* = 8.4 Hz, 2H), 7.15 (d, *J* = 8.4 Hz, 2H), 2.86 (ddt, *J* = 7.8, 7.0, 4.6 Hz, 1H), 2.77 – 2.61 (m, 3H), 2.55 (s, 3H), 2.15 (d, *J* = 2.5 Hz, 1H), 1.97 (dddd, *J* = 13.6, 8.7, 7.5, 4.8 Hz, 1H), 1.73 (dtd, *J* = 14.2, 8.1, 6.3 Hz, 1H) ppm. ^{13}C NMR (126 MHz, $CDCl_3$) δ 144.7, 139.2, 135.1, 132.0, 129.8, 129,8 128.6, 128.1, 39.5, 34.1, 33.1, 32.4, 21.7 ppm. IR (neat, cm^{-1}): 2926, 2862, 1597, 1492, 1452, 1405, 1320, 1305, 1231, 1157, 1090, 1015. HRMS calcd. for ($C_{17}H_{18}ClNNaO_2S$) $[M+Na]^+$: 358.0639 found 358.0633.

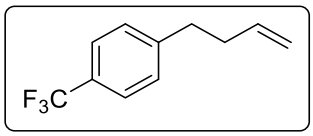

1-(But-3-en-1-yl)-4-trifluoromethylbenzene (S3): Following **GP5**, 4-trifluoromethylbenzyl bromide (1.5 ml, 10 mmol, 1.0 equiv.) afforded **S3** (1.4 g, 68%) as a colourless oil. In this case, no purification was carried out. ^{1}H NMR (400 MHz, $CDCl_3$) δ 7.53 (d, *J* = 7.8 Hz, 2H), 7.29 (d, *J* = 7.9 Hz, 2H), 5.83 (ddt, *J* = 16.9, 10.2, 6.6 Hz, 1H), 5.10 – 4.97 (m, 2H), 2.77 (dd, *J* = 8.7, 6.8 Hz, 2H), 2.39 (tdt, *J* = 7.8, 6.6, 1.4 Hz, 2H) ppm. ^{13}C NMR (101 MHz, $CDCl_3$) δ 146.1, 137.5, 128.9, 128.4 (q, *J* = 32.0 Hz), 125.9, 124.5 (q, *J* = 271.0 Hz), 125.4 (q, *J* = 3.8 Hz), 115.6, 35.3, 35.2 ppm. ^{19}F NMR (376 MHz, $CDCl_3$) δ -62.02. Spectroscopic data for **S3** match those previously reported in the literature.[135]

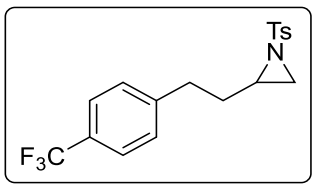

1-Tosyl-2-(4-(trifluoromethyl)phenethyl) aziridine (2.1z): Following **GP3** with **S3** (1.4 g, 7.0 mmol), purification by column chromatography on silica gel (hexane:EtOAc 9:1) afforded **2.1z** as a white solid (0.95 g, 37%). M.P: 80 – 83 °C. ^{1}H NMR (400 MHz, $CDCl_3$) δ 7.88 – 7.76 (m, 2H), 7.52 (d, *J* = 8.0 Hz, 2H), 7.38 – 7.31 (m, 2H), 7.24 (d, *J* = 8.0 Hz, 2H), 2.77 (ddt, *J* = 8.0, 6.9, 4.6 Hz, 1H), 2.72 – 2.66 (m, 2H), 2.61 (d, *J* = 6.9 Hz, 1H), 2.45 (s, 3H), 2.06 (d, *J* = 4.5 Hz, 1H), 1.94 (dddd, *J* = 13.2, 8.7, 7.6, 4.6 Hz, 1H), 1.65 (dtd, *J* = 14.4, 8.1, 6.6 Hz, 1H) ppm. ^{13}C NMR (126 MHz, $CDCl_3$) δ 144.9 (q, *J* = 1.1 Hz), 144.8, 134.9, 129.8, 128.8, 128.5 (q, *J* = 32.3 Hz), 128.1, δ 125.4 (q, *J* = 3.9 Hz), 124.3 (d, *J* = 269.4 Hz), 39.3, 34.1, 32.9, 32.8, 21.7 ppm. ^{19}F NMR (376 MHz, $CDCl_3$) δ -62.45. IR (neat, cm^{-1}): 3067, 2936, 1615, 1456, 1415, 1317, 1234, 1154, 1115, 1093, 1063, 1017. HRMS calcd. for ($C_{18}H_{18}F_3NNaO_2S$) $[M+Na]^+$: 392.0903 found 392.0892.

General procedure 6 (GP6): Cross-coupling of S5 with aryl-boronic acids

A flame dried Schlenk flask was charged with **S5**, boronic acid (1.3 equiv.), $PdCl_2$(dppf) (2.0 mol%) and Na_2CO_3 (aq. 1.0 M) under a flow of argon. Then a mixture of PhMe:EtOH:H_2O (3:2:1, 0.08 M), degassed in advance, was added into the flask. The resulting reaction was heated to 80 °C and stirred at this temperature overnight (the reaction progress can be monitored by TLC). Upon completion, the reaction was cooled to RT and diluted with H_2O. The organic phase was separated and the aqueous phase was extracted with EtOAc. The combined organic fractions were dried ($MgSO_4$) and concentrated *in vacuo*. The crude was purified by column chromatography on silica gel (hexane:EtOAc 2:1 → 1:1) to afford the product. If necessary, the product can be washed with Et_2O for additional purification.

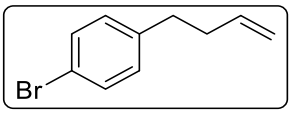

1-(But-3-en-1-yl)-4-chlorobenzene (S4): Following **GP5**, 4-bromobenzyl bromide (6.8 g, 27 mmol, 1.0 equiv.) gave **S4** (5.4 g, 89%) as a colourless oil. In this case, no purification was carried out. ^{1}H NMR (300 MHz, $CDCl_3$) δ 7.45 – 7.32 (m, 2H), 7.11 – 6.95 (m, 2H), 5.82 (ddt, *J* = 16.9, 10.2, 6.6 Hz, 1H), 5.10 – 4.93 (m, 2H), 2.66 (dd, *J* = 8.8, 6.6 Hz, 2H), 2.42 – 2.27 (m, 2H) ppm. Spectroscopic data for **S4** match those previously reported in the literature.[135]

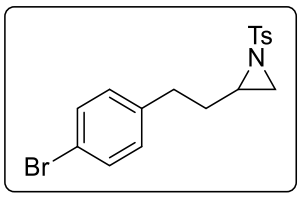

2-(4-Bromophenethyl)-1-tosylaziridine (S5): Following **GP3** with **S4** (3.2 g, 15 mmol, 1.0 equiv.), purification by column chromatography on silica gel (hexane:EtOAc 9:1) afforded **S5** (2.5 g, 44%) as a white solid. M.P: 46 – 49 °C. ^{1}H NMR (400 MHz, $CDCl_3$) δ 7.86 – 7.78 (m, 2H), 7.40 – 7.36 (m, 2H), 7.38 – 7.31 (m, 2H), 7.04 – 6.96 (m, 2H), 2.75 (ddt, *J* = 7.9, 7.0, 4.7 Hz, 1H), 2.62 – 2.54 (m, 3H), 2.45 (s, 3H), 2.04 (d, *J* = 4.6 Hz, 1H), 1.87 (dddd, *J* = 13.6, 8.7, 7.5, 4.7 Hz, 1H), 1.62 (dtd, *J* = 14.3, 8.1, 6.4 Hz, 1H) ppm. ^{13}C NMR (101 MHz, $CDCl_3$) δ 144.7, 139.8, 135.1, 131.7, 130.3, 129.8, 128.2, 120.1, 39.5, 34.1, 33.1, 32.6, 21.8 ppm. IR (neat, cm^{-1}): 3274, 3055, 2956, 2931, 2892, 1596, 1488, 1450, 1399, 1317, 1291, 1223, 1151, 1112, 1088, 1007. HRMS calcd. for ($C_{17}H_{18}BrNNaO_2S$) $[M+Na]^+$: 402.0134 found 402.0122.

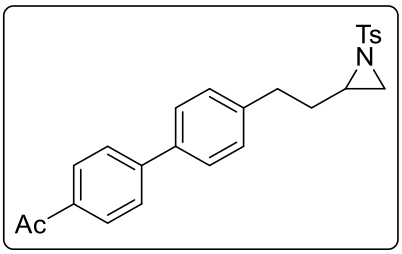

1-(4'-(2-(1-Tosylaziridin-2-yl)ethyl)-[1,1'-biphenyl]-4-yl) ethan-1-one (2.1ab): Following **GP6** with (4-acetylphenyl)boronic acid (0.49 g, 1.5 equiv.), **S5** (0.76 g, 2.0 mmol, 1.0 equiv.) afforded **2.1ab** as a white solid (0.72 g, 86%) after purification by column chromatography on silica gel (hexane:EtOAc 9:1). M.P: 126 – 127 °C. ^{1}H NMR (400 MHz, $CDCl_3$) δ 8.02 (d, *J* = 8.5 Hz, 2H), 7.85 (d, *J* = 8.3 Hz, 2H), 7.66 (d, *J* = 8.4 Hz, 2H), 7.54 (d, *J* = 8.2 Hz, 2H), 7.35 (d, *J* = 7.6 Hz,

2H), 7.24 (d, *J* = 8.2 Hz, 2H), 2.87 – 2.76 (m, 1H), 2.68 (m, 2H), 2.67 – 2.64 (m, 4H), 2.45 (s, 3H), 2.08 (d, *J* = 4.6 Hz, 1H), 1.94 (dddd, *J* = 13.6, 8.7, 7.5, 4.8 Hz, 1H), 1.70 (dtd, *J* = 14.2, 8.1, 6.4 Hz, 1H) ppm. ^{13}C NMR (126 MHz, $CDCl_3$) δ 197.9, 145.6, 144.7, 141.1, 137.9, 135.9, 135.2, 129.8, 129.2, 129.1, 128.2, 127.5, 127.2, 39.7, 34.2, 33.2, 32.8, 26.8, 21.8 ppm. IR (neat, cm^{-1}): 3004, 2925, 1672, 1601, 1527, 1493, 1446, 1421, 1398, 1360, 1336, 1308, 1264, 1234, 1160, 1088. HRMS calcd. for ($C_{25}H_{25}NO_3S$) $[M+Na]^+$: 442.1447 found 442.1463.

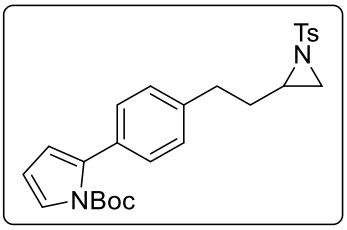

***tert*-Butyl 2-(4-(2-(1-tosylaziridin-2-yl)ethyl)phenyl)-1H-pyrrole-1-carboxylate (2.1ac)**: Following **GP6** with *N*-Boc-2-pyrroleboronic acid (0.82 g, 1.3 equiv.), **S5** (1.1 g, 2.9 mmol, 1.0 equiv.) afforded **2.1ac** as a yellow viscous oil (0.55 g, 39%) after purification by column chromatography on silica gel (hexane:EtOAc 8:2). ^{1}H NMR (400 MHz, $CDCl_3$) δ 7.85 (d, *J* = 8.3 Hz, 2H), 7.35 (d, *J* = 7.9 Hz, 2H), 7.33 (dd, *J* = 3.3, 1.8 Hz, 1H), 7.25 (d, *J* = 8.2 Hz, 2H), 7.09 (d, *J* = 8.2 Hz, 2H), 6.21 (t, *J* = 3.3 Hz, 1H), 6.15 (dd, *J* = 3.3, 1.8 Hz, 1H), 2.79 (ddt, *J* = 7.8, 6.9, 4.7 Hz, 1H), 2.66 – 2.58 (m, 3H), 2.45 (s, 3H), 2.09 (d, *J* = 4.6 Hz, 1H), 1.91 (dddd, *J* = 13.5, 8.6, 7.5, 4.8 Hz, 1H), 1.67 (dtd, *J* = 14.5, 8.0, 6.9 Hz, 1H), 1.36 (s, 9H) ppm. ^{13}C NMR (101 MHz, $CDCl_3$) δ 149.5, 144.7, 139.8, 135.2, 135.0, 132.4, 129.8, 129.4, 128.2, 127.7, 122.6, 114.4, 110.7, 83.6, 39.9, 34.1, 33.3, 32.9, 27.8, 21.8 ppm. IR (neat, cm^{-1}): 2979, 2931, 1734, 1597, 1515, 1474, 1456, 1393, 1370, 1309, 1255, 1144, 1091. HRMS calcd. for ($C_{26}H_{30}N_2NaO_4S$) $[M+Na]^+$: 489.1818 found 489.1822.

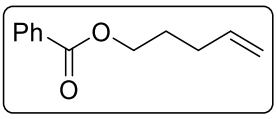

Pent-4-en-1-yl benzoate (S6): To a 100 mL round-bottomed flask under nitrogen, pent-4-en-1-ol (2.9 mL, 1.0 equiv., 28 mmol) and Et_3N (7.8 mL, 2.0 equiv., 56 mmol) were dissolved in CH_2Cl_2 (20 mL). To this solution cooled to 0 °C, benzoyl chloride (3.9 g, 3.3 mL, 28 mmol) was added drop wise over 10 min. The reaction mixture was stirred for an additional 50 min at 0 °C and at room temperature for 3 h. The reaction mixture was quenched with HCl (1.0 M, 50 mL), the layers were separated and the aqueous layer was extracted with Et_2O (30 mL). The combined organic layers were washed with aqueous $NaHCO_3$ (50 mL), dried ($MgSO_4$) and filtered. After evaporation of the solvent under reduced pressure, purification by column chromatography on silica gel, eluting with hexane:Et_2O (98:2) gave **S6** (4.6 g, 87 %). ^{1}H NMR (400 MHz, $CDCl_3$) δ 8.09 – 7.99 (m, 2H), 7.62 – 7.49 (m, 1H), 7.48 – 7.38 (m, 2H), 5.85 (ddt, *J* = 16.9, 10.2, 6.6 Hz, 1H), 5.07 (dq, *J* = 17.1, 1.7 Hz, 1H), 5.04 – 4.99 (m, 1H), 4.34 (t, *J* = 6.6 Hz, 2H), 2.27 – 2.17 (m, 2H), 1.93 – 1.80 (m, 2H) ppm. ^{13}C NMR (101 MHz, $CDCl_3$) δ 166.7, 137.6, 132.9, 130.5, 130.3, 129.6, 128.4, 115.5, 64.4, 30.3, 28.0 ppm. Spectroscopic data for **S6** match those previously reported in the literature.[136]

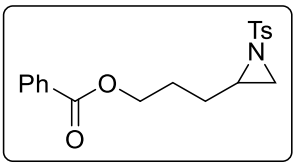

3-(1-Tosylaziridin-2-yl) propyl benzoate (2.1ae): Following **GP3** with **S6** (0.57 g, 3.0 mmol), purification by column chromatography on silica gel (hexane:EtOAc 9:1) afforded **2.1ae** as a white solid (0.44 g, 41%). ^{1}H NMR (400 MHz, $CDCl_3$) δ 8.04 – 7.97 (m, 2H), 7.87 – 7.73 (m, 2H), 7.61 – 7.52 (m, 1H), 7.49 – 7.39 (m, 2H), 7.33 (d, *J* = 7.9 Hz, 1H), 4.26 (td, *J* = 6.3, 2.2 Hz, 2H), 2.86 – 2.76 (m, 1H), 2.67 (d, *J* = 6.9 Hz, 1H), 2.42 (s, 3H), 2.11 (d, *J* = 4.5 Hz, 1H), 1.86 – 1.68 (m, 3H), 1.53 – 1.40 (m, 1H). ^{13}C NMR (101 MHz, $CDCl_3$) δ 166.6, 144.7, 135.2, 133.1, 130.3, 129.8, 129.7, 128.5, 128.2, 64.1, 39.7, 34.0, 28.1, 26.3, 21.7. LRMS (ESI): 359, 254, 237, 204, 155, 105, 91. Spectroscopic data for **2.1ae** match those previously reported in the literature.[121]

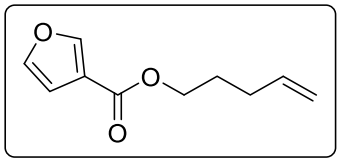

Pent-4-en-1-yl furan-3-carboxylate (S7): Following literature procedure,[137] a round-bottom flask was flame dried and charged with furan-3-carboxylic acid (0.56 g, 5.0 mmol), CH_2Cl_2 (25 ml), DMAP (61 mg, 0.50 mmol) and pent-4-en-1-ol (0.43 g, 5.0 mmol). A solution of DCC (1.0 g, 5.0 mmol) in CH_2Cl_2 (1.0 M, 5.0 ml) was then added and reaction was stirred at RT overnight. The resulting mixture was filtered through a pad of silica gel eluted with hexane:EtOAc (95:5) and the filtrate was concentrated *in vacuo* to afford **S7** as a colorless liquid (0.79 g, 88%). ^{1}H NMR (400 MHz, $CDCl_3$) δ 8.01 (dd, *J* = 1.6, 0.8 Hz, 1H), 7.42 (t, *J* = 1.7 Hz, 1H), 6.74 (dd, *J* = 1.9, 0.8 Hz, 1H), 5.83 (ddt, *J* = 16.9, 10.2, 6.6 Hz, 1H), 5.09 – 4.98 (m, 2H), 4.26 (t, *J* = 6.6 Hz, 2H), 2.22 – 2.14 (m, 2H), 1.87 – 1.78 (m, 2H) ppm. Spectroscopic data for **S7** match those previously reported in the literature.[137]

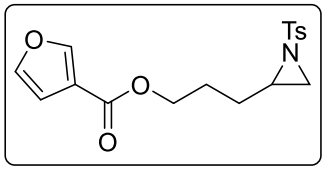

3-(1-Tosylaziridin-2-yl) propyl furan-3-carboxylate (2.1af): Following **GP3** with **S7** (0.80 g, 4.4 mmol), purification by column chromatography on silica gel (hexane:EtOAc 9:1 → 8:2) afforded **2.1af** as a colorless oil (0.53 g, 34%). ^{1}H NMR (400 MHz, $CDCl_3$) δ 7.98 (dd, *J* = 1.6, 0.8 Hz, 1H), 7.85 – 7.80 (m, 2H), 7.42 (t, *J* = 1.7 Hz, 1H), 7.36 – 7.31 (m, 2H), 6.72 (dd, *J* = 1.9, 0.8 Hz, 1H), 4.24 – 4.14 (m, 2H), 2.83 – 2.77 (m, 1H), 2.65 (d, *J* = 6.9 Hz, 1H), 2.43 (s, 3H), 2.09 (d, *J* = 4.6 Hz, 1H), 1.79 – 1.66 (m, 3H), 1.47 – 1.39 (m, 1H) ppm. ^{13}C NMR (101 MHz, $CDCl_3$) δ 163.1, 147.8, 144.8, 143.9, 135.1, 129.8, 128.1, 119.4, 109.9, 63.7, 39.7, 34.0, 28.2, 26.2, 21.8 ppm. IR (neat, cm^{-1}): 3149, 2957, 1718, 1597, 1578, 1507, 1452, 1404, 1304, 1234, 1155, 1076, 1007, 970, 942, 898, 873, 815, 762, 712, 691, 660, 603, 568, 550. HRMS calcd. for ($C_{17}H_{19}NNaO_5S$) $[M+H]^+$: 372.0876 found 372.0871.

General procedure 6 (GP7): Synthesis of pentenylated phenols (S8-11)

To the phenol (1.1 equiv.) and K_2CO_3 (2.0 equiv.) in MeCN (1.0 M) was added 5-bromopent-1-ene (1.0 equiv.). The reaction mixture was heated to 80 °C for 16 h and then allowed to cool to RT. The mixture was diluted with Et_2O (25 ml) and filtered, washing with Et_2O until all product had eluted. Purification was carried out by column chromatography (hexane:EtOAc 95:5).

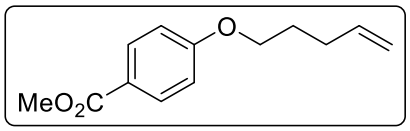

Methyl 4-(pent-4-en-1-yloxy) benzoate (S8): Following **GP7**, methyl 4-hydroxybenzoate (2.43 g, 1.1 equiv.) afforded **S8** (2.9 g, 87%) as an oil. ^{1}H NMR (400 MHz, $CDCl_3$) δ 8.02 – 7.94 (m, 2H), 6.94 – 6.86 (m, 2H), 5.85 (ddt, *J* = 16.9, 10.2, 6.7 Hz, 1H), 5.07 (dq, *J* = 17.1, 1.7 Hz, 1H), 5.01 (ddt, *J* = 10.2, 2.0, 1.2 Hz, 1H), 4.02 (t, *J* = 6.4 Hz, 2H), 3.88 (s, 3H), 2.30 – 2.19 (m, 2H), 1.96 – 1.85 (m, 2H) ppm. Spectroscopic data for **S8** match those previously reported in the literature.[138]

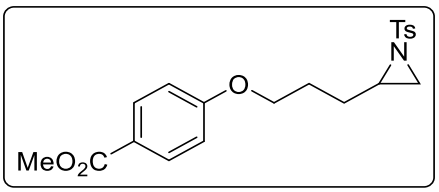

Methyl 4-(3-(1-tosylaziridin-2-yl)propoxy) benzoate (2.1aj): Following **GP3** with **S8** (0.44 g, 2.0 mmol) , purification by column chromatography on silica gel (hexane:EtOAc 9:1 → 8:2) afforded **2.1aj** as a white solid (0.21 g, 27%). M.P: 67 – 69 °C. ^{1}H NMR (500 MHz, $CDCl_3$) δ 7.99 – 7.95 (m, 2H), 7.83 – 7.78 (m, 2H), 7.33 – 7.29 (m, 2H), 6.87 – 6.83 (m, 2H), 3.97 (td, *J* = 6.2, 2.3 Hz, 2H), 3.88 (s, 3H), 2.83 (ddt, *J* = 8.1, 6.9, 4.5 Hz, 1H), 2.65 (d, *J* = 6.9 Hz, 1H), 2.42 (s, 3H), 2.09 (d, *J* = 4.6 Hz, 1H), 1.88 (dddd, *J* = 13.3, 8.9, 6.3, 4.4 Hz, 1H), 1.85 – 1.76 (m, 2H), 1.53 – 1.42 (m, 1H) ppm. ^{13}C NMR (126 MHz, $CDCl_3$) δ 167.0, 162.7, 144.7, 135.2, 131.7, 129.8, 128.1, 122.7, 114.2, 67.1, 52.0, 39.8, 34.0, 28.0, 26.6, 21.8 ppm. IR (neat, cm^{-1}): 2953, 2923, 2880, 1700, 1611, 1513, 1442, 1397, 1318, 1292, 1269, 1218, 1193, 1173, 1154, 1118, 1098, 1029, 1005. HRMS calcd. for ($C_{20}H_{23}NNaO_5S$) $[M+Na]^+$: 412.1189 found 412.1180.

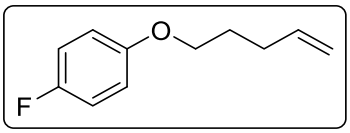

1-Fluoro-4-(pent-4-en-1-yloxy) benzene (S9): Following **GP7**, 4-fluorophenol (1.8 g, 1.1 equiv.) gave **S9** (2.0 g, 74%) as a colourless oil. ^{1}H NMR (400 MHz, $CDCl_3$) δ 7.01 – 6.91 (m, 2H), 6.87 – 6.78 (m, 2H), 5.85 (ddtd, *J* = 16.9, 10.1, 6.7, 0.9 Hz, 1H), 5.06 (dp, *J* = 17.2, 1.7 Hz, 1H), 5.00 (ddt, *J* = 10.2, 2.0, 1.2 Hz, 1H), 3.93 (t, *J* = 6.4 Hz, 2H), 2.29 – 2.19 (m, 2H), 1.93 – 1.81 (m, 2H) ppm. ^{19}F NMR (376 MHz, $CDCl_3$) δ -124.10 ppm. Spectroscopic data for **S9** match those previously reported in the literature.[139]

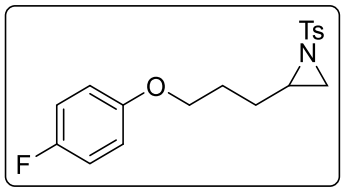

2-(3-(4-Fluorophenoxy)propyl)-1-tosylaziridine (2.1ak): Following **GP3** with **S9** (0.90 g, 5.0 mmol), purification by column chromatography on silica gel (hexane:EtOAc 9:1 → 8:2) afforded **2.1ak** as a colourless oil (0.37 g. 41%). M.P: 55 – 57 °C. ^{1}H NMR (400 MHz, $CDCl_3$) δ 7.84 – 7.77 (m, 2H), 7.34 – 7.30 (m, 2H), 7.01 – 6.90 (m, 2H), 6.85 – 6.73 (m, 2H), 3.94 – 3.79 (m, 2H), 2.82 (ddt, *J* = 8.1, 7.0, 4.5 Hz, 1H), 2.64 (d, *J* = 7.0 Hz, 1H), 2.43 (s, 3H), 2.09 (d, *J* = 4.6 Hz, 1H), 1.91 – 1.80 (m, 1H), 1.82 – 1.71 (m, 2H), 1.54 – 1.41 (m, 1H) ppm. ^{13}C NMR (101 MHz, $CDCl_3$) δ 158.5, 156.1, 155.1 (d, *J* = 2.2 Hz), 144.7, 135.2, 128.9 (d, *J* = 172.8 Hz), 115.9 (d, *J* = 23.0 Hz), 115.5 (d, *J* = 8.0 Hz).67.5, 39.9, 34.0, 28.1, 26.7, 21.7. ^{19}F NMR (376 MHz, $CDCl_3$) δ -124.19 (tt, *J* = 8.3, 4.3 Hz) ppm. IR (neat, cm^{-1}): 3071, 3055, 2953, 2932, 2879, 1595, 1504, 1474, 1392, 1318, 1293, 1245, 1200, 1154, 1095, 1028. HRMS calcd. for ($C_{18}H_{21}FNO_3S$) $[M+H]^+$: 350.1221 found 350.1225.

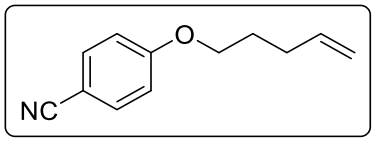

4-(Pent-4-en-1-yloxy) benzonitrile (S10): Following **GP7**, 4-hydroxybenzonitrile (1.2 g, 10 mmol), gave **S10** as a colourless oil (1.9 g, 99%). ^{1}H NMR (400 MHz, $CDCl_3$) δ 7.61 – 7.53 (m, 2H), 6.97 – 6.89 (m, 2H), 5.84 (ddt, *J* = 16.9, 10.2, 6.7 Hz, 1H), 5.06 (dq, *J* = 17.0, 1.6 Hz, 1H), 5.02 (ddt, *J* = 10.2, 1.8, 1.2 Hz, 1H), 4.01 (t, *J* = 6.4 Hz, 2H), 2.29 – 2.19 (m, 2H), 1.91 (tt, *J* = 7.0, 6.4 Hz, 2H) ppm. ^{13}C NMR (126 MHz, $CDCl_3$) δ 162.5, 137.5, 134.1, 119.4, 115.7, 115.3, 103.9, 67.7, 30.1, 28.2 ppm. Spectroscopic data for **S10** match those previously reported in the literature.[140]

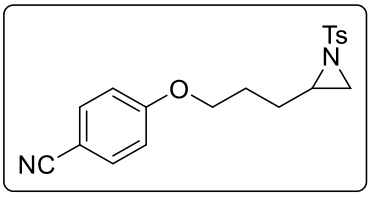

4-(3-(1-Tosylaziridin-2-yl)propoxy) benzonitrile (2.1al): Following **GP3** with **S10** (0.94 g, 5.0 mmol), purification by column chromatography on silica gel (hexane:EtOAc 9:1 → 6:4) gave **2.1al** as a white solid (0.93 g, 52%). M.P: 63 – 65 °C. ^{1}H NMR (400 MHz, $CDCl_3$) δ 7.82 (d, *J* = 8.3 Hz, 2H), 7.59 (d, *J* = 8.9 Hz, 2H), 7.32 (d, *J* = 8.0 Hz, 2H), 6.93 (d, *J* = 8.9 Hz, 2H), 4.02 (t, *J* = 6.0 Hz, 2H), 2.87 (ddt, *J* = 8.7, 7.0, 4.3 Hz, 1H), 2.65 (d, *J* = 7.0 Hz, 1H), 2.45 (s, 3H), 2.10 (d, *J* = 4.5 Hz, 1H), 1.99 – 1.79 (m, 3H), 1.55 – 1.42 (m, 1H) ppm. ^{13}C NMR (101 MHz, $CDCl_3$) δ 162.3, 144.8, 135.1, 134.1, 129.8, 128.1, 119.4, 115.3, 104.0, 67.2, 39.6, 34.1, 28.0, 26.5, 21.8 ppm. IR (neat, cm^{-1}): 2915, 2223, 1604, 1573, 1506, 1476, 1403, 1304, 1259, 1157, 1087, 1019. HRMS calcd. for ($C_{20}H_{21}N_2O_5S$) $[M+H]^+$: 357.1267 found 357.1260.

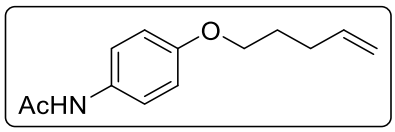

***N*-(4-(Pent-4-en-1-yloxy)phenyl) acetamide (S11)**: Following **GP6**, *N*-(4-hydroxyphenyl)acetamide (2.4 g, 16 mmol) gave **S11** as a colourless oil (2.4 g, 73%). ^{1}H NMR (400 MHz, $CDCl_3$) δ 7.41 – 7.32 (m, 2H), 7.09 (s, br, 1H), 6.91 – 6.80 (m, 2H), 5.85 (ddt, *J* = 16.9, 10.2, 6.6 Hz, 1H),

5.06 (dq, *J* = 17.1, 1.7 Hz, 1H), 4.99 (ddt, *J* = 10.2, 2.3, 1.3 Hz, 1H), 3.94 (t, *J* = 6.5 Hz, 2H), 2.28 – 2.17 (m, 2H), 2.15 (s, 3H), 1.87 (dq, *J* = 7.8, 6.5 Hz, 2H), 1.62 – 1.56 (m, 2H). Spectroscopic data for **S19** match those previously reported in the literature.[141]

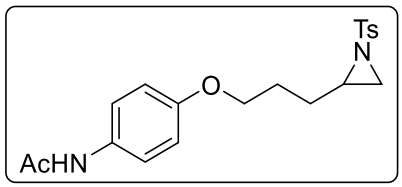

***N*-(4-(3-(1-Tosylaziridin-2-yl)propoxy)phenyl) acetamide (2.1am)**: Following **GP3** with **S11** (1.8 g, 8.0 mmol), purification by column chromatography (hexane:EtOAc 8:2 → 6:4) gave **2.1am** as a viscous oil (1.3 g, 43%). ^{1}H NMR (400 MHz, $CDCl_3$) δ 7.81 (d, *J* = 8.3 Hz, 2H), 7.37 (d, *J* = 9.0 Hz, 1H), 7.32 (d, *J* = 8.0 Hz, 2H), 7.17 (s, 1H), 6.79 (d, *J* = 9.0 Hz, 2H), 3.92 – 3.81 (m, 2H), 2.86 – 2.76 (m, 1H), 2.64 (d, *J* = 7.0 Hz, 1H), 2.43 (s, 3H), 2.14 (s, 3H), 2.09 (d, *J* = 4.6 Hz, 1H), 1.90 – 1.77 (m, 1H), 1.80 – 1.68 (m, 2H), 1.52 – 1.42 (m, 1H). ^{13}C NMR (101 MHz, $CDCl_3$) δ 168.1, 155.4, 144.4, 134.8, 130.9, 129.5, 127.8, 121.7, 114.5, 66.8, 39.7, 33.7, 27.8, 26.4, 24.1, 21.4. IR (neat, cm^{-1}): 3306, 3064, 2928, 1661, 1599, 1538, 1509, 1473, 1410, 1371, 1317, 1234, 1156, 1092, 1018. HRMS calcd. for ($C_{20}H_{25}N_2O_4S$) $[M+H]^+$: 389.1530 found 389.1532.

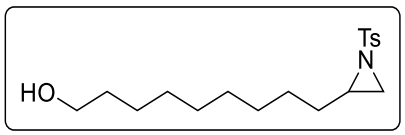

9-(1-Tosylaziridin-2-yl) nonan-1-ol (2.2aq): Following literature procedure[142] with 10-undecen-1-ol (4.0 ml, 20 mmol, 2.0 equiv.), **2.2aq** was isolated with trace uncyclized intermediate after purification by column chromatography on silica gel (CH_2Cl_2:Et_2O 2:1). This mixture was submitted to a base cyclization (**GP4**) to give **2.2aq** in >98% purity (2.5 g, 74%). ^{1}H NMR (400 MHz, $CDCl_3$) δ 7.86 – 7.79 (m, 2H), 7.37 – 7.29 (m, 2H), 3.63 (t, *J* = 6.6 Hz, 2H), 2.72 (tt, *J* = 7.3, 4.8 Hz, 1H), 2.63 (d, *J* = 7.0 Hz, 1H), 2.44 (s, 3H), 2.05 (d, *J* = 4.6 Hz, 1H), 1.61 – 1.47 (m, 4H), 1.41 – 1.13 (m, 12H) ppm. ^{13}C NMR (101 MHz, $CDCl_3$) δ 144.5, 135.4, 129.8, 128.1, 63.2, 40.6, 34.0, 32.9, 31.4, 29.5, 29.5, 29.4, 29.1, 26.9, 25.8, 21.8 ppm. LRMS (ESI): 701 (2M+Na), 679 (2M+H), 362 (M+Na), 340 (M+H). Spectroscopic data for **2.2aq** match those previously reported in the literature.[142]

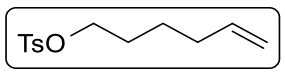

Hex-5-en-1-yl 4-methylbenzenesulfonate (S12): A solution of hex-5-en-1-ol (3.6 ml, 30 mmol, 1.0 equiv) in CH_2Cl_2 (60 mL) was cooled down to 0 °C. Et_3N (5.0 mL, 36 mmol, 1.2 equiv) and *p*-toluenesulfonyl chloride (5.7 g, 30 mmol, 1.0 equiv) were added subsequently. After addition, the reaction mixture was warmed to RT and stirred for 5 h. A aqueous solution of $NaHCO_3$ (sat.) was then added and the aqueous phase was extracted with EtOAc (3 x 60 ml). The combined organic phases were washed with brine (30 ml), dried ($MgSO_4$), filtered and concentrated *in vacuo*. Purification by column chromatography on silica gel (hexane:EtOAc 96:4 → 92:8) gave (6.4 g, 83 %) as a colorless liquid. ^{1}H NMR (400 MHz, $CDCl_3$): δ 7.81 – 7.77 (m, 2H), 7.37 – 7.31 (m, 2H), 5.72 (ddt, *J* = 17.0, 10.2, 6.7 Hz, 1H),

4.99 – 4.91 (m, 2H), 4.03 (t, *J* = 6.4 Hz, 2H), 2.45 (s, 3H), 2.00 (m, 2H), 1.65 (m, 2H), 1.46 – 1.36 (m, 2H) ppm. ^{13}C NMR (126 MHz, $CDCl_3$): δ 144.8, 138.0, 133.4, 130.0, 128.0, 115.2, 100.1, 70.6, 33.0, 28.4, 24.7, 21.8 ppm. Spectroscopic data for **S11** match those previously reported in the literature.[143]

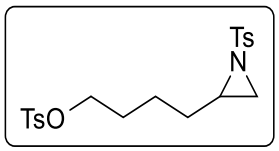

4-(1-Tosylaziridin-2-yl) butyl 4-methylbenzenesulfonate (2.1ar): Following **GP3** with **S12** (0.64 g, 2.5 mmol), purification by column chromatography on silica gel (hexane:EtOAc 9:1 → 8:2) afforded **2.1ar** as a colorless oil (0.57 g, 55%). ^{1}H NMR (400 MHz, $CDCl_3$) δ 7.84 – 7.76 (m, 2H), 7.80 – 7.73 (m, 2H), 7.38 – 7.33 (m, 2H), 7.36 – 7.30 (m, 2H), 3.91 (td, *J* = 6.4, 1.1 Hz, 2H), 2.67 (tt, *J* = 7.1, 4.5 Hz, 1H), 2.59 (d, *J* = 7.0 Hz, 1H), 2.45 (s, 6H), 2.01 (d, *J* = 4.5 Hz, 1H), 1.65 – 1.51 (m, 3H), 1.37 – 1.18 (m, 3H) ppm. ^{13}C NMR (126 MHz, $CDCl_3$) δ 144.9, 144.8, 135.1, 133.2, 130.0, 129.8, 128.1, 128.0, 70.2, 39.8, 33.8, 30.7, 28.2, 22.9, 21.8 ppm. IR (neat, cm^{-1}): 2927, 2867, 1597, 1495, 1455, 1354, 1320, 1232, 1174, 1157, 1094, 1019. HRMS calcd. for ($C_{20}H_{25}NNaO_5S_2$) $[M+Na]^+$: 446.1066 found 446.1060.

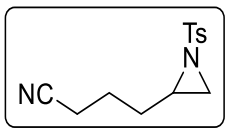

4-(1-Tosylaziridin-2-yl) butanenitrile (2.1as): Following **GP3** but keeping the reaction scale to 1.0 mmol, hex-5-enenitrile (3 × 0.12 mL, 3 × 1.0 mmol) afforded **2.1as** as a yellow oil (0.20 g, 25%) after purification of the combined reactions by column chromatography on silica gel (hexane:EtOAc 8:2 → 6:4). ^{1}H NMR (400 MHz, $CDCl_3$) δ 7.83 – 7.77 (m, 2H), 7.38 – 7.31 (m, 2H), 2.73 (ddt, *J* = 8.5, 7.0, 4.2 Hz, 1H), 2.61 (d, *J* = 7.0 Hz, 1H), 2.44 (s, 3H), 2.36 (td, *J* = 7.1, 2.5 Hz, 2H), 2.07 (d, *J* = 4.5 Hz, 1H), 1.89 (dddd, *J* = 14.3, 8.4, 6.5, 3.9 Hz, 1H), 1.67 (dqd, *J* = 8.9, 7.1, 1.9 Hz, 2H), 1.42 – 1.28 (m, 1H) ppm. ^{13}C NMR (101 MHz, $CDCl_3$) δ 145.0, 134.8, 129.9, 128.1, 119.2, 38.7, 33.8, 30.0, 23.0, 21.7, 16.5 ppm. IR (neat, cm^{-1}): 2941, 2246, 1597, 1455, 1404, 1319, 1291, 1233, 1157, 1091. HRMS calcd. for ($C_{13}H_{16}N_2NaO_2S$) $[M+Na]^+$: 287.0825 found 287.0820.

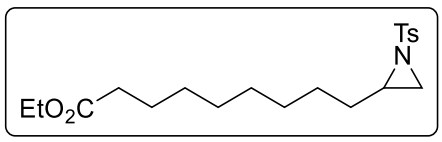

Ethyl 9-(1-tosylaziridin-2-yl) nonanoate (2.1at): Following **GP3** with ethyl undec-10-enoate (1.2 mL, 5.0 mmol), purification by column chromatography on silica gel (hexane:EtOAc 9:1 → 8:2) afforded **2.1at** as a colourless oil (1.2 g, 63%). ^{1}H NMR (400 MHz, $CDCl_3$) δ 7.92 (d, *J* = 8.3 Hz, 2H), 7.43 (d, *J* = 7.9 Hz, 2H), 4.22 (q, *J* = 7.1 Hz, 2H), 2.81 (tt, *J* = 7.3, 4.8 Hz, 1H), 2.73 (d, *J* = 7.0 Hz, 1H), 2.54 (s, 3H), 2.37 (t, *J* = 7.5 Hz, 2H), 2.15 (d, *J* = 4.6 Hz, 1H), 1.75 – 1.58 (m, 3H), 1.47 – 1.24 (m, 14H).^{13}C NMR (101 MHz, $CDCl_3$) δ 174.0, 144.5, 135.4, 129.8, 128.2, 60.3, 40.6, 34.5, 33.9, 31.4, 29.3, 29.2, 29.2, 29.1, 26.9, 25.1, 21.8, 14.4. IR (neat, cm^{-1}): 2928, 2855, 1731, 1597, 1457, 1373, 1323, 1305, 1232, 1184, 1158, 1090, 1033. HRMS calcd. for ($C_{20}H_{31}NNaO_4S$) $[M+Na]^+$: 404.1866 found 404.1859.

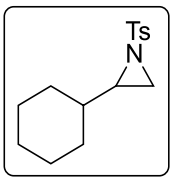

2-Cyclohexyl-1-tosylaziridine (2.1ao): Following **GP3** with vinylcyclohexane (0.79 g, 4.8 mmol), purification by column chromatography (hexane:EtOAc 9:1) gave **2.1ao** as a white solid (0.51 g, 38%). ^{1}H NMR (400 MHz, $CDCl_3$) δ 7.83 – 7.78 (m, 2H), 7.32 (d, *J* = 8.1 Hz, 2H), 2.59 (d, *J* = 7.0 Hz, 1H), 2.53 (td, *J* = 7.2, 4.5 Hz, 1H), 2.44 (s, 3H), 2.09 (d, *J* = 4.6 Hz, 1H), 1.73 – 1.55 (m, 4H), 1.49 (dtd, *J* = 12.4, 3.5, 1.7 Hz, 1H), 1.24 – 0.84 (m, 6H). ^{13}C NMR (101 MHz, $CDCl_3$) δ 144.5, 135.2, 129.7, 128.2, 45.3, 39.5, 32.8, 30.3, 29.7, 26.1, 25.7, 25.5, 21.8, 21.0. LRMS (ESI): 279 (M+), 252, 238, 210, 184, 155, 132, 91. Spectroscopic data for **2.1ao** match those previously reported in the literature.[121]

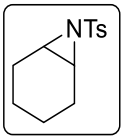

7-Tosyl-7-azabicyclo[4.1.0]heptane (2.8d): Following **GP3** with cyclohexene (4.1 ml, 40 mmol), purification by column chromatography on silica gel (hexane:EtOAc 9:1) afforded **2.8d** as a white solid (2.5 g, 25%). ^{1}H NMR (500 MHz, $CDCl_3$) δ 7.84 – 7.79 (m, 2H), 7.35 – 7.29 (m, 2H), 2.97 (p, *J* = 1.6 Hz, 2H), 2.44 (s, 3H), 1.83 – 1.73 (m, 4H), 1.45 – 1.33 (m, 2H), 1.27 – 1.16 (m, 2H) ppm. LRMS: 251, 223, 210, 197, 155, 96, 91. ^{13}C NMR (101 MHz, $CDCl_3$) δ 144.1, 136.1, 129.7, 127.8, 39.9, 22.9, 21.8, 19.6 ppm. Spectroscopic data for **1z** match those previously reported in the literature.[129]

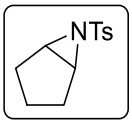

6-Tosyl-6-azabicyclo[3.1.0] hexane (2.8c): Following **GP3**, cyclopentene (1.8 ml, 20 mmol) gave **2.8c** as a white solid (4.2 g, 88%). ^{1}H NMR (400 MHz, $CDCl_3$) δ 7.83 – 7.78 (m, 2H), 7.36 – 7.28 (m, 2H), 3.33 (d, *J* = 1.4 Hz, 2H), 2.44 (s, 3H), 1.99 – 1.88 (m, 2H), 1.67 – 1.51 (m, 3H), 1.48 – 1.33 (m, 1H). Spectroscopic data for **2.8c** match those previously reported in the literature.[144]

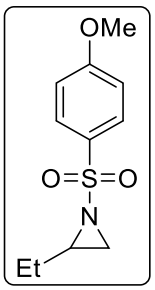

2-Ethyl-1-((4-methoxyphenyl)sulfonyl) aziridine (2.1ay): Following **GP1** but with 4-methoxybenzenesulfonyl chloride (6.7 g, 2.2 equiv., 33 mmol) instead of TsCl, (±)-2-amino-1-butanol (1.4 mL, 15 mmol) afforded **2.1ay** as a white solid (1.4 g, 39%) after purification by column chromatography on silica gel (hexane:EtOAc 3:1). M.P. = 59 – 61 °C. ^{1}H NMR (400 MHz, $CDCl_3$) δ 7.87 (d, *J* = 8.9 Hz, 2H), 7.00 (d, *J* = 8.9 Hz, 2H), 3.88 (s, 3H), 2.67 (tt, *J* = 7.4, 4.7 Hz, 1H), 2.61 (d, *J* = 6.7 Hz, 1H), 2.06 (d, *J* = 4.5 Hz, 1H), 1.64 – 1.56 (m, 1H), 1.30 –1.38 (m, 1H), 0.84 (t, *J* = 7.4 Hz, 3H). ^{13}C NMR (126 MHz, $CDCl_3$) δ 163.7, 130.3, 129.9, 114.3, 55.8, 41.8, 33.7, 24.6, 11.0. IR (neat, cm^{-1}): 3098, 3995, 2980, 2969, 2931, 2873, 2849, 1592, 1578, 1501, 1462, 1445, 1320, 1304, 1258, 1229, 1154, 1143, 1098, 1020. HRMS calcd. for ($C_{11}H_{15}NNaO_2S$) $[M+Na]^+$: 264.0665 found 264.0663.

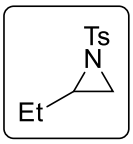

2-Ethyl-1-tosylaziridine (2.1az): Following **GP2**, (±)-2-amino-1-butanol (8.7 g, 98 mmol) afforded **2.1az** as a colourless oil (18 g, 81%) after purification by column chromatography on silica gel (hexane:EtOAc 9:1). ^{1}H NMR (400 MHz, $CDCl_3$) δ 7.82 (d, *J* = 8.3 Hz, 2H), 7.33 (d, *J* = 7.9 Hz, 2H), 2.69 (tt, *J* = 7.2, 4.7 Hz, 1H), 2.62 (d, *J* = 7.0 Hz, 1H), 2.44 (s, 3H), 2.07 (d, *J* = 4.6 Hz, 1H), 1.67 – 1.52 (m, 1H), 1.30 – 1.38 (m, 1H), 0.83 (t, *J* = 7.5 Hz, 3H) ppm. ^{13}C NMR (101 MHz, $CDCl_3$) δ 144.5, 135.3, 129.7, 128.1, 41.8, 33.7, 24.6, 21.7, 11.0 ppm. Spectroscopic data for **2.1az** match those previously reported in the literature.[145]

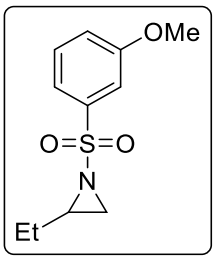

2-Ethyl-1-((3-methoxyphenyl)sulfonyl) aziridine (2.1ba): Following **GP1** but with 3-methoxybenzenesulfonyl chloride (3.6 g, 2.2 equiv., 18 mmol) instead of TsCl, (±)-2-amino-1-butanol (0.76 mL, 8.0 mmol) afforded **2.1ba** as a colourless oil (0.84 g, 44%) after purification by column chromatography on silica gel (hexane:EtOAc 3:1). ^{1}H NMR (500 MHz, $CDCl_3$) δ 7.50 (ddd, *J* = 7.7, 1.7, 1.0 Hz, 1H), 7.45 – 7.39 (m, 2H), 7.13 (ddd, *J* = 8.3, 2.7, 1.1 Hz, 1H), 3.85 (s, 3H), 2.71 (tt, *J* = 7.1, 4.8 Hz, 1H), 2.63 (d, *J* = 7.0 Hz, 1H), 2.08 (d, *J* = 4.7 Hz, 1H), 1.60 (dqd, *J* = 14.8, 7.5, 4.9 Hz, 1H), 1.35 (dp, *J* = 14.8, 7.4 Hz, 1H), 0.83 (t, *J* = 7.4 Hz, 3H) ppm. ^{13}C NMR (126 MHz, $CDCl_3$) δ 159.9, 139.3, 130.1, 120.2, 120.1, 112.6, 55.8, 41.9, 33.8, 24.5, 10.9 ppm. IR (neat, cm^{-1}): 3074, 2968, 2938, 2879, 2839, 1598, 1483, 1464, 1433, 1311, 1287, 1241, 1152, 1099, 1031. HRMS calcd. for ($C_{11}H_{15}NNaO_2S$) $[M+Na]^+$: 264.0665 found 264. 0668.

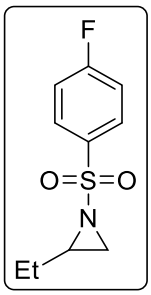

2-Ethyl-1-((4-fluorophenyl)sulfonyl) aziridine (2.1bb): Following **GP1** but with 4-fluorobenzenesulfonyl chloride (13 g, 66 mmol) instead of TsCl, (±)-2-amino-1-butanol (2.8 mL, 30 mmol) afforded **2.1bb** as a colourless oil (2.5 g, 36%) after purification by column chromatography on silica gel (hexane:EtOAc 9:1). ^{1}H NMR (400 MHz, $CDCl_3$) δ 7.99 – 7.94 (m, 2H), 7.24 – 7.19 (m, 2H), 2.72 (tt, *J* = 7.3, 4.7 Hz, 1H), 2.65 (d, *J* = 7.0 Hz, 1H), 2.10 (d, *J* = 4.6 Hz, 1H), 1.62 (dqd, *J* = 14.8, 7.4, 5.0 Hz, 1H), 1.34 (dq, *J* = 14.7, 7.4 Hz, 1H), 0.83 (t, *J* = 7.5 Hz, 3H) ppm. ^{13}C NMR (101 MHz, $CDCl_3$) 165.8 (d, *J* = 255.8 Hz), 134.5 (d, *J* = 3.3 Hz), 130.9 (d, *J* = 9.5 Hz), 116.4 (d, *J* = 22.7 Hz), 42.1, 33.9, 24.6, 10.9 ppm. ^{19}F NMR (376 MHz, $CDCl_3$) δ -103.63 (tt, *J* = 8.2, 5.0 Hz) ppm. IR (neat, cm^{-1}): 3106, 3075, 2970, 2937, 2880, 1591, 1493, 1461, 1405, 1323, 1291, 1230, 1166, 1152, 1096, 1085, 1026. 920. HRMS calcd. for ($C_{10}H_{12}FNNaO_2S$) $[M+Na]^+$: 252.0465 found 252.0461.

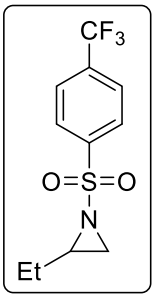

2-Ethyl-1-((4-(trifluoromethyl)phenyl)sulfonyl) aziridine (2.1bc): Following **GP1** but with a 3 h reaction time, using (±)-2-amino-1-butanol (0.11 mL, 1.2 mmol) and 4-trifluoromethylbenzenesulfonyl chloride (0.65 g, 2.6 mmol), purification by column chromatography on silica gel (hexane:EtOAc 9:1) afforded **2.1bc** as a colourless oil (0.56 g, 80%). ^{1}H NMR (400 MHz, $CDCl_3$) δ 8.14 – 8.06 (m, 2H), 7.86 – 7.77 (m, 2H), 2.82 (tt, *J* = 7.2, 4.8 Hz, 1H), 2.70 (d, *J* = 7.0 Hz, 1H), 2.14 (d, *J* = 4.7 Hz, 1H), 1.64 (dtd, *J* = 14.8, 7.4, 4.9 Hz, 1H), 1.40 (dp, *J* = 14.7, 7.4 Hz, 1H), 0.87 (t, *J* = 7.5 Hz, 3H). ^{13}C NMR (101 MHz, $CDCl_3$) δ 142.1 (q, *J* = 1.0 Hz), 135.3 (q, *J* = 33.0 Hz), 128.6, 126.3 (q, *J* = 3.7 Hz), 123.3 (q, *J* = 273.0 Hz), 42.4, 34.2, 24.5, 10.9. ^{19}F NMR (376 MHz, $CDCl_3$) δ -62.92. IR (neat, cm^{-1}): 2972, 2938, ,1461, 1404, 1319, 1233, 1162, 1129, 1106, 1087, 1061, 1016. HRMS calcd. for ($C_{11}H_{12}F_3NNaOS$) $[M+Na]^+$: 302.0433 found 302.0434.

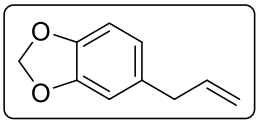

5-Allylbenzo[d][1,3]dioxole (S13): 5-bromobenzo[d][1,3]dioxole (6.0 g, 30 mmol) was dissolved in dry THF (20 ml) and Mg stirrings (1.1 g, 45 mmol) were added. Formation of the organomagnesium compound was promoted by addition of catalytic amount of I_2 at room temperature (caution! reaction is very exothermic; condenser is required). After reaction completion, the resulting solution was added drop wise to a solution of allyl bromide (2.6 ml, 30 mmol) in dry THF (20 ml). After addition reaction was stirred at room temperature for 1 hour. Then reaction mixture was quenched with aqueous NH_4Cl (sat.) and the organic phase was washed with water. After drying ($MgSO_4$) and concentrating *in vacuo*, the crude material was purified by column chromatography on silica gel (pure pentane) to afford **S13** (4.3 g, 88%) as a colorless liquid. ^{1}H NMR (400 MHz, $CDCl_3$) δ 6.75 (d, *J* = 7.9 Hz, 1H), 6.70 (d, *J* = 1.4 Hz, 1H), 6.67 – 6.63 (m, 1H), 5.98 – 5.94 (m, 1H), 5.93 (s, 2H), 5.11 – 5.04 (m, 2H), 3.34 – 3.29 (m, 2H) ppm. Spectroscopic data for **S12** match those previously reported in the literature.[146]

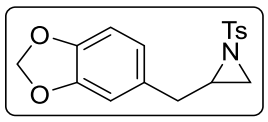

2-(Benzo[d][1,3]dioxol-5-ylmethyl)-1-tosylaziridine (2.1aw): Following **GP3** with **S13** (4.3 g, 27 mmol), purification by column chromatography on silica gel (hexane:EtOAc 9:1 → 5:1) afforded **2.1aw** as a white solid (2.9 g, 32%). ^{1}H NMR (400 MHz, $CDCl_3$) δ 7.71 – 7.65 (m, 2H), 7.25 – 7.21 (m, 2H), 6.60 – 6.56 (m, 1H), 6.50 – 6.46 (m, 2H), 5.90 (q, *J* = 1.4 Hz, 1H), 2.91 – 2.83 (m, 1H), 2.76 (dd, *J* = 14.5, 4.8 Hz, 1H), 2.72 (d, *J* = 6.9 Hz, 1H), 2.52 (dd, *J* = 14.5, 7.5 Hz, 1H), 2.43 (s, 3H), 2.15 (d, *J* = 4.5 Hz, 1H) ppm. ^{13}C NMR (101 MHz, $CDCl_3$) δ 147.6, 146.4, 144.5, 135.0, 130.9, 129.6, 128.1, 121.9, 109.3, 108.3, 101.0, 41.6, 37.3, 32.9, 21.7 ppm. LRMS (ESI): 331, 176, 161, 148, 135, 119, 105, 91, 77. Spectroscopic data for **2.1aw** match those previously reported in the literature.[147]

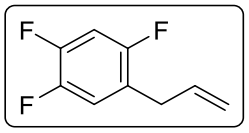

1-Allyl-2,4,5-trifluorobenzene (S14): Following a modified literature procedure,[147] a flame dried RBF was charged with 1-bromo-2,4,5-trifluorobenzene (4.4 g, 20 mmol) and THF (dry, 5.0 ml) under Ar atmosphere. The solution was cooled to –10 °C in an ice/salt bath and then *i*PrMgCl·LiCl (1.2 M in THF, 21 mmol) was added drop wise to reaction mixture. After stirring at 0 °C for 1 h, allyl bromide (1.8 ml, 21 mmol) was added drop wise. Obtained mixture was additionally stirred at 0 °C for 1 h and then warmed to RT and stirred overnight. The reaction was quenched with water and acidified to pH = 1 with aqueous HCl (2.0 M). The layers were separated and the aqueous phase was extracted with EtOAc. The combined organic fractions were washed with brine, dried ($MgSO_4$), filtered and concentrated *in vacuo*. The crude mixture was purified by flushing through a plug of silica gel using pentane as an eluent to afford **S14** as a colorless liquid (2.9 g, 85%). ^{1}H NMR (400 MHz, $CDCl_3$) δ 7.00 (ddd, *J* = 10.8, 8.8, 6.8 Hz, 1H), 6.89 (ddd, *J* = 10.2, 9.1, 6.6 Hz, 1H), 5.89 (ddt, *J* = 16.8, 10.1, 6.5 Hz, 1H), 5.13 (dq, *J* = 10.1, 1.4 Hz, 1H), 5.09 (dqd, *J* = 16.9, 1.6, 0.5 Hz, 1H), 3.36 – 3.32 (m, 2H) ppm.

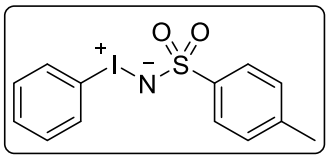

(Tosylimino) phenyliodinane (S15): Following literature procedure,[148] toluenesulfonamide (2.8 g, 16 mmol) and KOH (2.3 g, 41 mmol) were dissolved in MeOH (60 ml). The resulting solution was cooled to –10 °C in an ice/salt bath and (diacetoxy) iodosobenzene (5.3 g, 17 mmol) was added portion-wise. The reaction was stirring 30 minutes at –10 °C and then warmed up to room temperature and stirred additionally 3 hours. Ice cold water (100 ml) was then added and resulting mixture was cooled to 0 °C. Formed precipitate was collected by filtration and washed with cold MeOH (20 ml) and EtOAc (100 ml) to afford **S15** (3.2 g, 53%) as a colorless solid. ^{1}H NMR (400 MHz, DMSO-d_6) δ 7.71 – 7.67 (m, 2H), 7.49 – 7.41 (m, 3H), 7.29 (t, *J* = 7.7 Hz, 2H), 7.09 – 7.03 (m, 2H), 2.27 (s, 3H) ppm. Spectroscopic data for **S15** match those previously reported in the literature.[148]

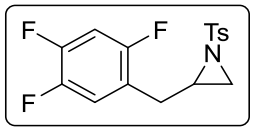

1-Tosyl-2-(2,4,5-trifluorobenzyl) aziridine (2.1ax): A flame dried Schlenk flask was charged with anhydrous $Cu(OTf)_2$ (0.27 mg, 0.74 mmol) and solution of 1-allyl-2,4,5-trifluorobenzene (**S14**) (1.3 g, 3.0 equiv., 7.5 mmol) in dry MeCN (8.0 ml). **S15** (0.93 g, 1.0 equiv., 2.5 mmol) was then added into the reaction solution in one portion under the flow of argon. The resulting mixture was stirred at room temperature for 2 hours. After time, reaction was diluted with EtOAc and filtered through a pad of silica gel followed by elution with additional amount of EtOAc. Obtained solution was concentrated *in vacuo*, and the crude material was purified by column chromatography on silica gel (hexane:EtOAc 9:1 → 5:1) afforded **2.1ax** as a colorless solid (0.53 g, 42%). ^{1}H NMR (400 MHz,

$CDCl_3$) δ 7.65 – 7.61 (m, 2H), 7.22 – 7.18 (m, 2H), 6.79 – 6.66 (m, 2H), 3.07 – 3.01 (m, 1H), 2.87 – 2.79 (m, 2H), 2.42 (s, 3H), 2.28 (ddd, *J* = 14.5, 8.3, 1.5 Hz, 1H), 2.20 (d, *J* = 4.2 Hz, 1H) ppm. ^{13}C NMR (101 MHz, $CDCl_3$) δ 155.6 (ddd, *J* = 244.5, 9.3, 2.7 Hz), 149.2 (ddd, *J* = 250.0, 14.5, 12.2 Hz), 146.4 (ddd, *J* = 244.8, 12.6, 3.7 Hz), 145.0, 134.6, 129.7, 127.9, 120.8 (ddd, *J* = 18.4, 5.7, 4.2 Hz), 118.7 (ddd, *J* = 19.2, 5.9, 1.4 Hz), 105.2 (dd, *J* = 28.2, 20.8 Hz), 40.1, 32.8, 30.5, 21.6 ppm. ^{19}F (367 MHz, $CDCl_3$) δ (-119.9) – (-120.1) (m), -135.64 (dtd, *J* = 21.9, 9.6, 3.4 Hz), -142.54 (dddd, *J* = 21.6, 15.2, 10.3, 6.5 Hz) ppm. LRMS (ESI): 321, 176, 161, 148, 135, 119, 105, 91, 77. Spectroscopic data for **2.1ax** match those previously reported in the literature.[147]

2.7.5 Synthesis of *β*-amino acids

General procedure 8 (GP8): Ni-catalyzed coupling of aziridines with CO_2

To an oven dried Schlenk tube in the glove box was added $NiCl_2$glyme (4.4 mg, 0.020 mmol), **L1** (9.8 mg, 0.040 mmol), Mn (33 mg, 0.60 mmol) and the aziridine (1.0 equiv., 0.20 mmol) if solid. A stirrer bar was added and the Schlenk was capped before being removed from the glove box. An atmosphere of CO_2 was generated by 3 cycles between vacuum (< 1 mbar pressure) and CO_2 line (1 atm). Under a flow of CO_2, dry DMPU (0.40 M, 0.50 ml) was added followed by the aziridine (1.0 equiv. 0.20 mmol) if liquid and MeOH (40 μl, 1.0 mmol). Note: between each addition, the Schlenk tube was manually agitated for ~10 s. The Schlenk tube was then capped and stirred at 10 °C for the specified time.[ii] The reaction was quenched by addition of HCl (1.0 M, 2.0 ml) at 10 °C, diluted with EtOAc and then stirred at RT. The layers were separated and the aq. layer extracted with EtOAc (3 × 5 ml). The combined organic layers were washed twice with HCl (1.0 M, 15 ml), dried ($MgSO_4$), filtered and concentrated *in vacuo*. Purification was carried out by column chromatography on silica gel. The crude reaction mixture was dissolved in CH_2Cl_2:Et_3N (1.0 ml:0.2 ml) and loaded onto a short plug of silica equilibrated with hexane:EtOAc (1:1). A second wash of the flask was performed using CH_2Cl_2:Et_3N (1.0 ml:0.2 ml) and a third with CH_2Cl_2 (1.0 ml). The impurities of the reaction were removed by flushing through hexane:EtOAc (1:1, 100 ml) and the product was eluted with EtOAc:AcOH (98:2).

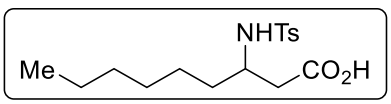

3-((4-Methylphenyl)sulfonamido) nonanoic acid (2.2a): Following **GP8** with a reaction time of 3 days, **2.1a** (52 μl, 0.20 mmol) gave **2.2a** (45 mg, 69%) as a white solid. In a scale up experiment **2.1a** (0.13 ml, 0.50 mmol) gave **2.2a** (0.12 g,73%) giving an average yield of 71%. ^{1}H NMR (400 MHz, $CDCl_3$) δ 7.78 (d, *J* = 8.3 Hz, 2H), 7.32 (d, *J* = 8.0 Hz, 2H), 5.39 (d, *J* = 9.1 Hz,

[ii] Although high yields and conversions can be obtained after 48 h, the inability to monitor the progress of these pressurized reactions meant that they were generally run for 72 h to ensure complete consumption of the aziridine and the maximum possible yield. In certain cases, the reaction stalled with significant aziridine remaining and prolonged reaction times did not lead to more acid being generated.

1H), 3.57 – 3.48 (m, 1H), 2.57 – 2.50 (m, 2H), 2.44 (s, 3H), 1.54 – 1.43 (m, 2H), 1.29 – 1.05 (m, 8H), 0.86 (t, *J* = 7.2 Hz, 3H) ppm. ^{13}C NMR (101 MHz, $CDCl_3$) δ 143.6, 138.0, 129.8, 127.2, 50.7, 39.0, 34.7, 31.7, 28.8, 25.8, 22.6, 21.6, 14.2 ppm. LRMS (ESI): 653 (2M-H), 440 (M+TFA$^-$), 326 (M-H). Spectroscopic data for **2.2a** match those previously reported in the literature.[149]

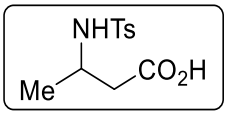

3-((4-Methylphenyl)sulfonamido) butanoic acid (2.2b): Following **GP8** with a reaction time of 3 days, **2.1b** (42 mg, 0.20 mmol) gave **2.2b** (34 mg, 66%) as a white solid. In a separate independent experiment **2.2b** (33 mg, 64%) was isolated giving an average yield of 65%. ^{1}H NMR (400 MHz, $CDCl_3$) δ 7.76 (d, *J* = 8.3 Hz, 2H), 7.32 – 7.29 (m, 2H), 5.38 (d, *J* = 8.5 Hz, 1H), 3.77 – 3.66 (m, 1H), 2.51 (d, *J* = 5.3 Hz, 2H), 2.42 (s, 3H), 1.16 (d, *J* = 6.7 Hz, 3H) ppm. ^{13}C NMR (101 MHz, $CDCl_3$) δ 176.0, 143.7, 137.9, 129.9, 127.2, 46.4, 40.6, 21.7, 21.0 ppm. Spectroscopic data for **2.2b** match those previously reported in the literature.[150]

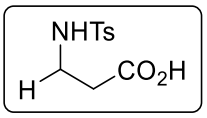

3-((4-Methylphenyl)sulfonamido) propanoic acid (2.2c): Following **GP8** with a reaction time of 2 days,[iii] *N*-tosylaziridine (40 mg, 0.20 mmol) gave **2.2c** (20 mg, 41%) as a white solid. In a separate independent experiment **2.2c** (19 mg, 39%) was isolated giving an average yield of 40%. ^{1}H NMR (400 MHz, $CDCl_3$) δ 7.75 (d, *J* = 8.3 Hz, 2H), 7.34 – 7.29 (m, 2H), 5.81 (t, *J* = 6.7 Hz, 1H), 3.23 – 3.15 (m, 2H), 2.62 (t, *J* = 5.7 Hz, 2H), 2.43 (s, 3H) ppm. ^{13}C NMR (101 MHz, $CDCl_3$) δ 176.0, 143.8, 137.0, 130.0, 127.2, 38.4, 34.0, 21.7 ppm. LRMS (ESI): 485 (2M-H), 278 (M+Cl), 242 (M-H). Spectroscopic data for **2.2c** match those previously reported in the literature.[150]

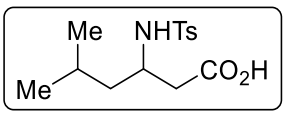

5-Methyl-3-((4-methylphenyl)sulfonamido) hexanoic acid (2.2d): Following **GP8** with a reaction time of 5 days,[iv] **2.1d** (46 μl, 0.20 mmol) gave **2.2d** (43 mg, 72%) as a white solid. In a separate independent experiment **2.2d** (49 mg, 82%) was isolated giving an average yield of 77%. ^{1}H NMR (400 MHz, $CDCl_3$) δ 7.76 (d, *J* = 8.3 Hz, 2H), 7.32 – 7.27 (m, 2H), 5.43 (d, *J* = 9.1 Hz, 1H), 3.57 (tq, *J* = 10.0, 5.1 Hz, 1H), 2.47 (d, *J* = 5.0 Hz, 2H), 2.42 (s, 3H), 1.59 – 1.47 (m, 1H), 1.41 (ddd, *J* = 14.4, 8.9, 5.6 Hz, 1H), 1.30 – 1.22 (m, 2H), 0.80 (d, *J* = 6.6 Hz, 3H), 0.69 (d, *J* = 6.5 Hz, 3H) ppm. ^{13}C NMR (101 MHz, $CDCl_3$) δ 176.7, 143.7, 138.0, 129.9, 127.2, 48.7, 43.9, 39.1, 24.6, 22.8, 21.8, 21.7

[iii] The reaction was complete after 48 h due to the reduced steric environment of the aziridine. Although most by-products generated in this reaction are volatile and hence not observed, the large amount of $TsNH_2$ (45%) generated suggests *β*-hydride and deamination pathways are more prevalent.
[iv] The steric hindrance of the *i*Bu group reduces the rate of the reaction but complete conversion is reached if a longer reaction time is used. Conversely, the reaction is more selective for the desired *β*-amino acid with only trace amounts of $TsNH_2$ (5-10%) observed.

ppm. LRMS (ESI): 597 (2M-H), 298 (M-H). Spectroscopic data for **2.2d** match those previously reported in the literature.[151]

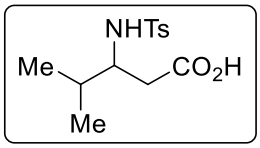

4-Methyl-3-((4-methylphenyl)sulfonamido) pentanoic acid (2.2e): Following **GP8** with a reaction time of 7 days,[v] **2.1e** (48 mg, 0.20 mmol) gave **2.2e** (24 mg, 42%) as a white solid. In a separate independent experiment **2.2e** (23 mg, 40%) was isolated giving an average yield of 41%. ^{1}H NMR (400 MHz, $CDCl_3$) δ 7.76 (d, *J* = 8.3 Hz, 2H), 7.29 (d, *J* = 8.0 Hz, 2H), 5.33 (d, *J* = 9.2 Hz, 1H), 3.40 – 3.28 (m, 1H), 2.50 (dd, *J* = 16.2, 5.1 Hz, 1H), 2.45 – 2.38 (m, 4H), 1.83 (hept, *J* = 6.8 Hz, 1H), 0.83 (dd, *J* = 6.8, 5.8 Hz, 6H) ppm. ^{13}C NMR (101 MHz, $CDCl_3$) δ 176.8, 143.6, 137.9, 129.8, 127.3, 56.2, 36.4, 31.7, 21.7, 19.1, 18.7 ppm. LRMS (ESI): 569 (2M-H), 284 (M-H). Spectroscopic data for **2e** match those previously reported in the literature.[152]

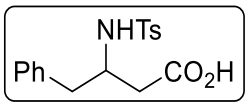

3-((4-Methylphenyl)sulfonamido)-4-phenyl butanoic acid (2.2f): Following **GP8** with a reaction time of 3 days and the temperature maintained at 10−13 °C for the duration, **2.1f** (0.29 g, 1.0 mmol) gave **2.2f** (0.21 g, 63%) as a white solid. In a separate independent experiment **2.2f** (0.20 g, 60%) was isolated giving an average yield of 62%. Note/ when performing the reaction on larger scale, it is important to ensure efficient stirring due to the non-homogenous nature of the reaction. M.P. = 103 – 106 °C. ^{1}H NMR (400 MHz, $CDCl_3$) δ 7.63 (d, *J* = 8.3 Hz, 2H), 7.24 – 7.18 (m, 5H), 7.04 – 7.00 (m, 2H), 5.58 (d, *J* = 8.5 Hz, 1H), 3.84 – 3.68 (m, 1H), 2.87 (dd, *J* = 13.7, 7.6 Hz, 1H), 2.79 (dd, *J* = 13.7, 6.7 Hz, 1H), 2.56 (d, *J* = 5.3 Hz, 2H), 2.40 (s, 3H) ppm. ^{13}C NMR (101 MHz, $CDCl_3$) δ 176.4, 143.6, 137.3, 136.9, 129.8, 129.4, 128.8, 127.1, 127.0, 51.9, 40.7, 37.9, 21.6 ppm. LRMS (ESI): 334 $(M+H)^+$, 356 $(M+Na)^+$. Spectroscopic data for **2.2f** match those previously reported in the literature.[150] HPLC: *rac* (CHIRALPAK® IC, hexane/ *i*-PrOH/ TFA = 75:25:0.1, 1 mL/min, 220 nm, t_R= 11.839; 14.084).

[v] After 3 days with this hindered substrate, 27% of **2.2e** was observed by ^{1}H NMR and 66% **2.1e** remained. After 7 days, 41% of **2.2e** was observed by and 45% **2.1e** remained. After 10 days, 42% of **2.2e** was observed and 50% **2.1e** still remained suggesting the reaction had stalled and the maximum amount of **2.2e** had been reached. Various reaction variables were modified to try and improve the yield such as increasing the [Ni] to 20mol%, switching to less hindered **L4** and increasing the temperature without success.

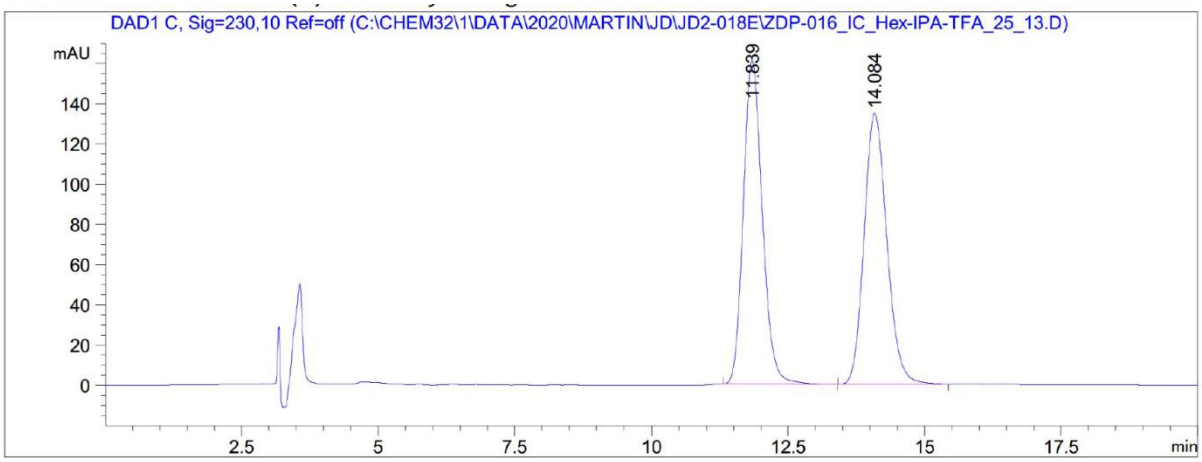

Peak #	RetTime [min]	Type	Width [min]	Area [mAU*s]	Height [mAU]	Area %
1	11.839	BB	0.3728	3899.17773	160.85664	49.9536
2	14.084	BB	0.4482	3906.41431	134.74947	50.0464
Totals :				7805.59204	295.60611	

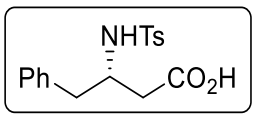

(S)-3-((4-Methylphenyl)sulfonamido)-4-phenyl butanoic acid ((S)-**2.2f)**: Following **GP8** with a reaction time of 3 days, (S)-**2.1f** (57 mg, 0.20 mmol) gave (S)-**2.2f** (47 mg, 70%) as a white solid. ^{1}H NMR (400 MHz, $CDCl_3$) δ 7.63 (d, *J* = 8.3 Hz, 2H), 7.24 – 7.18 (m, 5H), 7.04 – 7.00 (m, 2H), 5.58 (d, *J* = 8.5 Hz, 1H), 3.84 – 3.68 (m, 1H), 2.87 (dd, *J* = 13.7, 7.6 Hz, 1H), 2.79 (dd, *J* = 13.7, 6.7 Hz, 1H), 2.56 (d, *J* = 5.3 Hz, 2H), 2.40 (s, 3H) ppm. ^{13}C NMR (101 MHz, $CDCl_3$) δ 176.4, 143.6, 137.3, 136.9, 129.8, 129.4, 128.8, 127.1, 127.0, 51.9, 40.7, 37.9, 21.6 ppm. Spectroscopic data for (S)-**2.2f** match those previously reported in the literature.[150] HPLC: *rac* (CHIRALPAK® IC, hexane/ *i*-PrOH/ TFA = 75:25:0.1, 1 mL/min, 220 nm, t_R= 14.043).

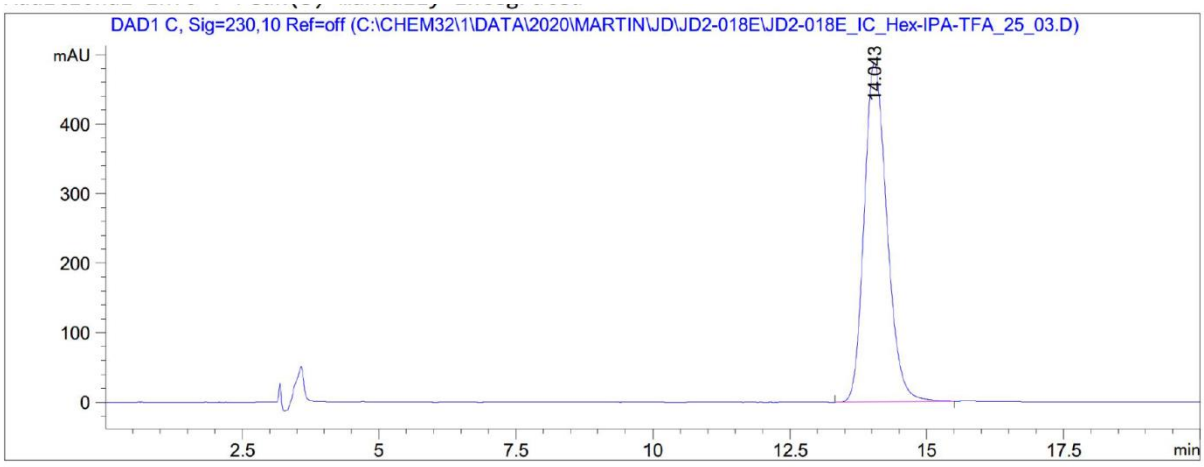

Peak #	RetTime [min]	Type	Width [min]	Area [mAU*s]	Height [mAU]	Area %
1	14.043	BB	0.4473	1.40904e4	487.42010	100.0000
Totals :				1.40904e4	487.42010	

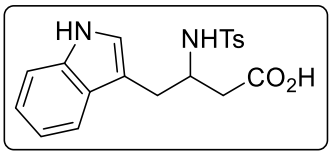

4-(1H-Indol-3-yl)-3-((4-methylphenyl)sulfonamido) butanoic acid (2.2g): Following **GP8** with a reaction time of 6 days,[vi] **2.1g** (65 mg, 0.20 mmol) gave **2.2g** (39 mg, 52%) as a pink solid. In a separate independent experiment **2.2g** (40 mg, 54%) was isolated giving an average yield of 53%. M.P: 178 – 180 °C. ^{1}H NMR (400 MHz, MeOD)[vii] δ 7.40 – 7.36 (m, 2H), 7.34 (dt, *J* = 8.0, 1.0 Hz, 1H), 7.24 (dt, *J* = 8.2, 0.9 Hz, 1H), 7.04 (ddd, *J* = 8.1, 7.0, 1.0 Hz, 1H), 6.97 (d, *J* = 8.0 Hz, 2H), 6.93 (s, 1H), 6.89 (ddd, *J* = 8.0, 7.0, 1.0 Hz, 1H), 3.82 (tt, *J* = 7.7, 5.4 Hz, 1H), 2.94 (dd, *J* = 14.4, 5.7 Hz, 1H), 2.74 (dd, *J* = 14.3, 7.9 Hz, 1H), 2.60 (dd, *J* = 15.9, 5.1 Hz, 1H), 2.48 (dd, *J* = 15.9, 7.7 Hz, 1H), 2.27 (s, 3H). ^{13}C NMR (101 MHz, MeOD) δ 144.0, 138.7, 138.1, 130.1, 128.5, 127.6, 124.5, 122.2, 119.6, 119.3, 112.2, 111.5, 52.6, 41.3, 31.7, 21.5. IR (neat, cm^{-1}): 3410, 3276, 3055, 2922, 1707, 1598, 1457, 1419, 1317, 1290, 1150, 1088, 1019. HRMS calcd. for ($C_{19}H_{19}N_2O_4S$) $[M–H]^–$: 371.1071 found 371.1073.

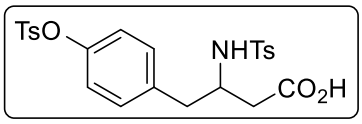

3-((4-Methylphenyl)sulfonamido)-4-(4-(tosyloxy)phenyl) butanoic acid (2.2l): Following **GP8** with a reaction time of 7 days,[viii] **2.1l** (92 mg, 0.20 mmol) gave **2.2l** (44 mg, 44%) as a white solid. In a separate independent experiment **2.2l** (38 mg, 38%) was isolated giving an average yield of 42%. ^{1}H NMR (400 MHz, $CDCl_3$) δ 7.68 (d, *J* = 8.0 Hz, 2H), 7.57 (d, *J* = 7.9 Hz, 2H), 7.30 (d, *J* = 8.0 Hz, 2H), 7.21 (d, *J* = 8.0 Hz, 2H), 6.93 (d, *J* = 8.1 Hz, 2H), 6.79 (d, *J* = 8.1 Hz, 2H), 5.62 (d, *J* = 8.8 Hz, 1H), 3.69 (h, *J* = 7.1 Hz, 1H), 2.82 (dd, *J* = 13.8, 7.0 Hz, 1H), 2.74 (dd, *J* = 13.9, 7.3 Hz, 1H), 2.60 – 2.44 (m, 2H), 2.44 (s, 3H), 2.40 (s, 3H) ppm. ^{13}C NMR (101 MHz, CD_2Cl_2) δ 176.2, 148.9, 146.2, 144.2, 137.6, 136.5, 132.6, 130.8, 130.3, 130.1, 128.8, 127.2, 122.8, 52.1, 40.3, 38.5, 21.8, 21.6. ppm IR (neat, cm^{-1}): 3590, 3366, 3290, 3239, 2929, 1728, 1701, 1598, 1502, 1416, 1374, 1318, 1300, 1199, 1175, 1152, 1093, 1071, 1019. HRMS calcd. for ($C_{24}H_{24}NO_7S_2$) $[M–H]^–$: 502.1000 found 502.0986.

[vi] A shorter reaction time was not attempted in this case but trace **2.1g** was observed in the crude ^{1}H NMR suggesting that the prolonged reaction time was necessary. The free indole may coordinate to Ni and slow the rate of reaction.
[vii] The NH indole and NHTs signals were not observed in MeOD.
[viii] After a 4-day reaction, 28% of **2.2l** was observed by ^{1}H NMR and 27% **2.1l** remained. Therefore, a prolonged reaction time was used to maximise the yield. Many trace by-products were observed in this reaction but were not identified.

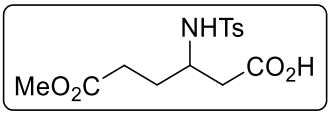

6-Methoxy-3-((4-methylphenyl)sulfonamido)-6-oxo hexanoic acid (2.2m): Following **GP8** with a reaction time of 3 days, **2.1m** 57 mg, 0.20 mmol) gave **2.2m** (37 mg, 56%) as a white solid. In a separate independent experiment **2i** (33 mg, 50%) was isolated giving an average yield of 53%. M.P: 108 – 108 °C. ^{1}H NMR (500 MHz, $CDCl_3$) δ 7.77 – 7.71 (m, 2H), 7.30 (d, *J* = 8.0 Hz, 2H), 5.69 (d, *J* = 9.3 Hz, 1H), 3.63 (s, 3H), 3.57 (tq, *J* = 9.5, 5.0 Hz, 1H), 2.45 (dd, *J* = 7.5, 4.9 Hz, 2H), 2.42 (s, 3H), 2.32 (t, *J* = 7.1 Hz, 2H), 1.91 – 1.76 (m, 2H) ppm. ^{13}C NMR (101 MHz, $CDCl_3$) δ 175.7, 174.0, 143.8, 137.8, 129.9, 127.1, 52.0, 50.1, 38.7, 30.4, 29.4, 21.7 ppm. IR (neat, cm^{-1}): 3289, 2964, 2931, 1711, 1598, 1436, 1417, 1342, 1327, 1255, 1232, 1192, 1157, 1080. HRMS calcd. for ($C_{14}H_{18}NO_6S$) $[M–H]^–$: 328.0860 found 328.0860.

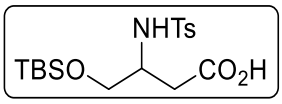

4-((*tert*-Butyldimethylsilyl)oxy)-3-((4-methylphenyl)sulfonamido) butanoic acid (2.2q): Following **GP8** with a reaction time of 6 days[ix] and quenching the reaction with $NH_4Cl_{(sat.)}$ instead of HCl, **2.1q** (68 mg, 0.20 mmol) gave **2.2q** (24 mg, 32%) as a white solid. In a separate independent experiment **2.2q** (25 mg, 32%) was isolated giving an average yield of 32%. ^{1}H NMR (400 MHz, $CDCl_3$) δ 7.79 – 7.72 (m, 2H), 7.33 – 7.26 (m, 2H), 5.30 (d, *J* = 8.5 Hz, 1H), 3.70 – 3.59 (m, 1H), 3.55 (dd, *J* = 10.1, 4.0 Hz, 1H), 3.49 (dd, *J* = 10.1, 5.5 Hz, 1H), 2.64 (dd, *J* = 16.6, 4.9 Hz, 1H), 2.50 (dd, *J* = 16.6, 7.0 Hz, 1H), 2.42 (s, 3H), 0.83 (s, 9H), -0.02 (s, 3H), -0.03 (s, 3H). ^{13}C NMR (101 MHz, $CDCl_3$) δ 175.6, 143.7, 137.8, 129.9, 127.2, 64.0, 51.6, 35.7, 25.9, 21.6, 18.3, -5.5, -5.5. IR (neat, cm^{-1}): 3259, 2928, 2857, 1777, 1598, 1540, 1452, 1408, 1320, 1252, 1156, 1091. HRMS calcd. for ($C_{17}H_{28}NO_5SSi$) $[M–H]^–$: 386.1463 found 386.1475.

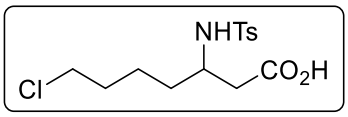

7-Chloro-3-((4-methylphenyl)sulfonamido) heptanoic acid (2.2t): Following **GP8** with a reaction time of 3 days, **2.1t** (57 mg, 0.20 mmol) gave **2.2t** (48 mg, 72%) as a white solid. In a separate independent experiment **2.2t** (45 mg, 67%) was isolated giving an average yield of 70%. ^{1}H NMR (400 MHz, $CDCl_3$) δ 9.02 (s, br, 1H), 7.75 (d, *J* = 8.1 Hz, 2H), 7.30 (d, *J* = 8.0 Hz, 2H), 5.56 (d, *J* = 9.1 Hz, 1H), 3.51 (q, *J* = 7.0, 6.5 Hz, 1H), 3.37 (t, *J* = 6.6 Hz, 2H), 2.56 – 2.45 (m, 2H), 2.41 (s, 3H), 1.59 (p, *J* = 7.1 Hz, 2H), 1.55 – 1.45 (m, 2H), 1.44 – 1.29 (m, 1H), 1.29 – 1.15 (m, 1H) ppm. ^{13}C NMR (101 MHz, $CDCl_3$) δ 176.4, 143.8, 137.8, 129.9, 127.2, 50.3, 44.7, 38.9, 33.9, 31.9, 23.2, 21.7 ppm. IR (neat, cm^{-1}): 3271, 2926, 2867, 1707, 1598, 1414, 1320, 1304, 1152, 1088. HRMS calcd. for ($C_{14}H_{19}ClNO_4S$) $[M–H]^–$: 332.0729 found 332.0736.

[ix] Crude NMR was not taken in this case due to the instability of the product. A long reaction time was used as it was proposed that the presence of the bulky TBS group would likely slow the reaction.

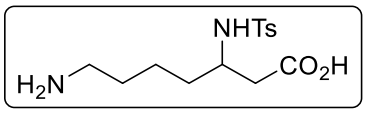

7-Amino-3-((4-methylphenyl)sulfonamido) heptanoic acid (2.2s): To **2.2t** (36 mg, 1.0 equiv, 1.1 mmol) in a Schlenk tube was added 5.0 M NH_4OH solution (0.44 ml, 20 equiv., 2.2 mmol) under Ar atmosphere. The tube was sealed and the reaction was heated to reflux for 4 h. After this time, the solvent was removed *in vacuo* and the product purified by column chromatography on silica gel, eluting with $CHCl_3$:MeOH:NH_4OH (80:15:2 → 70:30:4) to give **2.2s** (26 mg, 70%) as a white solid. M.P: 212 − 214 °C (decomposition at 220 °C). ^{1}H NMR (400 MHz, MeOD)[x] δ 7.72 – 7.65 (m, 2H), 7.32 – 7.27 (m, 2H), 3.56 – 3.41 (m, 1H), 3.28 (s, 1H), 2.76 (td, *J* = 7.5, 1.4 Hz, 2H), 2.35 (s, 3H), 2.16 (m, 2H), 1.60 – 1.43 (m, 3H), 1.43 – 1.20 (m, 3H) ppm. ^{13}C NMR (101 MHz, MeOD)[xi] δ 144.6, 140.2, 130.8, 130.8, 128.0, 52.4, 40.5, 35.3, 27.9, 23.5, 21.5 ppm. ^{13}C NMR (101 MHz, D_2O) δ 177.4, 144.9, 136.5, 130.1, 126.7, 51.0, 41.9, 39.2, 33.6, 26.2, 21.8, 20.7. IR (neat, cm^{-1}): 3327, 2918, 2861, 1634, 1557, 1396, 1315, 1229, 1155, 1093. HRMS calcd. for ($C_{14}H_{21}N_2O_4S$) $[M–H]^–$: 313.1228 found 313.1226.

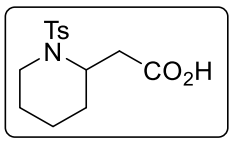

2-(1-Tosylpiperidin-2-yl) acetic acid (2.2u): To **2.2t** (44 mg, 1.0 equiv., 0.13 mmol) in dry DMF (1.0 ml) at 0 °C was added NaH (60% dispersion in mineral oil, 7.0 mg, 2.2 equiv. 0.29 mmol). The reaction mixture was warmed to RT and stirred overnight. After this time, the reaction was diluted with EtOAc and washed with 1.0 M HCl (2 times). The conversion was essentially quantitative and was purified by tituration with pentane to remove any grease, giving **2.2u** (24 mg, 88%) as a white solid. M.P: 107 − 109 °C. ^{1}H NMR (400 MHz, $CDCl_3$) δ 10.04 (s, 1H), 7.73 (d, *J* = 8.2 Hz, 2H), 7.30 (d, *J* = 8.0 Hz, 2H), 4.54 (m, 1H), 3.82 (dd, *J* = 13.9, 4.4 Hz, 1H), 2.94 (td, *J* = 13.3, 2.5 Hz, 1H), 2.70 (dd, *J* = 15.3, 9.4 Hz, 1H), 2.54 (dd, *J* = 15.3, 5.4 Hz, 1H), 2.43 (s, 3H), 1.68 – 1.32 (m, 6H) ppm. ^{13}C NMR (101 MHz, $CDCl_3$) δ 176.9, 143.4, 138.1, 129.9, 127.1, 49.5, 41.1, 34.8, 27.8, 24.7, 21.6, 18.4 ppm. IR (neat, cm^{-1}): 2930, 2860, 1698, 1596, 1474, 1428, 1406, 1337, 1292, 1228, 1190, 1152, 1091, 1034. HRMS calcd. for ($C_{14}H_{18}NO_4S$) $[M–H]^–$: 296.0962 found 296.0970.

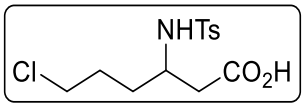

6-Chloro-3-((4-methylphenyl)sulfonamido) hexanoic acid (2.2w): Following **GP8** with a reaction time of 3 days, **2.1w** (55 mg, 0.20 mmol) gave **2.2w** (33 mg, 52%) as a colorless solid. In a separate independent experiment **2.2w** (38 mg, 58%) was isolated giving an average yield of 56%. M.P. = 118 – 121 °C. ^{1}H NMR (400 MHz, $CDCl_3$) δ 7.78 – 7.73 (m, 2H), 7.34 – 7.29 (m, 2H), 5.42 (d, *J* = 9.5 Hz, 1H), 3.58 – 3.50 (m, 1H), 3.49 – 3.39 (m, 2H), 2.46 (d, *J* = 4.9 Hz, 2H), 2.43 (s, 3H), 1.84 – 1.62 (m,

[x] The NH_2 and NHTs signals were not observed in the ^{1}H spectra when taken in in MeOD.
[xi] The carboxylic acid peak was not observed in the ^{13}C spectra when taken in MeOD. Therefore, the ^{13}C spectrum in D_2O is also reported.

4H) ppm. ^{13}C NMR (101 MHz, $CDCl_3$) δ 176.0, 143.9, 137.8, 130.0, 127.1, 49.9, 44.4, 38.6, 31.9, 28.9, 21.7 ppm. IR (neat, cm^{-1}): 3337, 3294, 3067, 2948, 2924, 2867, 2690, 2590, 1691, 1597, 1494, 1448, 1424, 1327, 1307, 1156, 1086, 1023, 984, 938, 903, 815, 729, 663, 580, 545, 514. HRMS calcd. for ($C_{13}H_{17}ClNO_4S$) $[M–H]^–$: 318.0572 found 318.0571.

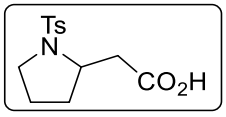

2-(1-Tosylpyrrolidin-2-yl) acetic acid (2.2v): NaH (60% in mineral oil, 9.5 mg, 0.23 mmol) was added in one portion to a solution of **2.2w** (33 mg, 0.11 mmol) in dry DMF (1.0 ml) and the resulting mixture was stirred at RT for 2 hours. The reaction mixture was diluted then with EtOAc (10 ml) and washed with 1 M HCl (2 × 10 ml). The organic phase was dried ($MgSO_4$), concentrated *in vacuo*, and crude was washed several times with pentane to remove traces of mineral oil. Final product **2.2v** was obtained as a white solid (24 mg, 81%). M.P. = 111 – 114 °C. ^{1}H NMR (400 MHz, $CDCl_3$) δ 7.76 – 7.71 (m, 2H), 7.36 – 7.30 (m, 2H), 3.94 (ddt, *J* = 10.7, 7.4, 3.9 Hz, 1H), 3.50 – 3.42 (m, 1H), 3.19 – 3.09 (m, 2H), 2.57 (dd, *J* = 16.4, 10.0 Hz, 1H), 2.44 (s, 3H), 1.86 – 1.75 (m, 2H), 1.74 – 1.64 (m, 1H), 1.59 – 1.48 (m, 1H) ppm. ^{13}C NMR (101 MHz, $CDCl_3$) δ 175.7, 143.8, 134.2, 129.9, 127.8, 56.5, 49.4, 41.1, 31.9, 23.9, 21.7. IR (neat, cm^{-1}): 3059, 2987, 2952, 2880, 2735, 2663, 1701, 1598, 1440, 1399, 1340, 1320, 1238, 1208, 1197, 1159, 1119, 1092, 1041, 988, 928, 821, 808, 709, 678, 659, 609, 583, 549. HRMS calcd. for ($C_{13}H_{16}NO_4S$) $[M–H]^–$: 282.0805 found 282.0802.

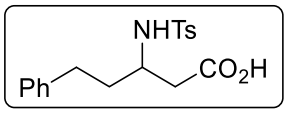

3-((4-Methylphenyl)sulfonamido)-5-phenyl pentanoic acid (2.2x): Following **GP8** with a reaction time of 3 days, **2.1x** (60 mg, 0.20 mmol) gave **2.2x** (48 mg, 69%) as a white solid. In a separate independent experiment **2.2x** (47 mg, 67%) was isolated giving an average yield of 68%. ^{1}H NMR (500 MHz, $CDCl_3$) δ 7.79 – 7.73 (m, 2H), 7.32 – 7.27 (m, 2H), 7.25 – 7.21 (m, 2H), 7.19 – 7.15 (m, 1H), 7.05 – 6.99 (m, 2H), 5.64 (d, *J* = 8.7 Hz, 1H), 3.69 – 3.46 (m, 1H), 2.60 (ddd, *J* = 14.0, 9.5, 6.2 Hz, 1H), 2.49 (d, *J* = 5.1 Hz, 2H), 2.50 – 2.43 (m, 1H), 2.42 (s, 3H), 1.90 – 1.74 (m, 2H) ppm. ^{13}C NMR (101 MHz, $CDCl_3$) δ 176.6, 143.8, 141.0, 138.0, 130.0, 128.7, 128.5, 127.3, 126.3, 50.3, 38.8, 36.4, 32.2, 21.8 ppm. LRMS (ESI): 693 (2M-H), 346 (M-H). Spectroscopic data for **2.2x** match those previously reported in the literature.[153]

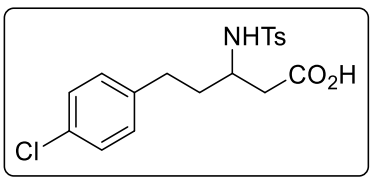

5-(4-Chlorophenyl)-3-((4-methylphenyl)sulfonamido) pentanoic acid (2.2y): Following **GP8** with a reaction time of 3 days, **2.1y** (67 mg, 0.20 mmol) gave **2.2y** (40 mg, 52%) as a white solid. In a separate independent experiment **2.2y** (38 mg, 50%) was isolated giving an average yield of 51%. M.P. = 150 – 152 °C. ^{1}H NMR (400 MHz, MeOD) δ 7.76 – 7.69 (m, 2H), 7.39 – 7.31 (m, 2H), 7.22 – 7.12 (m, 2H), 7.03 – 6.95 (m, 2H), 3.61 – 3.49 (m, 1H), 2.55 (ddd, *J* = 13.8, 9.8, 5.6 Hz, 1H), 2.42 (s, 3H), 2.45 – 2.34 (m, 3H), 1.76 (dddd, *J* =

14.3, 9.8, 6.4, 4.6 Hz, 1H), 1.62 (dddd, *J* = 13.9, 9.8, 8.4, 5.6 Hz, 1H) ppm. ^{13}C NMR (101 MHz, MeOD) δ 174.4, 144.7, 141.5, 140.0, 132.6, 130.9, 130.8, 129.3, 128.1, 51.5, 41.0, 37.4, 32.1, 21.5 ppm. IR (neat, cm^{-1}):3310, 2922, 1695, 1491, 1466, 1444, 1408, 1322, 1305, 1285, 1206, 1151, 1089, 1013. HRMS calcd. for ($C_{18}H_{19}ClNO_4S$) [M–H]$^-$: 380.0729 found 380.0725.

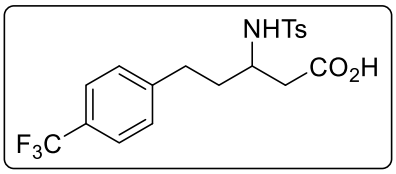

3-((4-Methylphenyl)sulfonamido)-5-(4-(trifluoromethyl)phenyl) pentanoic acid (2.2z): Following **GP8** with a reaction time of 3 days, **2.1z** (74 mg, 0.20 mmol) gave **2.2z** (48 mg, 58%) as a white solid. In a separate independent experiment **2.2z** (45 mg, 54%) was isolated giving an average yield of 56%. M.P. = 194–196 °C. ^{1}H NMR (400 MHz, MeOD)[xii] δ 7.79 – 7.72 (m, 2H), 7.52 (d, *J* = 8.0 Hz, 2H), 7.38 (d, *J* = 8.1 Hz, 2H), 7.24 (d, *J* = 8.0 Hz, 2H), 3.65 – 3.54 (m, 1H), 2.69 (ddd, *J* = 14.8, 9.8, 5.5 Hz, 1H), 2.54 (ddd, *J* = 14.0, 9.7, 6.5 Hz, 1H), 2.44 (s, 3H), 2.39 (d, *J* = 1.5 Hz, 1H), 2.38 (d, *J* = 3.1 Hz, 1H), 1.84 (dddd, *J* = 14.2, 9.8, 6.5, 4.5 Hz, 1H), 1.69 (dddd, *J* = 14.0, 9.8, 8.5, 5.6 Hz, 1H) ppm.^{13}C NMR (101 MHz, MeOD) δ 173.0, 146.0, 143.3, 138.7, 129.4, 128.6, 127.8 (q, *J* = 32.0 Hz),), 126.7, 125.8, 124.8 (q, *J* = 3.8 Hz), 124.5 (q, *J* = 270.8 Hz), 123.1, 50.1, 39.6, 35.8, 31.1, 20.1 ppm. ^{19}F NMR (376 MHz, MeOD, decoupled) δ -63.84 ppm. IR (neat, cm^{-1}): 3312, 2927, 1687, 1616, 1467, 1445, 1417, 1320, 1284, 1208, 1151, 1114, 1093, 1066, 1017. HRMS calcd. for ($C_{19}H_{19}F_3NO_4S$) [M–H]$^-$: 414.0992 found 414.0991.

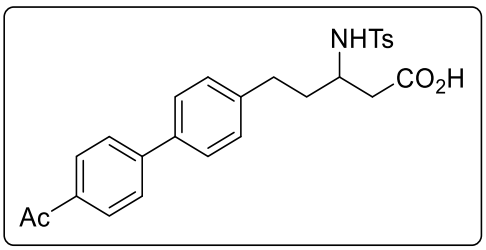

5-(4'-Acetyl-[1,1'-biphenyl]-4-yl)-3-((4-methylphenyl)sulfonamido) pentanoic acid (2.2ab): Following **GP8** with a reaction time of 5 days,[xiii] **2.1ab** (84 mg, 0.20 mmol) gave **2.2ab** (45 mg, 48%) as a white solid. In a separate independent experiment **2.2ab** (48 mg, 52%) was isolated giving an average yield of 50%. M.P. = 180 – 182 °C. ^{1}H NMR (400 MHz, DMSO)[xiv] δ 8.02 (d, *J* = 8.2 Hz, 2H), 7.79 (d, *J* = 8.3 Hz, 2H), 7.70 (d, *J* = 8.2 Hz, 2H), 7.61 (d, *J* = 8.2 Hz, 2H), 7.40 (d, *J* = 7.9 Hz, 2H), 7.11 (d, *J* = 7.8 Hz, 2H), 3.56 – 3.43 (m, 1H), 2.60 (s, 3H), 2.39 (s, 3H), 2.36 – 2.26 (m, 3H), 1.75 – 1.49 (m, 2H) ppm. ^{1}H NMR (400 MHz, $CDCl_3$) δ 8.06 – 7.97 (m, 2H), 7.80 – 7.73 (m, 2H), 7.67 – 7.63 (m, 2H), 7.54 – 7.48 (m, 2H), 7.30 (d, *J* = 8.1 Hz,

[xii] The NH signal was not observed in MeOD.
[xiii] After a 3-day reaction, 47% **2.2ab** was observed by ^{1}H NMR and 15% **2.1ab** remained. Therefore, a prolonged reaction time was used to maximise the yield. The high molecular weight allowed the accurate quantification of by-products with 26% terminal olefin and 40% $TsNH_2$ observed along with other trace by-products.
[xiv] The NH signal was not observed and the α-carboxylic acid protons were obscured by the DMSO-*d*$_6$ solvent peak. The solubility of **2.2ab** in $CDCl_3$ is very low and the ^{1}H NMR has been included for clarity.

2H), 7.18 – 7.12 (m, 2H), 5.50 (d, *J* = 9.4 Hz, 1H), 3.65 – 3.53 (m, 1H), 2.69 (ddd, *J* = 15.2, 9.5, 5.9 Hz, 1H), 2.64 (s, 3H), 2.61 – 2.51 (m, 1H), 2.49 (d, *J* = 4.8 Hz, 2H), 2.42 (s, 3H), 1.98 – 1.77 (m, 2H) ppm. ^{13}C NMR (101 MHz, DMSO) δ 197.4, 172.0, 144.4, 142.5, 141.8, 138.9, 136.3, 135.4, 129.6, 128.9, 128.9, 126.8, 126.6, 126.5, 50.2, 35.8, 30.6, 26.7, 21.0 ppm. IR (neat, cm^{-1}): 3248, 2957, 2916, 1722, 1645, 1600, 1451, 1427, 1399, 1362, 1327, 1280, 1244, 1152, 1092, 1073. HRMS calcd. for ($C_{26}H_{26}NO_5S$) [M–H]$^-$: 464.1537 found 414.1530.

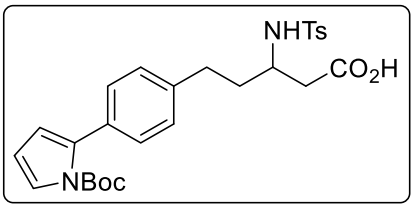

5-(4-(1-(*tert*-Butoxycarbonyl)-1*H*-pyrrol-2-yl)phenyl)-3-((4-methylphenyl)sulfonamido) pentanoic acid (2.2ac): Following **GP8** with a reaction time of 6 days,[xv] **2.1ac** (93 mg, 0.20 mmol) gave **2.2ac** (63 mg, 61%) as a purple oil. In a separate independent experiment **2.2ac** (52 mg, 51%) was isolated giving an average yield of 56%. ^{1}H NMR (400 MHz, $CDCl_3$) δ 7.78 (d, *J* = 8.3 Hz, 2H), 7.33 (dd, *J* = 3.3, 1.8 Hz, 1H), 7.31 (d, *J* = 8.0 Hz, 2H), 7.21 (d, *J* = 8.1 Hz, 2H), 7.00 (d, *J* = 8.1 Hz, 2H), 6.21 (t, *J* = 3.3 Hz, 1H), 6.15 (dd, *J* = 3.3, 1.8 Hz, 1H), 5.61 (d, *J* = 9.2 Hz, 1H), 3.65 – 3.52 (m, 1H), 2.63 (ddd, *J* = 15.1, 9.6, 6.0 Hz, 1H), 2.55 – 2.42 (m, 3H), 2.42 (s, 3H), 1.94 – 1.75 (m, 2H), 1.37 (s, 9H) ppm. ^{13}C NMR (101 MHz, $CDCl_3$) δ 176.3, 149.5, 143.7, 139.8, 137.9, 135.0, 132.3, 129.9, 129.3, 127.6, 127.2, 122.6, 114.4, 110.7, 83.7, 50.2, 38.7, 36.3, 27.8, 21.7 ppm. IR (neat, cm^{-1}): 3275, 2890, 2930, 1709, 1394, 1370, 1310, 1256, 1144, 1092, 1074. HRMS calcd. for ($C_{27}H_{31}N_2O_6S$) [M–H]$^-$: 511.1908 found 511.1888.

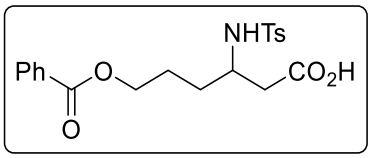

6-(Benzoyloxy)-3-((4-methylphenyl)sulfonamido) hexanoic acid (2.2ae): Following **GP8** with a reaction time of 3 days, **2.1ae** (72 mg, 0.20 mmol) gave **2.2ae** (51 mg, 62%) as a white solid. In a separate independent experiment **2.2ae** (56 mg, 69%) was isolated giving an average yield of 65%. M.P. = 122 – 124 °C. ^{1}H NMR (400 MHz, $CDCl_3$) δ 8.02 – 7.94 (m, 2H), 7.75 (d, *J* = 8.3 Hz, 2H), 7.59 – 7.50 (m, 1H), 7.46 – 7.38 (m, 2H), 7.25 (d, *J* = 8.3 Hz, 2H), 6.46 (s, br, 1H), 5.71 (d, *J* = 4.7 Hz, 1H), 4.25 – 4.08 (m, 2H), 3.60 (s, br, 1H), 2.49 (d, *J* = 4.4 Hz, 1H), 2.34 (s, 3H), 1.80 – 1.56 (m, 4H) ppm. ^{13}C NMR (101 MHz, $CDCl_3$) δ 175.5, 166.8, 143.8, 137.8, 133.1, 130.2, 129.9, 129.7, 128.5, 127.1, 64.3, 50.3, 38.9, 31.1, 25.3, 21.6 ppm. IR (neat, cm^{-1}): 3301, 3212, 2963, 2934, 1727, 1687, 1587, 1492, 1464, 1451, 1423, 1395, 1317, 1301, 1283, 1212, 1156, 1141, 1121, 1089, 1060, 1037. HRMS calcd. for ($C_{20}H_{22}NO_6S$) [M–H]$^-$: 404.1173 found 404.1164.

[xv] After a 3-day reaction, 40% of **2.2ac** was observed by ^{1}H NMR and 31% **2.1ac** remained. Therefore, a prolonged reaction time was used to reach completion.

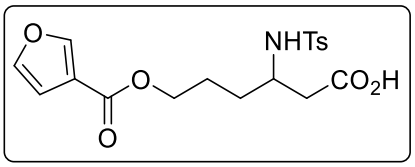

6-((Furan-3-carbonyl)oxy)-3-((4-methylphenyl)sulfonamido) hexanoic acid (2.2af): Following **GP8** with a reaction time of 3 days, **2.1af** (70 mg, 0.20 mmol) gave **2.2af** (49 mg, 62%) as a pale-yellow oil. In a separate independent experiment **2.2af** (54 mg, 68 %) was isolated giving an average yield of 65%. ^{1}H NMR (400 MHz, $CDCl_3$) δ 7.97 (dd, *J* = 1.6, 0.8 Hz, 1H), 7.77 – 7.72 (m, 2H), 7.41 (t, *J* = 1.7 Hz, 1H), 7.30 – 7.25 (m, 2H), 6.70 (dd, *J* = 1.9, 0.8 Hz, 1H), 5.62 (d, *J* = 9.2 Hz, 1H), 4.17 – 4.06 (m, 2H), 3.63 – 3.53 (m, 1H), 2.47 (d, *J* = 5.1 Hz, 2H), 2.38 (s, 3H), 1.78 – 1.52 (m, 4H) ppm. ^{13}C NMR (101 MHz, $CDCl_3$) δ 176.0, 163.3, 147.9, 143.9, 143.8, 137.8, 129.9, 127.1, 119.4, 109. 9, 63.8, 50.2, 38.7, 31.1, 25.2, 21.6 ppm. IR (neat, cm^{-1}): 3270, 2958, 1708, 1598, 1406, 1305, 1152, 1090, 968, 873, 814, 765, 707, 663, 575, 548. HRMS calcd. for ($C_{18}H_{20}NO_7S$) $[M–H]^–$: 394.0966 found 394.0983.

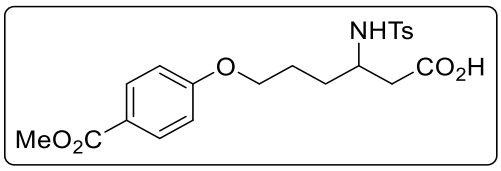

6-(4-(Methoxycarbonyl)phenoxy)-3-((4-methylphenyl)sulfonamido) hexanoic acid (2.2aj): Following **GP8** with a reaction time of 3 days, **2.1aj** (78 mg, 0.20 mmol) gave **2.2aj** (41 mg, 47%) as a white solid. In a separate independent experiment **2.2aj** (43 mg, 48%) was isolated giving an average yield of 48%. M.P: 122 – 124 °C. ^{1}H NMR (400 MHz, $CDCl_3$) δ 8.01 – 7.92 (m, 2H), 7.79 – 7.71 (m, 2H), 7.27 (d, *J* = 7.5 Hz, 2H), 6.87 – 6.79 (m, 2H), 5.53 (d, *J* = 8.0 Hz, 1H), 3.92 – 3.83 (m, 5H), 3.59 (s, br, 1H), 2.50 (dd, *J* = 5.0, 2.2 Hz, 2H), 2.38 (s, 3H), 1.85 – 1.64 (m, 4H). ^{13}C NMR (101 MHz, $CDCl_3$) δ 176.0, 167.1, 162.7, 143.8, 137.9, 131.7, 129.9, 127.2, 122.8, 114.2, 67.3, 52.1, 50.2, 38.7, 31.3, 25.6, 21.7. IR (neat, cm^{-1}):3187, 2955, 2874, 1713, 1607, 1511, 1434, 1280, 1259, 1193, 1153, 1091, 1935. HRMS calcd. for ($C_{21}H_{24}NO_7S$) $[M–H]^–$: 434.1279 found 434.1286.

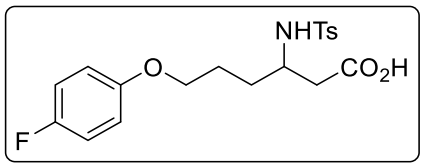

6-(4-Fluorophenoxy)-3-((4-methylphenyl)sulfonamido) hexanoic acid (2.2ak): Following **GP8** with a reaction time of 3 days, **2.1ak** (70 mg, 0.20 mmol) gave **2.2ak** (49 mg, 62%) as a white solid. In a separate independent experiment **2.2ak** (52 mg, 66%) was isolated giving an average yield of 64%. M.P: 93 – 94 °C. ^{1}H NMR (400 MHz, $CDCl_3$) δ 8.92 (s, 1H), 7.75 (d, *J* = 8.0 Hz, 2H), 7.27 (d, *J* = 7.8 Hz, 2H), 6.99 – 6.89 (m, 2H), 6.75 (m, 2H), 5.62 (d, *J* = 9.0 Hz, 1H), 3.78 (t, *J* = 5.1 Hz, 2H), 3.58 (m, 1H), 2.59 – 2.43 (m, 2H), 2.39 (s, 3H), 1.79 – 1.58 (m, 4H) ppm. ^{13}C NMR (101 MHz, $CDCl_3$) δ 176.5, 157.4 (d, *J* = 238.3 Hz), 154.9 (d, *J* = 2.1 Hz), 143.8, 137.8, 129.9, 127.2, 115.9 (d, *J* = 23.0 Hz), 115.5 (d, *J* = 7.9 Hz), 67.8, 50.3, 38.9, 31.3, 25.7, 21.6 ppm. ^{19}F NMR (376 MHz, $CDCl_3$) δ -123.99 (tt, *J* = 8.4, 4.3 Hz)

ppm. IR (neat, cm^{-1}): 3325, 3288, 2926, 2872, 1696, 1598, 1506, 1465, 1435, 1419, 1332, 1295, 1256, 1155, 1092, 1038. HRMS calcd. for ($C_{19}H_{21}FNO_5S$) $[M–H]^–$: 394.1130 found 392.1138.

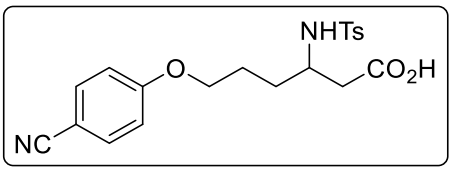

6-(4-Cyanophenoxy)-3-((4-methylphenyl)sulfonamido) hexanoic acid (2.2al): Following **GP8** with a reaction time of 6 days,[xvi] **2.1al** (71 mg, 0.20 mmol) gave **2.2al** (32 mg, 40%) as a white solid. In a separate independent experiment **2.2al** (34 mg, 42%) was isolated giving an average yield of 41%. M.P: 150 – 152 °C. ^{1}H NMR (400 MHz, $CDCl_3$) δ 7.75 (d, *J* = 8.2 Hz, 2H), 7.56 (m, 2H), 7.29 (d, *J* = 8.1 Hz, 2H), 6.90 – 6.85 (m, 2H), 5.44 (d, *J* = 9.3 Hz, 1H), 3.93 – 3.89 (m, 2H), 3.59 (m, 1H), 2.48 (d, *J* = 1.6 Hz, 1H), 2.46 (d, *J* = 2.4 Hz, 1H), 2.40 (s, 3H), 1.83 (m, 1H), 1.72 (m, 3H) ppm. ^{13}C NMR (101 MHz, $CDCl_3$)[xvii] δ 175.3, 162.2, 143.9, 137.9, 134.2, 130.0, 127.2, 119.3, 115.3, 104.2, 67.5, 50.2, 38.4, 31.3, 25.6, 21.7 ppm. ^{13}C NMR (101 MHz, CD_3OD) δ 174.4, 163.9, 144.7, 139.9, 135.1, 130.7, 128.0, 116.5, 104.5, 68.8, 51.5, 41.2, 32.2, 26.2, 21.4. IR (neat, cm^{-1}): 3265, 2921, 2215, 1712, 1605, 1574, 1508, 1450, 1404, 1302, 1259, 1172, 1152, 1095, 1022. HRMS calcd. for ($C_{20}H_{21}N_2O_5S$) $[M–H]^–$: 401.1177 found 401.1183

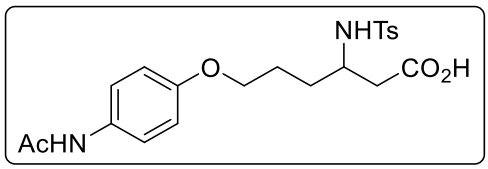

6-(4-Acetamidophenoxy)-3-((4-methylphenyl)sulfonamido) hexanoic acid (2.2am): Following **GP8** with a reaction time of 6 days,[xviii] **2.1am** (78 mg, 0.20 mmol) gave **2.2am** (27 mg, 31%) as a colorless solid. In a separate independent experiment **2.2am** (23.5 mg, 27%) was isolated giving an average yield of 29%. M.P. = 112 – 116 °C. ^{1}H NMR (400 MHz, MeOD) δ 7.77 – 7.71 (m, 2H), 7.44 – 7.35 (m, 2H), 7.33 (d, *J* = 7.9 Hz, 2H), 6.82 – 6.74 (m, 2H), 3.75 (t, *J* = 6.0 Hz, 2H), 3.64 – 3.52 (m, 1H), 2.45 – 2.29 (m, 5H), 2.09 (s, 3H), 1.68 (m, 2H), 1.62 – 1.44 (m, 2H). ^{13}C NMR (101 MHz, MeOD) δ 174.5, 171.4, 157.1, 144.7, 139.9, 132.8, 130.7, 128.0, 123.0, 115.6, 68.5, 51.7, 41.4, 32.3, 26.5, 23.6, 21.4. IR (neat, cm^{-1}): 3273, 2925, 1711, 1660, 1600, 1541, 1509, 1411, 1303, 1240, 1152, 1090, 1024. HRMS calcd. for ($C_{21}H_{25}N_2O_6S$) $[M–H]^–$: 433.1439 found 433.1434.

[xvi] After a 3-day reaction, 34% of **2.2al** was observed by ^{1}H NMR and 25% **2.1al** remained. Therefore, a prolonged reaction time was used to maximise the yield.
[xvii] The solubility of **2.2al** in $CDCl_3$ is low so the ^{13}C NMR in CD_3OD has also been provided.
[xviii] In this case accurate quantification by NMR was not possible due to the poor solubility of **2.2am** in $CDCl_3$. After the 6-day reaction, however, small amount of **2.1am** remained suggesting the long reaction time was necessary.

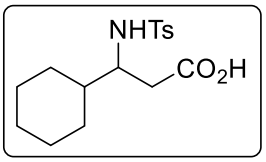

3-Cyclohexyl-3-((4-methylphenyl)sulfonamido) propanoic acid (2.2ao): Following **GP8** with a reaction time of 5 days,[xix] **2.1ao** (56 mg, 0.20 mmol) gave **2.2ao** (24 mg, 37%) as a white solid. In a separate independent experiment **2.2ao** (28 mg, 43%) was isolated giving an average yield of 40%. M.P. = 112 – 116 °C. ^{1}H NMR (400 MHz, $CDCl_3$) δ 7.75 (d, *J* = 7.8 Hz, 2H), 7.29 (d, *J* = 7.8 Hz, 2H), 5.33 (d, *J* = 9.4 Hz, 1H), 3.39 – 3.29 (m, 1H), 2.55 – 2.34 (m, 5H), 1.83 – 1.40 (m, 6H), 1.20 – 1.02 (m, 3H), 0.83 (dq, *J* = 46.2, 12.0 Hz, 2H). ^{13}C NMR (101 MHz, $CDCl_3$) δ 176.3, 143.6, 138.1, 129.8, 127.2, 55.4, 41.3, 35.9, 29.6, 29.3, 26.2, 26.1, 26.0, 21.7. IR (neat, cm^{-1}):3273, 2930, 2848, 1700, 1597, 1445, 1403, 1319, 1249, 1230, 1158, 1091, 1068, 1048. HRMS calcd. for ($C_{16}H_{22}NO_4S$) $[M–H]^–$: 324.1275 found 324.1280.

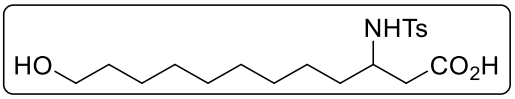

12-Hydroxy-3-((4-methylphenyl)sulfonamido) dodecanoic acid (2.2aq): Following **GP8** with a reaction time of 6 days,[xx] **2.1aq** (62 µl, 0.20 mmol) gave **2.2aq** (49 mg, 64%) as a white solid. In a separate independent experiment **2.2aq** (50 mg, 65%) was isolated giving an average yield of 65%. M.P.: 85 – 86 °C. ^{1}H NMR (400 MHz, $CDCl_3$) δ 7.78 – 7.71 (m, 2H), 7.28 (d, *J* = 8.0 Hz, 2H), 5.50 (d, *J* = 9.0 Hz, 1H), 5.38 (s, br, 2H), 3.63 (t, *J* = 6.6 Hz, 2H), 3.57 – 3.44 (m, 1H), 2.52 – 2.35 (m, 5H), 1.60 – 1.48 (m, 2H), 1.46 (q, *J* = 7.1 Hz, 2H), 1.37 – 1.04 (m, 13H) ppm. ^{13}C NMR (101 MHz, $CDCl_3$) δ 175.5, 143.5, 138.1, 129.8, 127.2, 63.1, 50.6, 38.8, 34.6, 32.5, 29.3, 29.2, 29.1, 28.9, 25.7, 25.6, 21.7 ppm. IR (neat, cm^{-1}): 3467, 3310, 2918, 2854, 1707, 1430, 1333, 1298, 1258, 1157, 1136, 1094, 1040, 1004. HRMS calcd. for ($C_{19}H_{30}NO_5S$) $[M–H]^–$: 384.1850 found 384.1842.

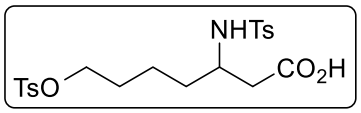

3-((4-Methylphenyl)sulfonamido)-7-(tosyloxy) heptanoic acid (2.2ar): Following **GP8** with a reaction time of 3 days, **2.1ar** (85 mg, 0.20 mmol) gave **2.2ar** (40 mg, 43%) as a colourless oil. In a separate independent experiment **2.2ar** (36 mg, 38%) was isolated giving an average yield of 41%. ^{1}H NMR (400 MHz, $CDCl_3$) δ 7.80 – 7.74 (m, 2H), 7.74 – 7.69 (m, 2H), 7.34 (d, *J* = 8.0 Hz, 2H), 7.29 (d, *J* = 8.0 Hz, 2H), 6.75 (s, br, 1H), 5.47 (d, *J* = 9.1 Hz, 1H), 3.96 – 3.83 (m, 2H), 3.46 (tq, *J* = 9.9, 5.6 Hz, 1H), 2.51 – 2.39 (m, 7H), 1.56 – 1.38 (m, 4H), 1.37 – 1.21 (m, 1H), 1.23 – 1.08 (m, 1H) ppm. ^{13}C NMR (101 MHz, $CDCl_3$) δ 176.0, 145.0, 143.8, 137.8, 133.1, 130.0, 129.9, 128.0, 127.1, 70.2, 50.4, 38.7, 33.9, 28.3, 21.8, 21.8, 21.6 ppm. IR (neat, cm^{-1}): 3278, 2926, 1709, 1598,

[xix] After a 5-day reaction, **2.1ao** (41%) was detected by ^{1}H NMR of the crude reaction mixture. Longer reaction times did not lead to better conversions suggesting the reaction had stalled. Other reaction variables such as increasing the temperature and changing the ligand were modified to try and improve the yield but without success.
[xx] In this case a shorter reaction was not carried out but trace **2.1aq** (7%) observed in the crude ^{1}H NMR suggested that the prolonged reaction time was necessary.

1422, 1326, 1173, 1154, 1092. HRMS calcd. for ($C_{21}H_{26}NO_7S_2$) $[M–H]^-$: 468.1156 found 468.1157.

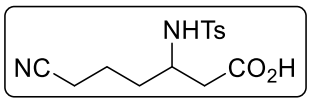

6-Cyano-3-((4-methylphenyl)sulfonamido) hexanoic acid (2.2as): Following **GP8** with a reaction time of 6 days,[xxi] **2.1as** (53 mg, 0.20 mmol) gave **2.2as** (31 mg, 50%) as a white solid. In a separate independent experiment **2.2as** (35 mg, 55%) was isolated giving an average yield of 53%. M.P.: 90 – 92 °C. ^{1}H NMR (400 MHz, $CDCl_3$) δ 7.75 (d, *J* = 7.9 Hz, 2H), 7.32 (d, *J* = 7.9 Hz, 2H), 6.61 (s, br, 1H), 5.72 (d, *J* = 9.3 Hz, 1H), 3.58 – 3.48 (m, 1H), 2.45 – 2.39 (m, 5H), 2.32 – 2.24 (m, 2H), 1.75 – 1.48 (m, 4H) ppm. ^{13}C NMR (101 MHz, $CDCl_3$) δ 175.5, 144.1, 137.7, 130.1, 127.1, 119.4, 49.7, 38.7, 33.4, 21.9, 21.7, 16.7 ppm. IR (neat, cm^{-1}): 3302, 2947, 2924, 2244, 1704, 1597, 1426, 1350, 1324, 1206, 1154, 1090, 1070, 1013. HRMS calcd. for ($C_{14}H_{17}N_2O_4S$) $[M–H]^-$: 309.0915 found 309.0916.

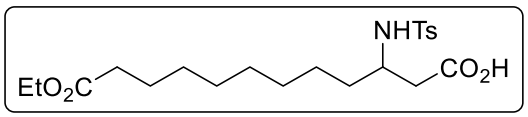

12-Ethoxy-3-((4-methylphenyl)sulfonamido)-12-oxo dodecanoic acid (2.2at): Following **GP8** with a reaction time of 3 days, **2.1at** (70 μl, 0.20 mmol) gave **2.2at** (59 mg, 69%) as a white solid. In a separate independent experiment **2.2at** (60 mg, 70%) was isolated giving an average yield of 70%. M.P.: 106 – 109 °C. ^{1}H NMR (400 MHz, $CDCl_3$) δ 7.80 – 7.71 (m, 2H), 7.29 (d, *J* = 8.3 Hz, 2H), 5.38 (d, *J* = 7.8 Hz, 1H), 4.12 (q, *J* = 7.1 Hz, 2H), 3.56 – 3.43 (m, 1H), 2.47 (dd, *J* = 5.2, 3.1 Hz, 2H), 2.41 (s, 3H), 2.27 (t, *J* = 7.5 Hz, 2H), 1.58 (apparent p, *J* = 7.5 Hz, 2H), 1.46 (d, *J* = 7.2 Hz, 2H), 1.24 (t, *J* = 7.1 Hz, 3H), 1.30 – 1.06 (m, 10H) ppm. ^{13}C NMR (101 MHz, $CDCl_3$) δ 176.26, 174.2, 143.6, 138.0, 129.8, 127.2, 60.4, 50.5, 38.8, 34.6, 34.5, 29.2, 29.1, 29.1, 29.0, 25.8, 25.0, 21.6, 14.4 ppm. IR (neat, cm^{-1}): 3271, 2937, 2859, 1703, 1597, 1451, 1422, 1329, 1290, 1258, 1188, 1156, 1093, 1004. HRMS calcd. for ($C_{21}H_{32}NO_6S$) $[M–H]^-$: 426.1956 found 426.1961.

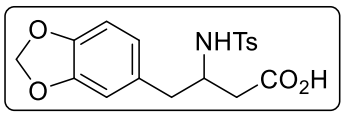

4-(Benzo[d][1,3]dioxol-5-yl)-3-((4-methylphenyl)sulfonamido) butanoic acid (2.2aw): Following **GP8** with a reaction time of 5 days,[xxii] **2.1aw** (66 mg, 0.20 mmol) gave **2.2aw** (45 mg, 60%) as a colorless solid. In a separate independent experiment **2.2aw** (48 mg, 64%) was isolated giving an average yield of 62%. M.P. = 113 – 116 °C. ^{1}H NMR (400 MHz, $CDCl_3$) δ 7.64 – 7.59 (m, 2H), 7.25 – 7.21 (m, 2H), 6.64 (d, *J* = 7.8 Hz, 1H), 6.50 – 6.42 (m, 2H), 5.93 – 5.90 (m, 2H), 5.40 – 5.10 (br. s., 1H), 3.72 – 3.62 (s, 1H), 2.78 (dd, *J* = 13.8, 7.1 Hz, 1H), 2.68 (dd, *J* = 13.8, 7.2 Hz,

[xxi] A shorter reaction was not carried out but trace **2.1as** (3%) observed in the crude ^{1}H NMR suggested that the prolonged reaction time was necessary. In this case, the cyano group may coordinate to Ni and slow the reaction.
[xxii] A shorter reaction was not carried out but trace **2.1aw** (5%) observed in the crude NMR suggested that the prolonged reaction time was necessary. 25% $TsNH_2$ was also observed.

1H), 2.58 (dd, *J* = 5.3, 2.6 Hz, 2H), 2.41 (s, 3H) ppm. ^{13}C NMR (101 MHz, $CDCl_3$) δ 175.7, 148.0, 146.7, 143.6, 137.2, 130.5, 129.7, 127.2, 122.5, 109.5, 108.5, 101.1, 52.0, 40.4, 38.0, 21.7 ppm. IR (neat, cm^{-1}): 3315, 2917, 2635, 1710, 1599, 1501, 1491, 1445, 1407, 1326, 1293, 1248, 1232, 1192, 1157, 1088, 1065, 1031, 927, 859, 806, 665, 583, 569, 546. HRMS calcd. for ($C_{18}H_{19}NNaO_6S$) $[M+Na]^+$: 400.0831 found 400.0821.

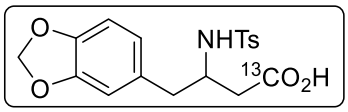

4-(Benzo[d][1,3]dioxol-5-yl)-3-((4-methylphenyl)sulfonamido) butanoic-1-^{13}C acid (2.2aw-^{13}C): Following a modified **GP8**: to **2.1aw** (66 mg, 0.20 mmol) and other solid reagents in a Schlenk tube under a flow of N_2 was added dry DMPU (0.50 ml, 0.40 M), MeOH (40 μl, 5.0 equiv.) and then frozen with liquid nitrogen. 3 × vacuum (<1 mbar) / $^{13}CO_2$ cycles were then performed using the head-space volume between the gas canister and valve filled with $^{13}CO_2$ for each addition. The Schlenk tube was then sealed, warmed to 10 °C and stirred for 5 days, giving **2.2aw-^{13}C** (47 mg, 63%) as a white solid. ^{1}H NMR (400 MHz, $CDCl_3$) δ 9.42 (s, br, 1H), 7.61 (d, *J* = 8.3 Hz, 2H), 7.22 (d, *J* = 8.0 Hz, 2H), 6.62 (d, *J* = 7.8 Hz, 1H), 6.50 – 6.42 (m, 2H), 5.96 – 5.86 (m, 2H), 5.46 (s, br, 1H), 3.76 – 3.61 (m, 1H), 2.76 (dd, *J* = 13.9, 7.0 Hz, 1H), 2.67 (dd, *J* = 13.9, 7.3 Hz, 1H), 2.63 – 2.49 (m, 2H), 2.40 (s, 3H) ppm.^{13}C NMR (101 MHz, $CDCl_3$) δ 176.6 (^{13}C), 147.9, 146.6, 143.6, 137.2, 130.5, 129.7, 127.1, 122.5, 109.5, 108.4, 101.1, 52.0, 40.4, 38.6, 38.0, 21.6 ppm. Spectroscopic data for **2.2aw-^{13}C** match that of the non-labelled analogue.

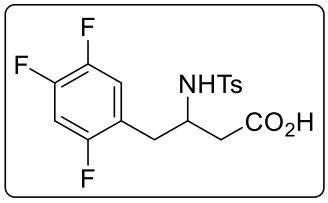

3-((4-Methylphenyl)sulfonamido)-4-(2,4,5-trifluorophenyl) butanoic acid (2.2ax): Following **GP8** with a reaction time of 5 days[xxiii], **2.1ax** (68 mg, 0.20 mmol) gave **2.2ax** (29 mg, 37%) as a white solid. In a separate independent experiment **2.2ax** (30 mg, 39%) was isolated giving an average yield of 38%. M.P. = 142 – 145 °C. ^{1}H NMR (400 MHz, $CDCl_3$) δ 7.57 – 7.52 (m, 2H), 7.21 – 7.16 (m, 2H), 6.83 – 6.67 (m, 2H), 5.48 (d, *J* = 9.4 Hz, 1H), 3.77 – 3.67 (m, 1H), 2.88 – 2.71 (m, 3H), 2.63 (dd, *J* = 17.1, 4.0 Hz, 1H), 2.41 (s, 3H) ppm. ^{13}C NMR (101 MHz, DMSO-d_6) δ 171.6, 142.3, 138.3, 129.3, 126.0, 121.6 (d, *J* = 18.6 Hz), 119.4 (dd, *J* = 19.4, 6.1 Hz), 105.4 (dd, *J* = 29.0, 20.9 Hz), 50.7, 40.8, 33.0, 20.9. ^{19}F (367 MHz, DMSO-d_6) δ -118.7 (ddt, *J* = 15.8, 10.1, 5.0 Hz), -137.2 (dtd, *J* = 23.5, 10.9, 10.2, 3.6 Hz), -144.2 (dddd, *J* = 22.5, 15.4, 11.2, 6.9 Hz) ppm. IR (neat, cm^{-1}): 3241, 3058, 2926, 2698, 2590, 1696, 1633, 1599, 1518, 1424, 1328, 1241, 1218, 1200,1155, 1097, 1083, 1068, 964, 917, 880, 845, 835, 813, 755,

[xxiii] After a 5-day reaction: 15% **2.1ax** was observed in the crude NMR along with 20% $TsNH_2$ Accurate quantification of **2.2ax** was not possible because of its' low solubility in $CDCl_3$. Increasing the reaction time to 7 days did not improve the yield in this case.

708, 654, 586, 547, 514, 483. HRMS calcd. for ($C_{17}H_{15}F_3NO_4S$) $[M–H]^-$: 386.0679 found 386.0676.

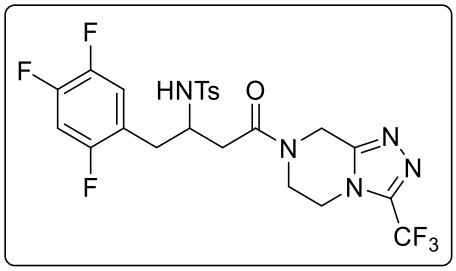

4-Methyl-N-(4-oxo-4-(3-(trifluoromethyl)-5,6-dihydro-[1,2,4]triazolo[4,3-a]pyrazin-7(8H)-yl)-1-(2,4,5-trifluorophenyl)butan-2-yl) benzenesulfonamide (2.4): Formally following literature procedure,[147] to a solution of 3-(trifluoromethyl)-5,6,7,8-tetrahydro-[1,2,4]triazolo[4,3-a]pyrazin-7-ium chloride (15 mg, 0.080 mmol), EDC**.**HCl (28 mg, 0.14 mmol) and DMAP (35 mg, 0.29 mmol) in CH_2Cl_2 (2.0 ml) was added drop wise a solution of **2.2ax** (28 mg, 0.070 mmol) in CH_2Cl_2 (2.0 ml) and the resulting mixture was stirred at room temperature overnight. The reaction was quenched with 4.0 M HCl and acidified to pH = 1. The aqueous phase was extracted with CH_2Cl_2. The combined organic fractions were dried ($MgSO_4$), filtered and concentrated. The crude material was purified by column chromatography on silica gel (CH_2Cl_2:MeOH 99:1 → 97:3) to afford **3** as a white solid (30 mg, 74%). The product appears as a mixture of rotamers (~1:1) at RT. M.P. = 204 – 207 °C. ^{1}H NMR (400 MHz, CD_3CN) δ 7.47 – 7.39 (m, 2H), 7.20 – 7.14 (m, 2H), 7.01 – 6.89 (m, 1H), 6.88 – 6.75 (m, 1H), 5.95 – 5.85 (m, 1H), 4.89 – 4.75 (m, 2H), 4.03 – 3.70 (m, 3H), 2.84 – 2.59 (m, 4H), 2.35 (s, 3H) ppm. ^{1}H NMR (500 MHz, DMSO-d_6, T = 115 °C)[xxiv] δ 7.52 – 7.43 (m, 2H), 7.33 (s, br, 1H), 7.20 (d, *J* = 8.0 Hz, 2H), 7.15 (ddd, *J* = 11.4, 9.2, 6.9 Hz, 1H), 7.09 (ddd, *J* = 10.9, 9.6, 6.8 Hz, 1H), 4.84 (s, 2H), 4.17 (m, 2H), 3.92 (t, *J* = 5.5 Hz, 2H), 3.86 (m, 1H), 2.83 (dd, *J* = 14.0, 5.1 Hz, 1H), 2.75 – 2.67 (m, 2H), 2.64 (dd, *J* = 15.5, 6.9 Hz, 1H), 2.34 (s, 3H) ppm. ^{13}C NMR (126 MHz, DMSO-d_6, T = 115 °C) δ 168.5, 155.3 (ddd, *J* = 243.5, 9.9, 2.4 Hz), 150.2, 147.6 (ddd, *J* = 247.1, 14.3, 12.7 Hz), 145.1 (ddd, *J* = 241.6, 12.3, 3.4 Hz), 142.1 (q, *J* = 39.6 Hz), 141.7, 138.3, 128.5, 125.5, 121.4 (ddd, *J* = 18.2, 5.8, 4.1 Hz), 118.7 (dd, *J* = 19.3, 6.2 Hz), 118.0 (q, *J* = 270.0 Hz), 104.6 (dd, *J* = 29.1, 21.1 Hz), 50.8, 42.9, 38.2 (2C), 32.9 (2C), 20.1. ^{19}F NMR (471 MHz, DMSO-d_6, T = 95 °C) δ -61.7, -118.34 (d, *J* = 15.3 Hz), -137.21 (dd, *J* = 22.1, 3.0 Hz), -144.12 (dd, *J* = 21.9, 16.0 Hz). IR (neat, cm^{-1}): 3157, 3057, 2927, 1626, 1515, 1477, 1445, 1425, 1336, 1272, 1236, 1201, 1162, 1136, 1095, 1073, 1034, 1016, 984, 969, 940, 854, 810, 709, 671, 575, 547. HRMS calcd. for ($C_{23}H_{20}F_6N_5O_3S$) $[M–H]^-$: 560.1197 found 560.1184.

[xxiv] The presence of rotamers of **2.4** at RT resulted in complicated NMR spectrum, particularly for the ^{13}C in which ^{13}C-^{19}F couplings' make analysis challenging. Therefore, variable temperature NMR was carried out in DMSO-d^6 with complete resolution of the rotamers observed at 115 °C.

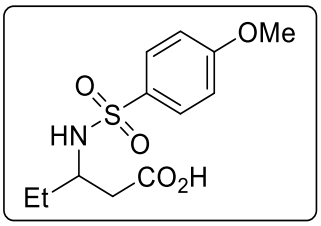

3-((4-Methoxyphenyl)sulfonamido) pentanoic acid (2.2ay): Following **GP8** with a reaction time of 5 days,[xxv] **2.1ay** (40 µl, 0.20 mmol) gave **2.2ay** (38 mg, 66%) as a white solid. In a separate independent experiment **2.2ay** (41 mg, 73%) was isolated giving an average yield of 70%. M.P.: 104 − 106 °C. ^{1}H NMR (400 MHz, $CDCl_3$) δ 8.58 (s, 1H), 7.93 – 7.74 (m, 2H), 7.09 – 6.83 (m, 2H), 5.42 (d, *J* = 8.2 Hz, 1H), 3.85 (s, 3H), 3.56 – 3.33 (m, 1H), 2.47 (m, 2H), 1.53 (p, *J* = 7.2 Hz, 2H), 0.80 (t, *J* = 7.2 Hz, 3H) ppm. ^{13}C NMR (126 MHz, $CDCl_3$) δ 176.7, 163.0, 132.5, 129.3, 114.4, 55.7, 52.1, 38.6, 27.8, 10.4 ppm. IR (neat, cm^{-1}): 3278, 2974, 2918, 1709, 1596, 1579, 1497, 1455, 1433, 1412, 1314, 1299, 1284, 1260, 1192, 1144, 1121, 1096, 1073, 1038, 1016. HRMS calcd. for ($C_{12}H_{16}NO_5S$) $[M–H]^–$: 286.0755 found 286.0757.

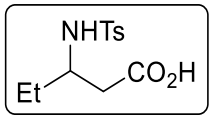

3-((4-Methylphenyl)sulfonamido) pentanoic acid (2.2az): Following **GP8** with a reaction time of 3 days, **2.1az** (39 µl, 0.20 mmol) gave **2.2az** (39 mg, 73%) as a white solid. In a separate independent experiment **2.2az** (41 mg, 77%) was isolated giving an average yield of 75%. ^{1}H NMR (500 MHz, $CDCl_3$) δ 7.75 (d, *J* = 8.3 Hz, 2H), 7.29 (d, *J* = 8.0 Hz, 2H), 5.41 (s, br, 1H), 3.46 (s, br, 1H), 2.56 – 2.41 (m, 2H), 2.41 (s, 3H), 1.52 (m, 2H), 0.79 (t, *J* = 7.4 Hz, 3H) ppm. ^{13}C NMR (126 MHz, $CDCl_3$) δ 176.8, 143.6, 138.0, 129.8, 127.2, 52.1, 38.6, 27.7, 21.6, 10.4 ppm. LRMS (ESI): 541 (2M-H), 270 (M-H). Spectroscopic data for **2.2az** match those previously reported in the literature.[153]

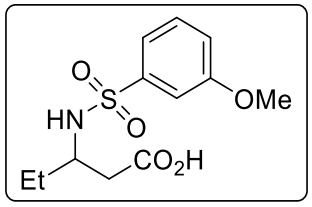

3-((3-Methoxyphenyl)sulfonamido) pentanoic acid (2.2ba). Following **GP8** with a reaction time of 5 days,[xxvi] **2.1ba** (48 mg, 0.20 mmol) gave **2.2ba** (33 mg, 57%) as a white solid. In a separate independent experiment **2.2ba** (34 mg, 59%) was isolated giving an average yield of 58%. M.P.: 89 − 91 °C.^{1}H NMR (500 MHz, $CDCl_3$) δ 8.35 (s, 1H), 7.46 (d, *J* = 7.8 Hz, 1H), 7.43 – 7.37 (m, 2H), 7.09 (dd, *J* = 8.5, 2.6 Hz, 1H), 5.45 (d, *J* = 9.0 Hz, 1H), 3.84 (s, 3H), 3.50 (q, *J* = 7.0 Hz, 1H), 2.54 – 2.41 (m, 2H), 1.54 (p, *J* = 7.3 Hz, 2H), 0.81 (t, *J* = 7.4 Hz, 3H) ppm. ^{13}C NMR (126 MHz, $CDCl_3$) δ 176.7, 160.1, 142.1, 130.3, 119.3, 119.3, 111.8, 55.8, 52.2, 38.5, 27.8, 10.4 ppm. IR (neat, cm^{-1}): 3230, 2975, 2945, 1704, 1595, 1581, 1475, 1427, 1333, 1283, 1237, 1155, 1035. HRMS calcd. for ($C_{12}H_{16}NO_5S$) $[M–H]^–$: 286.0755 found 286.0754.

[xxv] After a 3 day reaction, ~67% of **2.2ay** was observed by ^{1}H NMR and 18% **2.1ay** remained. Therefore, a prolonged reaction time was used to reach completion.
[xxvi] A shorter reaction was not carried out but trace **2.1ba** (10%) observed in the crude NMR suggested that the prolonged reaction time was necessary.

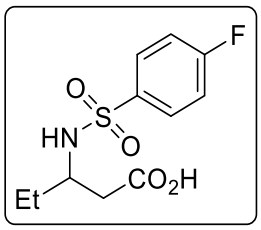

3-((4-Fluorophenyl)sulfonamido) pentanoic acid (2.2bb): Following **GP8** with a reaction time of 3 days, **2.1bb** (36 µl, 0.20 mmol) gave **2.2bb** (25 mg, 45%) as a white solid. In a separate independent experiment **2.2bb** (26 mg, 47%) was isolated giving an average yield of 46%. M.P.: 97 − 99 °C.^{1}H NMR (400 MHz, $CDCl_3$) δ 8.00 – 7.83 (m, 2H), 7.22 – 7.12 (m, 2H), 5.50 (d, *J* = 9.0 Hz, 1H), 3.59 – 3.38 (m, 1H), 2.50 (d, *J* = 5.4 Hz, 2H), 1.54 (p, *J* = 7.3 Hz, 2H), 0.79 (t, *J* = 7.4 Hz, 3H) ppm. ^{13}C NMR (101 MHz, $CDCl_3$) ^{13}C NMR (101 MHz, $CDCl_3$) δ 176.6, 165.2 (d, *J* = 254.7 Hz), 137.1 (d, *J* = 3.3 Hz), 129.9 (d, *J* = 9.2 Hz), 116.4 (d, *J* = 22.5 Hz), 52.3, 38.7, 27.9, 10.4. ^{19}F NMR (376 MHz, $CDCl_3$) δ -105.31 (tt, *J* = 8.6, 4.9 Hz) ppm. IR (neat, cm^{-1}): 3206, 2980, 2960, 2925, 1695, 1593, 1496, 1451, 1430, 1407, 1332, 1289, 1238, 1152, 1117, 1091, 1070, 1034, 1011. HRMS calcd. for ($C_{11}H_{13}FNO_4S$) $[M–H]^–$: 274.0555 found 274.0544.

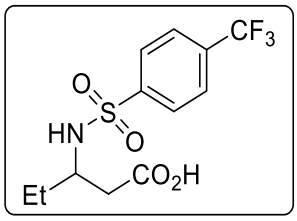

3-((4-(Trifluoromethyl)phenyl)sulfonamido) pentanoic acid (2.2bc): Following **GP8** with a reaction time of 5 days,[xxvii] **2.1bc** (43 µl, 0.20 mmol) gave **2.2bc** (14 mg, 22%) as a white solid. In a separate independent experiment **2.2bc** (15 mg, 23%) was isolated giving an average yield of 23%. M.P.: 100 − 102 °C. ^{1}H NMR (400 MHz, $CDCl_3$) δ 8.01 (d, *J* = 8.1 Hz, 2H), 7.77 (d, *J* = 8.2 Hz, 2H), 6.25 (s, br, 1H), 5.48 (d, *J* = 9.1 Hz, 1H), 3.60 – 3.47 (m, 1H), 2.52 (d, *J* = 5.2 Hz, 2H), 1.57 (p, *J* = 7.3 Hz, 2H), 0.81 (t, *J* = 7.4 Hz, 3H) ppm. ^{13}C NMR (101 MHz, $CDCl_3$) δ 176.4, 144.7, 134.51 (q, *J* = 33.1 Hz), 127.7, 126.39 (q, *J* = 3.8 Hz), 123.36 (q, *J* = 273.1 Hz), 52.5, 38.5, 28.0, 10.5 ppm. ^{19}F NMR (376 MHz, $CDCl_3$) δ -63.2. IR (neat, cm^{-1}):3300, 2968, 2918, 1699, 1422, 1406, 1320, 1292, 1160, 1127, 1109, 1093, 1061, 1026. HRMS calcd. for ($C_{12}H_{13}F_3NO_4S$) $[M–H]^–$: 324.0523 found 324.0522.

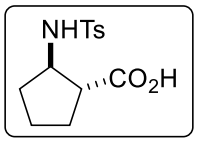

(*trans*)-2-((4-Methylphenyl)sulfonamido)cyclopentane-1-carboxylic acid (S26). Following **GP8** with a reaction time of 10 days,[xxviii] **2.8c** (48 mg, 0.20 mmol) gave **2.9c** (13 mg, 22%, > 10:1 *trans:cis*) as a white solid. In a separate independent experiment with a reaction time of 7 days, **2.9c** (9 mg, 27%) was isolated.^{1}H NMR (400 MHz, $CDCl_3$, diastereomers) δ 7.79 – 7.73 (m, 2H), 7.30 (d, *J* = 8.1 Hz, 2H), 5.27 (d, *J* = 8.3 Hz, 0.08H), 5.14 (d, *J* = 6.4 Hz, 0.92H), 3.78 (p, *J* = 7.1 Hz, 1H), 2.83 (dt, *J* = 12.1, 6.2 Hz, 0.08H), 2.72 (dt, *J* = 9.3, 7.4 Hz, 0.92H), 2.41 (s, 3H), 2.09 – 1.90 (m, 1H), 1.80 (tdd, *J* = 15.4, 8.0, 5.9 Hz, 1H), 1.75 – 1.57 (m, 1H), 1.46 (dq, *J* = 12.9, 7.9 Hz, 1H). ^{13}C NMR (101 MHz, $CDCl_3$, major diastereomer) δ 179.3, 143.8, 137.1, 129.9, 127.4, 57.7, 50.8, 33.6, 28.3, 23.1, 21.7. LRMS (ESI):

[xxvii] After a 3-day reaction, 16% of **2.2bc** was observed by ^{1}H NMR and 12% **2.1bc** remained.
[xxviii] After a 7-day reaction, 17% of **2.9c** was detected by ^{1}H NMR and 50% **2.8c** still remained. After a 10-day reaction, 25% of **2.9c** was detected by ^{1}H NMR and 35% **2.8c** still remained.

565 (2M-H), 396 (M+TFA), 282 (M-H). Spectroscopic data for **2.9c** match those previously reported in the literature.[154]

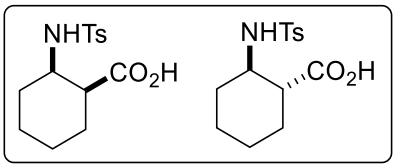

2-((4-Methylphenyl)sulfonamido)cyclohexane-1-carboxylic acid (2.9d): Following **GP8** with a reaction time of 10 days,[xxix] **2.8d** (50 mg, 0.20 mmol) gave **2.9d** (25 mg, 42%, d.r. 1:0.9 *cis:trans*) as a white solid. In a separate independent experiment **2.8d** (56 mg, 0.22 mmol) gave **2.9d** (25 mg, 38%) was isolated giving an average yield of 40%. H NMR (400 MHz, $CDCl_3$, diastereomers) δ 7.79 – 7.72 (m, 2H), 7.33 – 7.24 (m, 2H), 5.89 (d, *J* = 9.4 Hz, 0.55H), 5.17 (d, *J* = 8.0 Hz, 0.45H), 3.48 – 3.30 (m, 1H), 2.75 (q, *J* = 4.7 Hz, 0.55H), 2.42 (s, 1.65H), 2.40 (s, 1.35H), 2.32 (ddd, *J* = 11.3, 10.2, 3.8 Hz, 0.45H), 2.10 – 2.01 (m, 0.55H), 2.01 – 1.92 (m, 1H), 1.83 – 1.71 (m, 0.55H), 1.71 – 1.61 (m, 1.45H), 1.60 – 1.41 (m, 2H), 1.37 – 1.14 (m, 2.45H). ^{13}C NMR (101 MHz, $CDCl_3$, diastereomers)[xxx] δ 178.8^m, 178.5^M, 143.5^m, 143.5^M, 138.4^M, 138.0^m, 129.9^M, 129.7^m, 127.3^m, 127.0^M, 54.0^m, 52.5^M, 49.6^m, 45.1^M, 33.2^m, 29.9^M, 28.7^m, 27.4^M, 24.4^m, 24.1^M, 24.1^m, 22.2^M, 21.7^m, 21.7^M. LRMS (ESI): 594 (2M-H), 410 (M+TFA$^-$), 296 (M-H). Spectroscopic data for **2z** match those previously reported in the literature.[154]

2.7.6 Synthesis of *β*-amino acid 2.2a-*d*$_1$ and subsequent modification

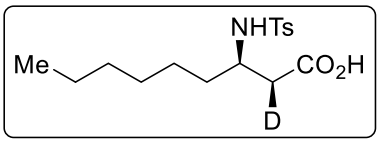

(2S,3R)-3-((4-|Methylphenyl)sulfonamido) nonanoic-2-*d* acid (2.2a-*d*$_1$): Following **GP8** with a reaction time of 3 days, **2.1a-*d*$_1$** (51 µl, 0.20 mmol) gave **2.2a-*d*$_1$** (43 mg, 66%, d.r 4:1 (major shown)) as a white solid. ^{1}H NMR (500 MHz, $CDCl_3$) δ 7.76 (d, *J* = 8.0 Hz, 2H), 7.29 (d, *J* = 7.9 Hz, 2H), 5.48 – 5.36 (m, 1H), 3.50 (p, *J* = 7.0 Hz, 1H), 2.47 (m, 1H), 2.48 (d, *J* = 4.5 Hz)^m & 2.46 (d, *J* = 5.8 Hz)^M (1H), 2.41 (s, 3H), 1.63 – 1.36 (m, 2H), 1.24 – 0.98 (m, 8H), 0.83 (t, *J* = 7.2 Hz, 3H). Note: NMR was also taken in CD_2Cl_2 which gave better but not perfect resolution of the isotopic doublets ^{1}H NMR (500 MHz, CD_2Cl_2) δ 9.24 (s, br, 1H), 7.79 – 7.70 (m, 2H), 7.32 (d, *J* = 8.0 Hz, 2H), 5.39 – 5.14 (m, 1H), 3.50 (q, *J* = 6.6 Hz, 1H), 2.49 (d, *J* = 4.6 Hz, 0.3H), 2.45 (d, *J* = 5.9 Hz, 0.8H), 2.42 (s, 3H), 1.45 (q, *J* = 7.0 Hz, 1H), 1.25 – 1.01 (m, 8H), 0.84 (t, *J* = 7.2 Hz, 3H) ppm. ^{13}C NMR (126 MHz, $CDCl_3$) δ 176.7, 143.6, 138.0, 129.8, 127.2, 50.5, 38.8 (t, *J* = 18.0 Hz), 34.7, 31.7, 28.8, 25.8, 22.6, 21.6, 14.1 ppm. ^{13}C NMR (101 MHz, CD_2Cl_2) δ 176.9, 144.1, 138.3, 130.1, 127.4, 50.9, 39.3, 39.1, 38.9, 35.0, 35.0, 32.0, 3.1, 26.0, 22.9, 21.7, 14.2. To confirm

[xxix] After a 7-day reaction, ~30% of **2.9d** was observed by ^{1}H NMR and 40% **2.8d** remained. After a 10-day reaction, ~40% of **2.9d** was observed and 25% **2.8d** remained. A 14-day reaction was also performed; no crude NMR was taken but the isolated yield of **2.9d** was again 42%. Various reaction variables were modified to improve the yield such as switching to less hindered **L4** and increasing the temperature but without success.
[xxx] Major (M) and minor (m) isomers have been assigned.

the presence of isomers in the isolated **2.2a-*d*$_1$** and to determine their relative conformation, **2.2a** and **2.2a-*d*$_1$** were converted to the cyclic carbamate derivatives.

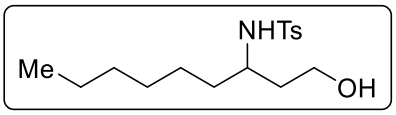

***N*-(1-Hydroxynonan-3-yl)-4-methylbenzenesulfonamide (S16)**: To a slurry of $LiAlH_4$ (34 mg, 6.6 eq.) in dry THF (1.0 ml) cooled to 0 °C was added **2.2a** (45 mg) as a solution in THF (2.0 ml) drop wise. The mixture was then allowed to warm to RT and stirred for 2 h. After this time, the reaction was quenched by careful addition of H_2O (~5 drops) and stirred until it turned white. CH_2Cl_2 (10 ml) was added and the mixture was filtered, washing with CH_2Cl_2 (2 × 5.0 ml). This gave **S15** (41 mg, 95%) which was used in the following step without further purification. ^{1}H NMR (400 MHz, $CDCl_3$) δ 7.76 (d, *J* = 7.9 Hz, 2H), 7.30 (d, *J* = 7.9 Hz, 2H), 4.79 (d, *J* = 8.4 Hz, 1H), 3.92 – 3.81 (m, 1H), 3.68 – 3.58 (m, 1H), 3.43 – 3.34 (m, 1H), 2.42 (s, 3H), 1.75 (ddt, *J* = 14.1, 9.2, 4.0 Hz, 1H), 1.47 – 1.35 (m, 1H), 1.37 – 1.26 (m, 2H), 1.16 (q, *J* = 6.8 Hz, 2H), 1.10 – 0.88 (m, 6H), 0.82 (t, *J* = 7.2 Hz, 3H) ppm. ^{13}C NMR (101 MHz, $CDCl_3$) δ 143.5, 138.1, 129.8, 127.2, 59.0, 51.6, 37.6, 35.8, 31.7, 29.0, 25.5, 22.5, 21.6, 14.2 ppm.

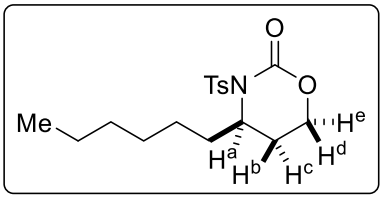

4-Hexyl-3-tosyl-1,3-oxazinan-2-one (S17): Following a modified literature procedure,[155] to **S16** (41 mg, 0.13 mmol, 1.0 eq.) and pyridine (0.42 ml, 5.2 mmol, 40 eq.) in dry CH_2Cl_2 (10 ml) cooled to 0 °C was added triphosgene (0.22 g, 0.65 mmol, 5.0 eq.) as a solution in CH_2Cl_2 (6.0 ml). After stirring for an hour at this temperature, the solution was warmed to RT and stirred overnight. The solution was again cooled to 0 °C, quenched with NH_4Cl (sat.) and diluted with EtOAc (20 ml). The layers were separated and the aqueous layer was extracted with EtOAc (2 × 10 ml). The combined organic fractions were dried ($MgSO_4$), filtered and concentrated under reduced pressure. Purification by column chromatography gave **S17** (16 mg, 36%) as a white solid. M.P: 80 − 82 °C. ^{1}H NMR (500 MHz, CD_2Cl_2) δ 7.88 – 7.81 (m, 2H), 7.36 – 7.31 (m, 2H), 4.61 – 4.54 (m, H^a), 4.37 (td, *J* = 11.6, 3.8 Hz, H^d), 4.27 (dddd, *J* = 11.3, 5.2, 2.8, 1.1 Hz, H^e), 2.44 (s, 3H), 2.12 (ddtd, *J* = 14.8, 11.5, 5.2, 0.9 Hz, H^c), 2.04 (ddt, *J* = 14.6, 3.9, 3.0 Hz, H^b), 1.99 – 1.90 (m, 1H), 1.73 – 1.62 (m, 1H), 1.42 – 1.24 (m, 8H), 0.91 (t, *J* = 6.8 Hz, 3H). ^{13}C NMR (126 MHz, CD_2Cl_2) δ 148.9, 145.4, 136.7, 129.7, 129.2, 65.2, 55.7, 34.4, 32.1, 29.3, 26.1, 25.7, 23.0, 21.8, 14.2. IR (neat, cm^{-1}): 2925, 2858, 1708, 1597, 1490, 1458, 1411, 1368, 1340, 1265, 1168, 1144, 1087, 1020. HRMS calcd. for ($C_{17}H_{26}NO_4S$) $[M+H]^+$: 340.1577 found 340.1572. Note: As for **2.2a-*d*$_1$**, better resolution was obtained taking the NMR in CD_2Cl_2 and allowed quantification of the isotopic ratio in the case of **2.16-*d*$_1$**.

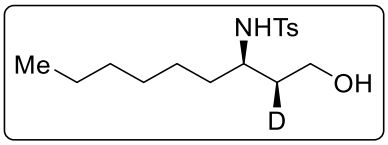

***N*-((2S,3R)-1-Hydroxynonan-3-yl-2-d)-4-methylbenzenesulfonamide (S18)**: Following the above procedure for the synthesis of **S16**, **2.2a-*d*$_1$** (43 mg) gave **S18** (38 mg, 93%) which was used in the following step without further purification. ^{1}H NMR (400 MHz, $CDCl_3$) δ 7.79 – 7.73 (m, 2H), 7.32 – 7.27 (m, 2H), 3.87 – 3.80 (m, 1H), 3.62 (dd, *J* = 11.4, 4.9 Hz, 1H), 3.36 (tq, *J* = 6.5, 2.8 Hz, 1H), 2.41 (s, 3H), 1.76 – 1.65 (m, 1H), 1.36 – 1.23 (m, 2H), 1.15 (q, *J* = 6.8 Hz, 2H), 1.09 – 0.91 (m, 6H), 0.81 (t, *J* = 7.2 Hz, 3H) ppm.

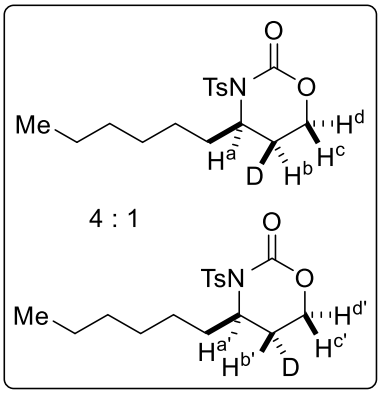

(4R,5S)-4-Hexyl-3-tosyl-1,3-oxazinan-2-one-5-d (2.16-*d*$_1$): Following the above procedure for the synthesis of **S17**, **S18** (38 mg) gave **2.16-*d*$_1$** (15 mg, 37%, 4:1 d.r) as a white solid. ^{1}H NMR (500 MHz, CD_2Cl_2) δ 7.87 – 7.83 (m, 2H), 7.36 – 7.32 (m, 2H), 4.59 – 4.53 (m, H$^{a/a'}$), 4.37 (t, *J* = 11.7 Hz, H^{c}) & 4.37 (dd, *J* = 11.3, 3.3 Hz, H$^{c'}$) , 4.26 (ddd, *J* = 11.3, 5.3, 1.1 Hz, H^{d}) & 4.26 (m, H$^{d'}$), 2.44 (s, 3H), 2.10 (dt, *J* = 11.5, 5.3 Hz, 0.8H^{b}), 2.03 (dt, *J* = 4.1, 2.6 Hz, 0.2H$^{b'}$), 2.00 – 1.90 (m, 1H), 1.73 – 1.64 (m, 1H), 1.43 – 1.24 (m, 9H), 0.94 – 0.87 (m, 3H) ppm. ^{13}C NMR (126 MHz, CD_2Cl_2, diastereomers)[xxxi] δ 149.0^{M} & 148.9^{m}, 145.4, 136.7, 129.7, 129.2, 65.2, 55.6^{M} & 55.6^{m}, 34.4^{M} & 34.3^{m}, 32.1, 29.3, 26.1^{m} & 26.1^{M}, 25.42 (t, *J* = 20.0 Hz)$^{M\&m}$, 23.0, 21.8, 14.2 ppm. Based on the closest available literature,[156] (**9**) has been assigned as a 4:1 *cis:trans* mixture of isomers.

[xxxi] The major (M) and minor (m) isomers have been assigned where the resolution was sufficient to detect separate peaks.

2.7.6 NMR spectra

^{1}H ($CDCl_3$, 500 MHz)

(L1)$NiCl_2$ (Ni-1)

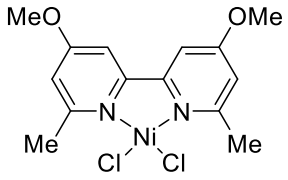

^{1}H ($CDCl_3$, 500 MHz)

(L2)$NiCl_2$ (Ni-2)

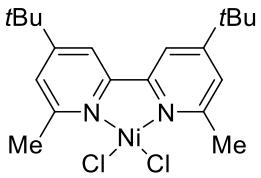

^{1}H ($CDCl_3$, 400 MHz)

2.1a-*d*$_1$

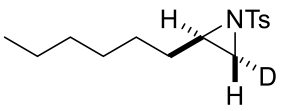

^{13}C ($CDCl_3$, 101 MHz)

2.1a-*d*$_1$

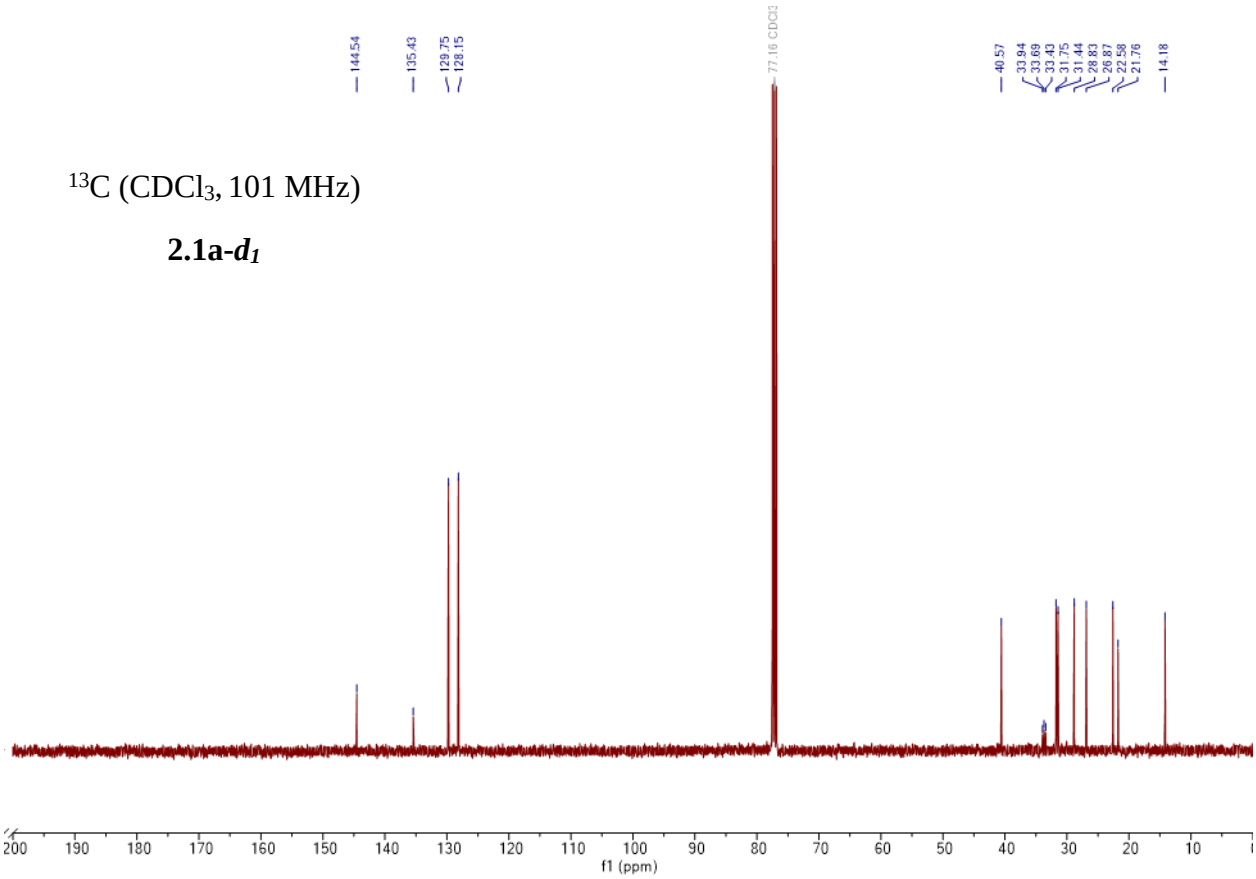

^{1}H ($CDCl_3$, 400 MHz)

2.1m

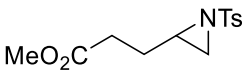

^{13}C ($CDCl_3$, 101 MHz)

2.1m

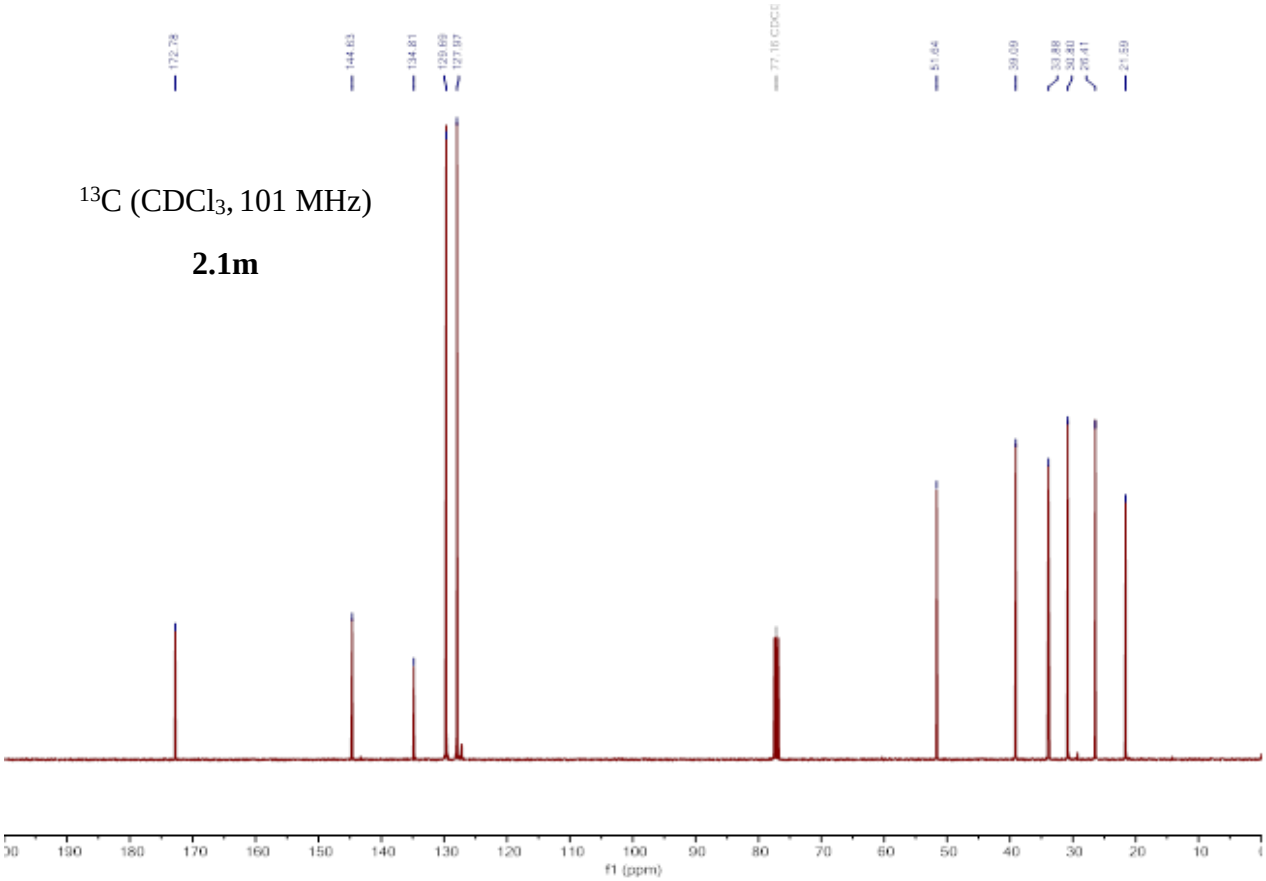

^{1}H ($CDCl_3$, 400 MHz)

2.1w

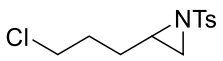

^{13}C ($CDCl_3$, 101 MHz)

2.1w

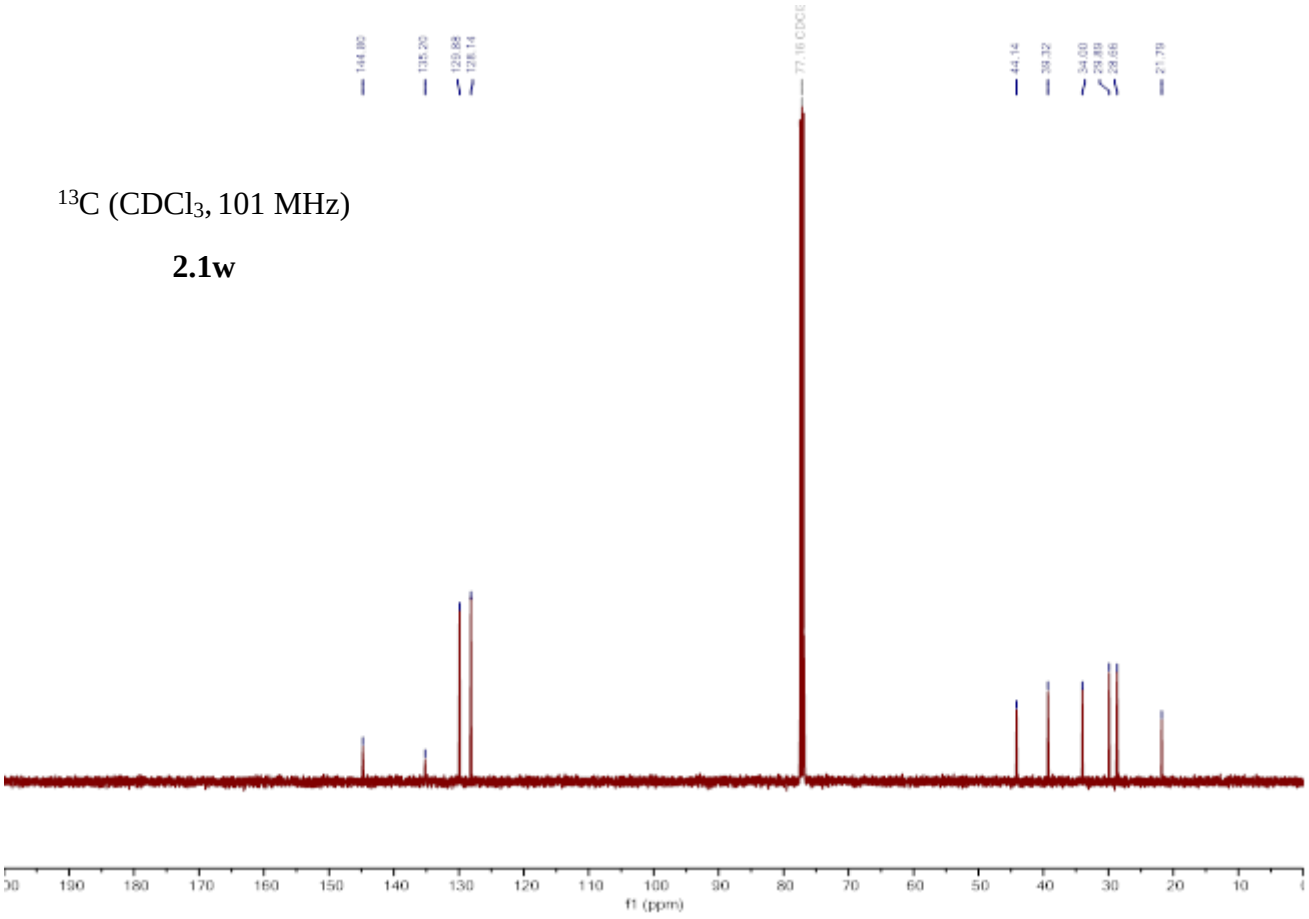

^{1}H ($CDCl_3$, 400 MHz)

2.1y

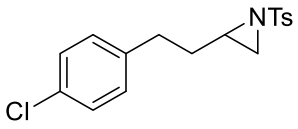

^{13}C ($CDCl_3$, 101 MHz)

2.1y

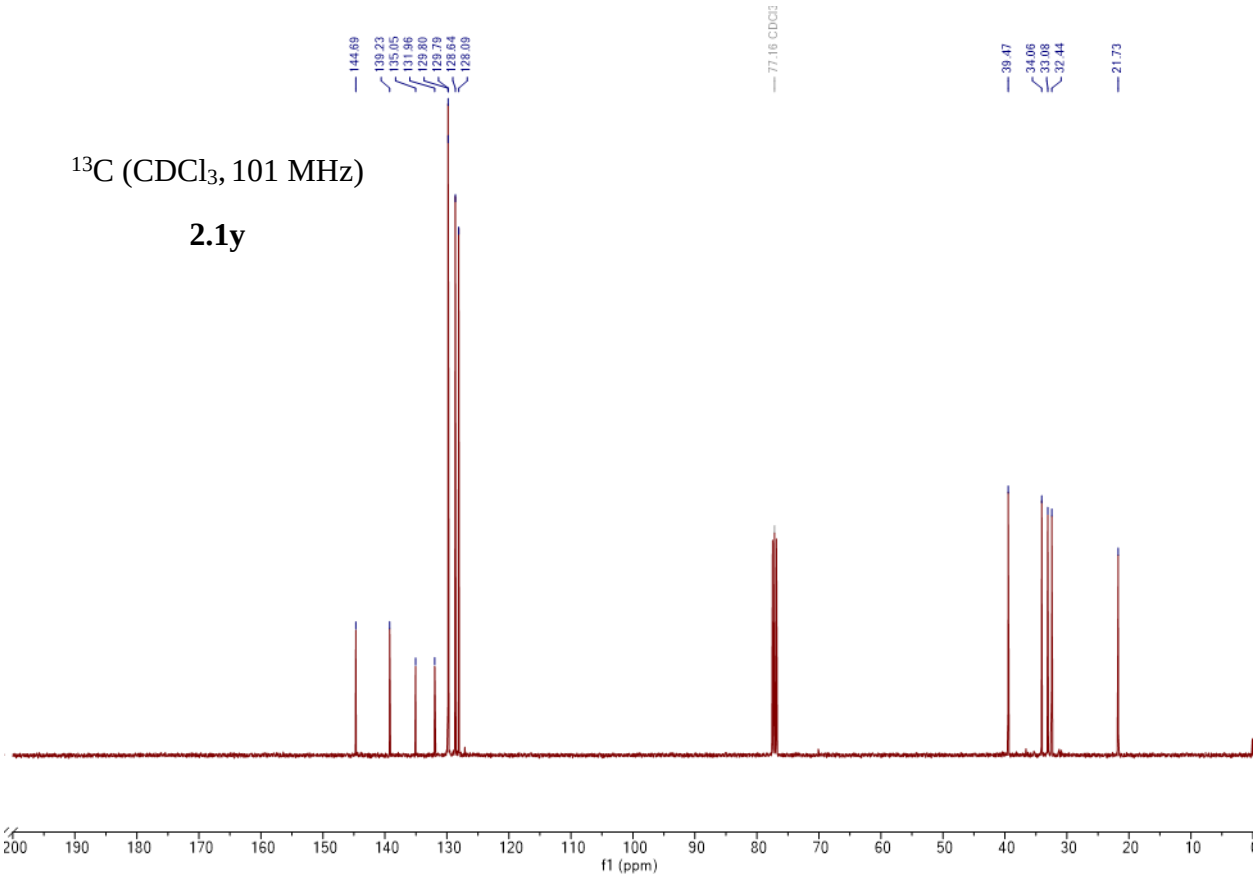

^{1}H ($CDCl_3$, 400 MHz)

2.1z

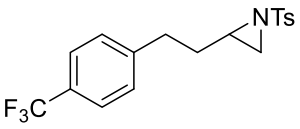

^{13}C ($CDCl_3$, 101 MHz)

2.1z

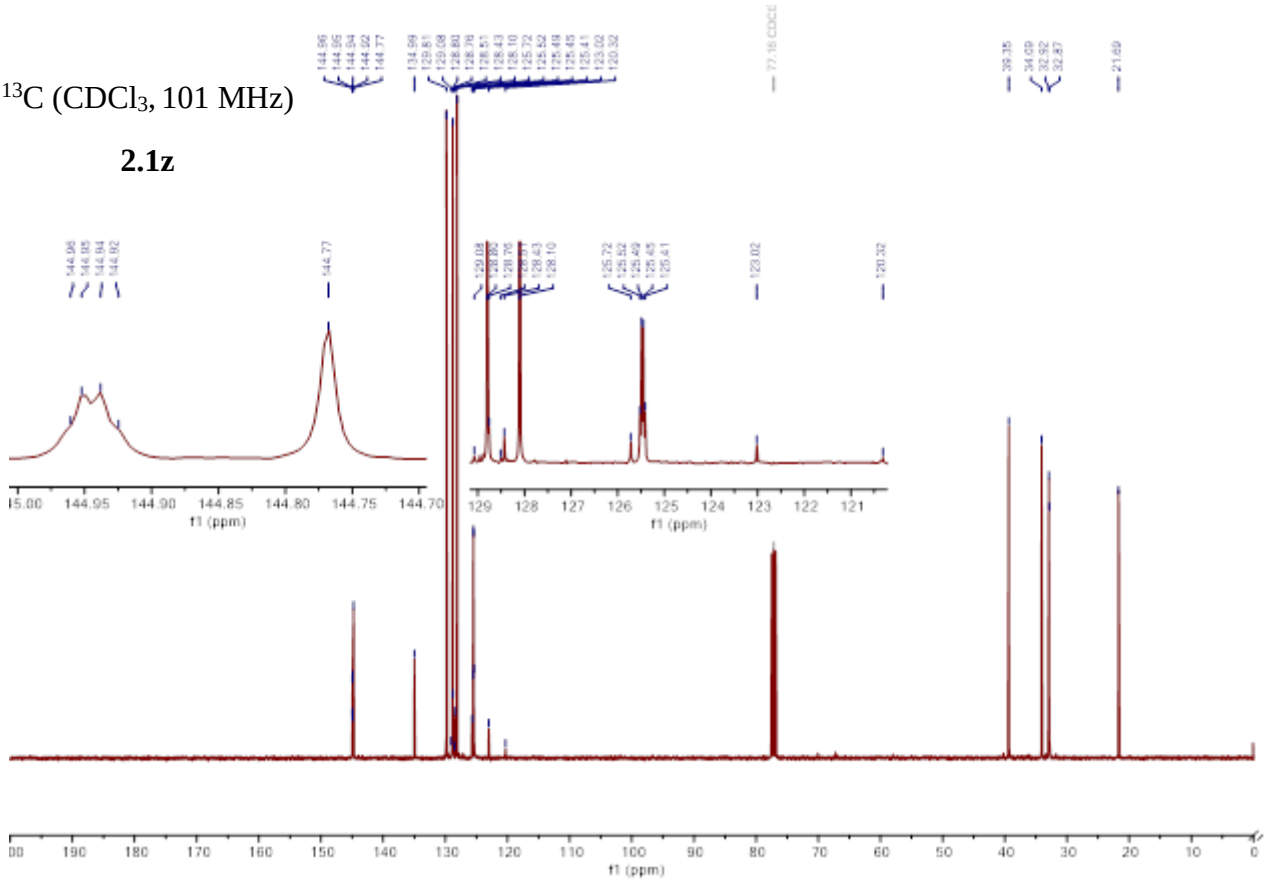

^{19}F ($CDCl_3$, 376 MHz)

2.1z

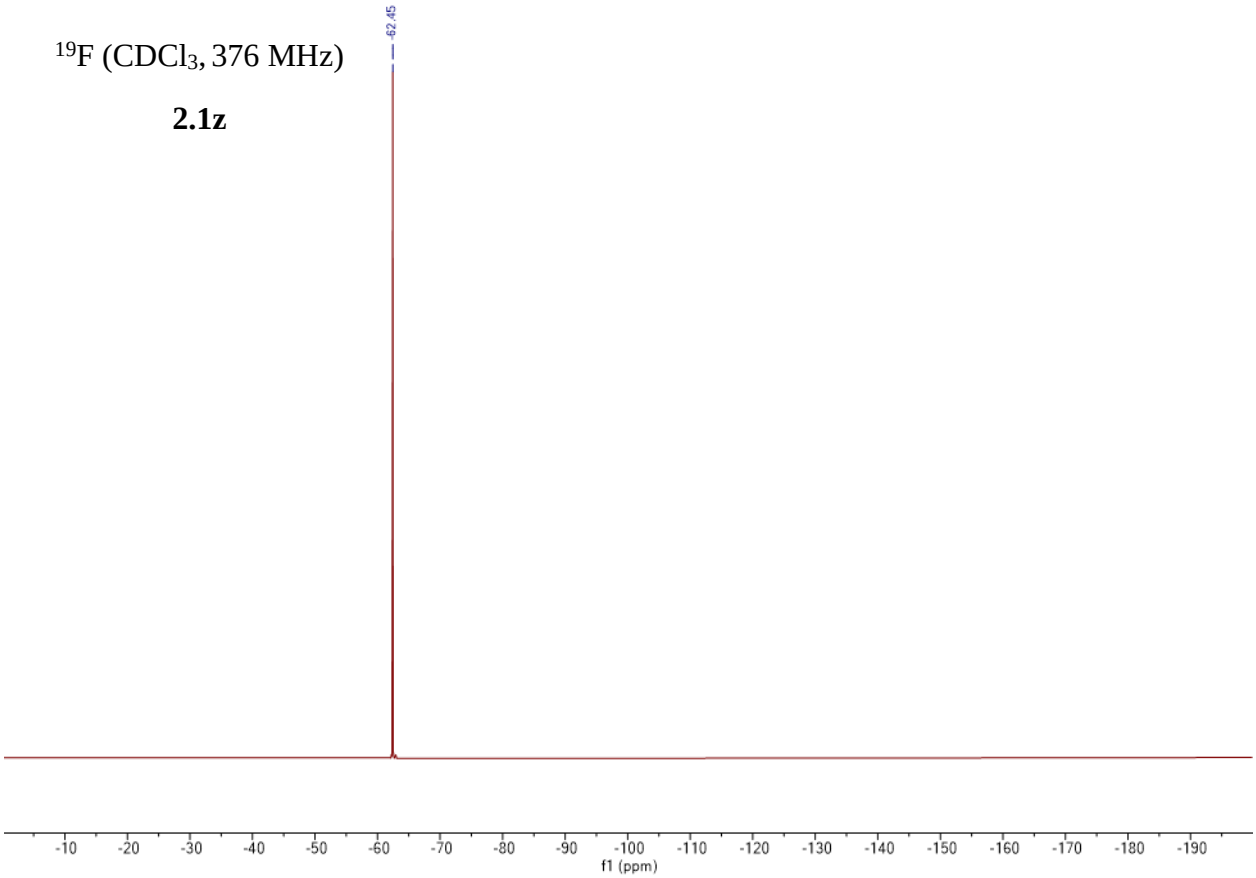

^{1}H ($CDCl_3$, 400 MHz)

2.1aa

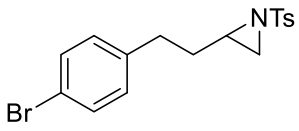

^{13}C ($CDCl_3$, 101MHz)

2.1aa

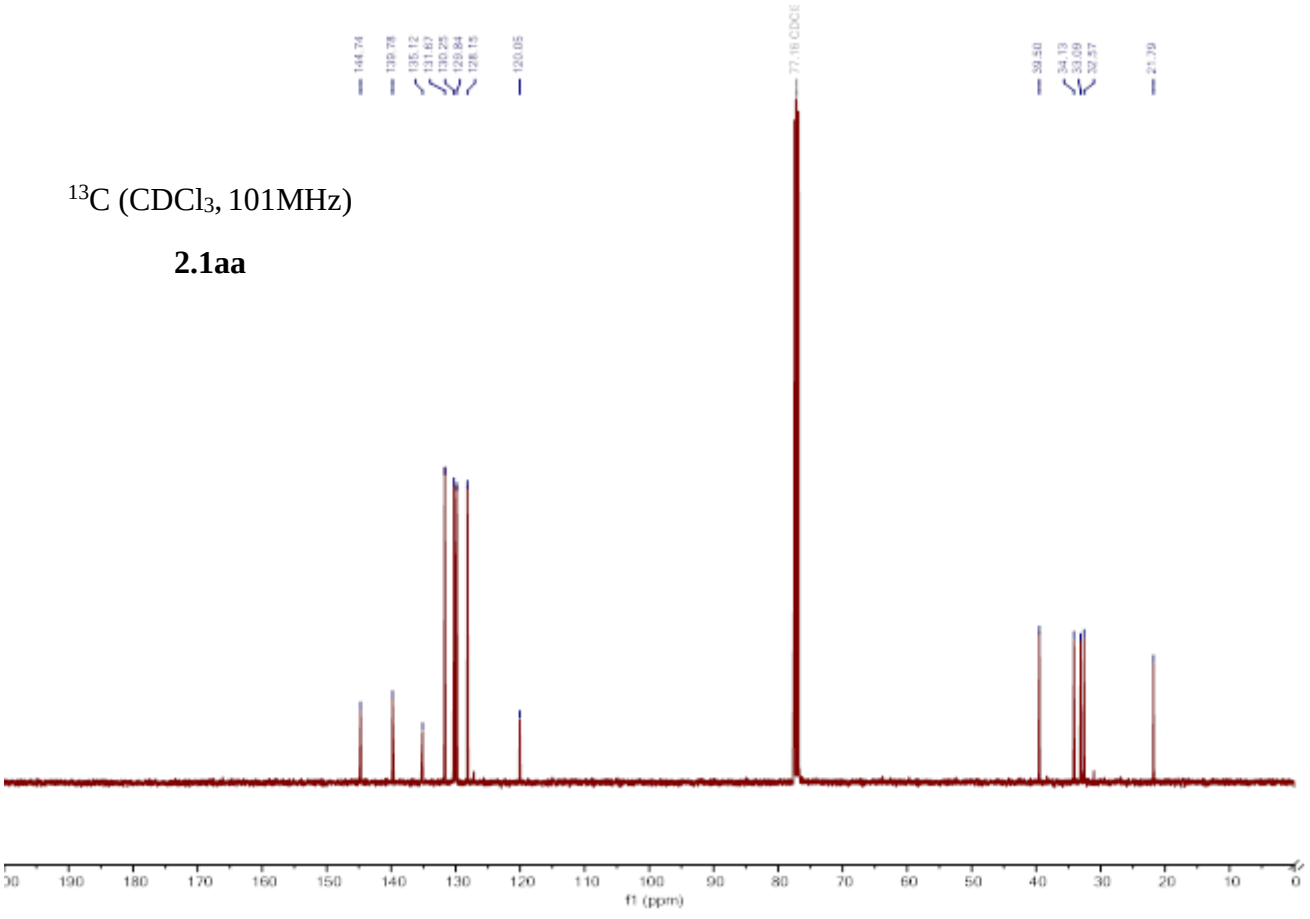

^{1}H ($CDCl_3$, 400 MHz)

2.1ab

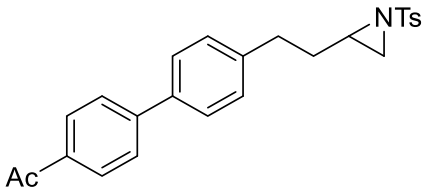

^{13}C ($CDCl_3$, 101 MHz)

2.1ab

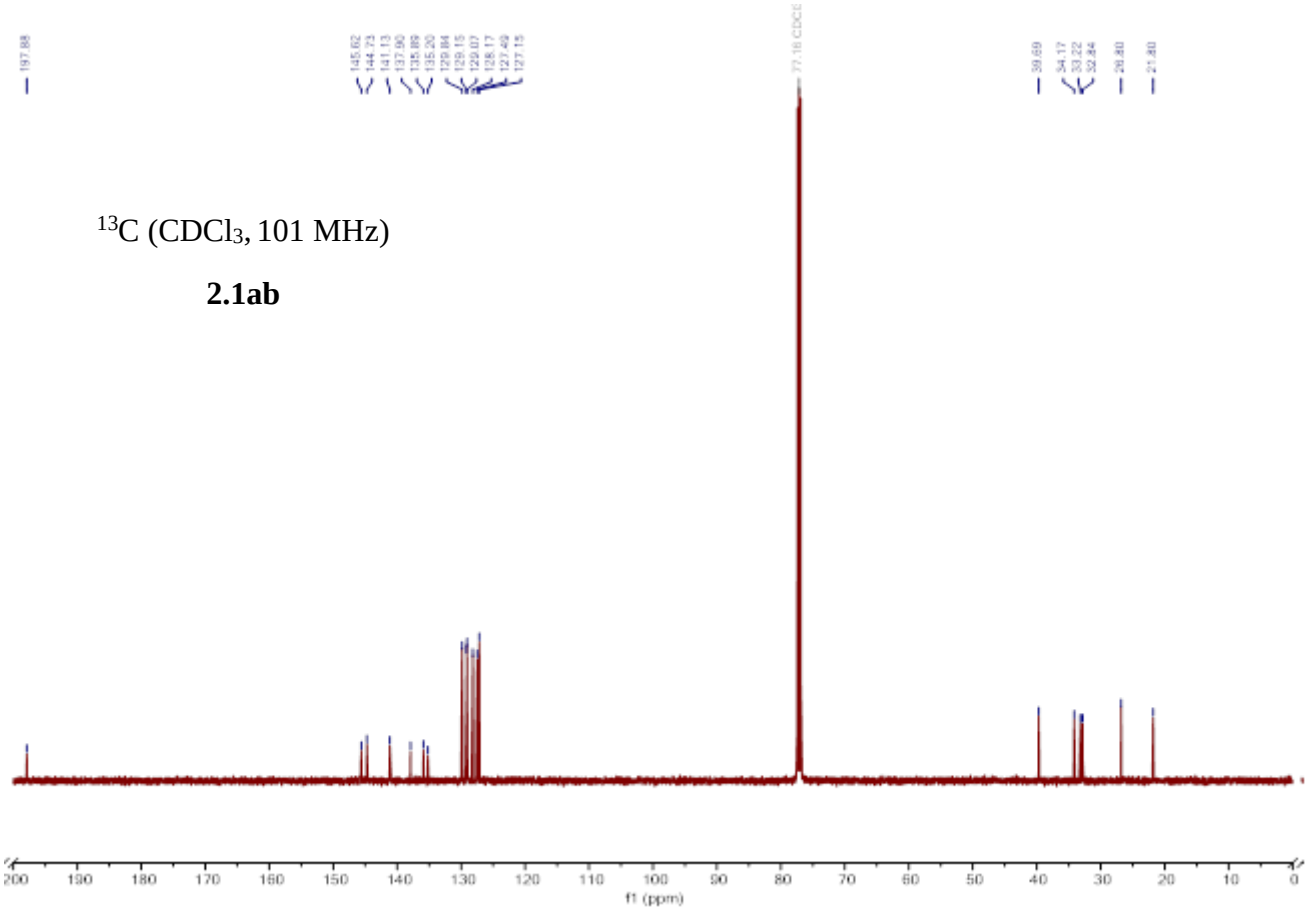

^{1}H ($CDCl_3$, 400 MHz)

2.1ac

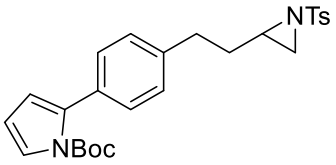

^{13}C ($CDCl_3$, 101 MHz)

2.1ac

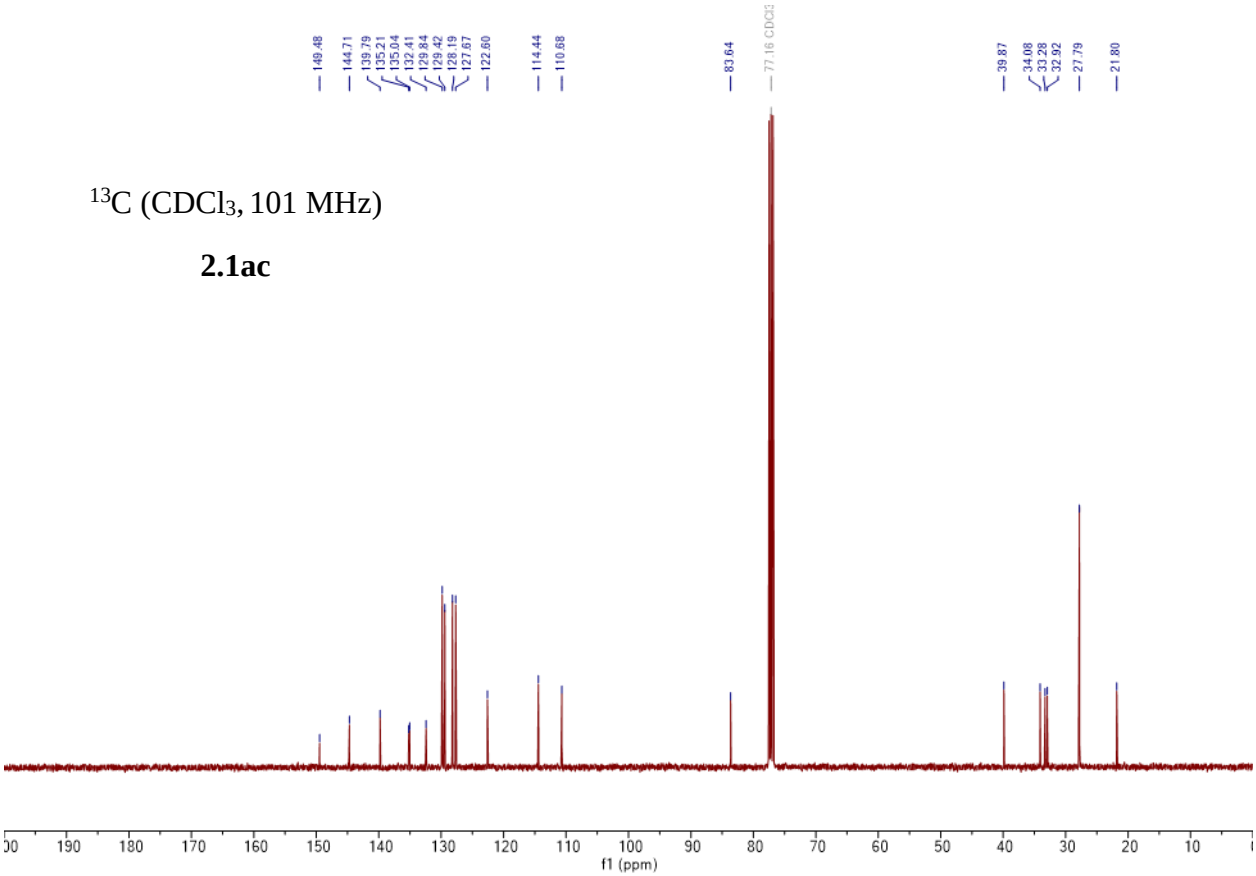

^{1}H ($CDCl_3$, 400 MHz)

2.1af

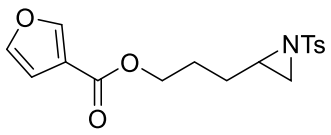

^{13}C ($CDCl_3$, 101 MHz)

2.1af

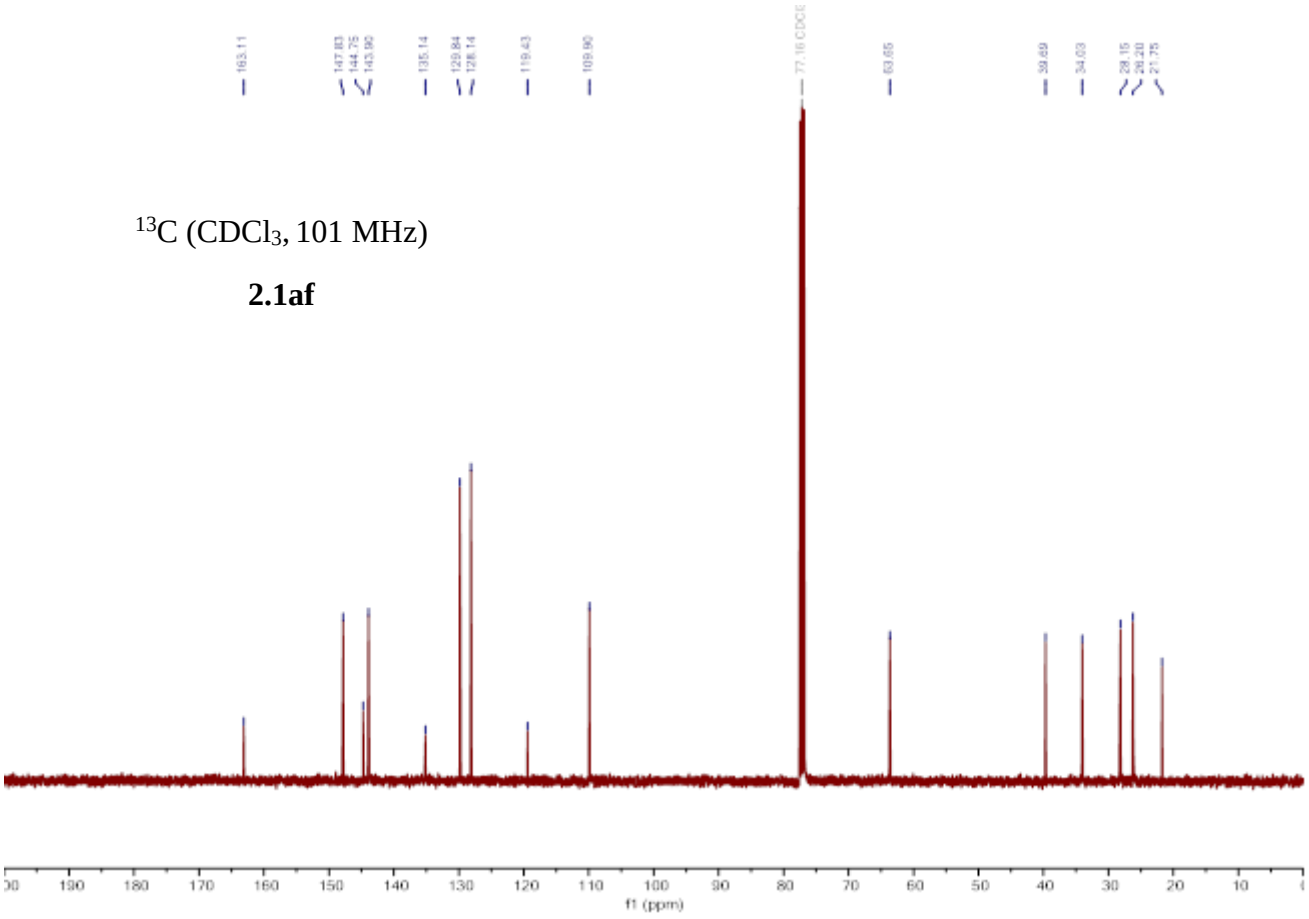

^{1}H ($CDCl_3$, 400 MHz)

2.1aj

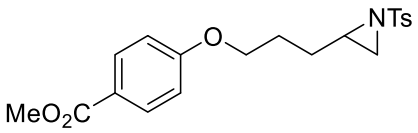

^{13}C ($CDCl_3$, 101 MHz)

2.1aj

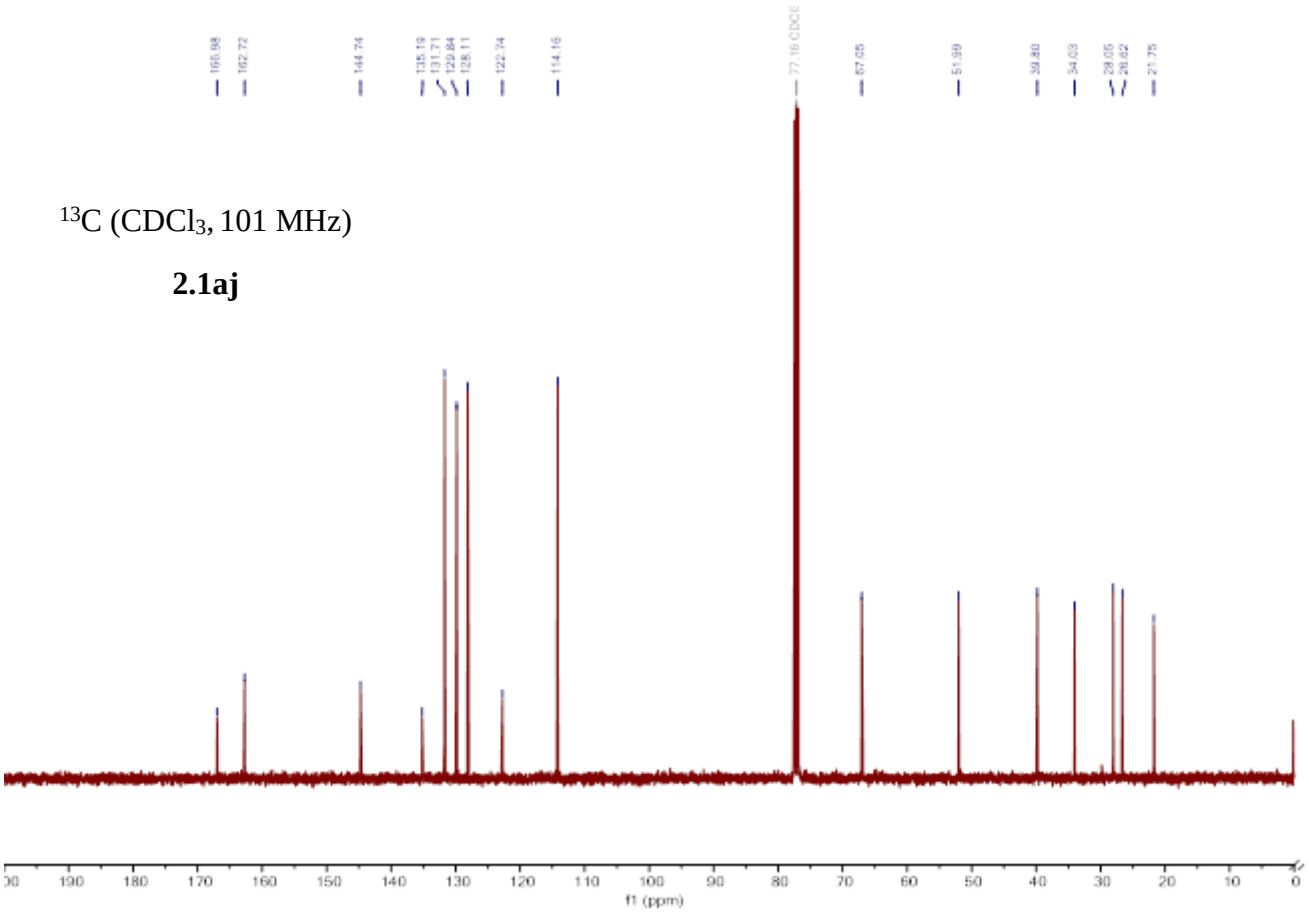

^{1}H ($CDCl_3$, 400 MHz)

2.1ak

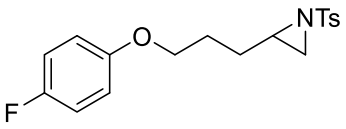

^{13}C ($CDCl_3$, 101 MHz)

2.1ak

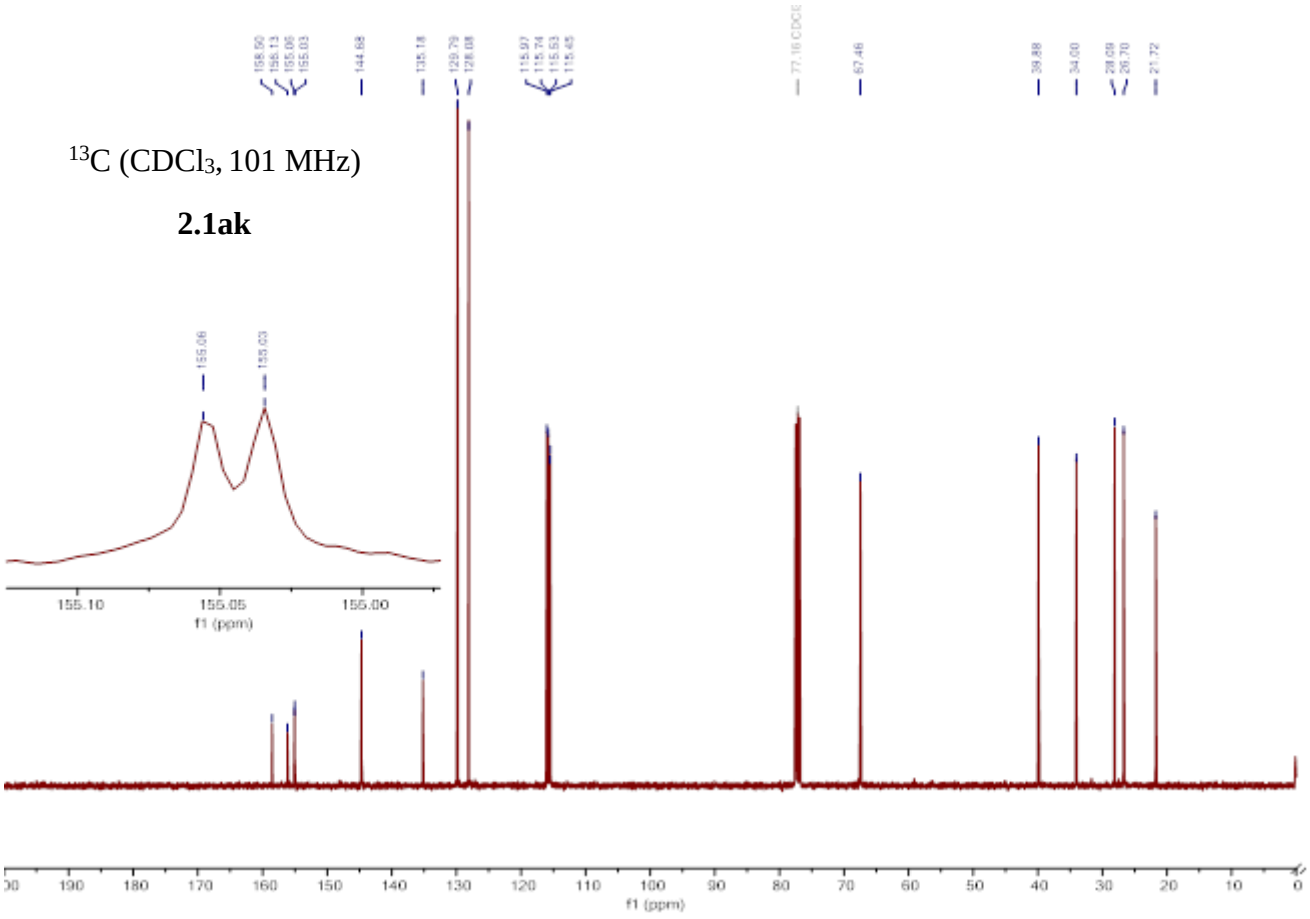

^{19}F ($CDCl_3$, 376 MHz)

2.1ak

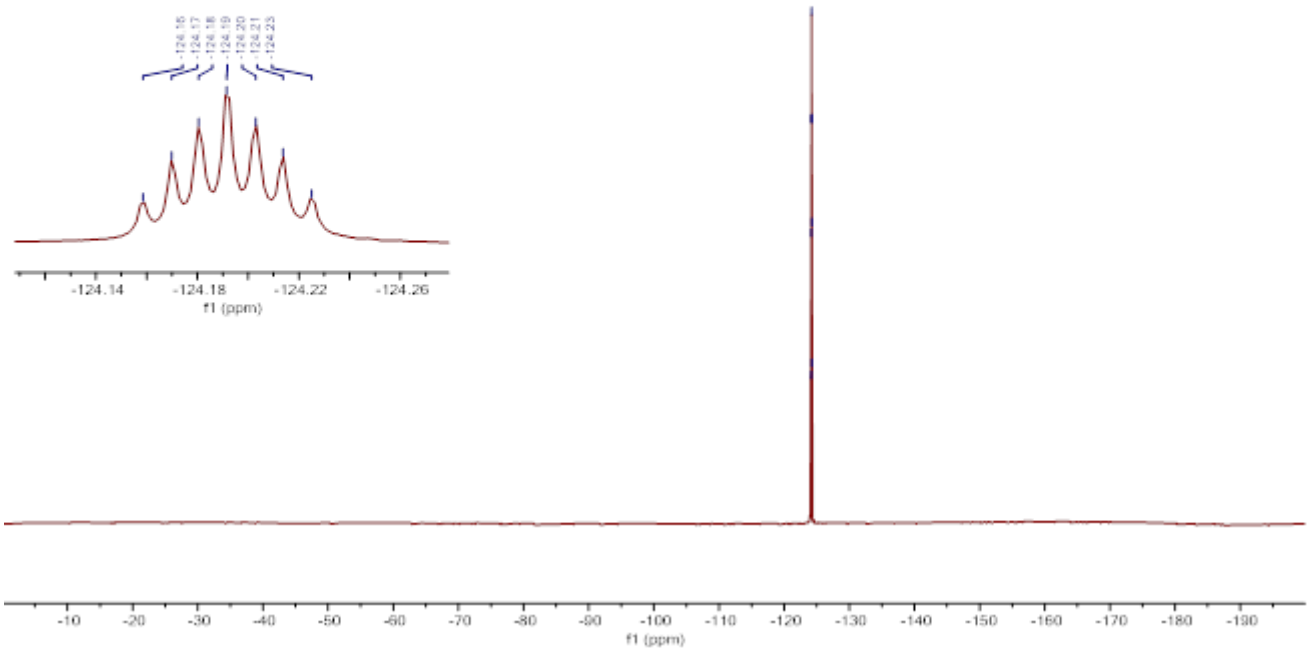

^{1}H ($CDCl_3$, 400 MHz)

2.1al

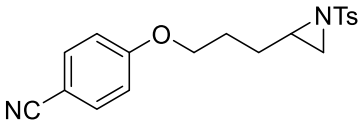

^{13}C ($CDCl_3$, 101 MHz)

2.1al

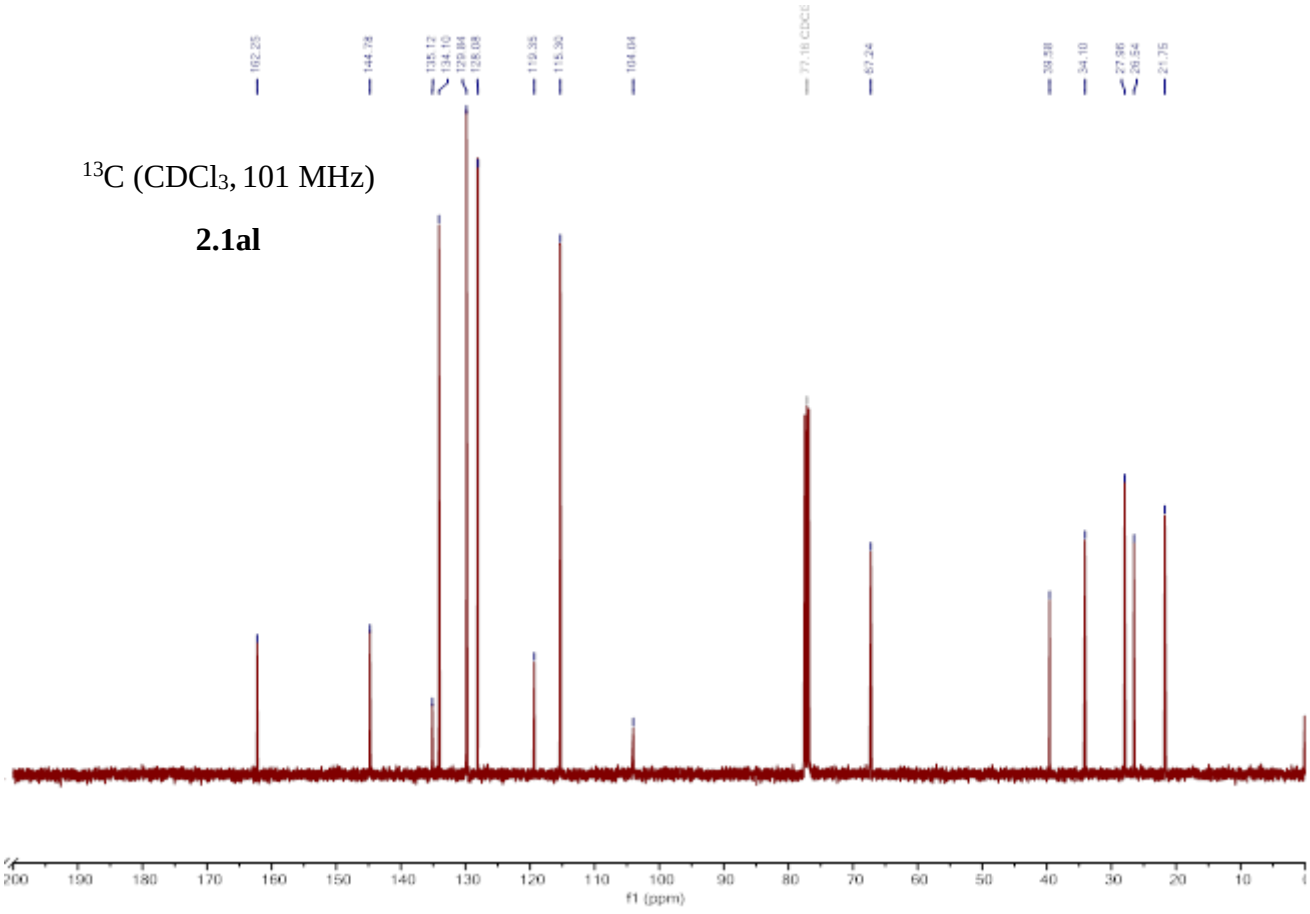

^{1}H ($CDCl_3$, 400 MHz)

2.1am

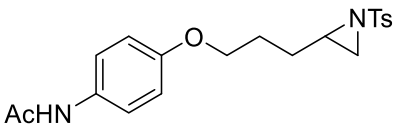

^{13}C ($CDCl_3$, 101 MHz)

2.1am

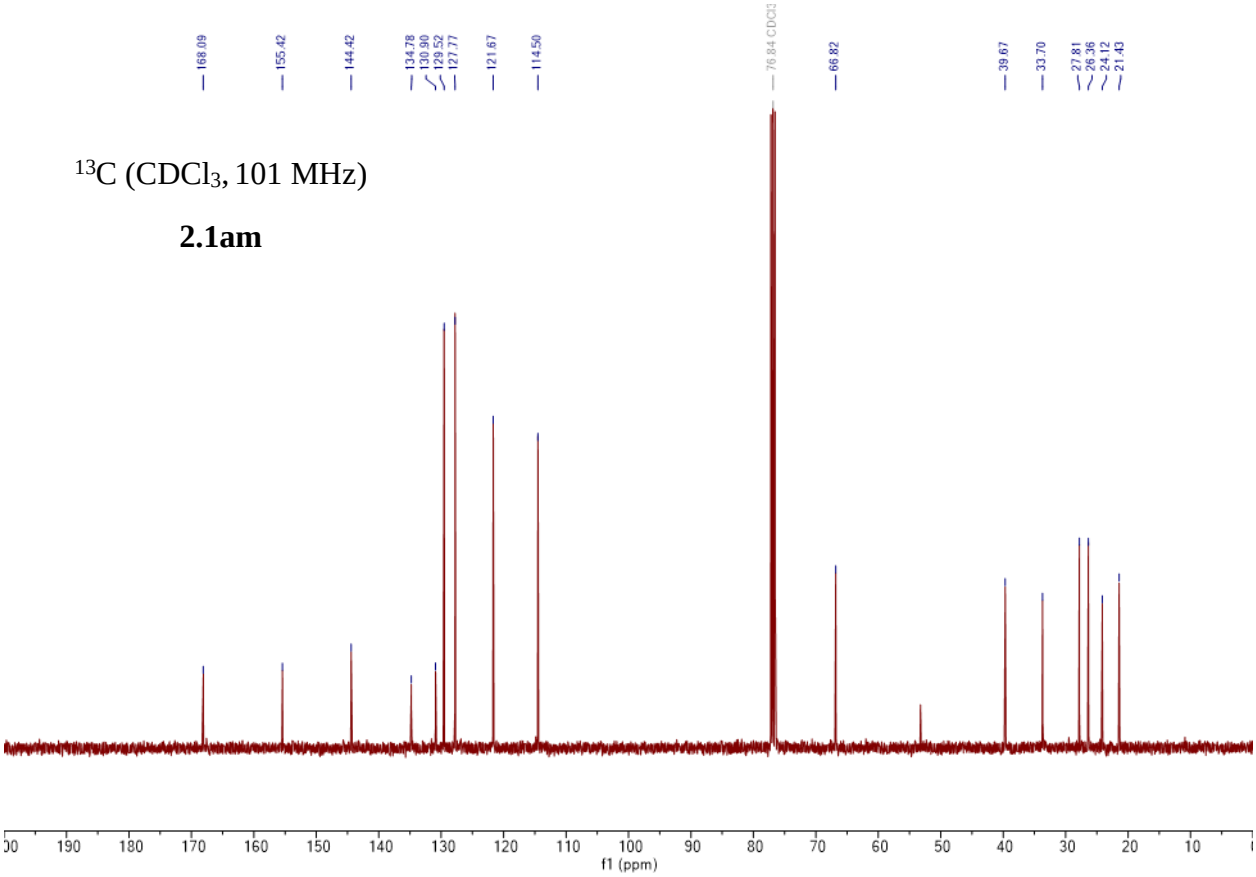

^{1}H ($CDCl_3$, 400 MHz)

2.1ar

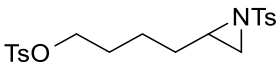

^{13}C ($CDCl_3$, 101 MHz)

2.1ar

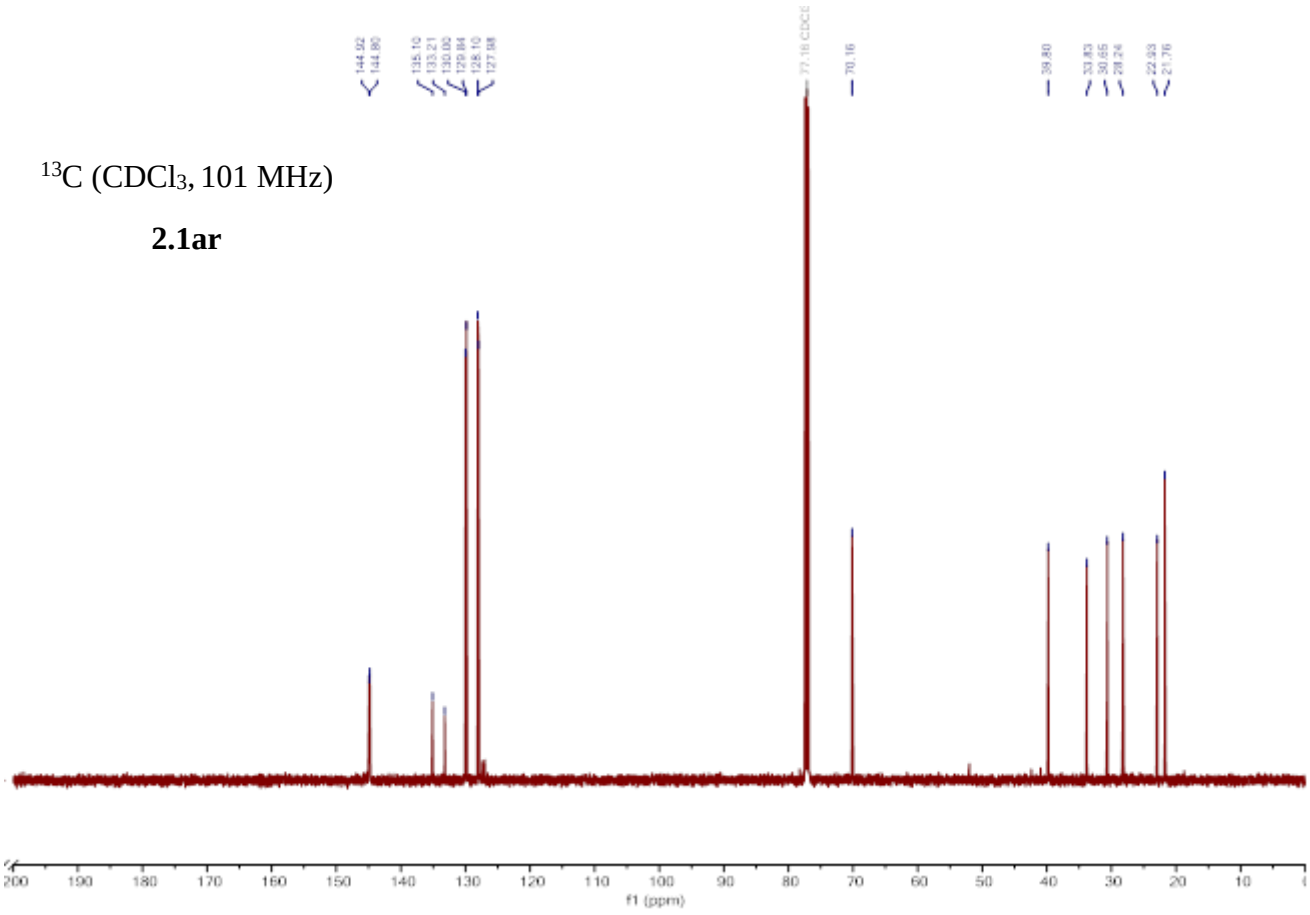

^{1}H ($CDCl_3$, 400 MHz)

2.1as

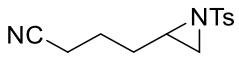

^{13}C ($CDCl_3$, 101 MHz)

2.1as

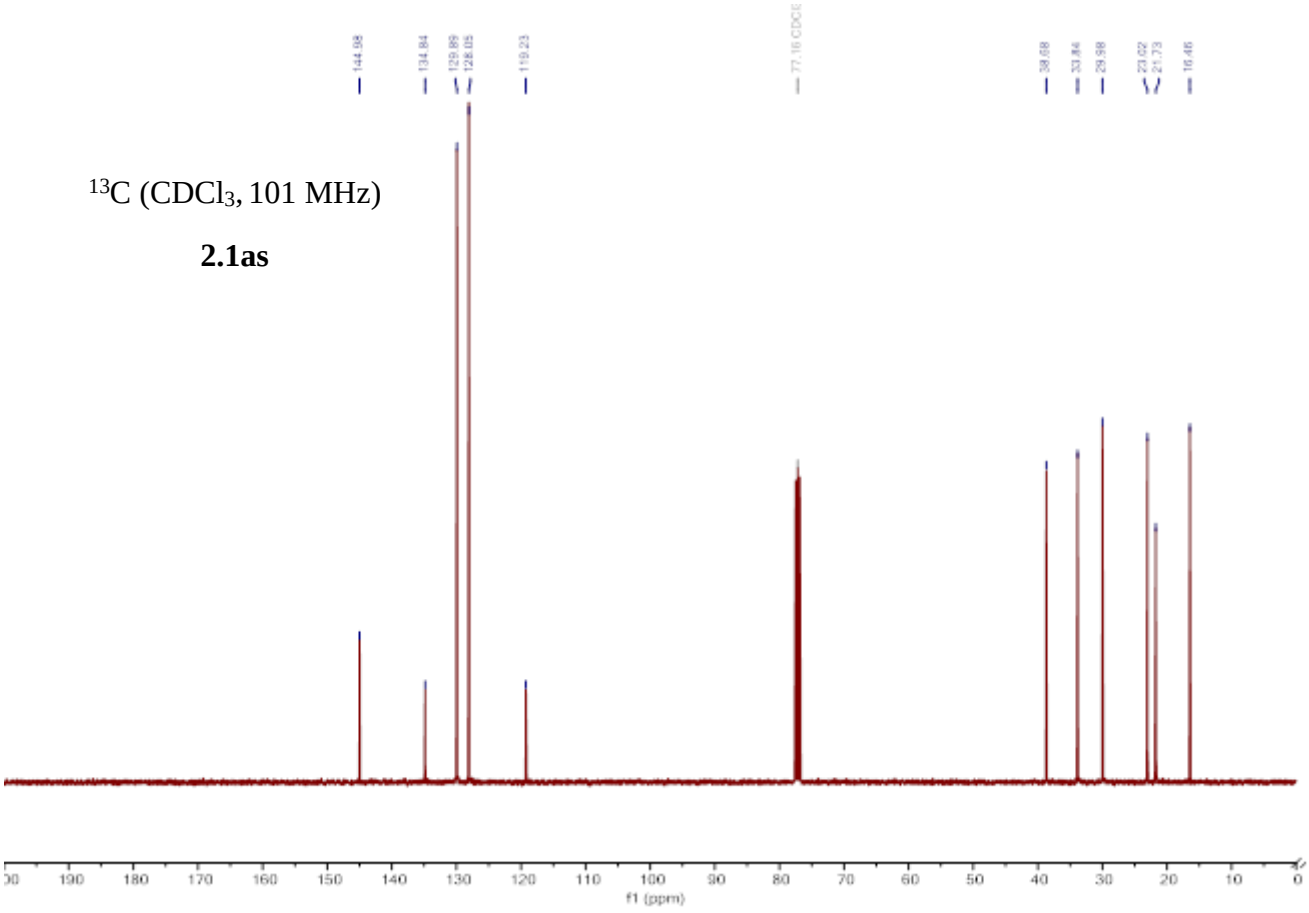

^{1}H ($CDCl_3$, 400 MHz)

2.1ay

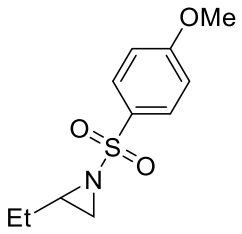

^{13}C ($CDCl_3$, 101 MHz)

2.1ay

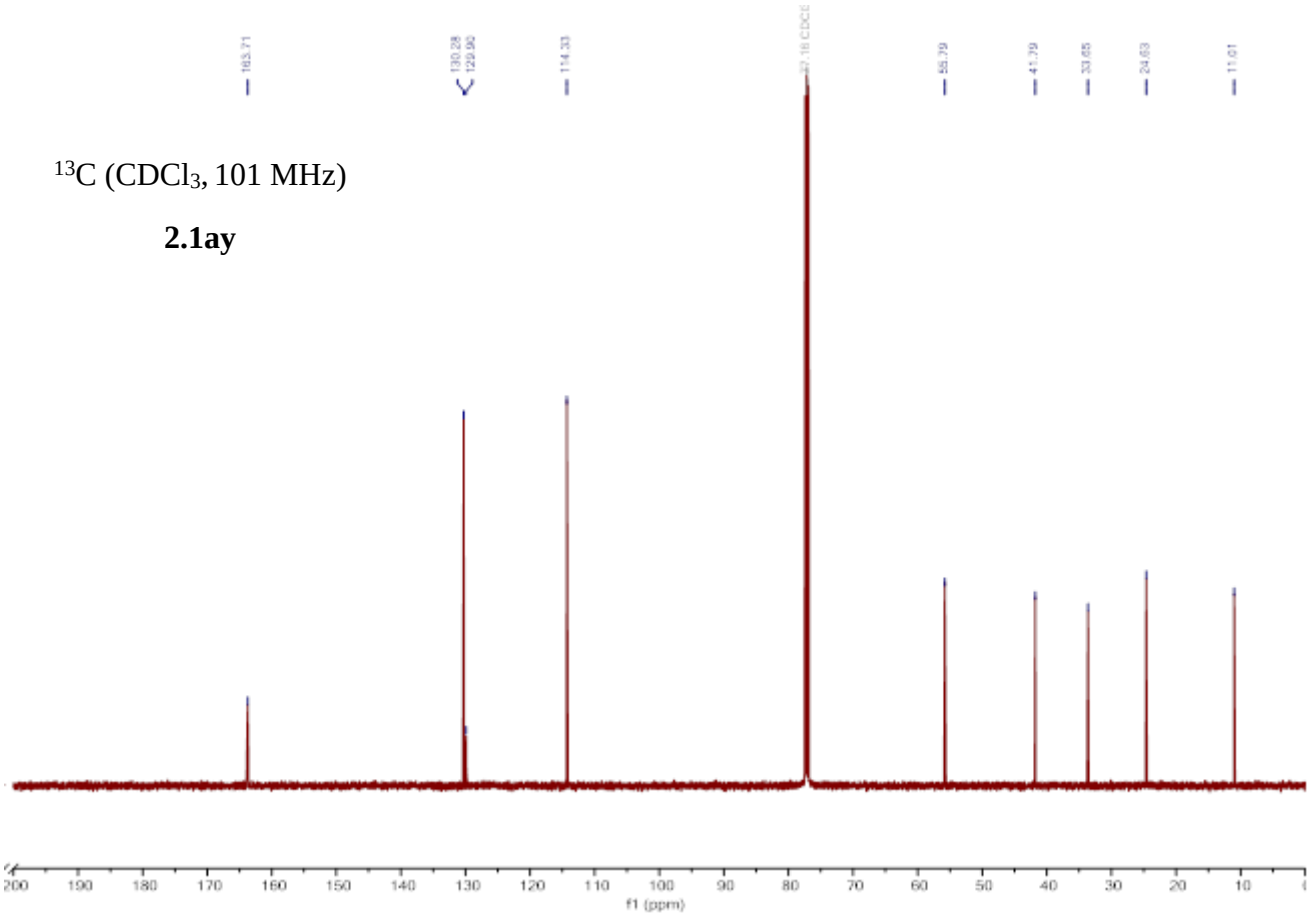

^{1}H ($CDCl_3$, 500 MHz)

2.1ba

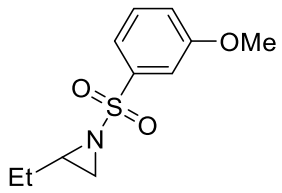

^{13}C ($CDCl_3$, 126 MHz)

2.1ba

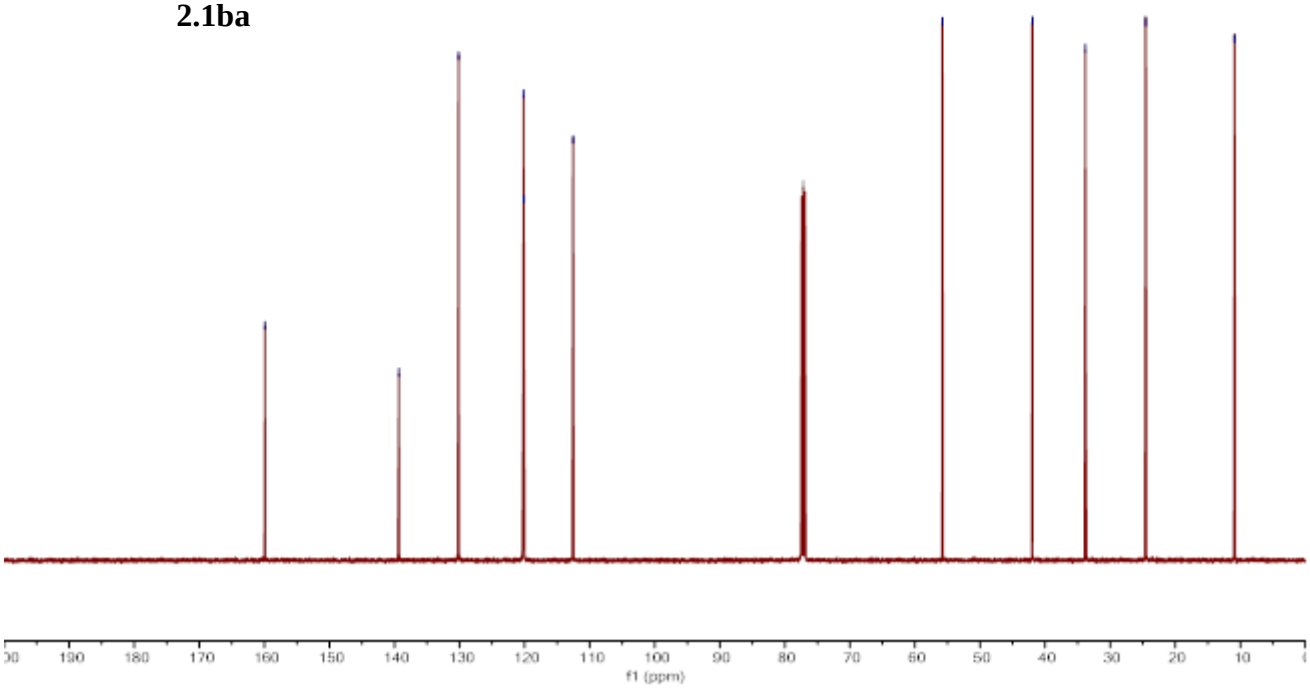

^{1}H ($CDCl_3$, 400 MHz)

2.1bb

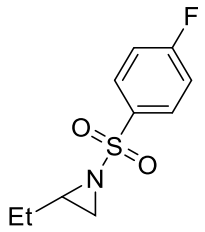

^{13}C ($CDCl_3$, 101 MHz)

2.1bb

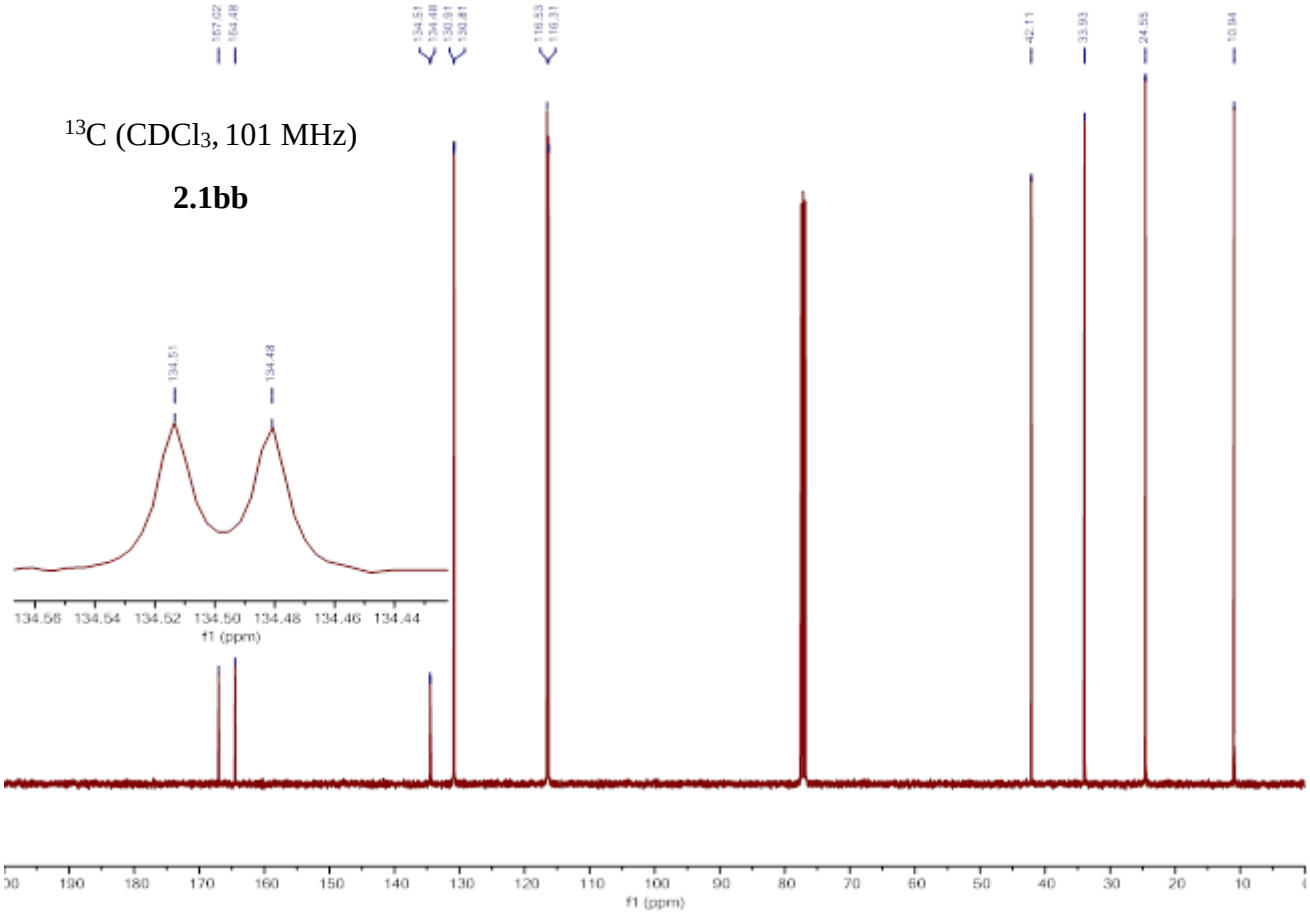

^{19}F ($CDCl_3$, 376 MHz)

2.1bb

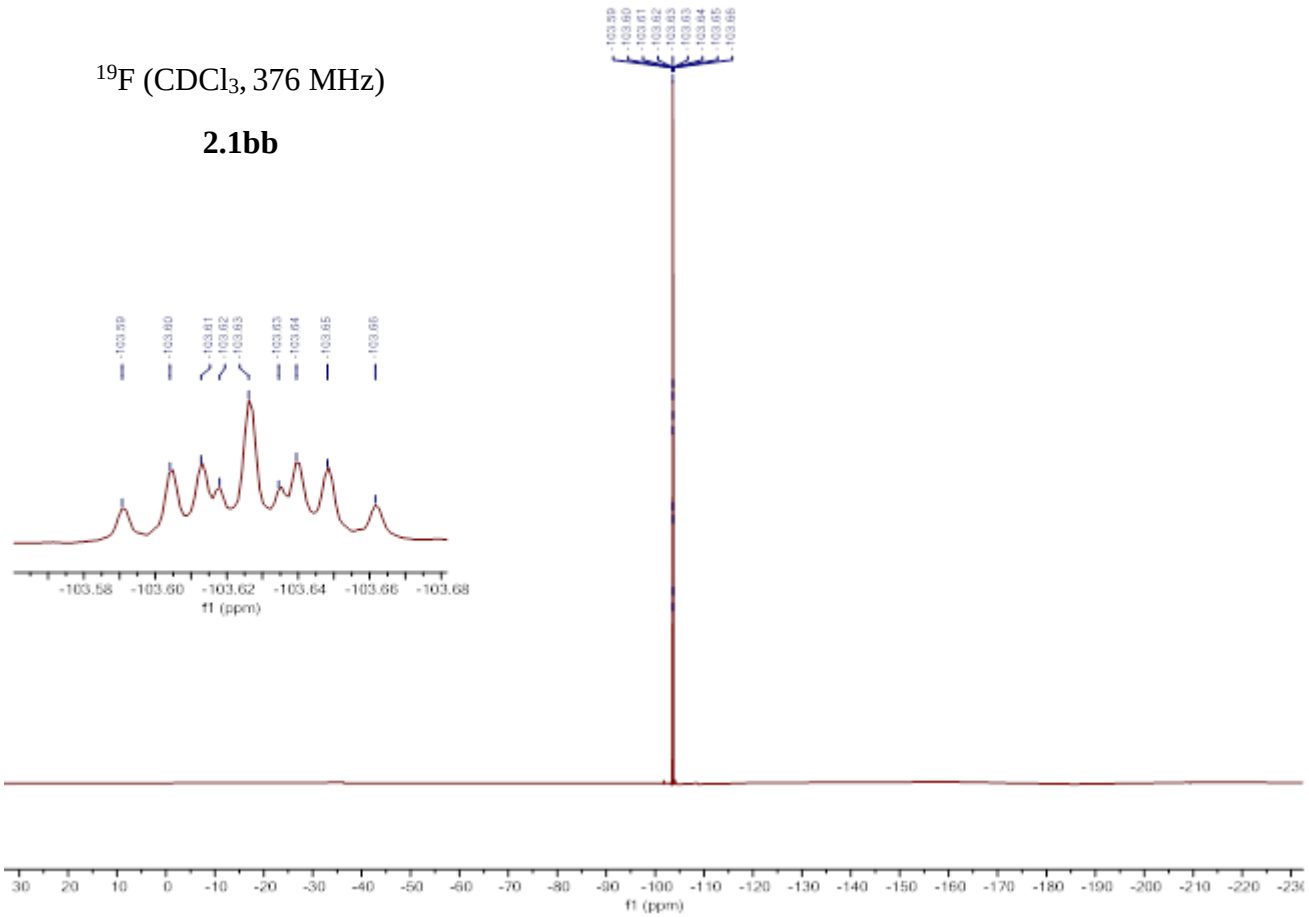

^{1}H ($CDCl_3$, 400 MHz)

2.1bc

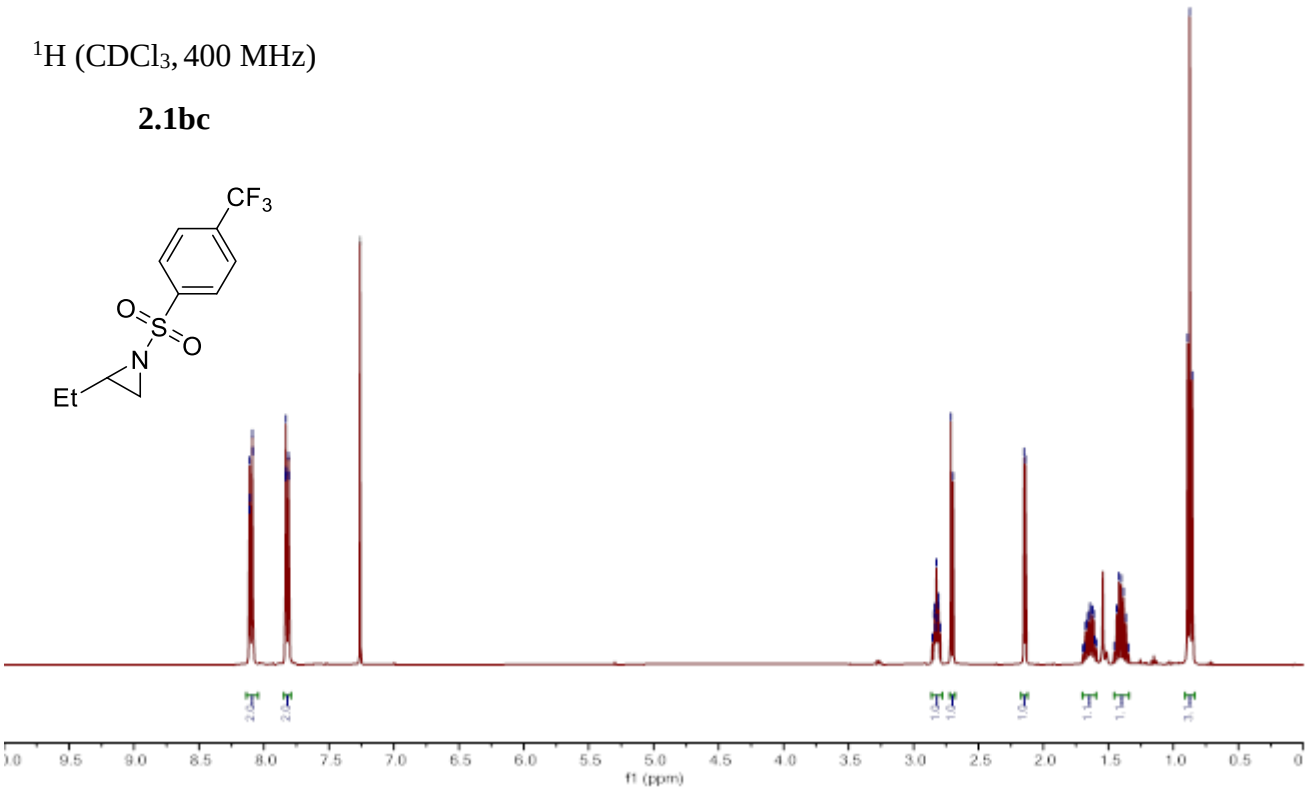

^{13}C ($CDCl_3$, 101 MHz)

2.1bc

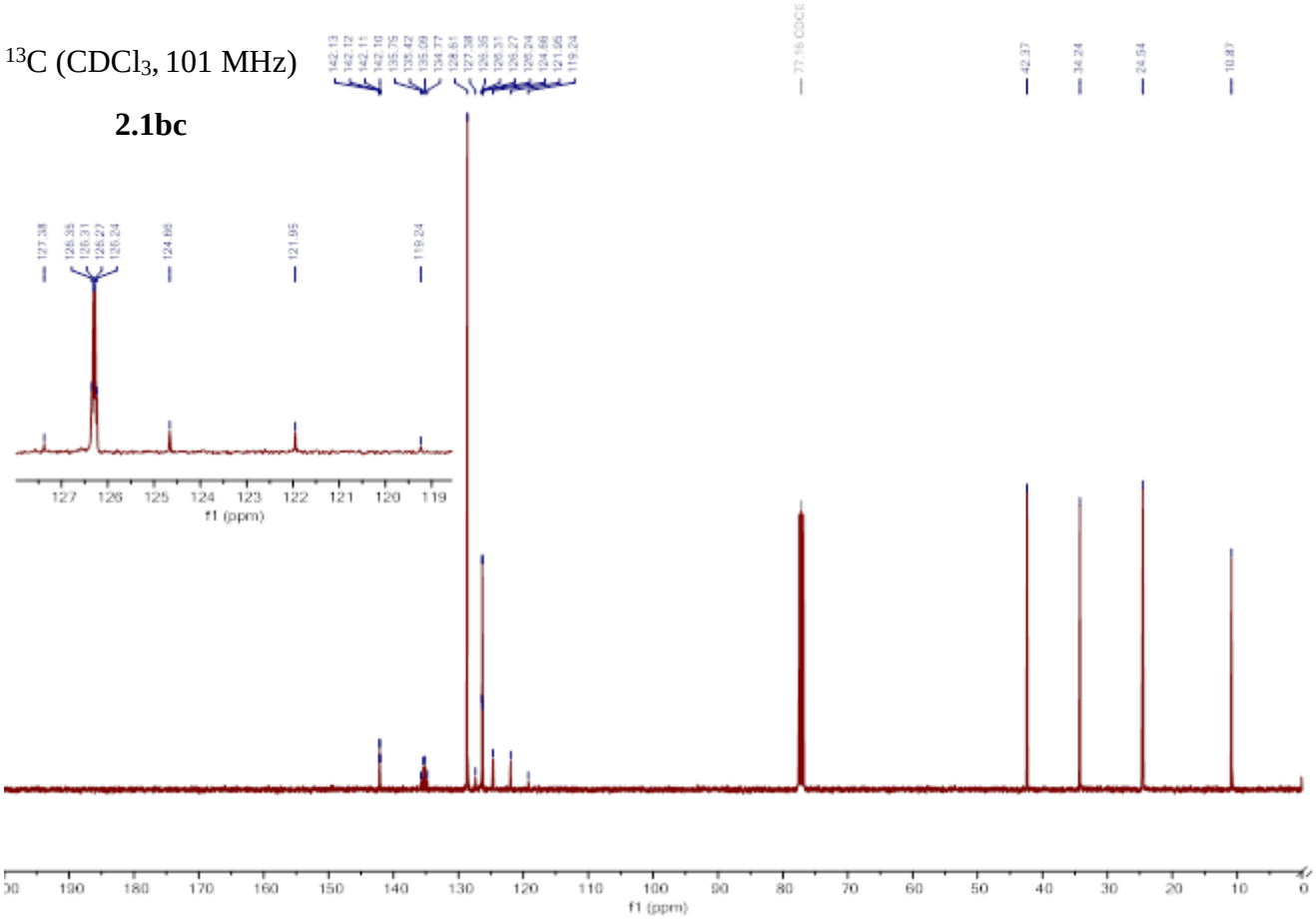

^{19}F ($CDCl_3$, 376 MHz)

2.1bc

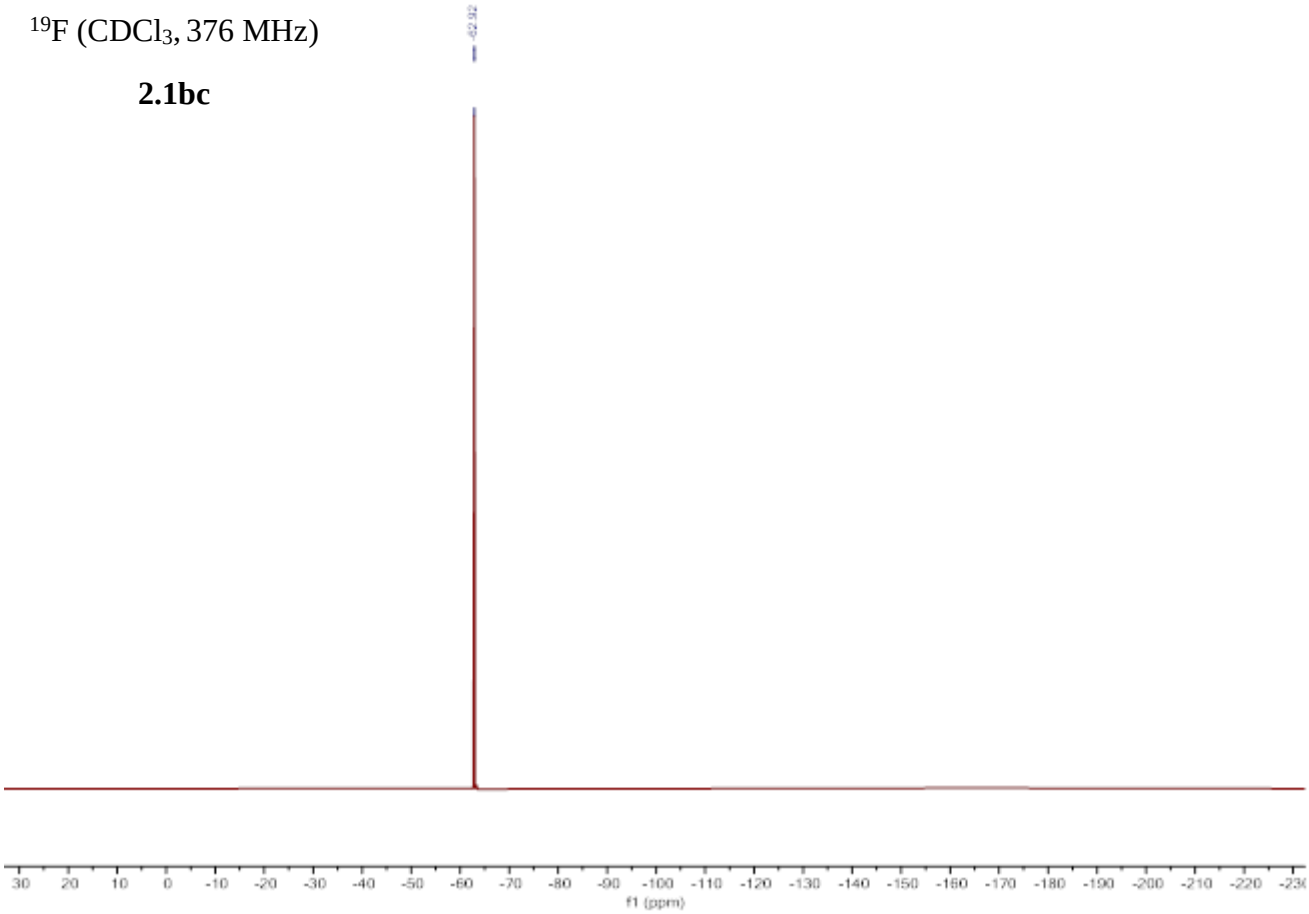

^{1}H (CD_3OD, 400 MHz)

2.2g

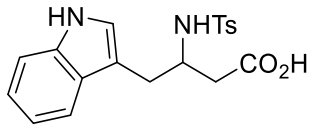

^{1}H (CD_3OD, 400 MHz)

2.2g

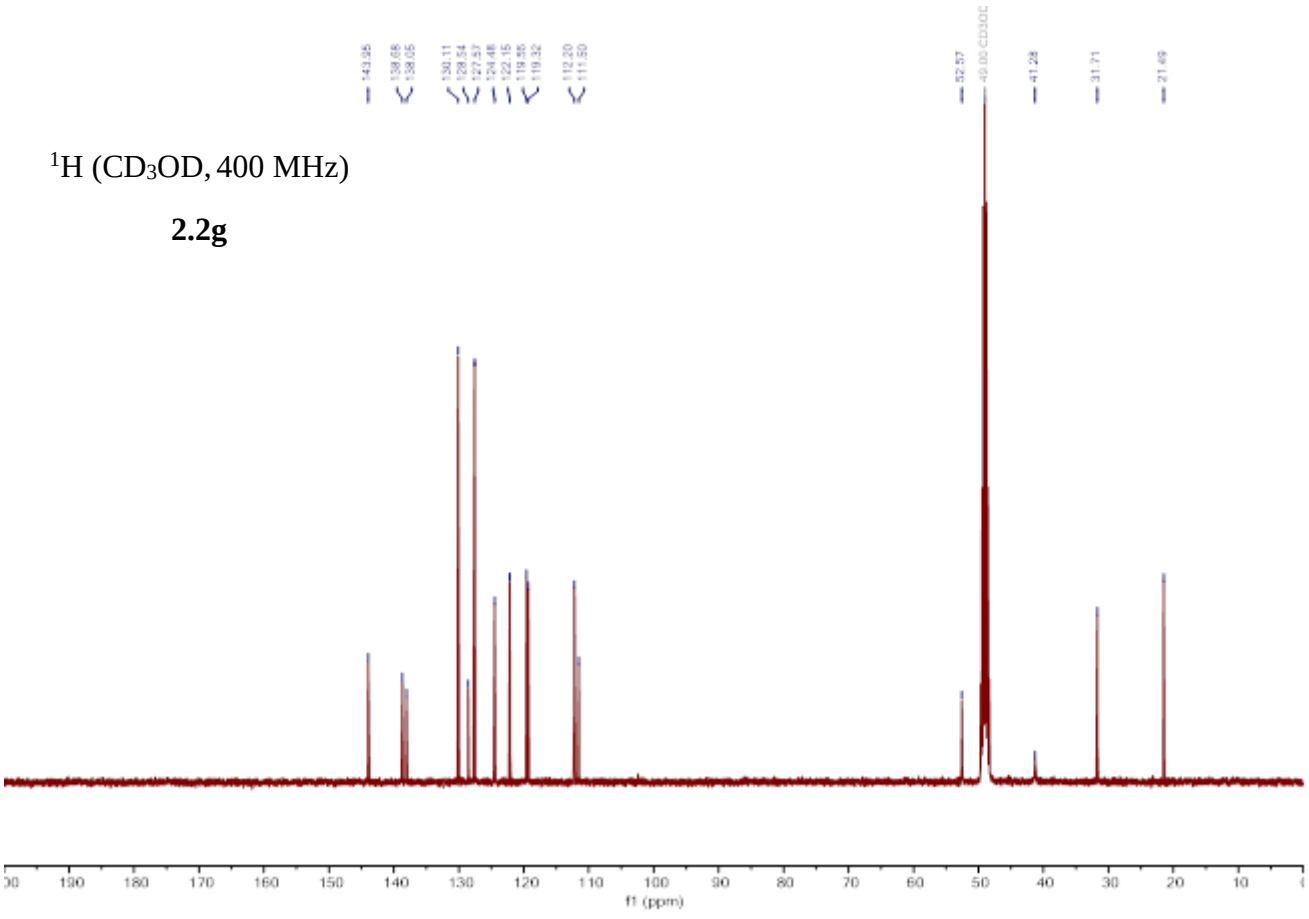

^{1}H ($CDCl_3$, 400 MHz)

2.2l

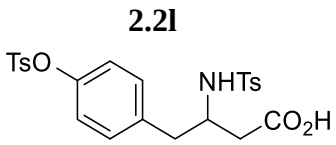

^{13}C (CD_2Cl_2, 101 MHz)

2.2l

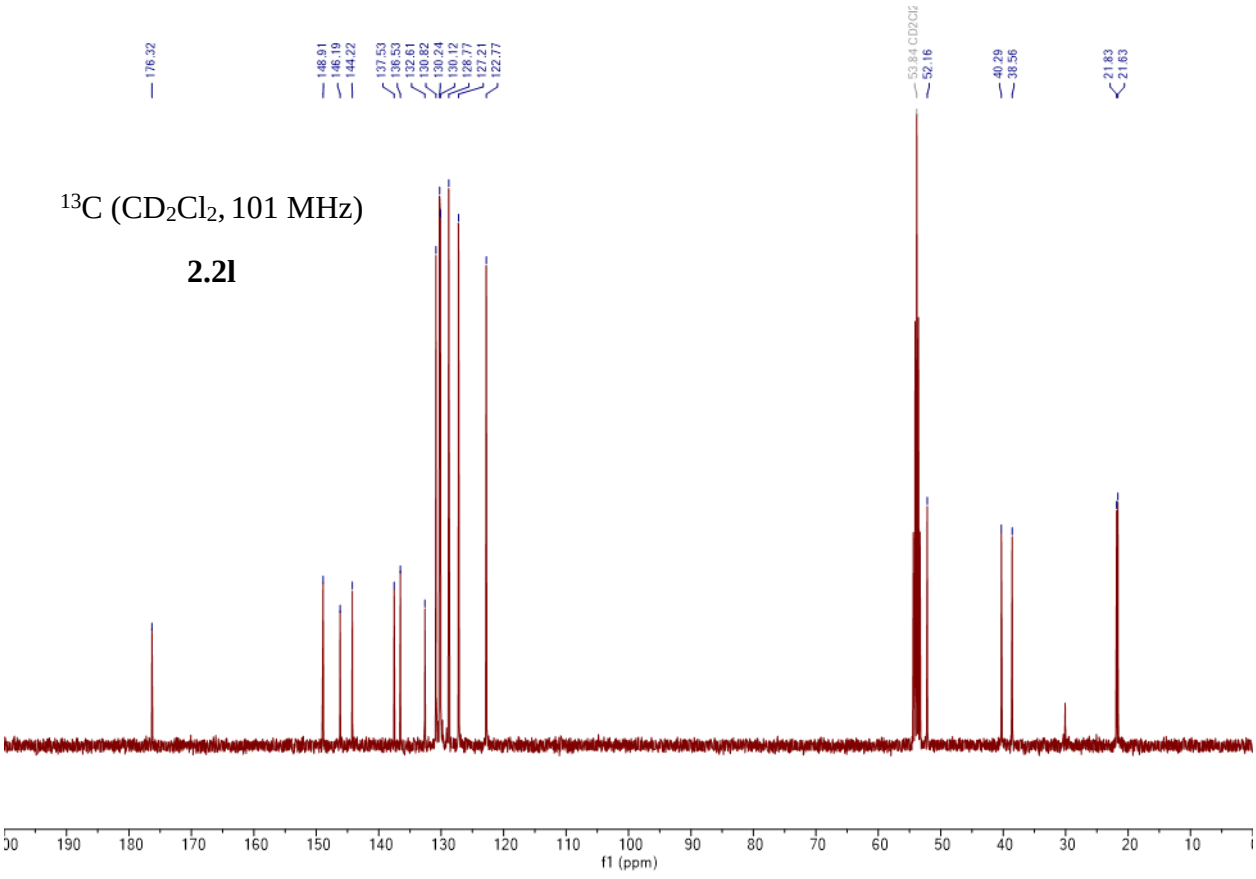

^{1}H ($CDCl_3$, 400 MHz)

2.2q

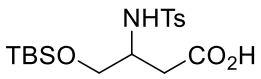

^{13}C ($CDCl_3$, 101 MHz)

2.2q

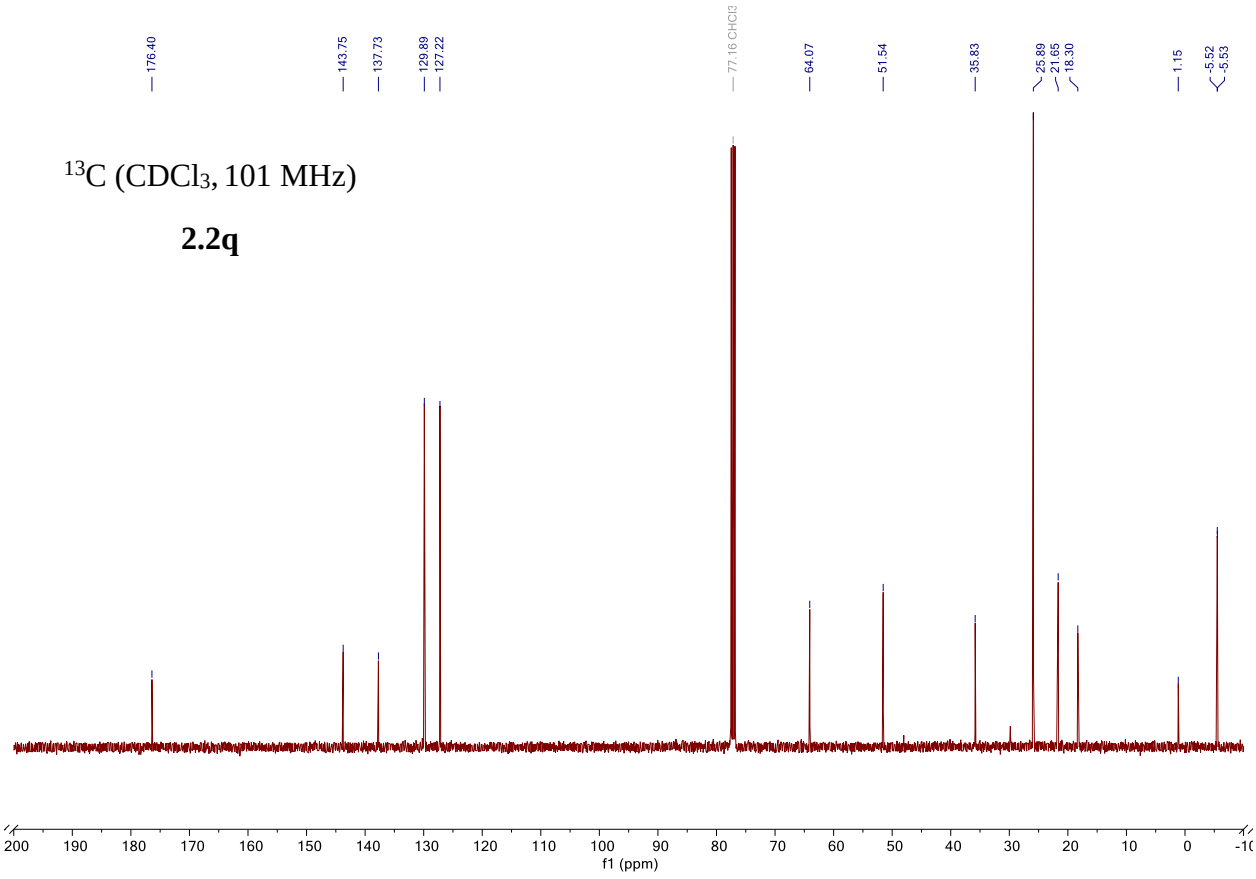

^{1}H ($CDCl_3$, 500 MHz)

2.2m

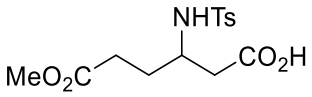

^{13}C ($CDCl_3$, 101 MHz)

2.2m

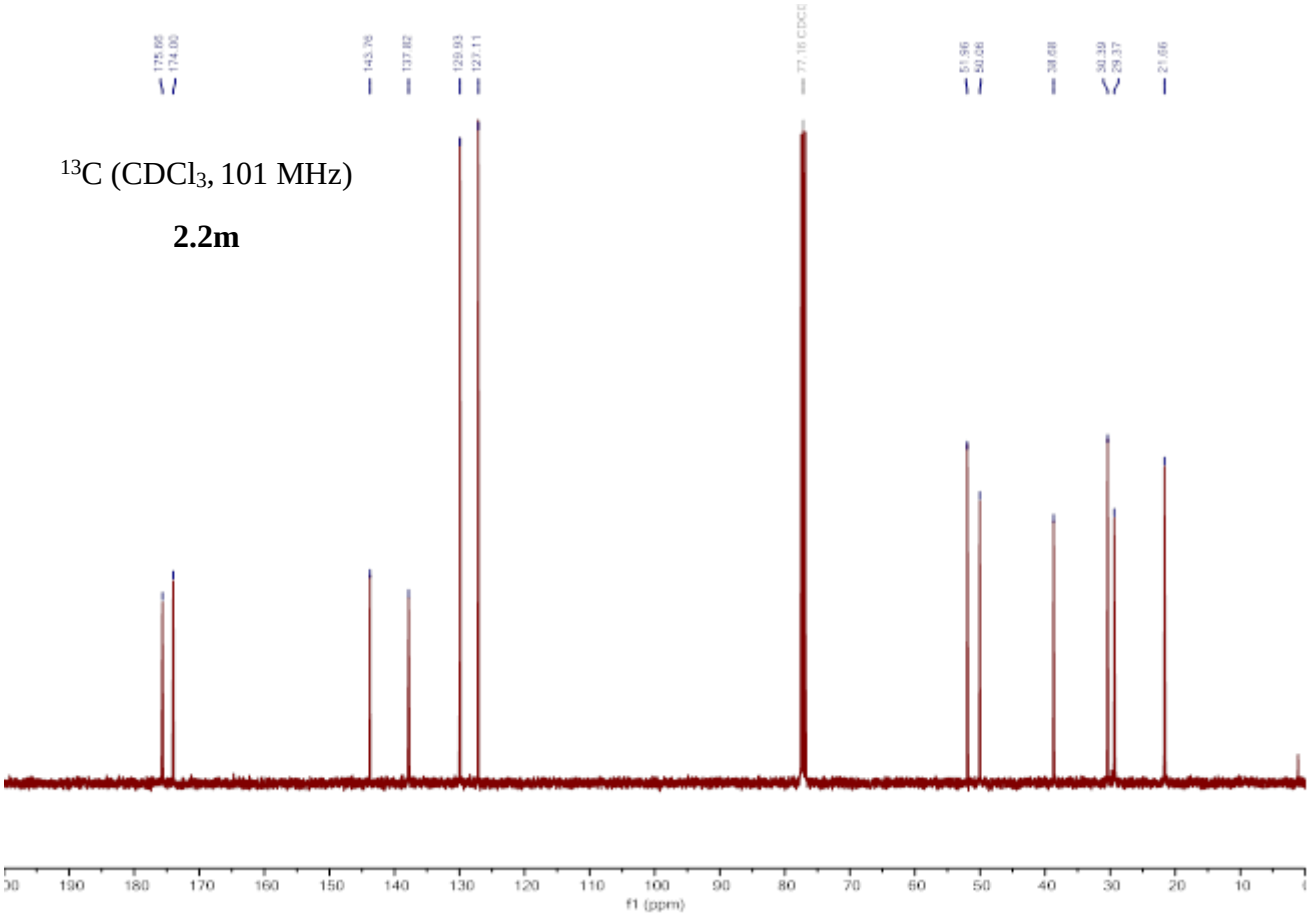

^{1}H ($CDCl_3$, 400 MHz)

2.2w

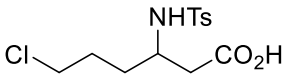

^{13}C ($CDCl_3$, 101 MHz)

2.2w

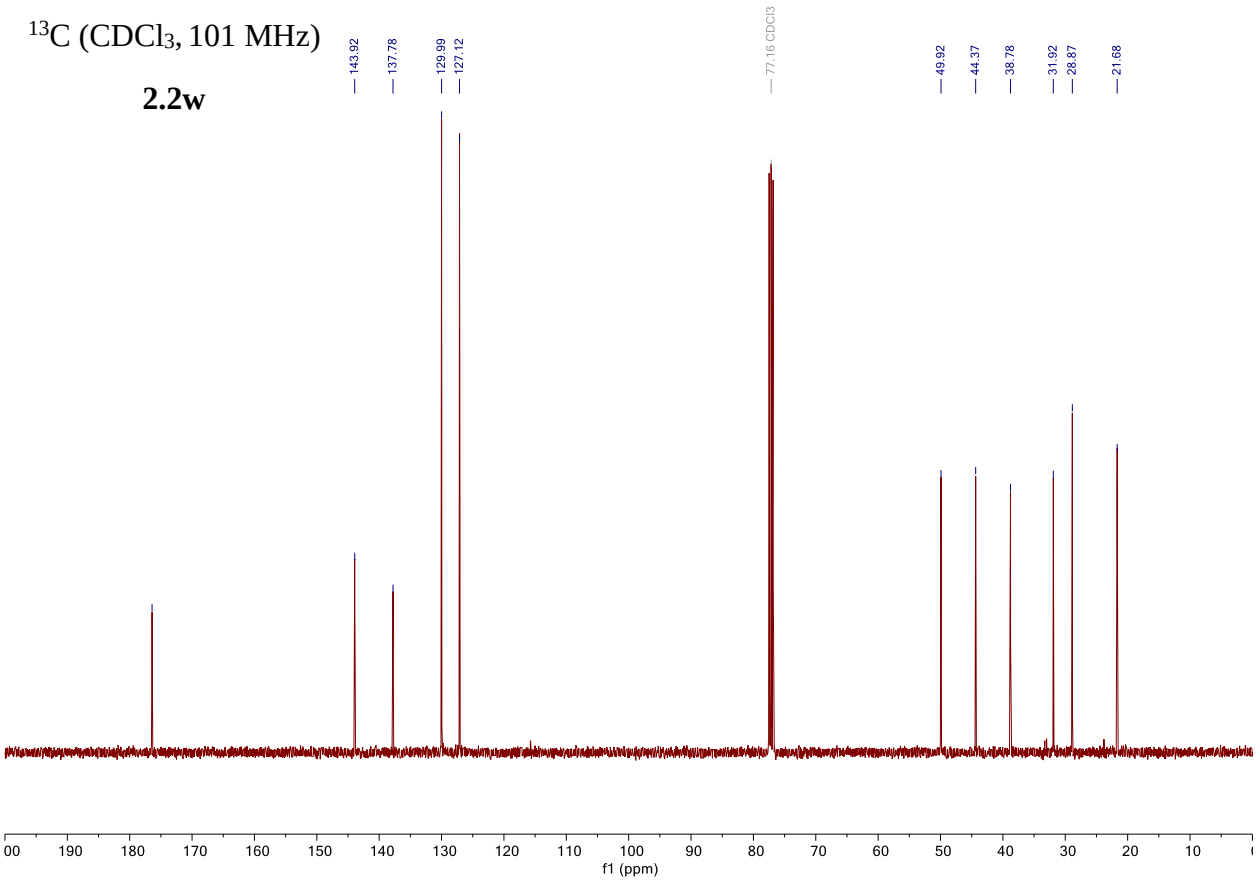

^{1}H ($CDCl_3$, 400 MHz)

2.2t

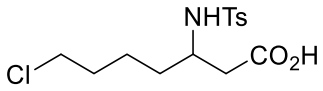

^{13}C ($CDCl_3$, 101 MHz)

2.2t

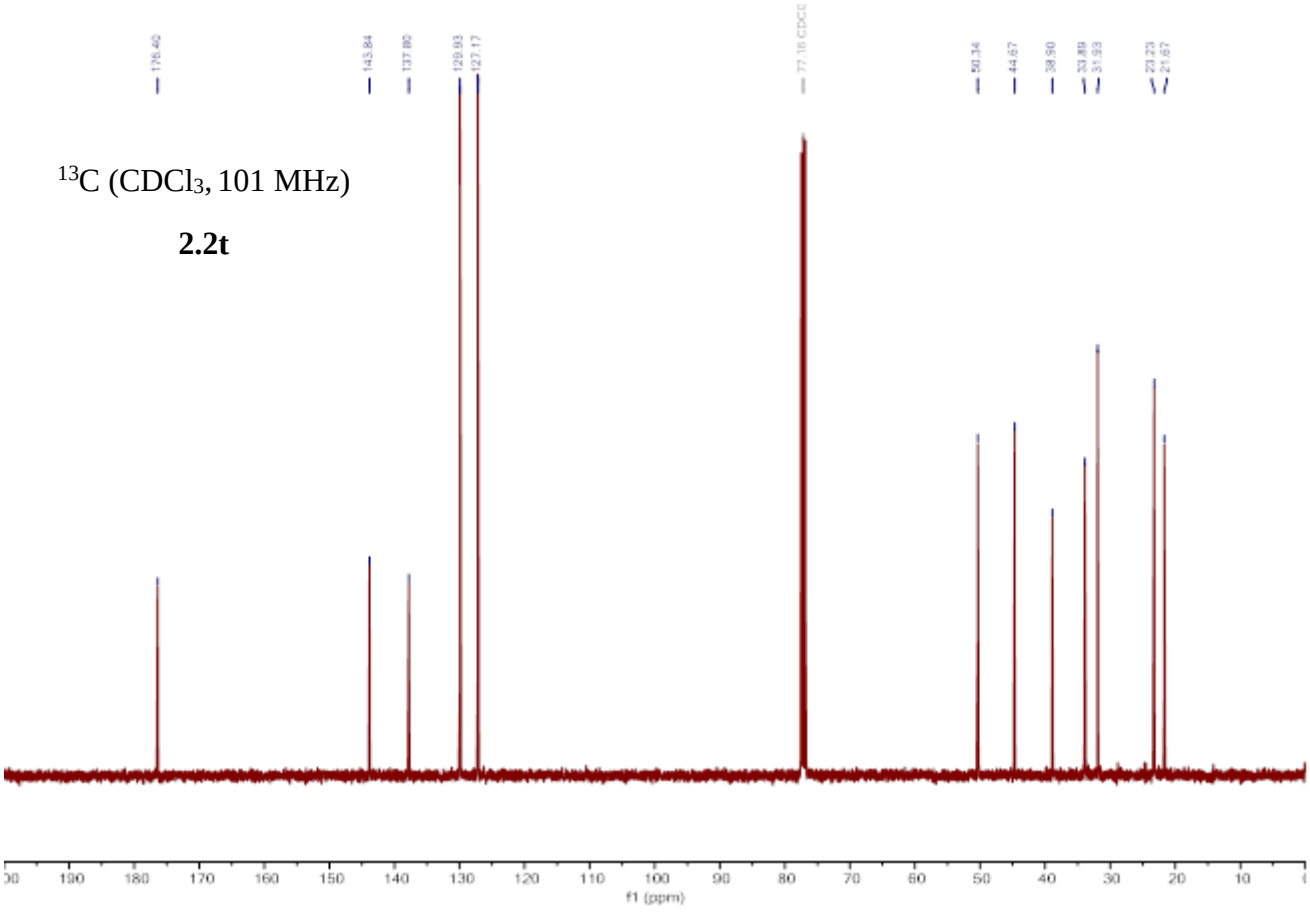

^{1}H (CD_3OD, 400 MHz)

2.2y

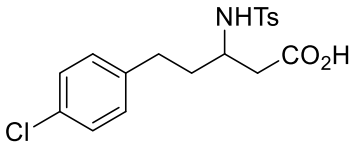

^{13}C (CD_3OD, 101 MHz)

2.2y

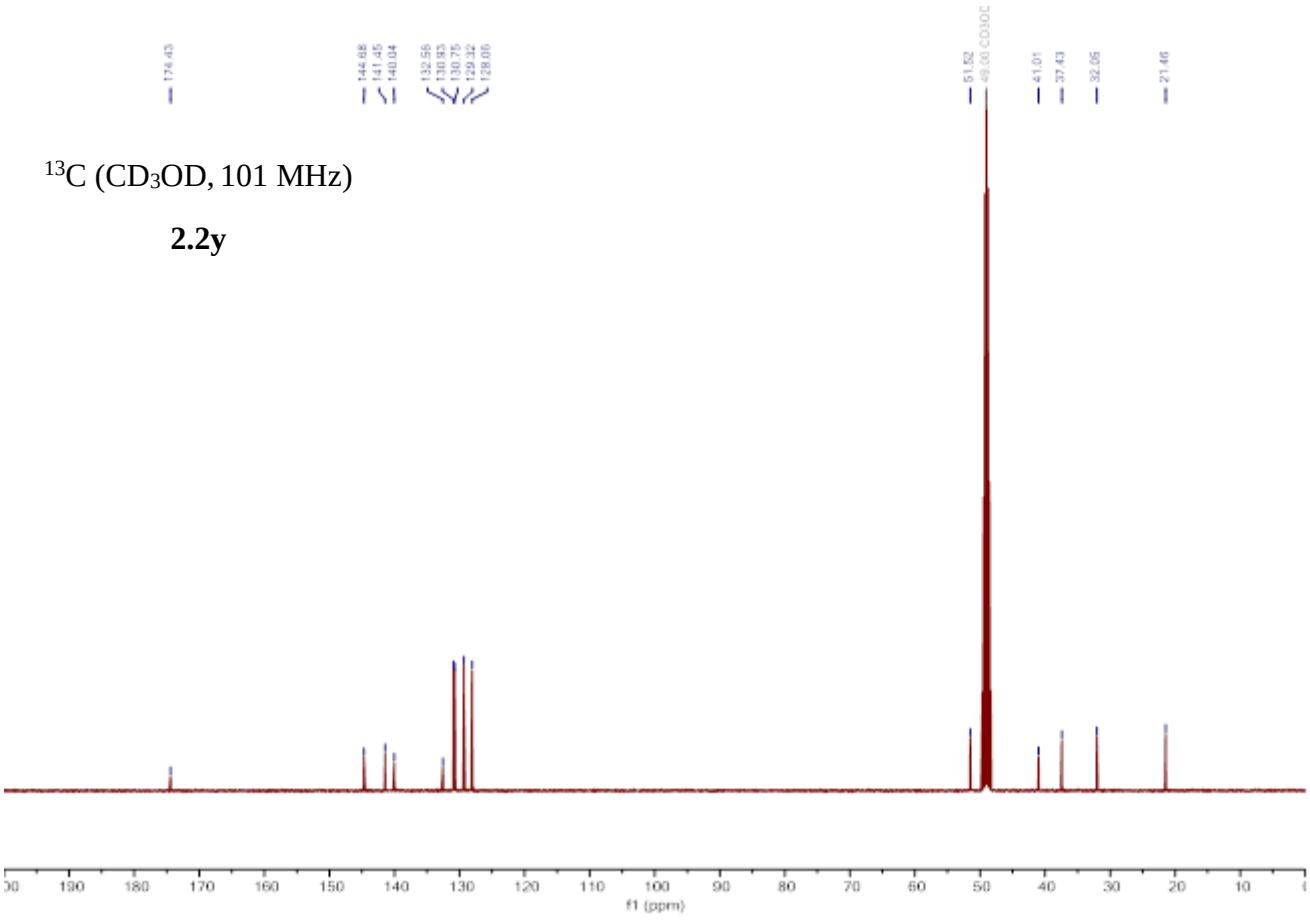

^{1}H (CD_3OD, 400 MHz)

2.2z

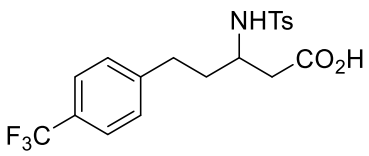

^{13}C (CD_3OD, 101 MHz)

2.2z

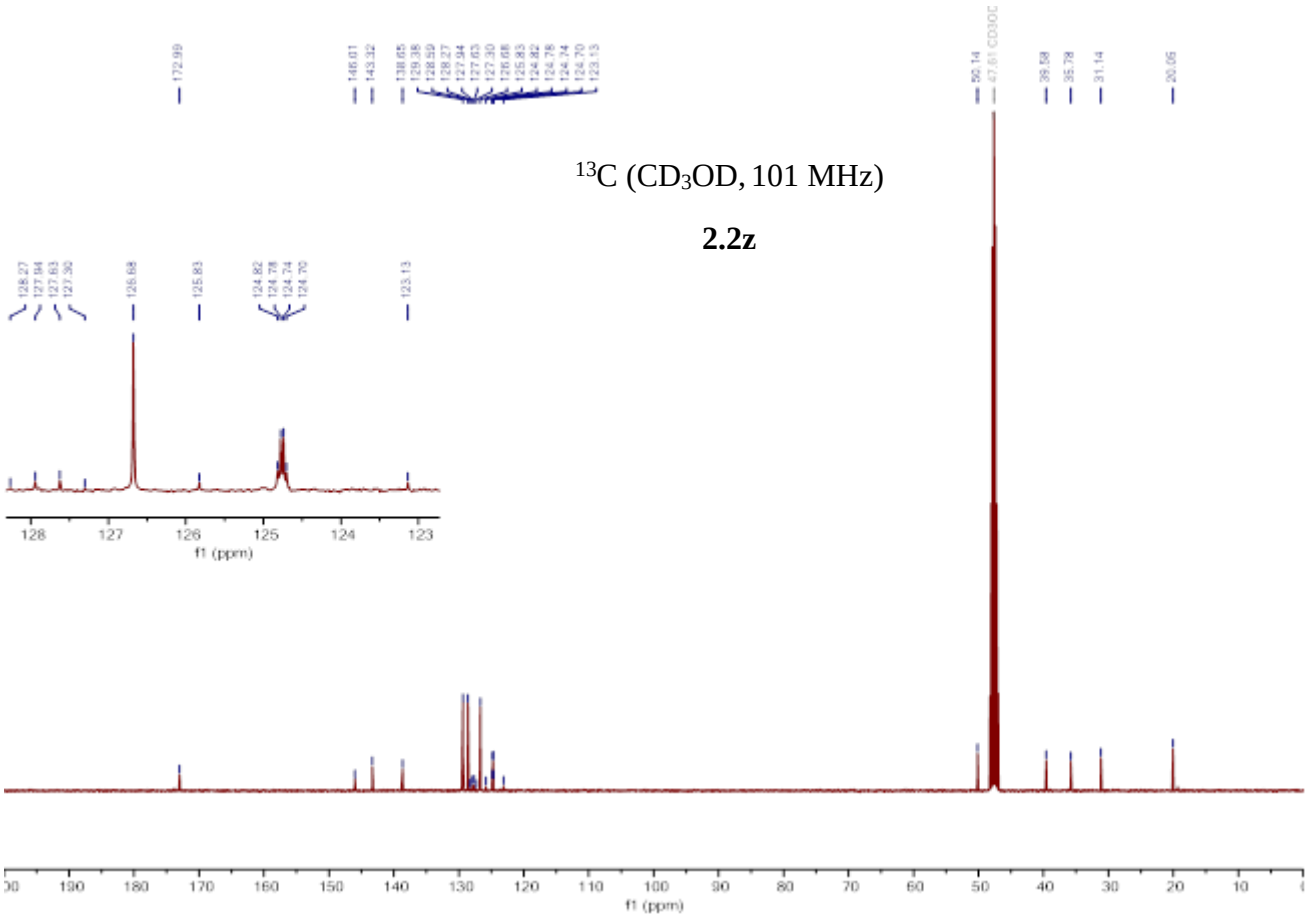

^{19}F (CD_3OD, 376 MHz)

2.2z

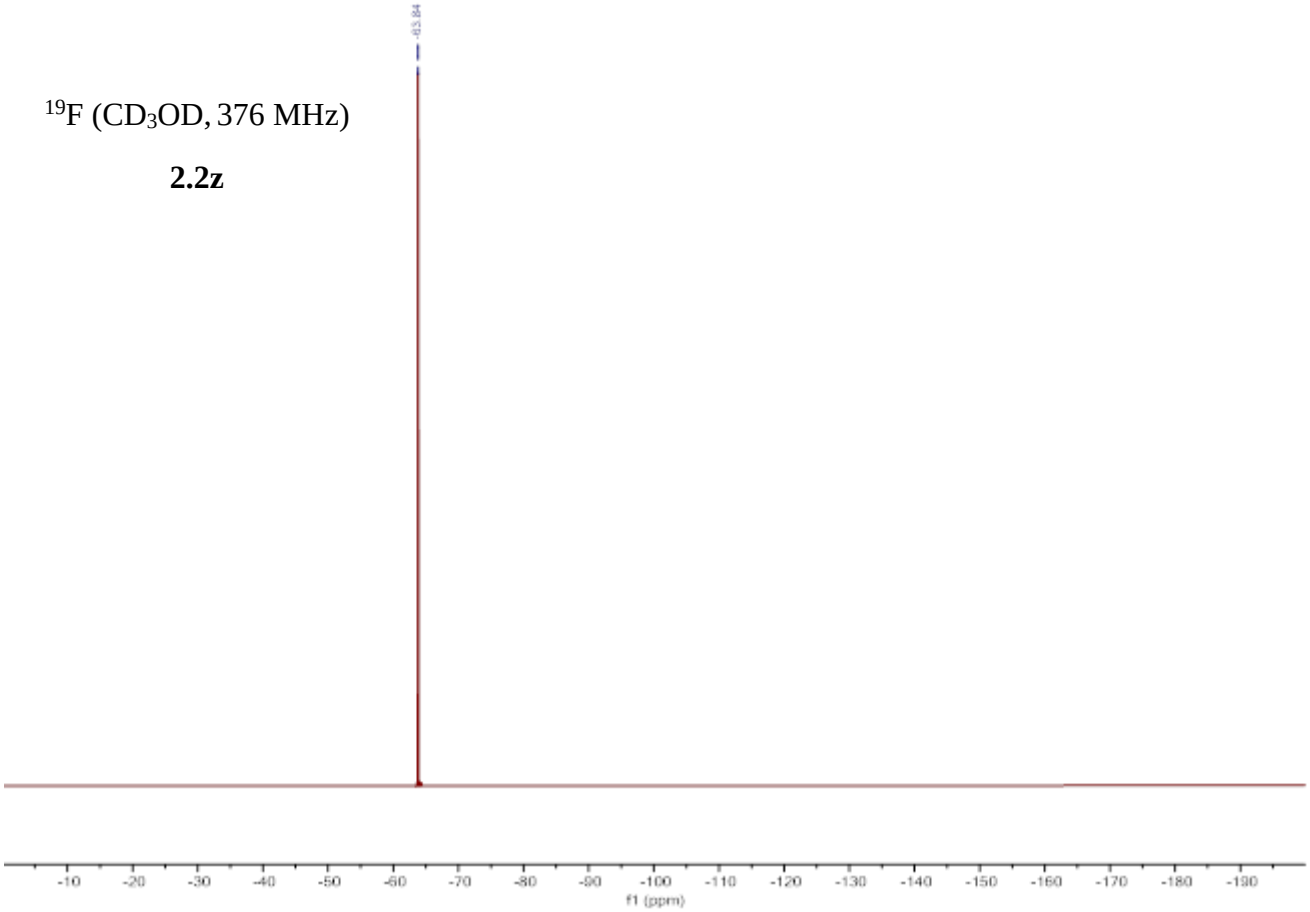

^{1}H (DMSO-d_6, 400 MHz)

2.2ab

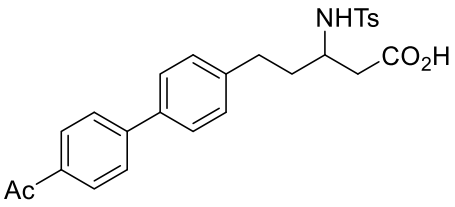

^{13}C (DMSO-d_6, 101 MHz)

2.2ab

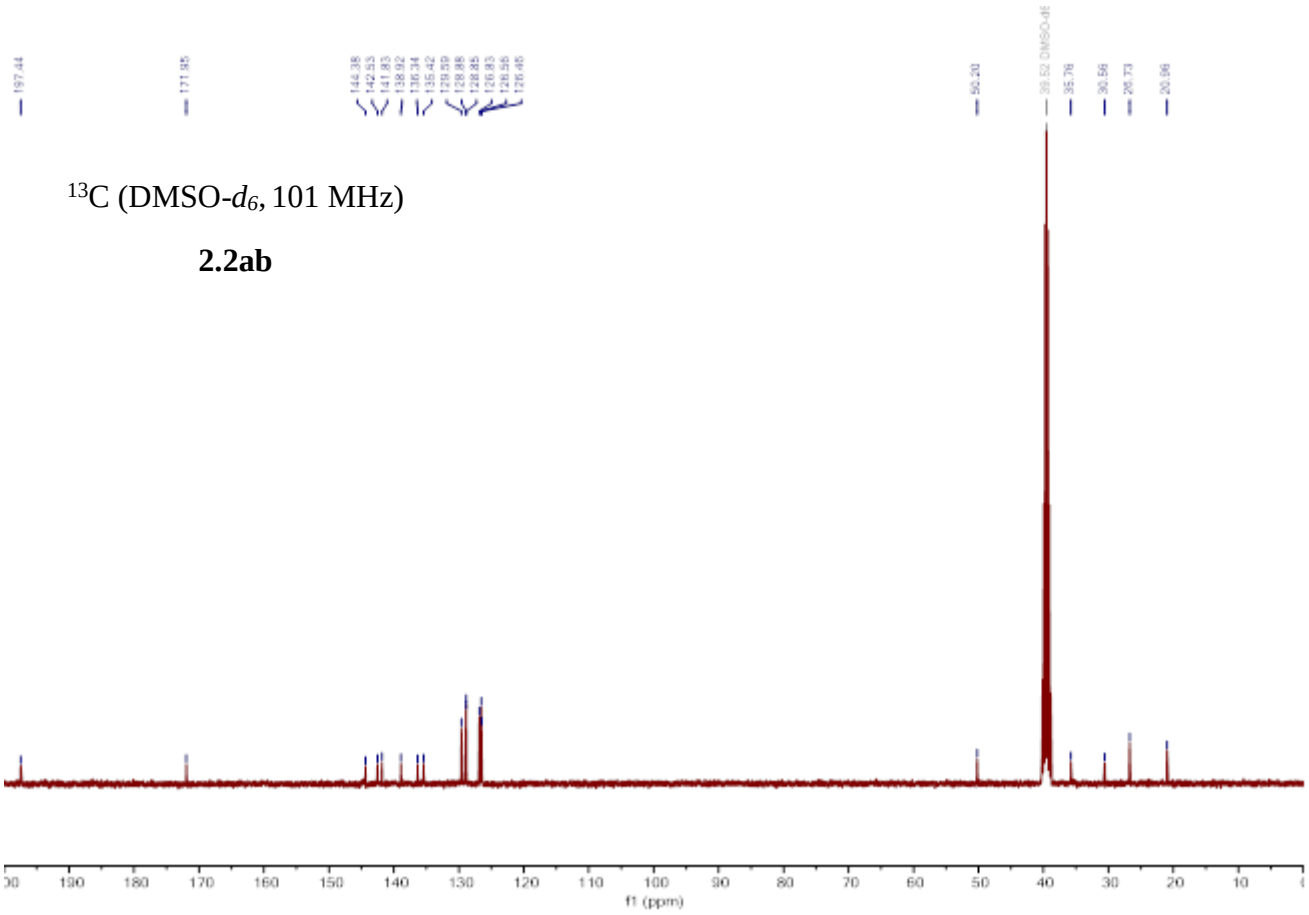

^{1}H ($CDCl_3$, 400 MHz)

2.2ac

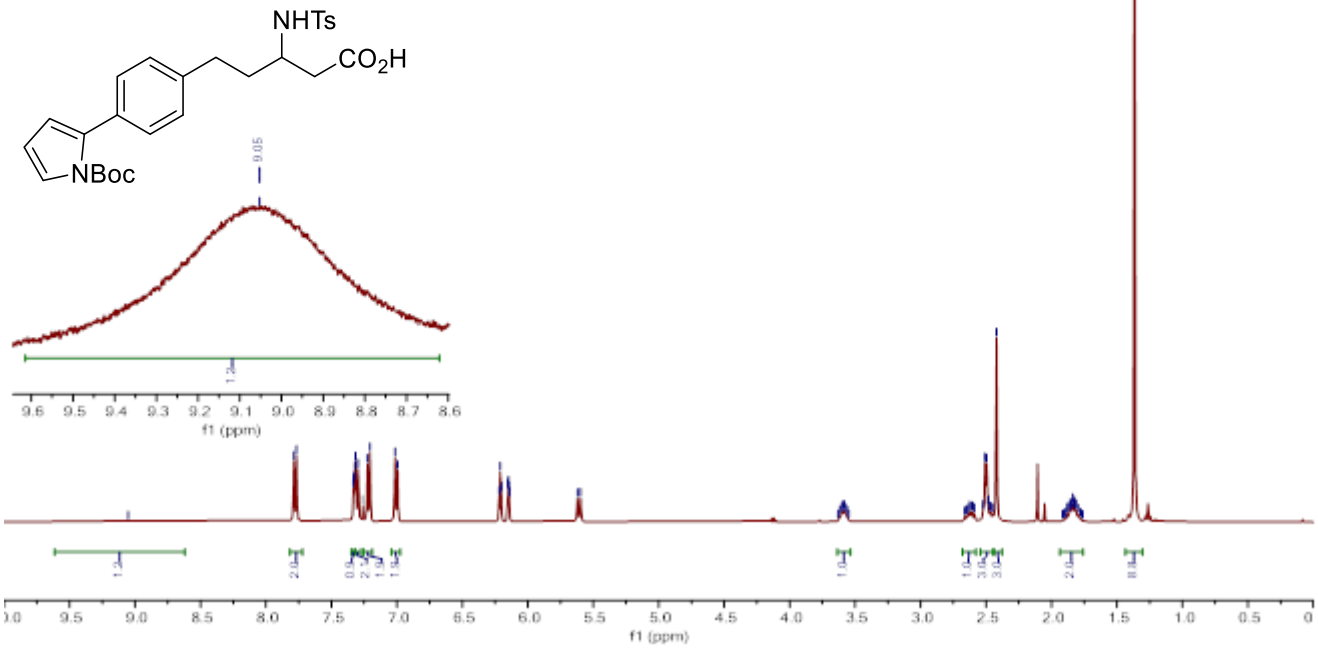

^{13}C ($CDCl_3$, 101 MHz)

2.2ac

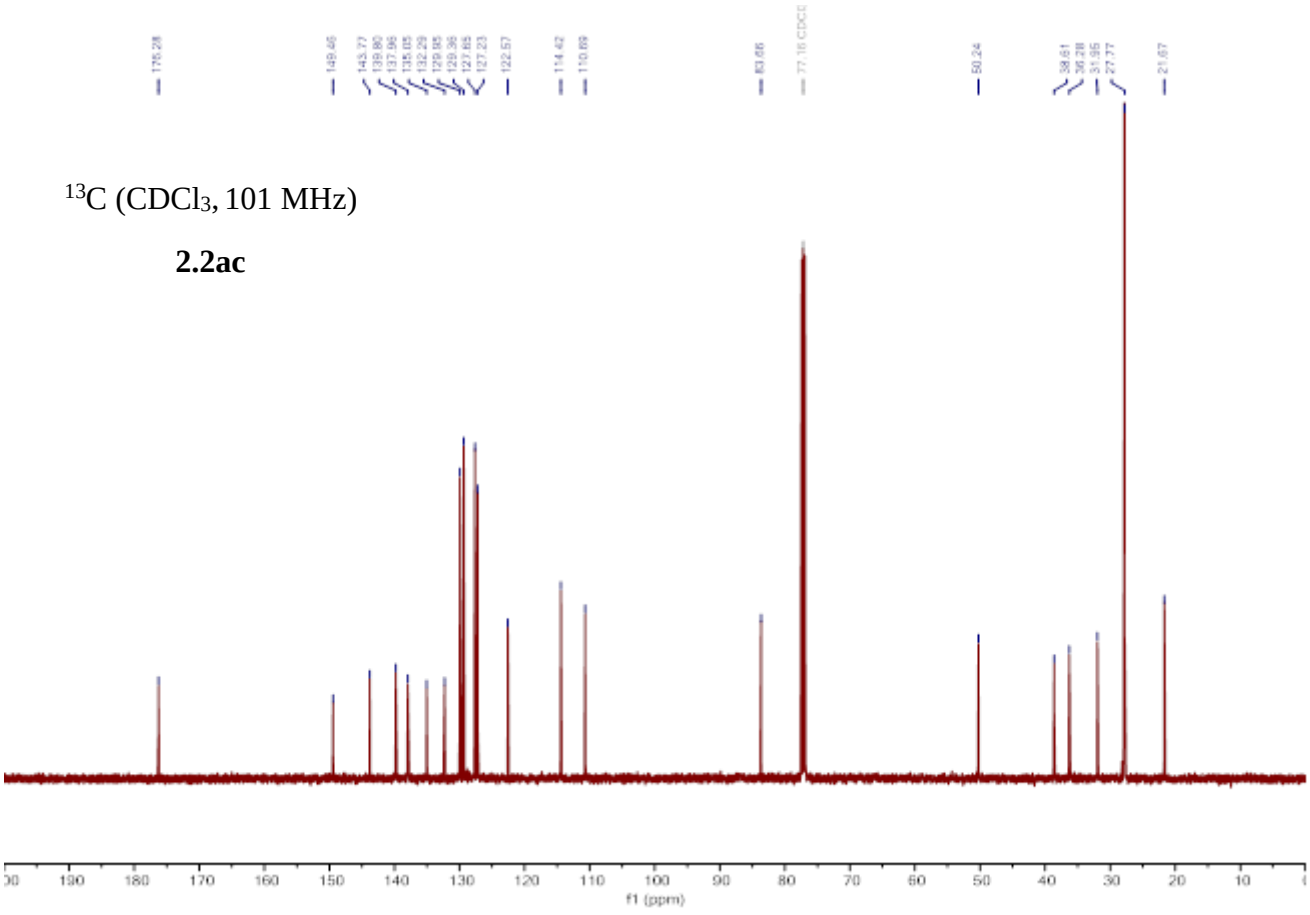

^{1}H ($CDCl_3$, 400 MHz)

2.2ae

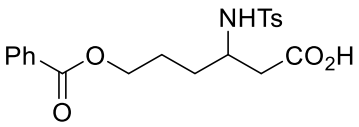

^{13}C ($CDCl_3$, 101 MHz)

2.2ae

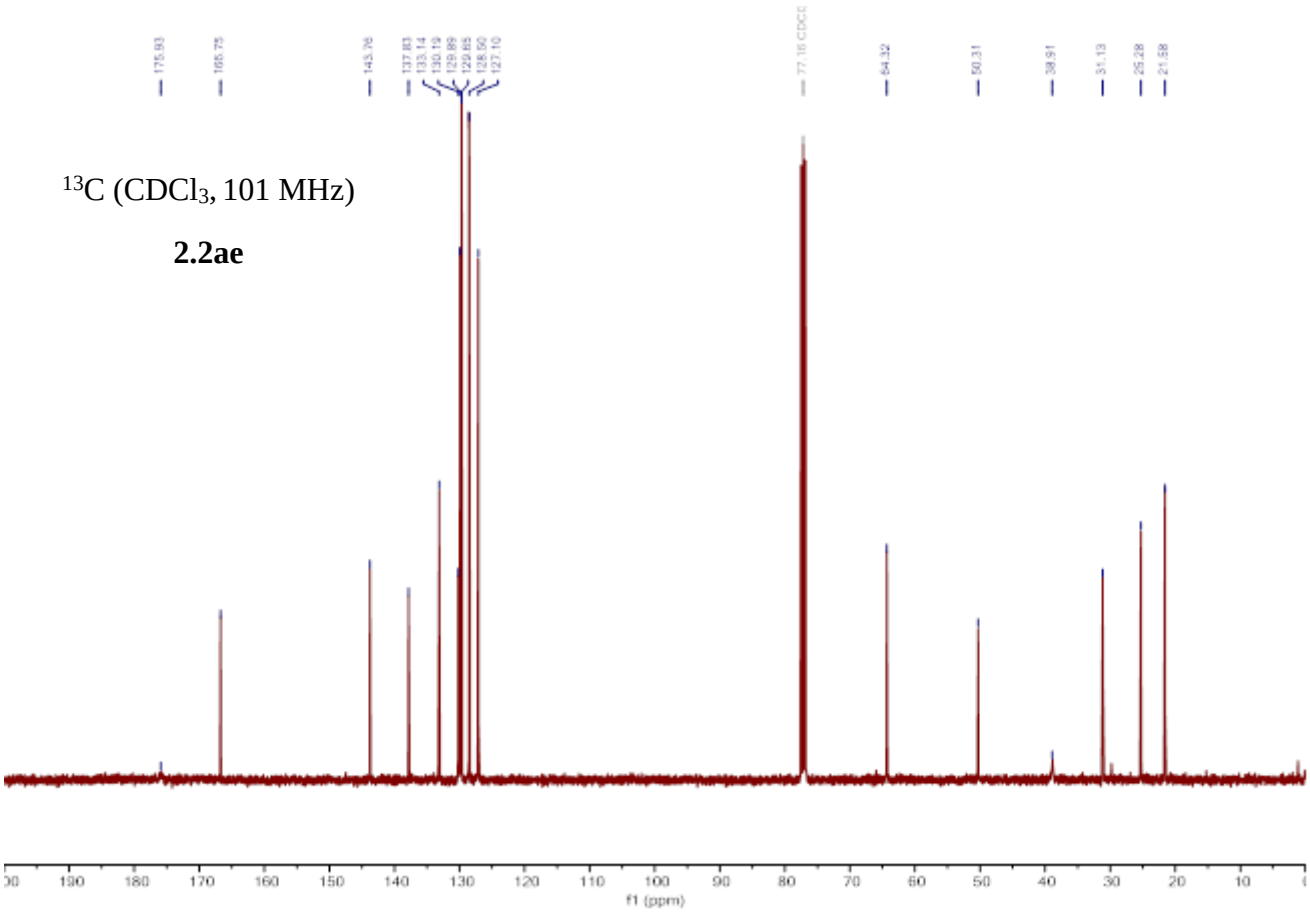

^{1}H ($CDCl_3$, 400 MHz)

2.2af

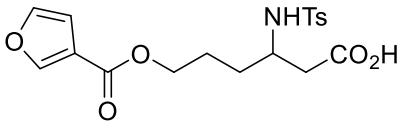

^{13}C ($CDCl_3$, 101 MHz)

2.2af

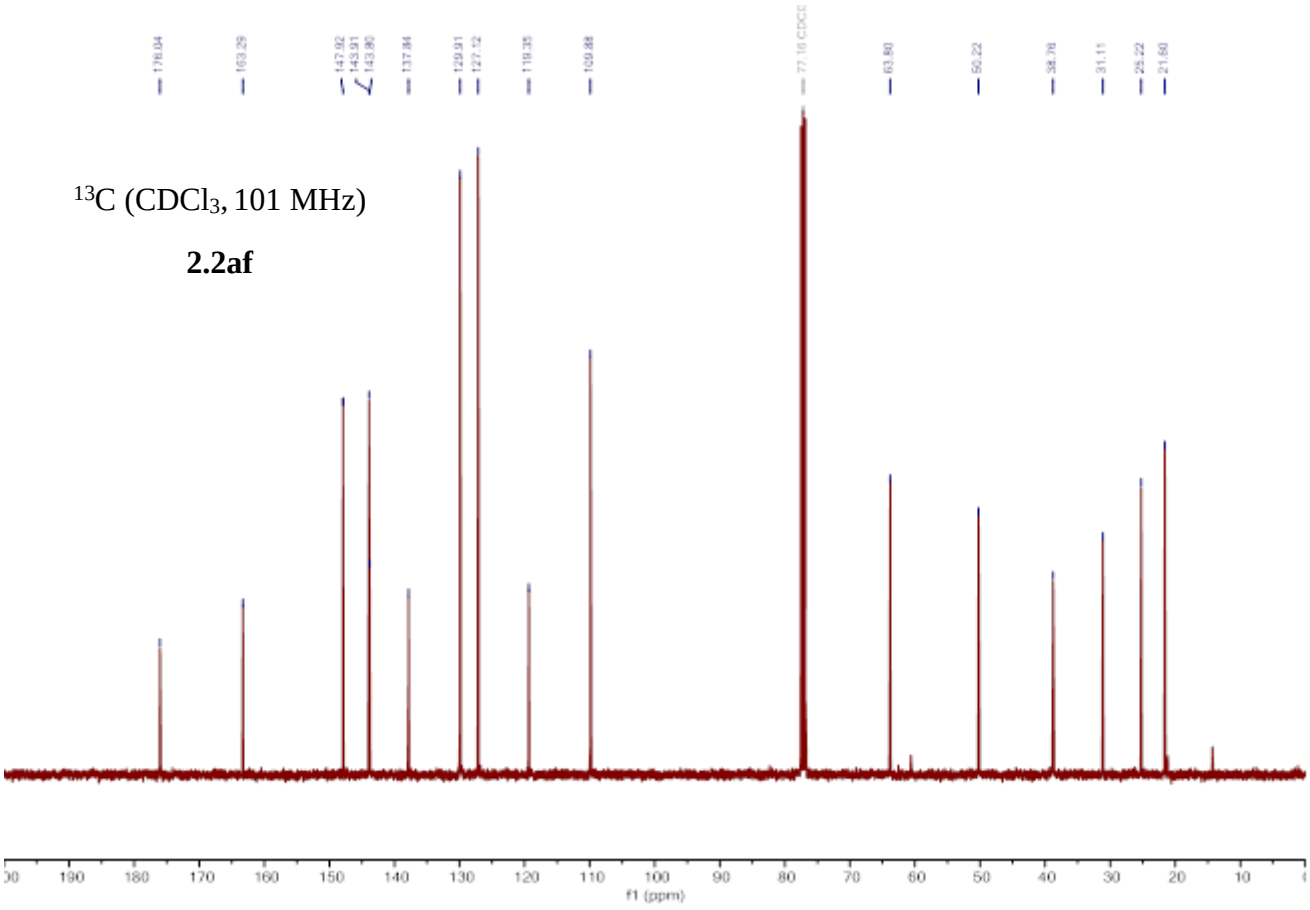

^{1}H ($CDCl_3$, 400 MHz)

2.2aj

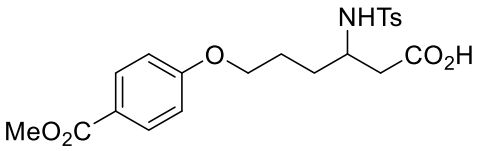

^{13}C ($CDCl_3$, 101 MHz)

2.2aj

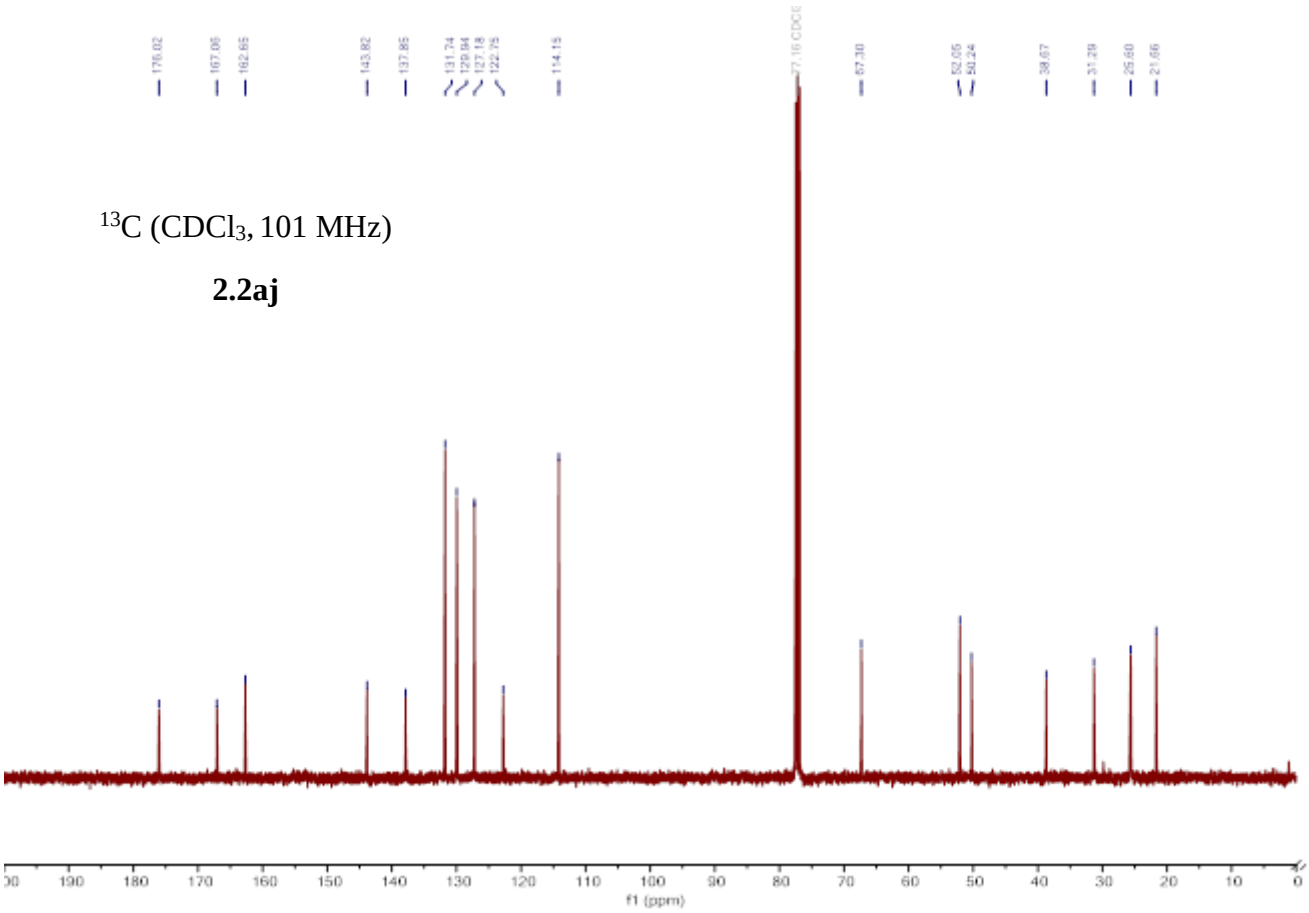

^{1}H ($CDCl_3$, 400 MHz)

2.2ak

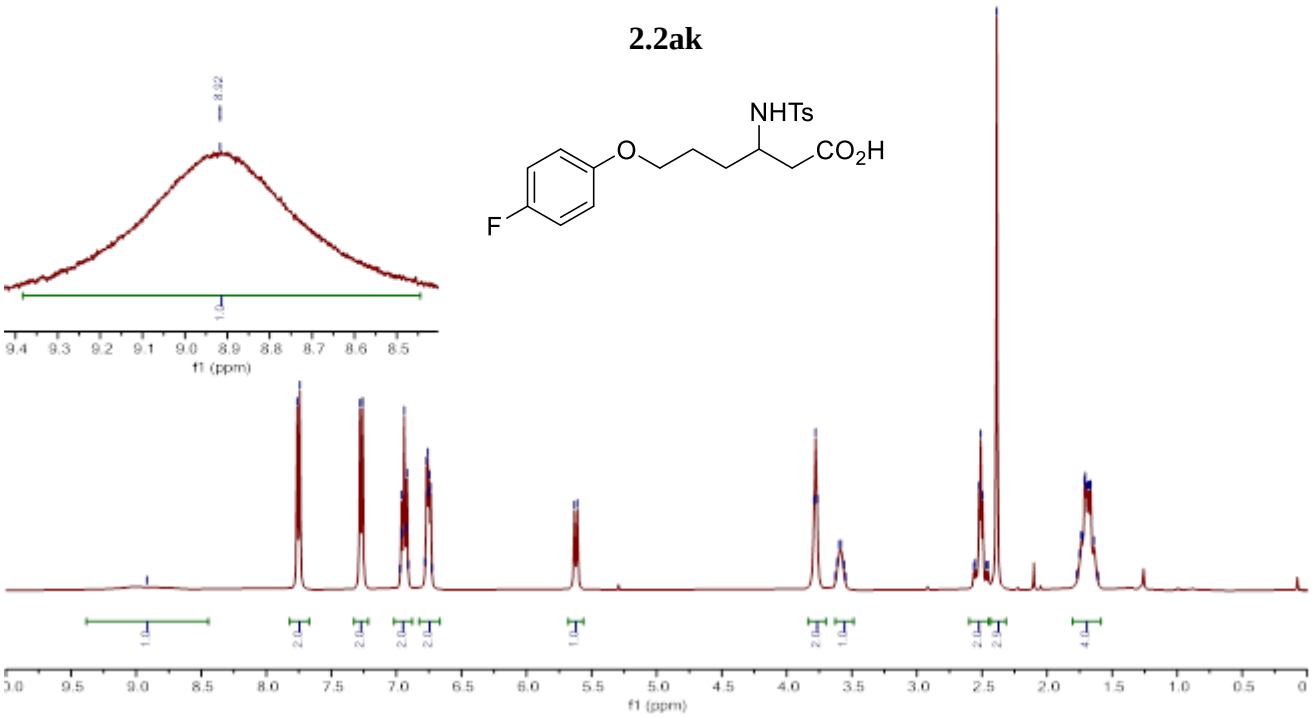

^{13}C ($CDCl_3$, 101 MHz)

2.2ak

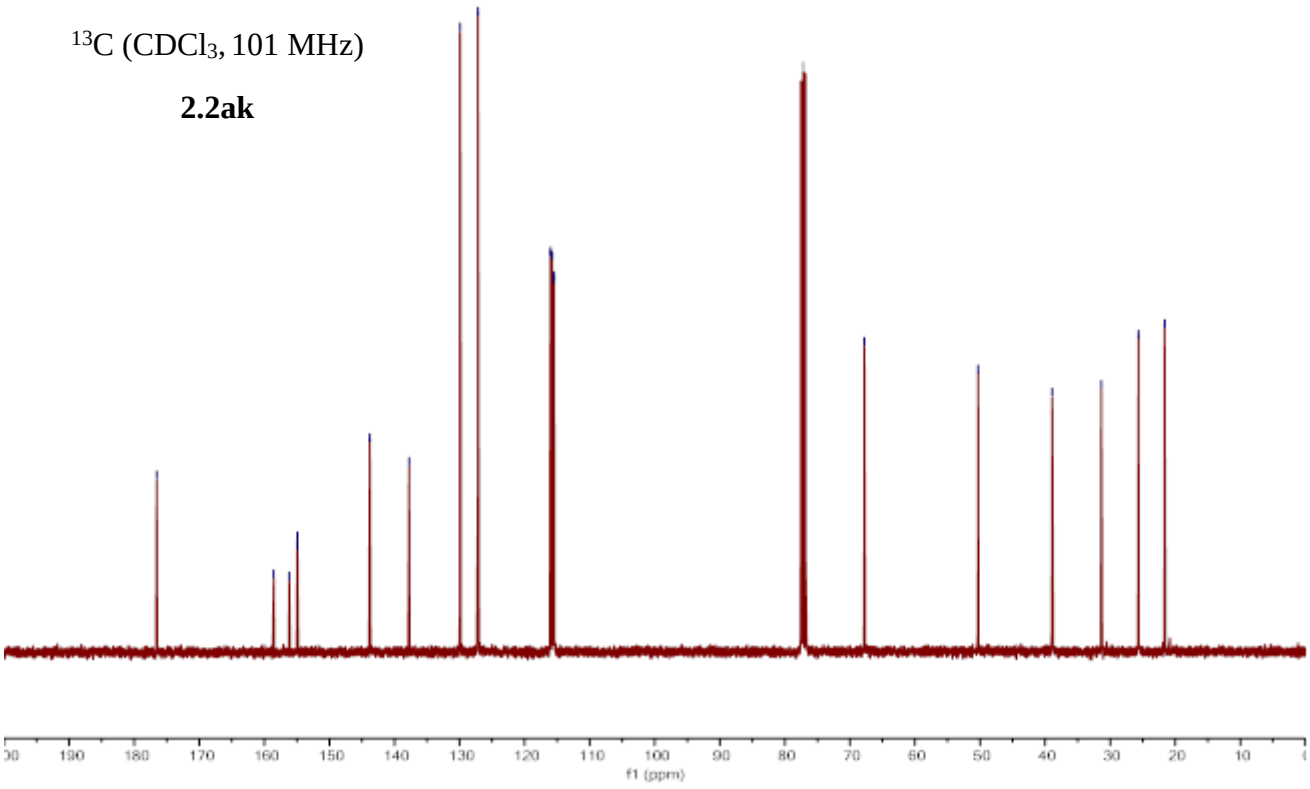

^{19}F ($CDCl_3$, 376 MHz)

2.2ak

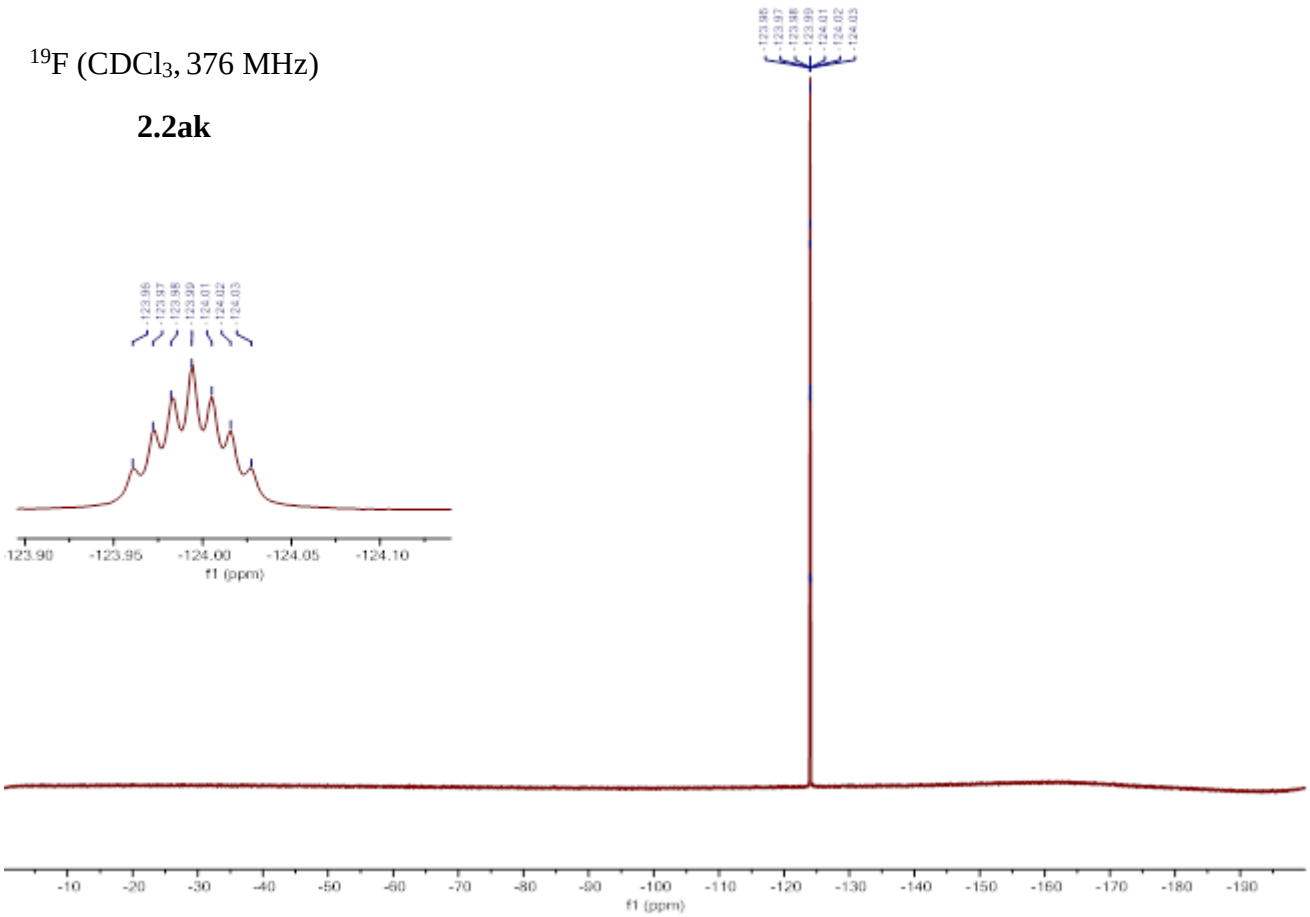

^{1}H ($CDCl_3$, 400 MHz)

2.2al

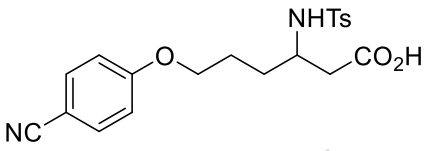

^{13}C ($CDCl_3$, 101 MHz)

2.2al

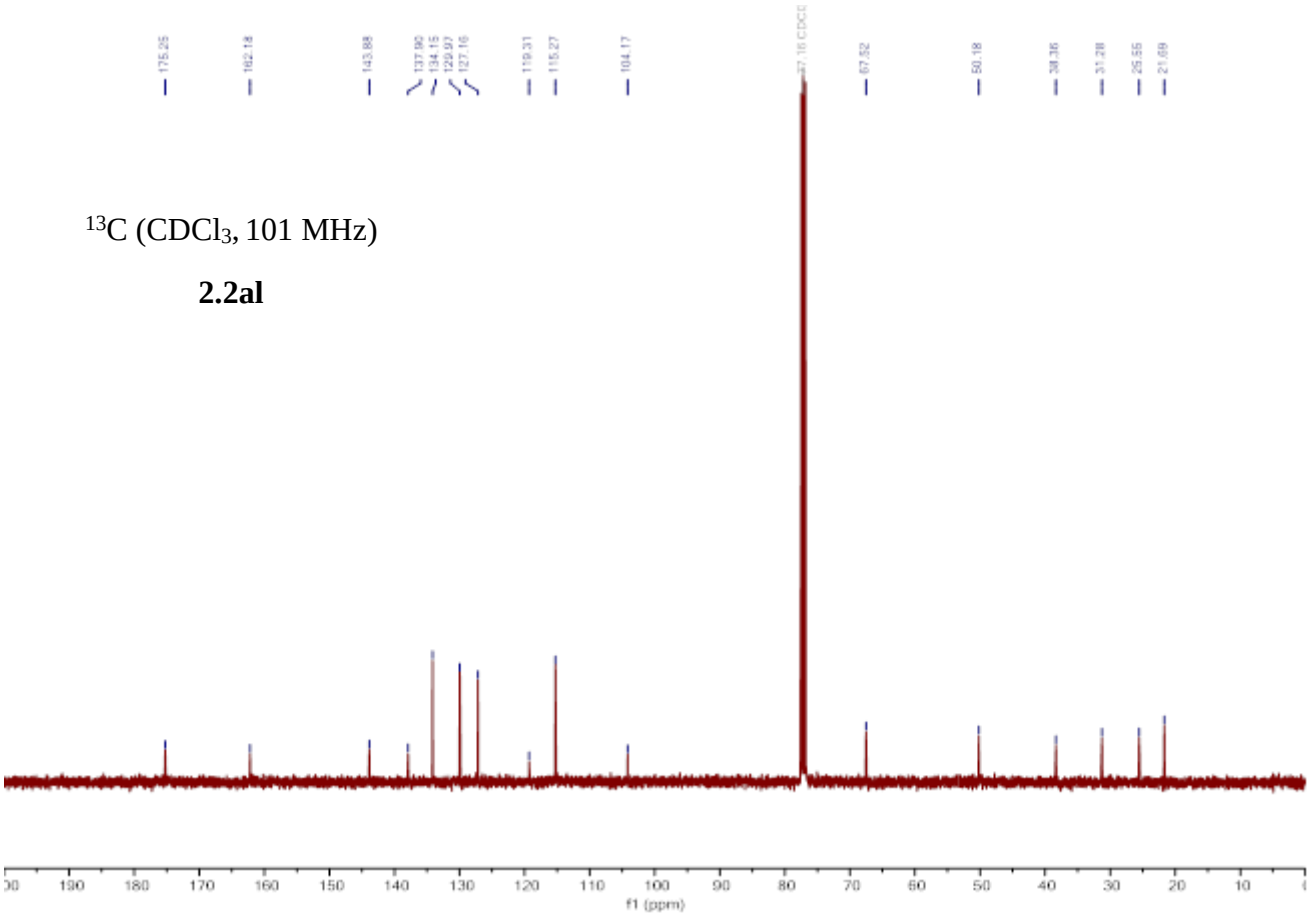

^{1}H (CD_3OD, 400 MHz)

2.2am

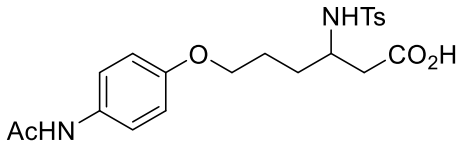

^{13}C (CD_3OD, 101 MHz)

2.2am

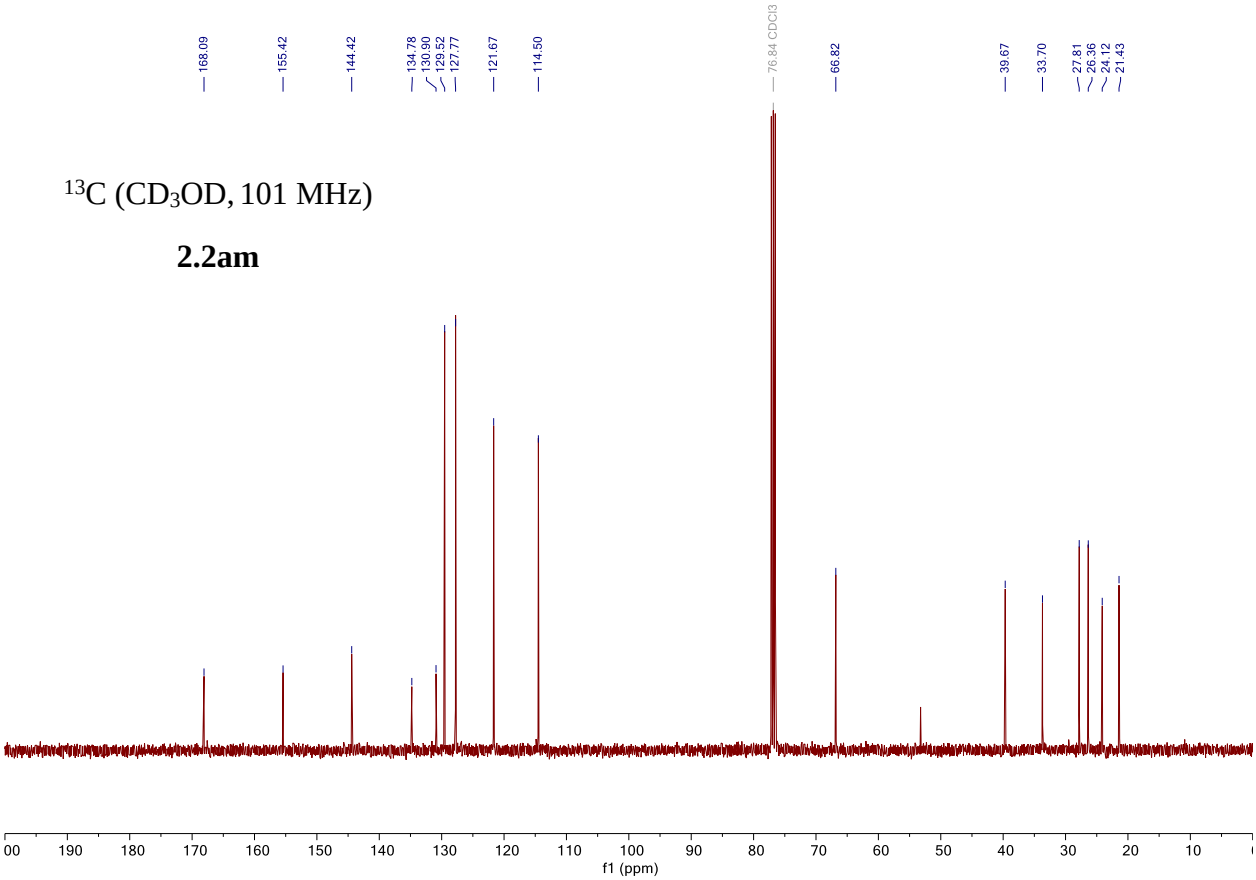

^{1}H ($CDCl_3$, 400 MHz)

2.2ao

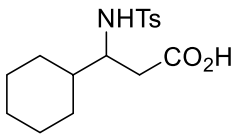

^{13}C ($CDCl_3$, 101 MHz)

2.2ao

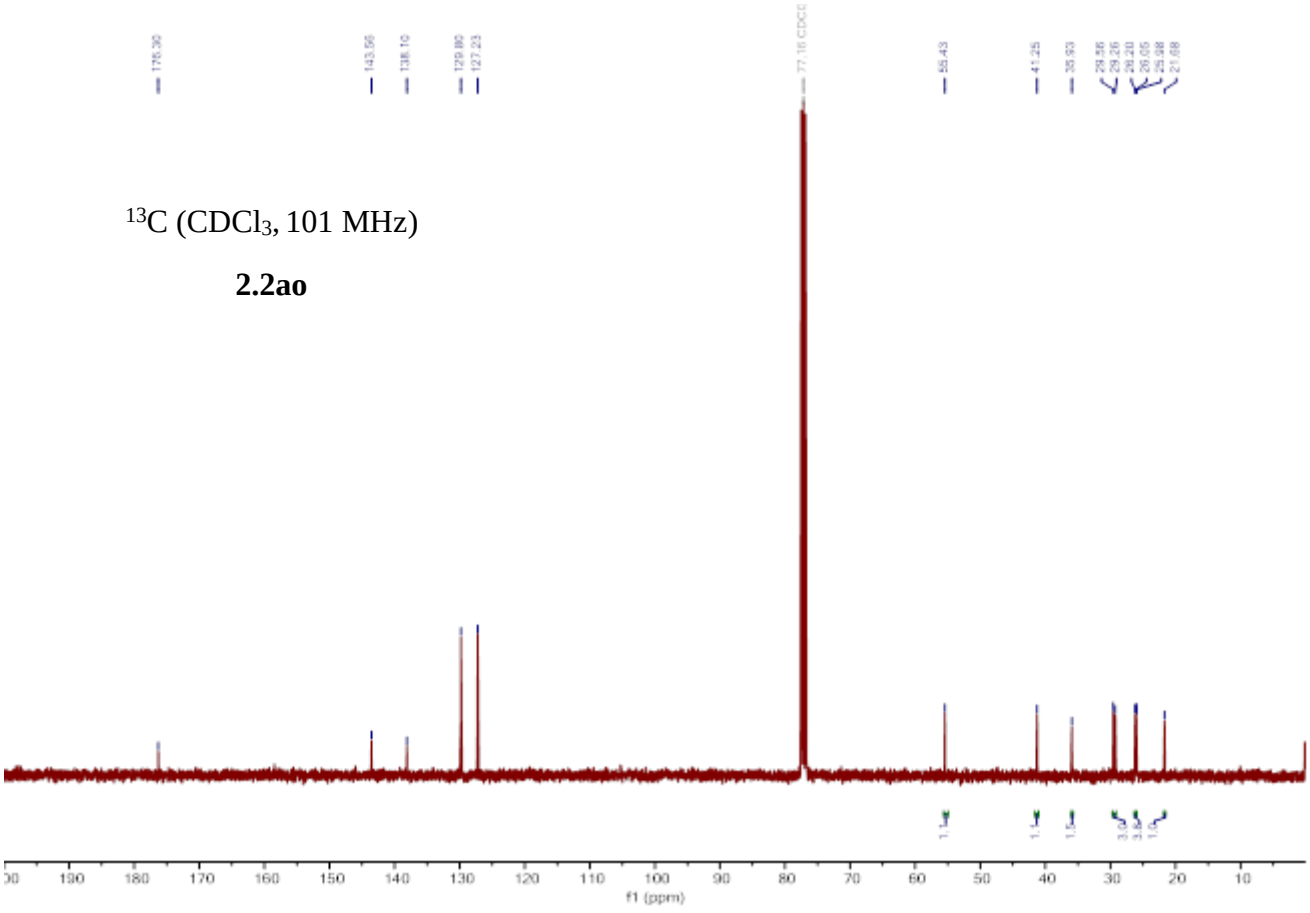

^{1}H ($CDCl_3$, 400 MHz)

2.2aq

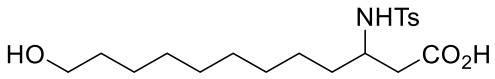

^{13}C ($CDCl_3$, 101 MHz)

2.2aq

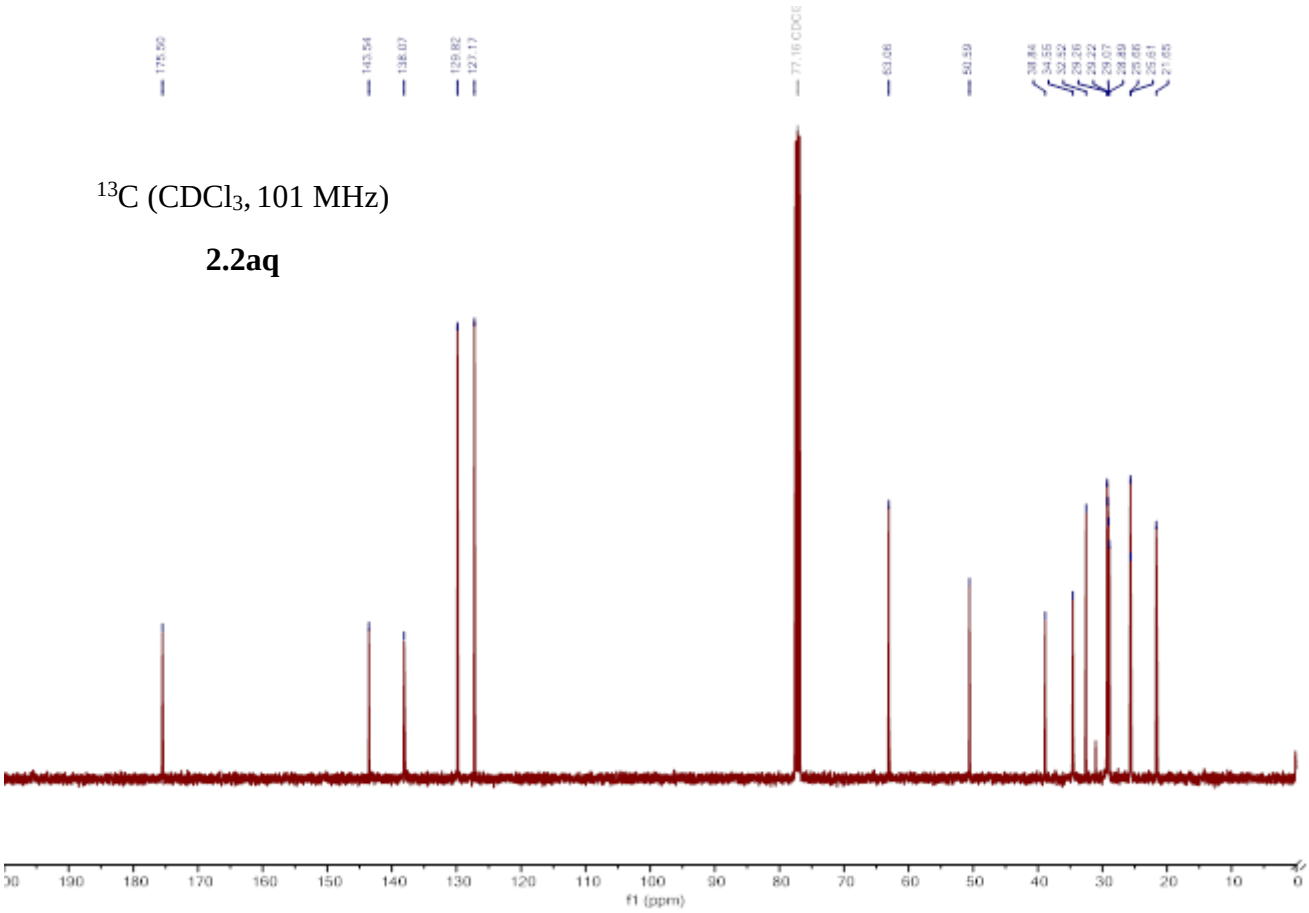

^{1}H ($CDCl_3$, 400 MHz)

2.2ar

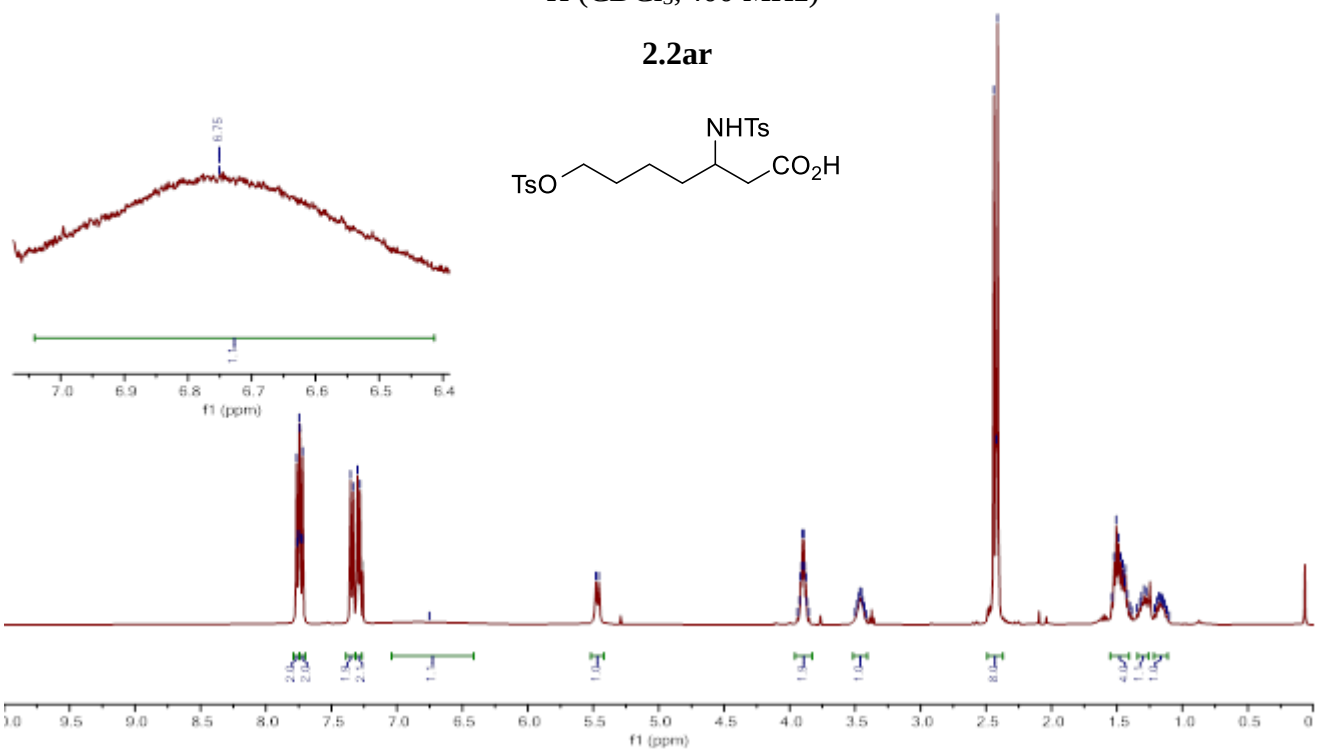

^{13}C ($CDCl_3$, 101 MHz)

2.2ar

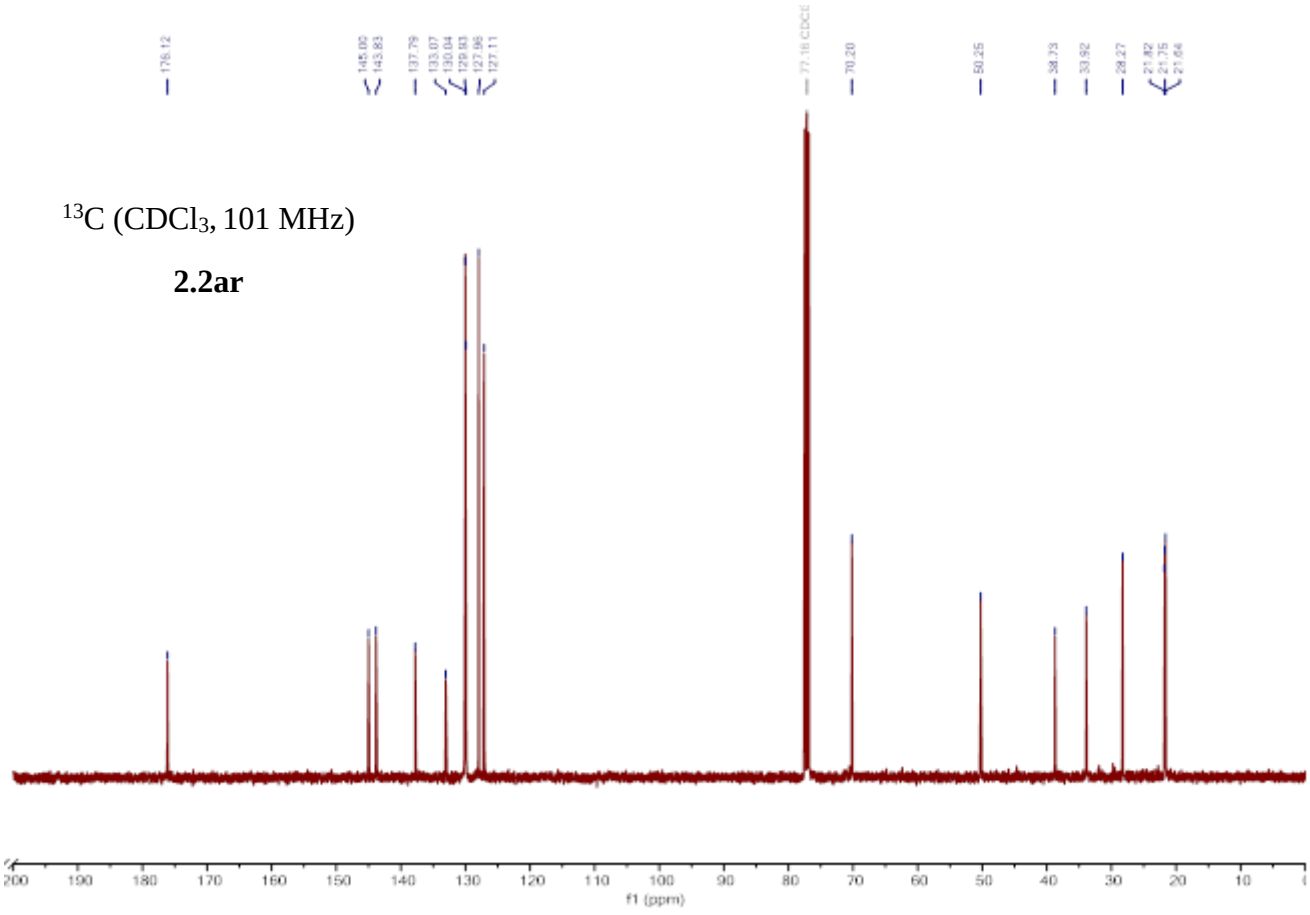

^{1}H ($CDCl_3$, 400 MHz)

2.2as

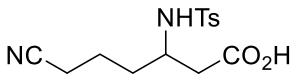

^{13}C ($CDCl_3$, 101 MHz)

2.2as

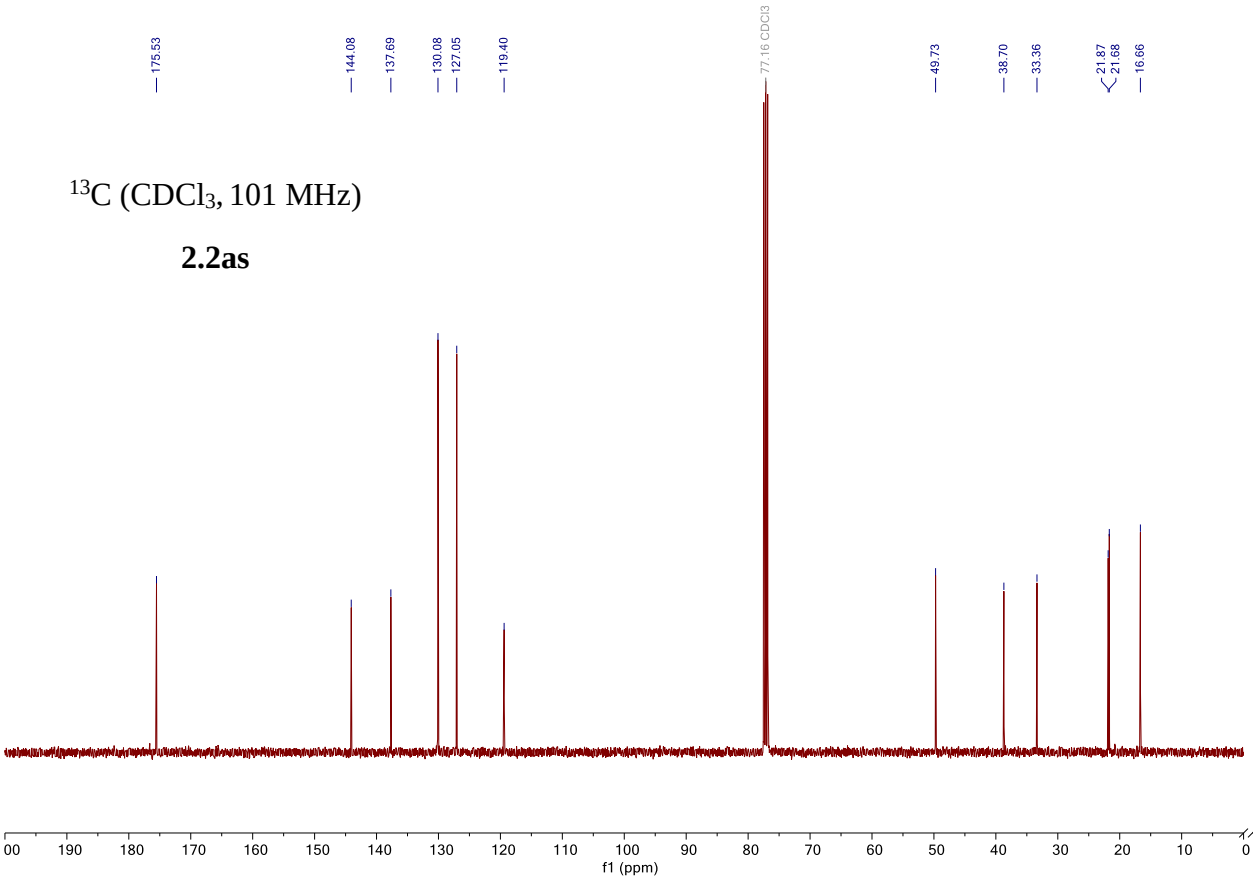

^{1}H ($CDCl_3$, 400 MHz)

2.2at

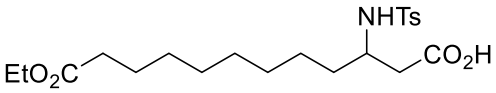

^{13}C ($CDCl_3$, 101 MHz)

2.2at

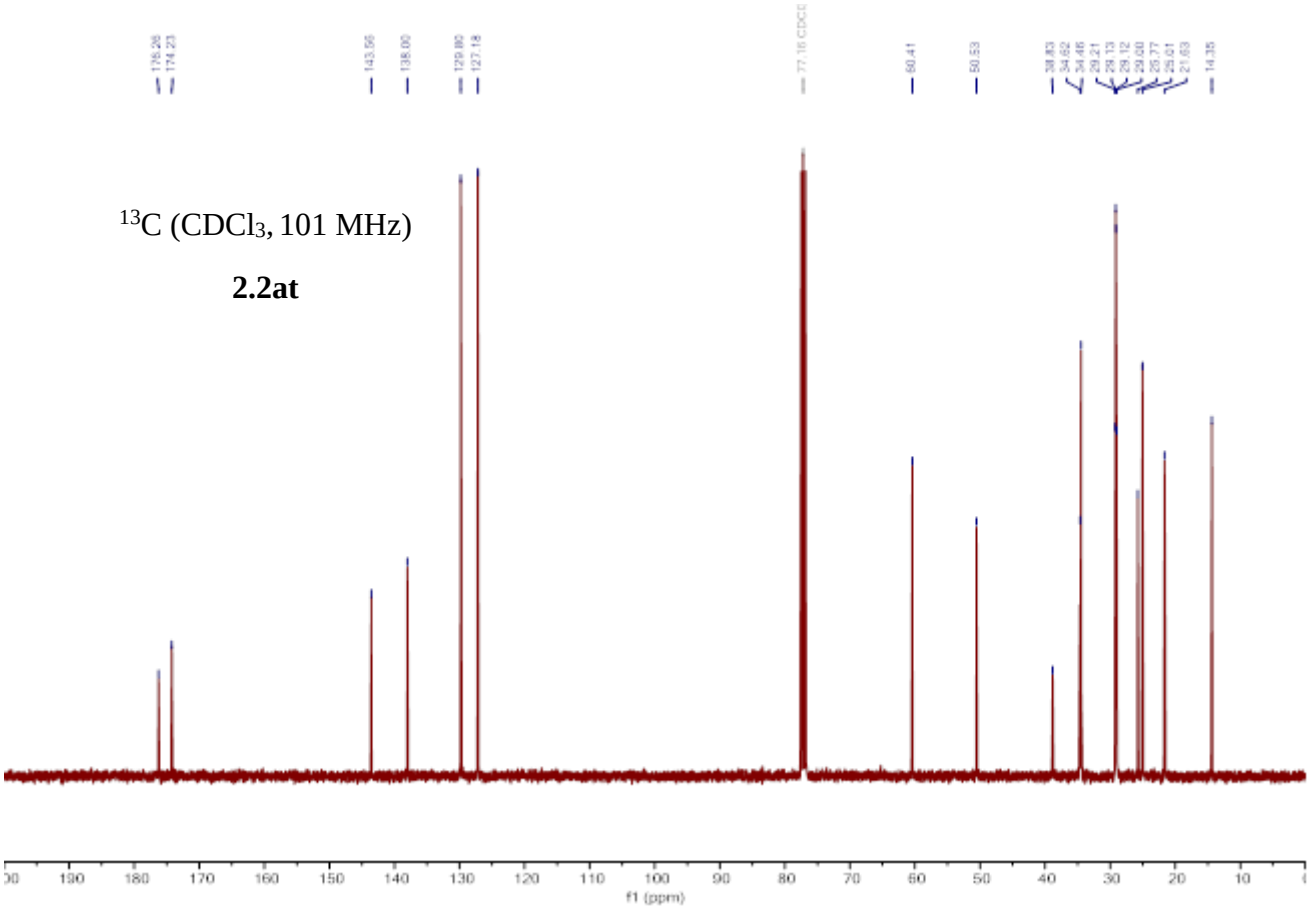

^{1}H ($CDCl_3$, 400 MHz)

2.9d (1:0.9 *trans:cis*)

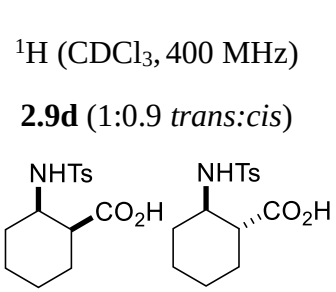

^{13}C ($CDCl_3$, 101 MHz)

2.9d (1:0.9 *trans:cis*)

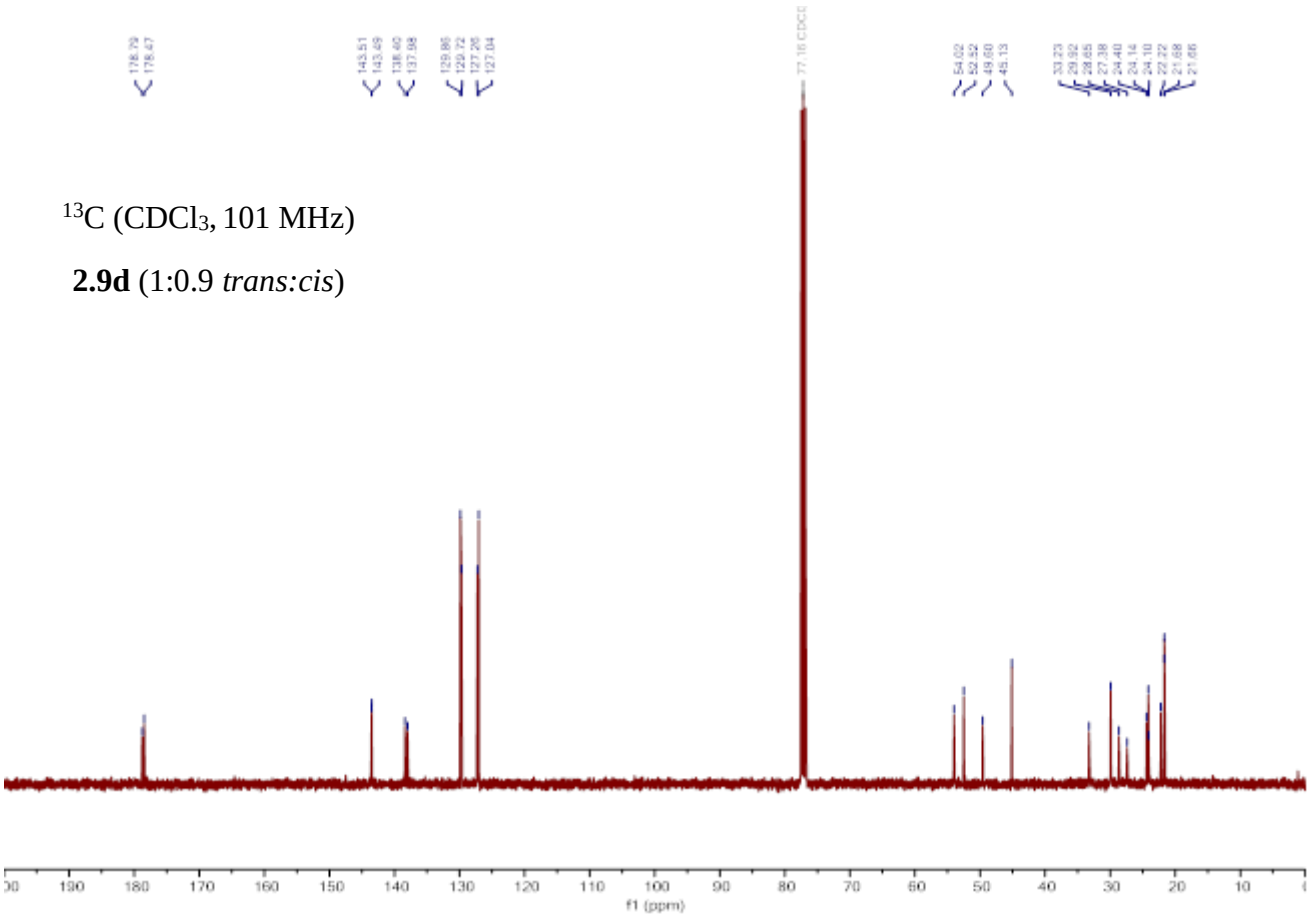

^{1}H ($CDCl_3$, 400 MHz)

2.2ay

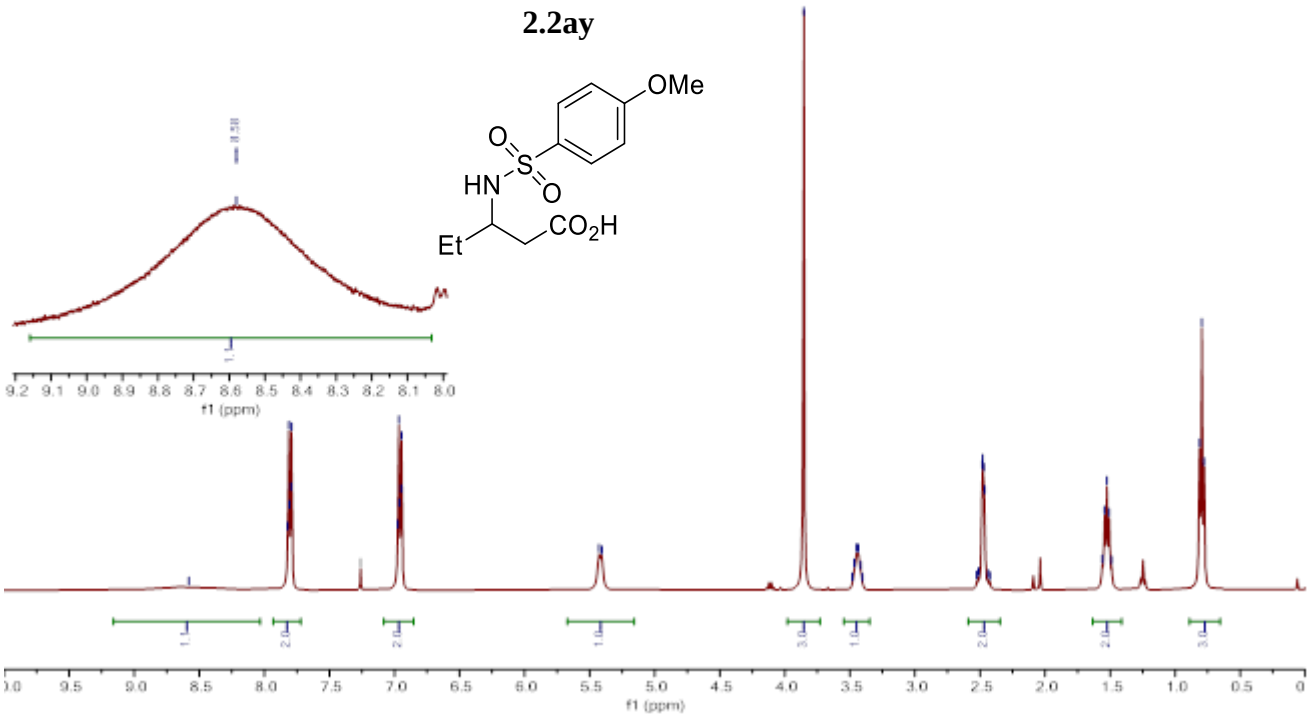

^{13}C ($CDCl_3$, 101 MHz)

2.2ay

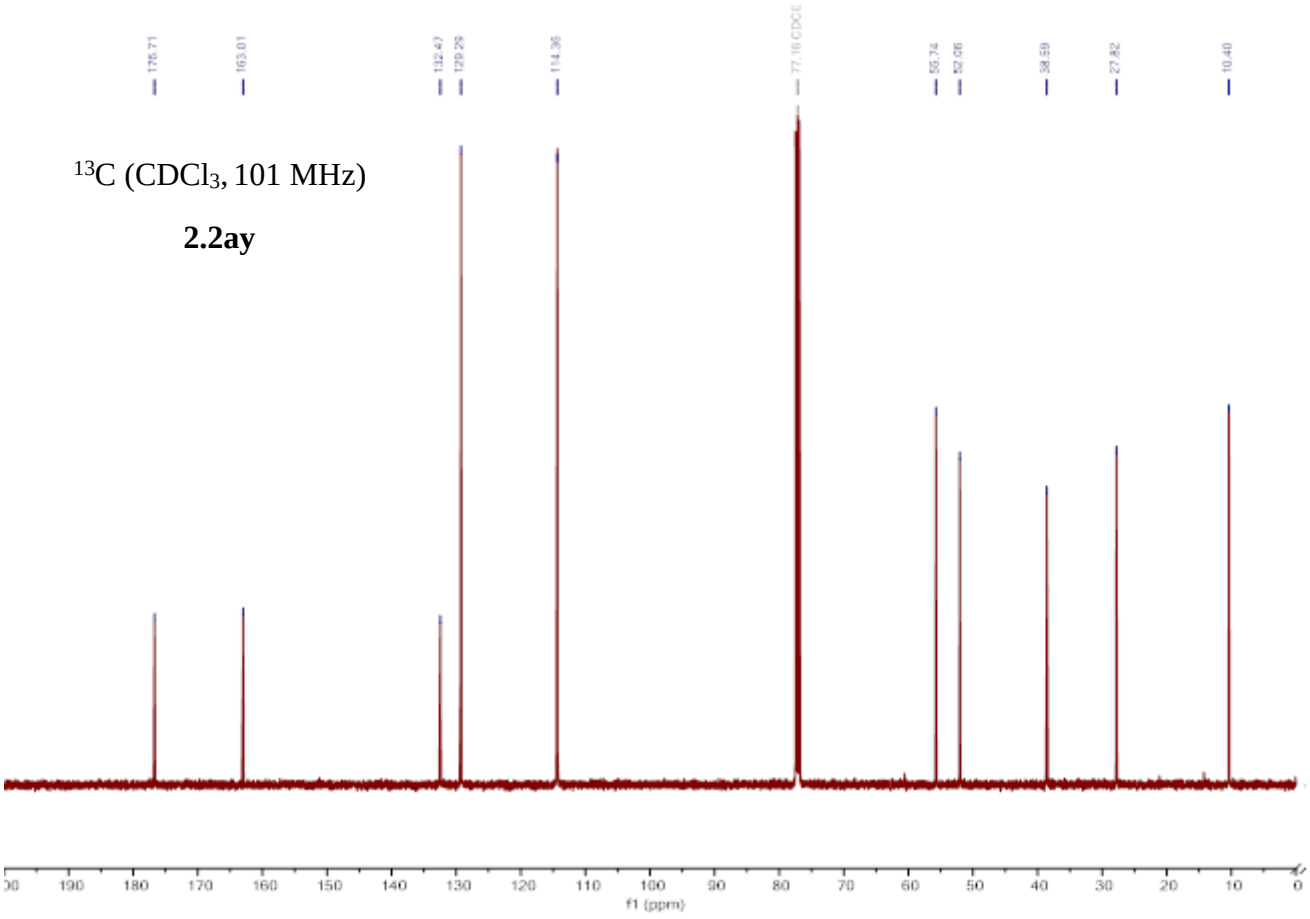

^{1}H ($CDCl_3$, 500 MHz)

2.2ba

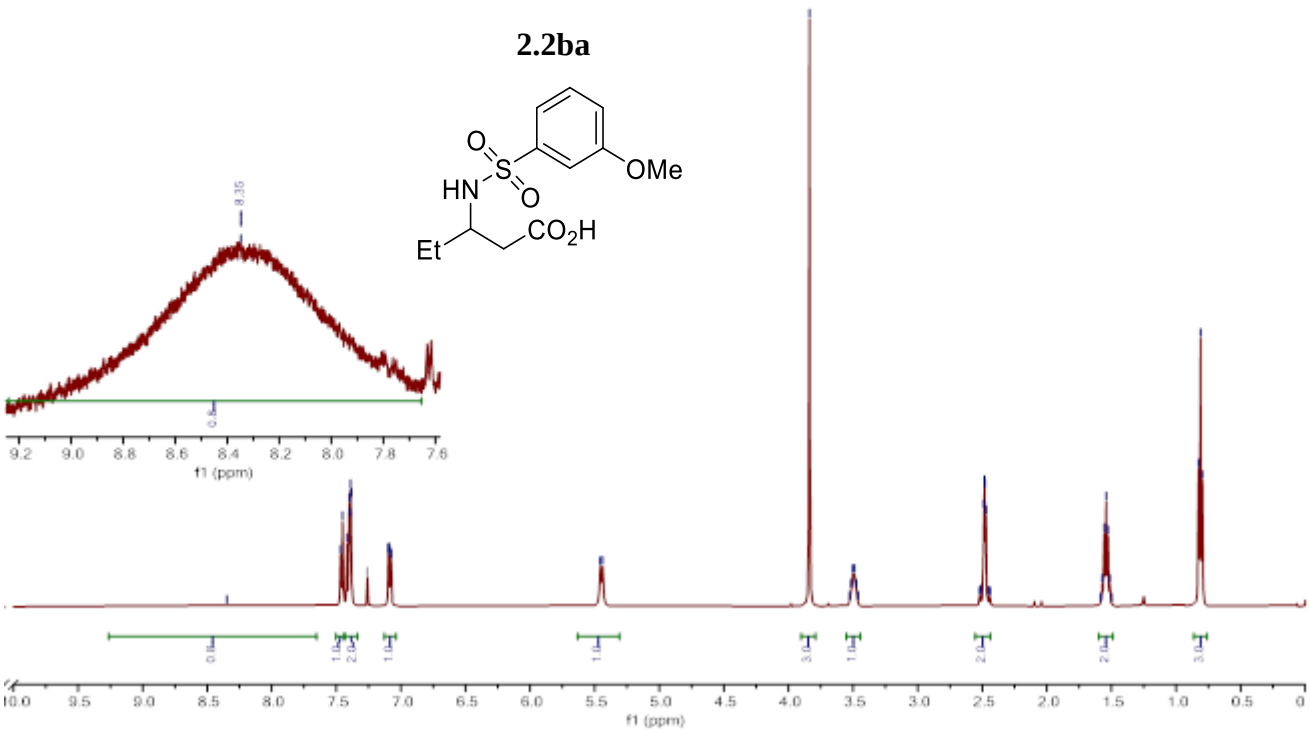

^{13}C ($CDCl_3$, 126 MHz)

2.2ba

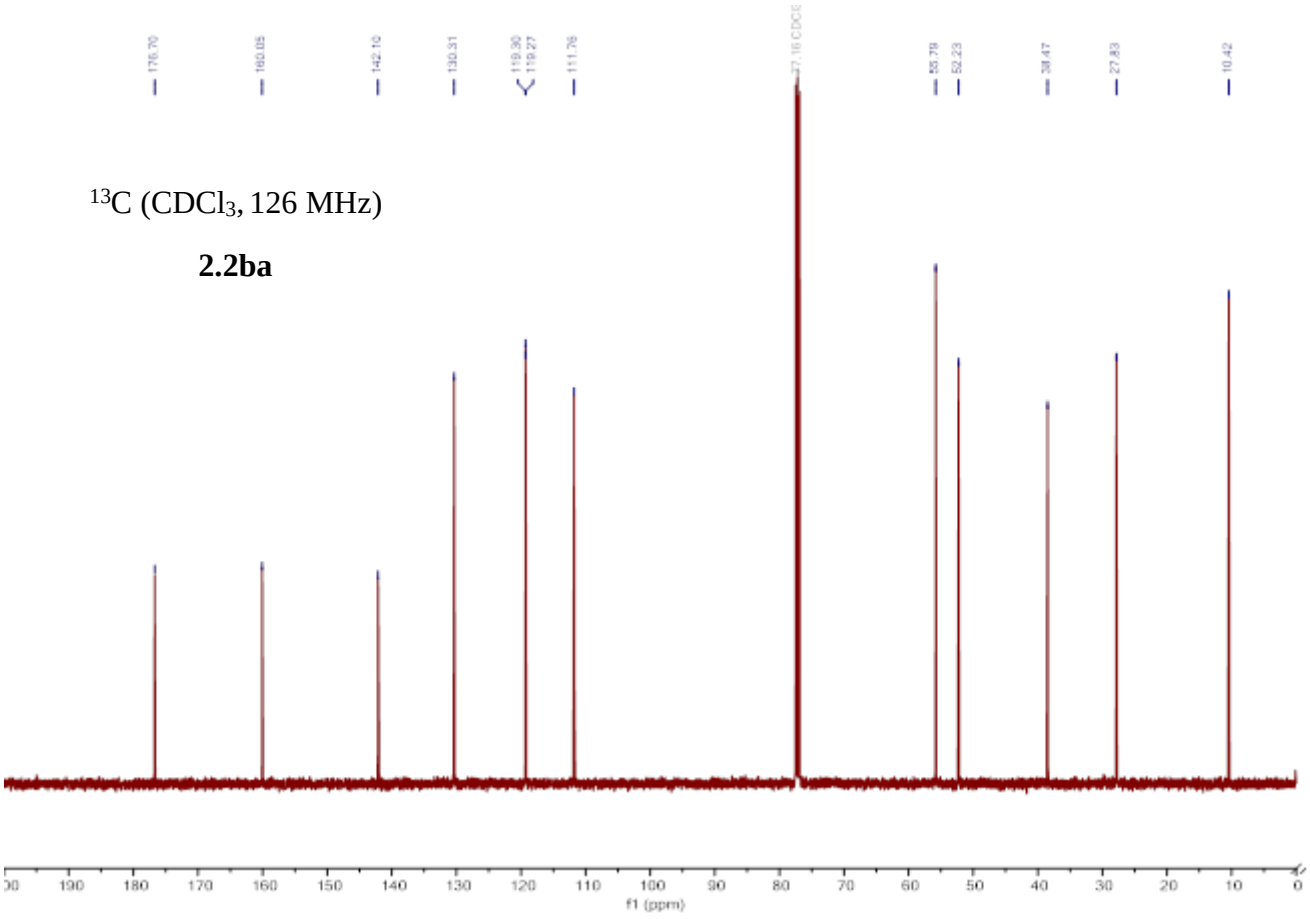

^{1}H ($CDCl_3$, 400 MHz)

2.2bb

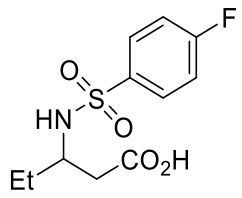

^{13}C ($CDCl_3$, 101 MHz)

2.2bb

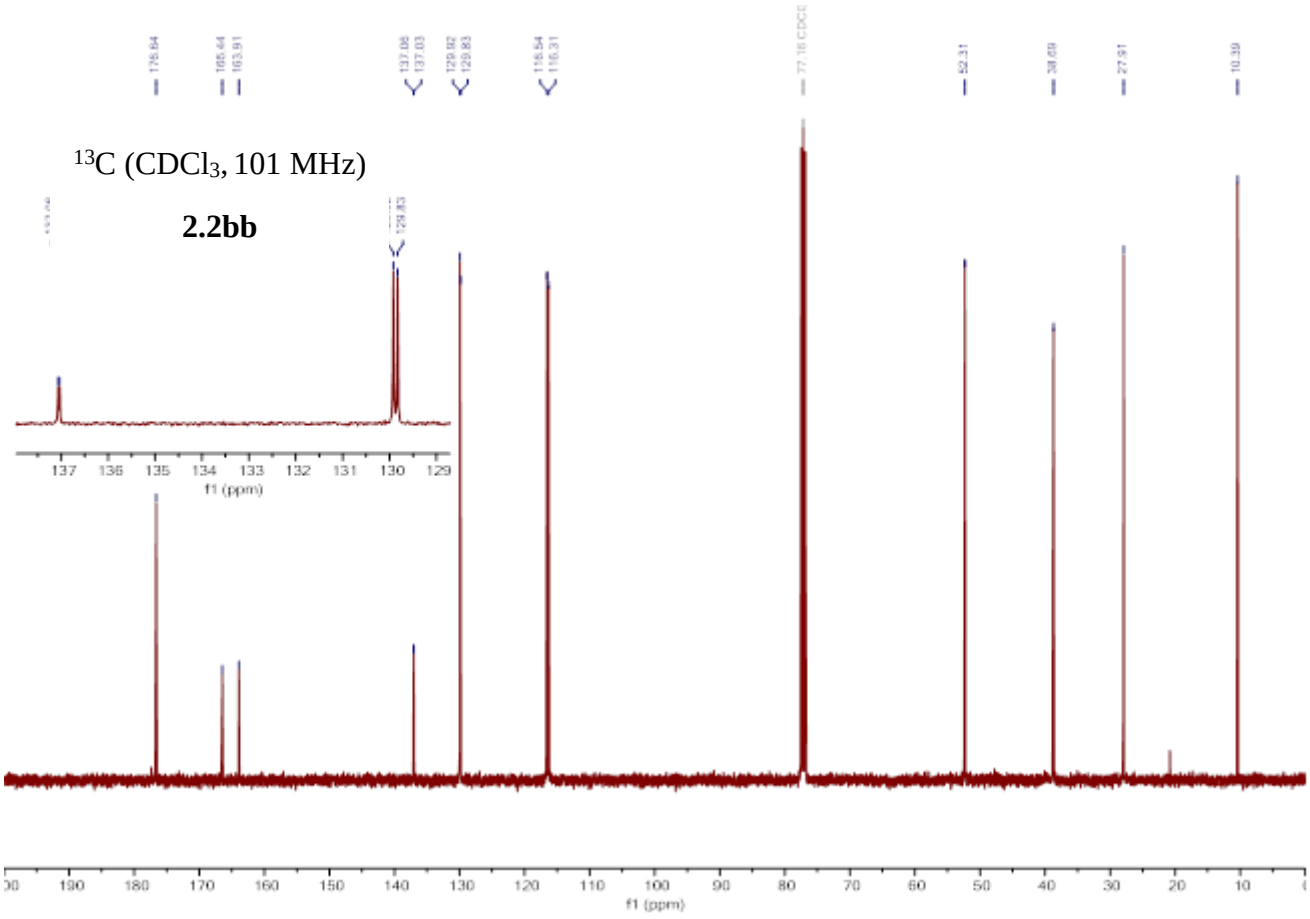

^{19}F ($CDCl_3$, 376 MHz)

2.2bb

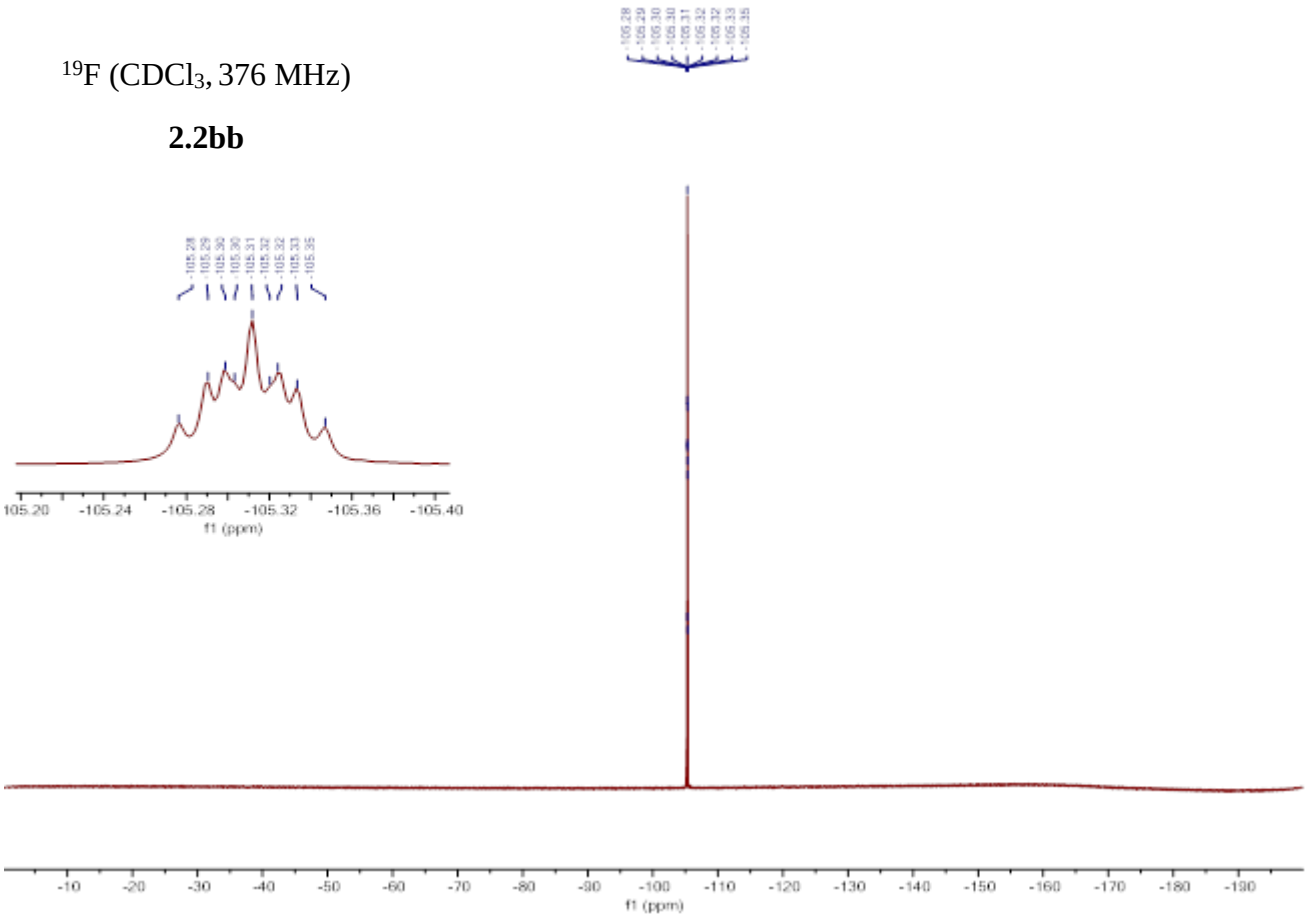

^{1}H ($CDCl_3$, 400 MHz)

2.2bc

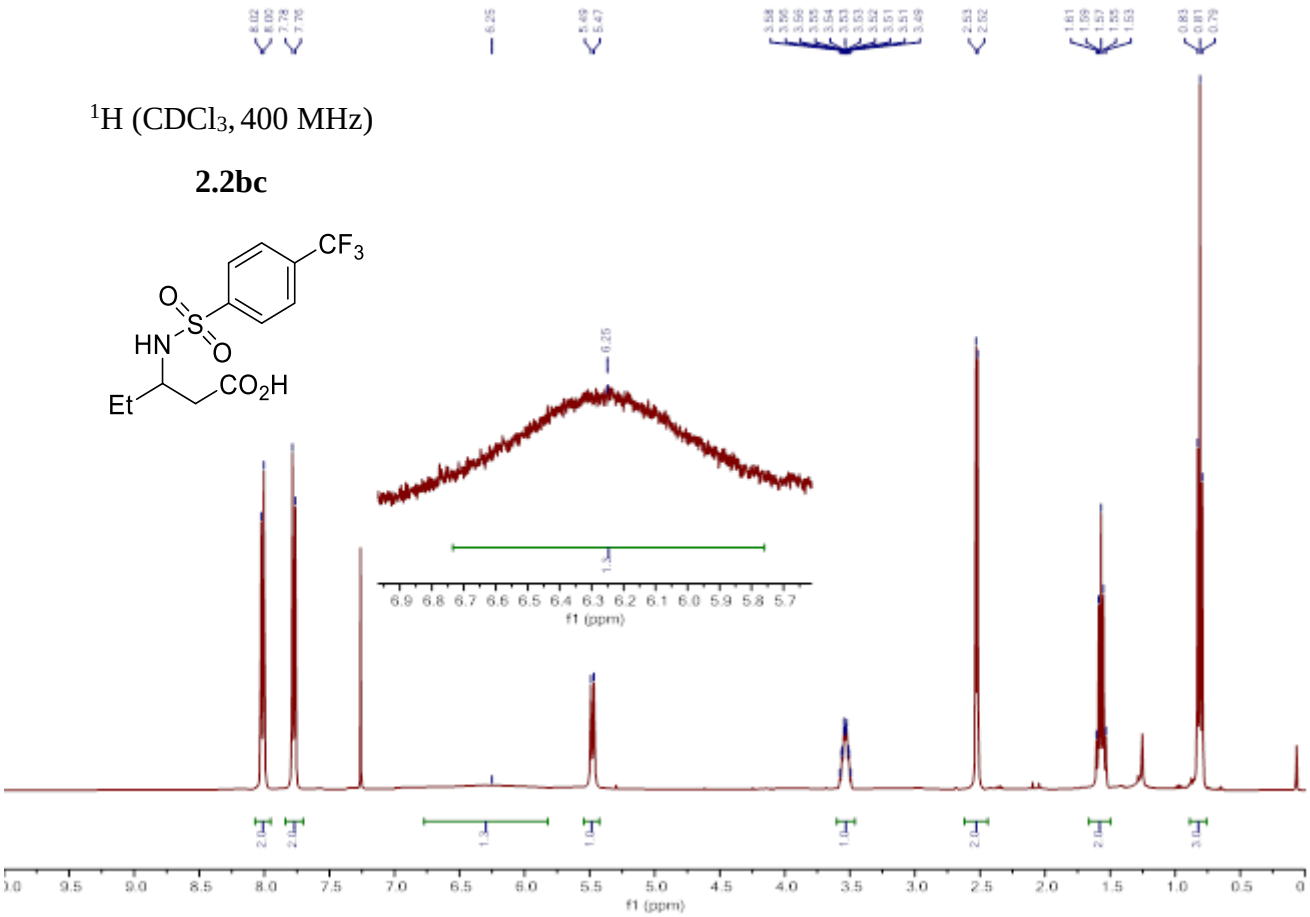

^{13}C ($CDCl_3$, 101 MHz)

2.2bc

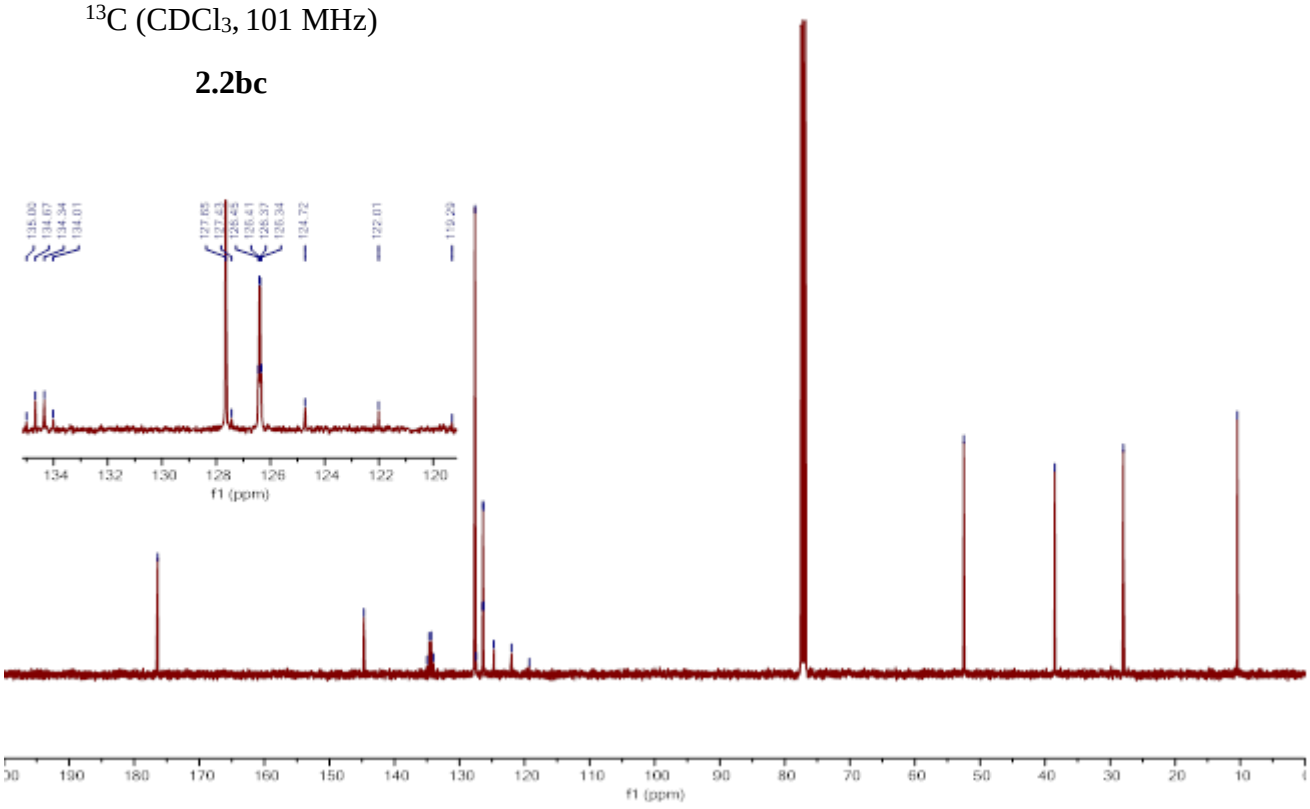

^{19}F ($CDCl_3$, 376 MHz)

2.2bc

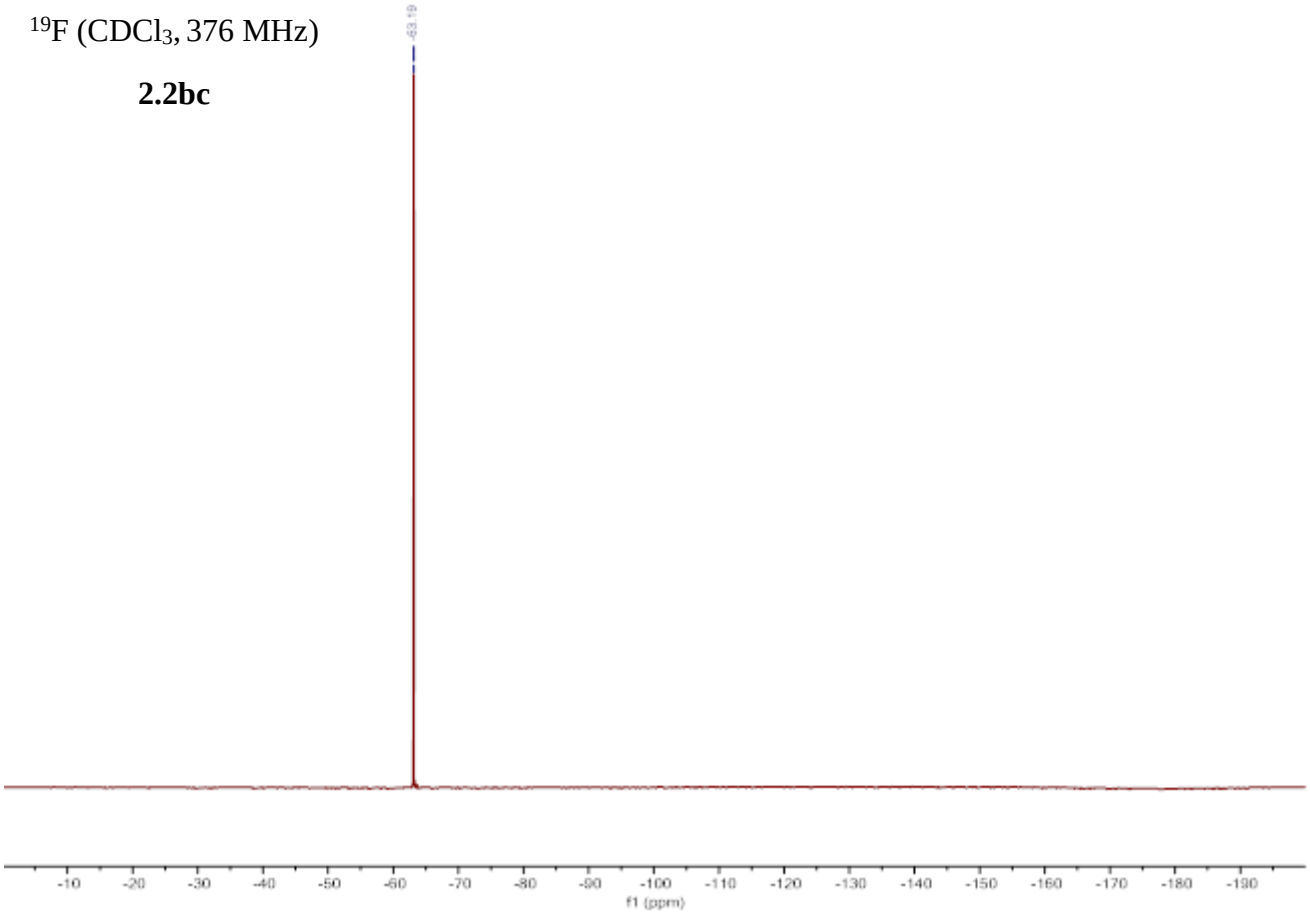

^{1}H ($CDCl_3$, 400 MHz)

2.2aw

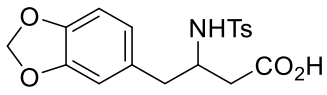

^{13}C ($CDCl_3$, 101 MHz)

2.2aw

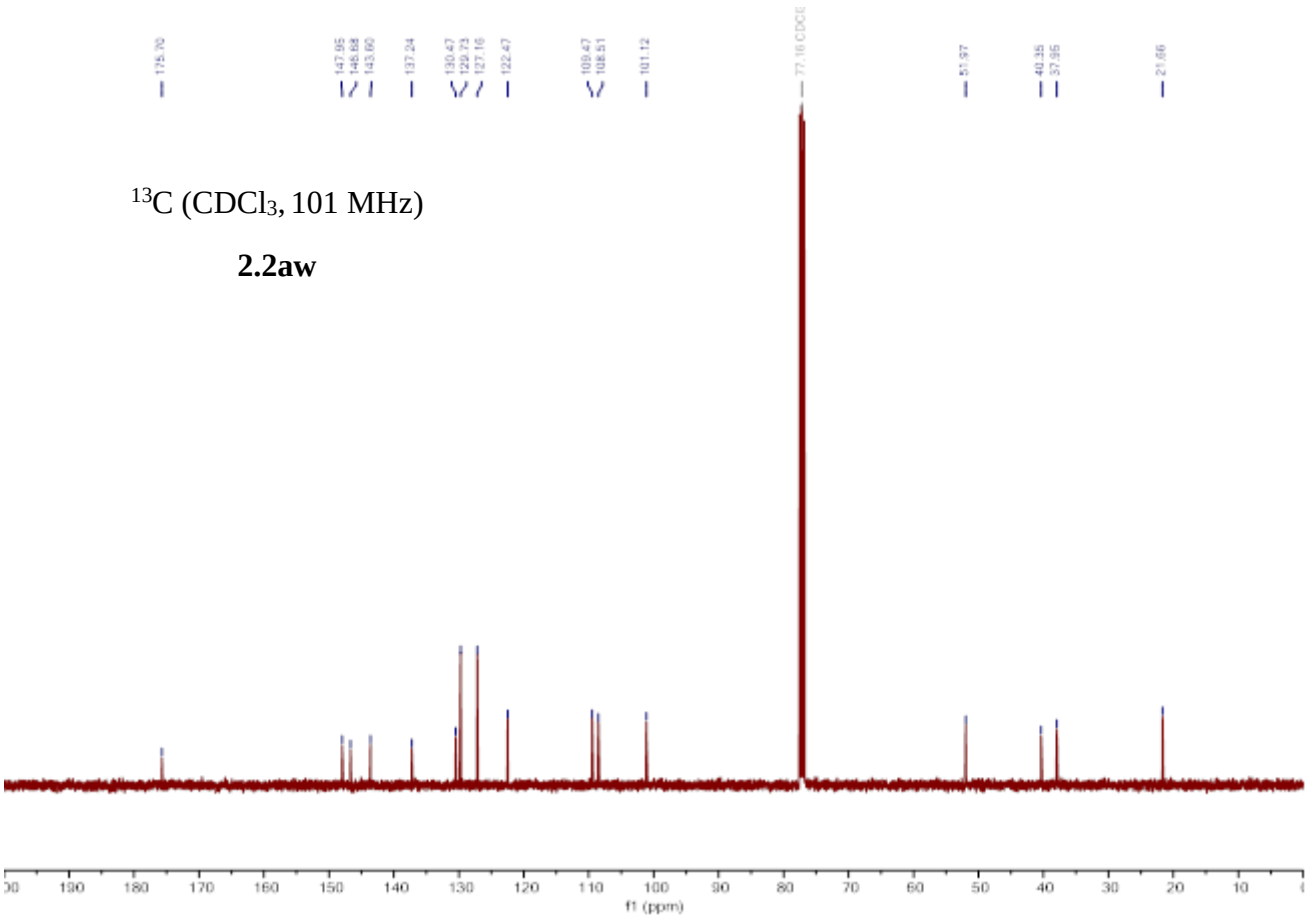

^{1}H ($CDCl_3$, 400 MHz)

2.2aw-^{13}C

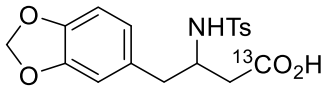

^{13}C ($CDCl_3$, 101 MHz)

2.2aw^{13}C

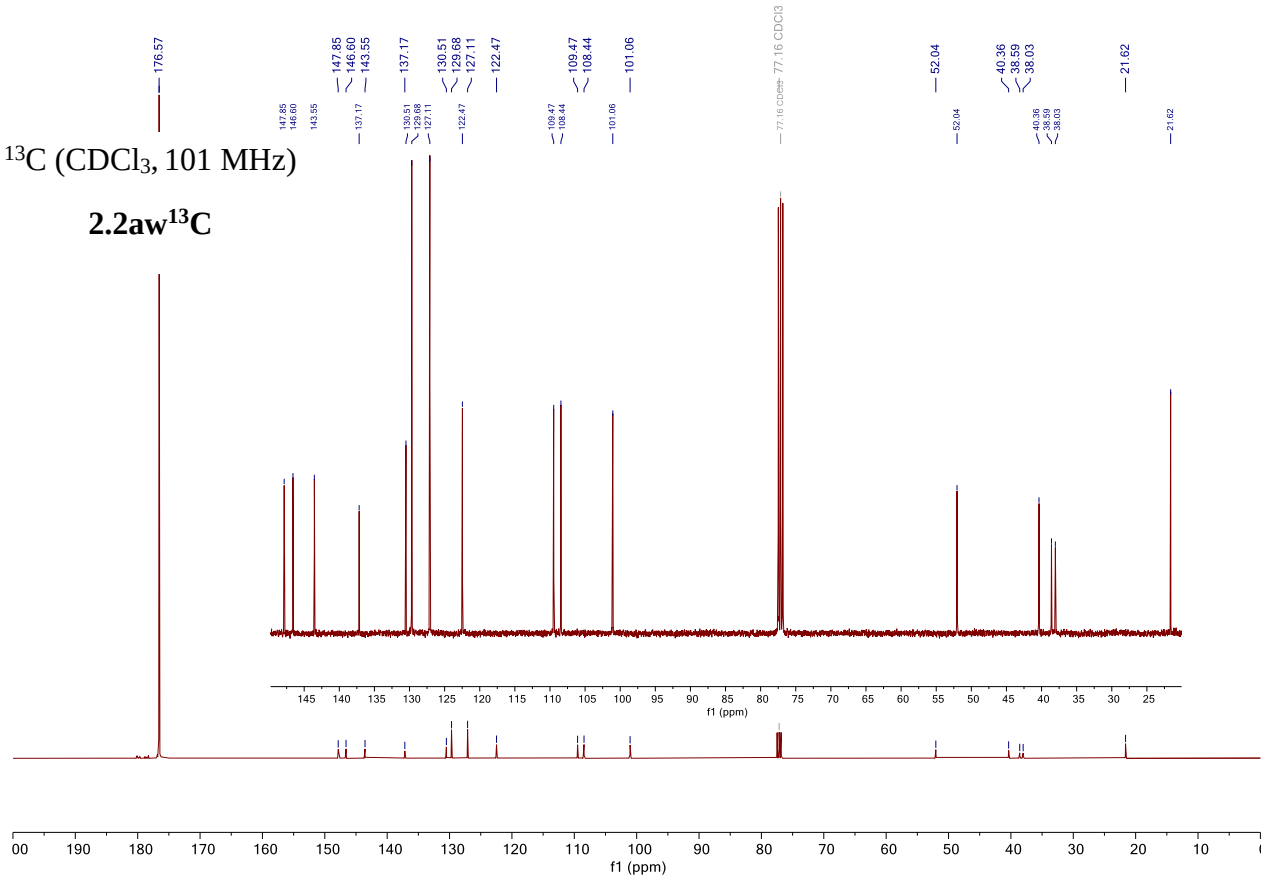

^{1}H ($CDCl_3$, 400 MHz)

2.2ax

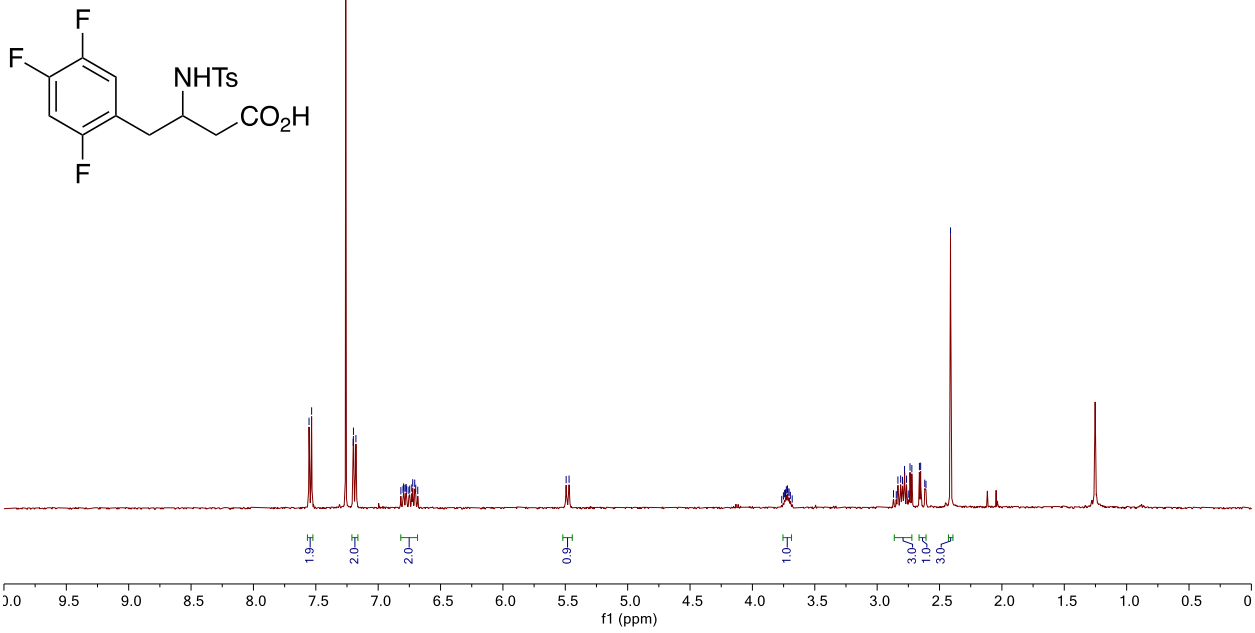

^{13}C (DMSO-d_6, 101 MHz)

2.2ax

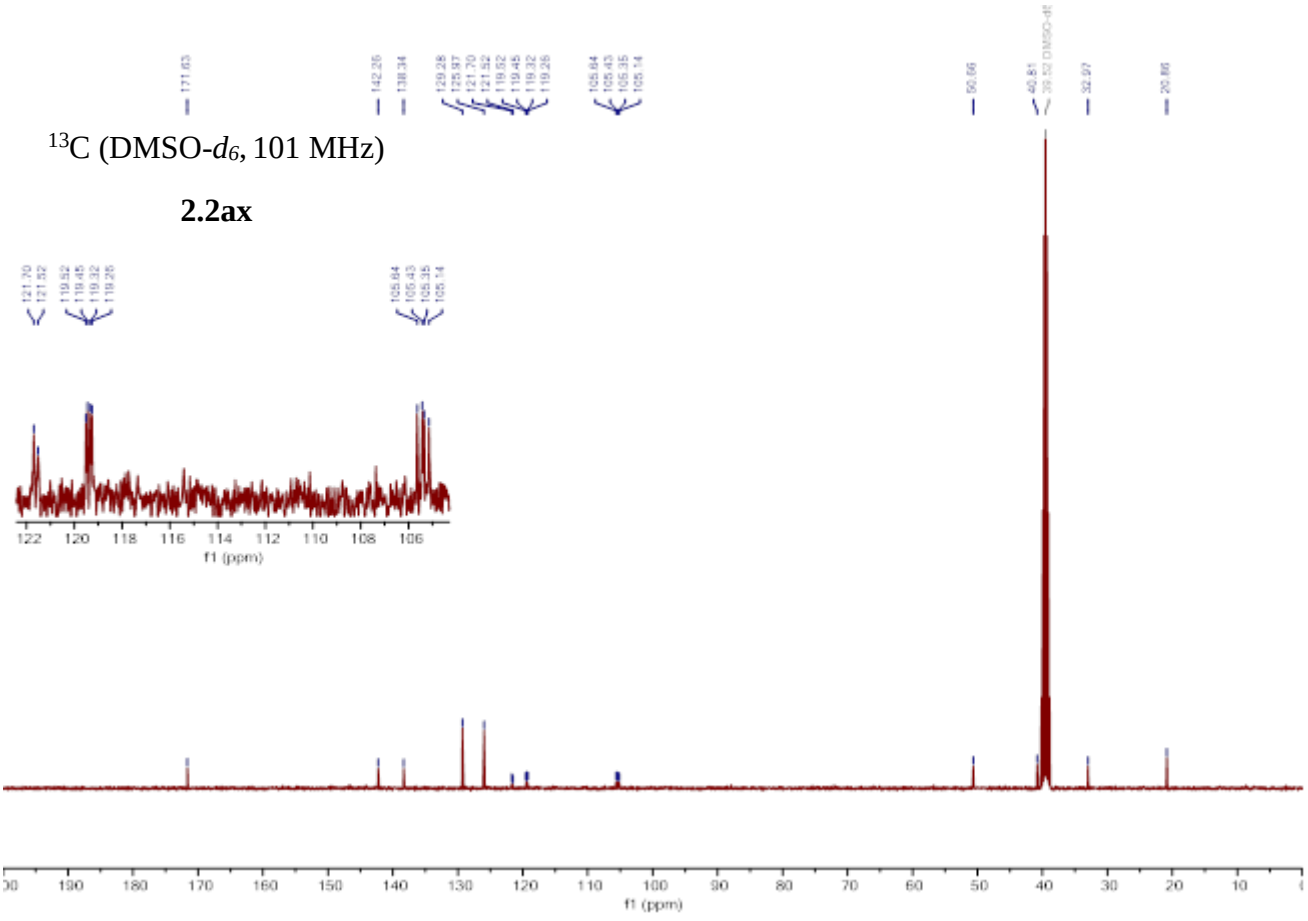

^{19}F (DMSO-d_6, 376 MHz)

2.2ax

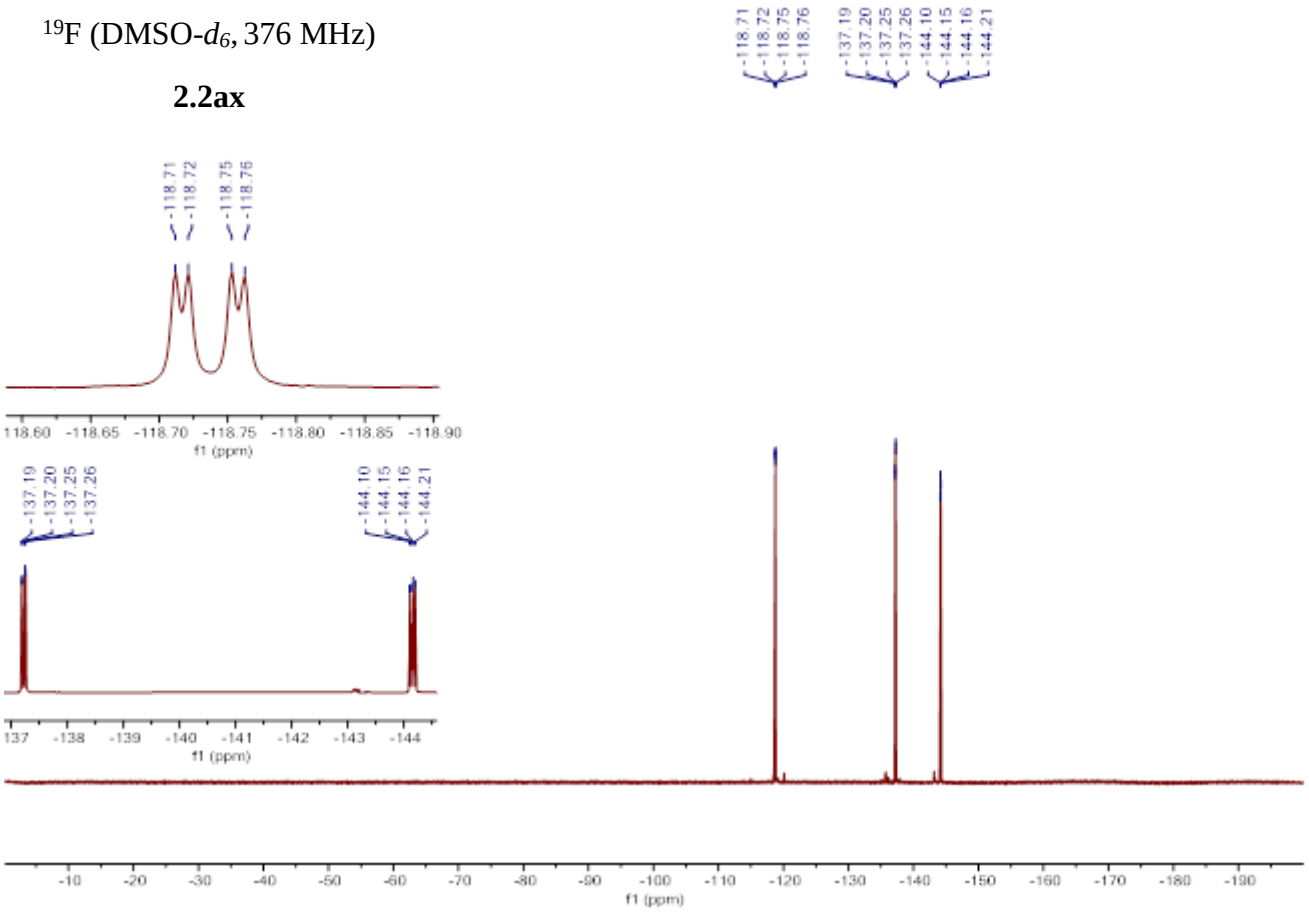

^{1}H (CD_3CN, 400 MHz)

2.4

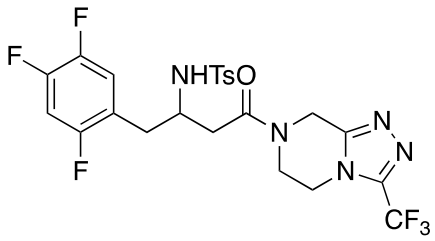

^{1}H (DMSO-d_6, 500 MHz, 115 °C)

2.4

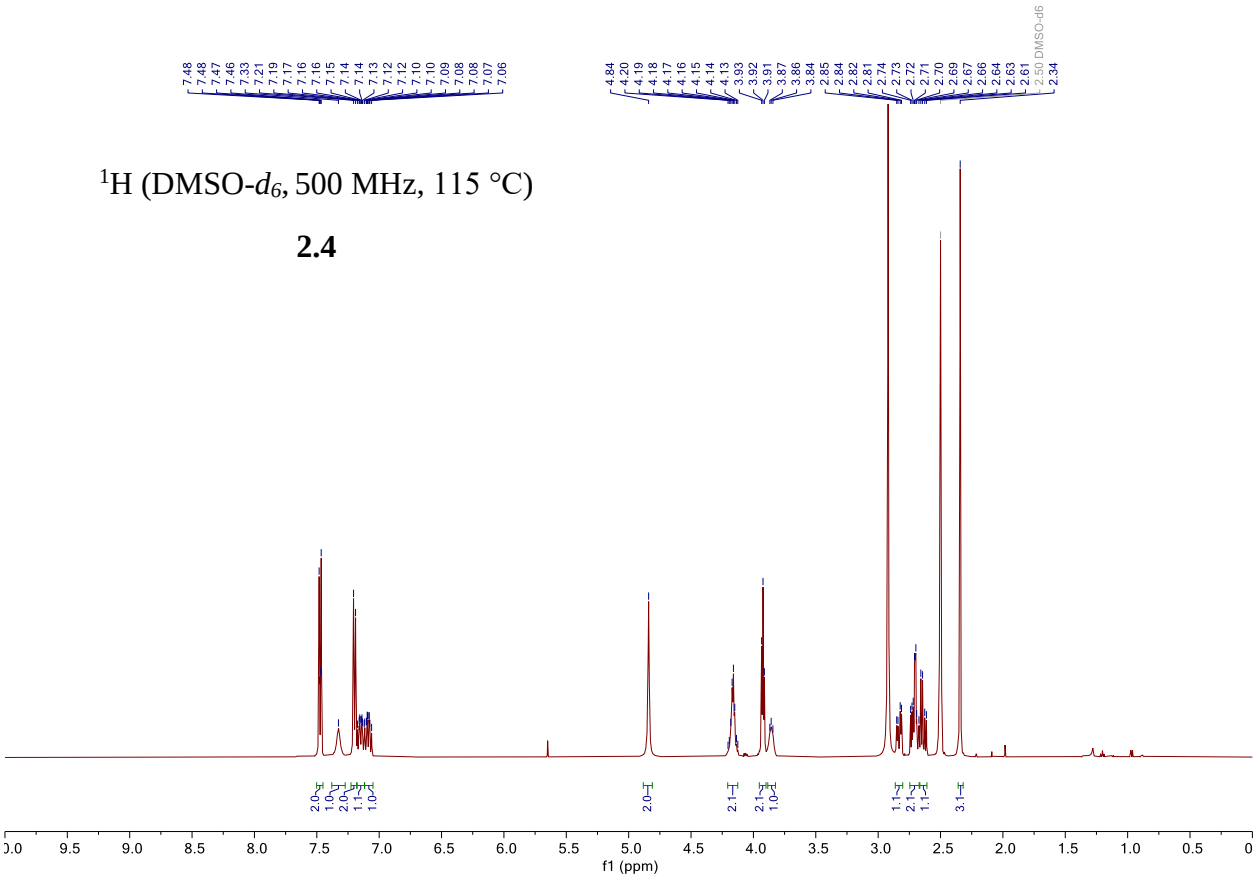

^{13}C (DMSO-d_6, 126 MHz, 115 °C)

2.4

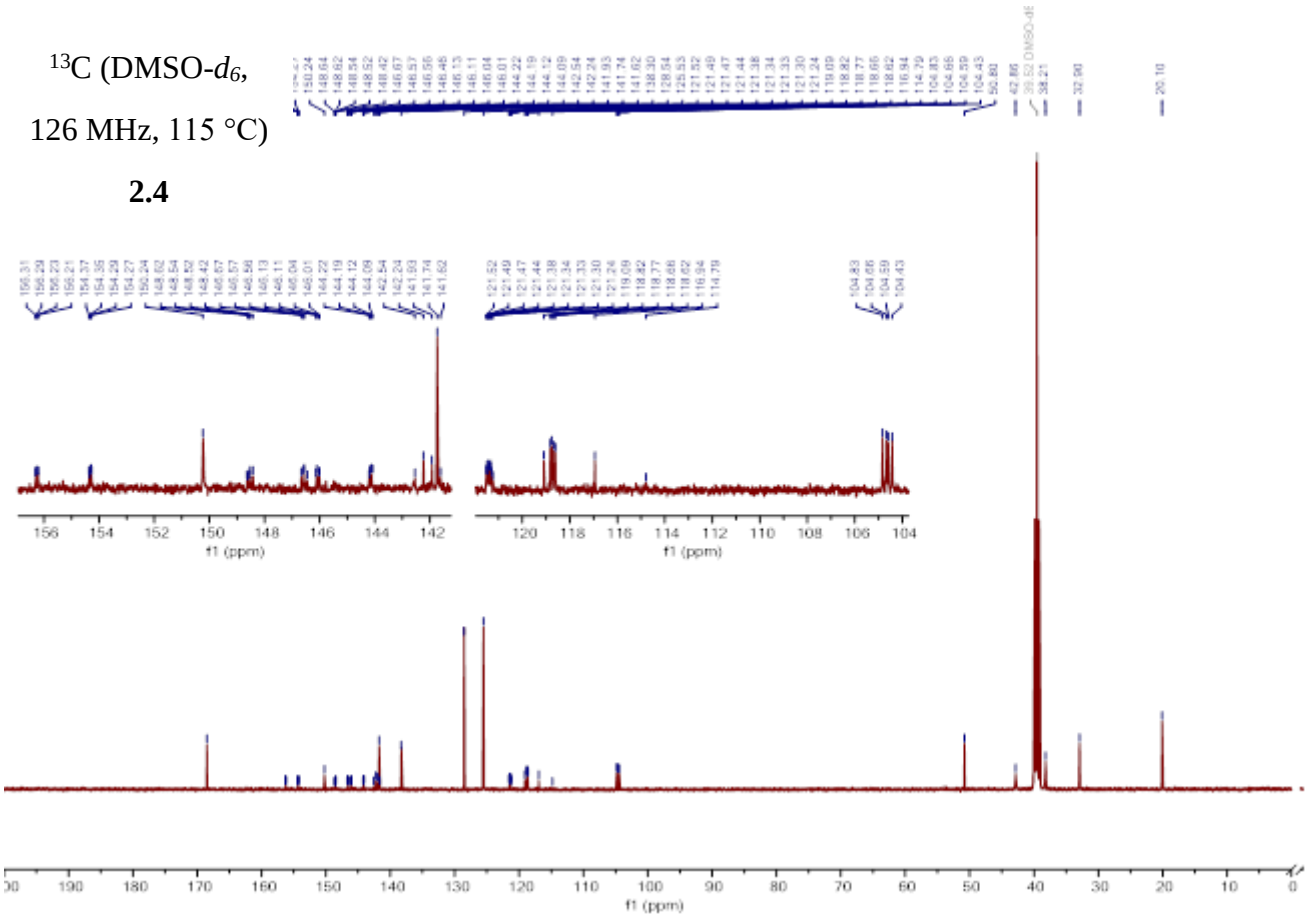

^{19}F (DMSO-d_6, 471 MHz, 115 °C)

2.4

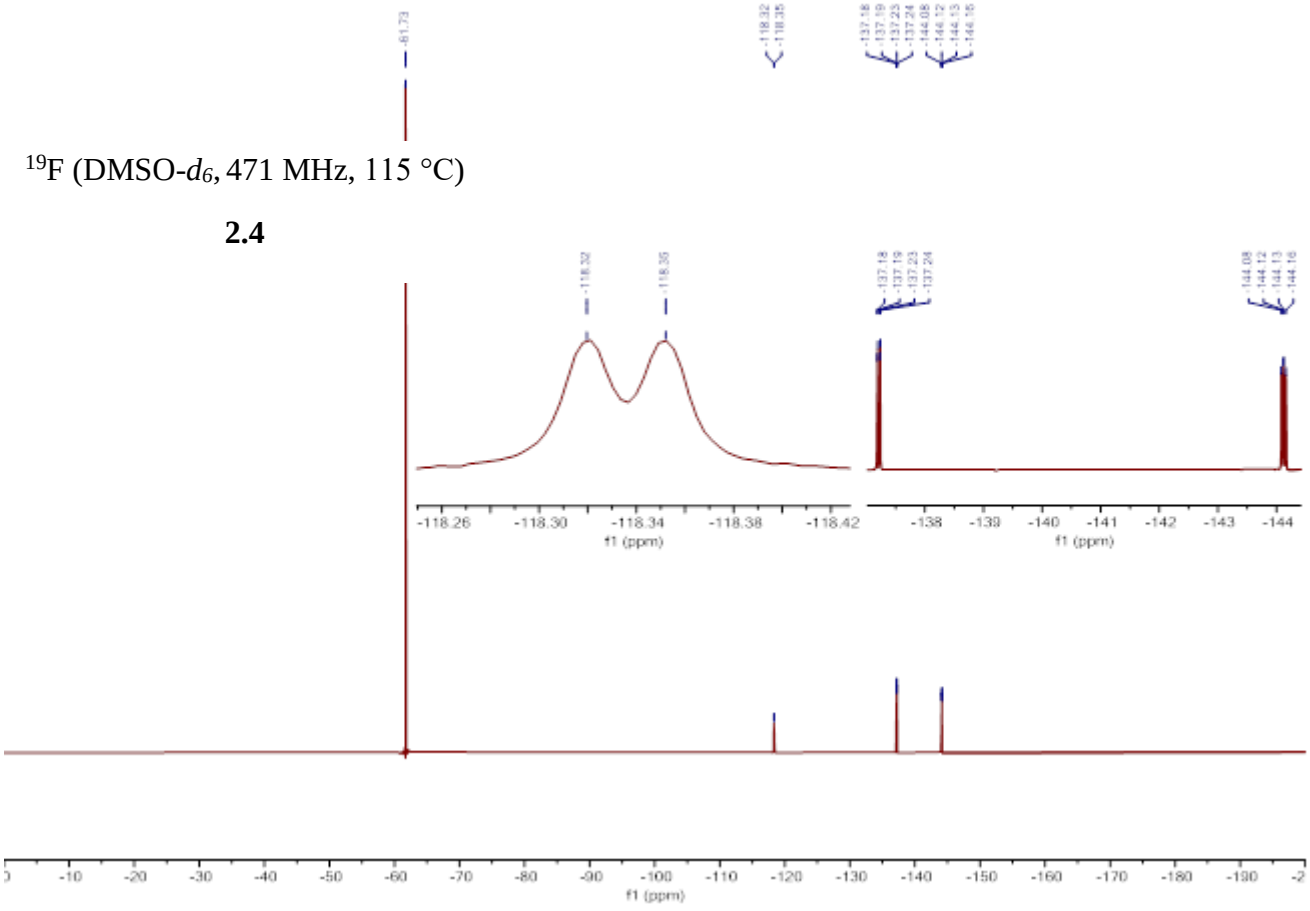

^{1}H (CD_3OD, 400 MHz)

2.2s

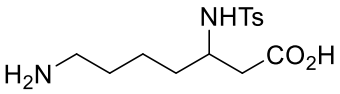

^{13}C (CD_3OD, 101 MHz)

2.2s

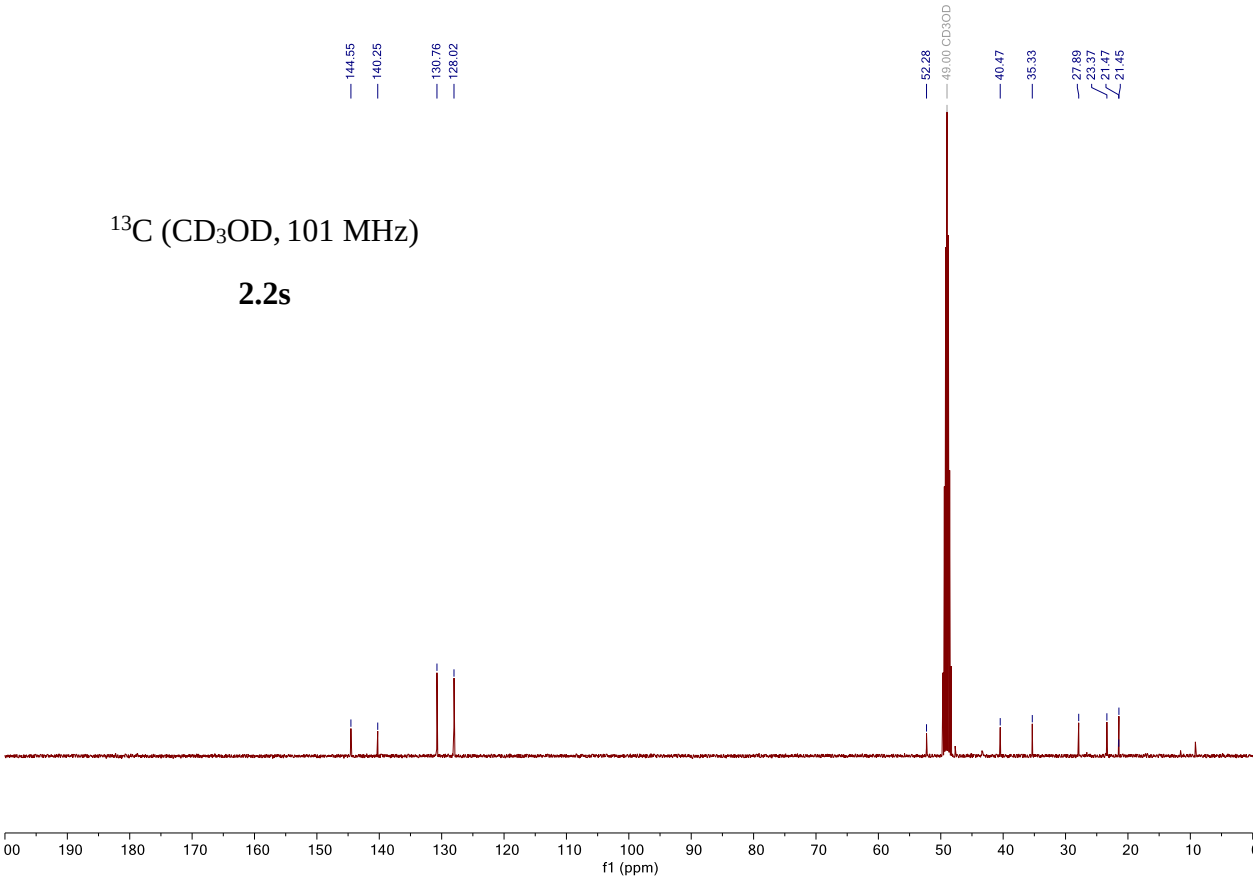

^{13}C (D_2O, 101 MHz)

2.2s

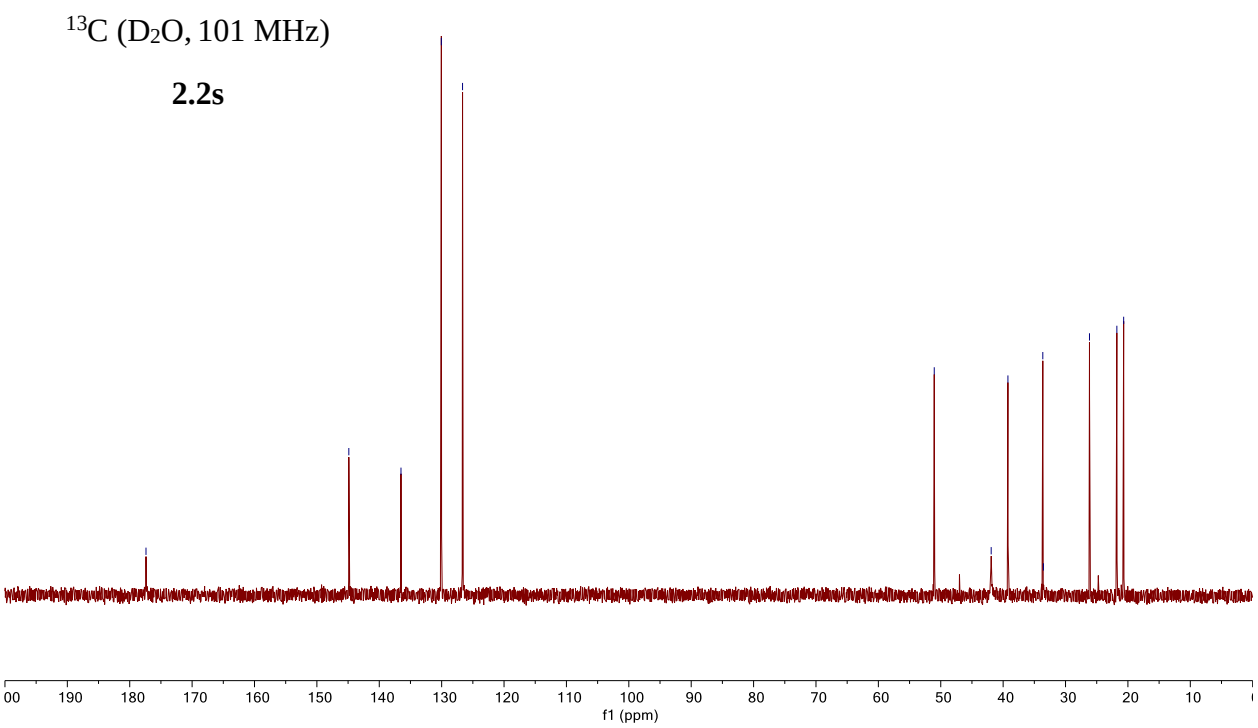

^{1}H ($CDCl_3$, 400 MHz)

2.2v

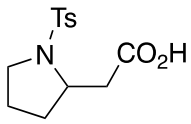

^{13}C ($CDCl_3$, 101 MHz)

2.2v

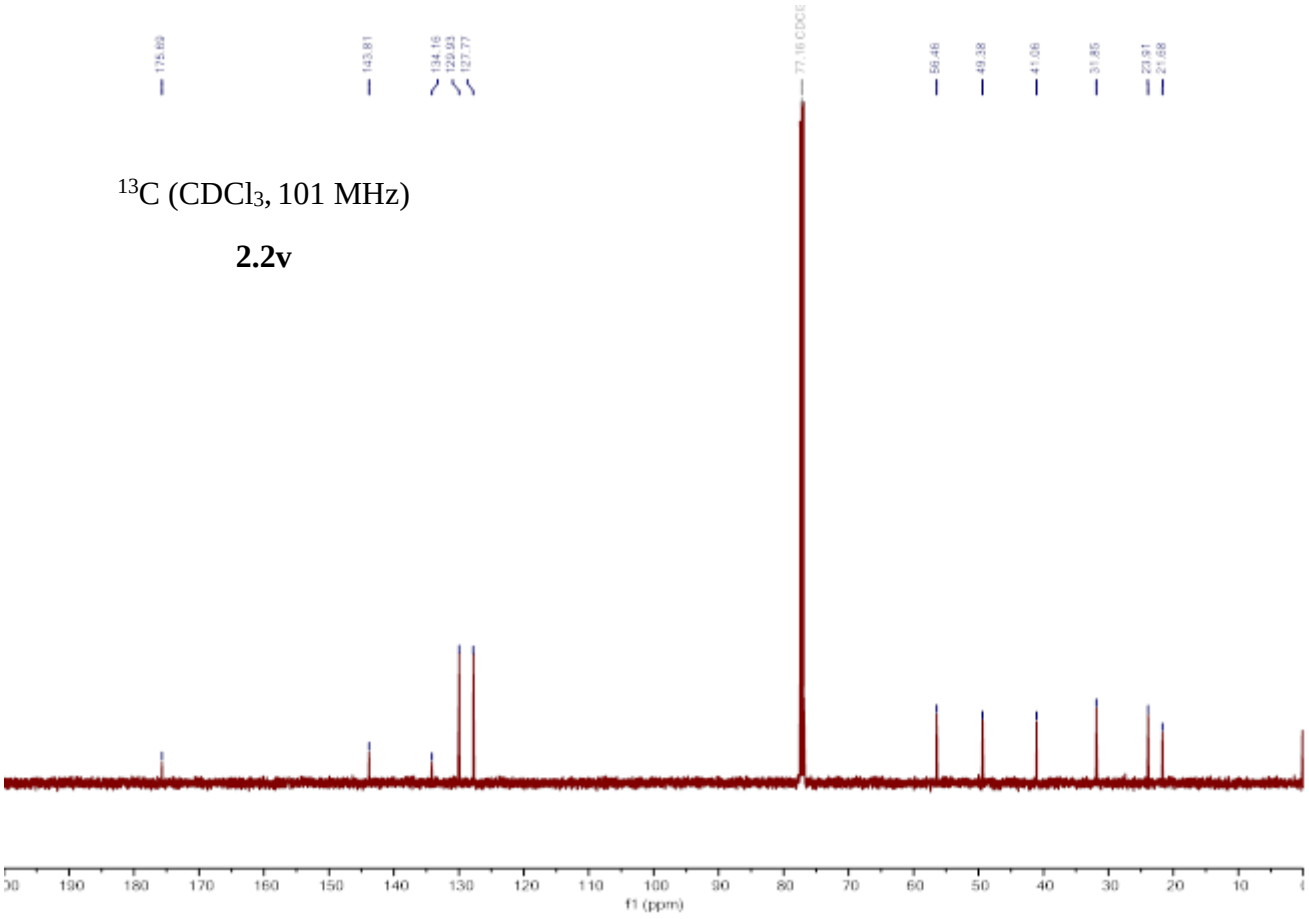

^{1}H ($CDCl_3$, 400 MHz)

2.2u

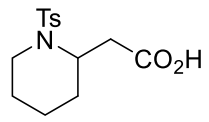

^{13}C ($CDCl_3$, 101 MHz)

2.2u

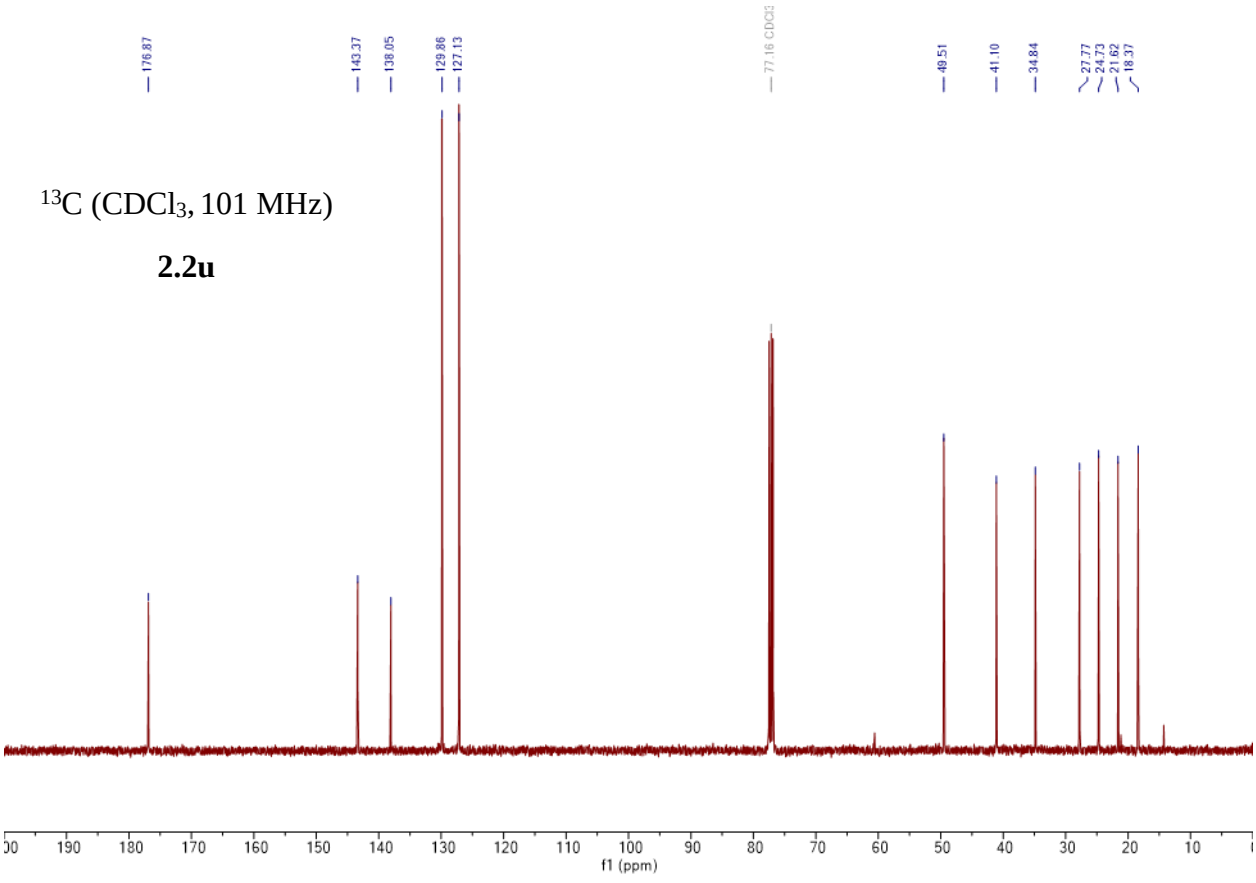

^{1}H ($CDCl_3$, 500 MHz)

2.2a-d_1

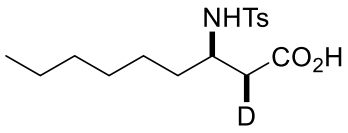

^{13}C ($CDCl_3$, 126 MHz)

2.2a-d_1

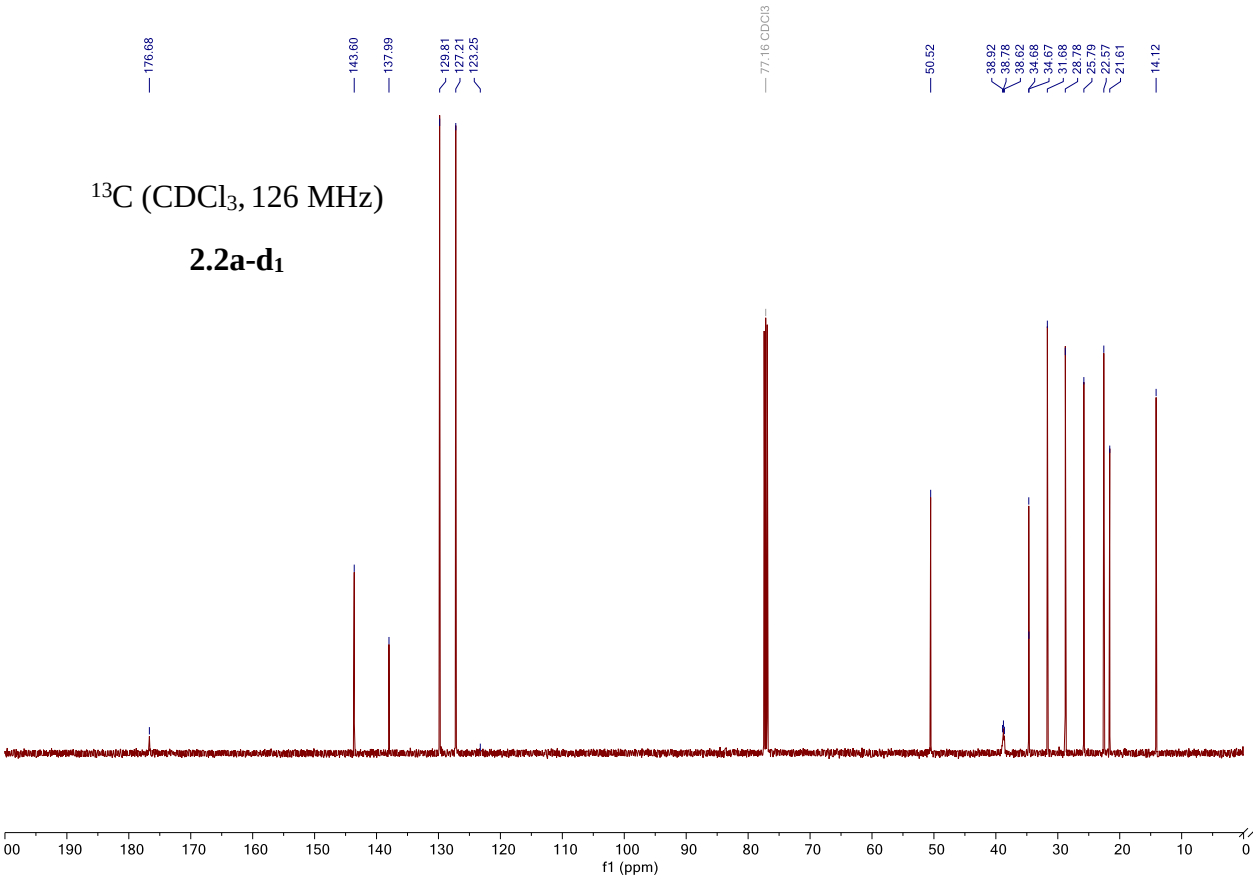

^{1}H (CD_2Cl_2, 500 MHz)

2.2a-d$_1$

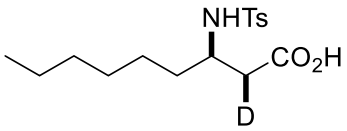

^{13}C (CD_2Cl_2, 126 MHz)

2.2a-d$_1$

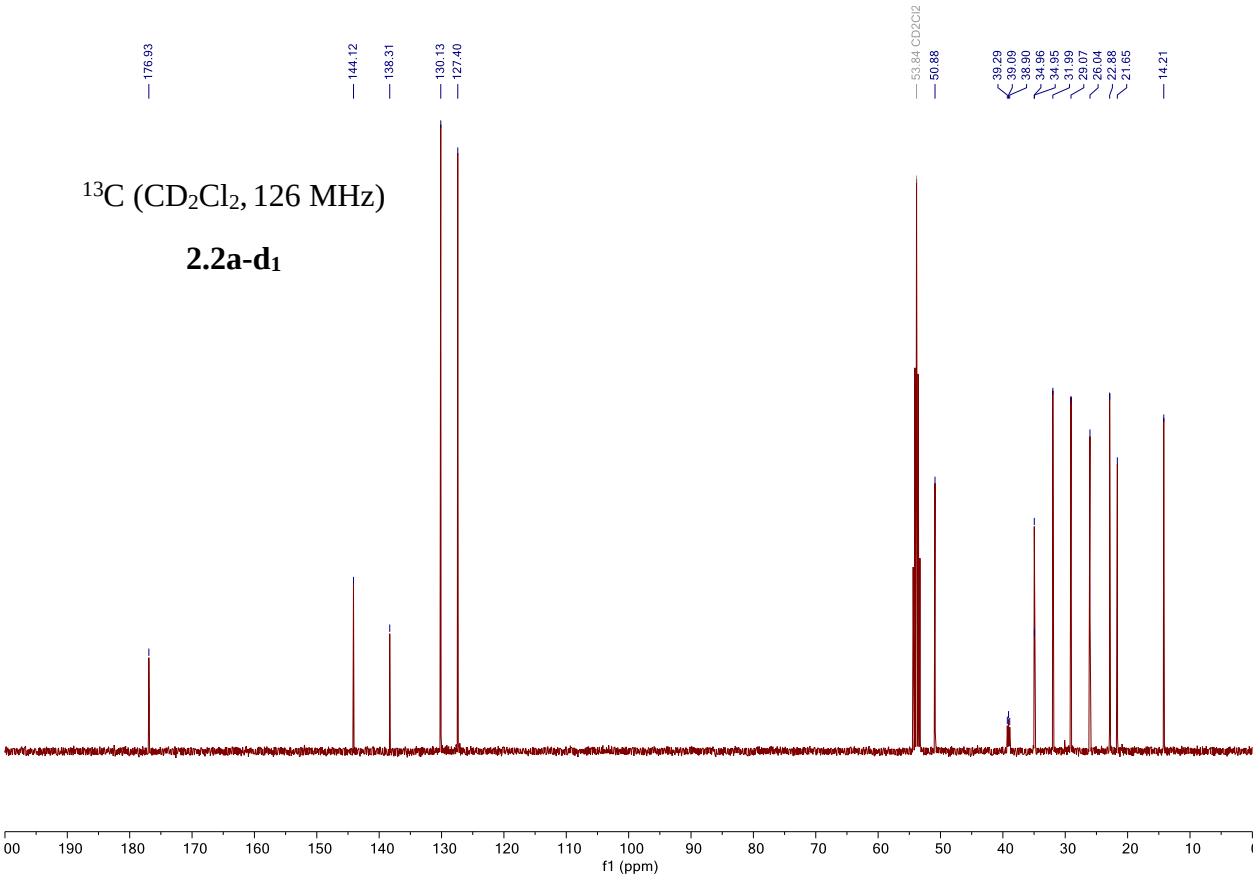

^{1}H ($CDCl_3$, 400 MHz)

S16

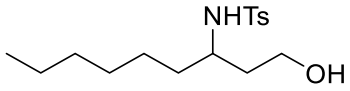

^{13}C ($CDCl_3$, 101 MHz)

S16

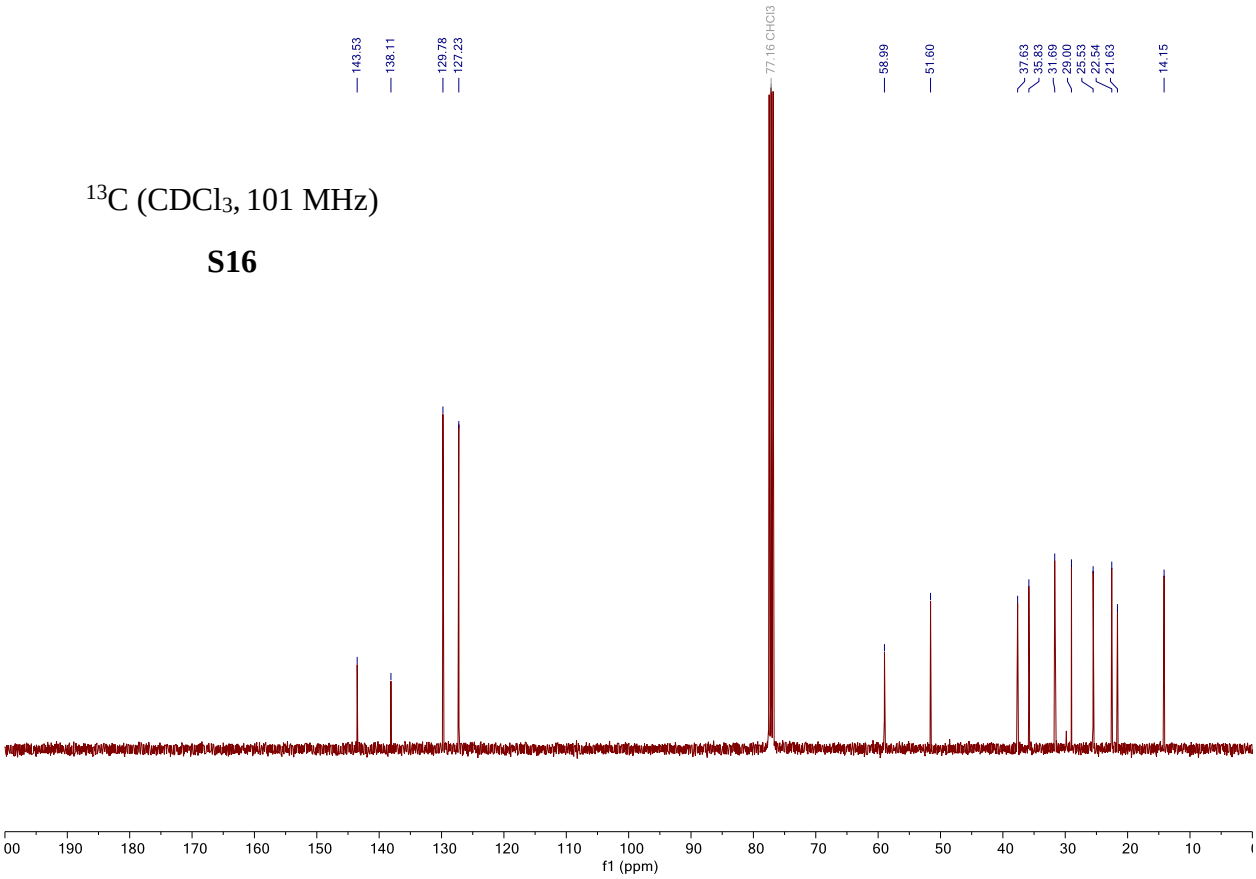

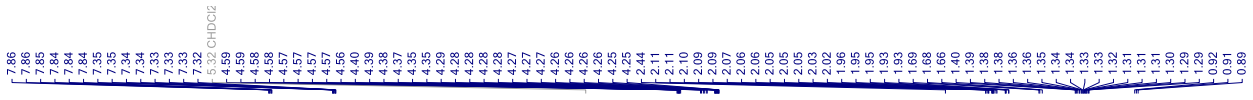

^{1}H (CD_2Cl_2, 500 MHz)

S17

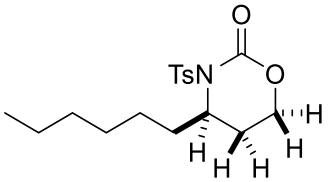

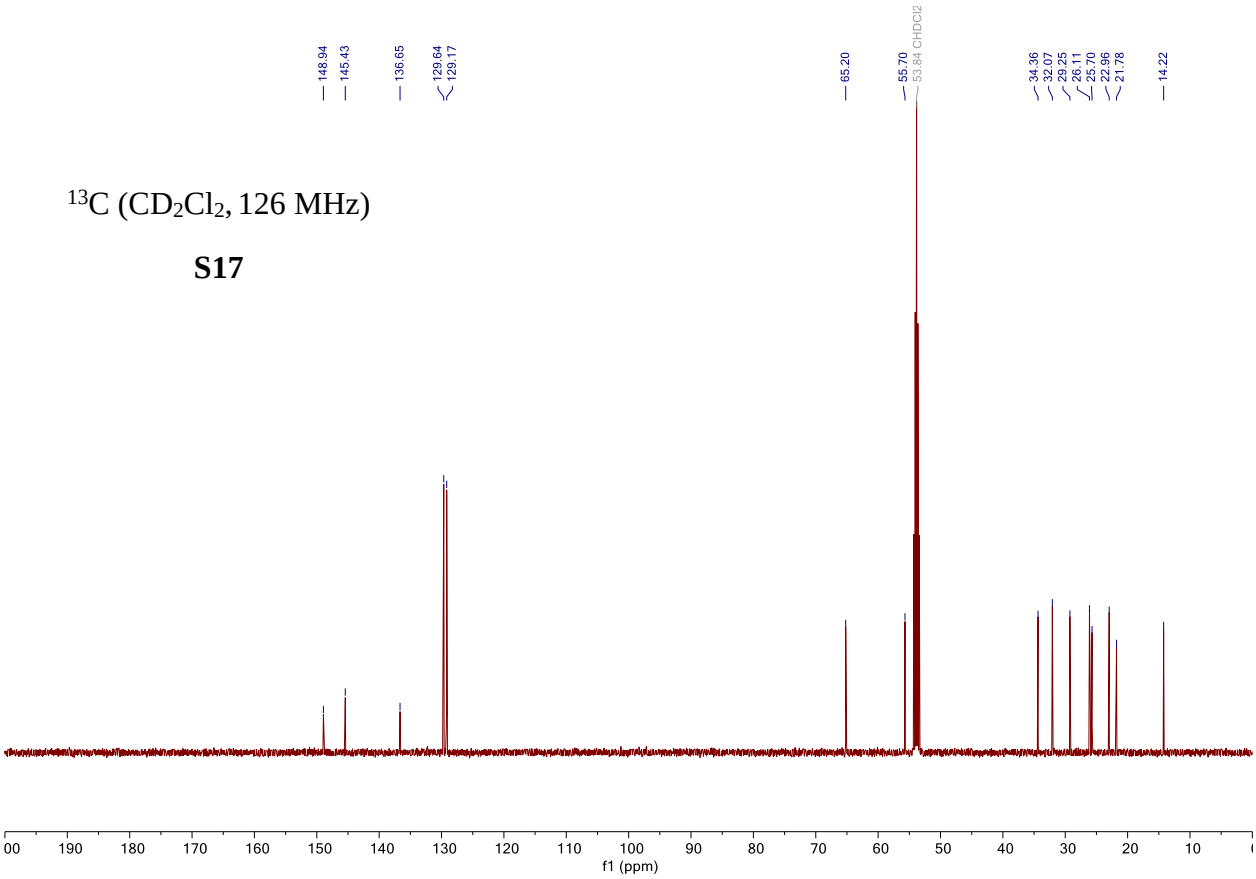

^{13}C (CD_2Cl_2, 126 MHz)

S17

^{1}H (CD_2Cl_2, 500 MHz)

2.16-*d*$_1$ (diastereomers 4:1)

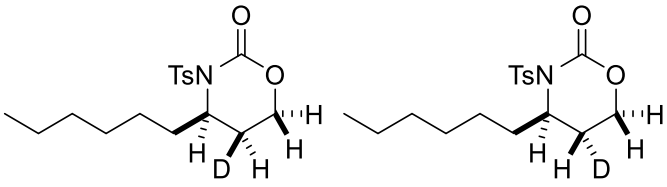

^{13}C (CD_2Cl_2, 126 MHz)

2.16-*d*$_1$ (diastereomers 4:1)

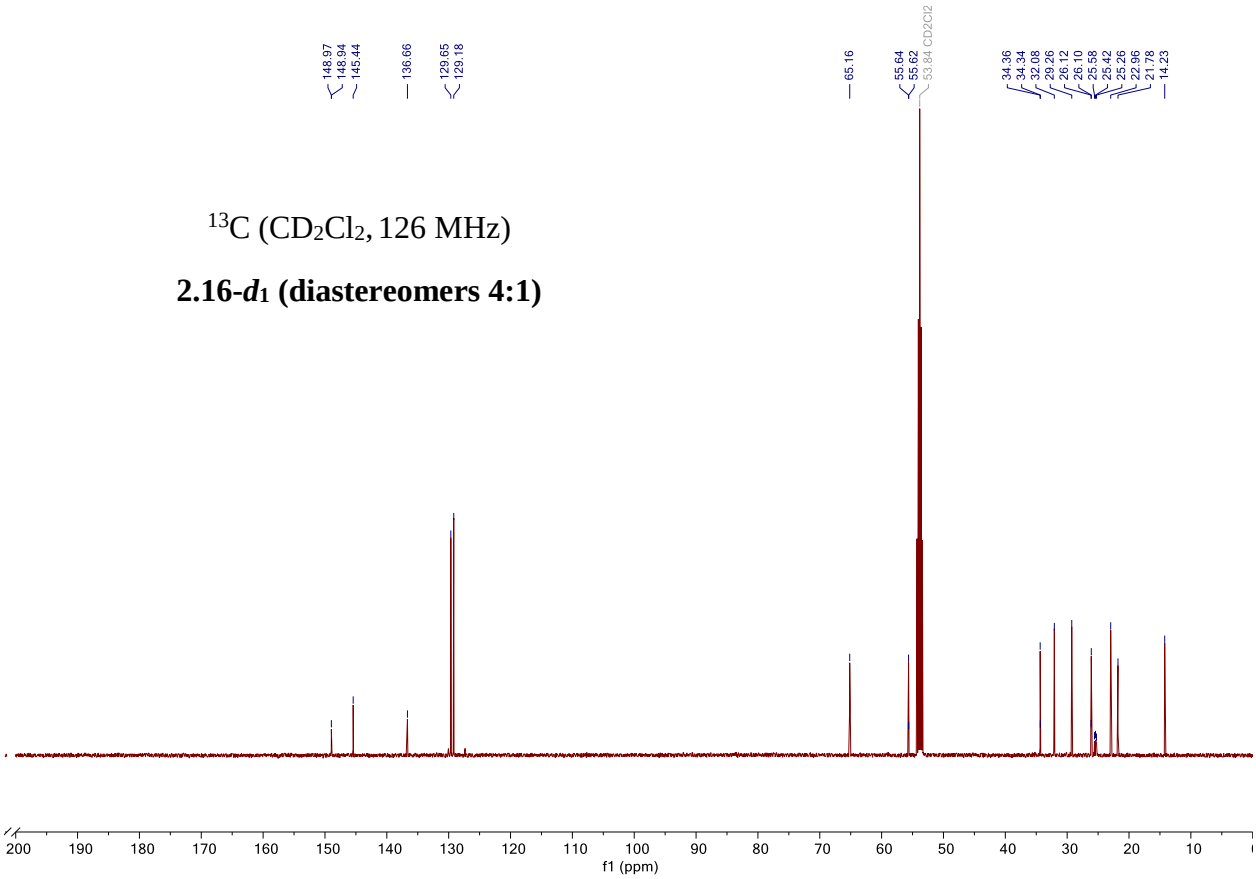

Chapter III. Ni-catalyzed reductive hydroalkenylation of aziridines to access homoallylamines

3.1 Ni-catalyzed functionalization of alkynes and project hypothesis

Functionalization of alkynes with the formation of complex alkenes is among the biggest topics of organic chemistry research.[157] One of the features of nickel is the high affinity to the triple carbon-carbon bonds, making nickel a metal of choice for catalytic processes involving alkynes as coupling partners.[158] Complex and diverse reactivity of nickel opens up room for a list of possible catalytic transformations. First, the metal can be involved in the indirect manner by trapping the vinyl radical formed *in situ* (Figure 3.1, *path a*).[159]

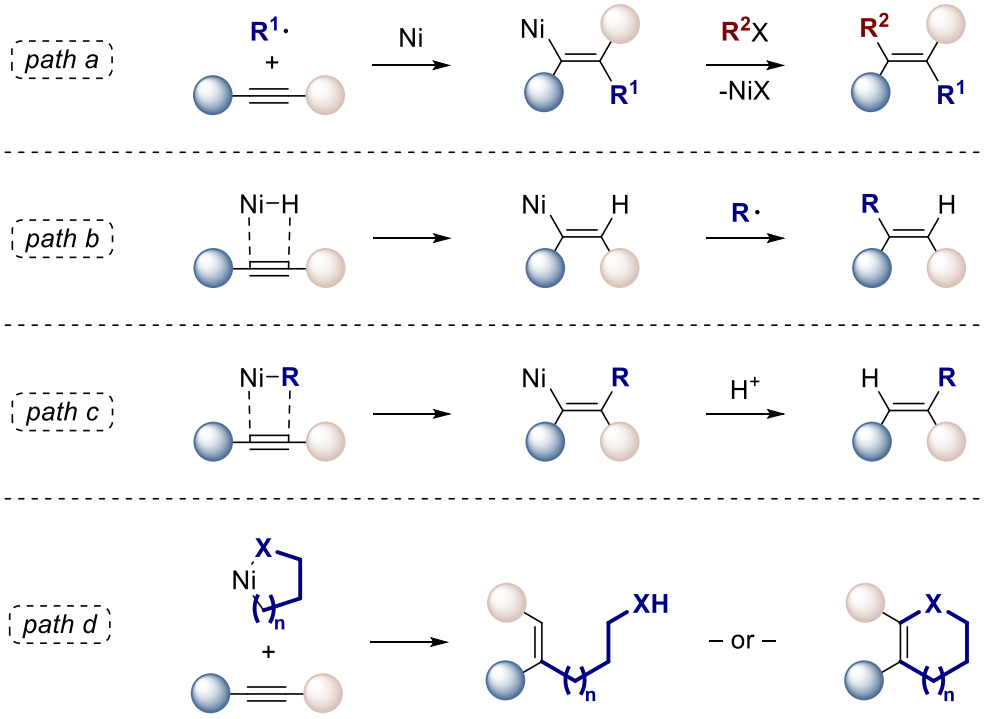

Figure 3.1 Ni-catalyzed functionalization of alkynes

Alternatively, a Ni-vinyl intermediate can be formed by inserting Ni-H species into the alkyne (Figure 3.1, *path b*).[160] The direct insertion of Ni-R species forming the Ni-vinyl complex is also possible (Figure 3.1, *path c*).[161] Finally, the insertion of alkynes into nickellacycle intermediates is also known (Figure 3.1, *path d*). It is worth mentioning, that an example of such transformation was reported in 2003 by Jamison for Ni-catalyzed reductive coupling of alkynes **3.1** and epoxides **3.2**, proposing the reaction proceed via oxanickellacyclobutane ring expansion through alkyne insertion (Scheme 3.1).[162]

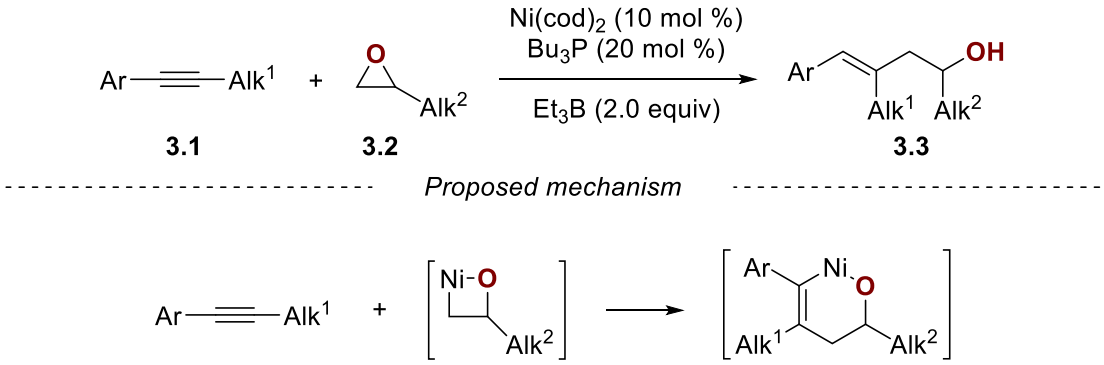

Scheme 3.1 Nickel-catalyzed reductive coupling of alkynes and epoxides

Based on the known data for Ni-catalyzed coupling reactions with alkynes and with experience gained after developing a Ni-catalyzed reductive carboxylation of aziridines **2.1** (see Chapter II) a new route to the synthesis of homoallylamines **3.5** was proposed. The reaction potentially could follow either through the direct expansion of azanickellacyclobutane intermediate with alkyne **3.4** (Scheme 3.2, *top*), or through the insertion of alkyne **3.4** into ring-opened Ni(II) intermediate (Scheme 3.2, *bottom*).

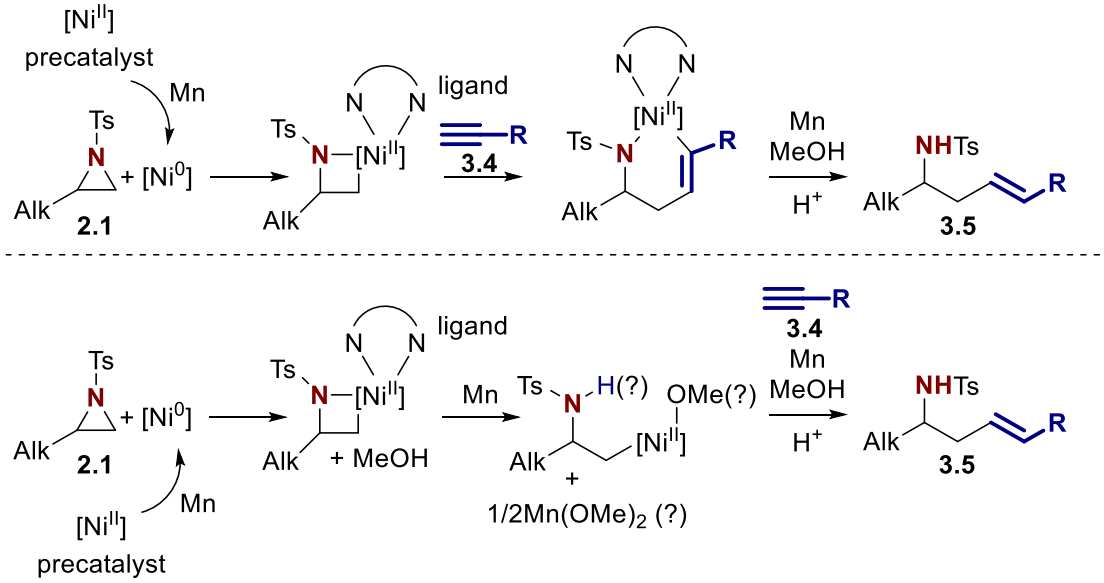

Scheme 3.2 Proposed synthesis of homoallylamines from aziridines **2.1** and alkynes **3.4**

By applying reaction conditions similar to the ones developed for the aziridine carboxylation process the desired product **3.5a** was formed in the range of 20-30% NMR yield (Scheme 3.3).

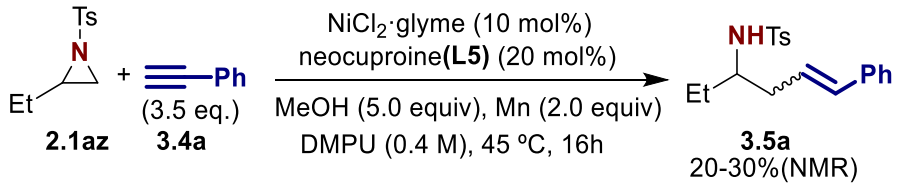

Scheme 3.3 Initial attempts to form product **3.5a** from aziridine **2.1az** and alkyne **3.4a**

This result became a starting point for the further reaction optimization described in the following section.

3.2 Reaction optimization

3.2.1 Different conditions

The crucial change in the reaction conditions which led to the increase in the yield of the desired product **3.5a** was a precise choice of the proton source. Among different alcohols tested the TFE demonstrated the best result with the final product formed in 69% yield (Scheme 3.4).

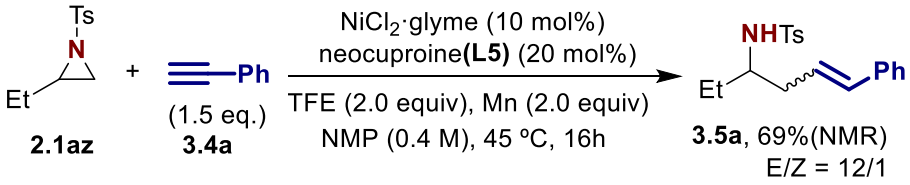

Scheme 3.4 Initially optimized conditions with model substrates **2.1az** and **3.4a**

However, some critical observations were made trying to use these conditions as optimized in present studies. First, some ambiguous and inconsistent results were obtained regarding the reaction reproducibility. For example, executing regular control experiments with model substrates **2.1az** and **3.4a** to control possible intrusion of environmental factors into reaction system it was observed inconsistency in the reaction yields (varying from 45% to 65% approx.). Another example was an ambiguous result with a precatalyst $NiCl_2$(**L5**) used instead of $NiCl_2$*glyme giving a significant drop in the yield of product **3.5a** (Table 3.1, entries 2 and 3).

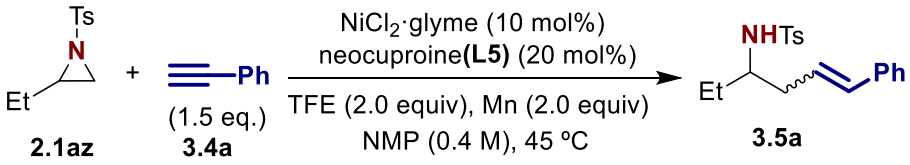

entry	deviation standard conditions	**3.5a** (%)[a]
1	none	69
2	using $NiCl_2$**L5** as precatalyst	31
3	using $NiCl_2$**L5** + **L5** (10 mol%)	45

[a]NMR yields using 1,3,5-trimethoxybenzene as internal standard.

Table 3.1 Results obtained using $NiCl_2$(**L5**) precatalyst

This result could not be rationalized by referring to the problem with the purity of aziridine arising from the aziridination procedure using Chorlamine-T*3H_2O discovered in *Chapter 2*. The aziridine **2.1az** was synthesized from parent *β*-amino alcohol using TsCl. Nevertheless, trying different solutions to that problem among them repurification of the starting material **2.1az** using column chromatography it was found that compound **2.1az** is unstable upon storage at RT. Trace amounts of impurities were generated within months. These impurities are not visible in ^{1}H NMR but can be detected on TLC plate using $KMnO_4$ stain and isolated in milligram quantities performing a multigram scale purification. After a careful literature check was found in one of the published protocols it was claimed that liquid aziridines are unstable at RT and undergo a slow degradation supporting our observation.[163] To avoid this problem the model substrate was changed from aziridine **2.1az** to aziridine **2.1f** which is solid at RT (Scheme 3.5).

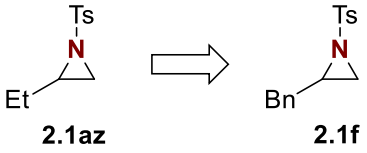

Scheme 3.5 Change of the model substrate from aziridine **2.1az** to aziridine **2.1f**

Second, among the problems found was uncontrolled and unavoidable formation of by-product **3.6a** in trace amounts (5-10%) (Scheme 3.6).

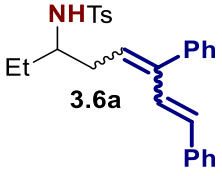

Scheme 3.6 Structure of by-product **3.6a**

Despite all the efforts to isolate the final product **3.5a** with at least 95% purity using standard column chromatography this result was never achieved. For demonstrative purposes alkyne **3.4b** was chosen as an alternative model substrate and with the increased polarity the separation of product **3.5b** from by-product **3.6b** was achieved (Scheme 3.7).

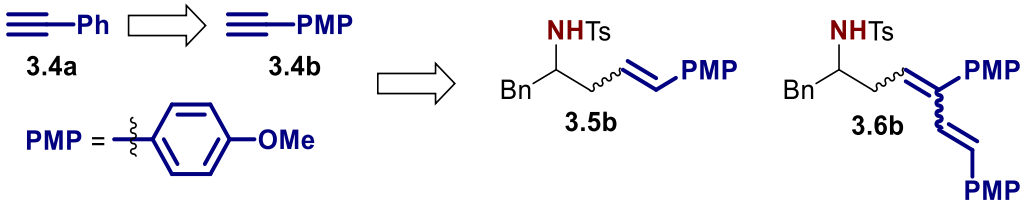

Scheme 3.7 Change of the model substrate from alkyne **3.4a** to alkyne **3.4b**

Finally, during initial reaction scope studies we observed that using DMPU instead of NMP led to more consistent results with lower amounts of $TsNH_2$ and **3.6b** formed and gave slightly higher yields testing different alkynes.

After three different parameters have been changed the optimization of reaction conditions was repeated by rescreening different reaction parameters and with the new optimized reaction conditions the product **3.5b** was formed in 67% NMR yield (Scheme 3.8).

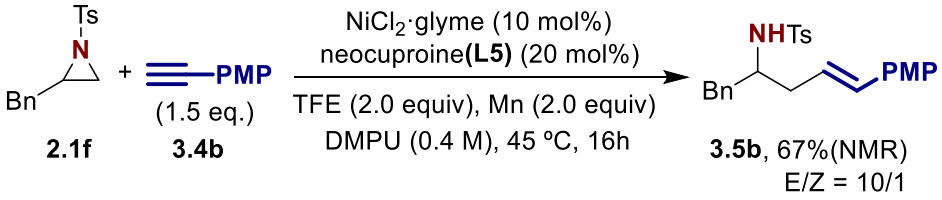

Scheme 3.8 Optimized reaction conditions after changes in model system

Under new conditions the desired reproducibility and consistency in the reaction yield were achieved. Additionally, repeated experiments with $NiCl_2$(**L5**) precatalyst gave rational results (Table 3.2).

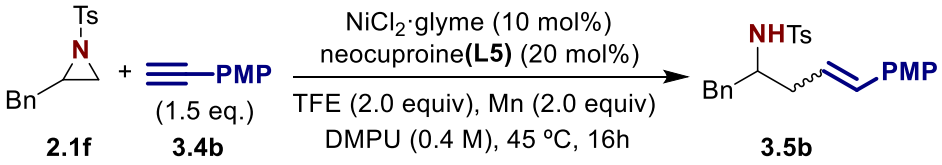

entry	deviation standard conditions	**3.5a** (%)[a]
1	none	67
2	using $NiCl_2$**L5** as precatalyst	54
3	using $NiCl_2$**L5 + L5** (10 mol%)	65

[a]NMR yields using 1,3,5-trimethoxybenzene as internal standard.

Table 3.2 Repeated experiments using $NiCl_2$(**L5**) precatalyst

Nevertheless, formation of the product **3.5b** as an E/Z-isomers mixture remained the problem. The optimization study was continued to achieve the formation of exclusively E-isomer remaining high reaction yield. This result was obtained within two different deviations in reaction conditions: by increasing the equivalent of alkyne **3.4b** or by running reaction at 10 °C (Table 3.3).

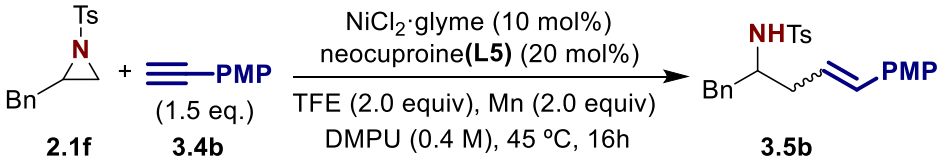

entry	deviation standard conditions	E/Z	**3.5a** (%)[a]
1	none	10/1	67
2	using 2.0 equiv. **of 3.4b**	20/1	66
3	at 10 ºC	20/1	66

[a]NMR yields using 1,3,5-trimethoxybenzene as internal standard.

Table 3.3 Reaction conditions giving the formation of exclusively E-isomer of **3.5b**

To give a complete overview of various deviations in the reaction conditions related results discussed in the following section.

3.2.2 Deviations ligand screening

A series of phenanthroline ligands was tested under reaction conditions (Table 3.4). When ligands **L12** (bearing EDG) and **L26** (bearing EWG) were used product **3.5b** was formed with a lower yield but only as an E-isomer (Table 3.4, *entries 2* and *3*). This observation can be rationalized by referring to the result obtained with 2.0 equivalents of alkyne **3.4b** (see Table 3.3 and Table 3.8). Using different ligands might affect the conversion of **2.1f** toward the formation of side-products, resulting in a higher concentration of **3.4b** which prevents undesired isomerization of the olefin bond.

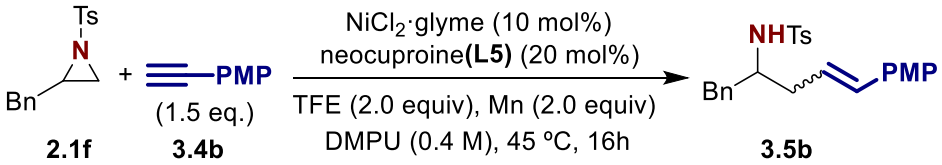

entry	deviation standard conditions	E/Z	**3.5a** (%)[a]
1	none	10/1	67
2	using **L12** instead of **L5**	20/1	29
3	using **L26** instead of **L5**	20/1	43
4	using **L27** instead of **L5**	–	0
5	using **L28** instead of **L5**	20/1	48
6	using **L14** instead of **L5**	–	trace
7	using **L1** instead of **L5**	–	trace

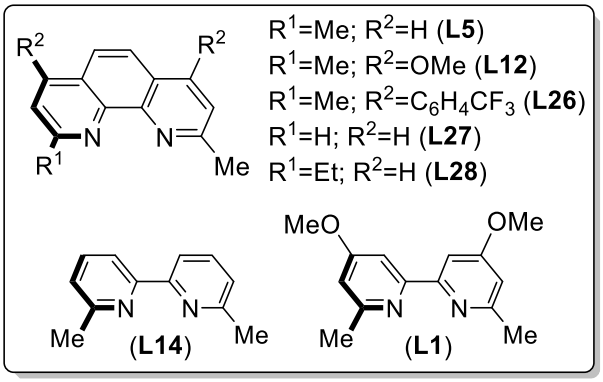

[a]NMR yields using 1,3,5-trimethoxybenzene as internal standard.

Table 3.4 Ligand screening

Notably, in case of **L27** when steric bulkiness was reduced no formation of product **3.5b** was observed (Table 3.4, *entry 4*). By increasing steric bulkiness in case of **L28** result similar to L **L12** and **L26** was observed with lower yield of **3.5b** and E/Z ratio = 20/1 (Table 3.4, *entry 5*) Finally, it was found that by changing from the *phen* family of ligands to the *bipy* one (**L14** and **L1**) only traces of the product **3.5b** have been observed (Table 3.4, *entries 6* and *7*), even though, ligand **L1** demonstrated the best performance in the case of Ni-catalyzed aziridine carboxylation (See Chapter II).

Next, by testing different loading of **L5** it was confirmed that 20 mol % is the optimal amount with the reaction yield dropping down with lower catalysis loadings (Table 3.5).

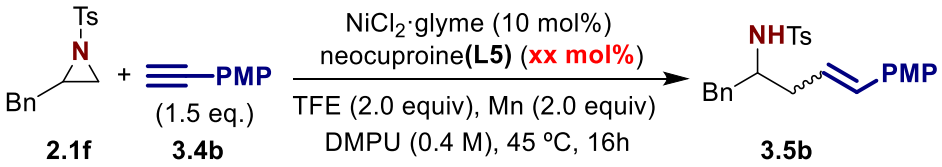

entry	L5 mol %	E/Z	**3.5a** (%)[a]
1	10	10/1	44
2	15	7/1	58
3	20	10/1	67
4	25	7/1	66

[a]NMR yields using 1,3,5-trimethoxybenzene as internal standard.

Table 3.5 Screening of **L5** loading

Neither was observed improvement in the reaction yield with extra ligand added. Additionally, there was no correlation between ligand loading and the ratio of E/Z isomers for the product **3.5b**.

3.2.3 Deviations solvents screening

Different amide-type solvents were tested and DMPU was confirmed as the optimal solvent giving the highest yield of the product **3.5b** (Table 3.6, *entry 1*).

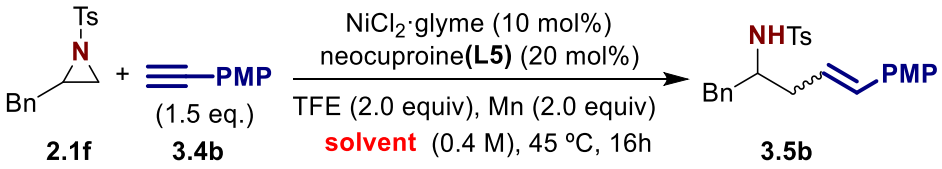

entry	solvent	E/Z	**3.5a** (%)[a]
1	DMPU	10/1	67
2	NMP	8/1	55
3	DMI	13/1	54
4	DMA	7/1	46
5	DMF	5/1	45

[a]NMR yields using 1,3,5-trimethoxybenzene as internal standard.

Table 3.6 Solvent screening

In any case no significant improvement in the E/Z ratio was observed (Table 3.6, *entries 2-5*).

3.2.4 Deviations in reagents stoichiometry and temperature screening

Expecting proton-transfer side-reaction to cause of the olefin bond isomerization different stoichiometry of TFE was tested (Table 3.7).

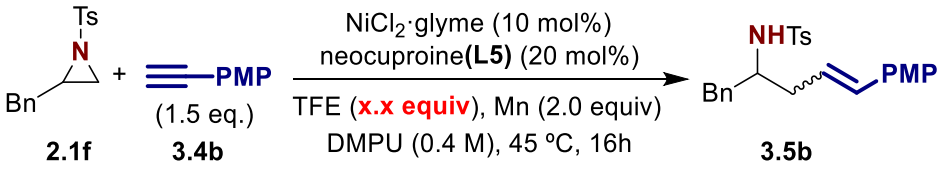

entry	TFE eq.	E/Z	**3.5a** (%)[a]
1	1.1	11/1	48
2	2.0	10/1	67
3	3.0	7/1	67
4	5.0	8/1	63

[a]NMR yields using 1,3,5-trimethoxybenzene as internal standard.

Table 3.7 Screening of TFE loading

Some increase in the formation of Z-isomer of the product **3.5b** was observed with the increase of TFE equivalents (Table 3.7, *entries 3* and *4*). However, no difference was observed between 3.0 equiv and 5.0 equiv and this result gives only indirect evidence to the initial proton-transfer side-reaction hypothesis.

Next, by testing different stoichiometry of alkyne **3.4b** a clear correlation between the amount of **3.4b** and the E/Z ratio was observed (Table 3.8).

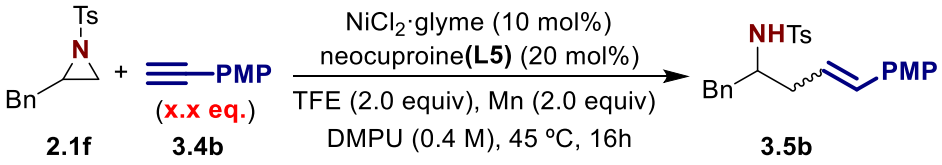

entry	alkyne eq.	E/Z	**3.5a** (%)[a]
1	1.1	7/1	61
2	1.5	10/1	67
3	2.0	20/1	66

[a]NMR yields using 1,3,5-trimethoxybenzene as internal standard.

Table 3.8 Screening of alkyne **3.4b** loading

With higher amounts of alkyne **3.4b** added into the reaction pot the formation of exclusively E-isomer of the product **3.5b** was achieved (Table 3.8, *entry 3*). This result indicates the involvement of the π-component into isomerization side-reaction.

No direct correlation was observed between E/Z ratio and Mn stoichiometry (Table 3.9).

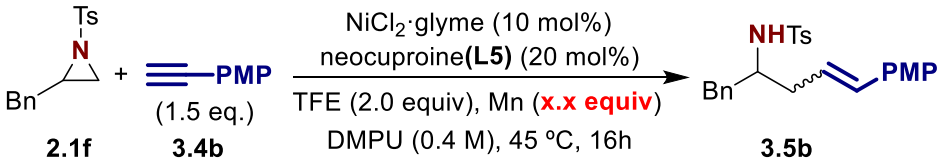

entry	Mn eq.	E/Z	**3.5a** (%)[a]
1	1.1	20/1	50
2	2.0	10/1	67
3	3.0	15/1	65

[a]NMR yields using 1,3,5-trimethoxybenzene as internal standard.

Table 3.9 Screening of Mn loading

No improvement was achieved in the reaction yield using higher amounts on the reductant and the drop in the reaction yield was observed for the lower reductant loading (Table 3.9, *entries 3* and *1*).

Finally, a trend in the increased Z-isomer formation was observed while increasing the reaction temperature (Table 3.10).

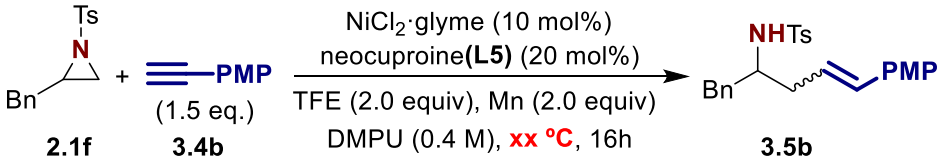

entry	ºC	E/Z	**3.5a** (%)[a]
1	10	20/1	66
2	45	10/1	67
3	60	7/1	66

[a]NMR yields using 1,3,5-trimethoxybenzene as internal standard.

Table 3.10 Screening of reaction temperature

This result as well gives an indirect evidence that olefin isomerization happens off-cycle potentially through the proton mediated side-reaction.

3.2.5 Undesired side-product formation

Bearing optimized conditions in hands and driven by the motivation to study the synthetic applicability of the designed transformation a substrate scope investigation was initiated. At this point, while isolating desired product **3.5b** using the standard flash chromatography technique it was observed that the isolated sample contained unexpected impurity. After careful elucidation of the potential structure of this side product, it was determined as a Sonogashira-type by-product **3.7b** (Scheme 3.9, *top*).

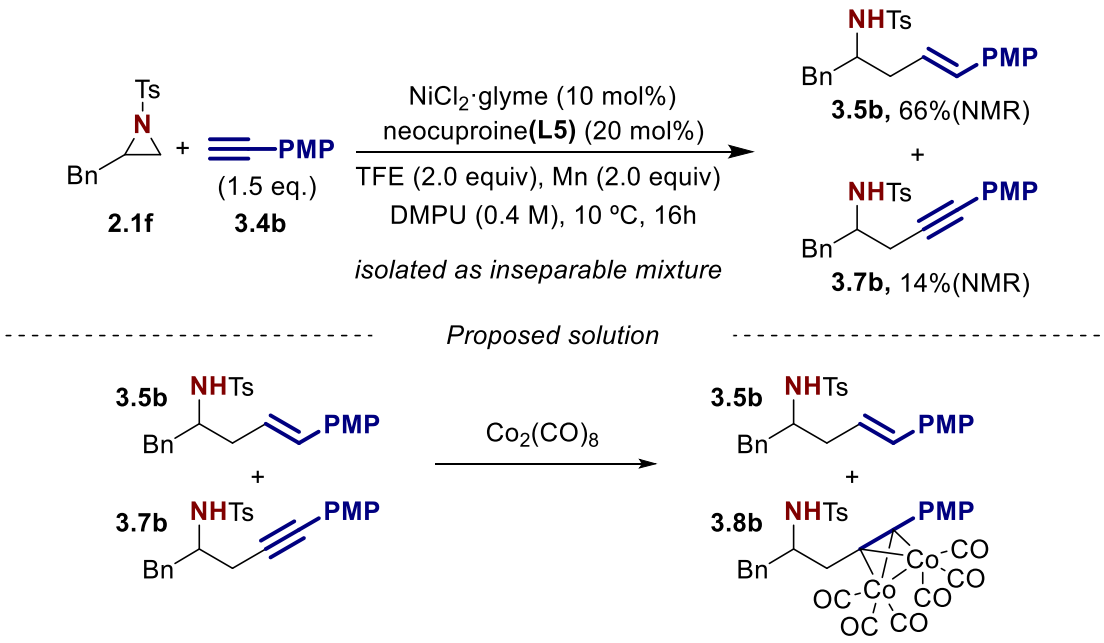

Scheme 3.9 Proposed purification procedure using $CO_2(CO)_8$

This impurity could not be removed using trivial separation on silica gel due to the absence of differences in the retention time. However, it was proposed that upon addition of $Co_2(CO)_8$ to the mixture of **3.5b** and **3.7b** and subjection of resulted sample to the column chromatography, the compound **3.5b** could be successfully separated from the compound **3.7b** which will form an adduct **3.8b** with cobalt complex (Scheme 3.9, *bottom*). The hypothesis was confirmed and the product **3.5b** was isolated with excellent purity in 50% isolated yield after 2 purification steps (Scheme 3.9, *top*). This purification procedure was used further in the reaction scope studies. For demonstrative purposes NMR yields were compared while elucidating differences in substrates reactivity which are discussed in the following section.

3.3 Reaction scope studies

3.3.1 Alkyne scope

The substrate scope study was initiated by elucidating the influence of electronic effects on reaction performance in the series of phenylacetylene derivatives. For para-substituted alkynes **3.4a-c**, starting from the strong π-donating p-OMe group **3.4b** to the strong σ-donating p-^{t}Bu group **3.4c** and then to the unsubstituted phenylacetylene **3.4a** was observed a drop in the reaction yield under standard conditions at 10 °C (Scheme 3.10).

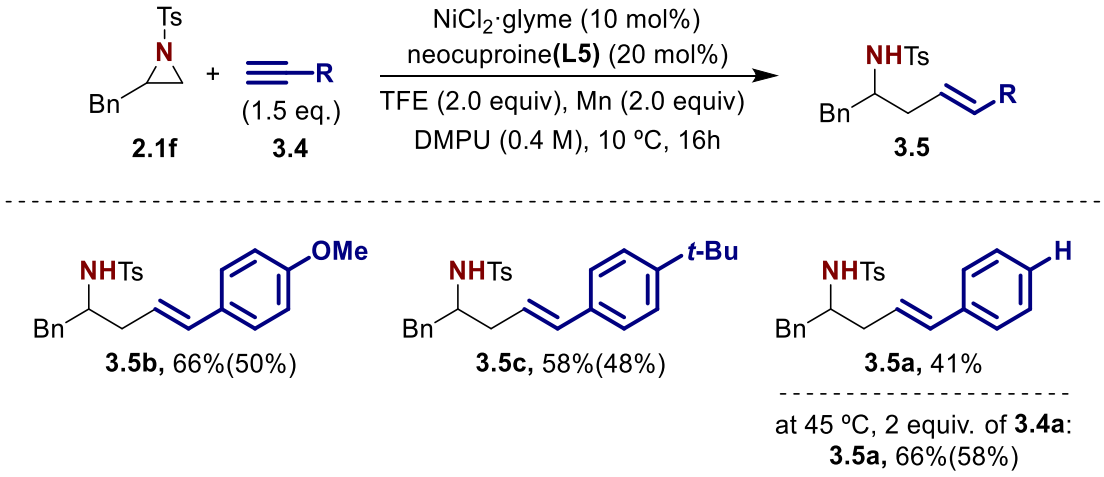

Scheme 3.10 Synthesis of homoallylamines **3.5a-c**

Alternative optimized reaction conditions at 45 °C with 2.0 alkyne equivalents were tested additionally for alkyne **3.4a** and reactivity was recovered with the product **3.5a** formed in 66% NMR yield.

Once the electron-withdrawing group (*p*-F) was introduced in the case of the alkyne **3.4d** the reactivity was completely suppressed under optimized conditions at 10 ºC (10% by NMR, 80% of **2.1f** remained) (Scheme 3.11).

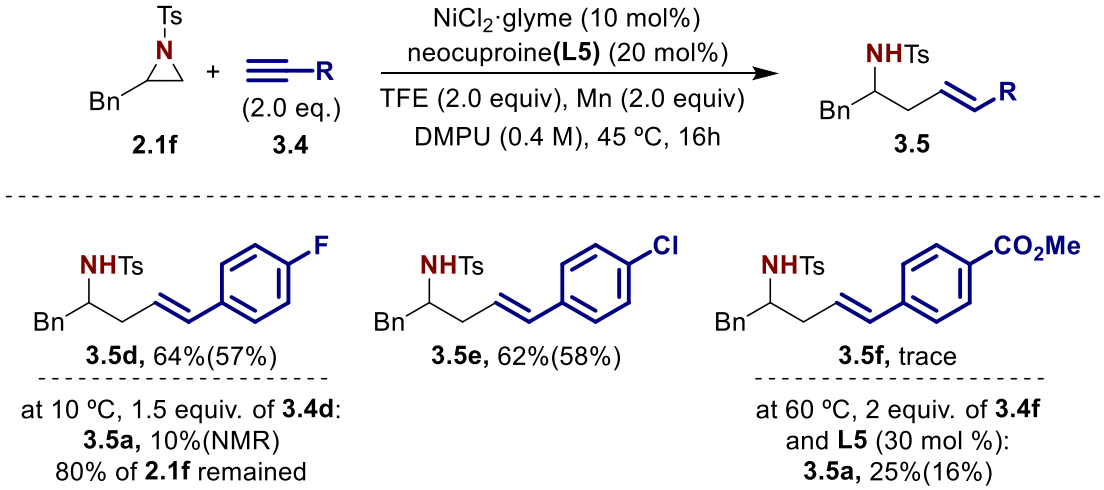

Scheme 3.11 Synthesis of homoallylamines **3.5d-f**

Such a low conversion of aziridine **2.1f** indicates that the catalytic activity of nickel toward aziridine ring-opening is suppressed in the presence of electron-deficient alkynes. This can be rationalized due to a high affinity of Ni(0)-center to the electron-deficient unsaturated bonds.[164] Thus, coordination of electron-deficient alkynes might prevent the formation of catalytic species essential for successful reaction endeavor. Formation of the products **3.5d** and **3.5e** was achieved by increasing the reaction temperature to 45 °C. Nevertheless, only traces of product **3.5f** were

observed using alkyne **3.4f** as a coupling partner running the reaction at 45 °C. Only by increasing the reaction temperature even higher to 60 °C and with extra **L5** loading (30 mol %) the formation of the product **3.5f** with a 25% yield. This result indicates that conjugation with a triple carbon-carbon bond in the case of alkynes bearing strong EWG groups in para-position plays a crucial role in suppressing the reactivity of Ni-catalyst through strong coordination of alkyne to the metal-center.

In a series of *meta*-substituted alkyne tested no difference in reactivity was observed for the *m*-OMe substituted phenylacetylene **3.4g** compared to the model substrate **3.4b** (Scheme 3.12).

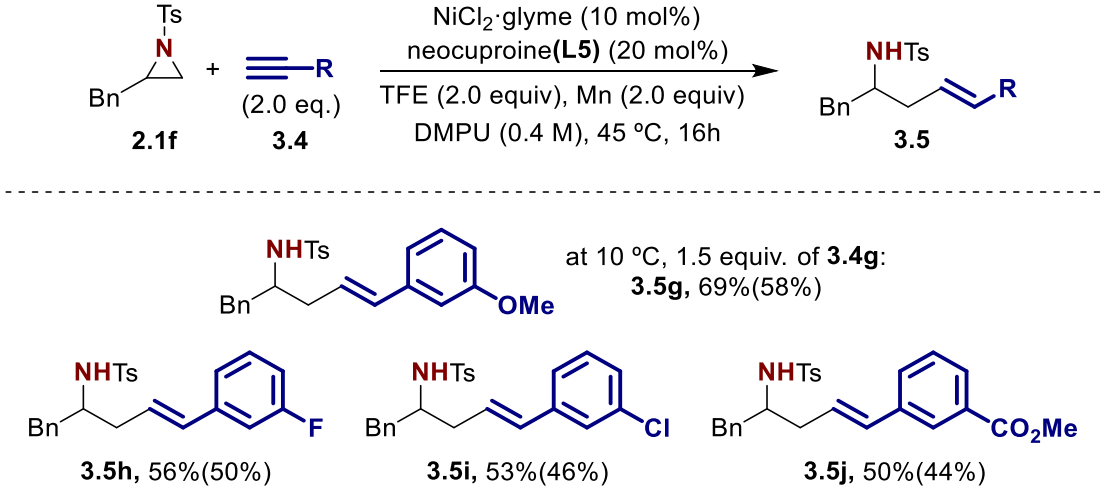

Scheme 3.12 Synthesis of homoallylamines **3.5g-j**

In the case of halides in *meta* position in both cases for *m*-F **3.4h** and *m*-Cl **3.4i** was observed a slight (around 10%) drop in the product yields compared to para-substituted analogs **3.4d** and **3.4e**. This result can be rationalized due to the absence of a positive mesomeric effect in the case of *meta*-substituted alkynes. The biggest difference in the influence of electronic effects (compared to para-substituted analogs) was observed for the alkyne **3.4j** bearing *m*-CO_2Me group. The product **3.5j** was formed in 50% yield under the same conditions as for halide-*meta*-substituted phenylacetylene derivatives **3.4h** and **3.4i**. This result supports previously observed low reactivity while running reaction with alkyne **3.4f** bearing *p*-CO_2Me group. In the absence of conjugation with CO_2Me group electron-deficiency of unsaturated bond is significantly reduced resulting in worse alkyne coordination with Ni(0)-center.

To evaluate an influence of the steric effect in alkyne core substrates **3.4k** and **3.4l** were tested under reaction conditions to achieve products **3.5k** and **3.5l** (Scheme 3.13).

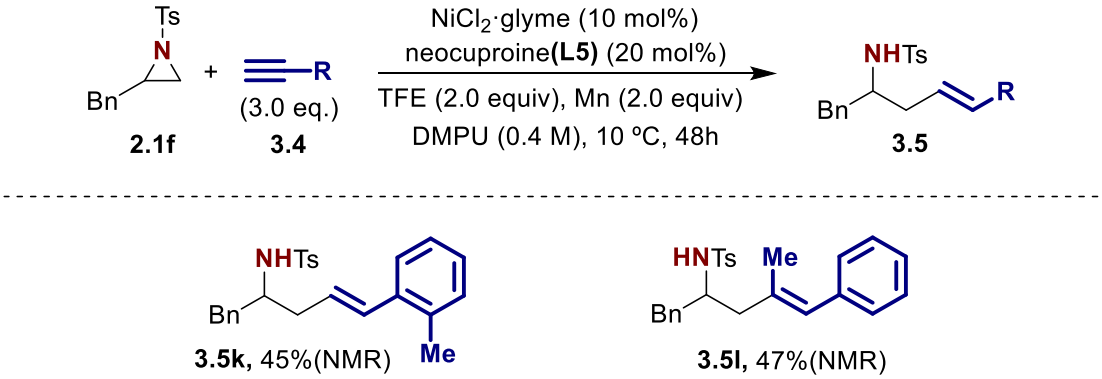

Scheme 3.13 Synthesis of homoallylamines **3.5k-l**

In both cases the reaction rate was found to be slower and to achieve a complete conversion of aziridine **2.1f** the longer reaction time (48h) and higher alkyne loading (3.0 equivalents) were used. Notably, product **3.5l** was formed exclusively as one regioisomer and regioselectivity of carbon-carbon bond formation is in agreement with previously reported Ni-catalyzed cross-coupling reactions with alkynes.[165]

Next, it was demonstrated that enyne **3.4m** also can serve as a coupling partner reacting with aziridine **2.1f** with the formation of diene **3.5m** (Scheme 3.14).

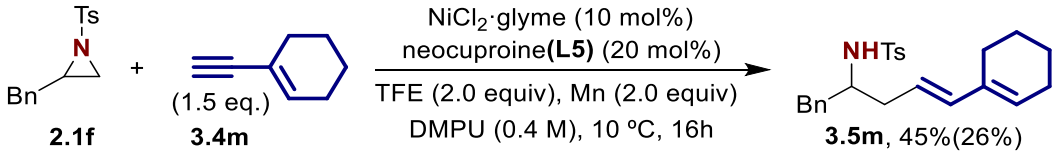

Scheme 3.14 Synthesis of homoallylamine **3.5m**

It is worth mentioning, that product **3.5m** was found to be sensitive to the purification procedure using $Co_2(CO)_8$. A significant amount of by-products formed was detected by TLC and nearly half of the organic material was irrevocably lost.

While testing under reaction conditions an alkyne **3.4n** bearing alkyl substituent it was formed a complex mixture of products containing the desired product **3.5n** among other compounds (Scheme 3.15).

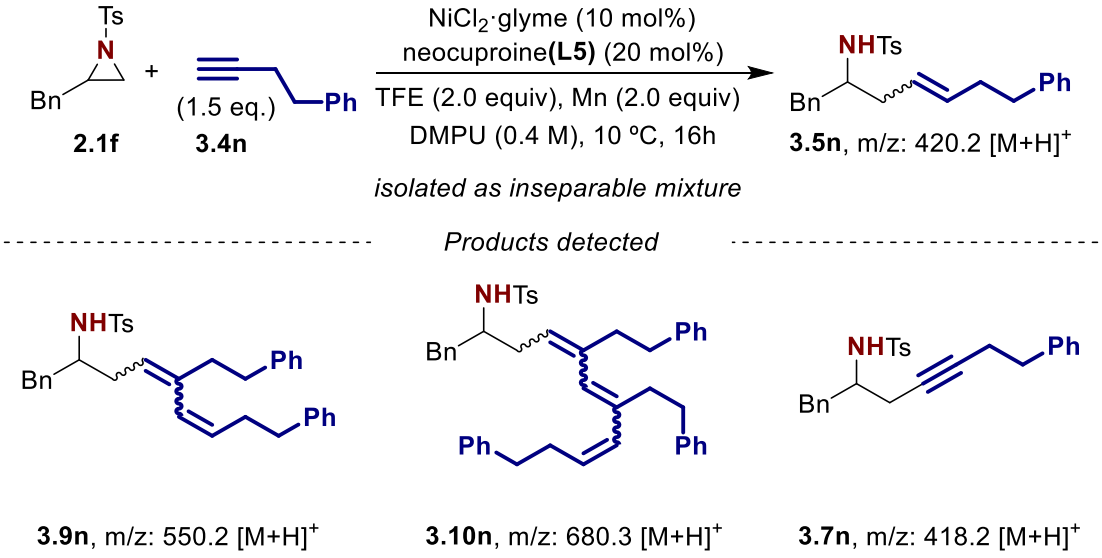

Scheme 3.15 Synthesis of homoallylamine **3.5n** and side-products detected using HPLC-MS technique

Using HPLC-MS technique to analyzed the obtained mixture some mass-peaks were detected and assigned based on characters of signals in ^{1}H NMR as oligomerization products **3.9n** and **3.10n**. Additionally, the Sonogashira-type side-product **3.7n** was also present in the isolated mixture of products.

To explore further the reaction synthetic applicability a series of alkynes adjacent to heteroatom was tested under reaction conditions (Scheme 3.16).

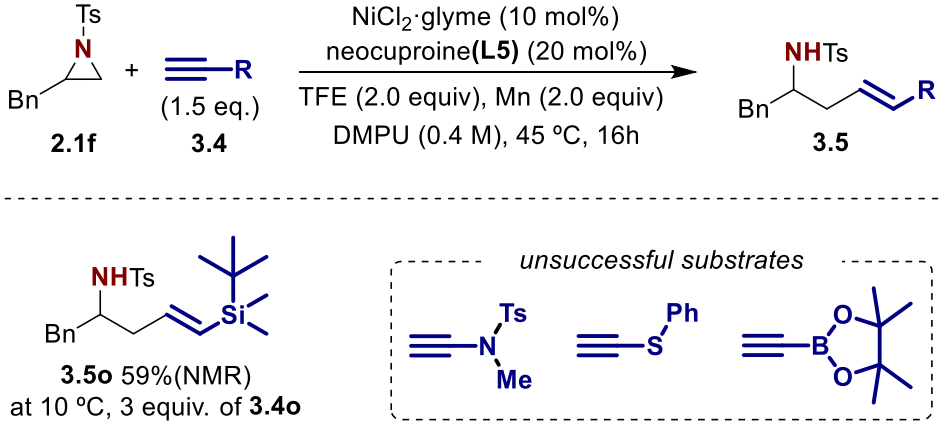

Scheme 3.16 Synthesis of homoallylamine **3.5o** and unsuccessful alkynes bearing heteroatoms

Whereas alkynes bearing –N, -S, or –B atoms did not show the desired reactivity, a TBS-protected alkyne **3.4o** gave promising results. After some additional optimization it was found that similar to alkynes **3.4k** and **3.4l** the reaction rate was slower compared to less sterically hindered alkynes. A longer reaction time with a higher equivalent of alkyne **3.4o** gave the desired product **3.5o** in 59% yield.

Finally, with the idea to expand reaction scope to other unsaturated coupling partners a series of allenes and olefins was tested under reaction conditions (Scheme 3.17).

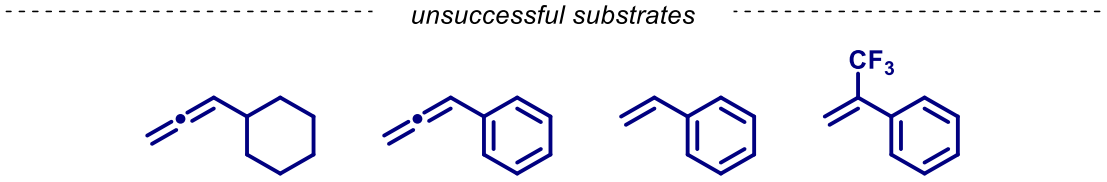

Scheme 3.17 Unsuccessful substrates bearing different unsaturated bonds

However, the formation of the coupling product was not observed in any of the cases, and optimized conditions are only suitable for the coupling of aziridines with alkynes.

3.3.2 Aziridine scope

To evaluate the influence of the steric effect of substituents adjacent to the aziridine ring the substrates containing isopropyl **2.2e** and isobutyl **2.2d** groups as well as non-substituted aziridine **2.2c** were tested under reaction conditions (Scheme 3.18).

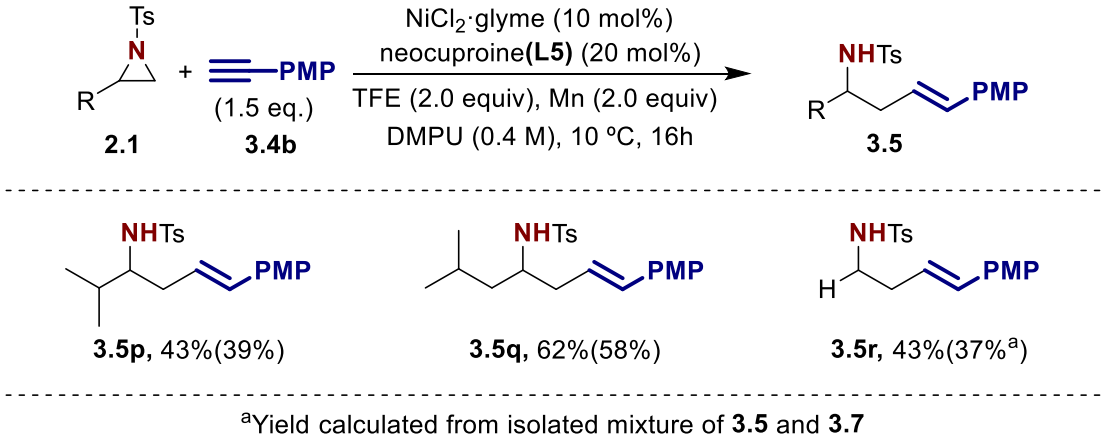

Scheme 3.18 Synthesis of homoallylamines **3.5p-r**

It was observed that the more sterically hindered product **3.5p** was formed with 20% less yield than the less sterically hindered **3.5q**. The product **3.5r** was formed in moderate yield (43% by NMR), which we rationalize by a higher number of *β*-H atoms which could be involved in the *β*-H elimination side reaction. These results agree with the results obtained for carboxylation of aziridines **2.2e**, **2.2d**, and **2.2c** (see Chapter II).

When enantiopure aziridine (*S*)-**2.1f** was subjected under reaction conditions the resulting product (*R*)-**3.5b** was formed remaining enantiopurity (Scheme 3.19).

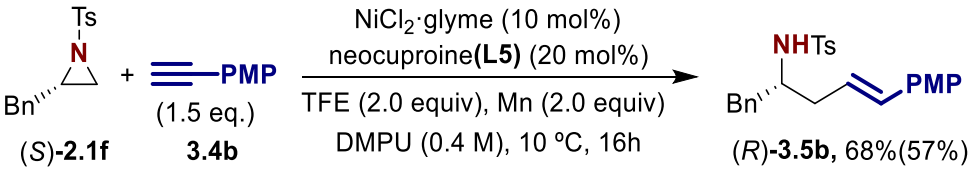

Scheme 3.19 Synthesis of enantiopure homoallylamine (*R*)-**3.5b** from enantiopure aziridine (*S*)-**2.1f**

This result demonstrates that the developed transformation can serve as a platform to access enantiopure homoallylic amines **3.5** starting from enantiopure aziridines **2.1**.

To complement reaction scope studies homoallylic amines possessing different functional groups adjacent to the alkyl substituent have been synthesized (Scheme 3.20).

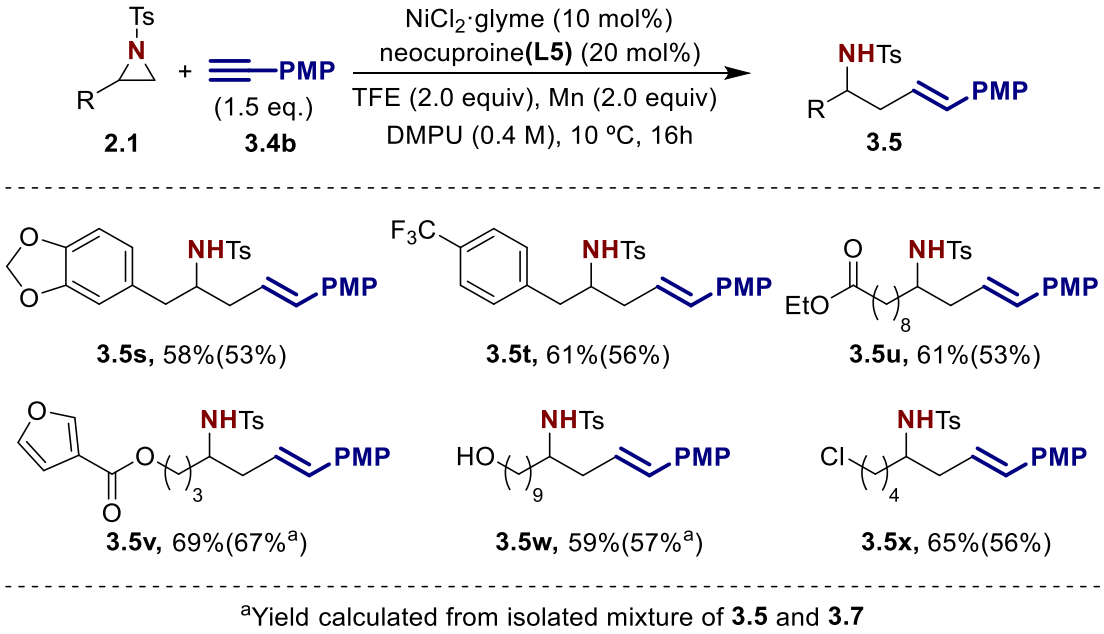

Scheme 3.20 Synthesis of homoallylamines **3.5s-x**

In all cases desired products have been formed with good yields. However, in the case of products **3.5v** and **3.5w** the purification procedure using $CO_2(CO)_8$ did not demonstrate the desired efficiency due to an almost complete lack of difference in retention times for products **3.5** and Co-additives **3.8**.

Finally, when styrene-derived aziridine **2.5** was tested under reaction conditions, the desired product **3.5y** formation was observed in a good yield (Scheme 3.21).

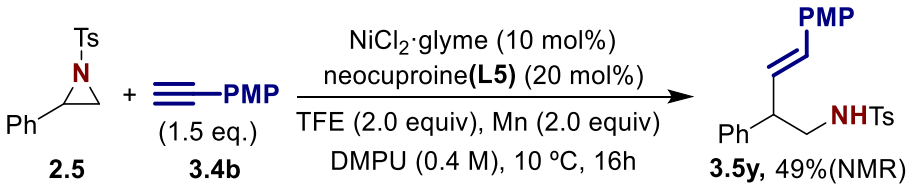

Scheme 3.21 Synthesis of homoallylamines **3.5s**

Interestingly, this result is partially in contrast with the aziridine carboxylation, where carboxylation of styrene-derived aziridine **2.5** was not achieved. Nevertheless, the aziridine **2.5** was very reactive toward ring-opening under carboxylation conditions and a full conversion was observed.

With the idea to see if the addition of phenyl substituent into homolog of aziridine **2.5** – the azetidine **3.11** will make it reactive toward ring-opening at the benzylic position the compound **3.11** was synthesized and tested under reaction conditions (Scheme 3.22)

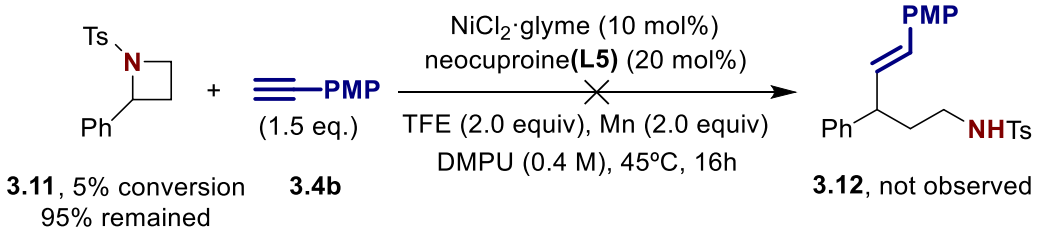

Scheme 3.22 Reaction with azetidine **3.11**

Only a trace amount of conversion for material **3.11** was observed highlighting that azetidines are unreactive in the presence of our particular catalytic system.

3.4 Labeling studies

For the better understanding of the olefin bond involvement into reaction mechanism a series of labeling experiments were conducted.

First, substrates **2.1f** and **3.4b** were subjected under reaction conditions in the presence of deuterium-labeled TFE (Scheme 3.23).

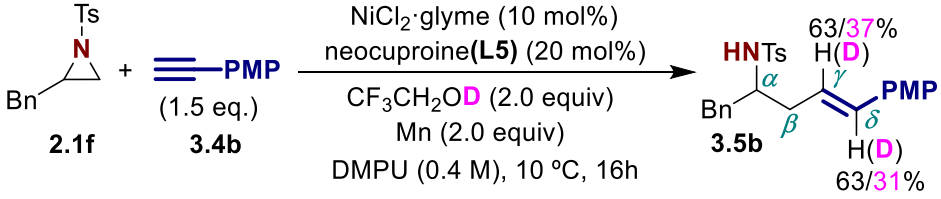

Scheme 3.23 Labeling experiment with deuterium-labeled TFE

The incorporation of deuterium was expected to occur exclusively into δ-position of homoallylamine **3.5b**. Instead, almost equal incorporation of deuterium atom into positons γ and δ was observed with additional lack of isotope mass balance.

Next, the experiment with deuterium-labeled alkyne **3.4b-*d*$_1$** was conducted (Scheme 3.24).

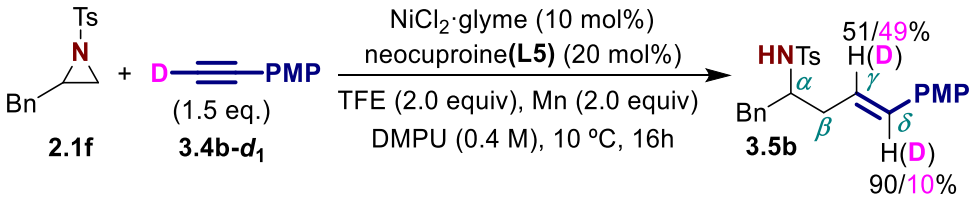

Scheme 3.24 Labeling experiment with deuterium-labeled alkyne **3.4b-*d*$_1$**

A slight incorporation of the deuterium into the δ-position was observed with a major part of deuterium remaining at γ-carbon. Additionally, a lack of deuterium mass balance was also detected in that case.

Vinyl-manganese species might be formed during the reaction after Ni reduction step. A loss of deuterium mass balance might originate from hydrolysis of these species during reaction work up with aqueous HCl. To confirm or refute this hypothesis a reaction of **2.1f** and **3.4b** runned under standard conditions was quenched with DCl/D_2O solution (Scheme 3.25).

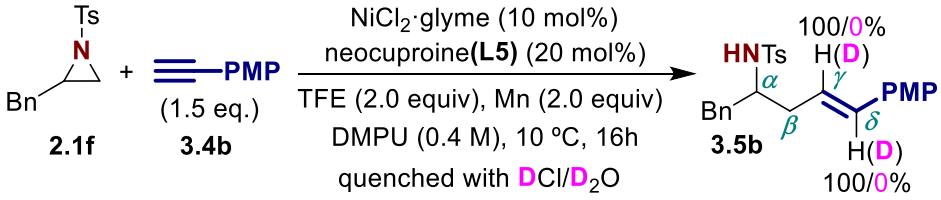

Scheme 3.25 Reaction under standard conditions quenched with DCl/D_2O solution

Notably, no deuterium incorporation was observed in that case. Thus, the hypothesis of vinyl-manganese species was refuted.

Finally, to see if the olefin bond remains intact once formed the product **3.5b** was subjected under reaction conditions in the separate experiment (Scheme 3.26).

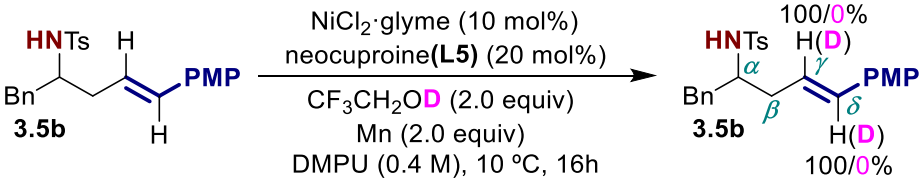

Scheme 3.26 Reaction of 3.5b under standard conditions with deuterium-labeled TFE

No deuterium incorporation into the olefin bond was observed in that case. Potential product of olefin bond reduction with Ni-H species was not detected either.

3.5 Chapter conclusions

- A novel methodology for Ni-catalyzed reductive hydroalkenylation of aziridines was developed
- Optimal reaction yield was achieved after careful choice of proton source viz. TFE
- The reaction was found to be sensitive regarding the electronic effects of phenylacetylene derivatives. Electron-deficient alkynes suppress catalytic activity of Ni-catalyst
- Reaction was found to be not applicable for the coupling of aziridines with terminal alkynes bearing alkyl substituent as the reaction undergoes uncontrolled oligomerization
- A diverse range of functional groups was found to be tolerant under reaction conditions demonstrating a high synthetic potential of the developed transformation
- The stereochemical course of the reaction was studied and the reaction was found to be applicable for the synthesis of enantiopure homoallylamines from enantiopure aziridines
- Results of labeling studies suggest a complex mechanism of olefin bond isomerization and more complex studies are needed to elucidate the reaction mechanism

3.6 Experimental section

3.6.1 General synthetic procedure (GP)

To an oven dried Schlenk tube in the glove box was added $NiCl_2$*glyme (4.4 mg, 0.020 mmol), neocuproine (8.3 mg, 0.040 mmol), Mn (22 mg, 0.60 mmol), the aziridine **2.1** (1.0 equiv., 0.20 mmol) if solid and the alkyne **3.4** (see **GP1** and **GP2**) if solid. The tube then was sealed with screw cap containing septum and transferred to the Schlenk line (vacuum, needle is going through the septum of reaction tube) located in the fume hood and run through argon/vacuum cycles three times. The solvent DMPU (dry, Sure/Seal packed, 0.40M => 0.5ml) was added first under the flow of argon. Then the aziridine **2.1** (if liquid) and/or alkyne **3.4** (if liquid) were added with micro syringes. The addition of TFE (2.0 equiv., 0.40 mmol, 29 μl) was performed in the end. All needles were removed and reaction tube was placed into the metallic lock connected with chiller or heating block (see **GP1** and **GP2**) and stirred for 24 hours. After the lapse of noted time reaction mixture was quenched with HCl (1 M, 2.0 ml) (saturated, 4.0 ml) and diluted with EtOAc. 1,3,5-Trimethoxybenzene (11 mg, 0.33 equiv.) internal standard was added as a stock solution in EtOAc at this step. Organic and aqueous layers were separated and the aqueous layer was additionally extracted with EtOAc (3 × 5.0 ml). The combined organic layers were washed three times with HCl (1 M, 10 ml), dried over $MgSO_4$, filtered and concentrated *in vacuo*. Quantification of crude NMR yields was carried out by integration of ^{1}H NMR against the TMB internal standard.

GP1: Alkyne **3.4** (1.5 equiv., 0.30 mmol). The reaction tube was placed into the metallic cooling block at 10 °C.

GP2: Alkyne **3.4** (2.0 equiv., 0.40 mmol). The reaction tube was placed into the metallic heating block at 45 °C

3.6.2 Purification of final products (PP)

Purification of crude mixtures was carried out by column chromatography on silica to give a final product **3.5**. Mobile phase acetone/n-hexane, gradient 1/12 => 1/10 => 1/8 => 1/6 => 1/4. If a mixture of products **3.5** and **3.7** was isolated, then $Co_2(CO)_8$ was used for further purification. Molar quantities of **3.5** and **3.7** were quantified knowing the mass of the isolated mixture and their molar ratio from ^{1}H NMR in every specific case. Based on quantification the molar quantity for $Co_2(CO)_8$ was calculated as 1.05 equivalent concerning **3.7**. Next, $Co_2(CO)_8$ was added in the glovebox to the round bottom flask containing a mixture of **3.5** and **3.7**. The flask was sealed with a septum and transferred to the bench. Dry toluene (3.0 ml) was added via a syringe. Resulted brown solution was stirred for approx. 30-60 minutes at RT. Toluene was concentrated *in vacuo*, remained crude mixture was purified by column chromatography on silica (DCM as mobile phase) to give a final product **3.5**.

3.6.3 Synthesis of homoallylamines

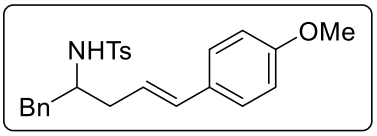

(*E*)-*N*-(5-(4-methoxyphenyl)-1-phenylpent-4-en-2-yl)-4-methylbenzenesulfonamide (**3.5b**): Following **GP1** product **3.5b** was formed with 65% NMR yield. In the separate independent experiment **3.5b** was formed with 66% NMR yield. Crude mixtures were combined and purified on silica giving an isolated mixture of **3.5b** and **3.7b**. The mixture of **3.5b** and **3.7b** was subsequently purified using $Co_2(CO)_8$ giving pure compound **3.5b** (84 mg, colorless solid) with an average 50% isolated yield after two purification steps. M.P. = 82 – 84 °C. ^{1}H NMR (500 MHz, $CDCl_3$): δ 7.64–7.59 (m, 2H), 7.27–7.18 (m, 3H), 7.17–7.12 (m, 4H), 7.12–7.08 (m, 2H), 6.86–6.80 (m, 2H), 6.25 (d, *J* = 15.7 Hz, 1H), 5.75–5.65 (m, 1H), 4.67 (d, *J* = 7.2 Hz, 1H, NH), 3.81 (s, 3H), 3.50 (h, *J* = 7.3 Hz, 1H), 2.90–2.75 (m, 2H), 2.37 (s, 3H), 2.42–2.30 (m, 1H), 2.26–2.15 (m, 1H) ppm. ^{13}C NMR (126 MHz, $CDCl_3$): δ 159.2, 143.2, 137.5, 137.4, 133.3, 129.9, 129.7, 129.6, 128.6, 127.4, 127.1, 126.7, 122.7, 114.0, 55.4, 55.0, 41.5, 37.7, 21.6 ppm. IR (neat, cm^{-1}): 3294, 2927, 1603, 1508, 1413, 1331, 1238, 1154, 1062, 1024, 986, 885, 803, 747, 702, 663, 582, 548, 506. HRMS calcd. for ($C_{25}H_{28}NO_3S$) $[M+H]^+$: 422.1784 found 422.1790.

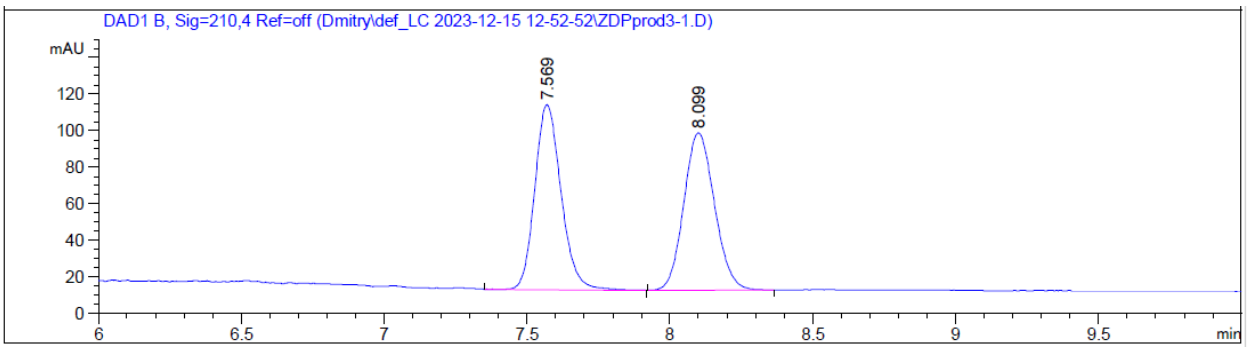

Signal 2: DAD1 B, Sig=210,4 Ref=off

Peak #	RetTime [min]	Type	Width [min]	Area [mAU*s]	Height [mAU]	Area %
1	7.569	VV R	0.0967	648.77692	101.31462	50.2513
2	8.099	BV R	0.1165	642.28687	86.12937	49.7487

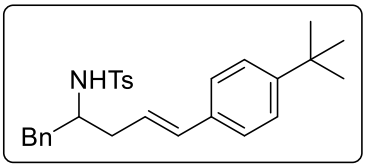

(E)-N-(5-(4-(tert-butyl)phenyl)-1-phenylpent-4-en-2-yl)-4-methylbenzenesulfonamide (3.5c): Following **GP1** product **3.5c** was formed with 58% NMR yield. The crude was purified on silica giving an isolated mixture of **3.5c** and **3.7c**. The mixture of **3.5c** and **3.7c** was subsequently purified using $Co_2(CO)_8$ giving pure compound **3.5c** (43 mg, colorless solid) with 48% isolated yield after two purification steps. M.P. = 118 – 120 °C. ^{1}H NMR (500 MHz, $CDCl_3$): δ 7.63–7.58 (m, 2H), 7.34–7.30 (m, 2H), 7.27–7.19 (m, 3H), 7.18–7.14 (m, 2H), 7.14–7.07 (m, 4H), 6.30 (d, *J* = 16.0 Hz, 1H), 5.85–5.76 (m, 1H), 4.50 (d, *J* = 7.2 Hz, 1H, NH),

3.51 (dtd, *J* = 12.7, 7.1, 5.7 Hz, 1H), 2.87–2.77 (m, 2H), 2.42–2.33 (m, 1H), 2.37 (s, 3H), 2.26–2.17 (m, 1H), 1.33 (s, 9H) ppm. ^{13}C NMR (126 MHz, $CDCl_3$): δ 150.7, 143.2, 137.5, 137.3, 134.3, 133.7, 129.7, 129.6, 128.7, 127.2, 126.8, 126.0, 125.5, 124.2, 55.0, 41.5, 37.8, 34.7, 31.4, 21.7 ppm. IR (neat, cm^{-1}): 3272, 3029, 2961, 1599, 1452, 1411, 1319, 1161, 1081, 972, 854, 812, 698, 669, 590. HRMS calcd. for ($C_{28}H_{33}NNaO_2S$) $[M+Na]^+$: 470.2124 found 470.2126.

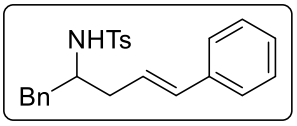

(E)-N-(1,5-diphenylpent-4-en-2-yl)-4-methylbenzenesulfonamide (3.5a): Following **GP2** product **3.5a** was formed with 65% NMR yield. In the separate independent experiment **3.5a** was formed with 66% NMR yield. Crude mixtures were combined and purified on silica giving an isolated mixture of **3.5a** and **3.7a**. The mixture of **3.5a** and **3.7a** was subsequently purified using $Co_2(CO)_8$ giving pure compound **3.5a** (91 mg, colorless solid) with an average 58% isolated yield after two purification steps. M.P. = 104 – 106 °C. ^{1}H NMR (500 MHz, $CDCl_3$): δ 7.63–7.58 (m, 2H), 7.32–7.27 (m, 2H), 7.27–7.18 (m, 6H), 7.15–7.07 (m, 4H), 6.31 (d, *J* = 15.8 Hz, 1H), 5.89–5.80 (m, 1H), 4.52 (d, *J* = 7.2 Hz, 1H, NH), 3.52 (qt, *J* = 7.2, 5.6 Hz, 1H), 2.83 (qd, *J* = 13.7, 6.6 Hz, 2H), 2.42–2.34 (m, 1H), 2.37 (s, 3H), 2.27–2.19 (m, 1H) ppm. ^{13}C NMR (126 MHz, $CDCl_3$): δ 143.3, 137.4, 137.3, 137.0, 133.9, 129.7, 129.6, 128.7, 128.6, 127.6, 127.2, 126.8, 126.3, 125.1, 54.9, 41.5, 37.8, 21.6 ppm. IR (neat, cm^{-1}): 3281, 3032, 1596, 1493, 1412, 1316, 1159, 1084, 970, 812, 746, 698, 665, 588, 553. HRMS calcd. for ($C_{24}H_{25}NNaO_2S$) $[M+Na]^+$: 414.1500 found 414.1498.

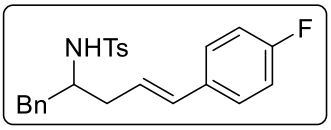

(E)-N-(5-(4-fluorophenyl)-1-phenylpent-4-en-2-yl)-4-methylbenzenesulfonamide (3.5d): Following **GP2** product **3.5d** was formed with 59% NMR yield. In the separate independent experiment **3.5d** was formed with 69% NMR yield. Crude mixtures were combined and purified on silica giving an isolated mixture of **3.5d** and **3.7d**. The mixture of **3.5d** and **3.7d** was subsequently purified using $Co_2(CO)_8$ giving pure compound **3.5d** (93 mg, colorless solid) with an average 57% isolated yield after two purification steps. M.P. = 71 – 73 °C. ^{1}H NMR (400 MHz, $CDCl_3$): δ 7.62–7.57 (m, 2H), 7.27–7.20 (m, 3H), 7.20–7.11 (m, 4H), 7.10–7.05 (m, 2H), 6.27 (d, *J* = 15.8 Hz, 1H), 5.78 (dt, *J* = 15.7, 7.3 Hz, 1H), 4.44 (d, *J* = 7.3 Hz, 1H, NH), 3.57–3.47 (m, 1H), 2.87–2.74 (m, 2H), 2.43–2.33 (m, 1H), 2.37 (s, 3H), 2.27–2.17 (m, 1H) ppm. ^{13}C NMR (101 MHz, $CDCl_3$): δ 162.3 (d, *J* = 246.6 Hz), 143.3, 137.5, 137.2, 133.22 (d, *J* = 3.3 Hz), 132.7, 129.7, 129.6, 128.7, 127.8 (d, *J* = 7.8 Hz), 127.2, 126.9, 124.9 (d, *J* = 2.2 Hz), 115.5 (d, *J* = 21.6 Hz), 54.9, 41.5, 37.8, 21.6 ppm. ^{19}F NMR (376 MHz, proton-decoupled, $CDCl_3$): -114.79 (s) δ ppm. IR (neat, cm^{-1}): 3280, 3033, 2922, 1600, 1507, 1454, 1315, 1227, 1156, 1083, 970, 855, 811, 757, 701, 663, 587, 552. HRMS calcd. for ($C_{24}H_{24}FNNaO_2S$) $[M+Na]^+$: 432.1404 found 432.1398.

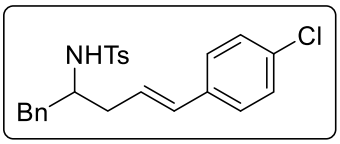

(E)-N-(5-(4-chlorophenyl)-1-phenylpent-4-en-2-yl)-4-methylbenzenesulfonamide (3.5e): Following **GP2** (note: 1.5 equiv. of **3.4e** were used) product **3.5e** was formed with 60% NMR yield. In the separate independent experiment **3.5e** was formed with 63% NMR yield. Crude mixtures were combined and purified on silica giving pure compound **3.5e** (99 mg, yellowish oil) with an average 58% isolated yield. Formation of Sonogashira-type side-product **3.7e** was not observed in this case. ^{1}H NMR (500 MHz, $CDCl_3$): δ 7.62–7.57 (m, 2H), 7.26–7.20 (m, 5H), 7.14–7.10 (m, 4H), 7.09–7.06 (m, 2H), 6.26 (d, *J* = 15.8 Hz, 1H), 5.89–5.80 (m, 1H), 4.65 (d, *J* = 7.4 Hz, 1H, NH), 3.57–3.48 (m, 1H), 2.86–2.74 (m, 2H), 2.43–2.35 (m, 1H), 2.36 (s, 3H), 2.26–2.18 (m, 1H) ppm. ^{13}C NMR (126 MHz, $CDCl_3$): δ 143.3, 137.5, 137.2, 135.6, 133.1, 132.6, 129.7, 129.6, 128.71, 128.70, 127.5, 127.1, 126.8, 126.0, 55.0, 41.6, 37.8, 21.6 ppm. IR (neat, cm^{-1}): 3277, 2923, 1598, 1490, 1454, 1324, 1153, 1088, 967, 812, 745, 700, 662, 548. HRMS calcd. for ($C_{24}H_{24}ClNNaO_2S$) $[M+Na]^+$: 448.1100 found 448.1108.

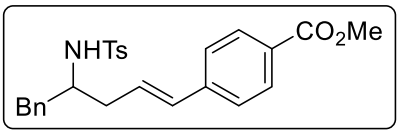

Methyl (E)-4-(4-((4-methylphenyl)sulfonamido)-5-phenylpent-1-en-1-yl)benzoate (3.5f): Following **GP** (note: reaction was conducted at 60 °C; 2.0 equiv. of **3.4e** and 30 mol % of **L5** were used) product **3.5f** was formed with 28% NMR yield. In the separate independent experiment **3.5f** was formed with 21% NMR yield. Crude mixtures were combined and purified on silica giving pure compound **3.5f** (29 mg, colorless oil) with an average 16% isolated yield. Formation of Sonogashira-type side-product **3.7f** was not observed in this case. ^{1}H NMR (500 MHz, $CDCl_3$): δ 7.97–7.92 (m, 2H), 7.62–7.57 (m, 2H), 7.27–7.19 (m, 5H), 7.14–7.10 (m, 2H), 7.10–7.05 (m, 2H), 6.34 (d, *J* = 15.8 Hz, 1H), 6.04–5.95 (m, 1H), 4.55 (d, *J* = 7.4 Hz, 1H, NH), 3.92 (s, 3H), 3.60–3.49 (m, 1H), 2.88–2.75 (m, 2H), 2.50–2.39 (m, 1H), 2.36 (s, 3H), 2.31–2.22 (m, 1H) ppm. ^{13}C NMR (126 MHz, $CDCl_3$): δ 167.0, 143.4, 141.5, 137.4, 137.1, 132.9, 130.0, 129.7, 129.6, 129.0, 128.8, 128.3, 127.1, 126.9, 126.1, 54.9, 52.2, 41.6, 38.0, 21.6 ppm. IR (neat, cm^{-1}): 3278, 2950, 1715, 1605, 1434, 1275, 1153, 1108, 968, 812, 747, 700, 662, 548. HRMS calcd. for ($C_{26}H_{27}NNaO_4S$) $[M+Na]^+$: 472.1553 found 472.1559.

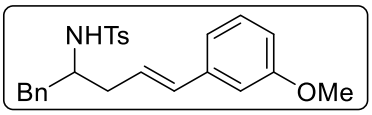

(E)-N-(5-(3-methoxyphenyl)-1-phenylpent-4-en-2-yl)-4-methylbenzenesulfonamide (3.5g): Following **GP1** product **3.5g** was formed with 68% NMR yield. In the separate independent experiment **3.5g** was formed with 69% NMR yield. Crude mixtures were combined and purified on silica giving an isolated mixture of **3.5g** and **3.7g**. The mixture of **3.5g** and **3.7g** was subsequently purified using $Co_2(CO)_8$ giving pure compound **3.5g** (98 mg, colorless solid) with an average 58% isolated yield after two purification steps. M.P. = 80 – 82 °C. ^{1}H NMR (500 MHz,

$CDCl_3$): δ 7.64–7.59 (m, 2H), 7.27–7.18 (m, 4H), 7.14–7.08 (m, 4H), 6.83–6.75 (m, 3H), 6.28 (dt, *J* = 15.7, 1.4 Hz, 1H), 5.90–5.80 (m, 1H), 4.75 (d, *J* = 7.3 Hz, 1H, NH), 3.81 (s, 3H), 3.56–3.48 (m, 1H), 2.89–2.77 (m, 2H), 2.42–2.34 (m, 1H), 2.36 (s, 3H), 2.27–2.19 (m, 1H) ppm. ^{13}C NMR (126 MHz, $CDCl_3$): δ 159.8, 143.2, 138.5, 137.4, 137.3, 133.7, 129.7, 129.6, 129.5, 128.6, 127.1, 126.7, 125.5, 119.0, 113.0, 111.7, 55.3, 55.0, 41.5, 37.7, 21.5 ppm. IR (neat, cm^{-1}): 3285, 2922, 1596, 1491, 1453, 1315, 1290, 1253, 1158, 1082, 1039, 969, 812, 753, 699, 665, 583, 552. HRMS calcd. for ($C_{25}H_{28}NO_3S$) $[M+H]^+$: 422.1784 found 422.1765.

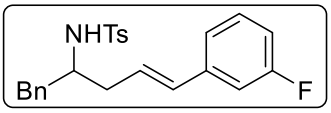

(E)-N-(5-(3-fluorophenyl)-1-phenylpent-4-en-2-yl)-4-methylbenzenesulfonamide (3.5h): Following **GP2** product **3.5h** was formed with 57% NMR yield. In the separate independent experiment **3.5h** was formed with 55% NMR yield. Crude mixtures were combined and purified on silica giving an isolated mixture of **3.5h** and **3.7h**. The mixture of **3.5h** and **3.7h** was subsequently purified using $Co_2(CO)_8$ giving pure compound **3.5h** (82 mg, colorless solid) with an average 50% isolated yield after two purification steps. M.P. = 110 – 112 °C. ^{1}H NMR (400 MHz, $CDCl_3$): δ 7.63–7.58 (m, 2H), 7.28–7.19 (m, 4H), 7.17–7.12 (m, 2H), 7.11–7.07 (m, 2H), 6.98–6.82 (m, 3H), 6.27 (d, *J* = 15.8 Hz, 1H), 5.88–5.76 (m, 1H), 4.46 (d, *J* = 7.3 Hz, 1H, NH), 3.58–3.46 (m, 1H), 2.83 (qd, *J* = 13.7, 6.5 Hz, 2H), 2.44–2.35 (m, 1H), 2.37 (s, 3H), 2.26–2.17 (m, 1H) ppm. ^{13}C NMR (101 MHz, $CDCl_3$): δ 163.2 (d, *J* = 245.2 Hz), 143.4, 139.4 (d, *J* = 7.6 Hz), 137.4, 137.1, 132.7 (d, *J* = 2.6 Hz), 130.1 (d, *J* = 8.5 Hz), 129.8, 129.7, 128.8, 127.2, 126.9, 126.8, 122.3 (d, *J* = 2.8 Hz), 114.4 (d, *J* = 21.4 Hz), 112.5 (d, *J* = 21.8 Hz), 54.9, 41.7, 37.7, 21.6 ppm. ^{19}F NMR (376 MHz, proton-decoupled, $CDCl_3$): δ -113.65 (s) ppm. IR (neat, cm^{-1}): 3280, 3034, 2921, 1579, 1492, 1412, 1316, 1246, 1159, 1084, 1047, 971, 880, 812, 783, 757, 699, 665, 580, 553. HRMS calcd. for ($C_{24}H_{24}FNNaO_2S$) $[M+Na]^+$: 432.1404 found 432.1399.

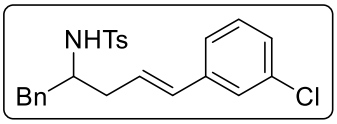

(E)-N-(5-(3-chlorophenyl)-1-phenylpent-4-en-2-yl)-4-methylbenzenesulfonamide (3.5i): Following **GP2** product **3.5i** was formed with 50% NMR yield. In the separate independent experiment **3.5i** was formed with 55% NMR yield. Crude mixtures were combined and purified on silica giving an isolated mixture of **3.5i** and **3.7i**. The mixture of **3.5i** and **3.7i** was subsequently purified using $Co_2(CO)_8$ giving pure compound **3.5i** (78 mg, colorless solid) with an average 46% isolated yield after two purification steps. M.P. = 121 – 123 °C. ^{1}H NMR (500 MHz, $CDCl_3$): δ 7.63–7.57 (m, 2H), 7.28–7.17 (m, 5H), 7.17–7.12 (m, 3H), 7.11–7.07 (m, 2H), 7.07–7.04 (m, 1H), 6.24 (d, *J* = 15.8 Hz, 1H), 5.87–5.79 (m, 1H), 4.54 (d, *J* = 7.3 Hz, 1H, NH), 3.51 (qt, *J* = 7.3, 5.4 Hz, 1H), 2.90–2.75 (m, 2H), 2.43 – 2.35 (m, 1H), 2.37 (s, 3H), 2.26–2.17 (m, 1H) ppm. ^{13}C NMR (126 MHz, $CDCl_3$): δ 143.4, 138.9, 137.3, 137.1, 134.5, 132.5, 129.8, 129.8, 129.6, 128.7, 127.5, 127.2,

126.9, 126.9, 126.0, 124.7, 54.9, 41.7, 37.7, 21.6 ppm. IR (neat, cm^{-1}): 3285, 2919, 1594, 1454, 1410, 1316, 1160, 1082, 1040, 967, 813, 705, 667, 591, 553. HRMS calcd. for ($C_{24}H_{24}ClNNaO_2S$) $[M+Na]^+$: 448.1108 found 448.1112.

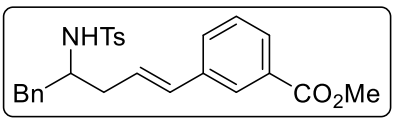

Methyl (E)-3-(4-((4-methylphenyl)sulfonamido)-5-phenylpent-1-en-1-yl)benzoate (3.5j): Following **GP2** product **3.5j** was formed with 50% NMR yield. In the separate independent experiment **3.5j** was formed with 49% NMR yield. Crude mixtures were combined and purified on silica giving an isolated mixture of **3.5j** and **3.7j**. The mixture of **3.5j** and **3.7j** was subsequently purified using $Co_2(CO)_8$ giving pure compound **3.5j** (79 mg, colorless oil) with an average 44% isolated yield after two purification steps. ^1H NMR (500 MHz, $CDCl_3$): δ 7.92–7.86 (m, 2H), 7.62–7.56 (m, 2H), 7.41–7.32 (m, 2H), 7.27–7.18 (m, 3H), 7.14–7.05 (m, 4H), 6.33 (d, *J* = 15.8 Hz, 1H), 6.02–5.90 (m, 1H), 4.65 (d, *J* = 7.4 Hz, 1H, NH), 3.93 (s, 3H), 3.53 (h, *J* = 7.2 Hz, 1H), 2.87–2.76 (m, 2H), 2.46–2.37 (m, 1H), 2.33 (s, 3H), 2.30–2.19 (m, 1H) ppm. ^{13}C NMR (126 MHz, $CDCl_3$): δ 167.1, 143.3, 137.4, 137.4, 137.2, 132.9, 130.7, 130.5, 129.7, 129.6, 128.7, 128.7, 128.5, 127.3, 127.1, 126.8, 126.6, 54.9, 52.3, 41.5, 37.8, 21.6 ppm. IR (neat, cm^{-1}): 3281, 2950, 1719, 1599, 1439, 1288, 1203, 1153, 1083, 967, 813, 746, 662, 580, 548. HRMS calcd. for ($C_{26}H_{27}NNaO_4S$) $[M+Na]^+$: 472.1553 found 472.1555.

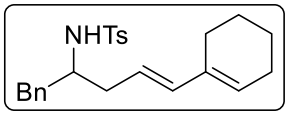

(E)-N-(5-(cyclohex-1-en-1-yl)-1-phenylpent-4-en-2-yl)-4-methylbenzenesulfonamide (3.5m): Following **GP1** product **3.5m** was formed with 46% NMR yield. In the separate independent experiment **3.5m** was formed with 43% NMR yield. Crude mixtures were combined and purified on silica giving an isolated mixture of **3.5m** and **3.7m**. The mixture of **3.5m** and **3.7m** was subsequently purified using $Co_2(CO)_8$ giving pure compound **3.5m** (41 mg, colorless oil) with an average 26%[xxxii] isolated yield after two purification steps. ^1H NMR (500 MHz, $CDCl_3$): δ 7.66–7.61 (m, 2H), 7.25–7.16 (m, 5H), 7.10–7.05 (m, 2H), 5.94 (d, *J* = 15.6 Hz, 1H), 5.63 (t, *J* = 4.2 Hz, 1H), 5.19 (dt, *J* = 15.1, 7.3 Hz, 1H), 4.47 (d, *J* = 7.1 Hz, 1H, NH), 3.47–3.38 (m, 1H), 2.85–2.70 (m, 2H), 2.41 (s, 3H), 2.25–2.17 (m, 1H), 2.14–2.05 (m, 3H), 2.00–1.86 (m, 2H), 1.68–1.54 (m, 4H) ppm. ^{13}C NMR (126 MHz, $CDCl_3$): δ 143.2, 137.9, 137.7, 137.5, 135.2, 129.7, 129.6, 129.1, 128.6, 127.2, 126.7, 55.0, 41.3, 37.4, 25.9, 24.6, 22.63, 22.56, 21.6 ppm. IR (neat, cm^{-1}): 3255, 3027, 2926, 1598, 1495, 1436, 1325, 1151, 1070, 976, 815, 741, 697, 666, 549. HRMS calcd. for ($C_{24}H_{29}NNaO_2S$) $[M+Na]^+$: 418.1812 found 418.1809.

[xxxii] Product **3.5m** was found to be reactive in the presence if $Co_2(CO)_8$ and formation of multiple side-products was observed on TLC plate.

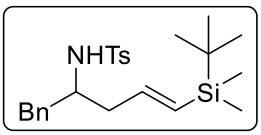

(E)-N-(5-(tert-butyldimethylsilyl)-1-phenylpent-4-en-2-yl)-4-methylbenzenesulfonamide (3.5o): Following **GP** (note: reaction was conducted at 10 °C; 3.0 equiv. of **3.4o** were used; 48 hours of reaction time) product **3.5o** was formed with 59% NMR yield. In the separate independent experiment **3.5o** was formed with 57% NMR yield. Crude mixtures were combined and purified on silica giving an isolated mixture of **3.5o** and **3.7o**. The mixture of **3.5o** and **3.7o** was subsequently purified using $Co_2(CO)_8$, however a minor difference in retention time was observed and only analytical quantity of pure compound **3.5o** (24 mg, colorless oil) was isolated after two purification steps. ^{1}H NMR (500 MHz, $CDCl_3$): δ 7.66–7.61 (m, 2H), 7.25–7.19 (m, 5H), 7.07–7.02 (m, 2H), 5.78 (dt, *J* = 18.6, 6.5 Hz, 1H), 5.66 (dt, *J* = 18.5, 1.2 Hz, 1H), 4.36 (d, *J* = 6.9 Hz, 1H, NH), 3.48 (h, *J* = 6.5 Hz, 1H), 2.80–2.71 (m, 2H), 2.41 (s, 3H), 2.34–2.26 (m, 1H), 2.24–2.17 (m, 1H), 0.85 (s, 9H), -0.03 (s, 3H), -0.05 (s, 3H) ppm. ^{13}C NMR (126 MHz, $CDCl_3$): δ 143.3, 142.7, 137.6, 137.3, 133.0, 129.8, 129.6, 128.7, 127.2, 126.8, 54.5, 41.8, 41.0, 26.5, 21.6, 16.5, -6.00, -6.1 ppm. IR (neat, cm^{-1}): 3277, 2926, 2854, 1599, 1455, 1326, 1247, 1156, 1083, 811, 778, 742, 700, 661, 581, 549. HRMS calcd. for ($C_{24}H_{36}NO_2SSi$) $[M+H]^+$: 430.2231 found 430.2231.

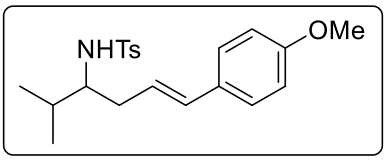

(E)-N-(6-(4-methoxyphenyl)-2-methylhex-5-en-3-yl)-4-methylbenzenesulfonamide (3.5p): Following **GP1** product **3.5p** was formed with 46% NMR yield. In the separate independent experiment **3.5p** was formed with 39% NMR yield. Crude mixtures were combined and purified on silica giving an isolated mixture of **3.5p** and **3.7p**. The mixture of **3.5p** and **3.7p** was subsequently purified using $Co_2(CO)_8$ giving pure compound **3.5p** (58 mg, colorless solid) with an average 39% isolated yield after two purification steps. M.P. = 94 – 96 °C. ^{1}H NMR (500 MHz, $CDCl_3$): δ 7.73–7.67 (m, 2H), 7.21–7.17 (m, 2H), 7.14–7.08 (m, 2H), 6.84–6.79 (m, 2H), 6.19 (d, *J* = 15.8 Hz, 1H), 5.66–5.57 (m, 1H), 4.37 (d, *J* = 8.3 Hz, 1H, NH), 3.81 (s, 3H), 3.18–3.11 (m, 1H), 2.38 (s, 3H), 2.26–2.12 (m, 2H), 1.88 (m, 1H), 0.88 (dd, *J* = 6.8, 4.8 Hz, 6H) ppm. ^{13}C NMR (126 MHz, $CDCl_3$): δ 159.1, 143.1, 138.2, 132.8, 129.9, 129.7, 127.4, 127.2, 123.3, 114.0, 59.3, 55.4, 35.2, 31.5, 21.6, 18.5, 18.2 ppm. IR (neat, cm^{-1}): 3285, 2961, 1606, 1511, 1454, 1314, 1287, 1247, 1179, 1153, 1091, 1028, 977, 812, 796, 667, 570, 544. HRMS calcd. for ($C_{21}H_{27}NNaO_3S$) $[M+Na]^+$: 396.1604 found 396.1596.

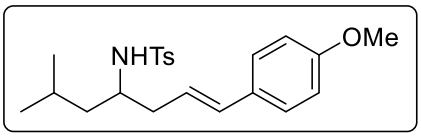

(E)-N-(1-(4-methoxyphenyl)-6-methylhept-1-en-4-yl)-4-methylbenzenesulfonamide (3.5q): Following **GP1** product **3.5q** was formed with 64% NMR yield. In the separate independent experiment **3.5q** was formed with 60% NMR yield. Crude mixtures were combined and purified on silica giving an isolated mixture of **3.5q** and **3.7q**. The mixture of **3.5q** and **3.7q**

was subsequently purified using $Co_2(CO)_8$ giving pure compound **3.5q** (90 mg, colorless solid) with an average 58% isolated yield after two purification steps. M.P. = 71 – 73 °C. ^{1}H NMR (500 MHz, $CDCl_3$): δ 7.77–7.72 (m, 2H), 7.26–7.22 (m, 2H), 7.19–7.14 (m, 2H), 6.85–6.80 (m, 2H), 6.18 (d, *J* = 15.9 Hz, 1H), 5.80–5.72 (m, 1H), 4.47 (d, *J* = 8.3 Hz, 1H, NH), 3.81 (s, 3H), 3.40 (tq, *J* = 8.2, 5.6 Hz, 1H), 2.40 (s, 3H), 2.30–2.15 (m, 2H), 1.67–1.57 (m, 2H), 1.30 (qdd, *J* = 13.9, 8.0, 6.1 Hz, 2H), 0.84 (d, *J* = 6.6 Hz, 3H), 0.76 (d, *J* = 6.6 Hz, 3H) ppm. ^{13}C NMR (126 MHz, $CDCl_3$): δ 159.2, 143.3, 138.4, 133.3, 129.9, 129.7, 127.4, 127.2, 122.5, 114.0, 55.4, 52.1, 44.5, 38.8, 24.6, 22.9, 22.2, 21.7 ppm. IR (neat, cm^{-1}): 3246, 2914, 1607, 1510, 1457, 1429, 1303, 1250, 1156, 1083, 1034, 998, 971, 810, 758, 665, 580, 544. HRMS calcd. for ($C_{22}H_{29}NNaO_3S$) $[M+Na]^+$: 410.1760 found 410.1758.

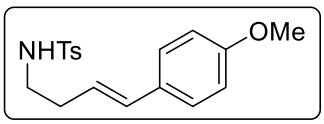

(E)-N-(4-(4-methoxyphenyl)but-3-en-1-yl)-4-methylbenzenesulfonamide (3.5r): Following **GP1** product **3.5r** was formed with 45% NMR yield. In the separate independent experiment **3.5r** was formed with 41% NMR yield. Crude mixtures were combined and purified on silica giving an isolated mixture of **3.5r** and **3.7r**. The mixture of **3.5r** and **3.7r** was subsequently purified using $Co_2(CO)_8$, however a minor difference in retention time was observed and only analytical quantity of pure compound **3.5r** (23 mg, colorless solid) was isolated after two purification steps. M.P. = 76 – 78 °C. ^{1}H NMR (500 MHz, $CDCl_3$), sample is as mixture of (E/Z) isomers, with a molar ratio ca. 20/1, signals of only major (E) isomer are described: δ 7.76–7.72 (m, 2H), 7.31–7.27 (m, 2H), 7.23–7.18 (m, 2H), 6.86–6.80 (m. 2H), 6.30 (d, *J* = 15.8 Hz, 1H), 5.82 (dt, *J* = 15.7, 7.1 Hz, 1H), 4.52 (t, *J* = 6.1 Hz, 1H, NH), 3.80 (s, 3H), 3.08 (q, *J* = 6.5 Hz, 2H), 2.42 (s, 3H), 2.37–2.30 (m, 2H) ppm. ^{13}C NMR (126 MHz, $CDCl_3$): δ 159.3, 143.6, 137.1, 132.8, 129.9, 129.7, 127.4, 127.3, 123.3, 114.1, 55.4, 42.8, 33.1, 21.7 ppm. IR (neat, cm^{-1}): 3289, 2966, 1603, 1510, 1443, 1411, 1323, 1306, 1242, 1157, 1093, 1026, 968, 815, 798, 668, 574, 548, 489. HRMS calcd. for ($C_{18}H_{21}NNaO_3S$) $[M+Na]^+$: 354.1134 found 354.1136.

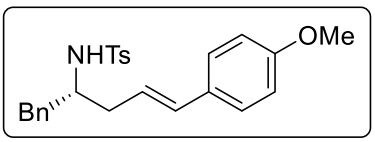

(R,E)-N-(5-(4-methoxyphenyl)-1-phenylpent-4-en-2-yl)-4-methylbenzenesulfonamide ((*R*)-3,5b): Following **GP1** product (R)-**3.5b** was formed with 69% NMR yield. In the separate independent experiment (R)-**3.5b** was formed with 67% NMR yield. Crude mixtures were combined and purified on silica giving an isolated mixture of (*R*)-**3.5b** and (*R*)-**3.7b**. The mixture of (*R*)-**3.5b** and (*R*)-**3.7b** was subsequently purified using $Co_2(CO)_8$ giving pure compound (*R*)-**3.5b** (96 mg, colorless oil) with an average 57% isolated yield after two purification steps. ^{1}H NMR (500 MHz, $CDCl_3$): δ 7.62–7.58 (m, 2H), 7.26–7.19 (m, 3H), 7.17–7.12 (m, 4H), 7.11–7.07 (m, 2H), 6.85–6.81 (m, 2H), 6.25 (d, *J* = 15.8 Hz, 1H), 5.72–5.65 (m, 1H), 4.39 (d, *J* = 7.1 Hz, 1H,

NH), 3.82 (s, 3H), 3.50 (m, 1H), 2.82 (qd, *J* = 13.7, 6.5 Hz, 2H), 2.38 (s, 3H), 2.37–2.31 (m, 1H), 2.24–2.15 (m, 1H) ppm. ^{13}C NMR (126 MHz, CDCl3): δ 159.2, 143.2, 137.5, 137.4, 133.3, 129.8, 129.7, 129.6, 128.6, 127.4, 127.2, 126.7, 122.7, 114.0, 55.4, 55.0, 41.5, 37.7, 21.6 ppm. IR (neat, cm^{-1}): 3279, 2932, 1606, 1510, 1454, 1324, 1245, 1153, 1083, 1032, 967, 812, 737, 701, 662, 578, 548. HRMS calcd. for ($C_{25}H_{28}NO_3S$) $[M+H]^+$: 422.1784 found 422.1784.

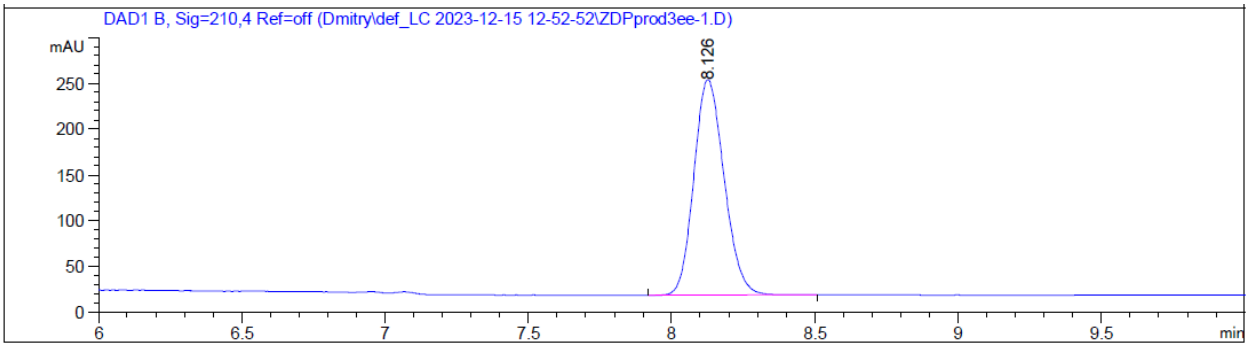

Signal 2: DAD1 B, Sig=210,4 Ref=off

Peak #	RetTime [min]	Type	Width [min]	Area [mAU*s]	Height [mAU]	Area %
1	8.126	BB	0.1152	1728.29187	235.32286	100.0000

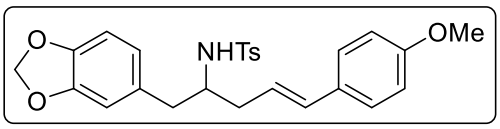

(E)-N-(1-(benzo[d][1,3]dioxol-5-yl)-5-(4-methoxyphenyl)pent-4-en-2-yl)-4-methylbenzenesulfonamide (3.5s): Following **GP1** product **3.5s** was formed with 61% NMR yield. In the separate independent experiment **3.5s** was formed with 55% NMR yield. Crude mixtures were combined and purified on silica giving an isolated mixture of **3.5s** and **3.7s**. The mixture of **3.5s** and **3.7s** was subsequently purified using $Co_2(CO)_8$ giving pure compound **3.5s** (99 mg, colorless solid) with an average 53% isolated yield after two purification steps. M.P. = 101 – 103 °C. ^{1}H NMR (500 MHz, $CDCl_3$): δ 7.63–7.57 (m, 2H), 7.18–7.12 (m, 4H), 6.86–6.79 (m, 2H), 6.69–6.64 (m, 1H), 6.55–6.49 (m, 2H), 6.26 (d, *J* = 15.8 Hz, 1H), 5.94–5.89 (m, 2H), 5.71 (dt, *J* = 15.2, 7.3 Hz, 1H), 4.54 (d, *J* = 7.1 Hz, 1H, NH), 3.81 (s, 3H), 3.41 (h, *J* = 6.6 Hz, 1H), 2.71 (d, *J* = 6.6 Hz, 2H), 2.38 (s, 3H), 2.42–2.32 (m, 1H), 2.28–2.18 (m, 1H) ppm. ^{13}C NMR (126 MHz, $CDCl_3$): δ 159.2, 147.8, 146.4, 143.2, 137.4, 133.3, 131.1, 129.9, 129.6, 127.43, 127.2, 122.7, 122.6, 114.0, 109.7, 108.4, 101.0, 55.4, 55.2, 41.1, 37.9, 21.6 ppm. IR (neat, cm^{-1}): 3267, 2913, 1606, 1505, 1449, 1417, 1316, 1242, 1180, 1154, 1090, 1034, 932, 811, 773, 663, 580, 548. HRMS calcd. for ($C_{26}H_{28}NO_5S$) $[M+H]^+$: 466.1683 found 466.1686.

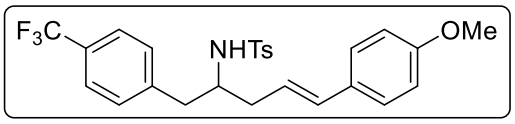

(E)-N-(5-(4-methoxyphenyl)-1-(4-(trifluoromethyl)phenyl)pent-4-en-2-yl)-4-methylbenzenesulfonamide (3.5t): Following **GP1** product **3.5t** was formed with 63% NMR yield. In the separate independent experiment **3.5t** was formed with 59% NMR yield. Crude mixtures were combined and purified on silica giving an isolated mixture of **3.5t** and **3.7t**. The mixture of **3.5t** and **3.7t** was subsequently purified using $Co_2(CO)_8$ giving pure compound **3.5t** (110 mg, colorless solid) with an average 56% isolated yield after two purification steps. M.P. = 115 – 117 °C. ^{1}H NMR (500 MHz, $CDCl_3$): δ 7.56–7.52 (m, 2H), 7.46–7.42 (m, 2H), 7.20–7.17 (m, 2H), 7.17–7.13 (m, 2H), 7.12–7.09 (m, 2H), 6.85–6.81 (m, 2H), 6.28 (d, *J* = 15.9 Hz, 1H), 5.70 (dt, *J* = 15.7, 7.4 Hz, 1H), 4.58 (d, *J* = 7.3 Hz, 1H, NH), 3.81 (s, 3H), 3.55–3.47 (m, 1H), 2.94–2.81 (m, 2H), 2.41–2.34 (m, 1H), 2.37 (s, 3H), 2.29–2.22 (m, 1H) ppm. ^{13}C NMR (101 MHz, $CDCl_3$): δ 159.4, 143.4, 141.7, 137.3, 133.8, 129.9, 129.69, 129.66, 129.0 (d, *J* = 32.4 Hz), 127.5, 127.1, 125.4 (q, *J* = 3.8 Hz), 124.3 (d, *J* = 271.9 Hz), 122.1, 114.1, 55.5, 55.0, 41.3, 38.3, 21.6 ppm. ^{19}F NMR (376 MHz, proton-decoupled, $CDCl_3$): δ -62.49 (s) ppm. IR (neat, cm^{-1}): 3311, 2925, 1607, 1510, 1420, 1322, 1291, 1249, 1147, 1109, 1062, 968, 803, 753, 655, 579, 547. HRMS calcd. for ($C_{26}H_{26}F_3NNaO_3S$) $[M+Na]^+$: 512.1478 found 512.1487.

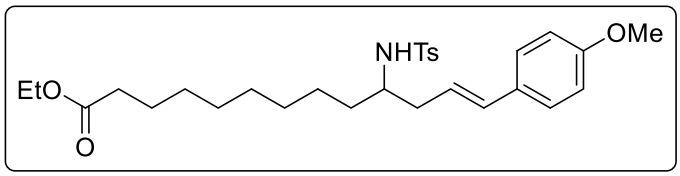

Ethyl (E)-13-(4-methoxyphenyl)-10-((4-methylphenyl)sulfonamido)tridec-12-enoate(3.5u): Following **GP1** product **3.5u** was formed with 58% NMR yield. In the separate independent experiment **3.5u** was formed with 64% NMR yield. Crude mixtures were combined and purified on silica giving an isolated mixture of **3.5u** and **3.7u**. The mixture of **3.5u** and **3.7u** was subsequently purified using $Co_2(CO)_8$ giving pure compound **3.5u** (109 mg, yellowish oil) with an average 53% isolated yield after two purification steps. ^{1}H NMR (500 MHz, $CDCl_3$): δ 7.75–7.70 (m, 2H), 7.25–7.22 (m, 2H), 7.19–7.13 (m, 2H), 6.85–6.80 (m, 2H), 6.20 (d, *J* = 15.7 Hz, 1H), 5.72 (dt, *J* = 15.3, 7.4 Hz, 1H), 4.30 (d, *J* = 8.1 Hz, 1H, NH), 4.13 (q, *J* = 7.1 Hz, 2H), 3.81 (s, 3H), 3.31 (h, *J* = 6.2 Hz, 1H), 2.40 (s, 3H), 2.31–2.16 (m, 4H), 1.64–1.56 (m, 2H), 1.51–1.36 (m, 2H), 1.30–1.22 (m, 8H), 1.20–1.15 (m, 5H) ppm. ^{13}C NMR (126 MHz, $CDCl_3$): δ ^{13}C NMR (126 MHz, $CDCl_3$) δ 174.0, 159.0, 143.2, 138.3, 133.1, 129.9, 129.7, 127.4, 127.2, 122.7, 114.0, 60.3, 55.4, 53.9, 38.5, 35.1, 34.5, 29.35, 29.32, 29.22, 29.17, 25.5, 25.0, 21.6, 14.4 ppm. IR (neat, cm^{-1}): 3284, 2927, 2854, 1731, 1607, 1510, 1443, 1324, 1246, 1155, 1093, 1031, 967, 813, 663, 548. HRMS calcd. for ($C_{29}H_{41}NNaO_5S$) $[M+Na]^+$: 538.2591 found 538.2598.

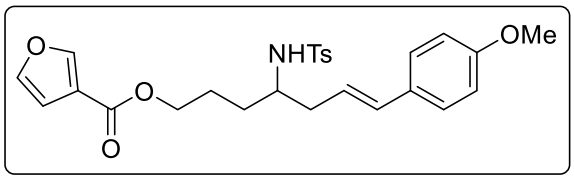

(E)-7-(4-methoxyphenyl)-4-((4-methylphenyl)sulfonamido)hept-6-en-1-yl furan-3-carboxylate (3.5v): Following **GP1** product **3.5v** was formed with 72% NMR yield. In the separate independent experiment **3.5v** was formed with 65% NMR yield. Crude mixtures were combined and purified on silica giving an isolated mixture of **3.5v** and **3.7v**. The mixture of **3.5v** and **3.7v** was subsequently purified using $Co_2(CO)_8$, however a minor difference in retention time was observed and only analytical quantity of pure compound **3.5v** (21 mg, yellowish oil) was isolated after two purification steps. ^{1}H NMR (500 MHz, $CDCl_3$): δ 7.98–7.96 (m, 1H), 7.74–7.70 (m, 2H), 7.41 (t, *J* = 1.7 Hz, 1H), 7.24–7.20 (m, 2H), 7.15–7.11 (m, 2H), 6.84–6.80 (m, 2H), 6.72–6.70 (m, 1H), 6.20 (d, *J* = 15.8 Hz, 1H), 5.67 (dt, *J* = 15.3, 7.4 Hz, 1H), 4.49 (d, *J* = 8.1 Hz, 1H, NH), 4.23–4.13 (m, 2H), 3.81 (s, 3H), 3.42–3.34 (m, 1H), 2.38 (s, 3H), 2.29–2.16 (m, 2H), 1.82–1.49 (br. m, 6H)[xxxiii] ppm. ^{13}C NMR (126 MHz, $CDCl_3$): δ 163.2, 159.3, 147.8, 143.8, 143.5, 138.1, 133.6, 129.8, 129.7, 127.5, 127.2, 122.1, 119.5, 114.1, 109.9, 64.1, 55.5, 53.5, 38.5, 31.7, 25.0, 21.7 ppm. IR (neat, cm^{-1}): 3279, 2930, 1718, 1606, 1509, 1442, 1305, 1246, 1154, 1091, 1030, 873, 814, 762, 663, 547. HRMS calcd. for ($C_{26}H_{29}NNaO_6S$) $[M+Na]^+$: 506.1608 found 506.1614.

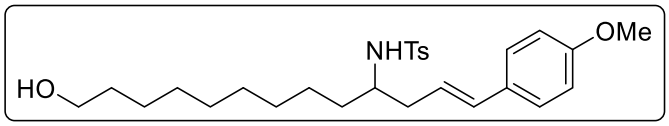

(E)-N-(13-hydroxy-1-(4-methoxyphenyl)tridec-1-en-4-yl)-4-methylbenzenesulfonamide (3.5w): Following **GP1** product **3.5w** was formed with 57% NMR yield. In the separate independent experiment **3.5w** was formed with 61% NMR yield. Crude mixtures were combined and purified on silica giving an isolated mixture of **3.5w** and **3.7w**. The mixture of **3.5w** and **3.7w** was subsequently purified using $Co_2(CO)_8$, however a minor difference in retention time was observed and only analytical quantity of pure compound **3.5w** (27 mg, colorless solid) was isolated after two purification steps. M.P. = 103 – 105 °C. ^{1}H NMR (500 MHz, $CDCl_3$): δ 7.76–7.68 (m, 2H), 7.25–7.19 (m, 2H), 7.18–7.12 (m, 2H), 6.85–6.78 (m, 2H), 6.20 (d, *J* = 15.7 Hz, 1H), 5.72 (dt, *J* = 15.3, 7.4 Hz, 1H), 4.51 (d, *J* = 8.1 Hz, 1H, NH), 3.81 (s, 3H), 3.64 (t, *J* = 6.5 Hz, 2H), 3.35–3.25 (m, 1H), 2.39 (s, 3H), 2.23 (tp, *J* = 13.9, 6.6 Hz, 2H), 1.70–1.00 (br. m, 20H)[xxxiv] ppm. ^{13}C NMR (126 MHz, $CDCl_3$): δ 159.2, 143.2, 138.3, 133.2, 129.9, 129.7, 127.4, 127.2, 122.7, 114.0, 63.2, 55.4, 54.0, 38.5, 35.1, 32.9, 29.54, 29.5, 29.4, 25.8, 25.5, 21.7 ppm. IR (neat, cm^{-1}): 3488, 3171, 2916, 2850, 1606, 1510, 1454, 1315, 1243, 1150, 1089, 1037, 967, 818, 668, 576. HRMS calcd. for ($C_{27}H_{40}NO_4S$) $[M+H]^+$: 474.2673 found 474.2686.

[xxxiii] Overlaps with signal of water; expected intensity is 4H.
[xxxiv] Overlaps with other signals; expected intensity is 16H.

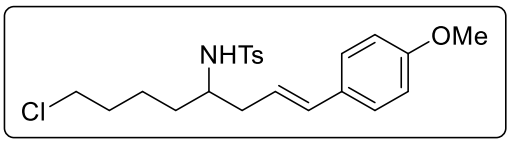

(E)-N-(8-chloro-1-(4-methoxyphenyl)oct-1-en-4-yl)-4-methylbenzenesulfonamide (3.5x): Following **GP1** product **3.5x** was formed with 63% NMR yield. In the separate independent experiment **3.5x** was formed with 67% NMR yield. Crude mixtures were combined and purified on silica giving an isolated mixture of **3.5x** and **3.7x**. The mixture of **3.5x** and **3.7x** was subsequently purified using $Co_2(CO)_8$ giving pure compound **3.5x** (95 mg, colorless solid) with an average 56% isolated yield after two purification steps. M.P. = 84 – 86 °C. ^{1}H NMR (500 MHz, $CDCl_3$): δ δ 7.77–7.67 (m, 2H), 7.25–7.19 (m, 2H), 7.18–7.11 (m, 2H), 6.87–6.77 (m, 2H), 6.21 (d, *J* = 15.7 Hz, 1H), 5.70 (dt, *J* = 15.3, 7.4 Hz, 1H), 4.69 (d, *J* = 8.0 Hz, 1H, NH), 3.80 (s, 3H), 3.43 (t, *J* = 6.6 Hz, 2H), 3.31 (h, *J* = 6.5 Hz, 1H), 2.39 (s, 3H), 2.23 (qt, *J* = 14.0, 6.7 Hz, 2H), 1.66 (p, *J* = 7.1 Hz, 2H), 1.58–1.22 (br. m, 5H)[xxxv] ppm. ^{13}C NMR (126 MHz, $CDCl_3$): δ 159.2, 143.4, 138.1, 133.3, 129.79, 129.76, 127.4, 127.2, 122.4, 114.0, 55.4, 53.7, 44.8, 38.5, 34.4, 32.3, 22.9, 21.6 ppm. IR (neat, cm^{-1}): 3263, 2935, 1606, 1510, 1463, 1410, 1318, 1291, 1248, 1161, 1084, 1007, 959, 816, 730, 668, 551. HRMS calcd. for ($C_{22}H_{29}ClNO_3S$) $[M+H]^+$: 422.1551 found 422.1553.

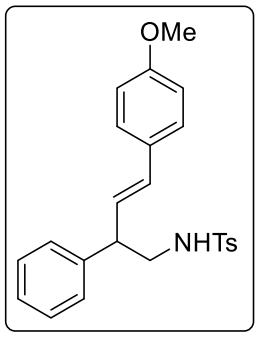

(E)-N-(4-(4-methoxyphenyl)-2-phenylbut-3-en-1-yl)-4-methylbenzenesulfonamide (3.5y): Following **GP1** product **3.5y** was formed with 51% NMR yield. In the separate independent experiment **3.5y** was formed with 46% NMR yield. Crude mixtures were combined and purified on silica giving an isolated mixture of **3.5y** with a series of identified side-products with similar retention time. Analytical quantity of pure compound **3.5y** (18 mg, colorless solid) was obtained after recrystallizing the isolated mixture from acetone/n-hexane (approx. 1/10, slow evaporation). M.P. = 116 – 118 °C. ^{1}H NMR (500 MHz, $CDCl_3$): δ 7.72–7.68 (m, 2H), 7.33–7.28 (m, 4H), 7.27–7.21 (m. 3H), 7.15–7.11 (m, 2H), 6.85–6.79 (m, 2H), 6.32 (d, *J* = 15.9 Hz, 1H), 6.02 (dd, *J* = 15.9, 8.0 Hz, 1H), 4.39 (t, *J* = 6.2 Hz, 1H), 3.80 (s, 3H), 3.54 (q, *J* = 7.2 Hz, 1H), 3.36–3.25 (m, 2H), 2.44 (s, 3H) ppm. ^{13}C NMR (126 MHz, $CDCl_3$): δ 159.4, 143.6, 140.6, 137.1, 131.9, 129.9, 129.4, 129.1, 127.8, 127.6, 127.4, 127.3, 127.1, 114.1, 55.4, 48.8, 47.7, 21.7 ppm. IR (neat, cm^{-1}): 3283, 2934, 1607, 1510, 1422, 1321, 1250, 1176, 1151, 1092, 1030, 963, 819, 668, 552. HRMS calcd. for ($C_{24}H_{25}NNaO_3S$) $[M+Na]^+$: 430.1447 found 430.1460.

[xxxv] Overlaps with signal of water; expected intensity is 4H.

3.6.4 NMR spectra

^{1}H ($CDCl_3$, 500 MHz)

3.5b

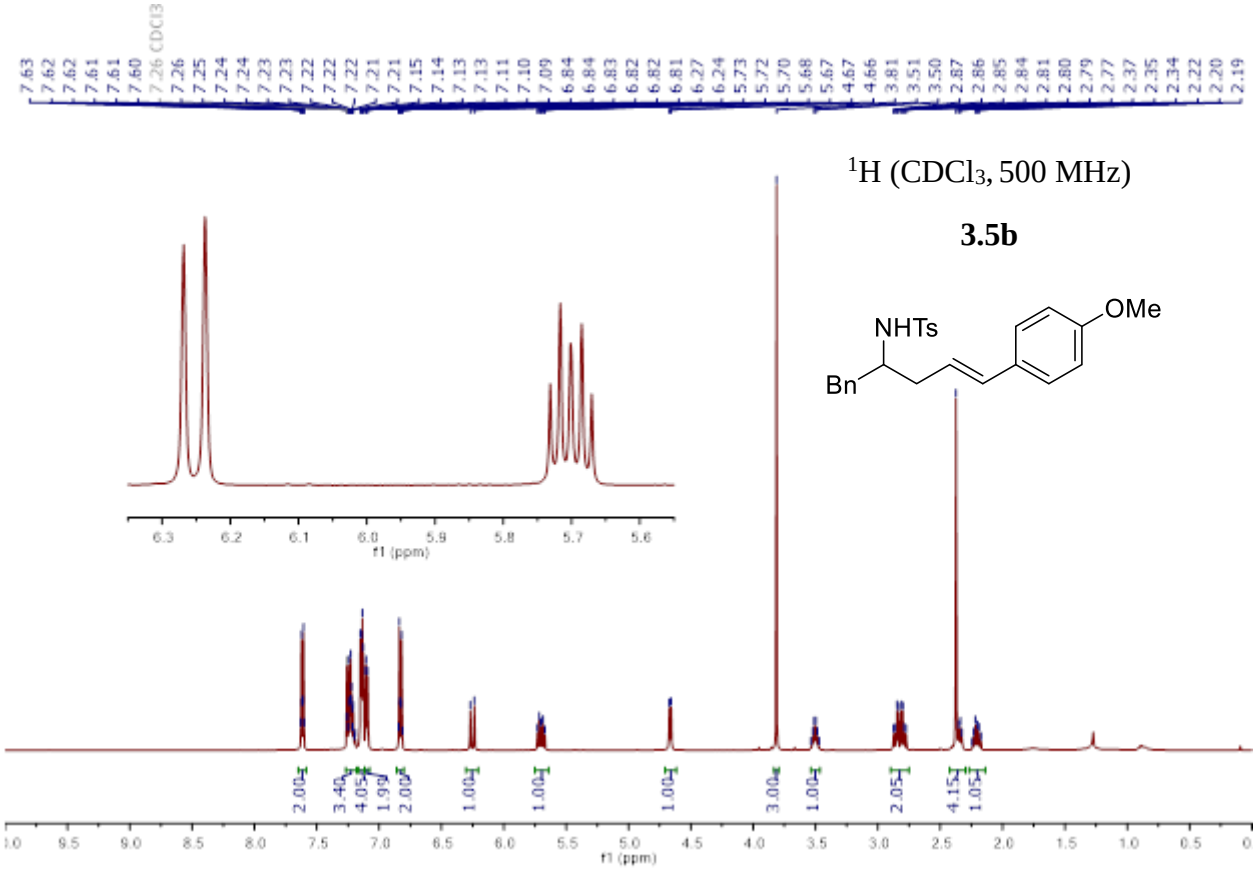

^{13}C ($CDCl_3$, 126 MHz)

3.5b

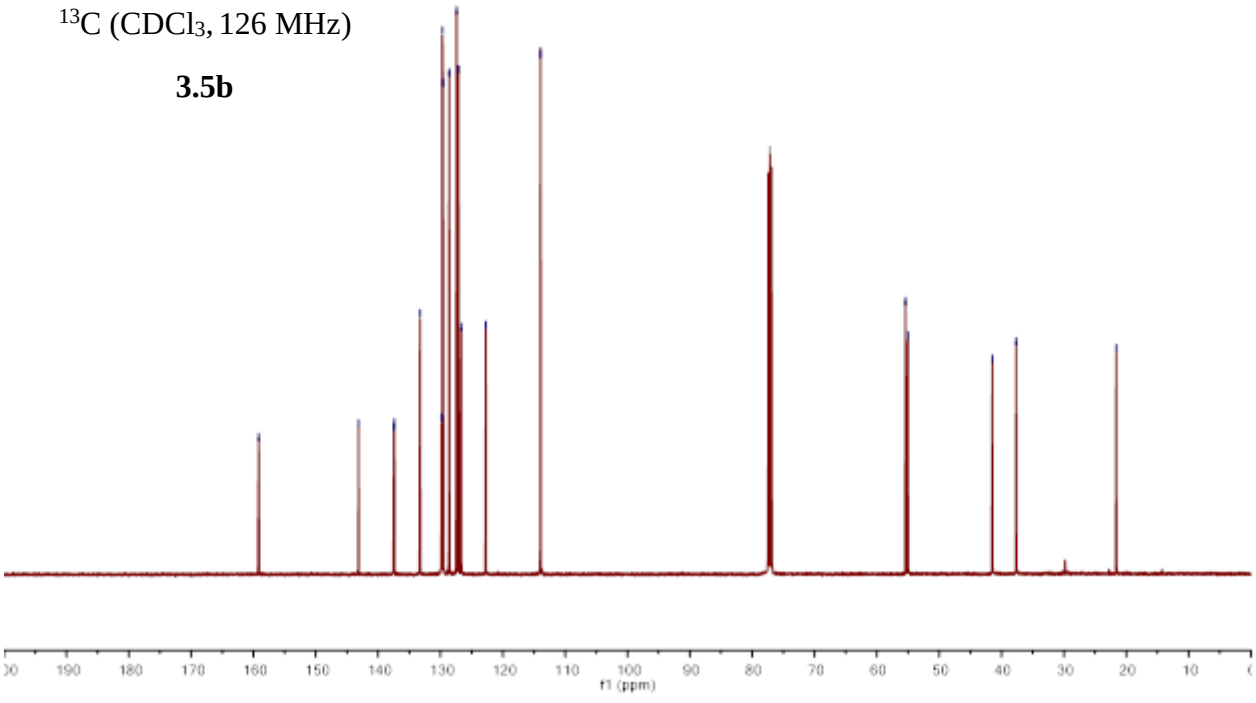

^{1}H ($CDCl_3$, 500 MHz)

3.5c

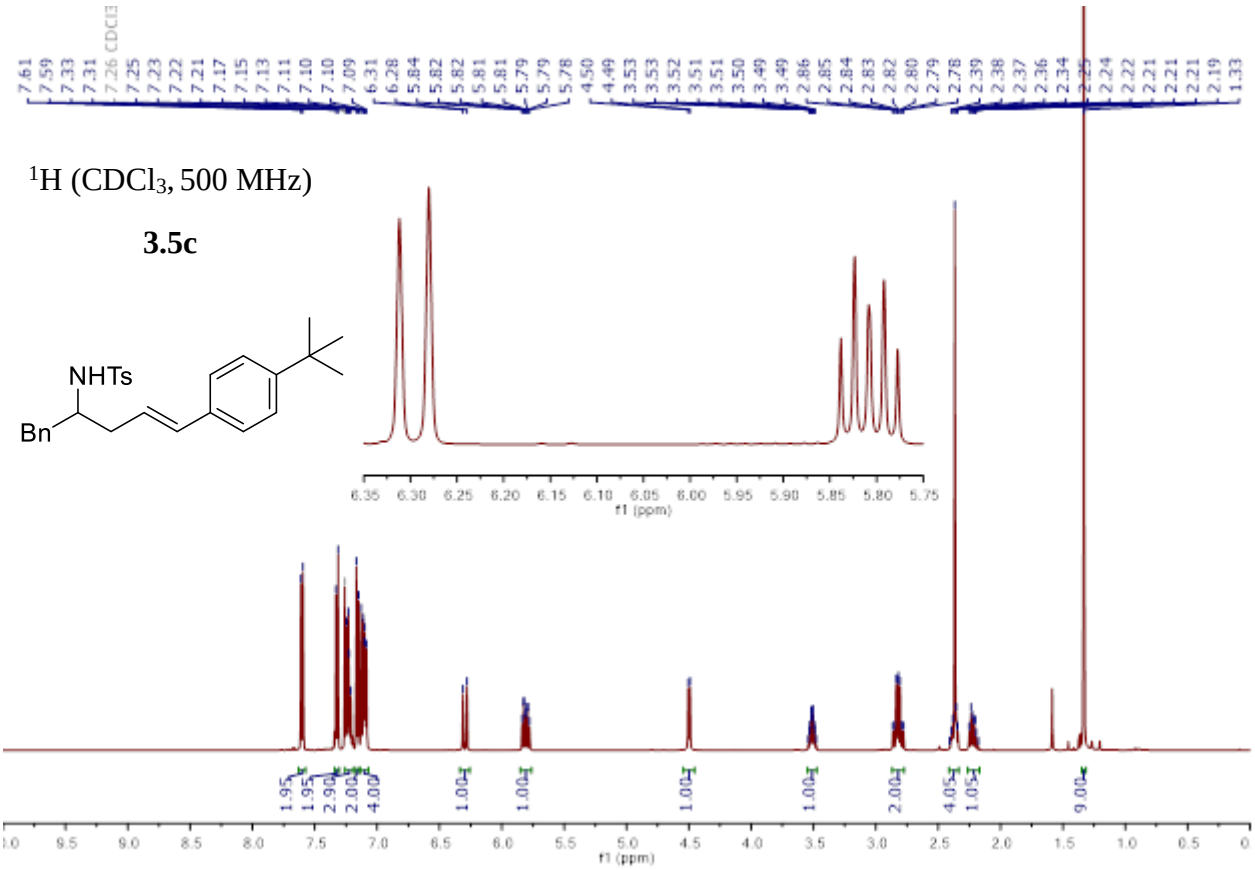

^{13}C ($CDCl_3$, 126 MHz)

3.5c

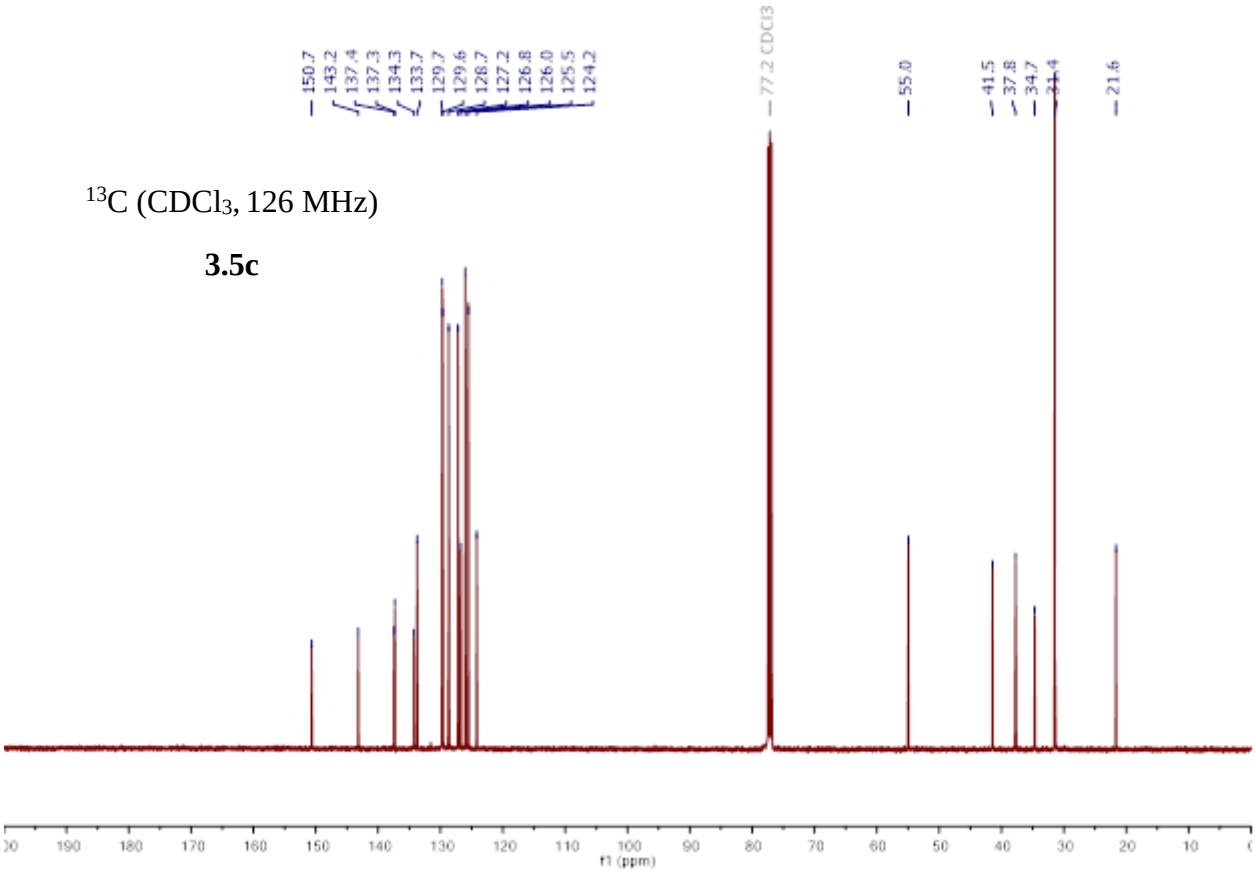

^{1}H ($CDCl_3$, 500 MHz)

3.5a

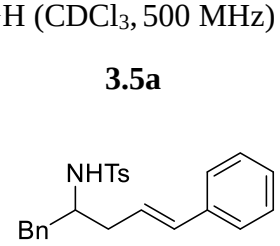

^{13}C ($CDCl_3$, 126 MHz)

3.5a

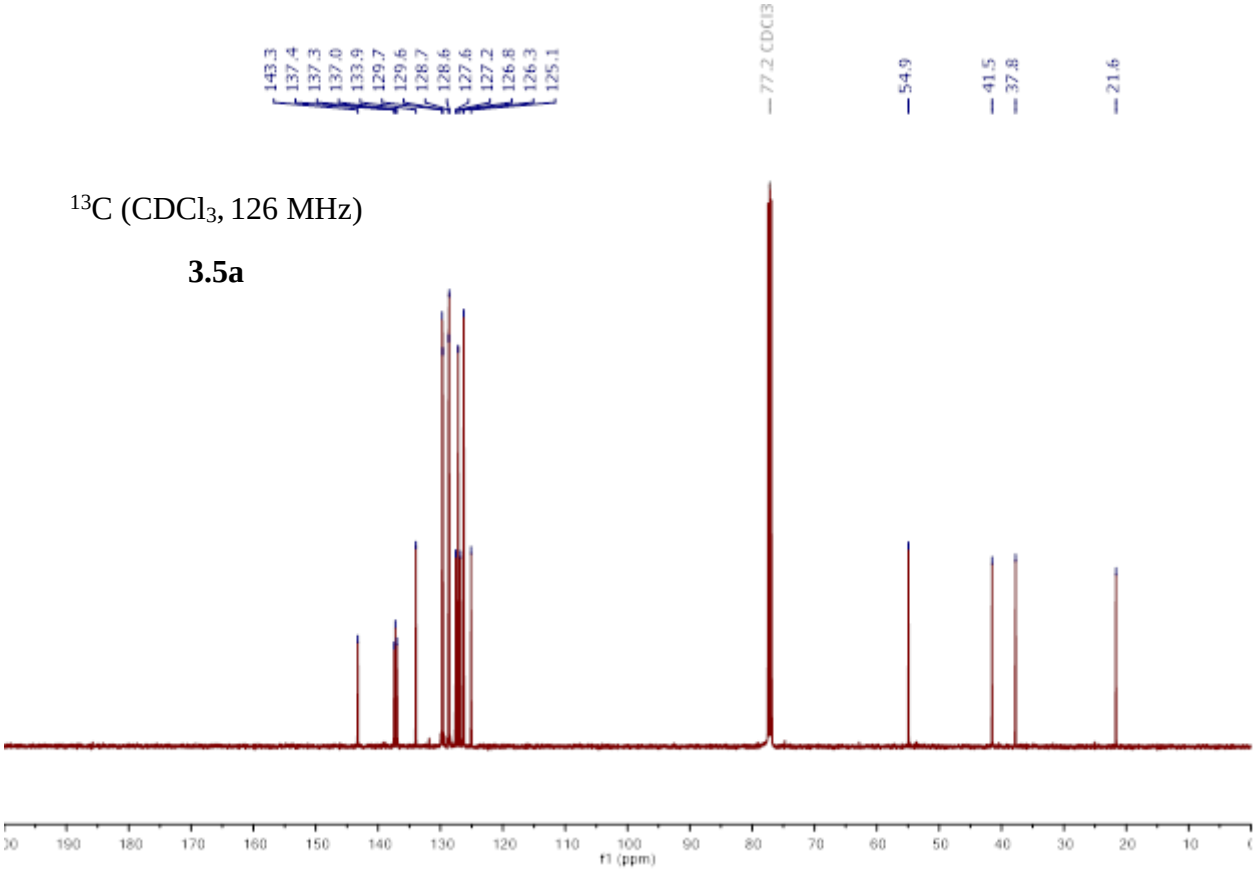

^{1}H ($CDCl_3$, 400 MHz)

3.5d

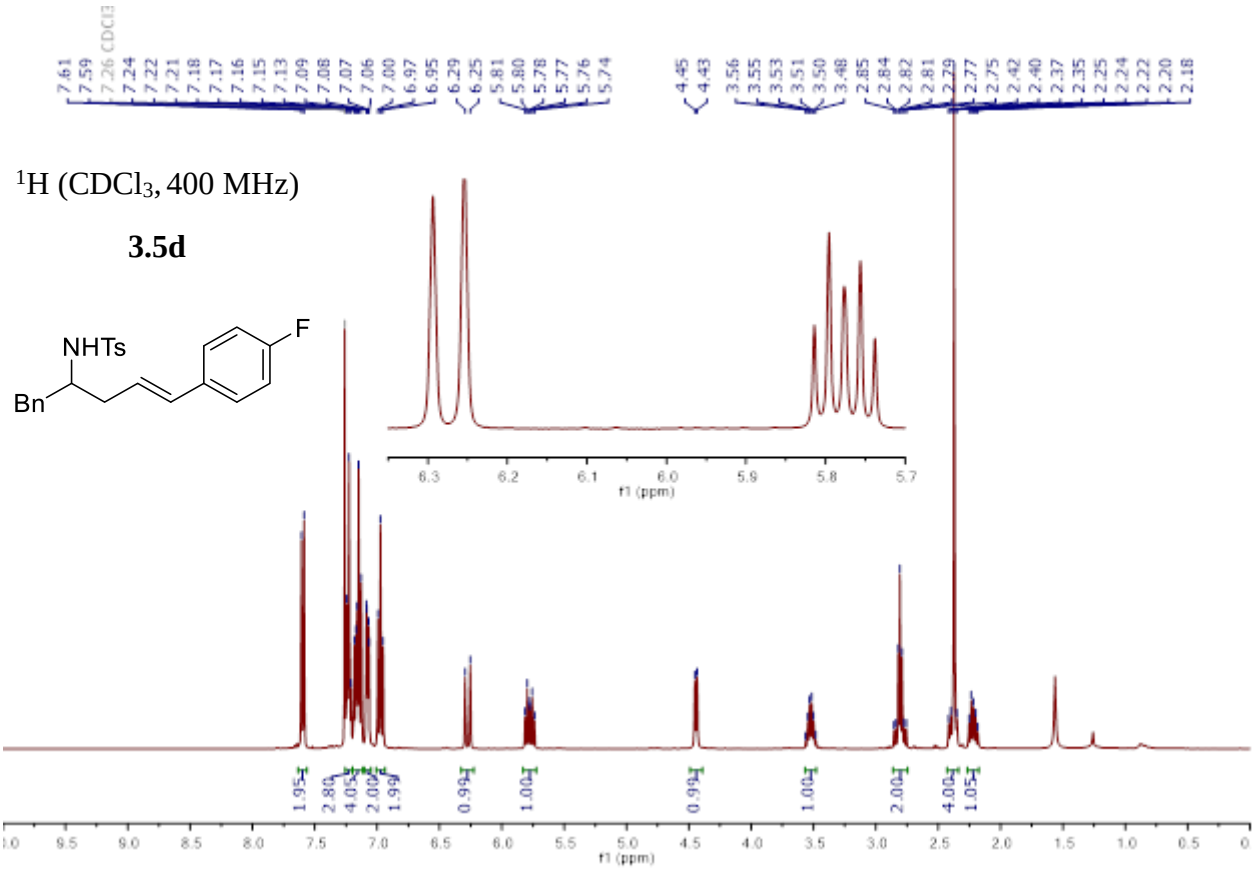

^{13}C ($CDCl_3$, 101 MHz)

3.5d

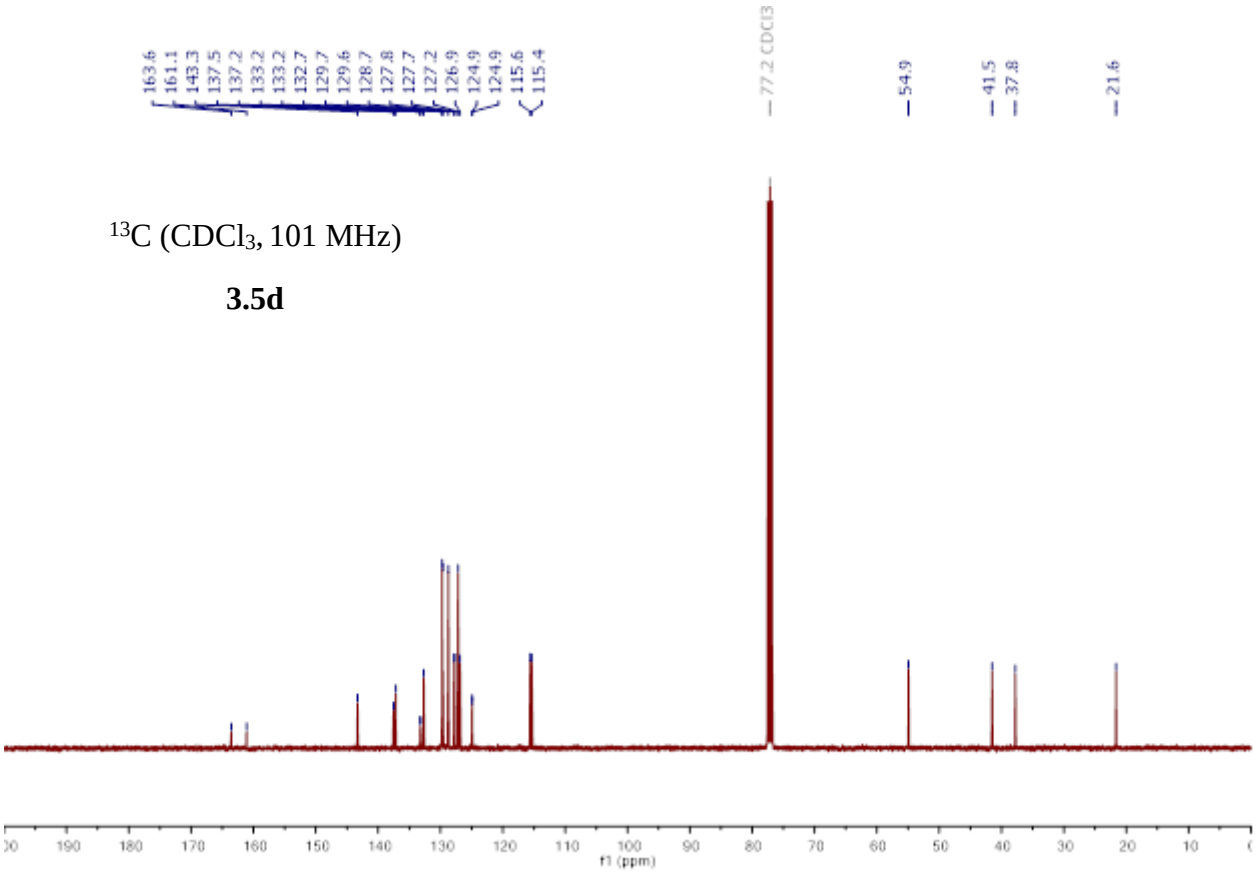

^{19}F ($CDCl_3$, 376 MHz)

Proton-decoupled

3.5d

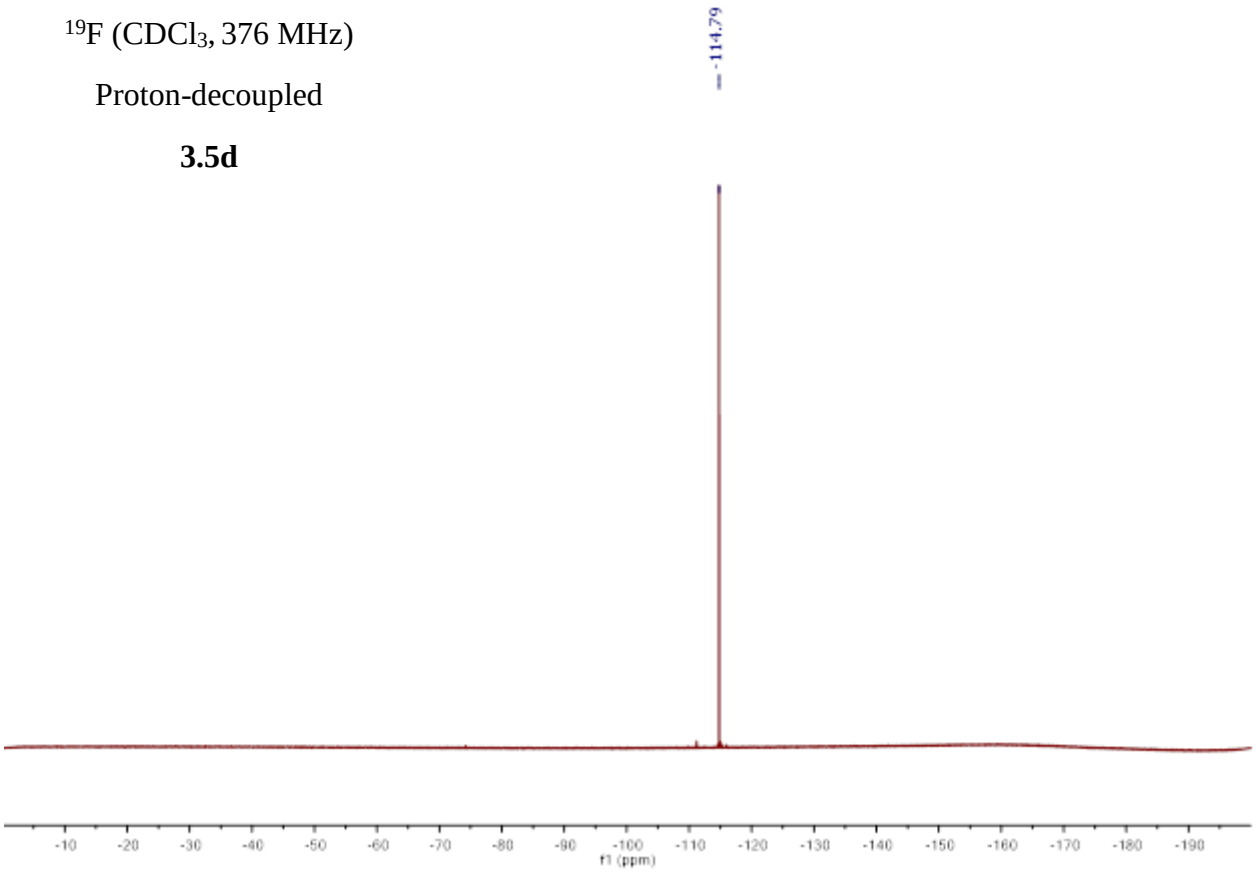

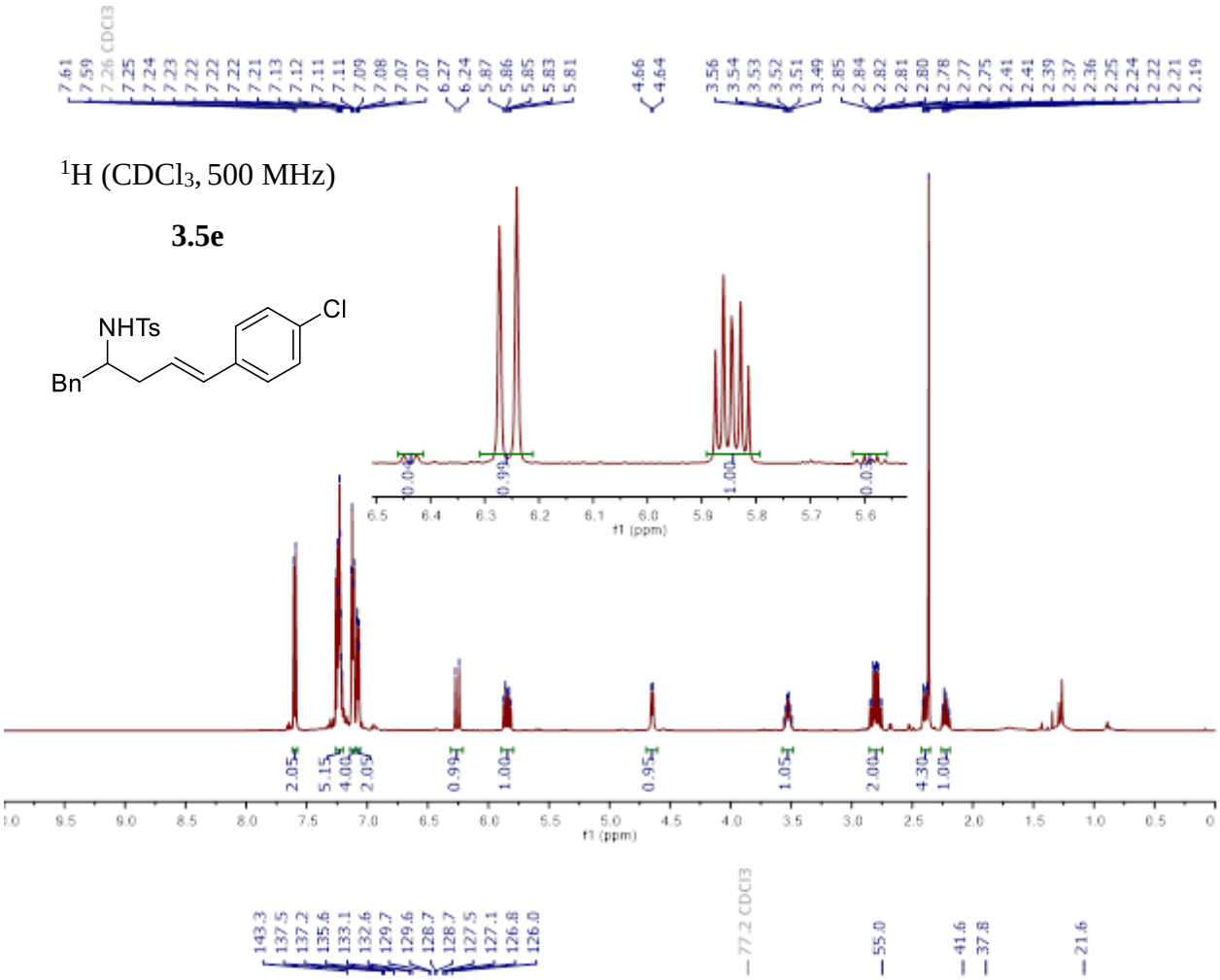

^{1}H ($CDCl_3$, 500 MHz)

3.5e

^{13}C ($CDCl_3$, 126 MHz)

3.5e

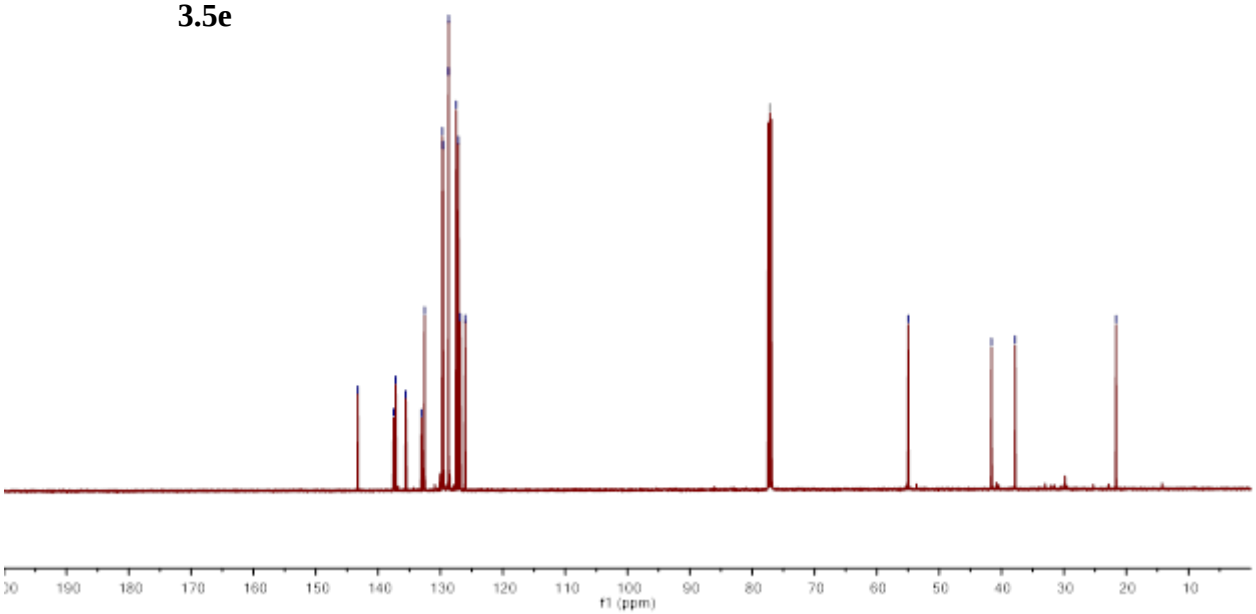

^{1}H ($CDCl_3$, 500 MHz)

3.5f

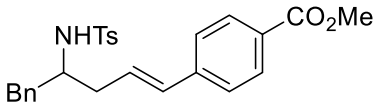

^{13}C ($CDCl_3$, 126 MHz)

3.5f

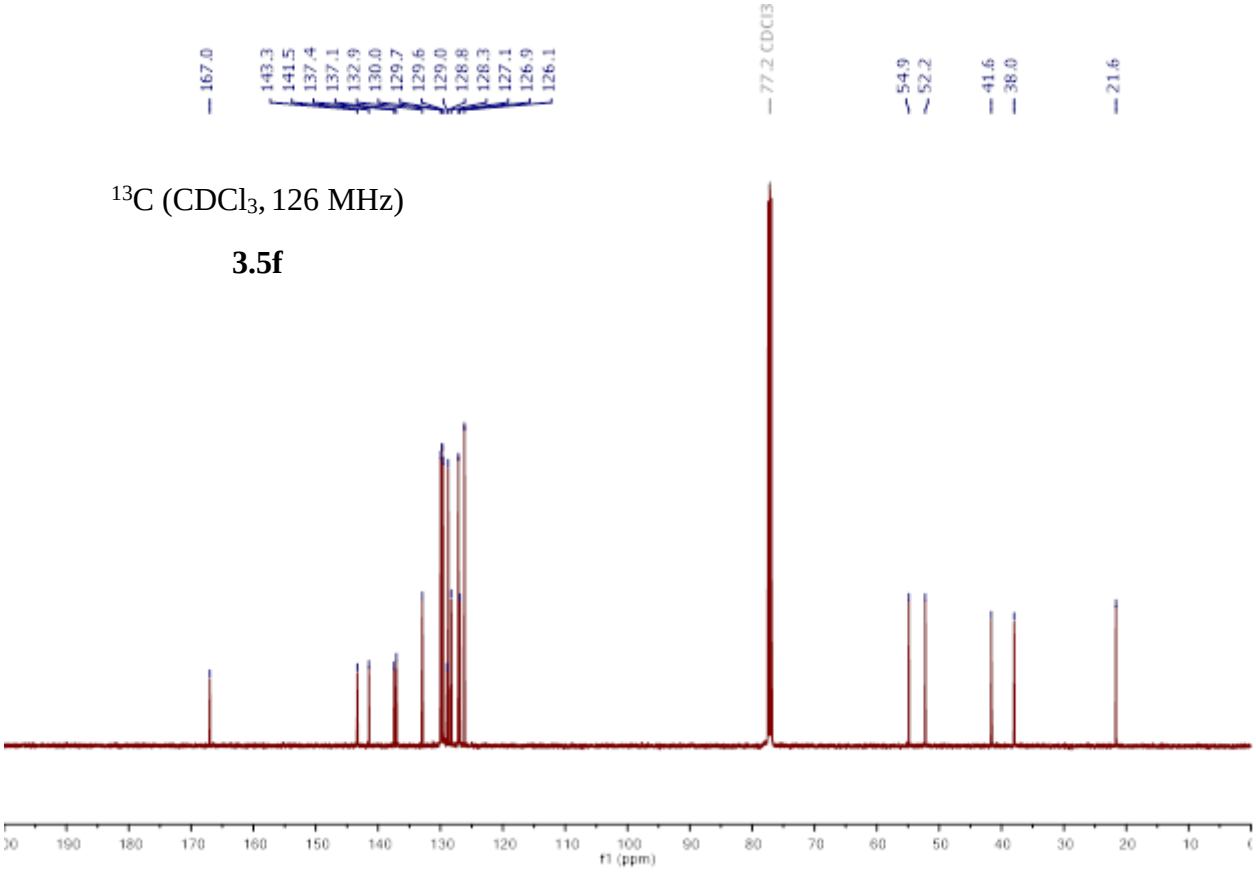

^{1}H ($CDCl_3$, 500 MHz)

3.5g

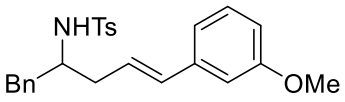

^{13}C ($CDCl_3$, 126 MHz)

3.5g

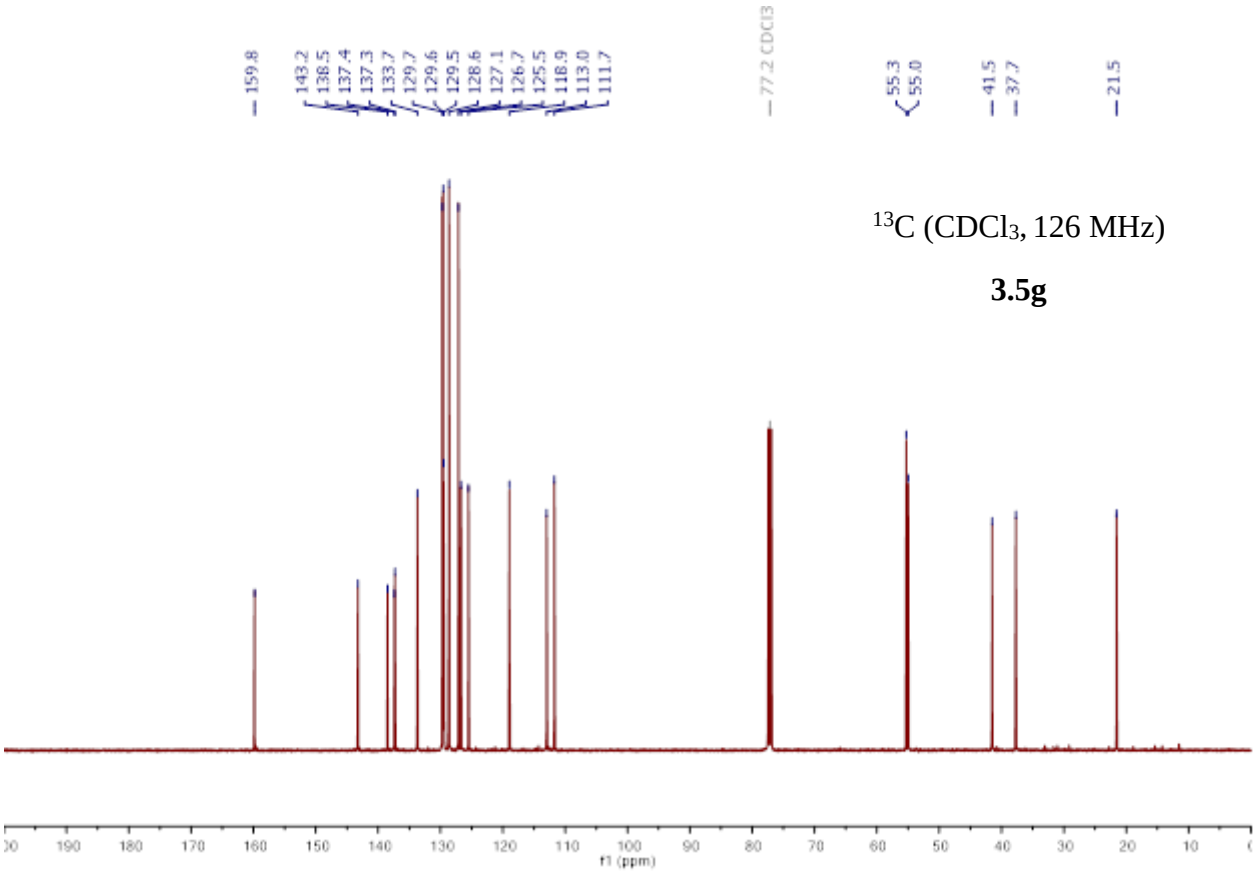

^{1}H ($CDCl_3$, 400 MHz)

3.5h

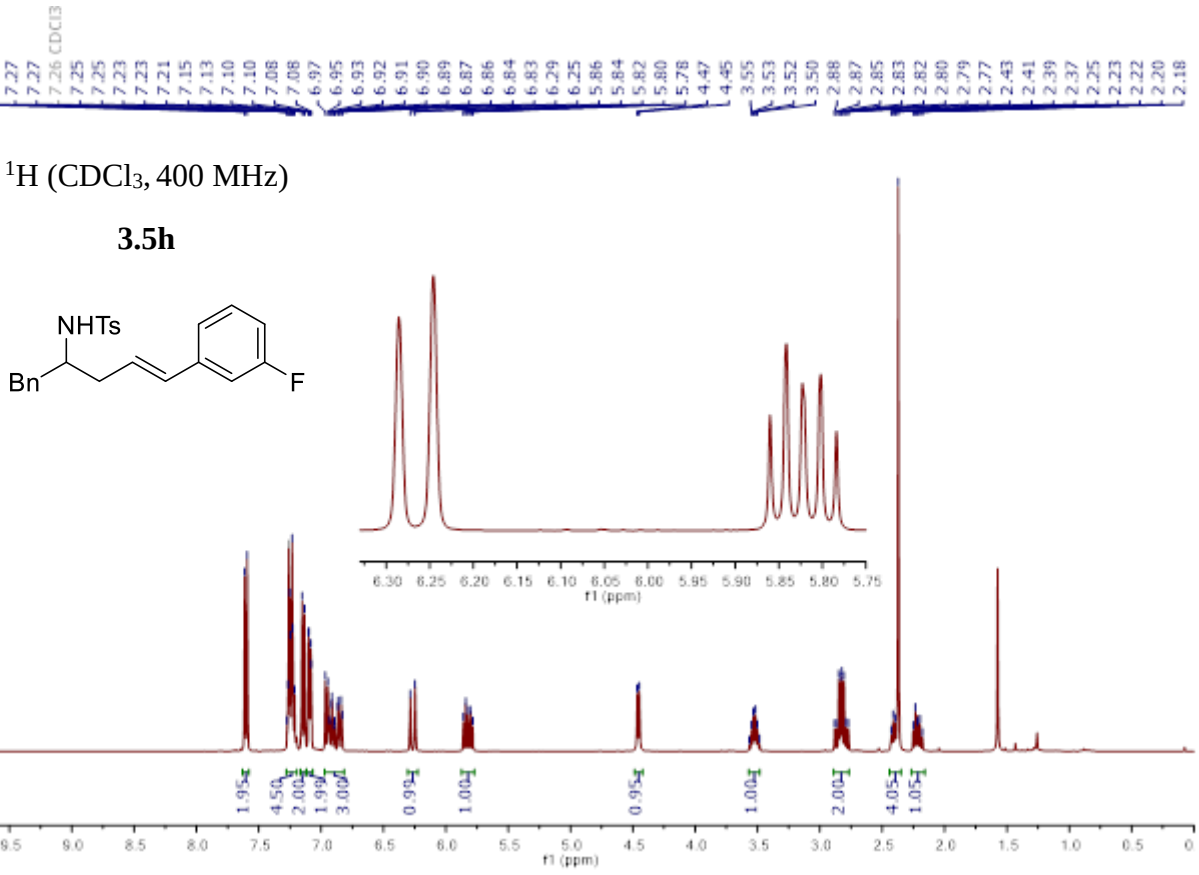

^{13}C ($CDCl_3$, 101 MHz)

3.5h

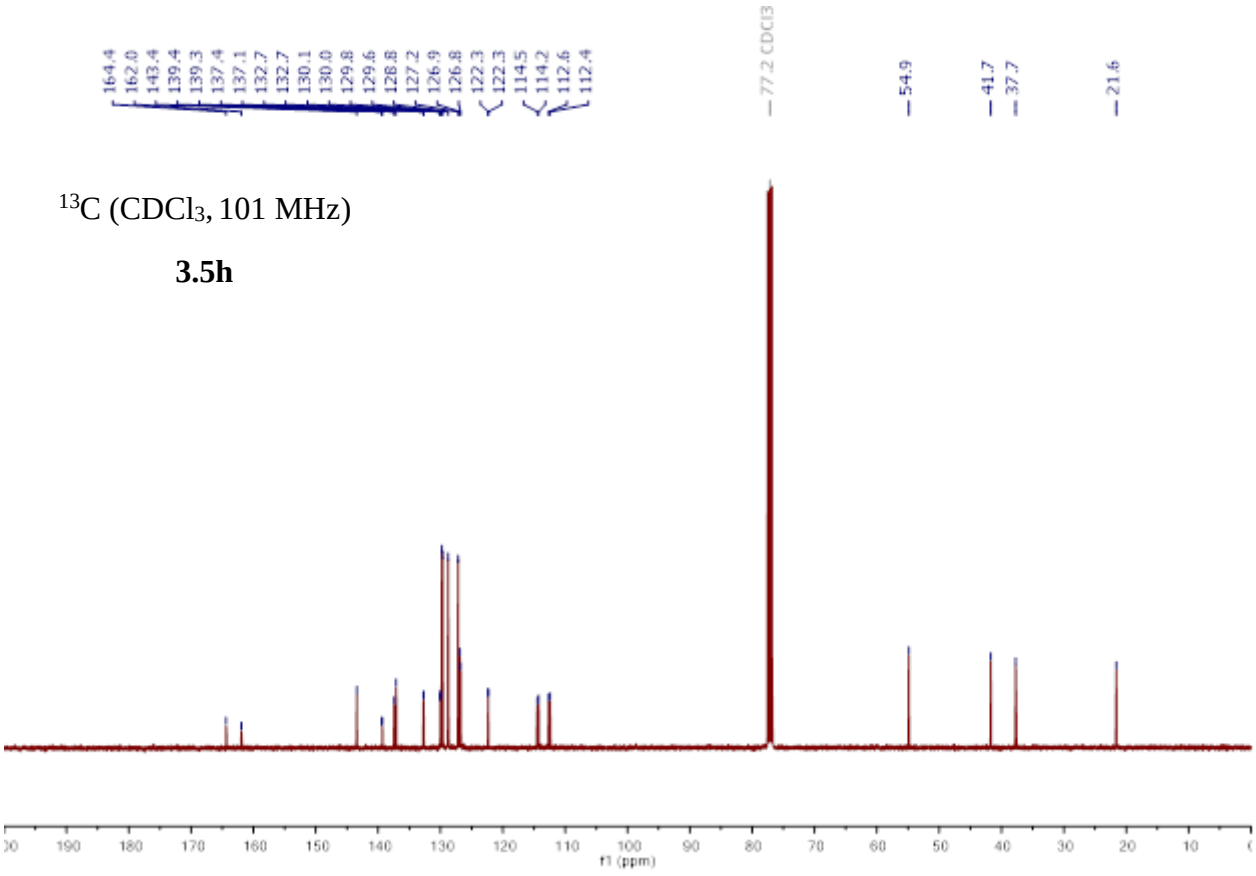

^{19}F ($CDCl_3$, 376 MHz)

Proton-decoupled

3.5h

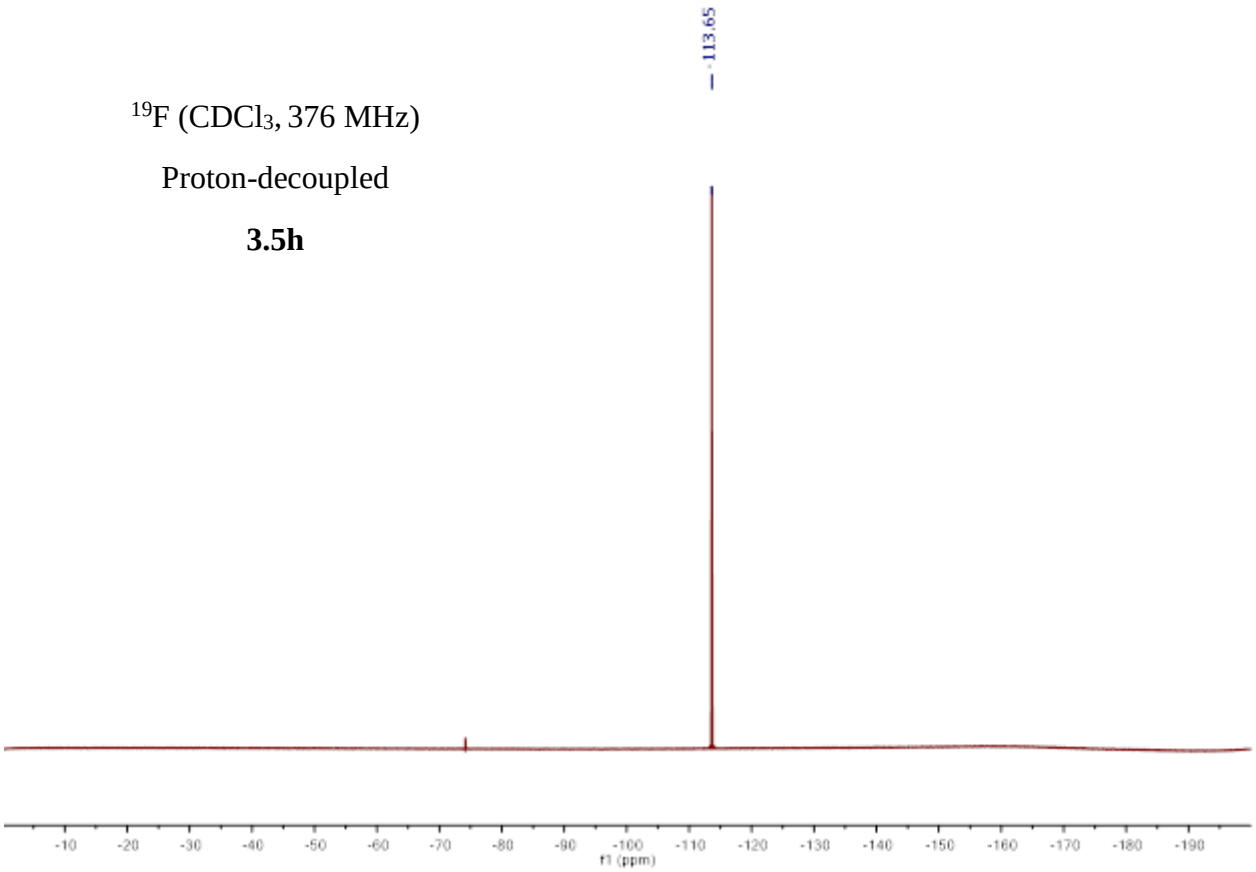

^{1}H ($CDCl_3$, 500 MHz)

3.5i

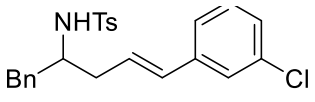

^{13}C ($CDCl_3$, 126 MHz)

3.5i

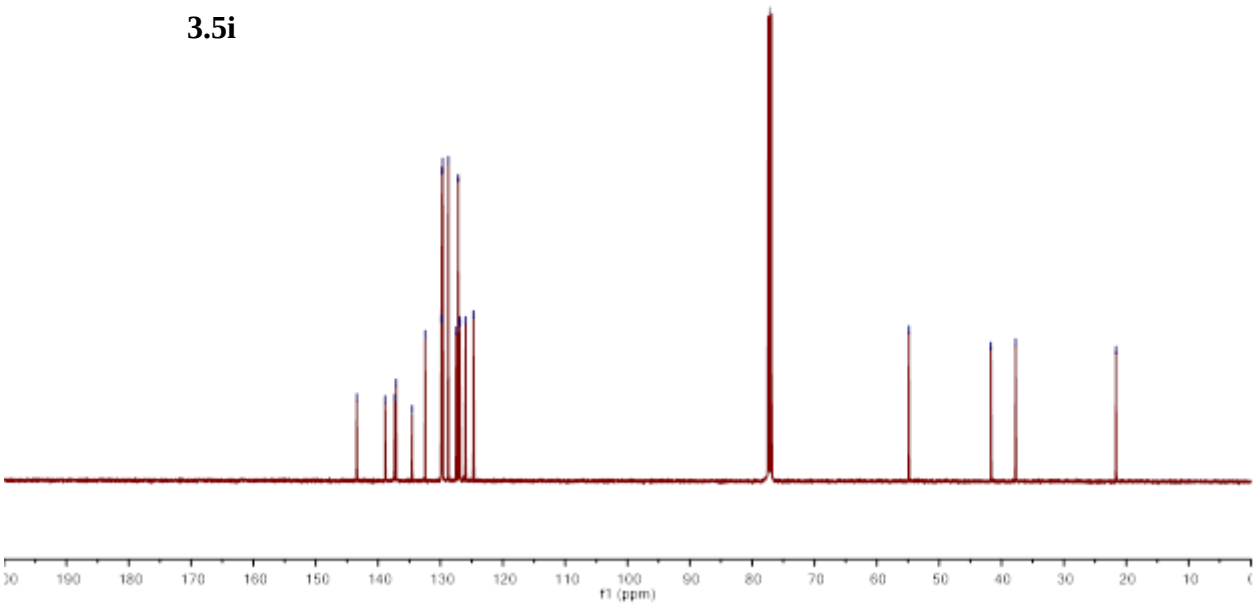

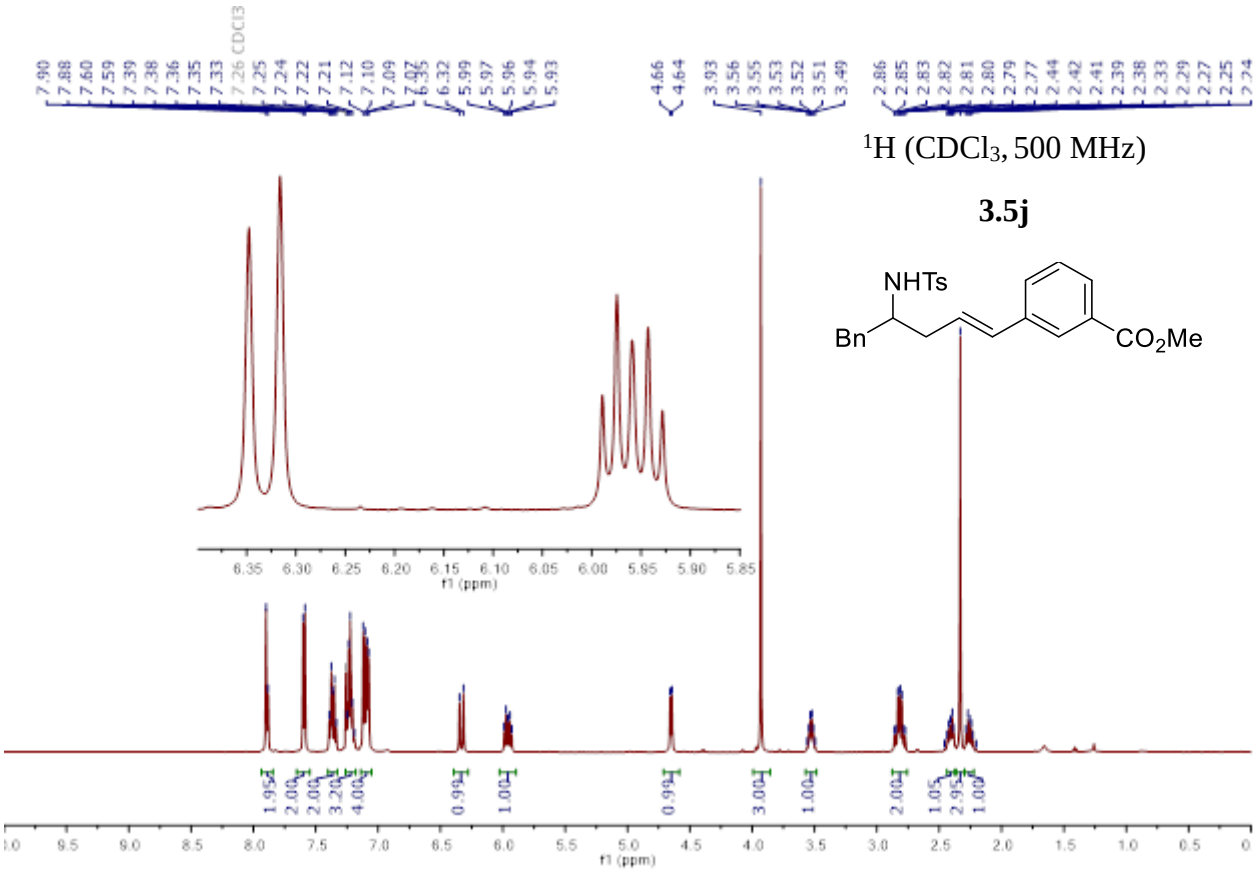

^{1}H ($CDCl_3$, 500 MHz)

3.5j

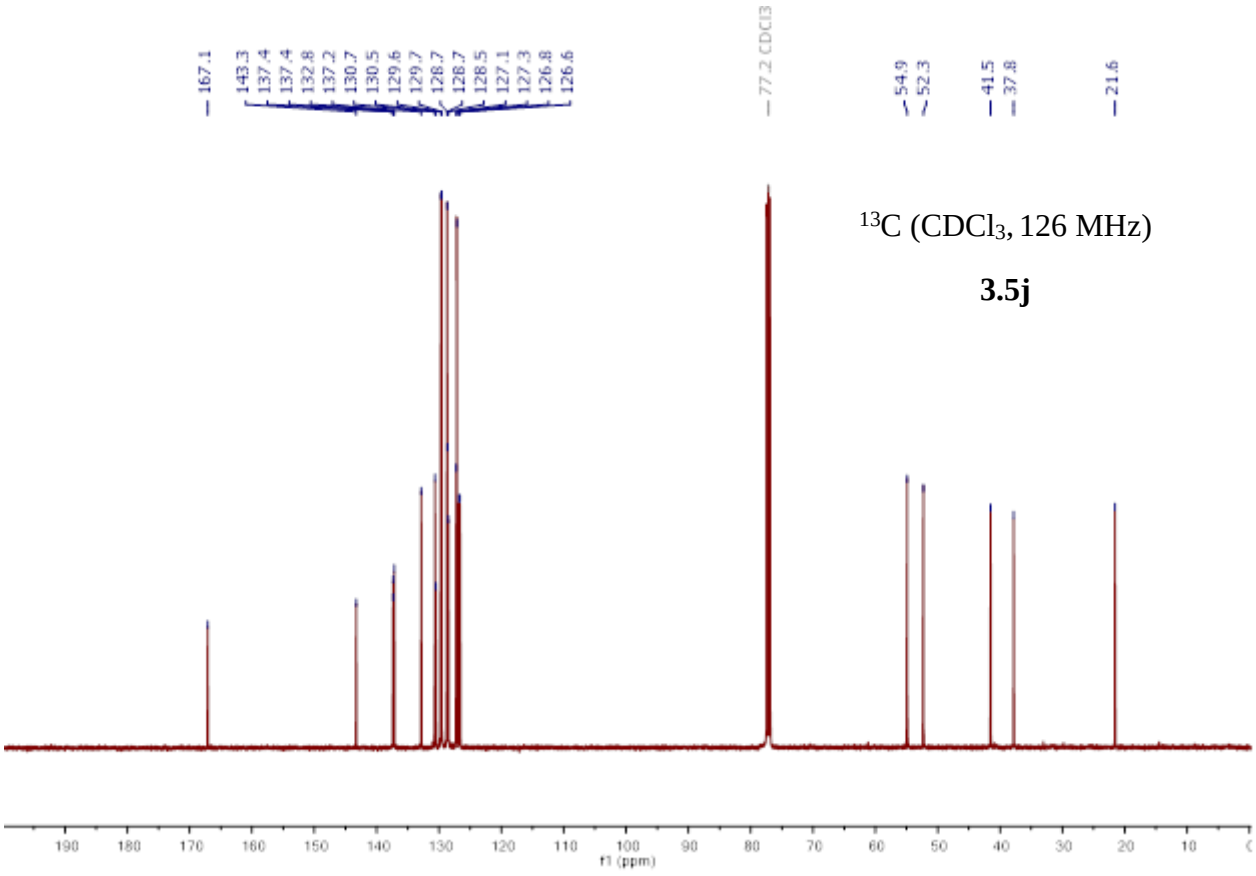

^{13}C ($CDCl_3$, 126 MHz)

3.5j

^{1}H ($CDCl_3$, 500 MHz)

3.5m

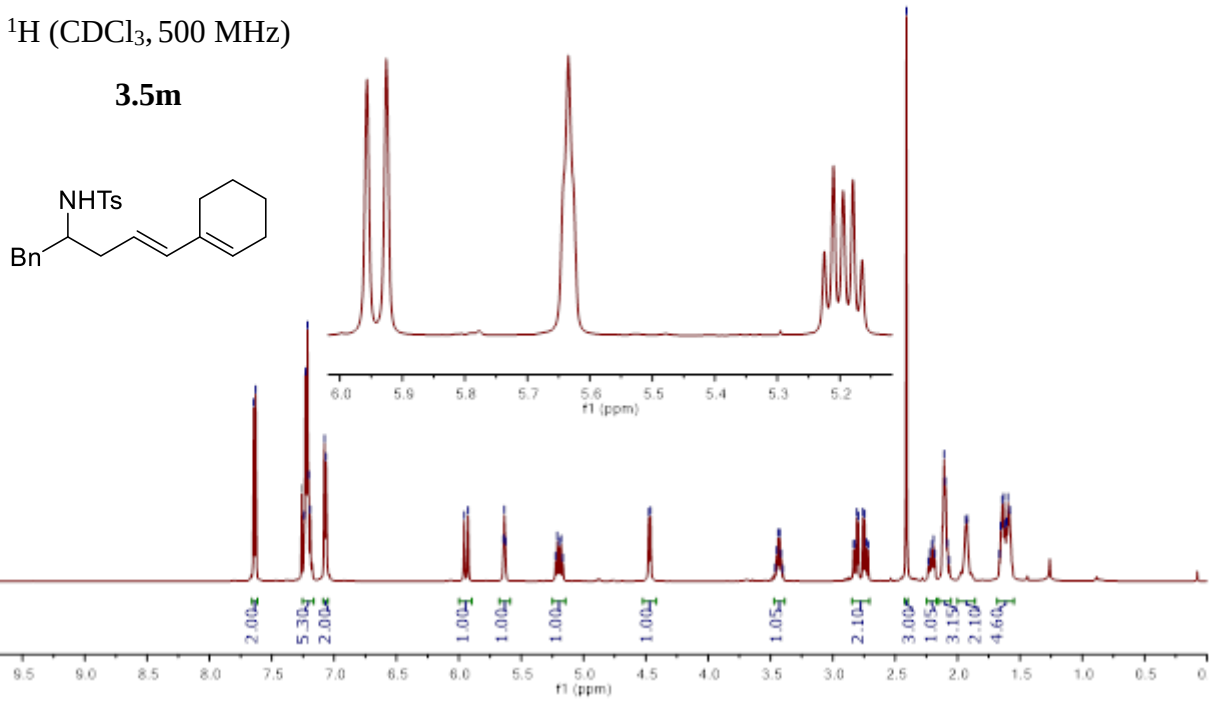

^{13}C ($CDCl_3$, 126 MHz)

3.5m

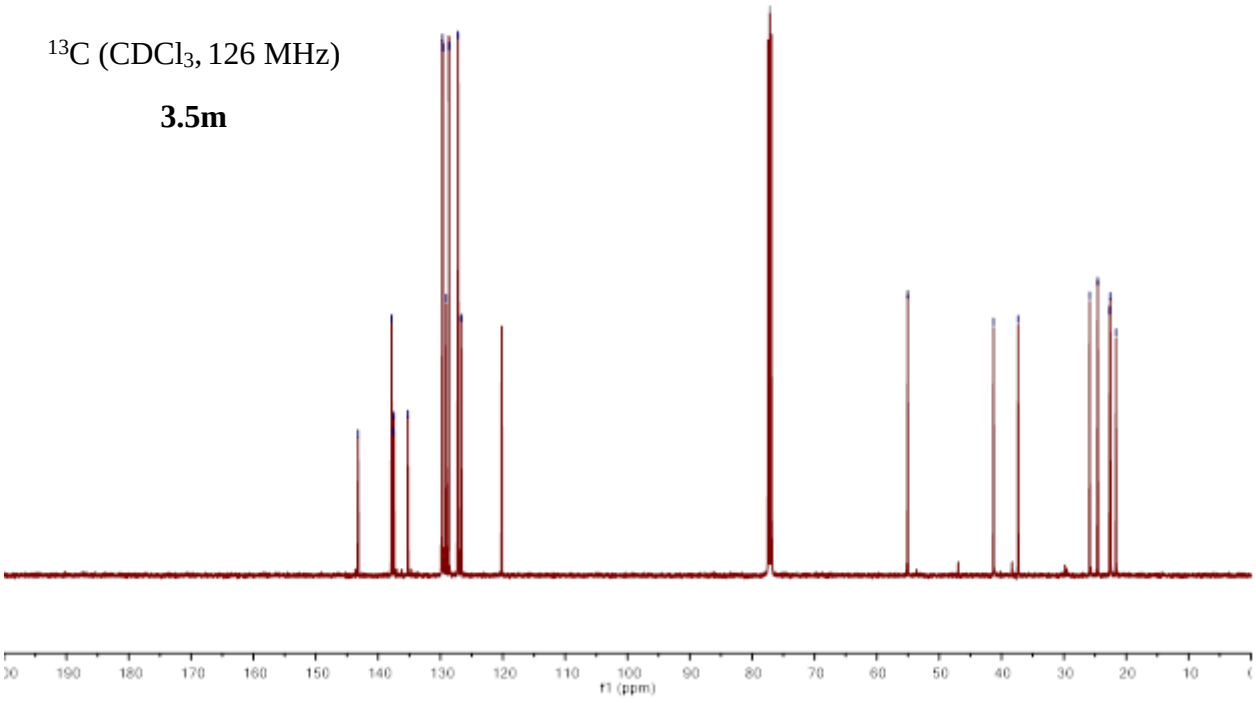

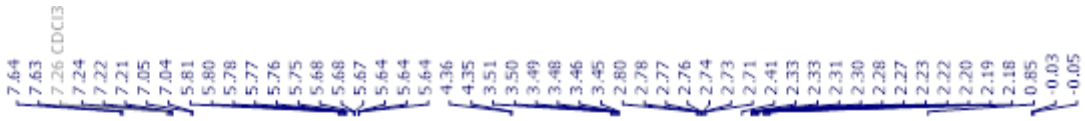

^{1}H ($CDCl_3$, 500 MHz)

3.5o

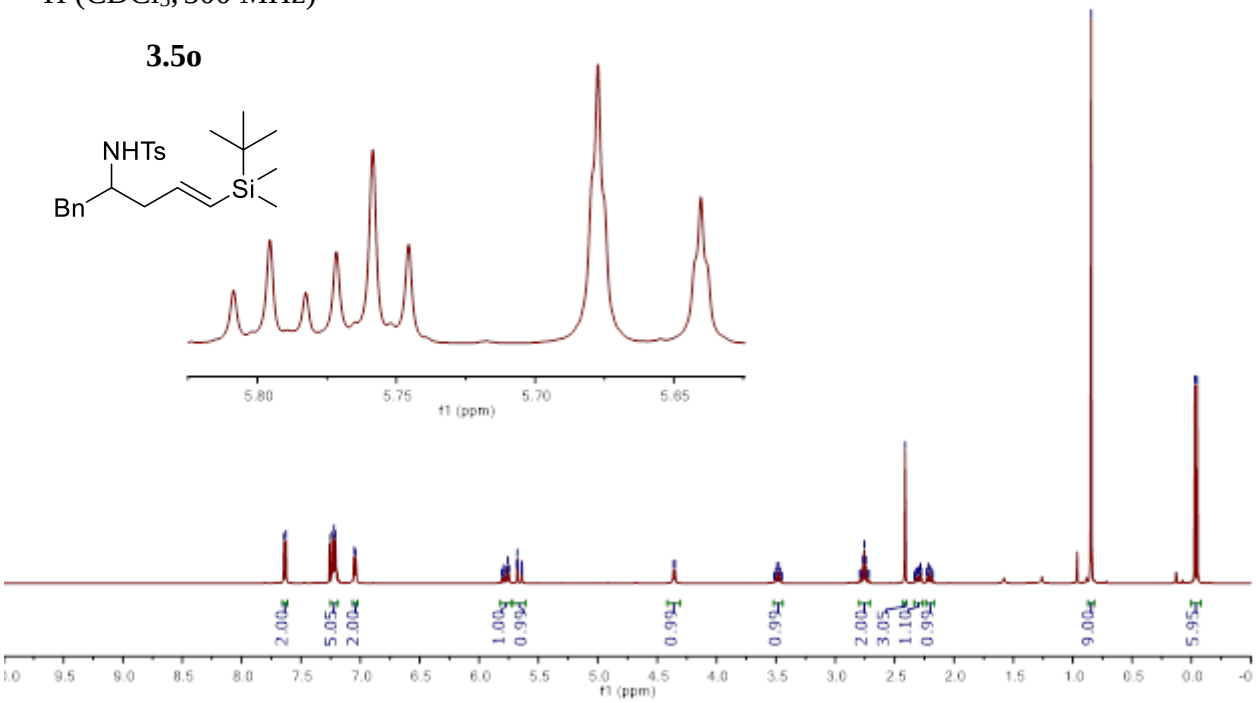

^{13}C ($CDCl_3$, 126 MHz)

3.5o

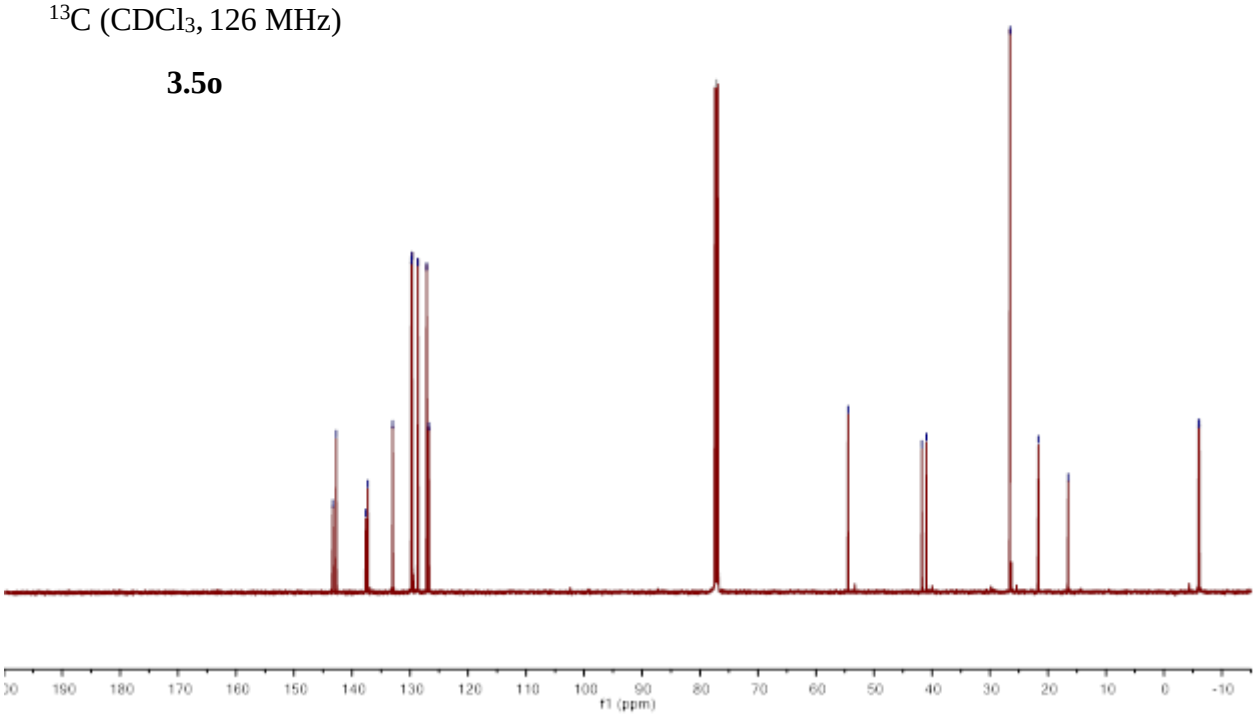

^{1}H ($CDCl_3$, 500 MHz)

(*R*)-**3.5b**

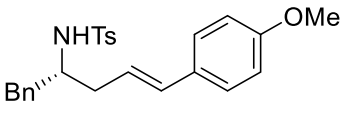

^{13}C ($CDCl_3$, 126 MHz)

(*R*)-**3.5b**

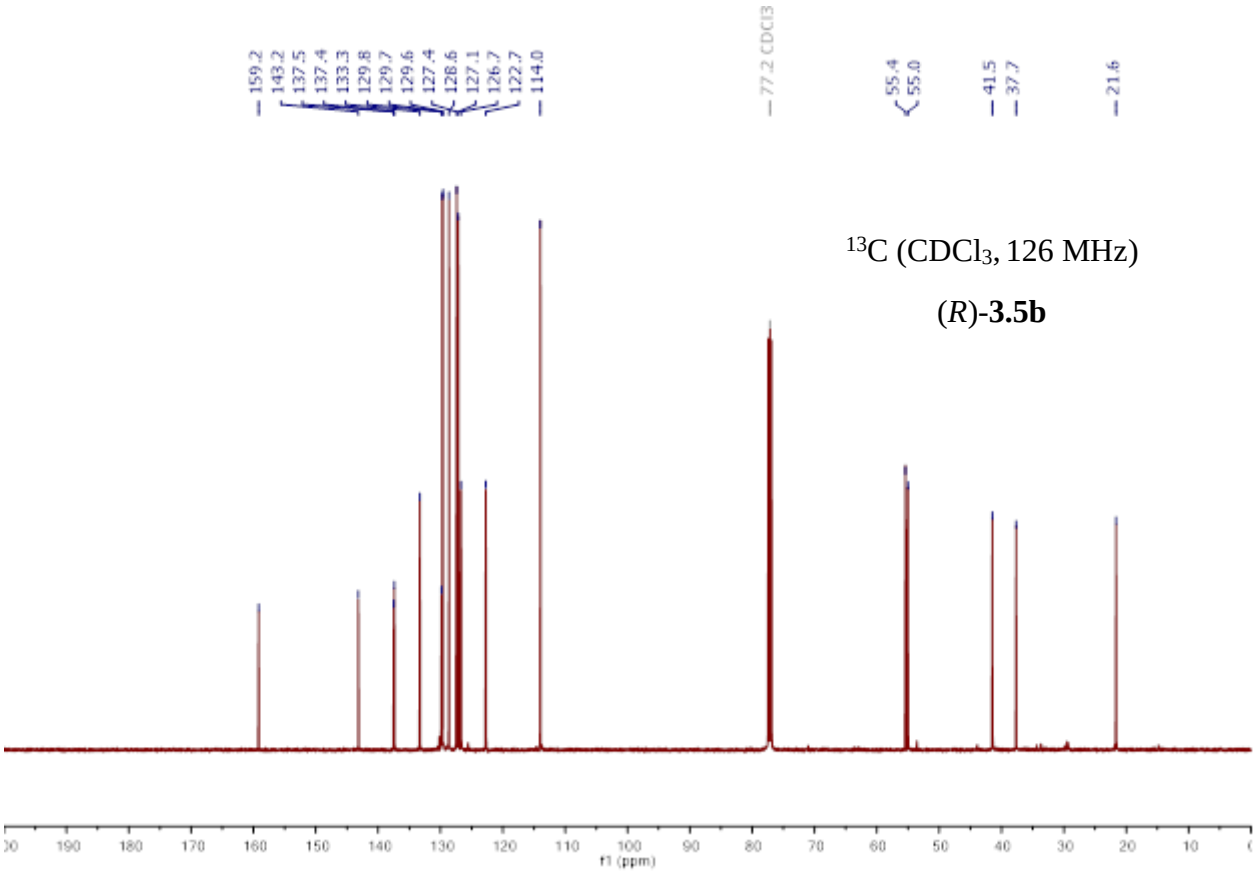

^{1}H ($CDCl_3$, 500 MHz)

3.5p

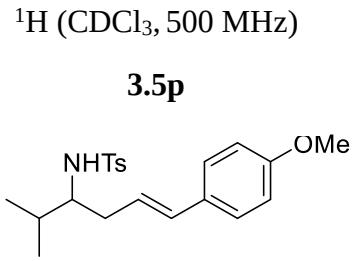

^{13}C ($CDCl_3$, 126 MHz)

3.5p

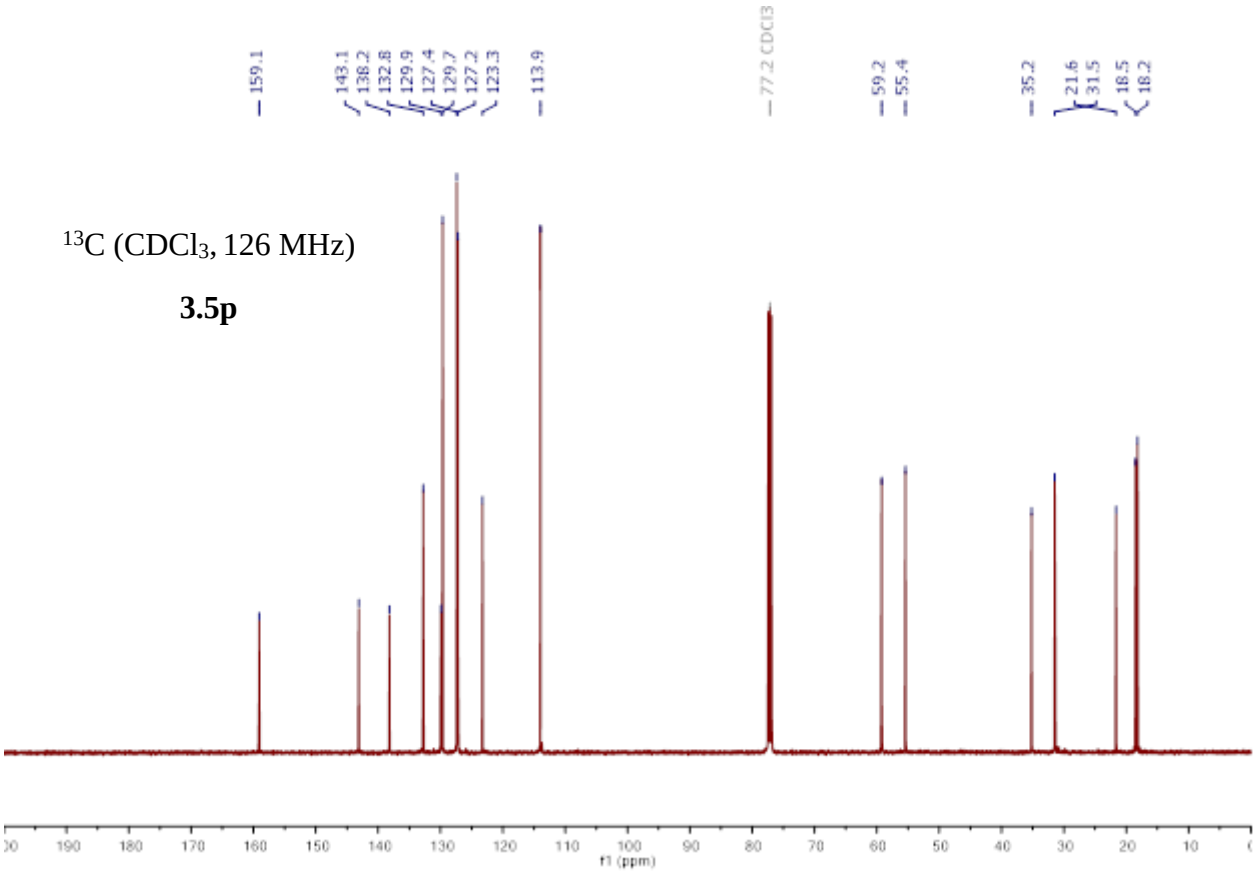

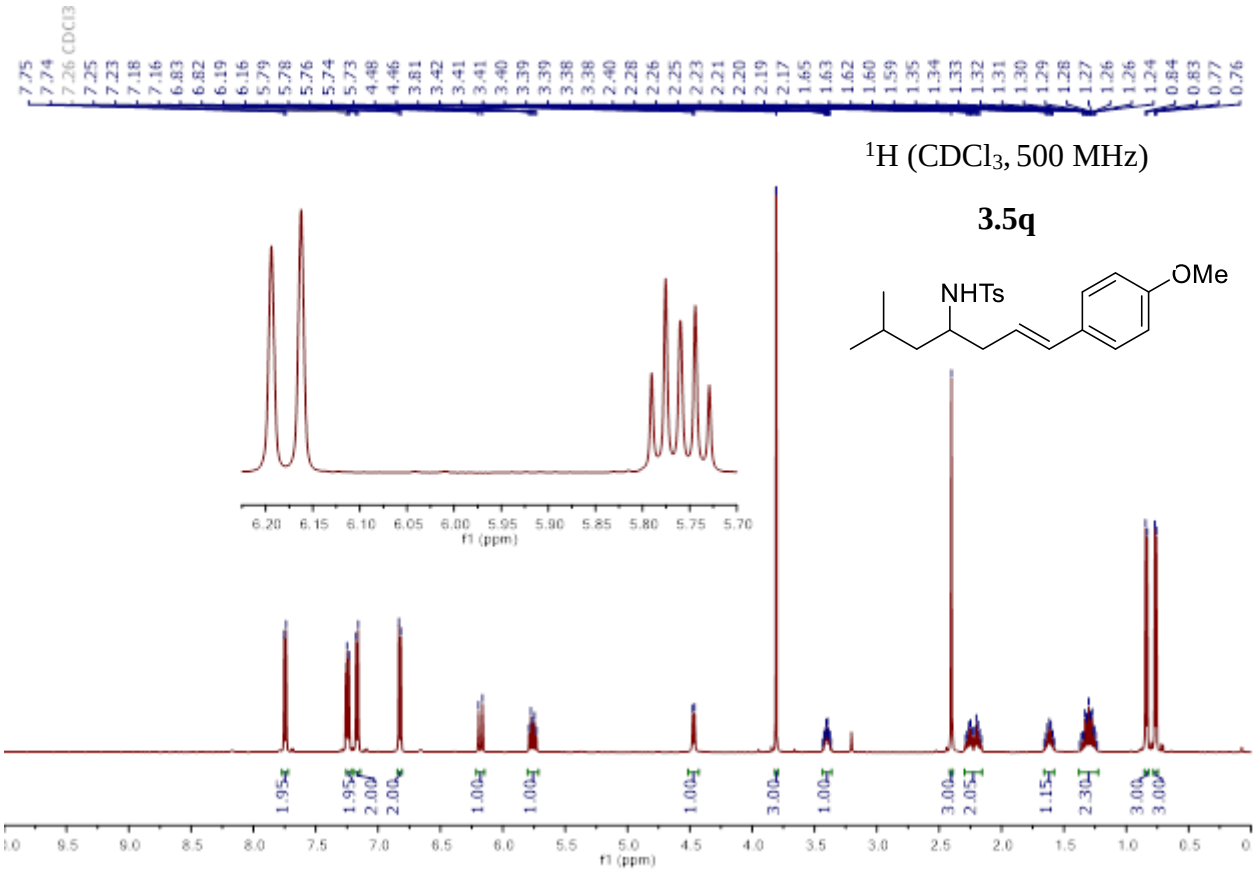

^{1}H ($CDCl_3$, 500 MHz)

3.5q

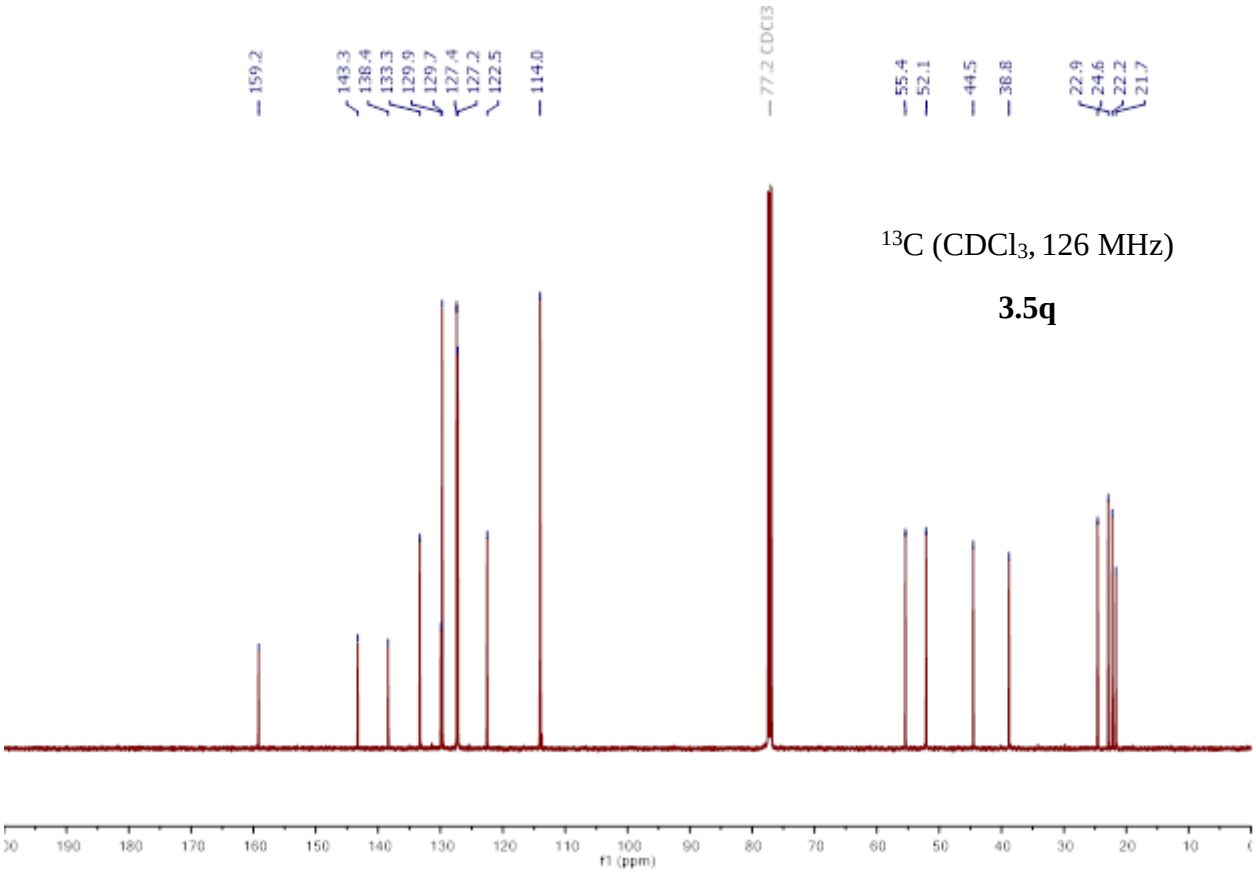

^{13}C ($CDCl_3$, 126 MHz)

3.5q

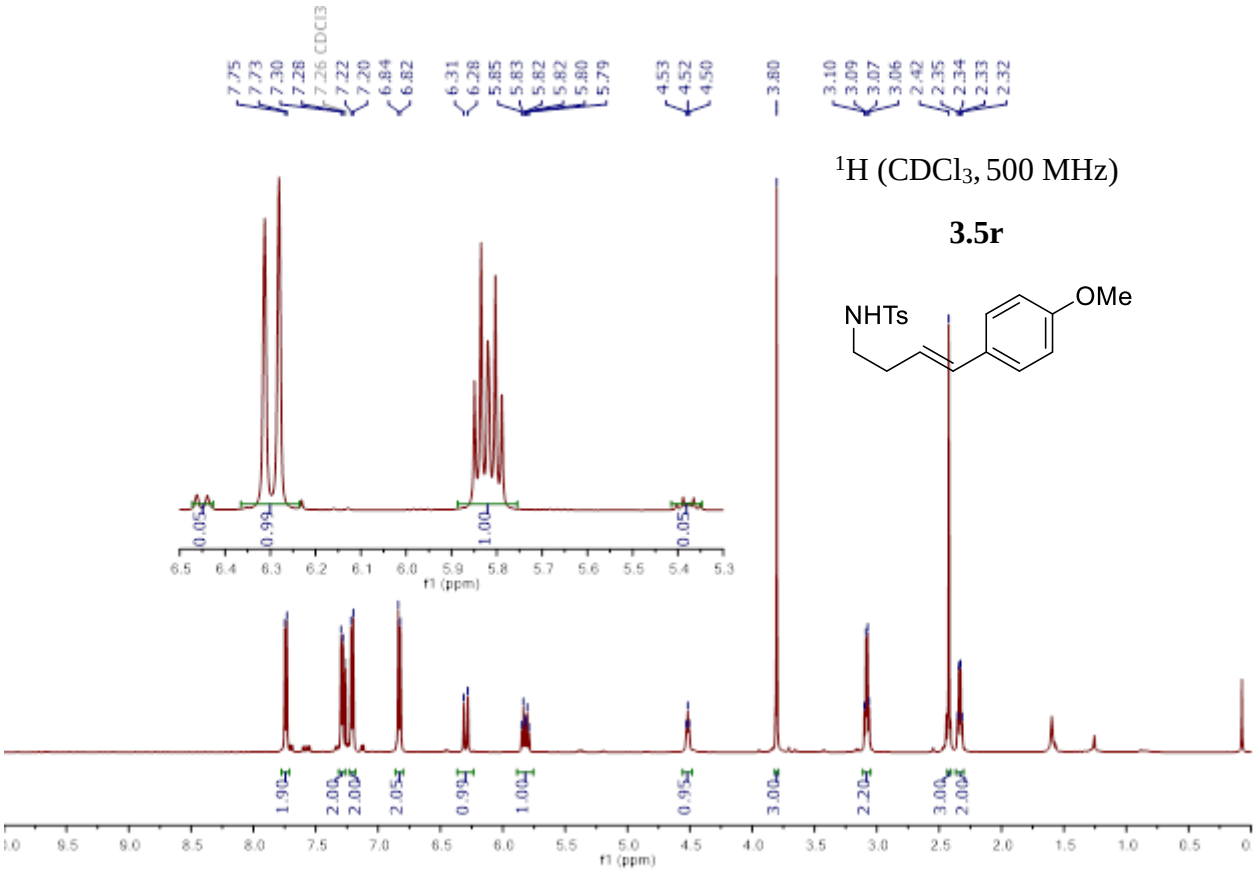

^{1}H ($CDCl_3$, 500 MHz)

3.5r

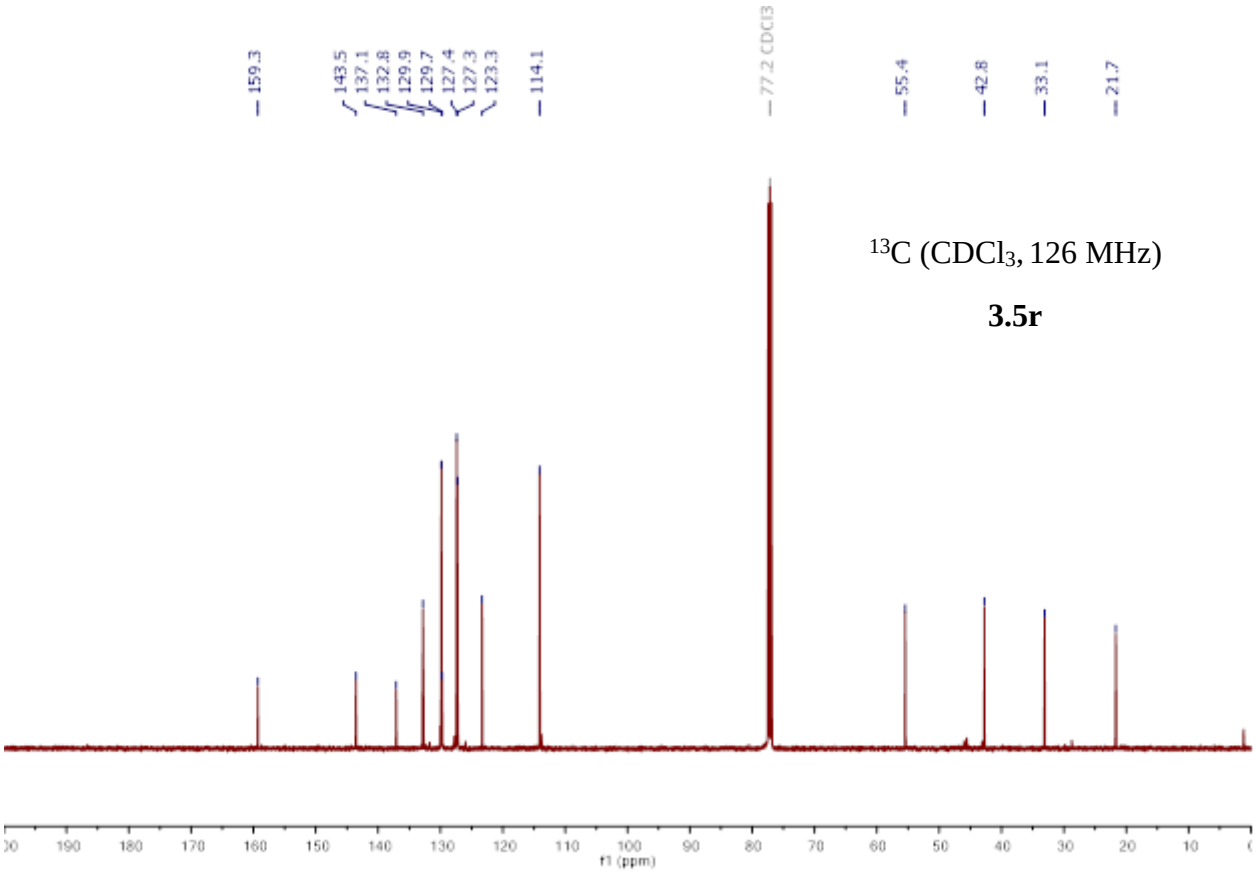

^{13}C ($CDCl_3$, 126 MHz)

3.5r

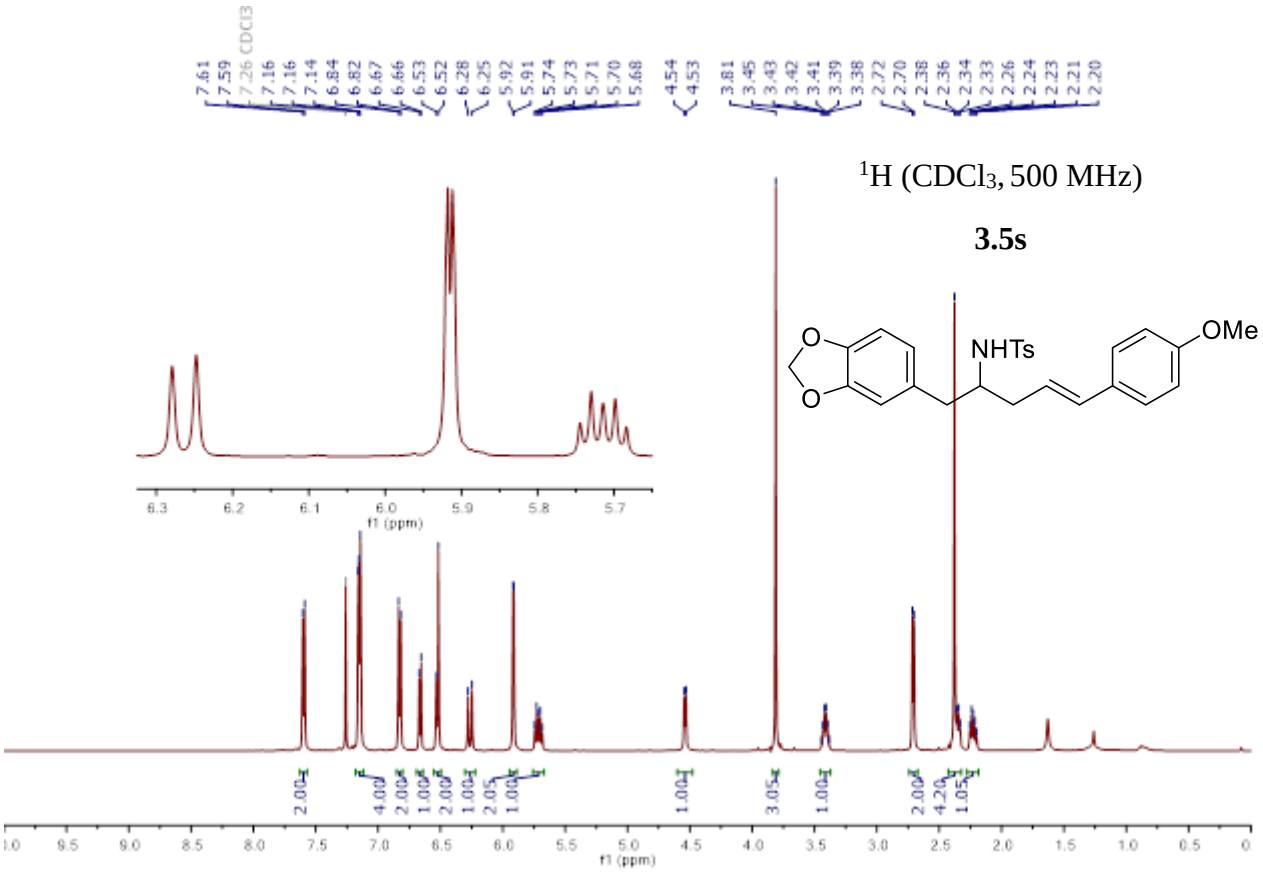

^{1}H ($CDCl_3$, 500 MHz)

3.5s

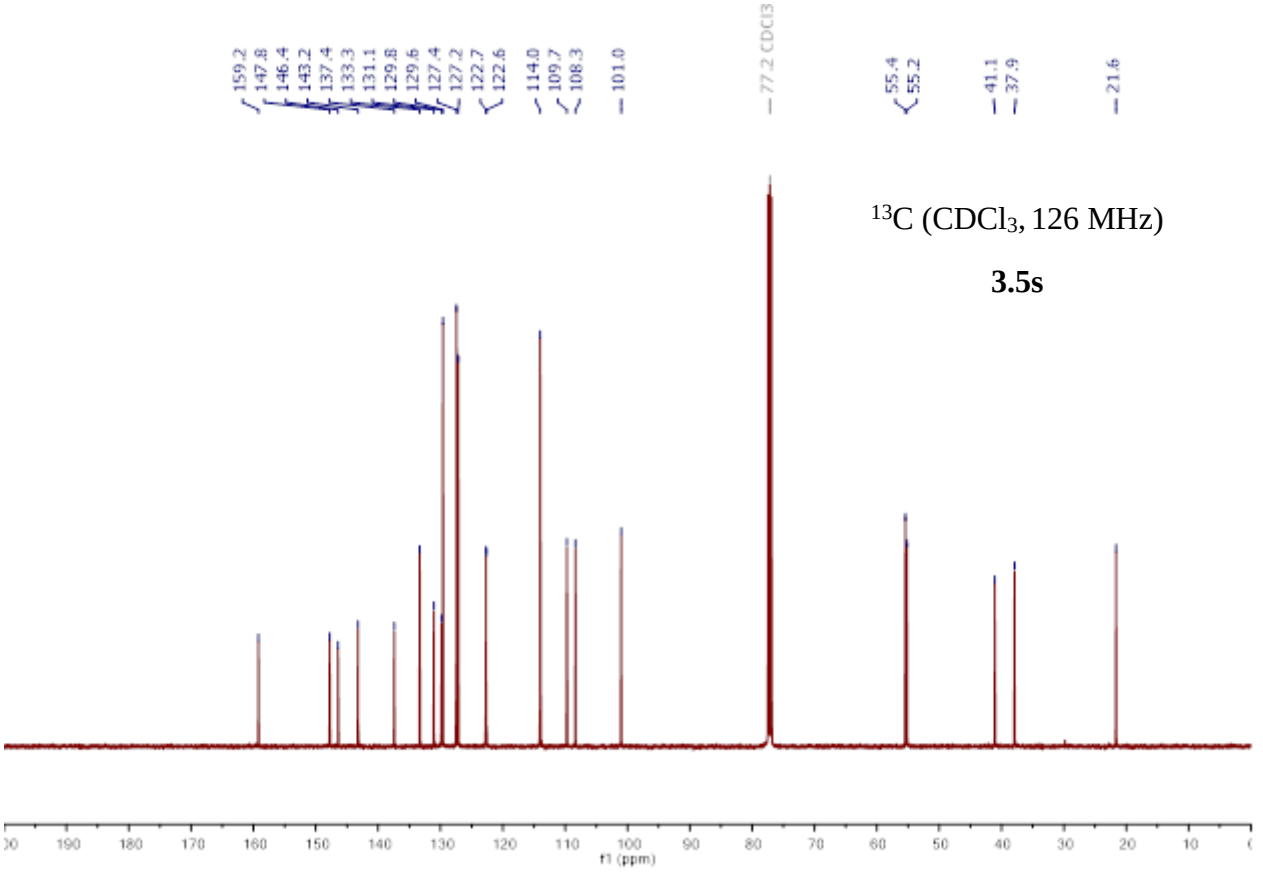

^{13}C ($CDCl_3$, 126 MHz)

3.5s

^{1}H ($CDCl_3$, 500 MHz)

3.5t

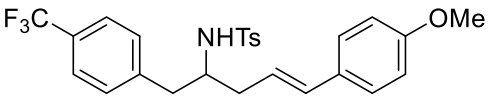

^{13}C ($CDCl_3$, 126 MHz)

3.5t

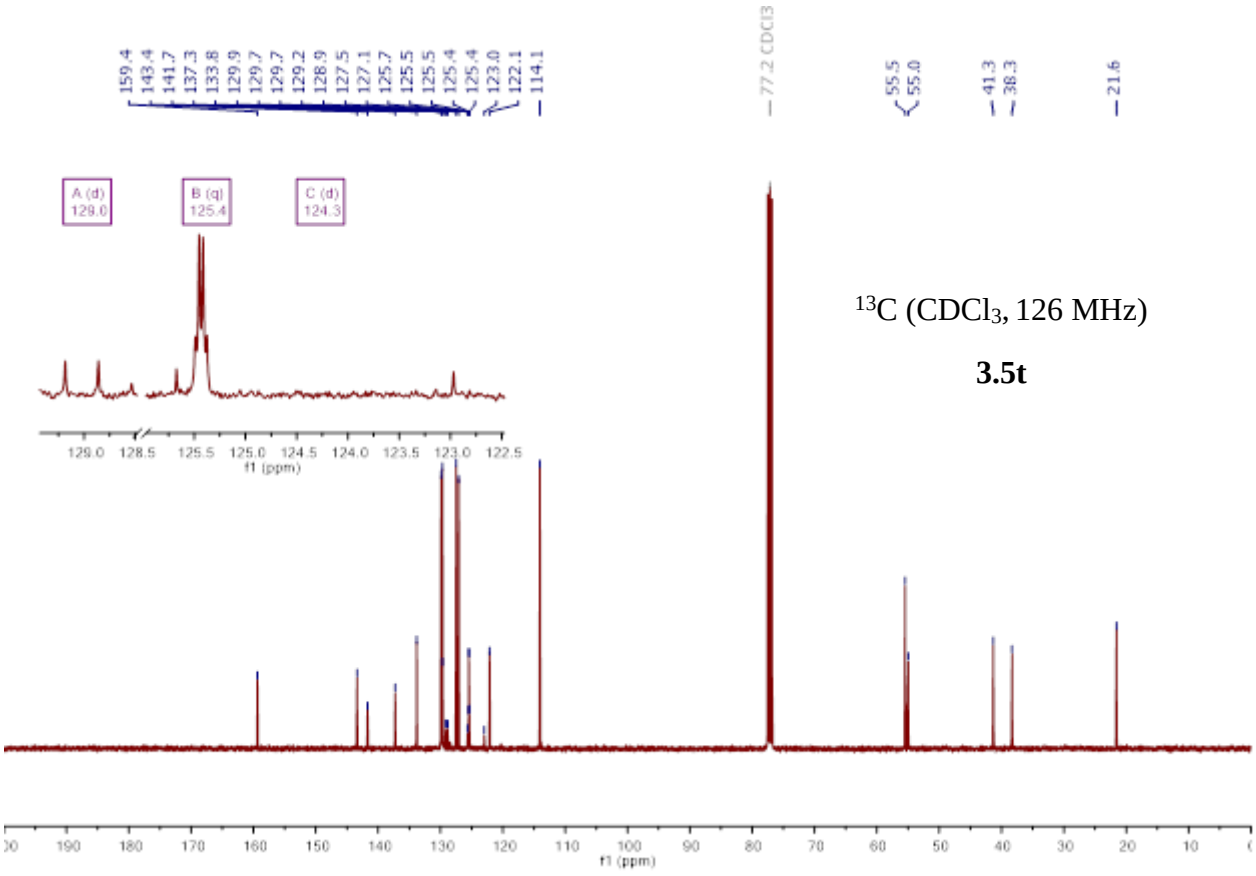

^{19}F ($CDCl_3$, 376 MHz)

3.5t

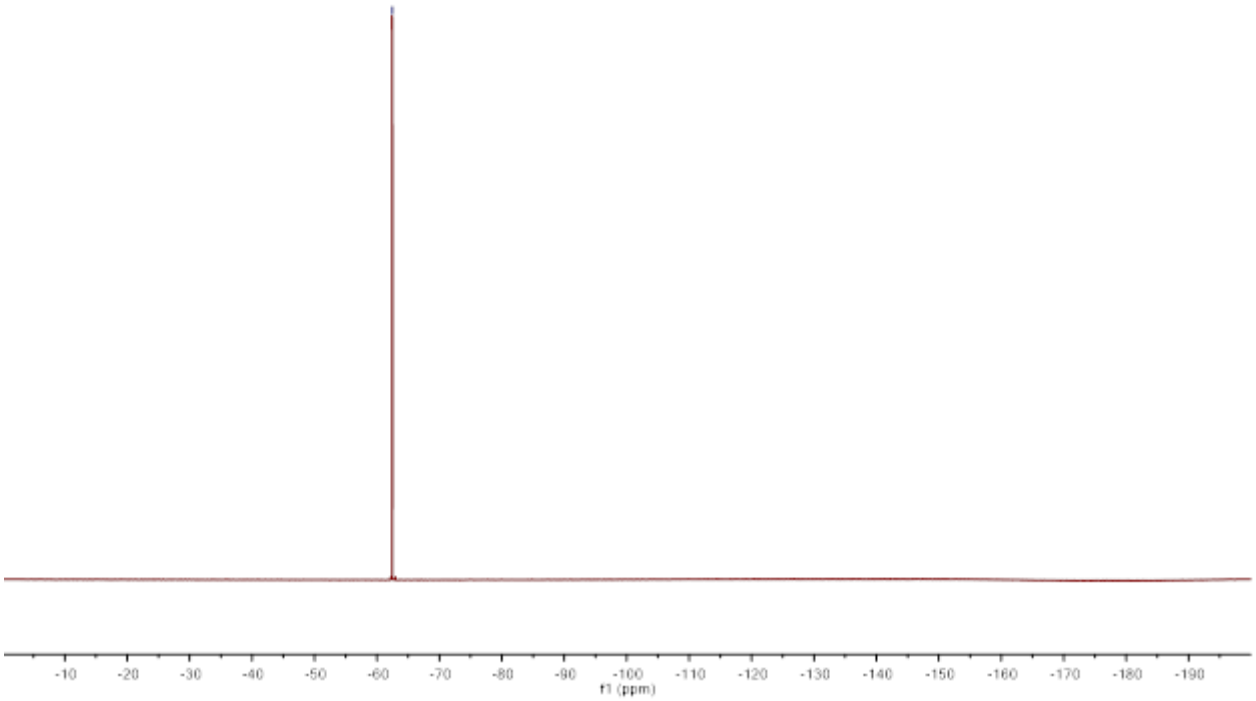

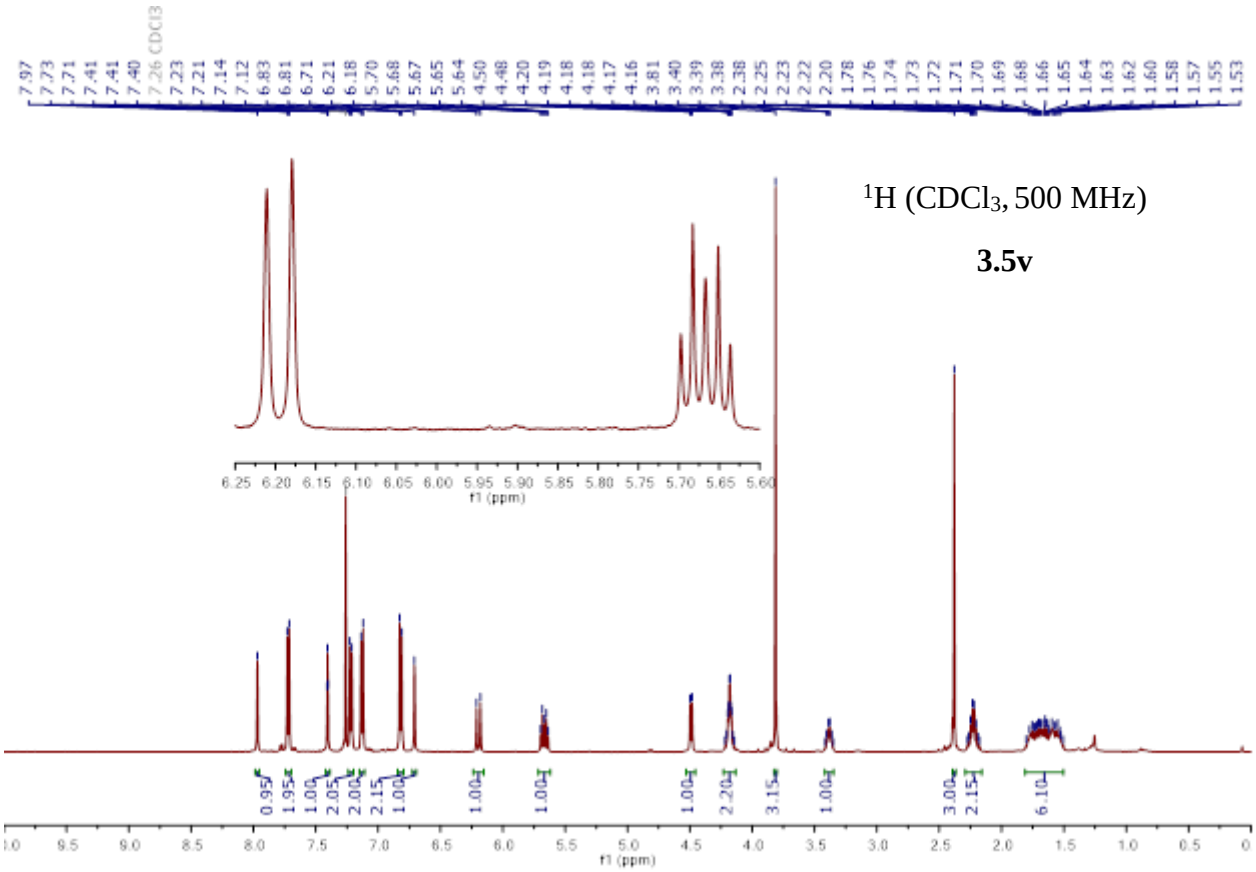

^{1}H ($CDCl_3$, 500 MHz)

3.5v

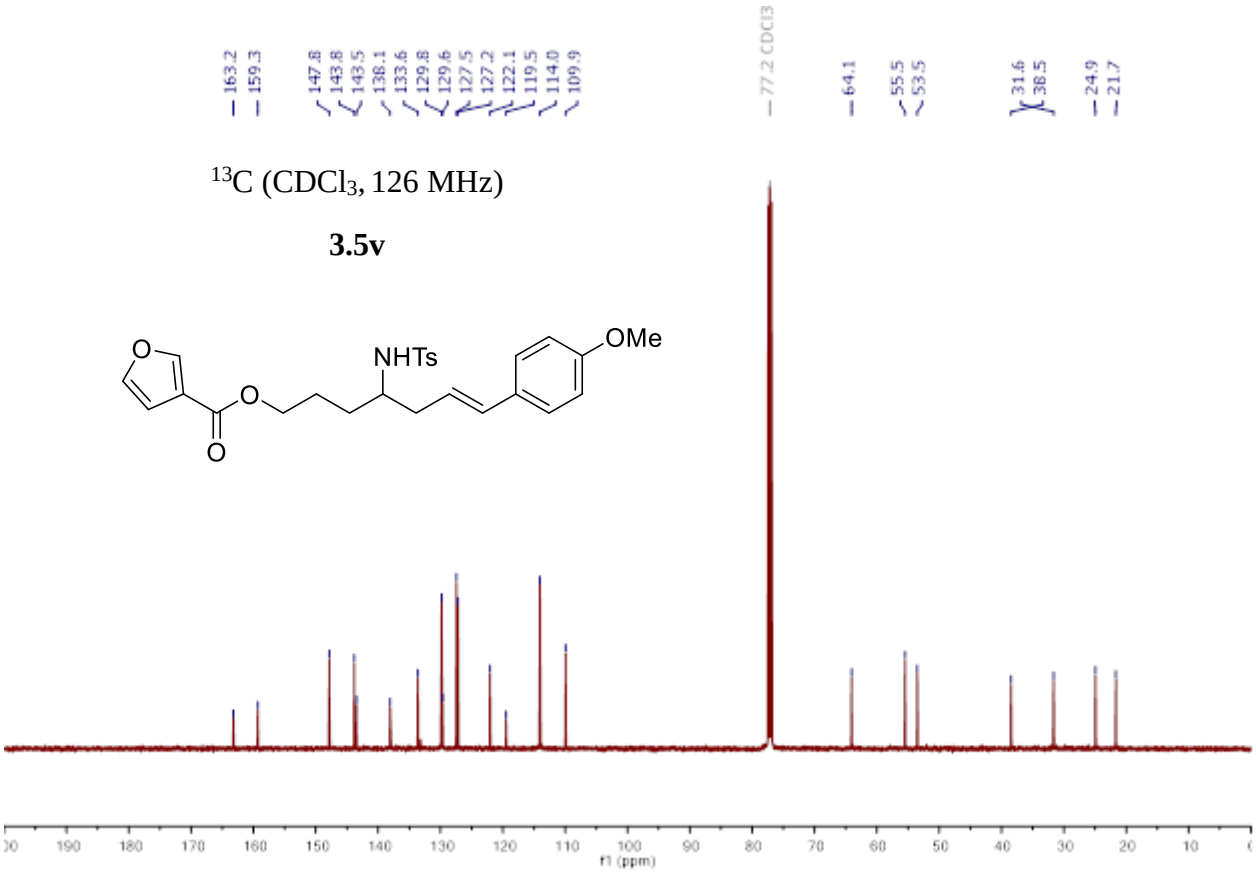

^{13}C ($CDCl_3$, 126 MHz)

3.5v

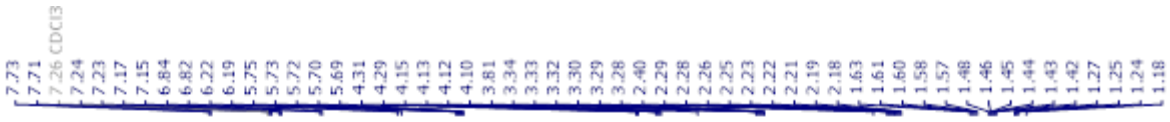

^{1}H ($CDCl_3$, 500 MHz)

3.5u

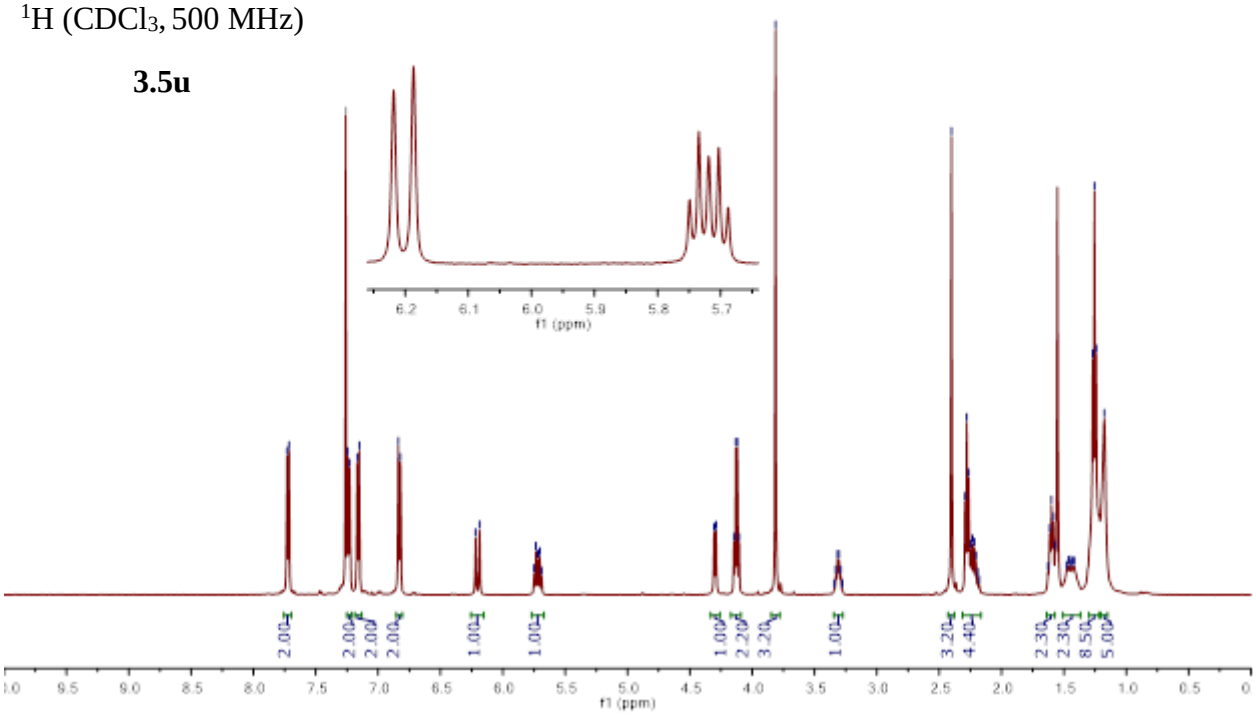

^{13}C ($CDCl_3$, 126 MHz)

3.5u

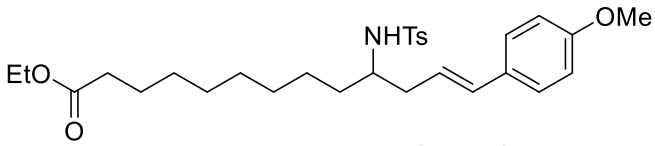

^{1}H ($CDCl_3$, 500 MHz)

3.5w

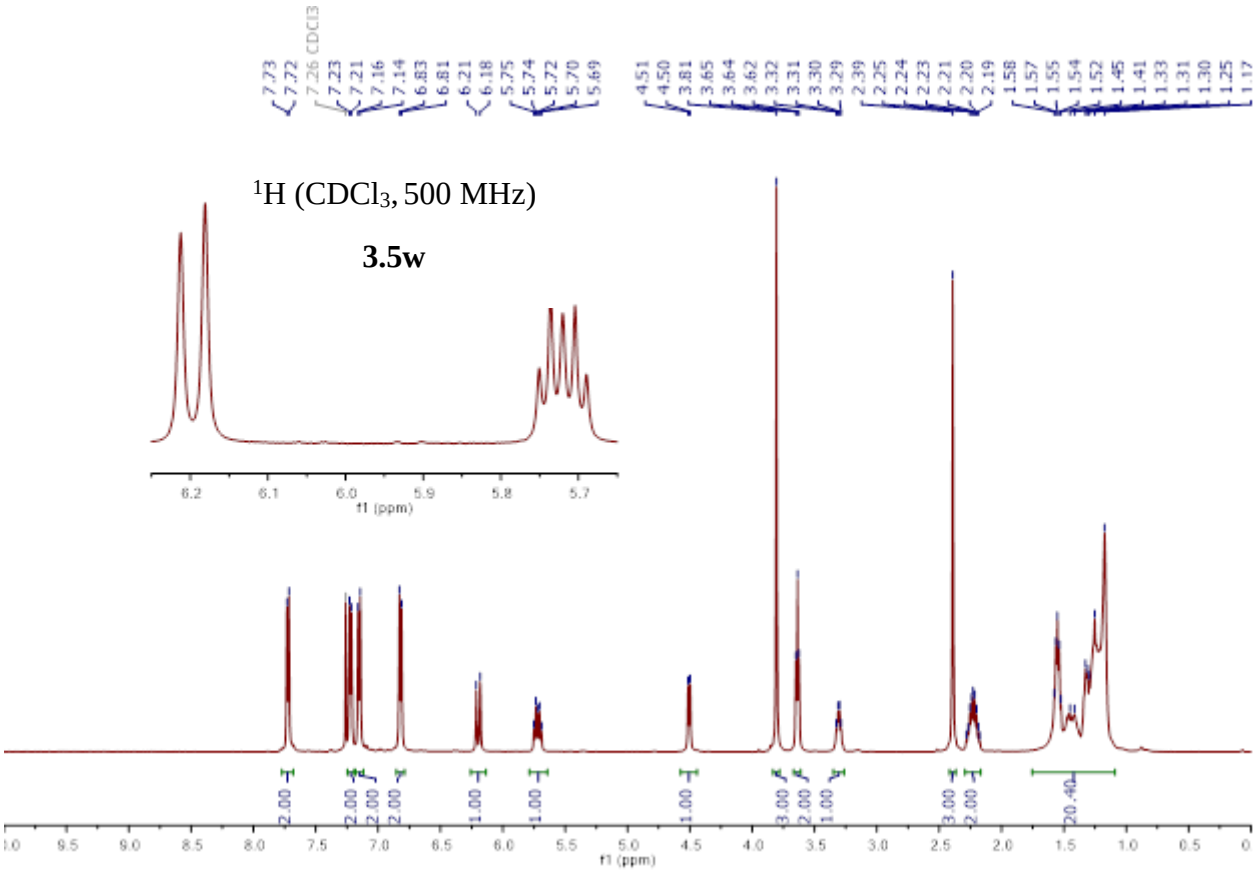

^{13}C ($CDCl_3$, 126 MHz)

3.5w

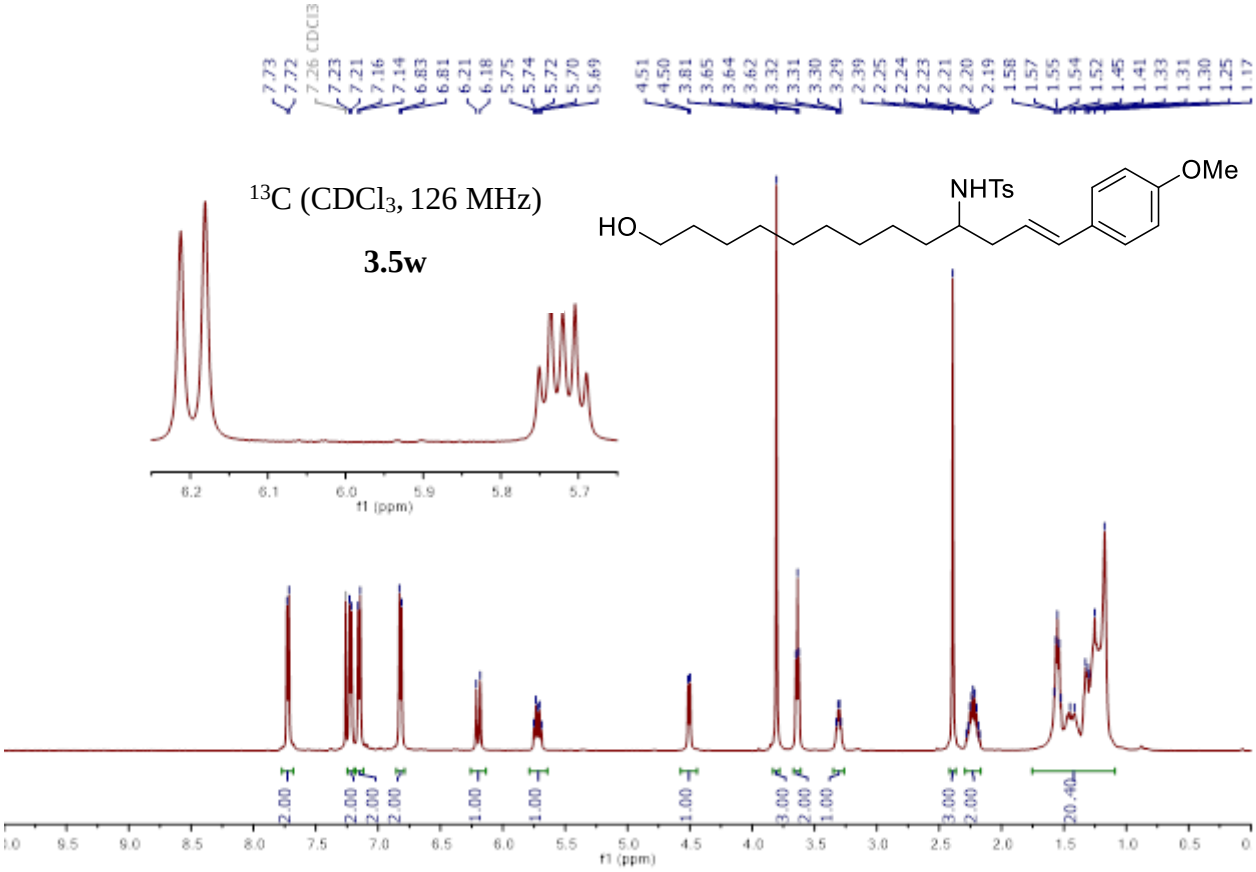

^{1}H ($CDCl_3$, 500 MHz)

3.5x

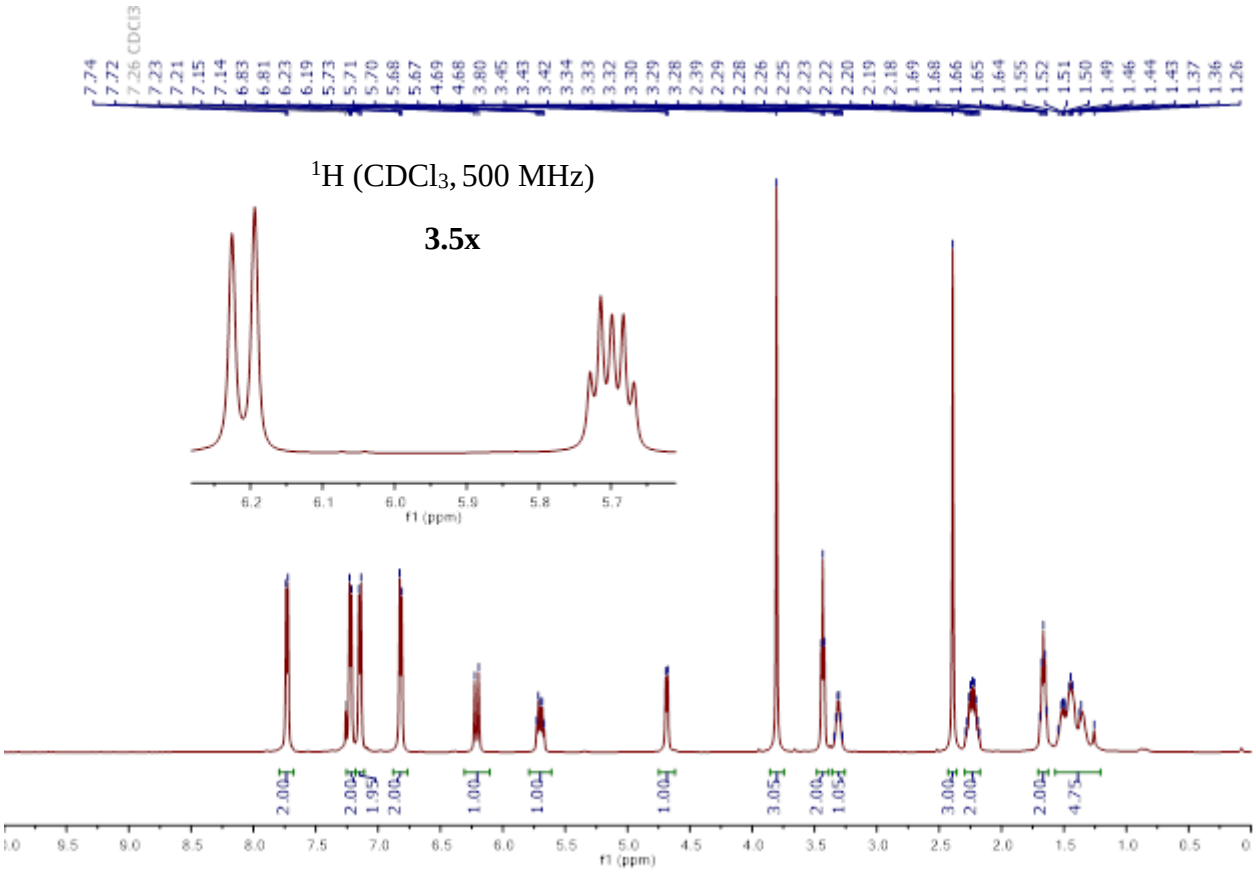

^{13}C ($CDCl_3$, 126 MHz)

3.5x

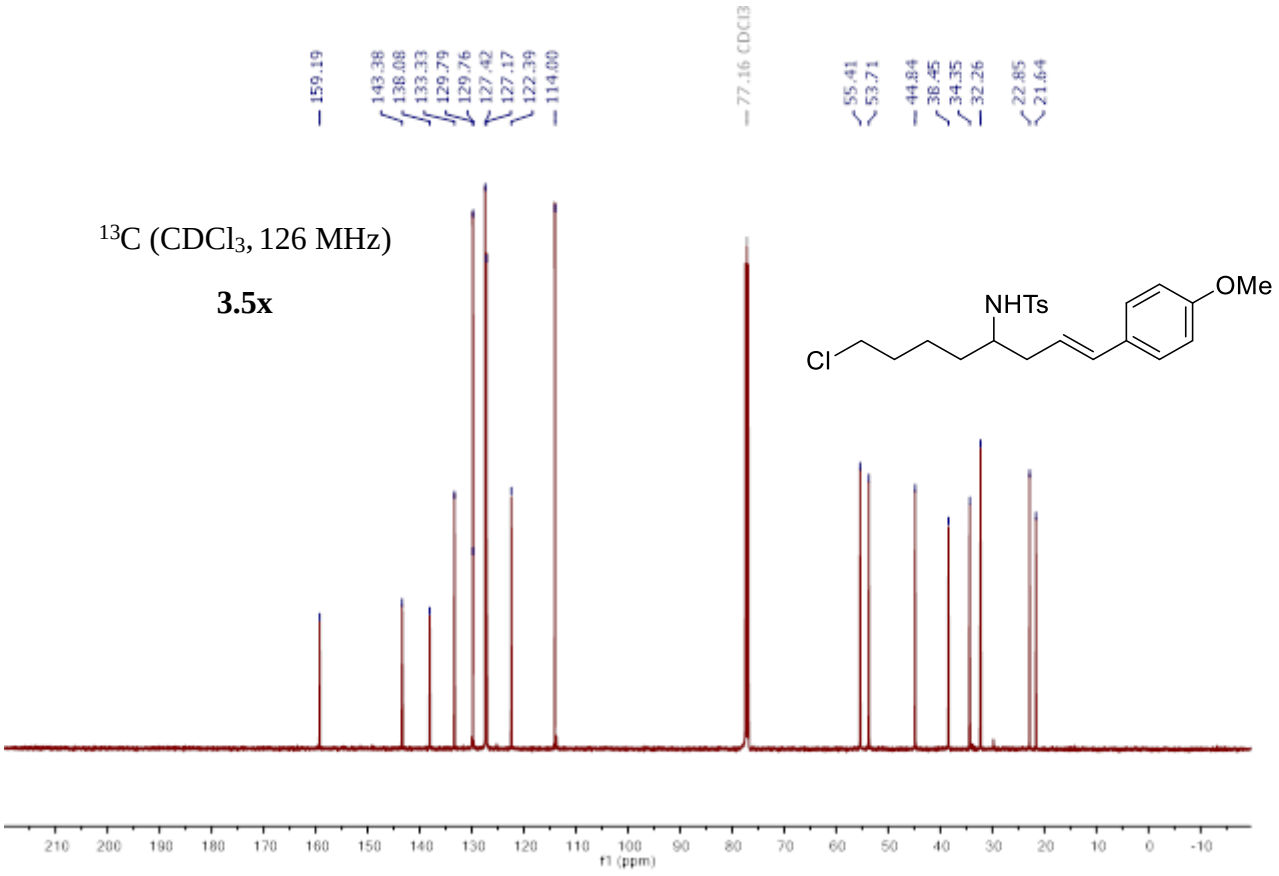

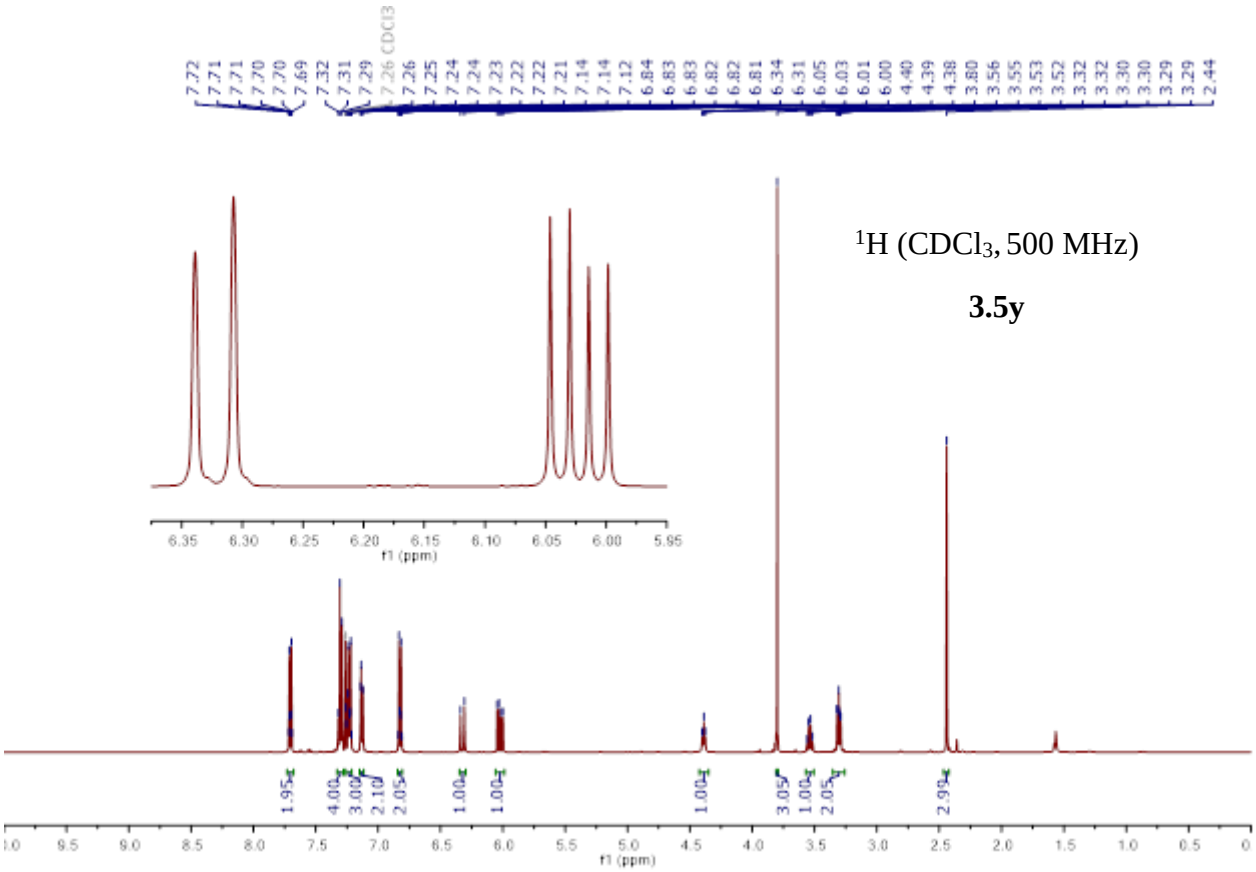

^{1}H ($CDCl_3$, 500 MHz)

3.5y

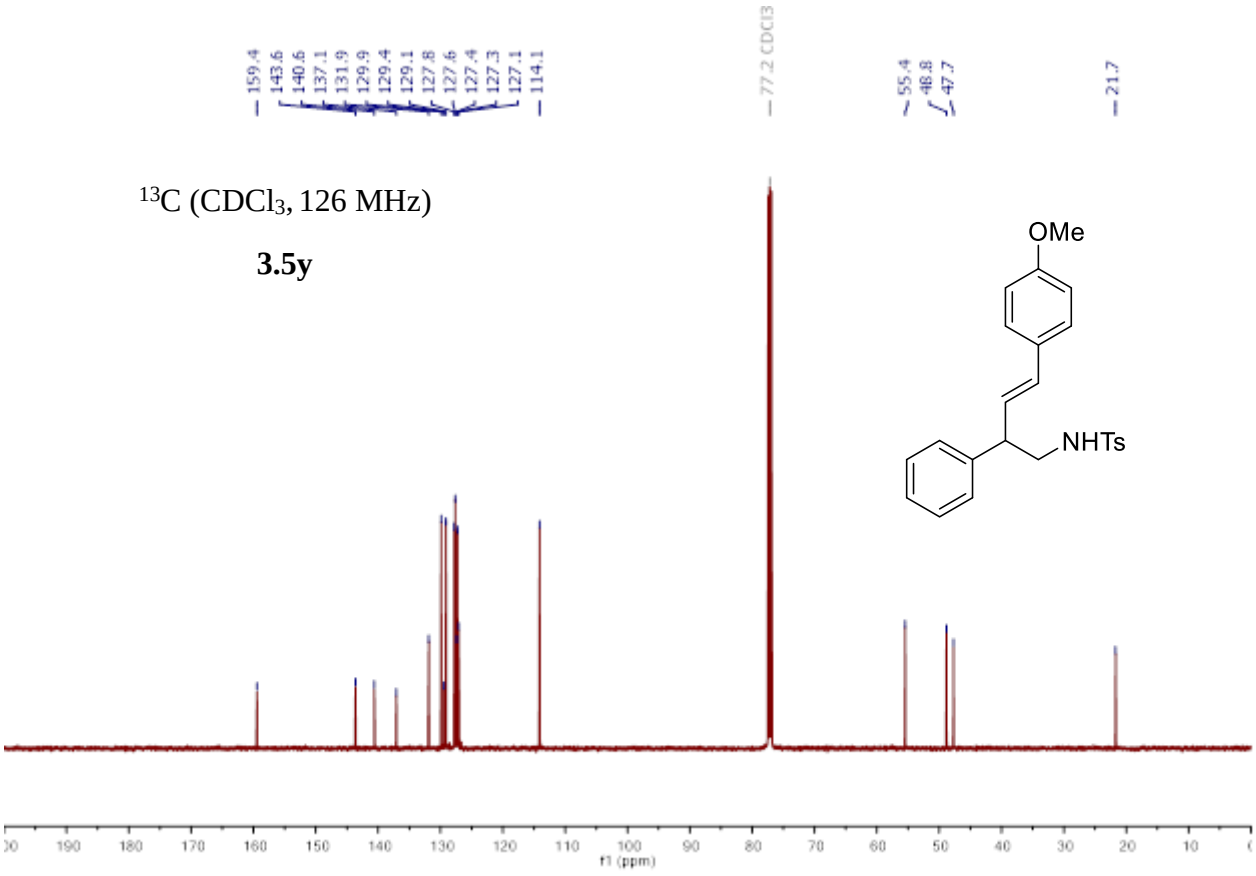

^{13}C ($CDCl_3$, 126 MHz)

3.5y

Chapter IV. Reactivity of aziridines in the presence of nickel complexes bearing sterically hindered phenanthroline ligands

4.1 Experiments with $(L5)_2Ni$

4.1.1 Stoichiometric experiments

To initiate mechanistic studies of aziridine reactivity in the presence of nickel and sterically hindered bidentate *N*-ligands the synthesis of azanickellacyclobutane **4.1** was approached (Scheme 4.1).

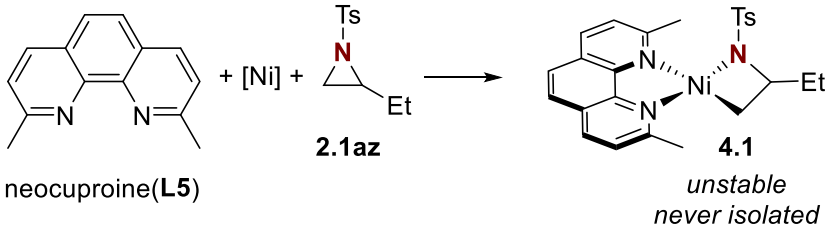

Scheme 4.1 Approach for the synthesis of azanickellacyclobutane **4.1**

However, any approach attempted did not lead to the formation of the desired product **4.1** potentially due to the high instability of this compound.

Nevertheless, the evidence of azanickellacyclobutane **4.1** formation was obtained upon mixing complex $(L5)_2Ni$ with aziridine **2.1az** and analyzing crude reaction mixture using MALDI-MS technique (Scheme 4.2).

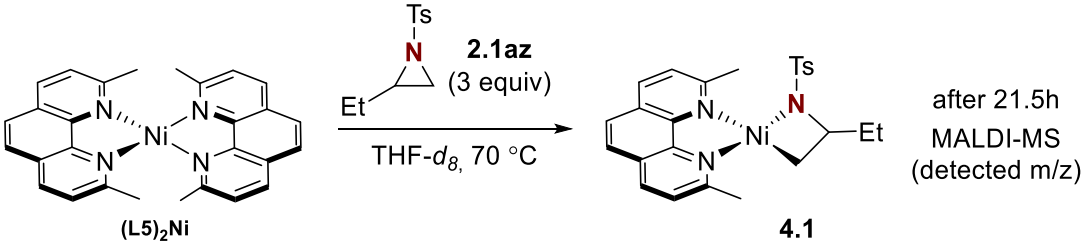

Scheme 4.2 Azanickellacyclobutane **4.1** detected using MALDI-MS

At any point of the crude reaction mixture monitoring with ^{1}H NMR signals of **4.1** were not detected. This result supports initial hypothesis of high instability of these species as they are present in the reaction mixture in the concentration below the detection limit of ^{1}H NMR. Notably, the formation of $TsNH_2$ and 1-butene was detected instead (Scheme 4.3).

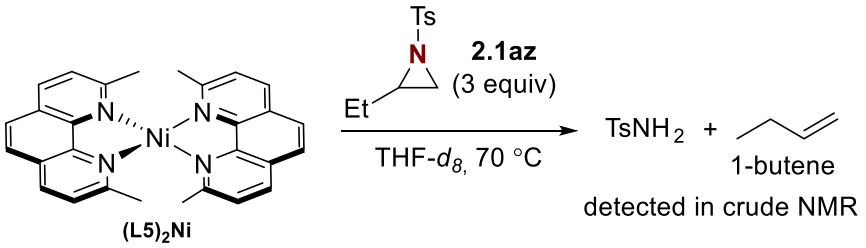

Scheme 4.3 Formation of $TsNH_2$ and 1-butene upon reaction of $(\mathbf{L5})_2$Ni with aziridine **2.1az**

After recrystallization of the crude mixture from reaction of complex $(\mathbf{L5})_2$Ni and aziridine **2.1az** another intriguing result was obtained. Crystals of a nickel complex **4.2** that has undergone ligand activation were formed (Scheme 4.4).

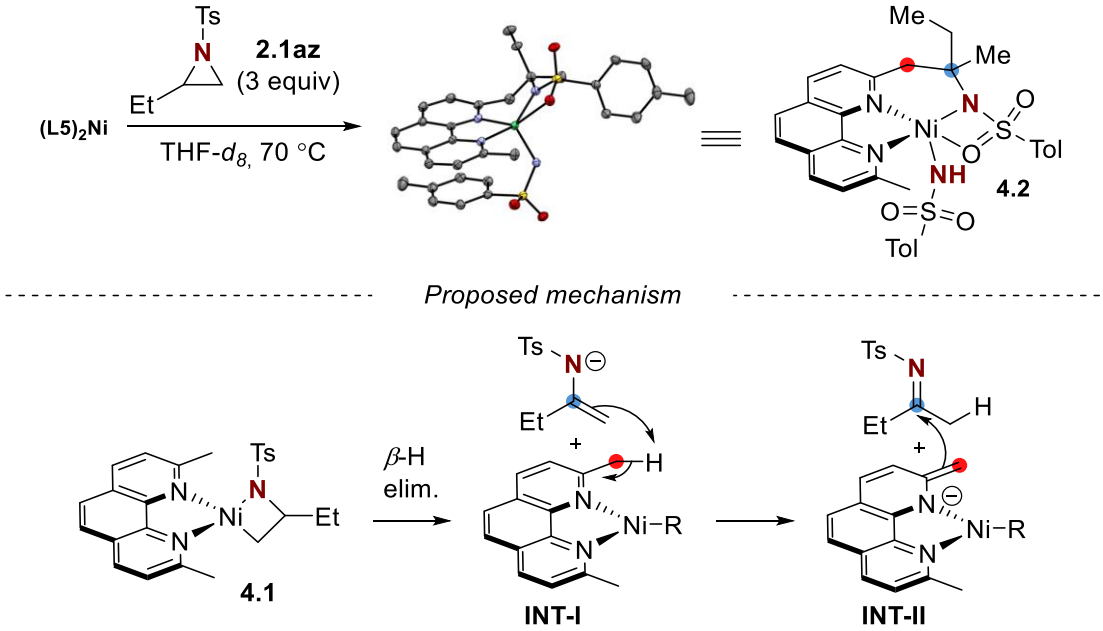

Scheme 4.3 Formation of nickel complex **4.2**

The mechanism by which this complex is generated is uncertain, particularly as the formation of a quaternary carbon is required in the ligand activation. The following mechanism was suggested: (1) the formation of an iminium intermediate through *β*-hydride elimination which acts as a base to deprotonate the *ortho*-Me of **L5** in **INT-I**; (2) addition of **INT-II** to the imine forms the quaternary center leading to **4.2**. The nature of **INT-I** is uncertain so it has been written with an ambiguous R group, but the presence of a ligated NHTs group in **Ni-II** suggests at the possibility of a nickel nitrene complex discussed next.

Finally, the nickel complex 4.3 was synthesized starting from $(\mathbf{L5})_2$Ni and aziridine **2.1az** (Scheme 4.4).

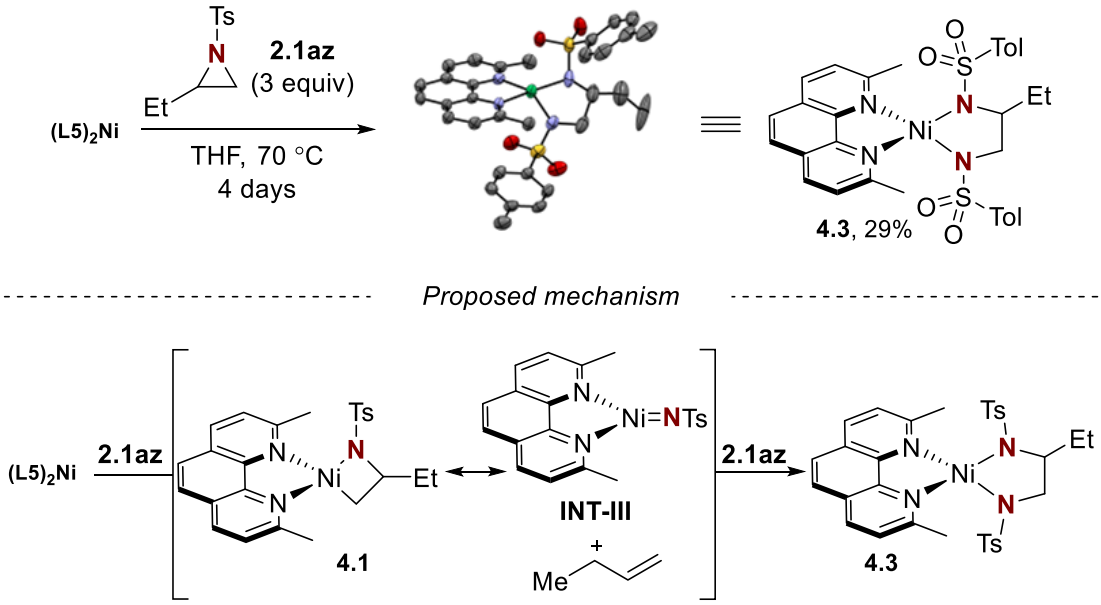

Scheme 4.4 Synthesis of nickel complex **4.3**

As a plausible mechanism can be suggested the formation of nitrene complex **INT-III** after *β*-deamination from **4.1**. The following cycloaddition of nitrene complex **INT-III** into another molecule of **2.1az** forms diazanickelacyclopentene **4.3**.

4.1.2 Carboxylation experiments with (L5)$_2$Ni

By applying (**L5**)$_2$Ni as a nickel source under aziridine carboxylation conditions it was confirmed as a competent catalyst (Scheme 4.5).

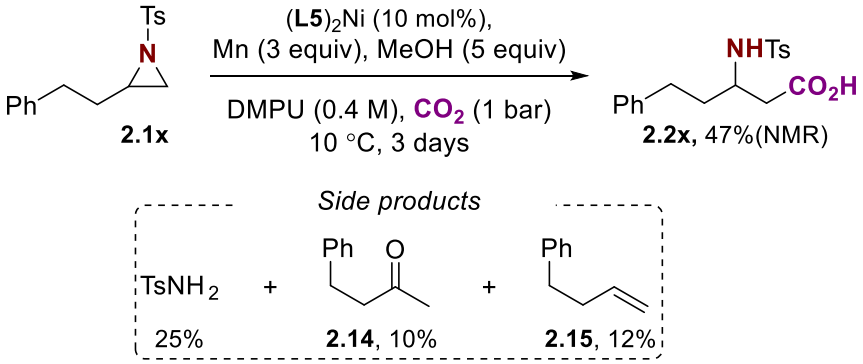

Scheme 4.5 Catalytic carboxylation with (**L5**)$_2$Ni

The side-products formed and their ratio are in agreement with priviously discussed aziridine reactivity under catalyztic conditions in the absence of CO_2.

Next, complex (**L5**)$_2$Ni was tested under carboxylation conditions in the absence either MeOH or Mn (Scheme 4.6).

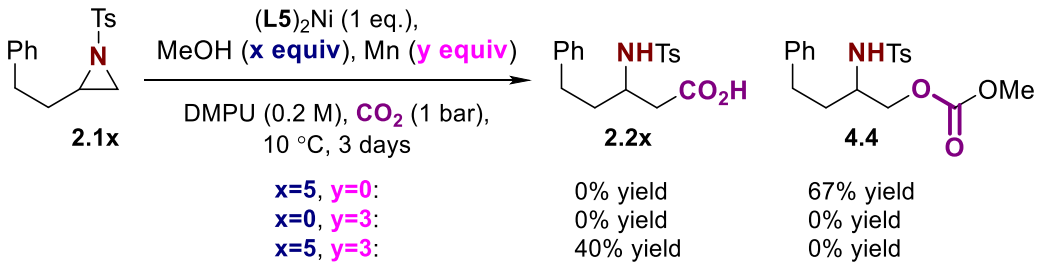

Scheme 4.6 Carboxylation experiments with (**L5**)$_2$Ni in the absence of MeOH or Mn

In the absence of Mn the formation of side-product **4.4** was observed with no formation of acid **2.2x**. Submitting compound **4.4** to the standard carboxylation reaction conditions in place of the aziridine **2.1x** did not generate any acid **2.2x**. Thus, it was confirmed that **4.4** is not a reaction intermediate. No formation of product **2.2x** was detected in the absence of MeOH additionally proving the crucial role of proton source for the successful reaction outcome. Notably, the acid **2.2x** was only observed in the presence of both MeOH and Mn, suggesting at the intervention of Ni(I) species within the catalytic cycle.

4.2 Experiments with (L)Ni(CH$_2$TMS)$_2$

As it was mentioned above any extensive attempts to access this nickellacycle intermediate **4.1** supported by neocuproine were met with failure. Nevertheless, it was crucial to elucidate the origin of synergy between bulky *phen* and *bipy* ligands and alcohols. As an alternative to the direct synthesis of azanickellacycle **4.1** a series of nickel complexes **4.5** with general formula (L)Ni(CH$_2$TMS)$_2$, where L is *phen* or *bipy* type ligands, were synthesized (Scheme 4.7).

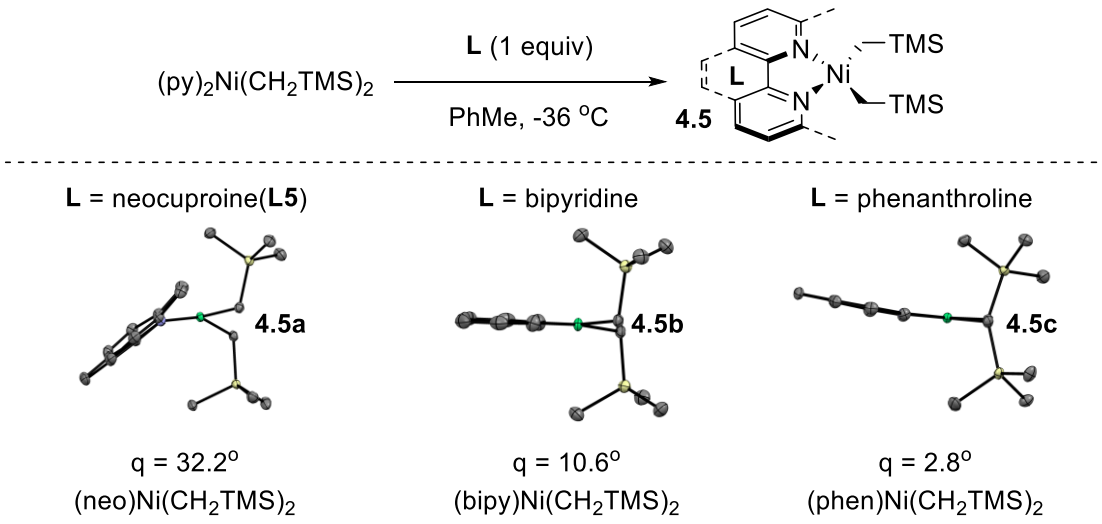

Scheme 4.7 Difference between (L)Ni(CH$_2$TMS)$_2$ complexes

Complex **4.5a** bearing neocuproine(**L5**) ligand showed an unusual binding mode where the N-Ni center is out of the plane determined by the N,N ligand and forms an angle of 51.3°. Furthermore,

the C-Ni-C plane reveals large deviations from a traditional square planar geometry and is highly distorted at 32.2°. The *bipy* and *phen* derivatives **4.5b** and **4.5c** compared to **4.5a** possess the expected square planar geometries with C-Ni-C planes of 10.6° and 2.76° respectively.

Turning to the reactivity of these complexes particularly facile protonolysis of **4.5a** with TFE to form paramagnetic TFE bridged dimer **4.6** was observed (Scheme 4.8).

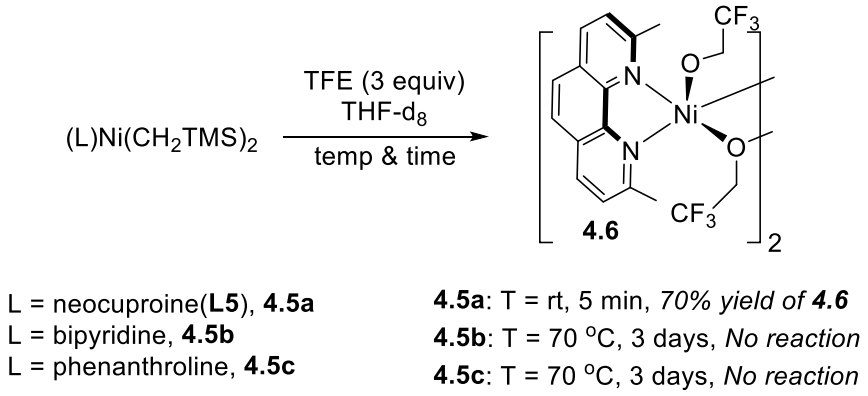

Scheme 4.8 Reactivity of complexes **4.5a-c** toward protonolysis with TFE

The reactivity of analogous bipyridine and phenanthroline complexes **4.5b** and **4.5c** was in stark contrast to **4.5a** as they did not undergo protonolysis, even under forcing conditions (70 ºC for 3 days). These results supported the suspicion that neocuproine-ligated Ni intermediates would be highly reactive compared to their bipyridine and phenanthroline analogues.

4.3 DFT studies

4.3.1 Azanickellacyclobutane geometry in different spin states

The DFT analysis was applied to study the reactivity of azanickellacyclobutanes *ab initio*.

First, the calculated structures of singlet **DFT_4.1a** and triplet **DFT_4.1b** spin states for azanickellacyclobutane bearing phenanthroline ligand were found (Scheme 4.9).

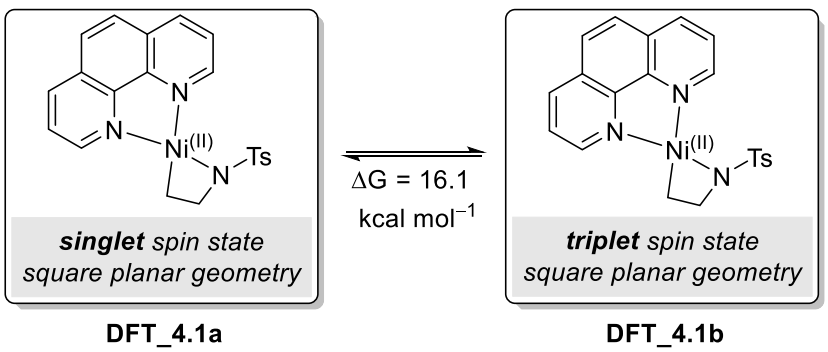

Scheme 4.9 Calculated structures **DFT_4.1a** and **DFT_4.1b**

The calculated difference in the Gibbs free energies between singlet and triplet states was 16.1 kcal×mol^{-1}.

Next, similar calculations were conducted to find calculated structures in different spin states for azanickellacyclobutane bearing neocuproine ligand (Scheme 4.10).

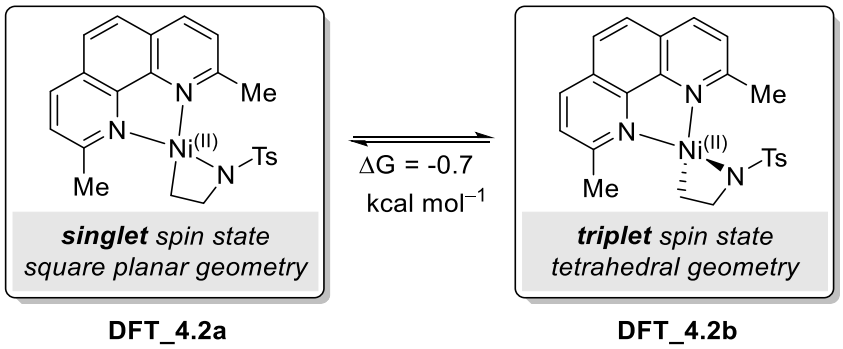

DFT_4.2a **DFT_4.2b**

Scheme 4.10 Calculated structures **DFT_4.2a** and **DFT_4.2b**

The calculated structure of azanickellacyclobutane in a triplet spin state **DFT_4.2b** was found to be slightly more stable (0.7 kcal×mol^{-1}) compared to a singlet spin state structure **DFT_4.2a**. Such a drastic change in the stability of the triplet spin state while changing the ligand from phenanthroline to neocuproine is remarkable. This result suggests the possibility of azanickellacyclobutanes intermediates existing in a triplet spin state under reaction conditions using bulky *phen* or *bipy* ligands. The importance of this phenomenon is discussed in the following section.

4.3.2 Reactivity of azanickellacyclobutane toward hydrolysis in different spin states

Next, the potential hydrolysis of azanickellacyclobutane bearing neocuproine(**L5**) ligand was studied applying DFT analysis.

First, when the molecule of MeOH was placed next to the nickel center of azanickellacyclobutane in a singlet spin state as a starting point for structure calculation (Scheme 4.11).

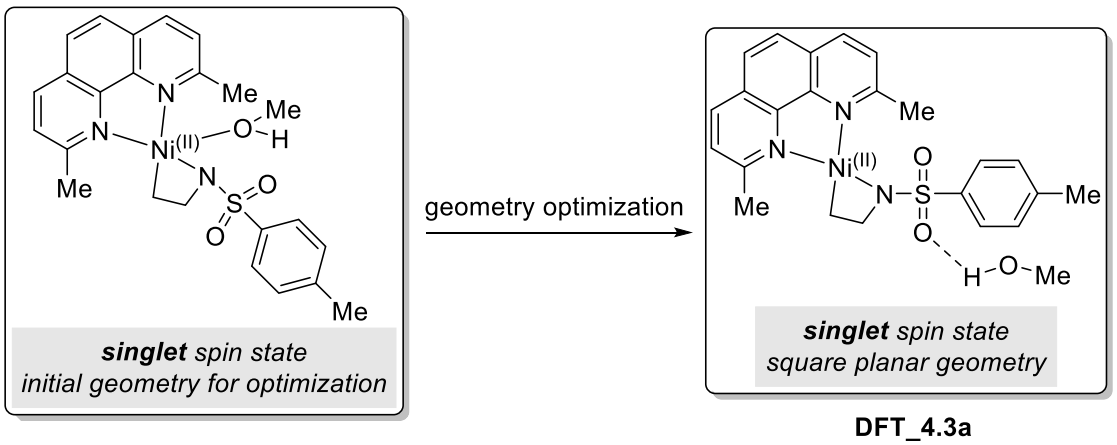

Scheme 4.11 Calculated structure **DFT_4.3a**

It was observed that coordination of MeOH to nickel center in that case is unfavorable and in calculated structure **DFT_4.3a** the azanickellacyclobutane remained four-coordinated with the molecule of MeOH placed by calculation algorithm away from the metal. This observation is in agreement with the general crystal field theory for d^8 transition metal complexes. The LUMO dx_2-y_2 orbital is expected to be high in energy in the low spin state of the nickel center and coordination of extra ligand to a square planar four-coordinated nickel complex to form trigonal bipyramidal penta-coordinated nickel complex in that case is unfavorable.

In contrast, in the high spin state coordination of extra ligand expected to be possible and calculated structure **DFT_4.3b** with nickel center in the triplet spin state in the presence of MeOH was found to be a penta-coordinated trigonal bipyramidal complex (Scheme 4.12).

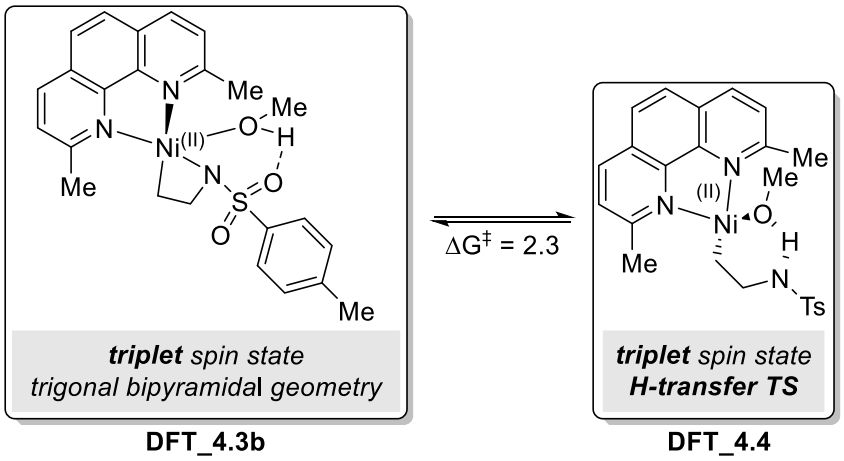

Scheme 4.11 Calculated structure **DFT_4.3b**

Using the optimized geometry **DFT_4.3b** the transition state structure **DFT_4.4** for intermolecular proton transfer from the oxygen atom of alcohol to the nitrogen atom of azanickellacyclobutane was calculated and free activation energy of this process was quantified ($\Delta G^{\ddagger}$ = 2.3 kcal×mol^{-1}).

4.4 Mechanistic hypothesis

Based on combined results of mechanistic studies it can be proposed with great certainty that developed transformations specifically aziridine carboxylation (Chapter 2) and aziridine hydroalkenylation (Chapter 3) occur through a similar mechanism of aziridine ring activation (Scheme 4.12).

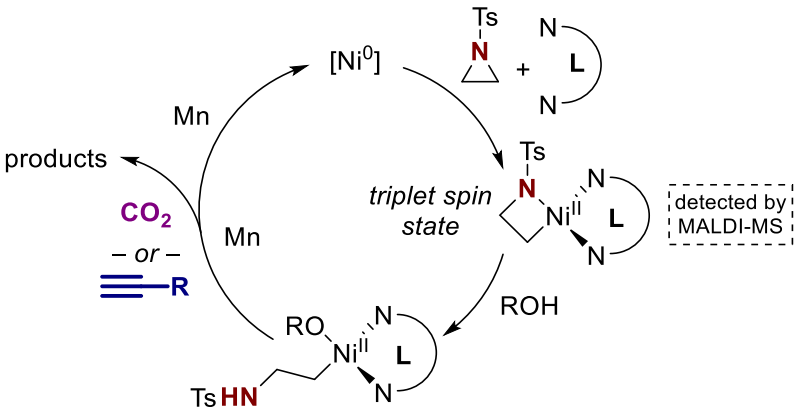

Scheme 4.12 Proposed hydrolysis of azanickellacyclobutane intermediate

The hydrolysis of azanickellacyclobutane intermediate happens when the Ni-center is in a triplet spin state. This high spin state is achieved in the presence of bulky bidentate N,N ligands which distort square planar nickel complex geometry toward the formation of tetrahedral one.

4.5 Design of novel synthetic transformation

Based on mechanistic hypothesis discussed above a mechanism for Ni-catalyzed alkylation of aziridines was proposed (Scheme 4.13).

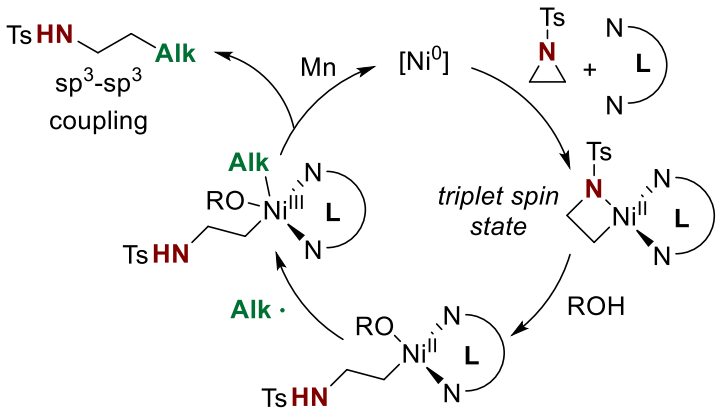

Scheme 4.13 Proposed mechanism for Ni-catalyzed alkylation of aziridines

It was suggested that ring-opened Ni(II) intermediate might trap generated *in situ* alkyl radical species forming Ni(III) intermediate. This intermediate will undergo reductive elimination even with the formation of Csp3-Csp3 cross-coupling product.

In order to test this working hypothesis aziridine **2.1f** and an electrophilic radical source - Katritzky salt **4.7** were subjected under hydroalkenylation (Scheme 4.14, *top*) and carboxylation (Scheme 4.14, *bottom*) reaction conditions (Scheme 4.14).

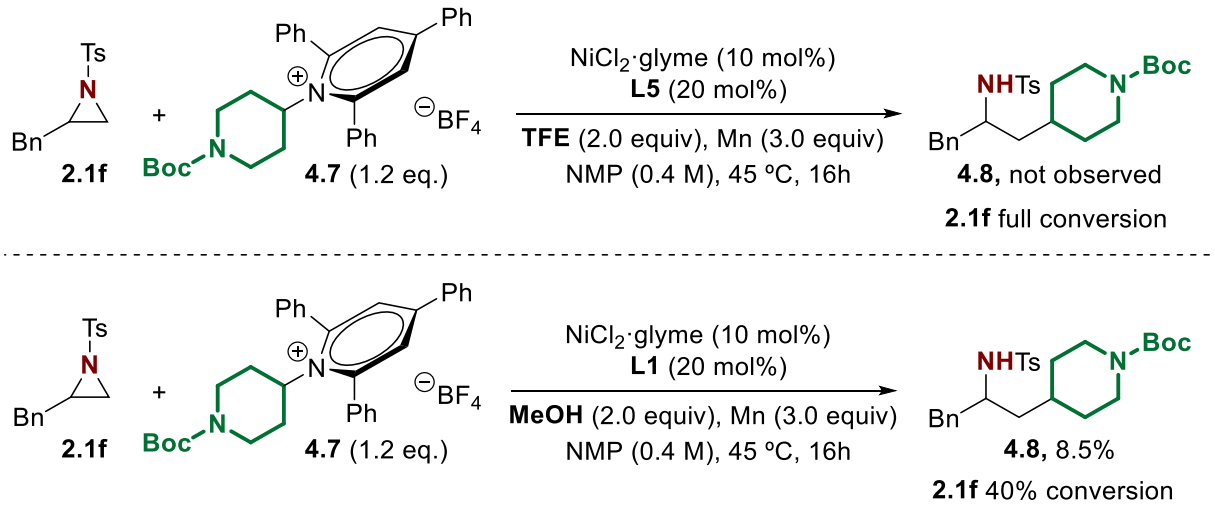

Scheme 4.14 Ni-catalyzed alkylation of aziridines using Katritzky salts

No product formation was detected under hydroalkenylation conditions. When the crude mixture of the second reaction was analyzed, despite a low conversion of aziridine **2.1f** signals of the product **4.8** were detected using UHPLC-MS. After careful purification of the mixture on silica the desired product **4.8** was isolated with 8.5% yield and its structure was confirmed by ^{1}H NMR and HRMS. Thus, the hypothesis was successfully confirmed and further studies regarding the development of Ni-catalyzed alkylation protocol will be continued in Prof. Ruben Martins group.

4.5 Chapter conclusions

- A series of mechanistic experiments were conducted to prove azanickellalactone as an active intermediate in the developed transformations and to study the reactivity of this intermediate
- The events of β-H elimination and β-deamination were proved to be the main competitive side-reactions in the developed transformations
- Reactivity of Ni-complexes bearing bidentate N,N-ligands was studied toward hydrolysis in the presence of alcohols. It was observed that in the presence of sterically hindered ligands Ni-complexes undergo facile hydrolysis, whereas for less bulky ligands a lack of reactivity was detected
- Applying DFT analysis it was found that the high reactivity of Ni-complexes in the presence of bulky ligands might be explained by the change of metal center spin state from a singlet spin state with less bulky ligands to a triplet spin state with bulkier ones
- Based on collected data a general mechanism of studied transformations was proposed with the hydrolysis and ring-opening of azanickellalactone intermediate as a key step
- Based on the mechanistic hypothesis a novel Ni-catalyzed alkylation of aziridines was proposed and successfully confirmed by isolating the desired alkylation product

4.6 Experimental section

4.6.1 Experiments with (L5)2Ni

Synthesis of (L5)2Ni

Following a modified literature procedure,[114] in the glovebox, $Ni(COD)_2$ (0.6 g, 2.17 mmol) and neocuproine (0.93 g, 4.46 mmol, 2.05 equiv.) were added to a 12 mL vial with a stirrer bar and charged with 6 mL of toluene. The reaction was left to stir for 16 h and the solvent was then removed to afford a brown solid. To the solid, 2 mL of toluene was added and stirred for 10 minutes followed by the addition of 5 mL of pentane. The solid was then filtered and washed with pentane (1 mL × 3) to afford **$(L5)_2Ni$** as a dark brown solid (1.0 g, 99 % yield). ^1H NMR (500 MHz, C_6D_6) δ 9.00 (d, *J* = 7.3 Hz, 2H), 7.68 (d, *J* = 7.3 Hz, 2H), 7.32 (s, 2H), 2.24 (s, 6H). Spectroscopic data for this compound matches with that reported in the literature.[166,167]

Stochiometric Monitoring of Ni(0) Undergoing Oxidative Addition to Aziridine and MALDI-MS Identification of (L5)Ni(Aza-metallacycle)

In the glovebox, **$(L5)_2Ni$** (5.5 mg, 0.01 mmol) and **2.1az** (6.7 mg, 0.03 mmol) were added to a 10 mL vial and dissolved in 1 mL THF-d_8. This solution was then added to a J-Young NMR tube and monitored by ^1H and paramagnetic ^1H NMR. After 7 h at 70 °C, a mixture of both diamagnetic (Figure S) and paramagnetic species (Figure S) had formed. Throughout the monitoring of this reaction, at no point were diamagnetic signals (δ = 12-0 ppm) corresponding to $(L5)Ni^{II}$(Aza-metallacycle) formed. However, analysis by MALDI-MS of the crude reaction mixture after 21.5 h (t_4) revealed the corresponding m/z-H signal of $(L5)Ni^{II}$(Aza-metallacycle) (Figure S).[168] These results suggest that if $(L5)Ni^{II}$(Aza-metallacycle) is formed in significant quantities, it may be as a paramagnetic species. Trace 1-butene was also detected after 7 h at 70 °C along with the formation of tosyl amide with increasing amounts observed at 12.5 and 21.5 h.

Note: MALDI-TOF mass spectra were collected on a Bruker Autoflex MALDI-TOF mass spectrometer. Samples were prepared by the dried-droplet protocol, from solutions containing the charge-transfer matrix pyrene or trans-2-[3-(4-tert-Butylphenyl)-2-methyl-2-propenylidene]malononitrile (DCTB) in THF.

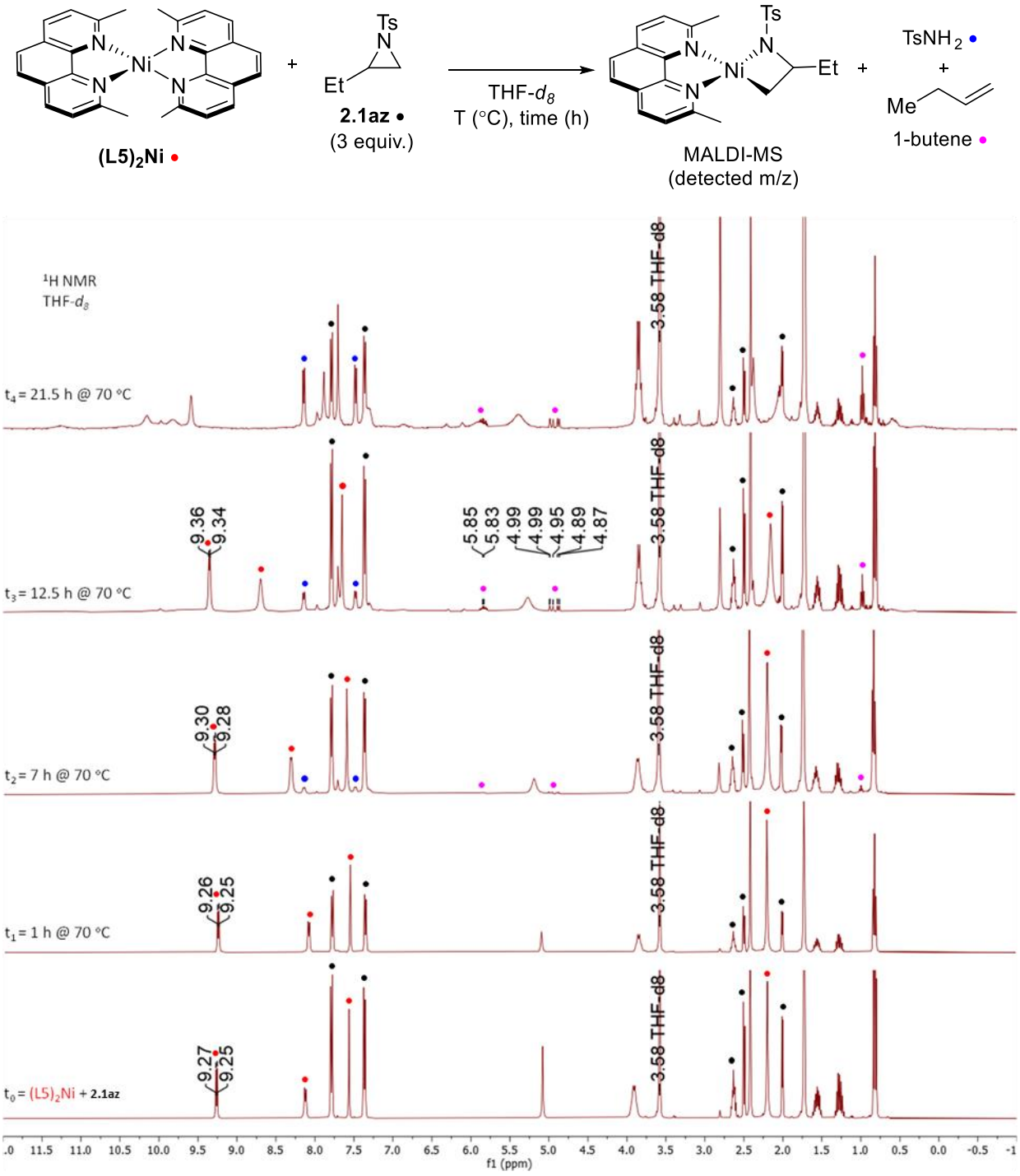

Figure S4.1 ^{1}H NMR spectra from monitoring the reaction between $(L5)_2Ni$ (grey) and **2.1az** (red) in THF-d_8 forming a mixture of products.

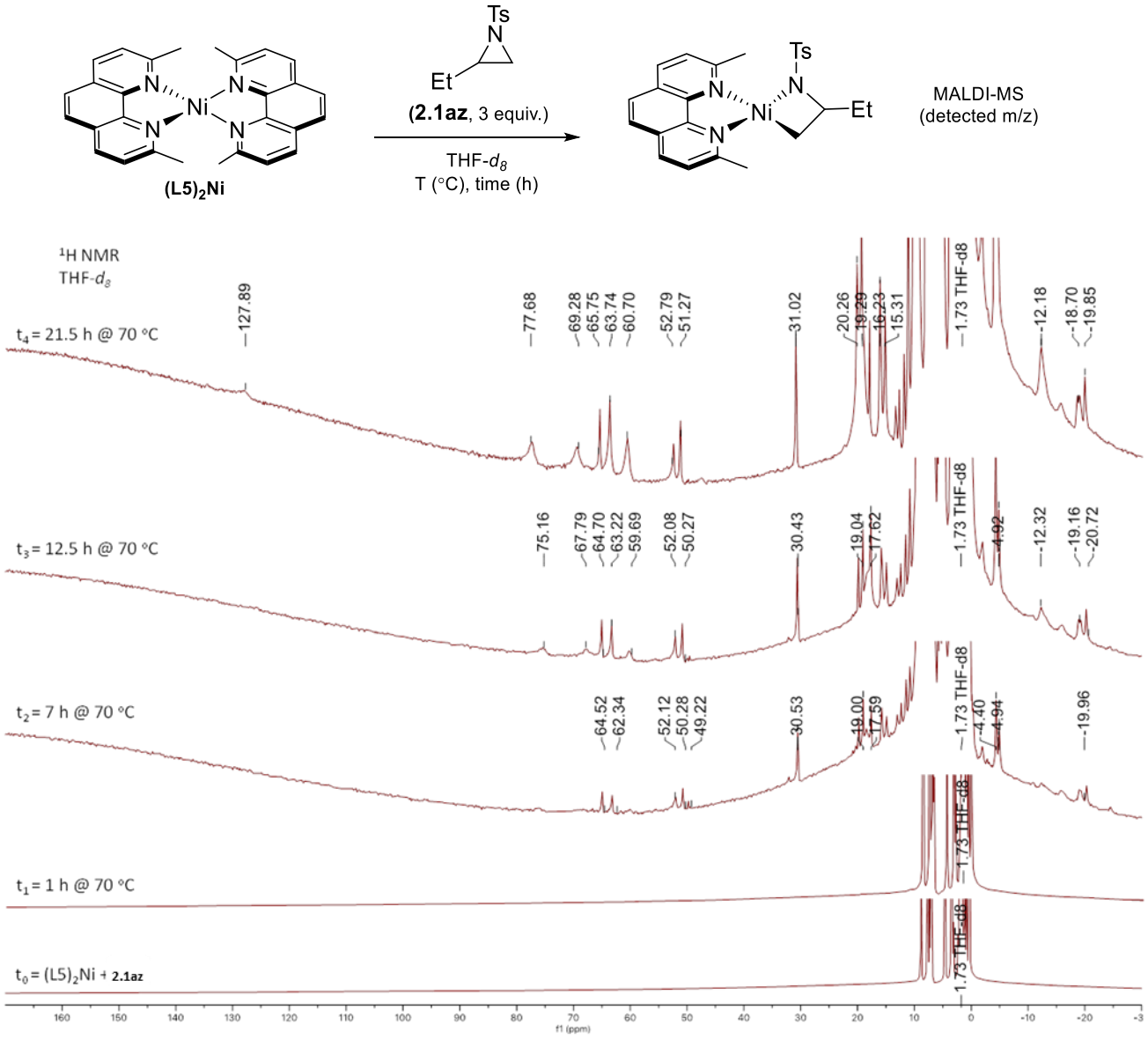

Figure S4.2 Paramagnetic ^{1}H NMR spectra from monitoring the reaction between $(L5)_2Ni$ and **2.1az** in THF-d_8 forming a mixture of products.

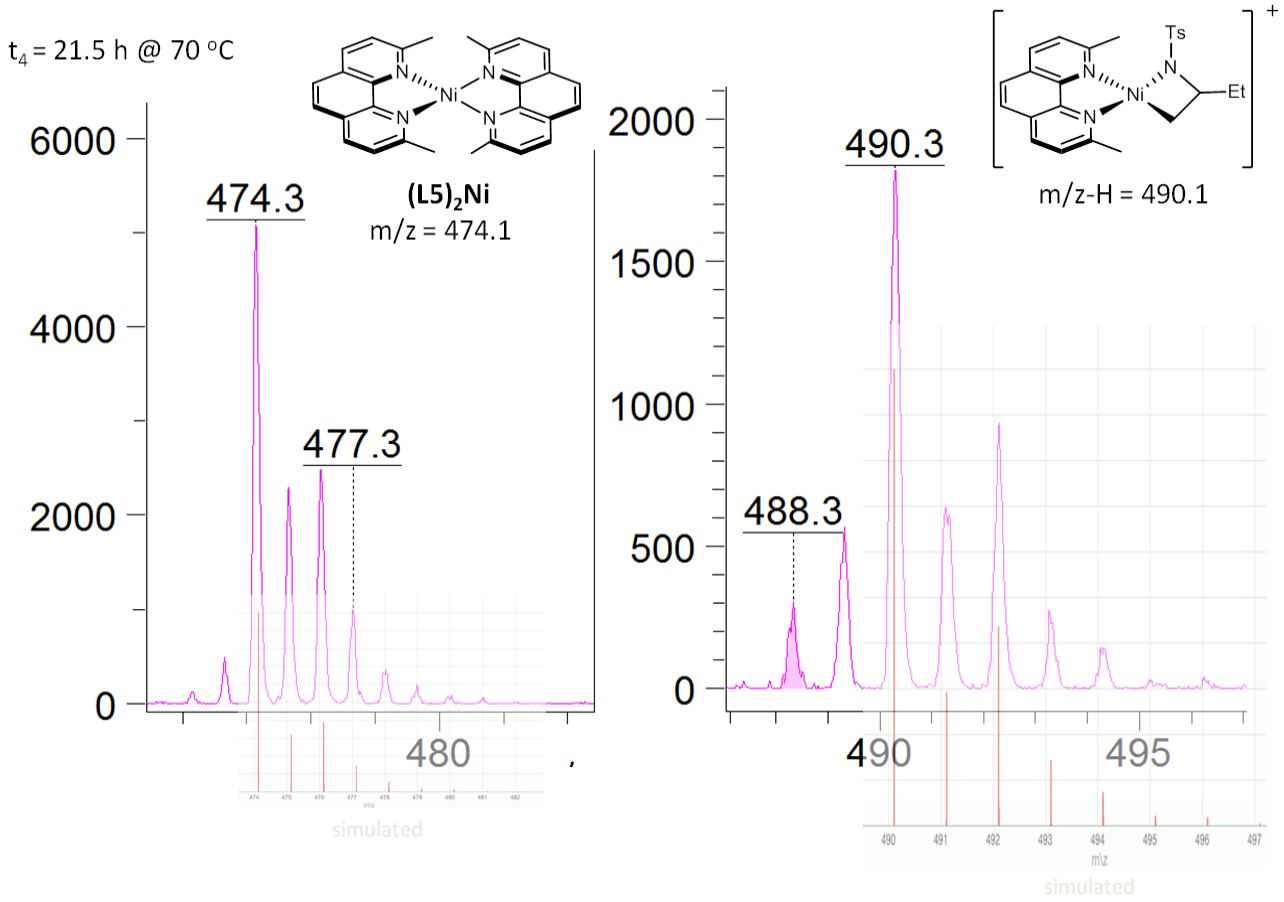

Figure S4.3 MALDI-MS of the crude reaction mixture after the final timepoint (t_4), identifying m/z-H signal of (L5)Ni^{II}(Aza-metallacycle) – right

Stochiometric Monitoring of Ni(0) Undergoing Oxidative Addition to Aziridine with Clean Formation of Organic Products Originating from Deamination of the Aziridine

In the glovebox, **(L5)$_2$Ni** (4.2 mg, 0.01 mmol), **2.1bb** (5.7 mg, 0.03 mmol) and LiCl (2.3 mg, 0.05 mmol) were added to a 10 mL vial and dissolved in 1 mL THF-d_8. This solution was then added to a J-Young NMR tube and monitored by ^{1}H, paramagnetic ^{1}H and ^{19}F NMR. Again, after 3 h at 60 °C, organic product 1-butene starts to be observed, followed by an increased amount after 18 h and full conversion of **(L5)$_2$Ni** (Figure **S**S4.4). While monitoring this and similar reactions, at no point were we able to identify signals that could correspond to (L5)Ni^{II}(Aza-metallacycle).

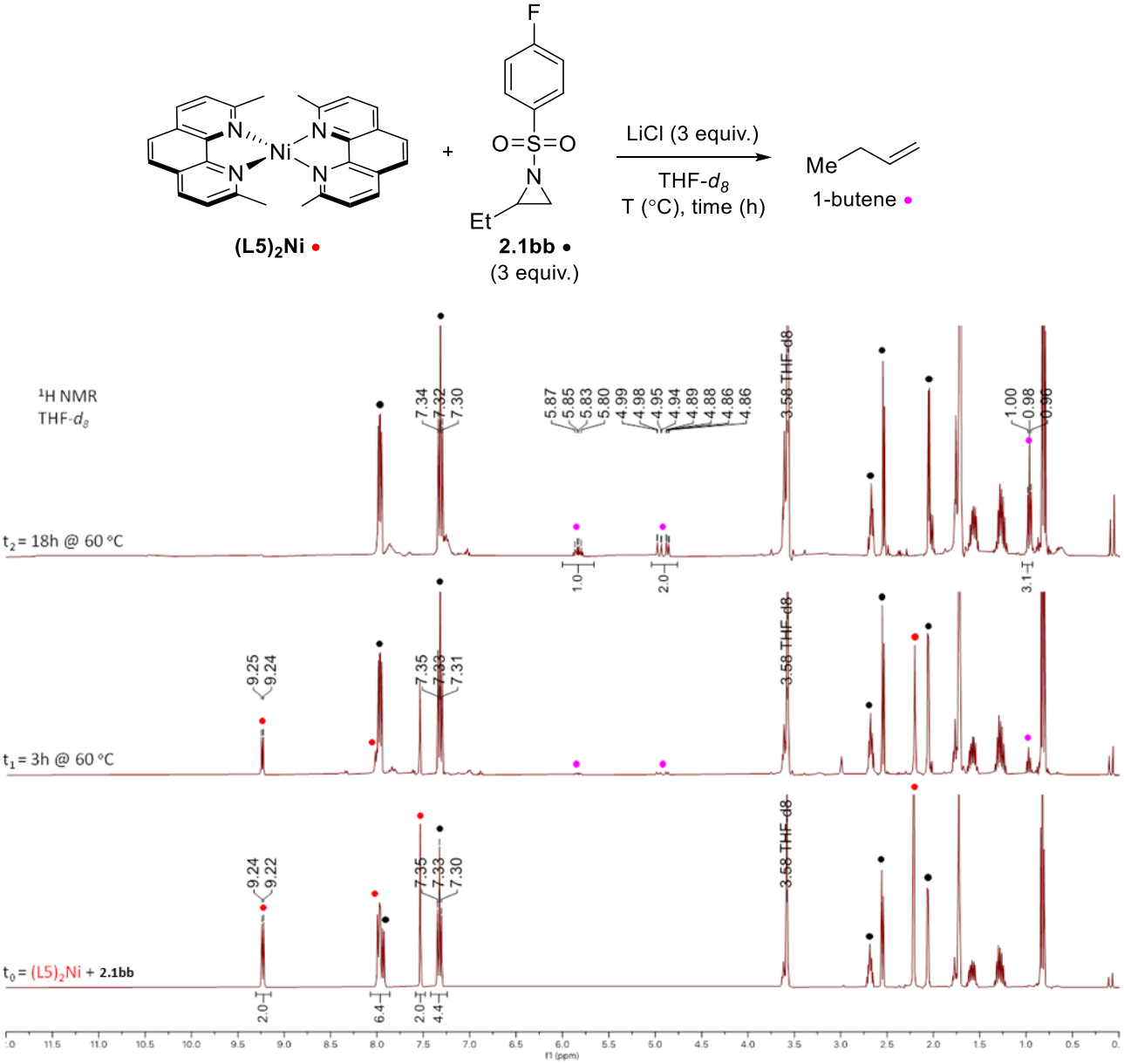

Figure S4.4 ^{1}H NMR spectra of monitoring the reaction between (L5)$_2$Ni (grey) and **2.1bb** (red) with clean formation of deamination product in THF-d_8.

Stochiometric Monitoring of Ni(0) Undergoing Oxidative Addition to Aziridine and Single Crystal Identification of Complexes Originating from Ligand Activation

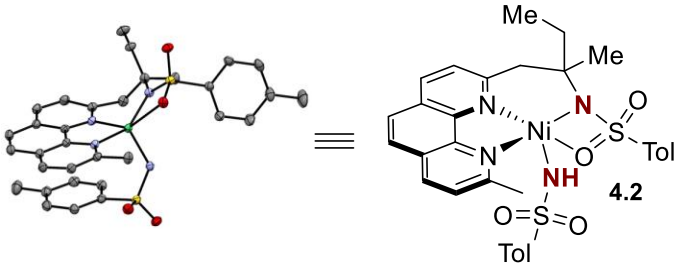

In the glovebox, $(L5)_2Ni$ (6.9 mg, 0.01 mmol) and **2.1az** (10.7 mg, 0.05 mmol) were added to a 10 mL vial and dissolved in 1 mL THF-d_8. This solution was then added to a J-Young NMR tube and monitored by ^1H and paramagnetic ^1H NMR. After 48 h at 50 ^oC a mixture of both diamagnetic (Figure **S**S4.5) and paramagnetic species (Figure **S**S4.6) had formed, with the identification of organic product 1-butene derived from deamination. Crystallization of the crude reaction mixture from THF/Pentane led to crystals of a nickel complex **4.2**.

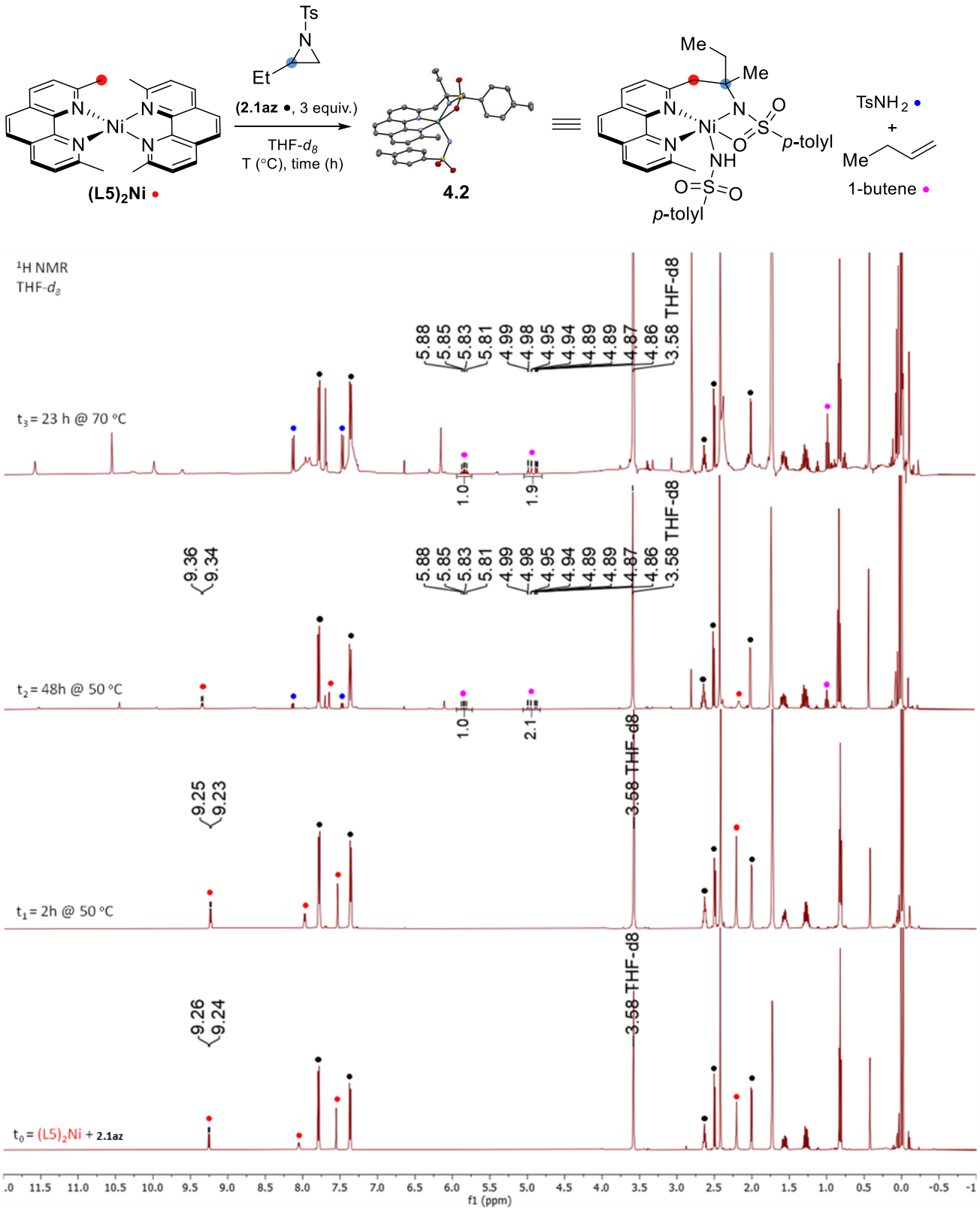

Figure S4.5 ^{1}H NMR spectra of monitoring the reaction between $(L5)_2Ni$ (grey) and 2.1az (red) in THF-d_8.

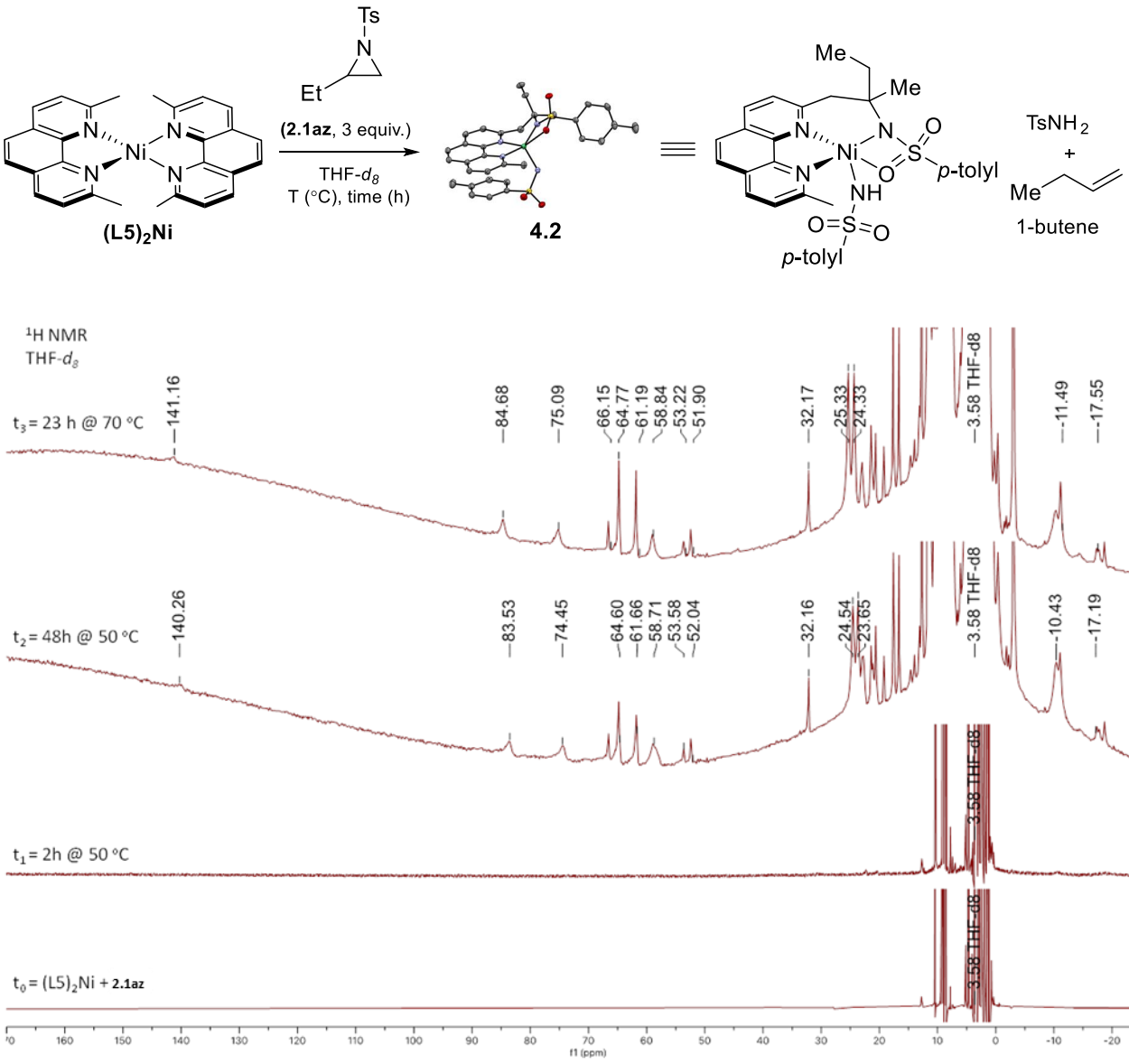

Figure S4.6 Paramagnetic ^{1}H NMR spectra monitoring the reaction between $(L5)_2Ni$ and **2.1az** in THF-d_8.

Isolating An Aziridine Derived Complex Post Oxidative Addition

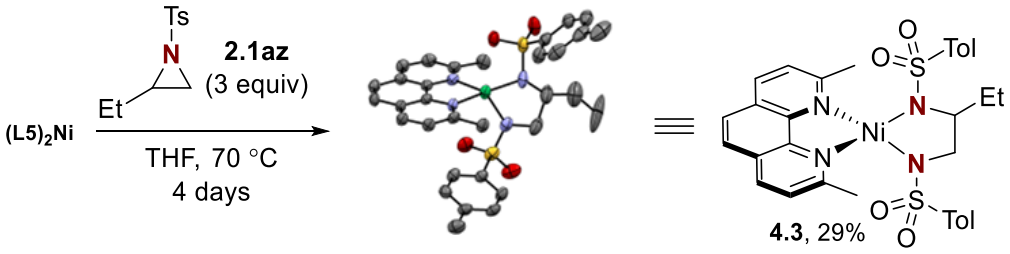

In the glovebox, **(L5)$_2$Ni** (30.6 mg, 0.05 mmol) and **2.1az** (37.0 mg, 0.16 mmol) were added to a 10 mL Schlenk flask and dissolved in 6 mL of THF with a stirrer bar. This stirred solution was then heated at 70 ºC for 4 days where a gradual color change from brown to purple/ blue was observed. To this solution, Et_2O (8 mL) was added and a blue solid precipitated which was then filtered and washed with pentane (1 mL × 3) to afford (L5)Ni(*N*,*N*-ditosyl-1-ethyl-diamine) **4.3** (12 mg, 29 % yield) as a blue powder. ^{1}H NMR (400 MHz, Toluene-d_8) δ 78.15 (s, 1H), 62.11 (s, 1H), 59.25 (s, 1H), 22.90 (s, 7H), 15.00 (d, J = 325.3 Hz, 2H), -4.05 (s, 3H), -11.47 (s, 1H). ^{13}C NMR is omitted due to paramagnetic line broadening.

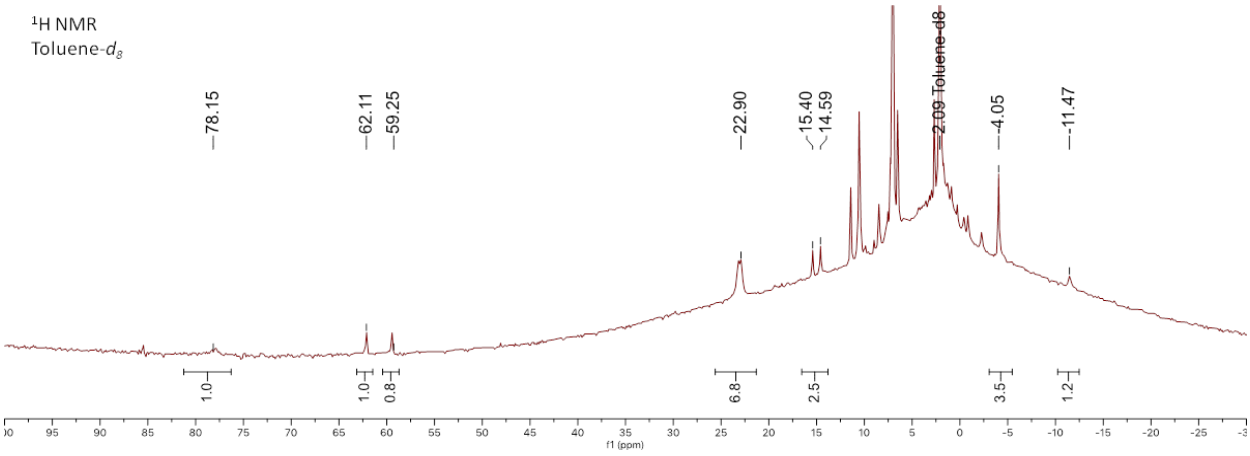

Figure S4.7: Paramagnetic ^{1}H NMR spectra of **4.3** in Toluene-d_8.

4.6.2 Experiments with (L)Ni($CH_2TMS)_2$

Synthesis of (Neocuproine)Ni($CH_2TMS)_2$ (4.5a)

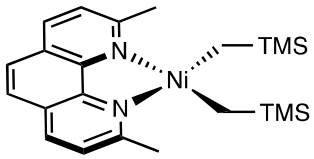

In the glovebox, $(py)_2Ni(CH_2TMS)_2$ (85 mg, 0.22 mmol) was added to a 10 mL vial and dissolved in cold toluene (-36 ºC) with a stirbar. Neocuproine (42 mg, 0.20 mmol) was then added, where a rapid colour change from brown to purple was observed. After 10 minutes, the solvent was removed and filtered through a pipette plug of celite in pentane. The solution was then concentrated to ca. 15 mL and let crystallize overnight. The purple crystals were then filtered and quickly washed with cold (-36 ºC) pentane (0.5 mL) to afford (Neocuproine)Ni$(CH_2TMS)_2$ (38 mg, 43 % yield) as purple crystals.

Note: (Neocuproine)Ni$(CH_2TMS)_2$ is unstable and readily undergoes reductive elimination to form Ni(0) species (Neocuproine)$_2$Ni and Ni black

^{1}H NMR (400 MHz, C_6D_6) δ 7.33 (d, *J* = 8.2 Hz, 2H), 7.05 (s, 2H), 6.67 (d, *J* = 8.2 Hz, 2H), 2.65 (s, 6H), 0.57 – 0.28 (m, 18H). **^{13}C NMR** (101 MHz, C_6D_6) δ 156.34, 149.21, 148.77, 138.51, 134.09, 124.11, 122.86, 116.21, 36.12, 28.24, 25.49, 9.07, -2.09.

NMR data of literature complexes (Bipy)Ni$(CH_2TMS)_2$ and (Phen)Ni$(CH_2TMS)_2$ are given below for convivence:

(Bipy)Ni$(CH_2TMS)_2$ (4.5b): ^{1}H NMR (400 MHz, Tol-d_8) δ 9.06 (dt, *J* = 5.6, 1.3 Hz, 2H), 6.75 (dt, *J* = 8.0, 1.1 Hz, 2H), 6.59 (ddd, *J* = 7.3, 5.7, 1.4 Hz, 2H), 0.38 (s, 18H), 0.25 (s, 4H).

(Phen)Ni$(CH_2TMS)_2$ (4.5c): ^{1}H NMR (400 MHz, THF-d_8) δ 9.40 (dd, *J* = 5.3, 1.3 Hz, 2H), 8.63 (dd, *J* = 8.1, 1.3 Hz, 2H), 7.97 (s, 2H), 7.88 (dd, *J* = 8.0, 5.2 Hz, 2H), -0.02 (s, 16H), -0.08 (s, 3H).

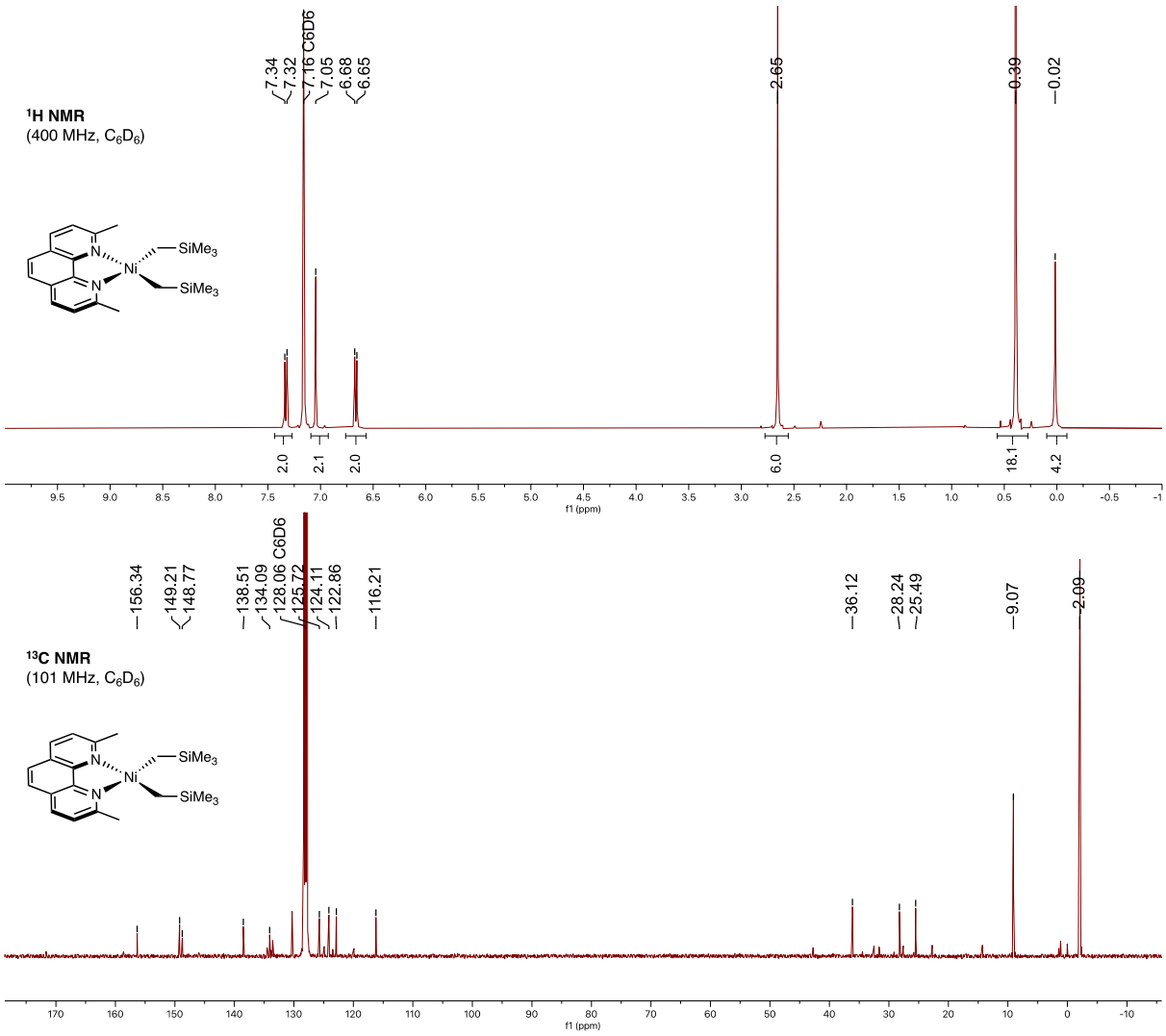

Figure S4.8 NMR spectra (C_6D_6, 400 MHz) of (Neocuproine)Ni($CH_2TMS)_2$.

Synthesis of [(Neocuproine)Ni(TFE)(μ^2-TFE)]$_2$ (4.6)

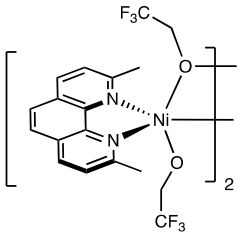

In the glovebox, (Neo)Ni(CH_2TMS)$_2$ (23 mg, 0.05 mmol) was added to a 10 mL vial and dissolved in 2 mL of THF where a stirbar was then added. To the stirred purple solution, a solution of TFE (12 μL, 0.17 mmol, 3.2 equiv.) in 0.5 mL THF was added dropwise where a colour change to white was observed. After 10 minutes the solvent was removed, dissolved in 0.5 mL THF and precipitated with 8 mL of pentane. The suspension was then cooled to -36 °C and filtered to afford [(Neo)Ni(OTFE)(μ2-OTFE)]$_2$ (17 mg, 70 % yield) as a grey powder.

^{1}H NMR (400 MHz, THF-d_8) δ 126.39 (br s, 2H), 52.95 (br s, 1H), 46.21 (br s, 10H), 14.68 (br s, 26H). Due to the paramagnetic nature of this complex, and accompanied line broadening, ^{13}C NMR are not reported.

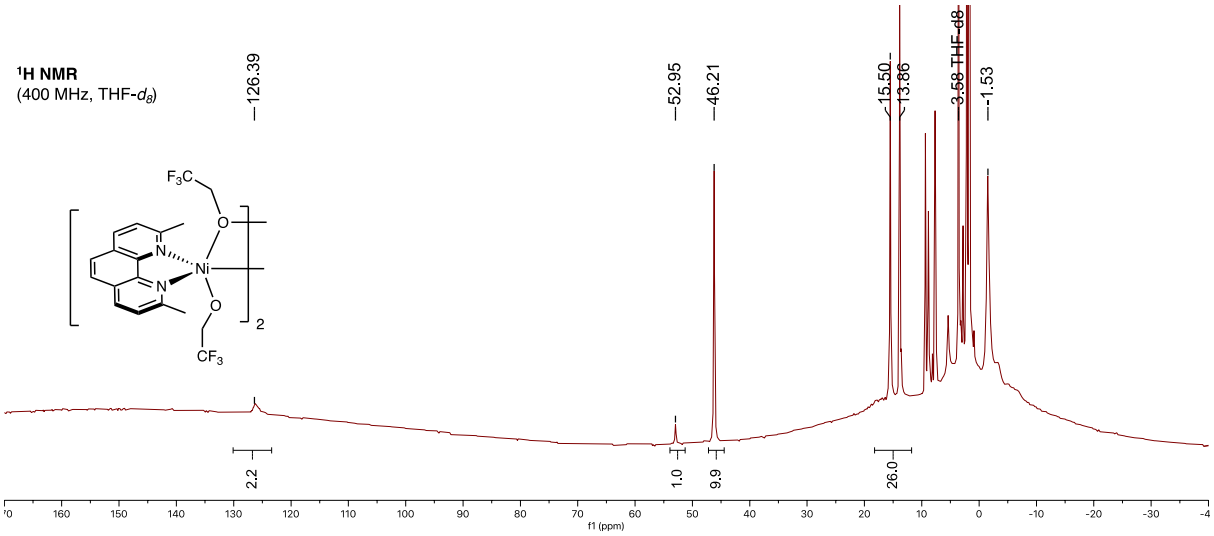

Figure S4.9 NMR spectra (THF-d_8, 400 MHz) of [(Neocuproine)Ni(TFE)(m^2-TFE)]$_2$.

Attempted protonolysis of (Phen)Ni($CH_2TMS)_2$ with TFE

In the glove (Phen)Ni($CH_2TMS)_2$ (9.7 mg, 0.02 mmol) and TMB (1.5 mg) were dissolved in 1 mL of THF-d_8 in a 3 mL vial. This solution was then added to a J. Young NMR tube, and the initial integration ratio of (Phen)Ni($CH_2TMS)_2$ and TMB was measured. This solution was then brought back into the glovebox and TFE (4 mL, 0.056 mmol, 2.4 equiv.) was added and then monitored by ^{1}H NMR spectroscopy with reaction times and conditions shown in the figure below where ultimately after heating at 70 °C no protonolysis was observed.

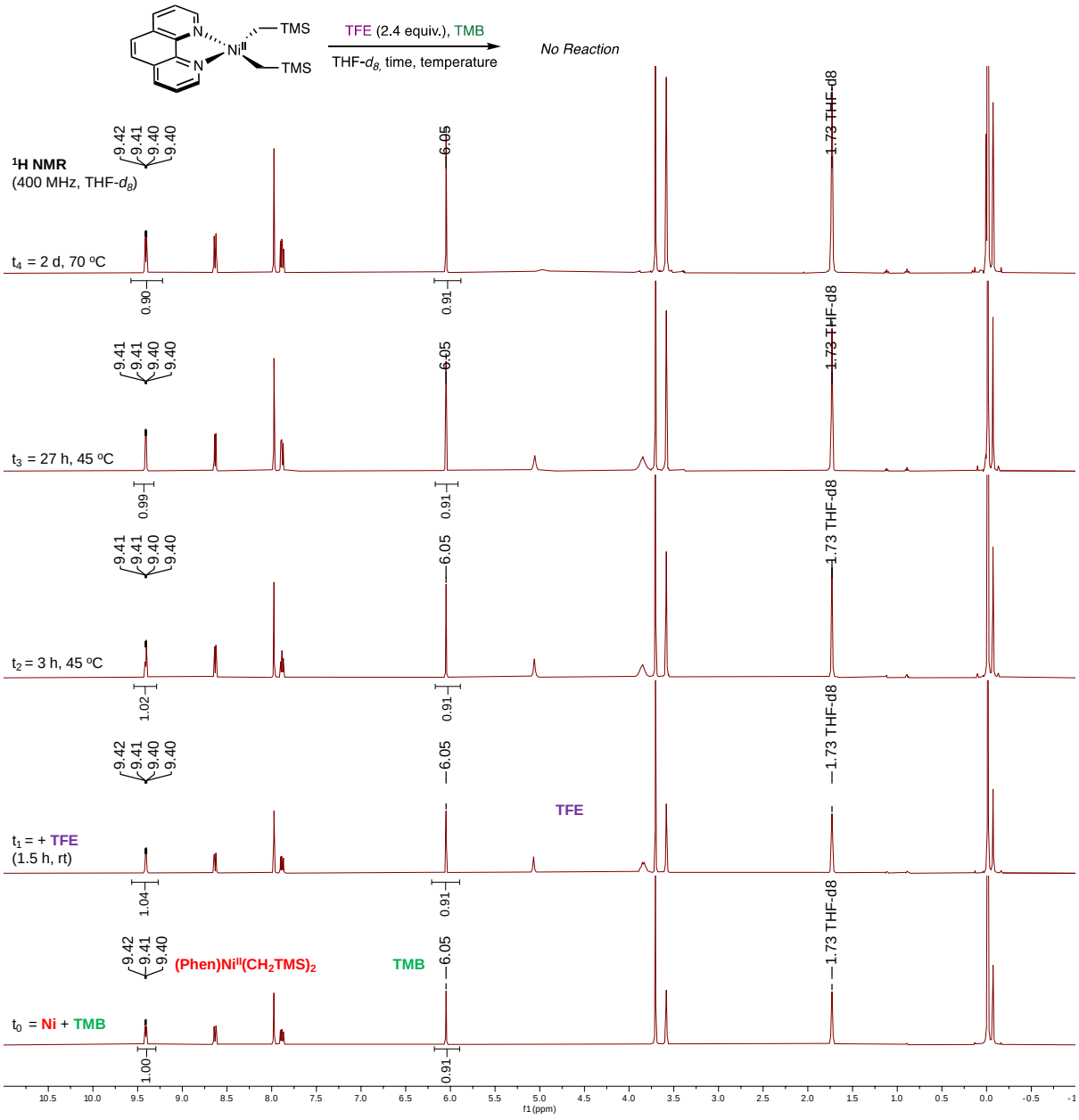

Figure S4.10 ^{1}H spectra (THF-d_8, 400 MHz) of the reaction between (Phen)Ni($CH_2TMS)_2$ (red) and trifluoroethanol (TFE) (purple) where no reaction is observed (internal standard = TMB (green).

Attempted protonolysis of (Bipy)Ni($CH_2TMS)_2$ with TFE

In the glove (Bipy)Ni($CH_2TMS)_2$ (7.3 mg, 0.02 mmol) was dissolved in 1 mL of THF-d_8 in a 3 mL vial and TFE (4 mL, 0.02 mmol, 1.1 equiv.) was added and then monitored by ^{1}H NMR spectroscopy with reaction times and conditions shown in the figure below where ultimately after heating at 70 ^{o}C no protonolysis was observed.

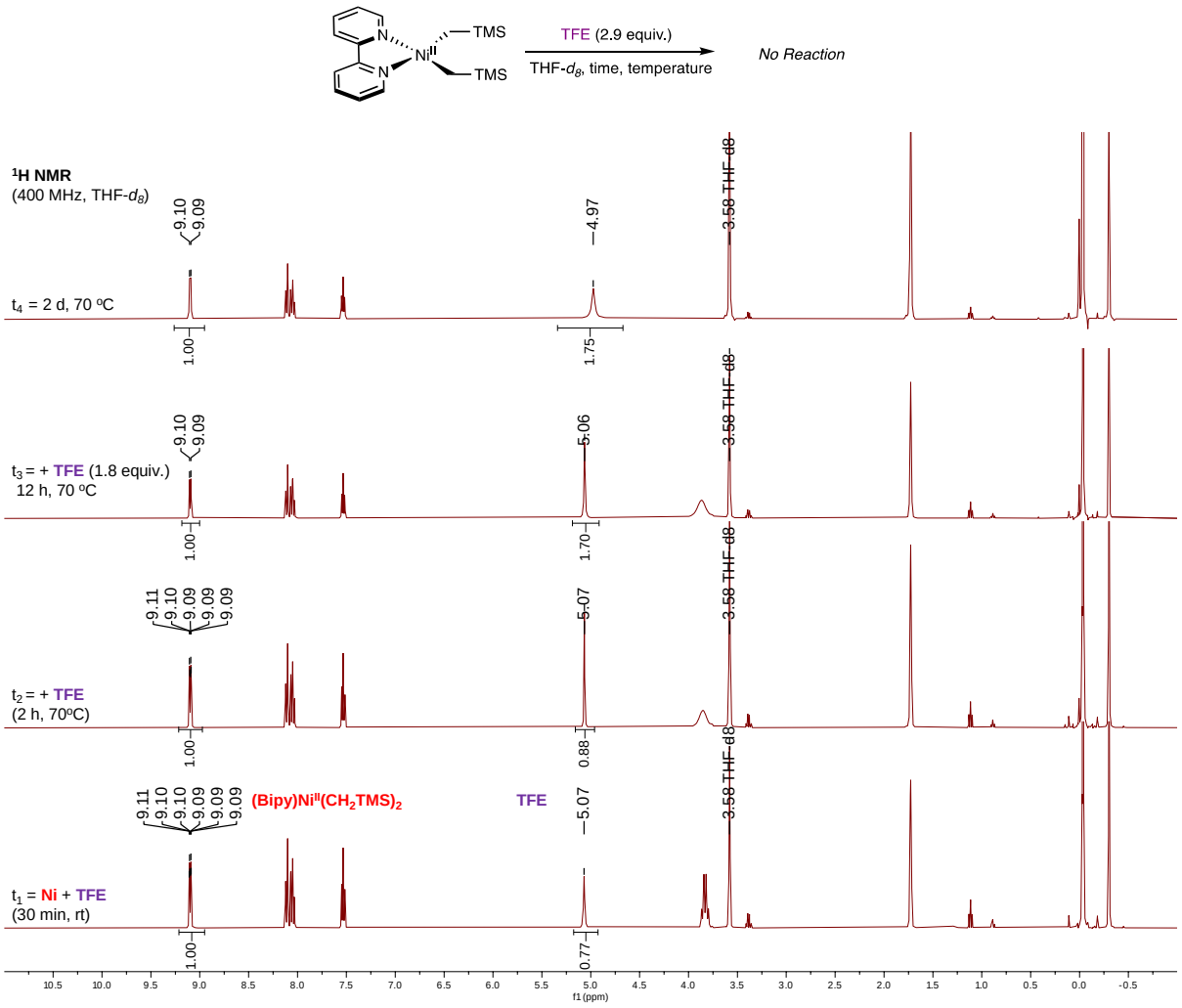

Figure S4.11 ^{1}H spectra (THF-d_8, 400 MHz) of the reaction between (Bipy)Ni($CH_2TMS)_2$ (red) and trifluoroethanol (TFE) (purple) where no reaction is observed.

4.6.3 Crystallographic Data

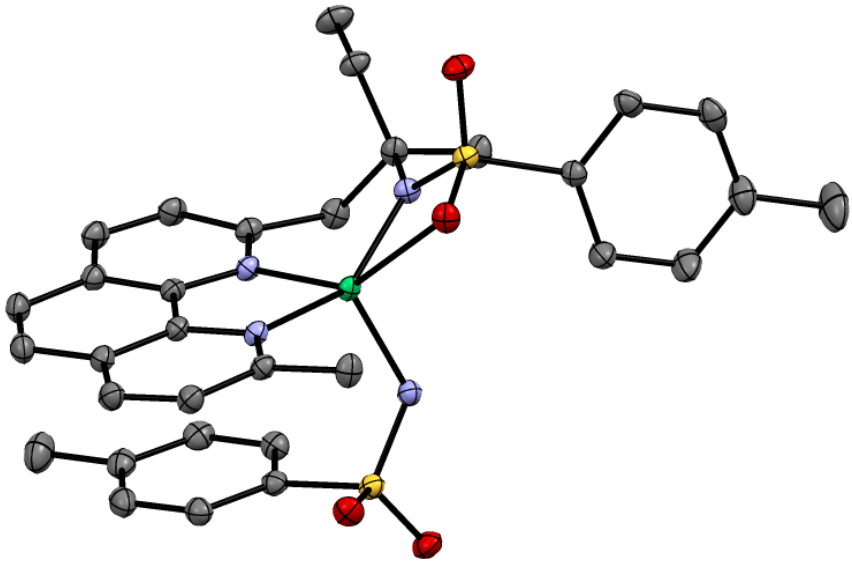

Figure S4.12 ORTEP Diagram of **4.2**

Crystal data and structure refinement for **4.2**.

Identification code	CSD-3-22	
Empirical formula	C32 H34 N4 Ni O4 S2	
Formula weight	661.46	
Temperature	100(2)K	
Wavelength	0.71073 Å	
Crystal system	triclinic	
Space group	P -1	
Unit cell dimensions	a = 10.03268(11)Å	α= 89.2731(7)°.
	b = 11.52248(10)Å	β = 71.8705(8)°.
	c = 14.40581(12)Å	γ = 70.1261(9)°.
Volume	1480.30(3) $Å^3$	
Z	2	
Density (calculated)	1.484 Mg/m^3	
Absorption coefficient	0.842 mm^{-1}	
F(000)	692	

Crystal size	0.300 x 0.200 x 0.050 mm^3
Theta range for data collection	2.284 to 32.185°.
Index ranges	-14<=h<=14,-17<=k<=17,-21<=l<=21
Reflections collected	113880
Independent reflections	10027[R(int) = 0.0364]
Completeness to theta =32.185°	96.0%
Absorption correction	Multi-scan
Max. and min. transmission	1.00 and 0.60
Refinement method	Full-matrix least-squares on F^2
Data / restraints / parameters	10027/ 0/ 418
Goodness-of-fit on F^2	1.048
Final R indices [I>2sigma(I)]	R1 = 0.0301, wR2 = 0.0799
R indices (all data)	R1 = 0.0329, wR2 = 0.0810
Largest diff. peak and hole	0.545 and -0.567 e.$Å^{-3}$

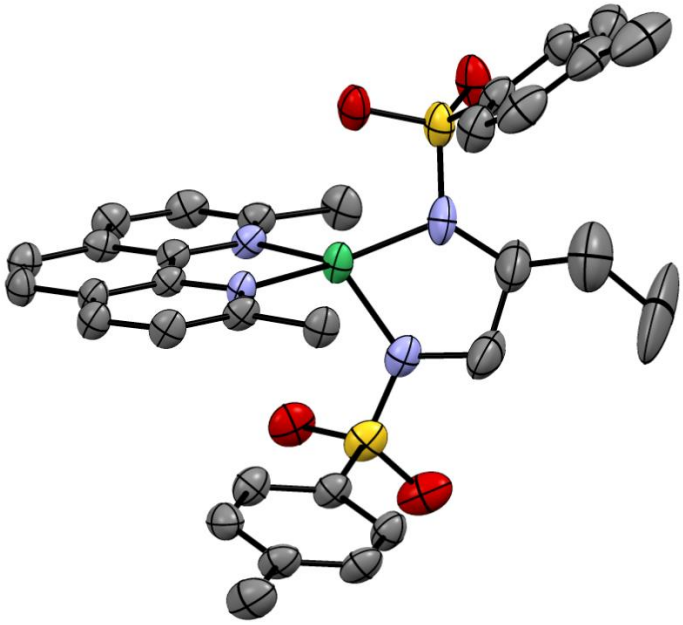

Figure S4.13 ORTEP Diagram of **4.3**

Crystal data and structure refinement for **4.3**

Identification code	mo_CSD0356A_0m	
Empirical formula	C36 H42 N4 Ni O5 S2	
Formula weight	733.56	
Temperature	100(2)K	
Wavelength	0.71073 Å	
Crystal system	triclinic	
Space group	P -1	
Unit cell dimensions	a = 10.3280(8)Å	α= 107.062(2)°.
	b = 11.2508(8)Å	β = 91.452(2)°.
	c = 15.8254(13)Å	γ = 95.082(2)°.
Volume	1748.5(2) $Å^3$	
Z	2	
Density (calculated)	1.393 Mg/m^3	
Absorption coefficient	0.722 mm^{-1}	
F(000)	772	

Crystal size	0.100 x 0.050 x 0.010 mm^3
Theta range for data collection	1.979 to 24.782°.
Index ranges	-12<=h<=8,-13<=k<=13,-18<=l<=18
Reflections collected	17694
Independent reflections	5870[R(int) = 0.0490]
Completeness to theta =24.782°	97.7%
Absorption correction	Multi-scan
Max. and min. transmission	0.74 and 0.63
Refinement method	Full-matrix least-squares on F^2
Data / restraints / parameters	5870/ 0/ 438
Goodness-of-fit on F^2	1.033
Final R indices [I>2sigma(I)]	R1 = 0.0623, wR2 = 0.1579
R indices (all data)	R1 = 0.1070, wR2 = 0.1824
Largest diff. peak and hole	1.531 and -0.403 e.$Å^{-3}$

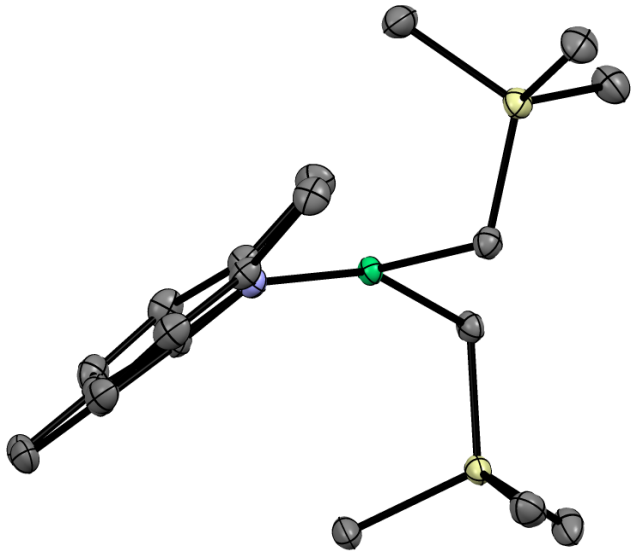

Figure S4.13 ORTEP Diagram of **4.5a**

Crystal data and structure refinement for **4.5a**.

Identification code	mo_CSD0230_0m	
Empirical formula	C22 H34 N2 Ni Si2	
Formula weight	441.40	
Temperature	100(2)K	
Wavelength	0.71073 Å	
Crystal system	monoclinic	
Space group	P 21/c	
Unit cell dimensions	a = 10.2120(4)Å	α= 90°.
	b = 9.9964(4)Å	β = 99.0060(10)°.
	c = 23.4038(9)Å	γ = 90°.
Volume	2359.68(16) $Å^3$	
Z	4	
Density (calculated)	1.242 Mg/m^3	
Absorption coefficient	0.933 mm^{-1}	
F(000)	944	
Crystal size	0.20 x 0.20 x 0.12 mm^3	
Theta range for data collection	1.762 to 35.076°.	
Index ranges	-16<=h<=16,-15<=k<=16,-31<=l<=35	
Reflections collected	51556	
Independent reflections	9756[R(int) = 0.0214]	
Completeness to theta =35.076°	93.4%	

Absorption correction	Multi-scan
Max. and min. transmission	0.74 and 0.71
Refinement method	Full-matrix least-squares on F^2
Data / restraints / parameters	9756/ 0/ 252
Goodness-of-fit on F^2	1.062
Final R indices [I>2sigma(I)]	R1 = 0.0257, wR2 = 0.0663
R indices (all data)	R1 = 0.0296, wR2 = 0.0682
Largest diff. peak and hole	0.519 and -0.285 e.$Å^{-3}$

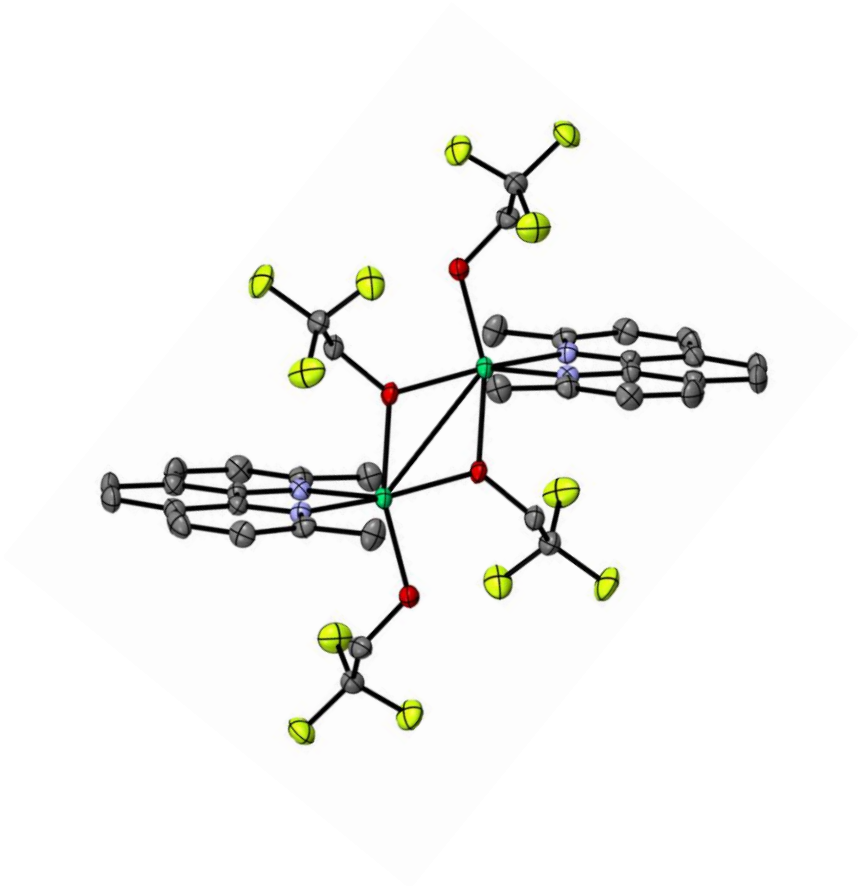

Figure S4.14 ORTEP Diagram of **4.6**

Crystal data and structure refinement for **4.6**.

Identification code	CSD-02-96	
Empirical formula	C36 H32 F12 N4 Ni2 O4	
Formula weight	930.07	
Temperature	100(2)K	
Wavelength	0.71073 E	
Crystal system	monoclinic	
Space group	I 2/a	
Unit cell dimensions	a = 17.9140(11)E	α= 90°.
	b = 9.5868(4)E	β = 107.781(6)°.
	c = 22.8440(12)E	γ = 90°.
Volume	3735.8(4) E^3	
Z	4	
Density (calculated)	1.654 Mg/m^3	
Absorption coefficient	1.114 mm^{-1}	
F(000)	1888	
Crystal size	0.050 x 0.050 x 0.030 mm^3	
Theta range for data collection	2.322 to 27.772°.	

Index ranges	-16<=h<=22,-12<=k<=12,-25<=l<=29
Reflections collected	13820
Independent reflections	3832[R(int) = 0.0981]
Completeness to theta =27.772°	86.7%
Absorption correction	Multi-scan
Max. and min. transmission	1.00 and 0.39
Refinement method	Full-matrix least-squares on F^2
Data / restraints / parameters	3832/ 0/ 264
Goodness-of-fit on F^2	0.970
Final R indices [I>2sigma(I)]	R1 = 0.0484, wR2 = 0.1119
R indices (all data)	R1 = 0.0718, wR2 = 0.1243
Largest diff. peak and hole	1.195 and -0.662 $e.E^{-3}$

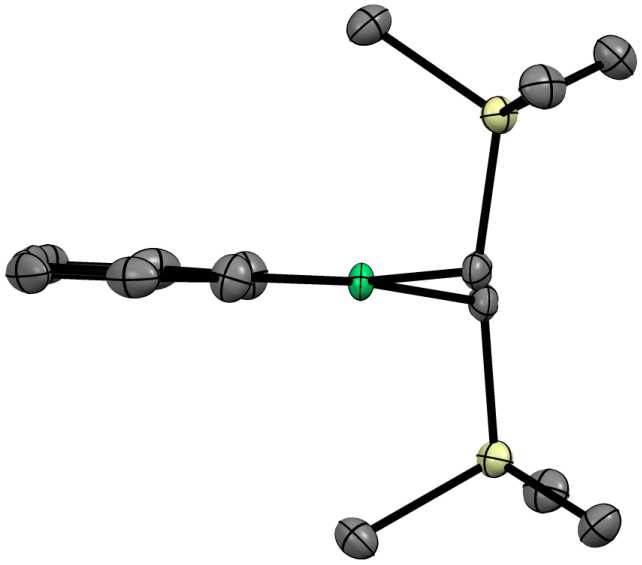

Figure S4.15 ORTEP Diagram of **4.5b**

Crystal data and structure refinement for **4.5b**.

Identification code	CSD-03-11	
Empirical formula	C18 H30 N2 Ni Si2	
Formula weight	389.33	
Temperature	100(2)K	
Wavelength	0.71073 E	
Crystal system	monoclinic	
Space group	I 2/a	
Unit cell dimensions	a = 17.8002(3)E	α= 90°.
	b = 9.38055(15)E	β = 98.7060(17)°.
	c = 36.3083(6)E	γ = 90°.
Volume	5992.74(18) E^3	
Z	12	
Density (calculated)	1.295 Mg/m^3	
Absorption coefficient	1.092 mm^{-1}	
F(000)	2496	
Crystal size	0.100 x 0.100 x 0.050 mm^3	
Theta range for data collection	2.244 to 29.805°.	
Index ranges	-21<=h<=24,-13<=k<=13,-50<=l<=49	
Reflections collected	45281	
Independent reflections	7962[R(int) = 0.0384]	
Completeness to theta =29.805°	92.7%	
Absorption correction	Multi-scan	
Max. and min. transmission	1.00 and 0.81	

Refinement method	Full-matrix least-squares on F^2
Data / restraints / parameters	7962/ 472/ 534
Goodness-of-fit on F^2	1.031
Final R indices [I>2sigma(I)]	R1 = 0.0366, wR2 = 0.0950
R indices (all data)	R1 = 0.0486, wR2 = 0.1017
Largest diff. peak and hole	2.108 and -0.636 e.E^{-3}

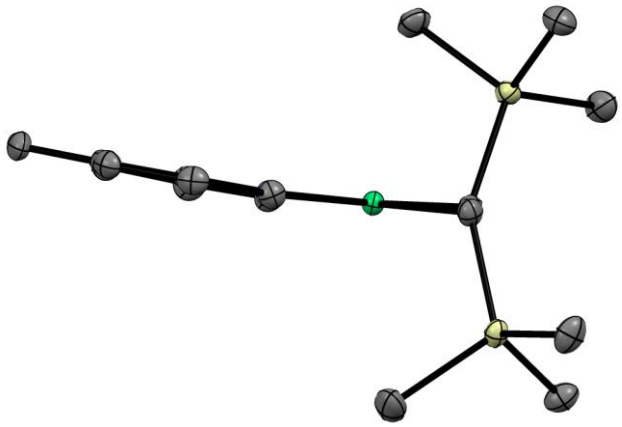

Figure S4.16 ORTEP Diagram of **4.5c**

Crystal data and structure refinement for **4.5c**.

Identification code	CSD-3-74	
Empirical formula	C20 H30 N2 Ni Si2	
Formula weight	413.35	
Temperature	100(2)K	
Wavelength	0.71073 E	
Crystal system	monoclinic	
Space group	P 21/n	
Unit cell dimensions	a = 7.16860(10)E	α= 90°.
	b = 12.0367(2)E	β = 94.8870(10)°.
	c = 24.5788(3)E	γ = 90°.
Volume	2113.10(5) E^3	
Z	4	
Density (calculated)	1.299 Mg/m^3	
Absorption coefficient	1.037 mm^{-1}	
F(000)	880	
Crystal size	0.100 x 0.100 x 0.100 mm^3	
Theta range for data collection	2.373 to 31.802°.	
Index ranges	-10<=h<=10,-17<=k<=17,-34<=l<=36	
Reflections collected	41226	
Independent reflections	6893[R(int) = 0.0211]	
Completeness to theta =31.802°	95.4%	
Absorption correction	Multi-scan	
Max. and min. transmission	1.00 and 0.37	
Refinement method	Full-matrix least-squares on F^2	
Data / restraints / parameters	6893/ 0/ 232	

Goodness-of-fit on F^2	1.273
Final R indices [I>2sigma(I)]	R1 = 0.0372, wR2 = 0.0932
R indices (all data)	R1 = 0.0389, wR2 = 0.0937
Largest diff. peak and hole	0.748 and -0.500 e.E^{-3}

4.6.4 DFT Data

All calculations were performed on the full molecular models without any truncations using Gaussian16, Revision B.01. Optimizations were done using hybrid functional B3LYP in combination with D3 version of the Grimme empirical dispersion correction and solvent model IEFPCM(DMA). For all calculations the basis set 6-31+G(d,p) was employed. Vibrational mode analysis was performed for all structures to ensure that they have zero (ground state) or exactly one (TS) imaginary frequency.

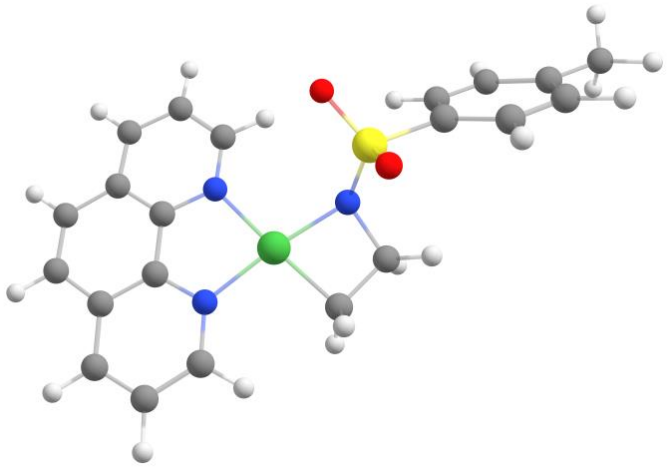

Figure S4.17 Calculated structure **DFT_4.1a** (B3LYP-D3/6-31+G(d,p)/IEFPCM(DMA))

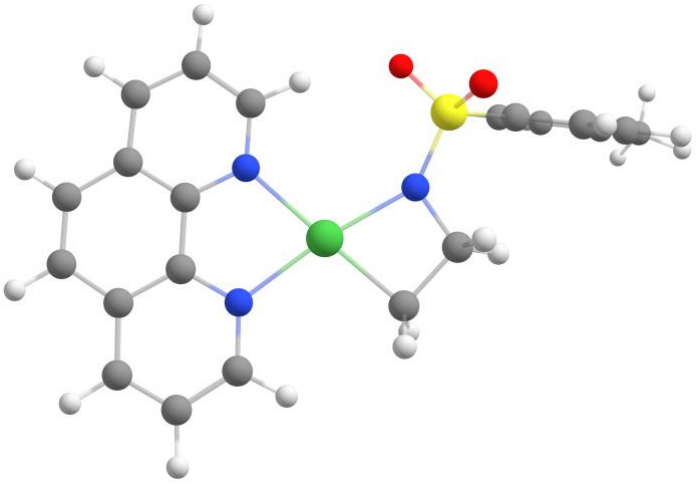

Figure S4.18 Calculated structure **DFT_4.1b** (B3LYP-D3/6-31+G(d,p)/IEFPCM(DMA))

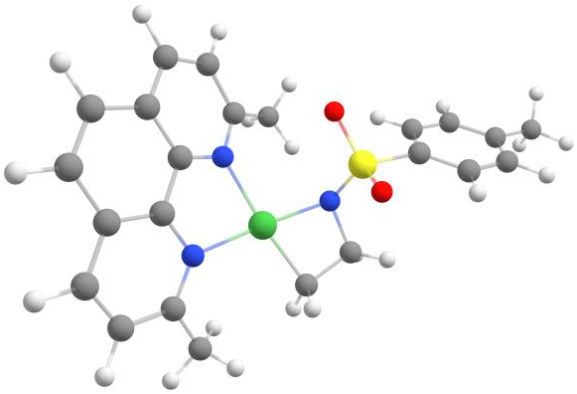

Figure S4.19 Calculated structure **DFT_4.2a** (B3LYP-D3/6-31+G(d,p)/IEFPCM(DMA))

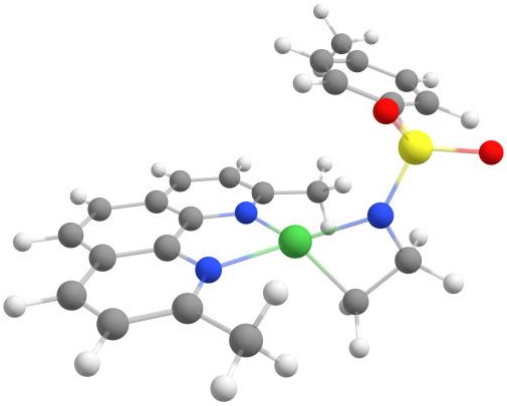

Figure S4.20 Calculated structure **DFT_4.2b** (B3LYP-D3/6-31+G(d,p)/IEFPCM(DMA))

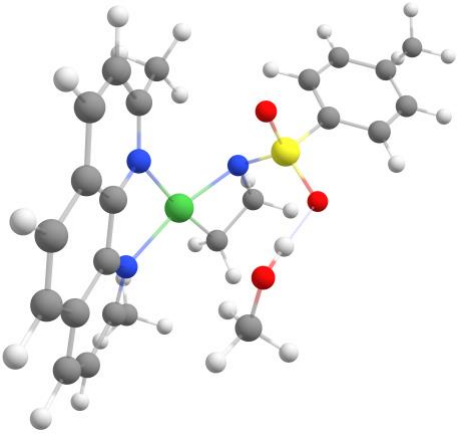

Figure S4.21 Calculated structure **DFT_4.3a** (B3LYP-D3/6-31+G(d,p)/IEFPCM(DMA))

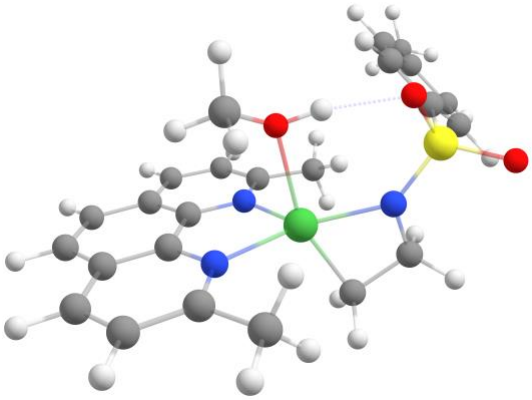

Figure S4.22. Calculated structure **DFT_4.3b** (B3LYP-D3/6-31+G(d,p)/IEFPCM(DMA))

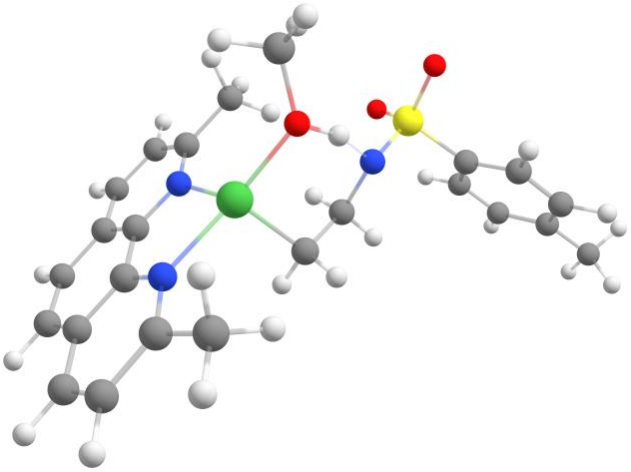

Figure S4.23. Calculated structure **DFT_4.4** (B3LYP-D3/6-31+G(d,p)/IEFPCM(DMA))

Cartesian coordinates of calculated structure **DFT_4.1a**:

Ni	0.766077000	-0.796378000	0.233281000
S	-1.958551000	-0.073581000	-0.997175000
O	-1.522041000	1.273817000	-1.453840000
N	2.619177000	-1.319286000	0.205565000
N	1.521766000	1.063684000	0.105131000
O	-1.998802000	-1.126897000	-2.054658000
N	-1.117342000	-0.469957000	0.342186000

C	-0.038167000	-2.511620000	0.554957000
C	-3.650431000	0.082983000	-0.390404000
C	2.881881000	1.035474000	0.083732000
C	3.138050000	-2.547636000	0.228129000
C	3.689735000	2.192031000	0.039104000
C	-3.936250000	1.059311000	0.571709000
C	4.884107000	-0.400216000	0.075925000
C	-5.238667000	1.190146000	1.045793000
C	1.636742000	3.460165000	0.087632000
C	3.479814000	-0.261787000	0.119499000
C	-5.957134000	-0.616455000	-0.381338000
C	-1.388847000	-1.869589000	0.833225000
C	4.524810000	-2.783017000	0.175693000
C	-4.653232000	-0.757834000	-0.869475000
C	0.916052000	2.248349000	0.116767000
C	5.402077000	-1.715386000	0.104437000
C	-6.270707000	0.354946000	0.578203000
C	3.019408000	3.437856000	0.040934000
C	-7.676331000	0.515209000	1.105580000
H	0.412488000	-3.042305000	1.401557000
H	-0.027144000	-3.135928000	-0.346292000
H	-1.613836000	-1.804264000	1.902464000
H	-3.147257000	1.704541000	0.944214000
H	-5.461570000	1.949182000	1.791179000
H	1.092743000	4.398019000	0.094642000

H	-6.737679000	-1.273519000	-0.755031000
H	4.885731000	-3.804913000	0.197219000
H	-4.415142000	-1.510145000	-1.613099000
H	6.475220000	-1.875879000	0.070348000
H	3.591817000	4.359931000	0.008965000
H	-8.354070000	-0.226803000	0.675276000
H	-8.069587000	1.511114000	0.871379000
H	-7.700082000	0.407985000	2.195848000
C	5.689815000	0.789733000	0.012095000
C	5.118207000	2.031736000	-0.000174000
H	5.738637000	2.921677000	-0.040695000
H	6.769348000	0.680835000	-0.020867000
H	-2.244313000	-2.344240000	0.336491000
H	-0.166101000	2.224783000	0.122919000
H	2.433394000	-3.367021000	0.292089000

Cartesian coordinates of calculated structure **DFT_4.1b**:

Ni	0.753515000	-0.825041000	-0.260203000
S	-2.279937000	0.686075000	-0.991584000
O	-1.813582000	2.023140000	-0.516967000
N	2.735597000	-1.460916000	0.099420000
N	1.794918000	1.048648000	-0.071115000
O	-2.563088000	0.594705000	-2.459073000
N	-1.269572000	-0.435954000	-0.446573000
C	-0.270071000	-2.576085000	-0.460928000

C	-3.868143000	0.382104000	-0.182304000
C	3.126249000	0.892064000	0.160051000
C	3.157877000	-2.718076000	0.174625000
C	4.016506000	1.981420000	0.311501000
C	-4.050513000	0.801070000	1.140344000
C	5.006888000	-0.681754000	0.489314000
C	-5.250887000	0.519591000	1.790479000
C	2.113758000	3.429040000	-0.020992000
C	3.630719000	-0.453168000	0.251090000
C	-6.072185000	-0.600591000	-0.179587000
C	-1.572120000	-1.853895000	-0.817042000
C	4.507384000	-3.046677000	0.409077000
C	-4.874136000	-0.321938000	-0.845086000
C	1.303466000	2.282958000	-0.158198000
C	5.431442000	-2.029038000	0.566355000
C	-6.281854000	-0.184176000	1.142549000
C	3.467642000	3.281547000	0.213259000
C	-7.586959000	-0.457225000	1.851612000
H	-0.330723000	-3.121077000	0.491071000
H	0.072900000	-3.265375000	-1.241849000
H	-2.461746000	-2.210251000	-0.273013000
H	-3.261586000	1.345325000	1.649318000
H	-5.392286000	0.850903000	2.816146000
H	1.661260000	4.411099000	-0.101170000
H	-6.853509000	-1.148725000	-0.699484000

H	4.803067000	-4.088267000	0.462824000
H	-4.722597000	-0.641443000	-1.870301000
H	6.478512000	-2.252195000	0.748042000
H	4.113625000	4.147549000	0.323160000
H	-8.159429000	-1.242213000	1.349600000
H	-8.210229000	0.445075000	1.876958000
H	-7.418390000	-0.763277000	2.889179000
C	5.886172000	0.444901000	0.638349000
C	5.409767000	1.722042000	0.552960000
H	6.080041000	2.568550000	0.666276000
H	6.940210000	0.260064000	0.820941000
H	-1.790331000	-1.935866000	-1.890779000
H	0.234974000	2.355368000	-0.338458000
H	2.397556000	-3.481166000	0.044197000

Cartesian coordinates of calculated structure **DFT_4.2a**:

Ni	0.766358000	-0.862837000	0.672016000
S	-1.711899000	0.064907000	-0.831861000
O	-1.288345000	1.488379000	-0.833302000
N	2.701665000	-1.159270000	0.385540000
N	1.328925000	1.080065000	0.793389000
O	-1.467925000	-0.681542000	-2.102613000
N	-1.133418000	-0.659263000	0.512186000
C	0.034223000	-2.646146000	0.522722000
C	-3.496447000	0.031080000	-0.570218000

C	2.487487000	1.205452000	0.087179000
C	3.452553000	-2.270742000	0.339361000
C	3.003459000	2.444834000	-0.349604000
C	-4.032585000	0.754883000	0.501828000
C	4.459712000	0.059297000	-0.825439000
C	-5.407686000	0.735427000	0.718520000
C	1.145695000	3.464754000	0.799276000
C	3.223722000	-0.003094000	-0.144107000
C	-5.702917000	-0.723303000	-1.179526000
C	-1.395776000	-2.136252000	0.565816000
C	4.697947000	-2.282523000	-0.338312000
C	-4.322829000	-0.710699000	-1.411908000
C	0.684269000	2.180434000	1.188517000
C	5.189188000	-1.145577000	-0.939497000
C	-6.265704000	-0.004357000	-0.116980000
C	2.271170000	3.599524000	0.016981000
C	-7.754057000	-0.011527000	0.136990000
H	0.303282000	-3.291373000	1.362461000
H	0.309336000	-3.115898000	-0.428367000
H	-1.904070000	-2.354030000	1.511632000
H	-3.379259000	1.323986000	1.154929000
H	-5.825509000	1.299778000	1.548215000
H	0.589811000	4.337558000	1.124571000
H	-6.346473000	-1.302043000	-1.836458000
H	5.262006000	-3.208287000	-0.366174000

H	-3.891714000	-1.266838000	-2.236859000
H	6.139754000	-1.157270000	-1.464228000
H	2.616322000	4.579786000	-0.298624000
H	-8.281895000	-0.640441000	-0.584772000
H	-8.166365000	1.001824000	0.071240000
H	-7.977631000	-0.385117000	1.142694000
C	4.928130000	1.320672000	-1.325626000
C	4.228652000	2.471523000	-1.094512000
C	2.989219000	-3.516486000	1.035236000
C	-0.492825000	2.046985000	2.107996000
H	2.347274000	-4.114626000	0.381077000
H	3.848635000	-4.130774000	1.313875000
H	2.419210000	-3.266906000	1.930346000
H	4.599591000	3.426653000	-1.453757000
H	5.865859000	1.342853000	-1.872243000
H	-0.935314000	1.055833000	2.017769000
H	-0.156932000	2.200184000	3.141660000
H	-1.245534000	2.807517000	1.886389000
H	-2.035679000	-2.491823000	-0.250716000

Cartesian coordinates of calculated structure **DFT_4.2b**:

Ni	0.535213000	-1.038037000	0.559260000
S	-2.325525000	-2.129129000	-0.668450000
O	-1.749538000	-2.382016000	-2.018020000
N	2.491279000	-0.936209000	-0.035121000

N	0.791856000	1.010715000	0.667298000
O	-3.415325000	-3.040949000	-0.214556000
N	-1.113252000	-2.070511000	0.392018000
C	-0.001896000	-1.758523000	2.422807000
C	-3.041953000	-0.475329000	-0.747182000
C	2.010681000	1.391301000	0.190957000
C	3.308918000	-1.950492000	-0.338663000
C	2.412972000	2.741537000	0.083728000
C	-2.364041000	0.517946000	-1.464256000
C	4.212486000	0.673591000	-0.661045000
C	-2.840717000	1.825798000	-1.439342000
C	0.261290000	3.319364000	1.010976000
C	2.922474000	0.345969000	-0.185075000
C	-4.654228000	1.154263000	0.000403000
C	-1.362157000	-2.182234000	1.861309000
C	4.616183000	-1.703838000	-0.819486000
C	-4.187498000	-0.164400000	-0.014428000
C	-0.063232000	1.943179000	1.099514000
C	5.064275000	-0.407693000	-0.984117000
C	-3.988308000	2.167882000	-0.701847000
C	1.479537000	3.718519000	0.502058000
C	-4.463444000	3.599696000	-0.648252000
H	-0.051121000	-1.009891000	3.218374000
H	0.625834000	-2.602797000	2.728262000
H	-2.160872000	-1.497498000	2.181454000

H	-1.470333000	0.266435000	-2.025473000
H	-2.311883000	2.596435000	-1.994149000
H	-0.463829000	4.050584000	1.351023000
H	-5.547721000	1.394825000	0.570246000
H	5.257591000	-2.545175000	-1.056864000
H	-4.707009000	-0.943793000	0.532270000
H	6.066184000	-0.211772000	-1.354213000
H	1.732915000	4.772000000	0.429844000
H	-5.496993000	3.667284000	-0.297751000
H	-4.399560000	4.077084000	-1.631306000
H	-3.839655000	4.185951000	0.038112000
C	4.587352000	2.054542000	-0.780484000
C	3.721087000	3.048884000	-0.422755000
C	2.776080000	-3.342552000	-0.155233000
C	-1.348599000	1.492511000	1.725488000
H	1.959086000	-3.526862000	-0.861831000
H	3.552259000	-4.093480000	-0.311533000
H	2.359372000	-3.454729000	0.850770000
H	4.011302000	4.091604000	-0.508107000
H	5.578073000	2.292726000	-1.155162000
H	-1.701175000	0.571972000	1.264301000
H	-1.183655000	1.291351000	2.790416000
H	-2.122334000	2.256544000	1.635285000
H	-1.677886000	-3.201483000	2.122738000

Cartesian coordinates of calculated structure **DFT_4.3a**:

Ni	-0.652478000	-0.710464000	-0.967793000
S	1.810695000	0.168791000	0.613692000
O	1.452625000	1.608114000	0.634151000
N	-2.587302000	-1.040343000	-0.756319000
N	-1.226848000	1.228655000	-0.949960000
O	1.478373000	-0.570889000	1.880228000
N	1.243323000	-0.516509000	-0.744449000
C	0.080769000	-2.498867000	-0.933770000
C	3.597917000	0.031680000	0.434592000
C	-2.390982000	1.286069000	-0.244487000
C	-3.328971000	-2.156864000	-0.817593000
C	-2.915560000	2.478297000	0.297081000
C	4.190271000	0.490398000	-0.747904000
C	-4.359459000	0.050432000	0.549370000
C	5.574468000	0.424605000	-0.885839000
C	-1.060207000	3.605390000	-0.752413000
C	-3.121297000	0.059109000	-0.128862000
C	5.763905000	-0.550662000	1.312468000
C	1.509341000	-1.991958000	-0.840964000
C	-4.577546000	-2.238995000	-0.151644000
C	4.375172000	-0.489980000	1.467423000
C	-0.588743000	2.362310000	-1.248994000
C	-5.079564000	-1.165168000	0.549372000
C	6.383800000	-0.097347000	0.139930000

C	-2.188375000	3.664672000	0.035843000
C	7.880964000	-0.176425000	-0.037642000
H	-0.133606000	-3.055817000	-1.849413000
H	-0.247935000	-3.064099000	-0.055419000
H	2.101798000	-2.173102000	-1.744700000
H	3.572601000	0.885278000	-1.547829000
H	6.036429000	0.780334000	-1.803031000
H	-0.509069000	4.506439000	-0.999474000
H	6.370140000	-0.958546000	2.116618000
H	-5.134134000	-3.167776000	-0.211095000
H	3.899118000	-0.845829000	2.374194000
H	-6.030839000	-1.232953000	1.068522000
H	-2.539664000	4.611466000	0.435635000
H	8.380754000	-0.467981000	0.889857000
H	8.290075000	0.786863000	-0.360691000
H	8.141963000	-0.912230000	-0.807483000
C	-4.835282000	1.257934000	1.162775000
C	-4.142435000	2.429353000	1.038336000
C	-2.848281000	-3.329973000	-1.619441000
C	0.590567000	2.313710000	-2.174017000
H	-2.231325000	-3.995907000	-1.007995000
H	-3.701175000	-3.906852000	-1.984952000
H	-2.248335000	-2.996312000	-2.466162000
H	-4.520011000	3.345420000	1.482275000
H	-5.773852000	1.225113000	1.707417000

H	1.009442000	1.308978000	-2.204653000
H	0.265443000	2.602669000	-3.181654000
H	1.361968000	3.017989000	-1.854396000
H	2.070964000	-2.383489000	0.015349000
O	-1.160418000	-0.255337000	2.785242000
H	-0.231862000	-0.298425000	2.479763000
C	-1.736111000	-1.545486000	2.586468000
H	-2.814338000	-1.457666000	2.744547000
H	-1.563503000	-1.906835000	1.566084000
H	-1.337801000	-2.285514000	3.295420000

Cartesian coordinates of calculated structure **DFT_4.3b**:

Ni	0.574215000	-0.791213000	0.507564000
S	-2.472656000	-2.055885000	-0.286912000
O	-1.960315000	-2.275012000	-1.682506000
N	2.622187000	-0.847555000	0.222752000
N	0.964634000	1.257954000	0.436508000
O	-3.337091000	-3.136852000	0.267677000
N	-1.204536000	-1.723280000	0.629724000
C	0.089341000	-1.163829000	2.501299000
C	-3.507914000	-0.581738000	-0.377644000
C	2.273429000	1.515658000	0.162435000
C	3.401446000	-1.929185000	0.151248000
C	2.788117000	2.824441000	0.017244000
C	-3.339752000	0.321239000	-1.431759000

C	4.533816000	0.595229000	-0.217370000
C	-4.054144000	1.518995000	-1.428336000
C	0.554399000	3.614885000	0.476100000
C	3.159850000	0.388061000	0.048097000
C	-5.085751000	0.916039000	0.664846000
C	-1.331611000	-1.586540000	2.110585000
C	4.786084000	-1.806296000	-0.111783000
C	-4.384569000	-0.291659000	0.671843000
C	0.117138000	2.273578000	0.614200000
C	5.347564000	-0.558208000	-0.299068000
C	-4.928959000	1.841669000	-0.378351000
C	1.871429000	3.890648000	0.173994000
C	-5.657745000	3.163718000	-0.360004000
H	0.123131000	-0.296993000	3.169567000
H	0.673740000	-1.985843000	2.932308000
H	-2.065154000	-0.806423000	2.364240000
H	-2.655527000	0.087058000	-2.239676000
H	-3.926527000	2.216311000	-2.252224000
H	-0.163006000	4.416937000	0.611933000
H	-5.767161000	1.139302000	1.481461000
H	5.395098000	-2.701758000	-0.167194000
H	-4.523737000	-1.002910000	1.478867000
H	6.408906000	-0.454069000	-0.504113000
H	2.212975000	4.915636000	0.063451000
H	-6.583927000	3.103041000	0.218741000

H	-5.903263000	3.498187000	-1.372467000
H	-5.032736000	3.940303000	0.098569000
C	5.024093000	1.934763000	-0.380310000
C	4.183974000	3.006416000	-0.267269000
C	2.737929000	-3.261732000	0.351540000
C	-1.295553000	1.957270000	1.009393000
H	2.033638000	-3.457924000	-0.464757000
H	3.465952000	-4.073858000	0.388409000
H	2.155210000	-3.251298000	1.278065000
H	4.560961000	4.017830000	-0.384761000
H	6.079703000	2.079237000	-0.589212000
H	-1.580119000	0.962202000	0.670843000
H	-1.380935000	1.975338000	2.102546000
H	-1.997785000	2.689252000	0.604322000
H	-1.681769000	-2.527618000	2.558101000
O	0.351592000	-0.773693000	-1.812355000
H	-0.431667000	-1.359330000	-1.912111000
C	1.380989000	-1.180138000	-2.719053000
H	2.228345000	-0.507536000	-2.573402000
H	1.708686000	-2.207870000	-2.521352000
H	1.040369000	-1.104175000	-3.758046000

Cartesian coordinates of calculated structure **DFT_4.4**:

Ni	-1.301927000	-0.423219000	1.014791000
S	3.161001000	1.032832000	0.747270000

O	2.973021000	2.336219000	0.039667000
N	-2.985640000	-1.381653000	0.379225000
N	-2.216675000	1.176645000	0.083759000
O	3.603854000	1.123342000	2.168205000
N	1.884555000	0.066055000	0.701409000
C	0.003578000	-1.036897000	-0.431552000
C	4.471970000	0.186172000	-0.165509000
C	-3.328181000	0.771456000	-0.595046000
C	-3.309715000	-2.667022000	0.553195000
C	-4.073012000	1.627423000	-1.438380000
C	4.790494000	0.575915000	-1.466614000
C	-4.874943000	-1.079175000	-1.127684000
C	5.769781000	-0.127622000	-2.175678000
C	-2.498181000	3.359993000	-0.857827000
C	-3.737727000	-0.597714000	-0.438293000
C	6.098411000	-1.591674000	-0.288949000
C	1.197664000	-0.099231000	-0.599838000
C	-4.435158000	-3.221447000	-0.098667000
C	5.121869000	-0.902228000	0.427366000
C	-1.802614000	2.443464000	-0.032072000
C	-5.211604000	-2.437930000	-0.930598000
C	6.439609000	-1.216399000	-1.601077000
C	-3.619449000	2.961267000	-1.555087000
C	7.517923000	-1.958028000	-2.354558000
H	0.347192000	-2.046540000	-0.155304000

H	-0.545502000	-1.111227000	-1.380244000
H	0.849625000	0.870607000	-0.988082000
H	4.281519000	1.422061000	-1.914701000
H	6.014032000	0.178349000	-3.189534000
H	-2.134454000	4.378895000	-0.930840000
H	6.604904000	-2.434328000	0.174756000
H	-4.678518000	-4.265378000	0.064347000
H	4.865542000	-1.202044000	1.438401000
H	-6.077201000	-2.856742000	-1.435167000
H	-4.155383000	3.659607000	-2.190959000
H	8.512495000	-1.660115000	-2.000646000
H	7.471519000	-1.751672000	-3.427495000
H	7.432599000	-3.039553000	-2.207385000
C	-5.613177000	-0.185748000	-1.974979000
C	-5.226786000	1.115984000	-2.123568000
C	-2.426638000	-3.476478000	1.458888000
C	-0.605747000	2.876827000	0.762056000
H	-2.388521000	-3.020976000	2.454327000
H	-2.778319000	-4.505219000	1.552349000
H	-1.402834000	-3.483521000	1.068923000
H	-5.786398000	1.788555000	-2.766329000
H	-6.485451000	-0.566731000	-2.497117000
H	0.149105000	2.091041000	0.800643000
H	-0.159366000	3.779038000	0.339696000
H	-0.908012000	3.098129000	1.791889000

H	1.915191000	-0.489965000	-1.343929000
O	0.082453000	-0.071904000	2.384579000
C	0.004689000	0.850642000	3.467874000
H	0.633260000	1.729159000	3.276066000
H	-1.030274000	1.184357000	3.601389000
H	0.344055000	0.375656000	4.396921000
H	1.018464000	0.045507000	1.726771000

General Conclusions

The content of the present Doctoral Thesis can be summarized in the following general conclusions.

In *Chapter I* a detailed analysis of state-of-the-art literature regarding Pd- and Ni-catalyzed cross-coupling transformations with aziridines was conducted. The analyzed data were arranged at the end of the chapter according to the mechanisms of discussed transformations and based on the type of products formed. The existing gaps and perspectives in the aziridine cross-coupling methodology were discussed highlighting the contribution of the present Doctoral Thesis to the field.

In *Chapter II* a Ni-catalyzed reductive carboxylation of aziridines was described. The developed methodology provides access to a broad range of valuable chemicals – *β*-amino acids. This transformation expands the list of known electrophilic coupling partners reacting with aziridines and has never been described in the literature before.

In *Chapter III* a Ni-catalyzed reductive hydroalkenylation of aziridines was described. The developed methodology provides access to a broad range of valuable chemicals – homoallylamines. This transformation expands the list of known electrophilic coupling partners reacting with aziridines and has never been described in the literature before.

In *Chapter IV* experimental evidences of azanickellacyclobutane intermediate formation were collected and the reactivity of this key reaction intermediate was broadly studied. Based on observed results a mechanistic hypothesis of aziridine activation in the presence of Ni-catalyst, bulky bidentate N,N-ligands and alcohols was given. Following the proposed mechanistic hypothesis, a new Ni-catalyzed cross-electrophile alkylation of aziridines was proposed and confirmed experimentally as a working hypothesis.

To conclude, the present Doctoral Thesis significantly contribute to the field of Ni-catalyzed cross-coupling transformations of aziridines by providing a new activation mode of azanickellacyclobutane intermediate. Following the discovered mechanism two elegant methodologies were fully developed and one novel transformation was proposed as an initial working hypothesis. These transformations significantly expand known methodologies for the synthesis of *β*-functionalized amines.

Literature

(1) Robinson, A. Chemistry's Visual Origins. *Nature* **2010**, *465* (7294), 36–36. https://doi.org/10.1038/465036a.
(2) Kirkpatrick, P.; Ellis, C. Chemical Space. *Nature* **2004**, *432* (7019), 823–823. https://doi.org/10.1038/432823a.
(3) Ruddigkeit, L.; van Deursen, R.; Blum, L. C.; Reymond, J.-L. Enumeration of 166 Billion Organic Small Molecules in the Chemical Universe Database GDB-17. *J. Chem. Inf. Model.* **2012**, *52* (11), 2864–2875. https://doi.org/10.1021/ci300415d.
(4) Reymond, J.-L.; Awale, M. Exploring Chemical Space for Drug Discovery Using the Chemical Universe Database. *ACS Chem. Neurosci.* **2012**, *3* (9), 649–657. https://doi.org/10.1021/cn3000422.
(5) For Chemists, the AI Revolution Has yet to Happen. *Nature* **2023**, *617* (7961), 438–438. https://doi.org/10.1038/d41586-023-01612-x.
(6) Charpentier, J.; Früh, N.; Togni, A. Electrophilic Trifluoromethylation by Use of Hypervalent Iodine Reagents. *Chem. Rev.* **2015**, *115* (2), 650–682. https://doi.org/10.1021/cr500223h.
(7) Bhawal, B. N.; Morandi, B. Shuttle Catalysis—New Strategies in Organic Synthesis. *Chem. – Eur. J.* **2017**, *23* (50), 12004–12013. https://doi.org/10.1002/chem.201605325.
(8) Pitzer, L.; Schwarz, J. L.; Glorius, F. Reductive Radical-Polar Crossover: Traditional Electrophiles in Modern Radical Reactions. *Chem. Sci.* **2019**, *10* (36), 8285–8291. https://doi.org/10.1039/C9SC03359A.
(9) Jablonka, K. M.; Patiny, L.; Smit, B. Making the Collective Knowledge of Chemistry Open and Machine Actionable. *Nat. Chem.* **2022**, *14* (4), 365–376. https://doi.org/10.1038/s41557-022-00910-7.
(10) Kolb, V. M. On the Applicability of the Principle of the Quantity-to-Quality Transition to Chemical Evolution That Led to Life. *Int. J. Astrobiol.* **2005**, *4* (3–4), 227–232. https://doi.org/10.1017/S1473550405002818.
(11) Carneiro, R. L. The Transition from Quantity to Quality: A Neglected Causal Mechanism in Accounting for Social Evolution. *Proc. Natl. Acad. Sci.* **2000**, *97* (23), 12926–12931. https://doi.org/10.1073/pnas.240462397.
(12) Lin, B. L.; Clough, C. R.; Hillhouse, G. L. Interactions of Aziridines with Nickel Complexes: Oxidative-Addition and Reductive-Elimination Reactions That Break and Make C−N Bonds. *J. Am. Chem. Soc.* **2002**, *124* (12), 2890–2891. https://doi.org/10.1021/ja017652n.
(13) Ney, J. E.; Wolfe, J. P. Synthesis and Reactivity of Azapalladacyclobutanes. *J. Am. Chem. Soc.* **2006**, *128* (48), 15415–15422. https://doi.org/10.1021/ja0660756.
(14) Wiberg, K. B. The Concept of Strain in Organic Chemistry. *Angew. Chem. Int. Ed. Engl.* **1986**, *25* (4), 312–322. https://doi.org/10.1002/anie.198603121.
(15) Howell, J.; Goddard, J. D.; Tam, W. A Relative Approach for Determining Ring Strain Energies of Heterobicyclic Alkenes. *Tetrahedron* **2009**, *65* (23), 4562–4568. https://doi.org/10.1016/j.tet.2009.03.090.
(16) Dudev, T.; Lim, C. Ring Strain Energies from Ab Initio Calculations. *J. Am. Chem. Soc.* **1998**, *120* (18), 4450–4458. https://doi.org/10.1021/ja973895x.
(17) Talaty, E. R.; Simons, G. Local Orbital Study of Bonding in Small Rings: Cyclopropane, Thiirane, Oxirane, and Aziridine. *Theor. Chim. Acta* **1978**, *48* (4), 331–335. https://doi.org/10.1007/PL00020132.
(18) Degennaro, L.; Mansueto, R.; Carenza, E.; Rizzi, R.; Florio, S.; Pratt, L. M.; Luisi, R. Nitrogen Dynamics and Reactivity of Chiral Aziridines: Generation of Configurationally Stable Aziridinyllithium Compounds. *Chem. – Eur. J.* **2011**, *17* (18), 4992–5003. https://doi.org/10.1002/chem.201003424.

(19) Luisi, R.; Capriati, V.; Florio, S.; Di Cunto, P.; Musio, B. Synthesis and Lithiation of Oxazolinylaziridines: The N-Substituent Effect. *Tetrahedron* **2005**, *61* (13), 3251–3260. https://doi.org/10.1016/j.tet.2005.01.045.

(20) Sabir, S.; Kumar, G.; Verma, V. P.; Jat, J. L. Aziridine Ring Opening: An Overview of Sustainable Methods. *ChemistrySelect* **2018**, *3* (13), 3702–3711. https://doi.org/10.1002/slct.201800170.

(21) Gleede, T.; Reisman, L.; Rieger, E.; Mbarushimana, P. C.; Rupar, P. A.; Wurm, F. R. Aziridines and Azetidines: Building Blocks for Polyamines by Anionic and Cationic Ring-Opening Polymerization. *Polym. Chem.* **2019**, *10* (24), 3257–3283. https://doi.org/10.1039/C9PY00278B.

(22) Jang, H.-J.; Lee, J. T.; Yoon, H. J. Aziridine in Polymers: A Strategy to Functionalize Polymers by Ring-Opening Reaction of Aziridine. *Polym. Chem.* **2015**, *6* (18), 3387–3391. https://doi.org/10.1039/C5PY00266D.

(23) Park, G.-S.; Kim, S.-C.; Kang, H.-Y. Substituents Effect on Aziridine Chemistry: N-Inversion Energy, Reactivity and Regioselectivity of Nucleophilic Ring-Opening. *Bull. Korean Chem. Soc.* **2005**, *26* (9), 1339–1343. https://doi.org/10.5012/bkcs.2005.26.9.1339.

(24) Dequina, H. J.; Jones, C. L.; Schomaker, J. M. Recent Updates and Future Perspectives in Aziridine Synthesis and Reactivity. *Chem* **2023**, *9* (7), 1658–1701. https://doi.org/10.1016/j.chempr.2023.04.010.

(25) Stanković, S.; D'hooghe, M.; Catak, S.; Eum, H.; Waroquier, M.; Speybroeck, V. V.; Kimpe, N. D.; Ha, H.-J. Regioselectivity in the Ring Opening of Non-Activated Aziridines. *Chem. Soc. Rev.* **2012**, *41* (2), 643–665. https://doi.org/10.1039/C1CS15140A.

(26) *Theoretical investigation of the regioselective ring opening of 2-methylaziridine. Lewis acid effect | Journal of Molecular Modeling*. https://link.springer.com/article/10.1007/s00894-018-3833-2 (accessed 2024-01-29).

(27) *"Orthogonal" Lewis Acids: Catalyzed Ring Opening and Rearrangement of Acylaziridines | The Journal of Organic Chemistry*. https://pubs-acs-org.sabidi.urv.cat/doi/10.1021/jo980558d (accessed 2024-01-29).

(28) Cardillo, G.; Gentilucci, L.; Gianotti, M.; Tolomelli, A. Influence of Lewis Acids on the Regioselectivity of N-Boc-Aziridine-2-Carboxylate Microwave-Assisted Rearrangement. *Synlett* **2000**, *2000* (9), 1309–1311. https://doi.org/10.1055/s-2000-7125.

(29) Cardoso, A. L.; Pinho e Melo, T. M. V. D. Aziridines in Formal [3+2] Cycloadditions: Synthesis of Five-Membered Heterocycles. *Eur. J. Org. Chem.* **2012**, *2012* (33), 6479–6501. https://doi.org/10.1002/ejoc.201200406.

(30) Tang, S.; Zhang, X.; Sun, J.; Niu, D.; Chruma, J. J. 2-Azaallyl Anions, 2-Azaallyl Cations, 2-Azaallyl Radicals, and Azomethine Ylides. *Chem. Rev.* **2018**, *118* (20), 10393–10457. https://doi.org/10.1021/acs.chemrev.8b00349.

(31) Li, J.; Du, T.; Zhang, G.; Peng, Y. 3-Bromooxindoles as Nucleophiles in Asymmetric Organocatalytic Mannich Reactions with N-Ts-Imines. *Chem. Commun.* **2013**, *49* (13), 1330–1332. https://doi.org/10.1039/C2CC38475B.

(32) Lai, B.-N.; Qiu, J.-F.; Zhang, H.-X.; Nie, J.; Ma, J.-A. Stereoselective Synthesis of Fused Aziridines via One-Pot Sequential Decarboxylative Mannich Reaction and Oxidative C–H Amination of Cyclic Imines with β-Ketoacids. *Org. Lett.* **2016**, *18* (3), 520–523. https://doi.org/10.1021/acs.orglett.5b03551.

(33) Nagata, Wataru.; Hirai, Shoichi.; Kawata, Kyozo.; Aoki, Tsutomu. One-Step Synthesis of Bridged Aziridines. *J. Am. Chem. Soc.* **1967**, *89* (19), 5045–5046. https://doi.org/10.1021/ja00995a040.

(34) Lowden, P. A. S. Aziridine Natural Products – Discovery, Biological Activity and Biosynthesis. In *Aziridines and Epoxides in Organic Synthesis*; John Wiley & Sons, Ltd, 2006; pp 399–442. https://doi.org/10.1002/3527607862.ch11.

(35) Singh, G. S. Synthetic Aziridines in Medicinal Chemistry: A Mini-Review. *Mini-Rev. Med. Chem. 16* (11), 892–904.

(36) Tanner, D. Chiral Aziridines—Their Synthesis and Use in Stereoselective Transformations. *Angew. Chem. Int. Ed. Engl.* **1994**, *33* (6), 599–619. https://doi.org/10.1002/anie.199405991.
(37) Wenker, H. The Preparation of Ethylene Imine from Monoethanolamine. *J. Am. Chem. Soc.* **1935**, *57* (11), 2328–2328. https://doi.org/10.1021/ja01314a504.
(38) Leighton, P. A.; Perkins, W. A.; Renquist, M. L. A Modification of Wenker's Method of Preparing Ethyleneimine. *J. Am. Chem. Soc.* **1947**, *69* (6), 1540–1540. https://doi.org/10.1021/ja01198a512.
(39) Steuerle, U.; Feuerhake, R. Aziridines. In *Ullmann's Encyclopedia of Industrial Chemistry*; John Wiley & Sons, Ltd, 2006. https://doi.org/10.1002/14356007.a03_239.pub2.
(40) Dank, C.; Ielo, L. Recent Advances in the Accessibility, Synthetic Utility, and Biological Applications of Aziridines. *Org. Biomol. Chem.* **2023**, *21* (22), 4553–4573. https://doi.org/10.1039/D3OB00424D.
(41) Sweeney, J. Aziridine Synthesis via Nucleophilic Attack of Carbene Equivalents on Imines: The Aza-Darzens Reaction. *Eur. J. Org. Chem.* **2009**, *2009* (29), 4911–4919. https://doi.org/10.1002/ejoc.200900211.
(42) Elgemeie, G. H.; Azzam, R. A.; Zaghary, W. A.; Aly, A. A.; Metwally, N. H.; Sarhan, M. O.; Abdelhafez, E. M.; Elsayed, R. E. Chapter 1 - Synthesis of N-Sulfonated Aziridines. In *N-Sulfonated-N-Heterocycles*; Elgemeie, G. H., Azzam, R. A., Zaghary, W. A., Aly, A. A., Metwally, N. H., Sarhan, M. O., Abdelhafez, E. M., Elsayed, R. E., Eds.; Elsevier, 2022; pp 1–36. https://doi.org/10.1016/B978-0-12-822179-2.00006-9.
(43) Qadir, T.; Amin, A.; Sarkar, D.; Sharma, P. K. A Review on Recent Advances in the Synthesis of Aziridines and Their Applications in Organic Synthesis. *Curr. Org. Chem. 25* (16), 1868–1893.
(44) Evans, D. A.; Bilodeau, M. T.; Faul, M. M. Development of the Copper-Catalyzed Olefin Aziridination Reaction. *J. Am. Chem. Soc.* **1994**, *116* (7), 2742–2753. https://doi.org/10.1021/ja00086a007.
(45) Davis, F. A.; Liu, H.; Zhou, P.; Fang, T.; Reddy, G. V.; Zhang, Y. Aza-Darzens Asymmetric Synthesis of N-(p-Toluenesulfinyl)Aziridine 2-Carboxylate Esters from Sulfinimines (N-Sulfinyl Imines). *J. Org. Chem.* **1999**, *64* (20), 7559–7567. https://doi.org/10.1021/jo990907j.
(46) Degennaro, L.; Trinchera, P.; Luisi, R. Recent Advances in the Stereoselective Synthesis of Aziridines. *Chem. Rev.* **2014**, *114* (16), 7881–7929. https://doi.org/10.1021/cr400553c.
(47) Pellissier, H. Recent Developments in Asymmetric Aziridination. *Adv. Synth. Catal.* **2014**, *356* (9), 1899–1935. https://doi.org/10.1002/adsc.201400312.
(48) Cheng, Q.-Q.; Zhou, Z.; Jiang, H.; Siitonen, J. H.; Ess, D. H.; Zhang, X.; Kürti, L. Organocatalytic Nitrogen Transfer to Unactivated Olefins via Transient Oxaziridines. *Nat. Catal.* **2020**, *3* (4), 386–392. https://doi.org/10.1038/s41929-020-0430-4.
(49) Holst, D. E.; Wang, D. J.; Kim, M. J.; Guzei, I. A.; Wickens, Z. K. Aziridine Synthesis by Coupling Amines and Alkenes via an Electrogenerated Dication. *Nature* **2021**, *596* (7870), 74–79. https://doi.org/10.1038/s41586-021-03717-7.
(50) Tan, H.; Samanta, S.; Maity, A.; Roychowdhury, P.; Powers, D. C. N-Aminopyridinium Reagents as Traceless Activating Groups in the Synthesis of N-Aryl Aziridines. *Nat. Commun.* **2022**, *13* (1), 3341. https://doi.org/10.1038/s41467-022-31032-w.
(51) Johansson Seechurn, C. C. C.; Kitching, M. O.; Colacot, T. J.; Snieckus, V. Palladium-Catalyzed Cross-Coupling: A Historical Contextual Perspective to the 2010 Nobel Prize. *Angew. Chem. Int. Ed.* **2012**, *51* (21), 5062–5085. https://doi.org/10.1002/anie.201107017.
(52) Biffis, A.; Centomo, P.; Del Zotto, A.; Zecca, M. Pd Metal Catalysts for Cross-Couplings and Related Reactions in the 21st Century: A Critical Review. *Chem. Rev.* **2018**, *118* (4), 2249–2295. https://doi.org/10.1021/acs.chemrev.7b00443.
(53) Ananikov, V. P. Nickel: The "Spirited Horse" of Transition Metal Catalysis. *ACS Catal.* **2015**, *5* (3), 1964–1971. https://doi.org/10.1021/acscatal.5b00072.

(54) Boit, T. B.; Bulger, A. S.; Dander, J. E.; Garg, N. K. Activation of C–O and C–N Bonds Using Non-Precious-Metal Catalysis. *ACS Catal.* **2020**, *10* (20), 12109–12126. https://doi.org/10.1021/acscatal.0c03334.

(55) Han, R.; Hillhouse, G. L. Sulfur-Atom Transfer from Elemental Sulfur to Nickel−Carbon Bonds as a New Route to Reactive Nickel(II) Thiolates. *J. Am. Chem. Soc.* **1998**, *120* (30), 7657–7658. https://doi.org/10.1021/ja981266x.

(56) Han, R.; Hillhouse, G. L. Carbon−Oxygen Reductive-Elimination from Nickel(II) Oxametallacycles and Factors That Control Formation of Ether, Aldehyde, Alcohol, or Ester Products. *J. Am. Chem. Soc.* **1997**, *119* (34), 8135–8136. https://doi.org/10.1021/ja9714999.

(57) Koo, K.; Hillhouse, G. L. Carbon-Nitrogen Bond Formation by Reductive Elimination from Nickel(II) Amido Alkyl Complexes. *Organometallics* **1995**, *14* (9), 4421–4423. https://doi.org/10.1021/om00009a054.

(58) Alper, H.; Perera, C. P.; Ahmed, F. R. A Novel Synthesis of .Beta.-Lactams. *J. Am. Chem. Soc.* **1981**, *103* (5), 1289–1291. https://doi.org/10.1021/ja00395a082.

(59) Alper, H.; Perera, C. P. Catalytic Homogeneous Carbonylation of Azirines by Palladium(0). Important Influence of Catalyst Ligands on the Reaction Pathway. *Organometallics* **1982**, *1* (1), 70–74. https://doi.org/10.1021/om00061a013.

(60) Alper, H.; Urso, F.; Smith, D. J. H. Regiospecific Metal-Catalyzed Ring Expansion of Aziridines to .Beta.-Lactams. *J. Am. Chem. Soc.* **1983**, *105* (22), 6737–6738. https://doi.org/10.1021/ja00360a045.

(61) Calet, S.; Urso, F.; Alper, H. Enantiospecific and Stereospecific Rhodium(I)-Catalyzed Carbonylation and Ring Expansion of Aziridines. Asymmetric Synthesis of .Beta.-Lactams and the Kinetic Resolution of Aziridines. *J. Am. Chem. Soc.* **1989**, *111* (3), 931–934. https://doi.org/10.1021/ja00185a023.

(62) Piotti, M. E.; Alper, H. Inversion of Stereochemistry in the Co2(CO)8-Catalyzed Carbonylation of Aziridines to β-Lactams. The First Synthesis of Highly Strained Trans-Bicyclic β-Lactams. *J. Am. Chem. Soc.* **1996**, *118* (1), 111–116. https://doi.org/10.1021/ja9531586.

(63) Alper, H.; Hamel, N. Regiospecific Synthesis of α-Methylene-β-Lactams by a Homogeneous Palladium Catalyzed Ring Expansion-Carbonylation Reaction. *Tetrahedron Lett.* **1987**, *28* (28), 3237–3240. https://doi.org/10.1016/S0040-4039(00)95481-9.

(64) Chamchaang, W.; Pinhas, A. R. The Conversion of an Aziridine to a .Beta.-Lactam. *J. Org. Chem.* **1990**, *55* (9), 2943–2950. https://doi.org/10.1021/jo00296a070.

(65) Klein, D. P.; Hayes, J. C.; Bergman, R. G. Insertion of (.Eta.5-C5Me5)(PMe3)Ir into the Carbon-Hydrogen Bonds of Functionalized Organic Molecules: A C-H Activation Route to 2-Oxa- and 2-Azametallacyclobutanes, Potential Models for Olefin Oxidation Intermediates. *J. Am. Chem. Soc.* **1988**, *110* (11), 3704–3706. https://doi.org/10.1021/ja00219a080.

(66) Matsunaga, P. T.; Hess, C. R.; Hillhouse, G. L. Reactions of Organoazides with Nickel Alkyls. Syntheses and Reactions of Nickel(II) Amido Complexes. *J. Am. Chem. Soc.* **1994**, *116* (8), 3665–3666. https://doi.org/10.1021/ja00087a089.

(67) Koo, K.; Hillhouse, G. L. Indoline Synthesis via Coupling of Phenethyl Grignard Reagents with Organoazides Mediated by (Alkylphosphine)Nickel(II) Complexes. *Organometallics* **1996**, *15* (12), 2669–2671. https://doi.org/10.1021/om960286+.

(68) Wolfe, J. P.; Ney, J. E. A New, Mild Synthesis of N-Sulfonyl Ketimines via the Palladium-Catalyzed Isomerization of Aziridines. *Org. Lett.* **2003**, *5* (24), 4607–4610. https://doi.org/10.1021/ol0357651.

(69) Huang, C.-Y. (Dennis); Doyle, A. G. Nickel-Catalyzed Negishi Alkylations of Styrenyl Aziridines. *J. Am. Chem. Soc.* **2012**, *134* (23), 9541–9544. https://doi.org/10.1021/ja3013825.

(70) Yamamoto, T.; Yamamoto, A.; Ikeda, S. Organo (Dipyridyl) Nickel Complexes. I. Stability and Activation of the Alkyl-Nickel Bonds of Dialkyl (Dipyridyl) Nickel by

Coordination with Various Substituted Olefins. *J. Am. Chem. Soc.* **1971**, *93* (14), 3350–3359. https://doi.org/10.1021/ja00743a009.

(71) Giovannini, R.; Stüdemann, T.; Dussin, G.; Knochel, P. An Efficient Nickel-Catalyzed Cross-Coupling Between Sp3 Carbon Centers. *Angew. Chem. Int. Ed.* **1998**, *37* (17), 2387–2390. https://doi.org/10.1002/(SICI)1521-3773(19980918)37:17<2387::AID-ANIE2387>3.0.CO;2-M.

(72) Hu, X. Nickel-Catalyzed Cross Coupling of Non-Activated Alkyl Halides: A Mechanistic Perspective. *Chem. Sci.* **2011**, *2* (10), 1867–1886. https://doi.org/10.1039/C1SC00368B.

(73) Nielsen, D. K.; Huang, C.-Y. (Dennis); Doyle, A. G. Directed Nickel-Catalyzed Negishi Cross Coupling of Alkyl Aziridines. *J. Am. Chem. Soc.* **2013**, *135* (36), 13605–13609. https://doi.org/10.1021/ja4076716.

(74) Duda, M. L.; Michael, F. E. Palladium-Catalyzed Cross-Coupling of N-Sulfonylaziridines with Boronic Acids. *J. Am. Chem. Soc.* **2013**, *135* (49), 18347–18349. https://doi.org/10.1021/ja410686v.

(75) Takeda, Y.; Ikeda, Y.; Kuroda, A.; Tanaka, S.; Minakata, S. Pd/NHC-Catalyzed Enantiospecific and Regioselective Suzuki–Miyaura Arylation of 2-Arylaziridines: Synthesis of Enantioenriched 2-Arylphenethylamine Derivatives. *J. Am. Chem. Soc.* **2014**, *136* (24), 8544–8547. https://doi.org/10.1021/ja5039616.

(76) Jensen, K. L.; Standley, E. A.; Jamison, T. F. Highly Regioselective Nickel-Catalyzed Cross-Coupling of N-Tosylaziridines and Alkylzinc Reagents. *J. Am. Chem. Soc.* **2014**, *136* (31), 11145–11152. https://doi.org/10.1021/ja505823s.

(77) Zultanski, S. L.; Fu, G. C. Nickel-Catalyzed Carbon–Carbon Bond-Forming Reactions of Unactivated Tertiary Alkyl Halides: Suzuki Arylations. *J. Am. Chem. Soc.* **2013**, *135* (2), 624–627. https://doi.org/10.1021/ja311669p.

(78) Tasker, S. Z.; Standley, E. A.; Jamison, T. F. Recent Advances in Homogeneous Nickel Catalysis. *Nature* **2014**, *509* (7500), 299–309. https://doi.org/10.1038/nature13274.

(79) Huang, C.-Y. (Dennis); Doyle, A. G. Electron-Deficient Olefin Ligands Enable Generation of Quaternary Carbons by Ni-Catalyzed Cross-Coupling. *J. Am. Chem. Soc.* **2015**, *137* (17), 5638–5641. https://doi.org/10.1021/jacs.5b02503.

(80) Chow, W. K.; Yuen, O. Y.; Choy, P. Y.; So, C. M.; Lau, C. P.; Wong, W. T.; Kwong, F. Y. A Decade Advancement of Transition Metal-Catalyzed Borylation of Aryl Halides and Sulfonates. *RSC Adv.* **2013**, *3* (31), 12518–12539. https://doi.org/10.1039/C3RA22905J.

(81) Hassan, M. M. M.; Guria, S.; Dey, S.; Das, J.; Chattopadhyay, B. Transition Metal–Catalyzed Remote C─H Borylation: An Emerging Synthetic Tool. *Sci. Adv.* **2023**, *9* (16), eadg3311. https://doi.org/10.1126/sciadv.adg3311.

(82) Takeda, Y.; Kuroda, A.; Sameera, W. M. C.; Morokuma, K.; Minakata, S. Palladium-Catalyzed Regioselective and Stereo-Invertive Ring-Opening Borylation of 2-Arylaziridines with Bis(Pinacolato)Diboron: Experimental and Computational Studies. *Chem. Sci.* **2016**, *7* (9), 6141–6152. https://doi.org/10.1039/C6SC01120A.

(83) Molander, G. A. Organotrifluoroborates: Another Branch of the Mighty Oak. *J. Org. Chem.* **2015**, *80* (16), 7837–7848. https://doi.org/10.1021/acs.joc.5b00981.

(84) Teh, W. P.; Michael, F. E. Palladium-Catalyzed Cross-Coupling of N-Sulfonylaziridines and Alkenylboronic Acids: Stereospecific Synthesis of Homoallylic Amines with Di- and Trisubstituted Alkenes. *Org. Lett.* **2017**, *19* (7), 1738–1740. https://doi.org/10.1021/acs.orglett.7b00504.

(85) Woods, B. P.; Orlandi, M.; Huang, C.-Y.; Sigman, M. S.; Doyle, A. G. Nickel-Catalyzed Enantioselective Reductive Cross-Coupling of Styrenyl Aziridines. *J. Am. Chem. Soc.* **2017**, *139* (16), 5688–5691. https://doi.org/10.1021/jacs.7b03448.

(86) Everson, D. A.; Jones, B. A.; Weix, D. J. Replacing Conventional Carbon Nucleophiles with Electrophiles: Nickel-Catalyzed Reductive Alkylation of Aryl Bromides and Chlorides. *J. Am. Chem. Soc.* **2012**, *134* (14), 6146–6159. https://doi.org/10.1021/ja301769r.

(87) Biswas, S.; Weix, D. J. Mechanism and Selectivity in Nickel-Catalyzed Cross-Electrophile Coupling of Aryl Halides with Alkyl Halides. *J. Am. Chem. Soc.* **2013**, *135* (43), 16192–16197. https://doi.org/10.1021/ja407589e.

(88) Cherney, A. H.; Kadunce, N. T.; Reisman, S. E. Catalytic Asymmetric Reductive Acyl Cross-Coupling: Synthesis of Enantioenriched Acyclic α,α-Disubstituted Ketones. *J. Am. Chem. Soc.* **2013**, *135* (20), 7442–7445. https://doi.org/10.1021/ja402922w.

(89) Cherney, A. H.; Reisman, S. E. Nickel-Catalyzed Asymmetric Reductive Cross-Coupling Between Vinyl and Benzyl Electrophiles. *J. Am. Chem. Soc.* **2014**, *136* (41), 14365–14368. https://doi.org/10.1021/ja508067c.

(90) Kadunce, N. T.; Reisman, S. E. Nickel-Catalyzed Asymmetric Reductive Cross-Coupling between Heteroaryl Iodides and α-Chloronitriles. *J. Am. Chem. Soc.* **2015**, *137* (33), 10480–10483. https://doi.org/10.1021/jacs.5b06466.

(91) Poremba, K. E.; Kadunce, N. T.; Suzuki, N.; Cherney, A. H.; Reisman, S. E. Nickel-Catalyzed Asymmetric Reductive Cross-Coupling To Access 1,1-Diarylalkanes. *J. Am. Chem. Soc.* **2017**, *139* (16), 5684–5687. https://doi.org/10.1021/jacs.7b01705.

(92) Ravn, A. K.; Vilstrup, M. B. T.; Noerby, P.; Nielsen, D. U.; Daasbjerg, K.; Skrydstrup, T. Carbon Isotope Labeling Strategy for β-Amino Acid Derivatives via Carbonylation of Azanickellacycles. *J. Am. Chem. Soc.* **2019**, *141* (30), 11821–11826. https://doi.org/10.1021/jacs.9b05934.

(93) Hermange, P.; Lindhardt, A. T.; Taaning, R. H.; Bjerglund, K.; Lupp, D.; Skrydstrup, T. Ex Situ Generation of Stoichiometric and Substoichiometric 12CO and 13CO and Its Efficient Incorporation in Palladium Catalyzed Aminocarbonylations. *J. Am. Chem. Soc.* **2011**, *133* (15), 6061–6071. https://doi.org/10.1021/ja200818w.

(94) Steiman, T. J.; Liu, J.; Mengiste, A.; Doyle, A. G. Synthesis of β-Phenethylamines via Ni/Photoredox Cross-Electrophile Coupling of Aliphatic Aziridines and Aryl Iodides. *J. Am. Chem. Soc.* **2020**, *142* (16), 7598–7605. https://doi.org/10.1021/jacs.0c01724.

(95) Fan, P.; Jin, Y.; Liu, J.; Wang, R.; Wang, C. Nickel/Photo-Cocatalyzed Regioselective Ring Opening of N-Tosyl Styrenyl Aziridines with Aldehydes. *Org. Lett.* **2021**, *23* (19), 7364–7369. https://doi.org/10.1021/acs.orglett.1c02514.

(96) Dongbang, S.; Doyle, A. G. Ni/Photoredox-Catalyzed C(Sp3)–C(Sp3) Coupling between Aziridines and Acetals as Alcohol-Derived Alkyl Radical Precursors. *J. Am. Chem. Soc.* **2022**, *144* (43), 20067–20077. https://doi.org/10.1021/jacs.2c09294.

(97) Wang, Y.-Z.; Wang, Z.-H.; Eshel, I. L.; Sun, B.; Liu, D.; Gu, Y.-C.; Milo, A.; Mei, T.-S. Nickel/Biimidazole-Catalyzed Electrochemical Enantioselective Reductive Cross-Coupling of Aryl Aziridines with Aryl Iodides. *Nat. Commun.* **2023**, *14* (1), 2322. https://doi.org/10.1038/s41467-023-37965-0.

(98) Hu, X.; Cheng-Sánchez, I.; Cuesta-Galisteo, S.; Nevado, C. Nickel-Catalyzed Enantioselective Electrochemical Reductive Cross-Coupling of Aryl Aziridines with Alkenyl Bromides. *J. Am. Chem. Soc.* **2023**, *145* (11), 6270–6279. https://doi.org/10.1021/jacs.2c12869.

(99) Kumar, G. S.; Zhu, C.; Kancherla, R.; Shinde, P. S.; Rueping, M. Metal Cations from Sacrificial Anodes Act as a Lewis Acid Co-Catalyst in Electrochemical Cross-Coupling of Aryl Bromides and Aziridines. *ACS Catal.* **2023**, *13* (13), 8813–8820. https://doi.org/10.1021/acscatal.3c01503.

(100) Tang, W.; Fan, P. Nickel-Catalyzed Cross-Electrophile Ring Opening/Gem-Difluoroallylation of Aziridines. *Org. Lett.* **2023**, *25* (31), 5756–5761. https://doi.org/10.1021/acs.orglett.3c01973.

(101) Williams, W. L.; Gutiérrez-Valencia, N. E.; Doyle, A. G. Branched-Selective Cross-Electrophile Coupling of 2-Alkyl Aziridines and (Hetero)Aryl Iodides Using Ti/Ni Catalysis. *J. Am. Chem. Soc.* **2023**, *145* (44), 24175–24183. https://doi.org/10.1021/jacs.3c08301.

(102) Hao, W.; Wu, X.; Sun, J. Z.; Siu, J. C.; MacMillan, S. N.; Lin, S. Radical Redox-Relay Catalysis: Formal [3+2] Cycloaddition of N-Acylaziridines and Alkenes. *J. Am. Chem. Soc.* **2017**, *139* (35), 12141–12144. https://doi.org/10.1021/jacs.7b06723.

(103) Zhang, Y.-Q.; Vogelsang, E.; Qu, Z.-W.; Grimme, S.; Gansäuer, A. Titanocene-Catalyzed Radical Opening of N-Acylated Aziridines. *Angew. Chem. Int. Ed.* **2017**, *56* (41), 12654–12657. https://doi.org/10.1002/anie.201707673.

(104) Chenniappan, V. K.; Silwal, S.; Rahaim, R. J. Ni/Ti Dual Catalytic Cross-Coupling of Nitriles and Organobromides To Access Ketones. *ACS Catal.* **2018**, *8* (5), 4539–4544. https://doi.org/10.1021/acscatal.8b00244.

(105) Smith, J. M.; Harwood, S. J.; Baran, P. S. Radical Retrosynthesis. *Acc. Chem. Res.* **2018**, *51* (8), 1807–1817. https://doi.org/10.1021/acs.accounts.8b00209.

(106) Davies, J.; Lyonnet, J. R.; Zimin, D. P.; Martin, R. The Road to Industrialization of Fine Chemical Carboxylation Reactions. *Chem* **2021**, *7* (11), 2927–2942. https://doi.org/10.1016/j.chempr.2021.10.016.

(107) Gaydou, M.; Moragas, T.; Juliá-Hernández, F.; Martin, R. Site-Selective Catalytic Carboxylation of Unsaturated Hydrocarbons with CO2 and Water. *J. Am. Chem. Soc.* **2017**, *139* (35), 12161–12164. https://doi.org/10.1021/jacs.7b07637.

(108) Davies, J.; Lyonnet, J. R.; Carvalho, B.; Sahoo, B.; Day, C. S.; Juliá-Hernández, F.; Duan, Y.; Álvaro Velasco-Rubio; Obst, M.; Norrby, P.-O.; Hopmann, K. H.; Martin, R. Kinetically-Controlled Ni-Catalyzed Direct Carboxylation of Unactivated Secondary Alkyl Bromides without Chain Walking. *J. Am. Chem. Soc.* **2024**, *146* (3), 1753–1759. https://doi.org/10.1021/jacs.3c11205.

(109) Somerville, R. J.; Odena, C.; Obst, M. F.; Hazari, N.; Hopmann, K. H.; Martin, R. Ni(I)–Alkyl Complexes Bearing Phenanthroline Ligands: Experimental Evidence for CO2 Insertion at Ni(I) Centers. *J. Am. Chem. Soc.* **2020**, *142* (25), 10936–10941. https://doi.org/10.1021/jacs.0c04695.

(110) Berman, R. S.; Kochi, J. K. Kinetics and Mechanism of Oxygen Atom Transfer from Nitro Compounds Mediated by Nickel(0) Complexes. *Inorg. Chem.* **1980**, *19* (1), 248–254. https://doi.org/10.1021/ic50203a050.

(111) Sun, S.-Z.; Romano, C.; Martin, R. Site-Selective Catalytic Deaminative Alkylation of Unactivated Olefins. *J. Am. Chem. Soc.* **2019**, *141* (41), 16197–16201. https://doi.org/10.1021/jacs.9b07489.

(112) Sun, S. Z.; Börjesson, M.; Martin-Montero, R.; Martin, R. Site-Selective Ni-Catalyzed Reductive Coupling of α-Haloboranes with Unactivated Olefins. *J. Am. Chem. Soc.* **2018**, *140*, 12765–12769. https://doi.org/10.1021/jacs.8b09425.

(113) Preston, H. S.; Kennard, C. H. L.; Plowman, R. A. STRUCTURAL STUDIES COMPLEXES OF SOME METAL CHLORIDES A TF . TRAHEDRAL Environment Surrounding M n Is Postulated for MnCI ~ Drop , from Spectral , Molecular Weight and Magnetic Susceptibility Evidence [1]. A Crystal Structure Analysis of ZnHC12 Dmp [2]. *J Inorg Nucl Chem* **1968**, *30* (1963), 1463–1467.

(114) Powers, D. C.; Anderson, B. L.; Nocera, D. G. Two-Electron HCl to H 2 Photocycle Promoted by Ni(II) Polypyridyl Halide Complexes. *J Am Chem Soc* **2013**, *135*. https://doi.org/10.1021/ja408787k.

(115) Dubey, A.; Rahaman, S. M. W.; Fayzullin, R. R.; Khusnutdinova, J. R. Transfer Hydrogenation of Carbonyl Groups, Imines and N-Heterocycles Catalyzed by Simple, Bipyridine-Based MnI Complexes. *ChemCatChem* **2019**, *11*, 3844–3852. https://doi.org/10.1002/cctc.201900358.

(116) Karpacheva, M.; Malzner, F. J.; Wobill, C.; Büttner, A.; Constable, E. C.; Housecroft, C. E. Cuprophilia: Dye-Sensitized Solar Cells with Copper(I) Dyes and Copper(I)/(II) Redox Shuttles. *Dyes Pigments* **2018**, *156* (April), 410–416. https://doi.org/10.1016/j.dyepig.2018.04.033.

(117) Lehn, J. -M; De Vains, J. R. Synthesis and Properties of Macrobicyclic Cryptates Incorporating Five- and Six-Membered Biheteroaryl Units. *Helv. Chim. Acta* **1992**, *75*, 1221–1236. https://doi.org/10.1002/hlca.19920750422.

(118) Kirsanov, D. O.; Borisova, N. E.; Reshetova, M. D.; Ivanov, A. V.; Korotkov, L. A.; Eliseev, I. I.; Alyapyshev, M. Yu.; Spiridonov, I. G.; Legin, A. V.; Vlasov, Yu. G.; Babain, V. A. Novel Diamides of 2 , 2 ′ Dipyridyl 6 , 6 ′ Dicarboxylic Acid : Synthesis , Coordination Properties , and Possibilities of Use in Electrochemical Sensors and Liquid Extraction. *Russ Chem Bull Int Ed* **2012**, *61* (4), 881–890.

(119) Regnouf De Vains, J. B.; Papet, A. L.; Marsura, A. New Symmetric and Unsymmetric Polyfunctionalized 2,2′-bipyridines. *Journal of Heterocyclic Chemistry*. 1994, pp 1069–1077. https://doi.org/10.1002/jhet.5570310463.

(120) Bieber, L. W.; De Araújo, M. C. F. Short and Efficient Synthesis of Optically Active N-Tosyl Aziridines from 2-Amino Alcohols. *Molecules* **2002**, *7* (12), 902–906. https://doi.org/10.3390/71200902.

(121) Jensen, K. L.; Standley, E. A.; Jamison, T. F. Highly Regioselective Nickel-Catalyzed Cross-Coupling of N -Tosylaziridines and Alkylzinc Reagents. *J. Am. Chem. Soc.* **2014**, *136* (31), 11145–11152. https://doi.org/10.1021/ja505823s.

(122) Jeong, J. U.; Tao, B.; Sagasser, I.; Henniges, H.; Sharpless, K. B. Bromine-Catalyzed Aziridination of Olefins. A Rare Example of Atom-Transfer Redox Catalysis by a Main Group Element. *J. Am. Chem. Soc.* **1998**, *120* (27), 6844–6845. https://doi.org/10.1021/ja981419g.

(123) Kong, D.-L.; He, L.-N.; Wang, J.-Q. Facile Synthesis of Oxazolidinones Catalyzed by N-Bu4NBr3/n-Bu4NBr Directly from Olefins, Chloramine-T and Carbon Dioxide. *Catal. Commun.* **2010**, *11* (11), 992–995. https://doi.org/10.1016/j.catcom.2010.04.003.

(124) Sevov, C. S.; Zhou, J.; Hartwig, J. F. Iridium-Catalyzed, Intermolecular Hydroamination of Unactivated Alkenes with Indoles. *J. Am. Chem. Soc.* **2014**, *136* (8), 3200–3207. https://doi.org/10.1021/ja412116d.

(125) Mahadevan, V.; Getzler, Y. D. Y. L.; Coates, G. W. [Lewis Acid]+[Co(CO)4] Complexes: A Versatile Class of Catalysts for Carbonylative Ring Expansion of Epoxides and Aziridines. *Angew. Chem. Int. Ed.* **2002**, *41* (15), 2781–2784. https://doi.org/10.1002/1521-3773(20020802)41:15<2781::AID-ANIE2781>3.0.CO;2-S.

(126) Samanta, K.; Panda, G. One Pot Synthesis of Amino Acid Derived Chiral Disubstituted Morpholines and 1,4-Oxazepanes via Tandem Aziridine/Epoxide Ring Opening Sequences. *Org. Biomol. Chem.* **2011**, *9* (21), 7365. https://doi.org/10.1039/c1ob05462g.

(127) Kawamura, K.; Fukuzawa, H.; Hayashi, M. Novel N,N,P -Tridentate Ligands for the Highly Enantioselective Copper-Catalyzed 1,4-Addition of Dialkylzincs to Enones. *Org. Lett.* **2008**, *10* (16), 3509–3512. https://doi.org/10.1021/ol801259u.

(128) Kumar, G. D. K.; Baskaran, S. Heteropoly Acid as a Novel Nitrene Transfer Agent: A Facile and Practical Aziridination of Olefins with Chloramine-TElectronic Supplementary Information (ESI) Available: Plot of % of Yield vs. Mol% PMA, Experimental Procedure and Spectral Data for All Com. *Chem. Commun.* **2004**, No. 8, 1026. https://doi.org/10.1039/b402371d.

(129) Kok, G. P. Y.; Yang, H.; Wong, M. W.; Zhao, Y. Cu-Catalyzed [3 + 3] Cycloaddition of Isocyanoacetates with Aziridines and Stereoselective Access to α,γ-Diamino Acids. *Org. Lett.* **2018**, *20*, 5112–5115. https://doi.org/10.1021/acs.orglett.8b01948.

(130) Sureshkumar, D.; Gunasundari, T.; Ganesh, V.; Chandrasekaran, S. Regio- and Stereospecific Synthesis of -Sulfonamidodisulfides and -Sulfonamidosulfides from Aziridines Using Tetrathiomolybdate as a Sulfur Transfer Reagent ‡. *J Org Chem* **2007**, *72* (6), 2106–2117. https://doi.org/10.1021/jo0624389.

(131) Righi, P.; Scardovi, N.; Marotta, E.; Holte, P.; Zwanenburg, B. Solution- and Solid-Phase Synthesis of Derivatives from Enantiomerically Pure N -Tosyl-2 , 3-Aziridine Alcohols. *Org Lett* **2002**, *7* (4), 497–500. https://doi.org/10.1021/ol0170152.

(132) McIntosh, J. M. Azapropellanes as Phase-Transfer Catalyst. 4. Conformational Stabilities of Substituted Azapropellanes: 2-Methyl-1-Azoniatricyclo[4.4.4.01,6]Tetradecane Salts. *J Org Chem* **1982**, *47* (19), 3777–3779. https://doi.org/10.1021/jo00140a042.
(133) Kabalka, G. W.; Gooch, E. E. A Mild and Convenient Procedure for Conversion of Alkenes into Alkyl Iodides via Reaction of Iodine Monochloride with Organoboranes. *J. Org. Chem.* **1980**, *45* (dl), 3578–3580. https://doi.org/10.1021/jo01306a007.
(134) Meng, Q. Y.; Schirmer, T. E.; Katou, K.; König, B. Controllable Isomerization of Alkenes by Dual Visible-Light-Cobalt Catalysis. *Angew. Chem. - Int. Ed.* **2019**, *58*, 5723–5728. https://doi.org/10.1002/anie.201900849.
(135) Bigi, M.; White, M. C. Terminal Olefins to Linear α,β-Unsaturated Ketones: Pd(II)/Hypervalent Iodine Co-Catalyzed Wacker Oxidation-Dehydrogenation. *J. Am. Chem. Soc.* **2013**, *135* (Ii), 7831–7834. https://doi.org/10.1021/ja402651q.
(136) Wang, X.; Ye, Y.; Zhang, S.; Feng, J.; Xu, Y.; Zhang, Y.; Wang, J. Copper-Catalyzed C(Sp 3)-C(Sp 3) Bond Formation Using a Hypervalent Iodine Reagent: An Efficient Allylic Trifluoromethylation. *J. Am. Chem. Soc.* **2011**, *133* (Table 2), 16410–16413. https://doi.org/10.1021/ja207775a.
(137) Nielsen, D. K.; Huang, C. Y.; Doyle, A. G. Directed Nickel-Catalyzed Negishi Cross Coupling of Alkyl Aziridines. *J. Am. Chem. Soc.* **2013**, *135*, 13605–13609. https://doi.org/10.1021/ja4076716.
(138) Lüning, U.; Mak, E.; Zindler, M.; Hartkopf, B.; Herges, R. 27- To 39-Membered Pyridine Macrocycles. *Eur J Org Chem* **2010**, 4932–4940. https://doi.org/10.1002/ejoc.201000505.
(139) Mao, L. L.; Cong, H. Atom-Transfer Radical Addition to Unactivated Alkenes by Using Heterogeneous Visible-Light Photocatalysis. *ChemSusChem* **2017**, *10*, 4461–4464. https://doi.org/10.1002/cssc.201701382.
(140) Hay, M. B.; Hardin, A. R.; Wolfe, J. P. Palladium-Catalyzed Synthesis of Tetrahydrofurans from γ-Hydroxy Terminal Alkenes: Scope, Limitations, and Stereoselectivity. *J. Org. Chem.* **2005**, *70*, 3099–3107. https://doi.org/10.1021/jo050022+.
(141) Oh, H.; Park, A.; Jeong, K. S.; Han, S. B.; Lee, H. Copper-Catalyzed 1,2-Bistrifluoromethylation of Terminal Alkenes. *Adv. Synth. Catal.* **2019**, *361* (Ii), 2136–2140. https://doi.org/10.1002/adsc.201801675.
(142) Rieger, E.; Manhart, A.; Wurm, F. R. Multihydroxy Polyamines by Living Anionic Polymerization of Aziridines. *ACS Macro Lett* **2016**, *5*, 195–198. https://doi.org/10.1021/acsmacrolett.5b00901.
(143) Kalyani, D.; Sanford, M. S. Oxidatively Intercepting Heck Intermediates: Pd-Catalyzed 1,2- and 1,1-Arylhalogenation of Alkenes. *J. Am. Chem. Soc.* **2008**, *130*, 2150–2151. https://doi.org/10.1021/ja0782798.
(144) Alagiri, K.; Prabhu, K. R. Catalyst-Free Regio- and Stereospecific Synthesis of β-Sulfonamido Dithiocarbamates: Efficient Ring-Opening Reactions of N-Tosyl Aziridines by Dialkyldithiocarbamates. *Chem. - Eur. J.* **2011**, *17*, 6922–6925. https://doi.org/10.1002/chem.201100817.
(145) D'hooghe, M.; Kerkaert, I.; Rottiers, M.; De Kimpe, N. Ring Opening Reactions of 1-Arenesulfonyl-2-(Bromomethyl)Aziridines. *Tetrahedron* **2004**, *60* (16), 3637–3641. https://doi.org/10.1016/j.tet.2004.02.059.
(146) Mohottalage, S.; Tabacchi, R.; Guerin, P. M. Components from Sri Lankan Piper betleL. Leaf Oil Andtheir Analogues Showing Toxicity against the Housefly,Musca Domestica. *Flavour Fragr J* **2007**, *22*, 130–138. https://doi.org/10.1002/ffj.
(147) Ravn, A. K.; Vilstrup, M. B. T.; Noerby, P.; Nielsen, D. U.; Daasbjerg, K.; Skrydstrup, T. Carbon Isotope Labeling Strategy for β - Amino Acid Derivatives via Carbonylation of Azanickellacycles. *Angew. Chem. Int. Ed.* **2019**. https://doi.org/10.1021/jacs.9b05934.
(148) Combee, L.; Raya, B.; Wang, D.; Hilinski, M. K. Organocatalytic Nitrenoid Transfer: Metal-Free Selective Intermolecular C(Sp3)-H Amination Catalyzed by an Iminium Salt. *Chem. Sci.* **2018**, *9*, 935–939. https://doi.org/10.1039/c7sc03968a.

(149) Jiang, H.; Albrecht, Ł.; Jørgensen, K. A. Organocatalytic Preparation of Simple -Hydroxy and -Amino Esters : Low Catalyst Loadings and Gram-Scale Synthesis. *Org Lett* **2010**, *12* (21), 2008–2011. https://doi.org/10.1021/ol102164y.

(150) Wang, J.; Hou, Y. Wol Ff Rearrangement of Diazo Ketones Derived from N - p - Tolylsulfonyl- Protected - and -Amino Acids Jianbo Wang * and Yihua Hou. *J Chem Soc Perkin Trans 1* **1998**, 1919–1923.

(151) Howson, W.; Osborn, H. M. I.; Sweeney, J. Ring-Opening of N-Tosyl Aziridines by 2-Lithiodithianes. *J. Chem. Soc. Perkin 1* **1995**, 2439–2445. https://doi.org/10.1039/p19950002439.

(152) Cariou, C. A. M.; Kariuki, B. M.; Snaith, J. S. Stereoselective Synthesis of 2 , 4 , 5-Trisubstituted Piperidines by Carbonyl Ene and Prins Cyclisations †. *Org Biomol Chem* **2008**, *6*, 3337–3348. https://doi.org/10.1039/b808644c.

(153) Seebach, D.; Bezençon, O.; Jaun, B.; Pietzonka, T.; Matthews, J. L.; Kühnle, F. N. M.; Schweizer, W. B. Furthefurther C-Alkylations of Cyclotetrapeptides via Lithium and Phosphazenium (P4) Enolates: Discovery of a New Conformationr C-Alkylations of Cyclotetrapeptides via Lithium and Phosphazenium (P4) Enolates: Discovery of a New Conformation. *Helv. Chim. Acta* **1996**, *79* (11350), 588–608. https://doi.org/10.1002/hlca.19960790303.

(154) Knall, A. C.; Winkler, M.; Martı, L.; Klempier, N. Synthesis and Microbial Transformation of b -Amino Nitriles. *Tetrahedron* **2005**, *61*, 4249–4260. https://doi.org/10.1016/j.tet.2005.02.057.

(155) Ogawa, Y.; Kuroda, K.; Mukaiyama, T. Highly Stereoselective Samarium(II) Iodide-Mediated Aldol Reactions of Acylaziridines with Aldehydes. *Bull. Chem. Soc. Jpn.* **2005**, *78*, 1309–1333. https://doi.org/10.1246/bcsj.78.1309.

(156) Bando, T.; Harayama, H.; Fukazawa, Y.; Shiro, M.; Fugami, K.; Tanaka, S.; Tamaru, Y. Regio- and Stereoselective Synthesis of 1,3-Hydroxyl Amines via Palladium-Catalyzed Carbonate-Carbamate Transformation with Unique Stereoselectivity: Synthesis of 3-Amino-4-Penten-1-Ols. *J. Org. Chem.* **1994**, *59* (5), 1465–1474. https://doi.org/10.1021/jo00085a039.

(157) Ramani, A.; Desai, B.; Patel, M.; Naveen, T. Recent Advances in the Functionalization of Terminal and Internal Alkynes. *Asian J. Org. Chem.* **2022**, *11* (5), e202200047. https://doi.org/10.1002/ajoc.202200047.

(158) Liu, W.; Kong, W. Ni-Catalyzed Stereoselective Difunctionalization of Alkynes. *Org. Chem. Front.* **2020**, *7* (23), 3941–3955. https://doi.org/10.1039/D0QO01097A.

(159) Li, Z.; García-Domínguez, A.; Nevado, C. Nickel-Catalyzed Stereoselective Dicarbofunctionalization of Alkynes. *Angew. Chem. Int. Ed.* **2016**, *55* (24), 6938–6941. https://doi.org/10.1002/anie.201601296.

(160) Deng, H.-P.; Fan, X.-Z.; Chen, Z.-H.; Xu, Q.-H.; Wu, J. Photoinduced Nickel-Catalyzed Chemo- and Regioselective Hydroalkylation of Internal Alkynes with Ether and Amide α-Hetero C(Sp3)–H Bonds. *J. Am. Chem. Soc.* **2017**, *139* (38), 13579–13584. https://doi.org/10.1021/jacs.7b08158.

(161) Till, N. A.; Smith, R. T.; MacMillan, D. W. C. Decarboxylative Hydroalkylation of Alkynes. *J. Am. Chem. Soc.* **2018**, *140* (17), 5701–5705. https://doi.org/10.1021/jacs.8b02834.

(162) Molinaro, C.; Jamison, T. F. Nickel-Catalyzed Reductive Coupling of Alkynes and Epoxides. *J. Am. Chem. Soc.* **2003**, *125* (27), 8076–8077. https://doi.org/10.1021/ja0361401.

(163) Bieber, L. W.; De Araújo, M. C. F. Short and Efficient Synthesis of Optically Active N-Tosyl Aziridines from 2-Amino Alcohols. *Molecules* **2002**, *7* (12), 902–906. https://doi.org/10.3390/71200902.

(164) Tran, V. T.; Kim, N.; Rubel, C. Z.; Wu, X.; Kang, T.; Jankins, T. C.; Li, Z.-Q.; Joannou, M. V.; Ayers, S.; Gembicky, M.; Bailey, J.; Sturgell, E. J.; Sanchez, B. B.; Chen, J. S.; Lin, S.; Eastgate, M. D.; Wisniewski, S. R.; Engle, K. M. Structurally Diverse Bench-Stable

Nickel(0) Pre-Catalysts: A Practical Toolkit for In Situ Ligation Protocols**. *Angew. Chem. Int. Ed.* **2023**, *62* (9), e202211794. https://doi.org/10.1002/anie.202211794.

(165) Zhu, Z.-F.; Tu, J.-L.; Liu, F. Ni-Catalyzed Deaminative Hydroalkylation of Internal Alkynes. *Chem. Commun.* **2019**, *55* (76), 11478–11481. https://doi.org/10.1039/C9CC05385A.

(166) Pallenberg, A. J.; Marschner, T. M.; Barnhart, D. M. Phenanthroline Complexes of the d 1 ° Metals Nickel (O), Zinc (Ll) and Silver (I) Comparison to Copper (I) Species. *Polyhedron* **1997**, *16* (16), 2711–2719.

(167) Moragas, T.; Cornella, J.; Martin, R. Ligand-Controlled Regiodivergent Ni-Catalyzed Reductive Carboxylation of Allyl Esters with CO2. *J. Am. Chem. Soc.* **2014**, *136*, 17702–17705. https://doi.org/10.1021/ja509077a.

(168) Bailey, G. a.; Fogg, D. E. Confronting Neutrality: Maximizing Success in the Analysis of Transition-Metal Catalysts by MALDI Mass Spectrometry. *ACS Catal.* **2016**, *6*, 4962–4971. https://doi.org/10.1021/acscatal.6b01105.

UNIVERSITAT
ROVIRA i VIRGILI